PNL-8278
AD-940

Hanford Tank Safety Project

Minutes of the Tank Waste Science Panel Meeting March 25-27, 1992

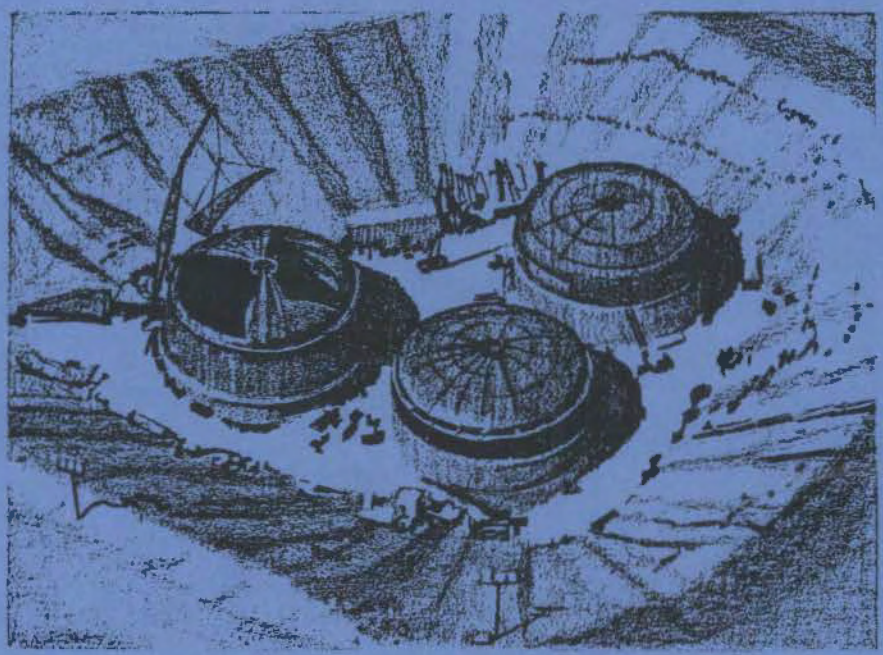

August 1992

Work Supported by the U.S. Department of Energy
under Contract DE-AC06-76RLO 1830

Pacific Northwest Laboratory
Operated for the U.S. Department of Energy
by Battelle Memorial Institute

Battelle

PNL-8278

DISCLAIMER

PACIFIC NORTHWEST LABORATORY
operated by
BATTELLE MEMORIAL INSTITUTE
for the
UNITED STATES DEPARTMENT OF ENERGY
under Contract DE-AC06-76RLO 1830

Printed in the United States of America

Available to DOE and DOE contractors from the Office of Scientific and Technical Information, P.O. Box 62, Oak Ridge, TN 37831; prices available from (615) 576-8401. FTS 626-8401.

Available to the public from the National Technical Information Service, U.S. Department of Commerce, 5285 Port Royal Rd., Springfield, VA 22161.

On the cover:

An aerial photograph of the SY waste tank farm under construction (circa 1975) on the Hanford site in southeastern Washington State. Tank 241-SY-101 is the tank in the foreground to the right.

PNL-8278
AD-940

Minutes of the Tank Waste Science Panel Meeting March 25-27, 1992

Compiled by
W. W. Schutz*
D. M. Strachan

August 1992

Prepared for
the U.S. Department of Energy
under Contract DE-AC06-76RLO 1830

Pacific Northwest Laboratory
Richland, Washington 99352

* Consultant
Wellington, Delaware

Preface

This document contains the minutes for the March 25-27, 1991, meeting of the Tank Waste Science Panel. The objective of this document is to provide an accurate recapitulation of the proceedings so that the diverse views of the Science Panel members can be documented. The content of this document has been reviewed by each of the Panel members to ensure its accuracy. Editorial comments are clearly marked in the text and are provided only for clarification. Because of this philosophy, this document may contain provocative statements, opinions which may run counter to facts, facts which are presented out of the context of the tank chemistry and physics, and information that may later be shown as incorrect. These meeting minutes, like the previous minutes and those which will follow, are intended to chronicle the Science Panel activities and progress toward understanding the chemical and physical mechanisms that are taking place in the waste tanks at Hanford.

Summary

The seventh meeting of the Tank Waste Science Panel was held March 25-27, 1992, in Denver, Colorado. The subject areas included the generation of gases in Tank 241-SY-101, the possible use of sonication as a mitigation method, and analysis for organic constituents in core samples.

The following important results were presented and discussed:

- Ferrocyanides appear to be rapidly dissolved in 1M NaOH. These data suggest that ferrocyanides would dissolve when highly alkaline wastes were pumped into the same tank and sufficient mixing occurred.

- Upon standing in the laboratory at ambient conditions oxalate precipitates from simulated wastes containing HEDTA. This suggests that one of the main components in the solids in Tank 241-SY-101 is oxalate.

- Hydrogen evolved from waste samples from Tank 241-SY-101 is five times that observed in the off gas from the tank. No good explanation is yet available for this discrepancy.

- The solubility of N_2O in simulated waste is in the range 0.003 to 0.01 g N_2O per kilogram of waste per atmosphere of N_2O. These data suggest that mitigation of Tank 241-SY-101 will not cause a high release of dissolved N_2O.

- When using a slurry for radiation studies, a portion of the generated gases is very difficult to remove. To totally recover the generated gases, the solids must first be dissolved. This result may have an impact on mitigation by mixing if the gases are not released.

- Using ^{13}C-labeled organics in thermal degradation studies has allowed researchers to illucidate much of the kinetic mechanism for the degradation of HEDTA and glycolate. In addition to some of the intermediate, more complex organic species, oxalate, formate, and Co_2 were identified. These data suggest that a large portion of the total organic carbon will be identified when analytic methods are available.

- Analytic methods for organics in radioactive complex solutions such as that found in Tank 241-SY-101 have been developed and others continue to be developed. Development of these methods has been assisted by the results from other parts of the program; results from the analyses of actual waste have proven useful in the other studies.

Contents

Minutes of the Tank Waste Science Panel Meeting
March 25-27, 1992

Introduction

The seventh meeting of the Tank Waste Science Panel (Science Panel) was convened March 25, 1992, in Denver, Colorado at the Red Lion Airport Hotel. A list of attendees at this meeting is provided in Appendix A; Appendix B lists the agenda followed at the March meeting.

Time at the meeting was allocated to presentation and discussion of recent information and results obtained in ongoing research programs at Argonne National Laboratory, Georgia Institute of Technology, Los Alamos National Laboratory, Pacific Northwest National Laboratory, and Westinghouse Hanford Co. Subjects discussed included the chemistry of ferrocyanide wastes; generation, retention, and release of gases from Tank 241-101-SY; and the potential application of sonic energy in mitigating gas retention in Tank 101-SY. Current approaches to and schedules for mitigating gas retention and periodic gas releases from Tank 101-SY were also reviewed.

In the following text, the Science Panel activities associated with each of the items listed in Appendix B are discussed.

Day 1, March 25, 1992

Ferrocyanide Tank Waste Chemistry (R. T. Hallen, Pacific Northwest Laboratory)

The only new items concerning the chemistry of ferrocyanide wastes present in 24 of the 149 single-shell tanks were presented and discussed by R. T. (Rich) Hallen, Pacific Northwest Laboratory. The material used in the presentation is included in Appendix C.

Solubilization of Ferrocyanides in Aqueous Base. Rich and his colleagues recently conducted extensive tests to investigate solubilization of solid ferrocyanides by reaction with aqueous solutions of sodium hydroxide according to the following reaction:

$$Na_2Ni[Fe(CN)_6] + 2NaOH = Na_4[Fe(CN)_6] + Ni(OH)_2 \quad (1)$$

These studies were motivated by suggestions made by D. O. Campbell and C. Forsberg at a recent Technical Advisory Panel meetings.

In their tests, Rich and coworkers varied widely several reaction parameters including initial pH and sodium concentration (0.01, 0.1, and 1.0 M) and ionic strength. Other reaction parameters to be examined include temperature and effects of added salts such as $NaNO_3$, $NaNO_2$, Na_3PO_4, Na_2SO_4, and Na_2CO_3. Typically, a 1-g portion of ferrocyanide solids was reacted with 50 mL of NaOH solution.

In all cases, Reaction 1 tended to completion as determined by the total iron in solution. As expected, the rate of the reaction was particularly rapid at higher temperatures and NaOH concentrations. Indeed, at 25°C the reaction between the ferrocyanide solid and 1 M NaOH was essentially complete in 1 to 2 h.

Infrared and x-ray diffraction analyses confirmed that solids remaining after reaction of the ferrocyanide solids with NaOH were $Ni(OH)_2$ that did not contain any detectable ferrocyanide. Only preliminary reflux experiments were analyzed for ammonia evolution during reaction of the ferrocyanide solids with NaOH. Also, the aqueous solution from the dissolution reaction contained very little CN^-, attesting to the known thermodynamic stability of the $Fe(CN)_6^{4-}$ moiety.

Rich also commented briefly on analytical plans for the core samples recently taken from Tank 112C. Ferrocyanide solids were precipitated in Tank 112C as part of the 1954-1957 In-Tank Scavenging Program. Tank 112C, from historical records, is believed to contain the highest concentration of ferrocyanide solids in any of the 24 waste tanks containing ferrocyanide. Rich stated that thermal properties of samples taken from Tank 112C would be examined using both DSC (Differential Scanning Calorimeter) and TGA (Thermal Gravimetric Analysis) techniques.

Gaseous Products from Thermal Decomposition of Ferrocyanides. Rich also described results of recent bench-scale experiments to determine, via GC-MS (gas chromatography-mass spectrometry) techniques, the composition of the gases evolved when a synthetic ferrocyanide waste containing 2 moles of nitrate per mole of ferrocyanide was decomposed in the temperature range of 50 to 500°C. Experiments were performed with rapid heating at the rate of 5°C per minute simulating TGA experiments. Material from this presentation is included in Appendix D. Identified gases include water, CO_2, N_2O, HCN, cyanogen (C_2N_2), NO, and N_2; the latter two gases appear to evolve only at temperatures above about 200°C.

The major amount of gas evolution is associated with exotherms observed in DSC analyses of solid ferrocyanide-nitrate mixtures. Some gas also appears to be released at temperatures as low as 100°C without any detectable exothermic reaction.

Day 2, March 26, 1992

All of March 26 was devoted to vugraph presentations by various speakers and ensuing discussion of various aspects of the chemistry in Tank 101-SY. The following text presents and discusses important results from ongoing bench-scale studies with simulated and actual tank waste.

Results from Tank 101-SY Core Sample Analyses (D. L. Herting, Westinghouse Hanford Co.)

D. L. (Dan) Herting provided an excellent summary of the complete results of analysis of cores taken from Tank 101-SY during Window C (May) in 1991. The complete analytical data for these cores are contained in the document WHC-SD-WM-DTR-024 Rev O. Dan's presentation materials are included in Appendix E.

Among the highlights of the analytical data were the following:

- The top 14 segments of the core samples represent the convecting layer in the tank.

- The organic content of the solids is about 50% higher than that in the liquid phase.
- The total organic content of the solids in the convecting layer is about the same as in the non-convecting layer.
- Solids in both the convecting and nonconvecting layers contain unexpectedly high amounts of chromium.
- Analyses of individual segments are not in good agreement with those of composite segment samples.
- Considerable scatter in ^{137}Cs analytical data probably reflects difficulties in pipetting samples.
- The cyanide content of the liquid ranges from 90 to 390 micrograms per gram of waste and from 150 to 400 micrograms per gram of waste in the solids. The accuracy of the cyanide analyses is still in question.

Bench-Scale Gas Generation Experiments (D. L. Herting, Westinghouse Hanford Co.)

Progress toward eventual bench-scale determination of the amount and composition of the gases evolved from a sample of Tank 101-SY waste was described by Dan Herting. Dan stated that he and his colleague, J. C. (Jim) Person, are currently planning to procure a flow-through apparatus, similar to an existing unit at the Savannah River Site, for conducting off gas measurements with a small quantity of actual Tank 101-SY waste.

Until the flow-through apparatus is available, Dan and Jim are conducting off gas generation measurements in a static system with both actual and various simulated Tank 101-SY wastes maintained at 100°C, under air or helium, for various times. The composition of the off gas thus produced is determined using mass spectrometric analyses. Significant results from static gas generation tests with simulated Tank 101-SY wastes containing either HEDTA or glycolic acid are:

- Ammonia is generated in all cases, even from simulated Tank 101-SY containing no organic material.
- No gas generation was observed from simulated wastes that did not contain $NaAlO_2$.
- White solids identified as sodium oxalate precipitated from simulated Tank 101-SY waste containing HEDTA when such solutions were allowed to stand 2 weeks at 25°C. But, according to Gene Ashby of the Georgia Institute of Technology, no precipitation of solids was observed when similar solutions under a nitrogen atmosphere were allowed to stand.
- In some cases, $Al(OH)_3$ solids can precipitate from simulated Tank 101-SY waste when it is allowed to stand at room temperature and after the simulated waste is clarified before standing. These two results indicate that great care must be taken when making up the so-called "Final Word Solution." Not only is the recipe important, but equally important are the sequence of chemical additions and the conditions under which the solution/slurry is made and stored. Solutions should be stored only briefly before use.

- Off gases from static experiments with both actual and simulated waste contained the expected components, namely, H_2, N_2, and N_2O. Considerable variability in gas generation rates was observed from experiment to experiment. Questions were raised at the meeting about the sensitivity of mass spectrometric analyses for hydrogen and nitrous oxide. Gene Ashby suggested that gas chromatographic analytical data should be obtained to verify mass spectrometric results.

- In one experiment with actual Tank 101-SY waste, the amount of evolved H_2 was about five times that of N_2O. Two possibilities may explain this difference.

  - The activation energies for generation of H_2 and N_2O are different.

  - Small laboratory samples of Tank 101-SY waste adsorb beta and gamma radiation differently than the waste in the tank, and the generation of N_2O is more sensitive to radiation than is generation of H_2.

- When metallic iron was included in one experiment with simulated waste, the gas generation rate increased significantly. The generation rate of nitrous oxide appeared to be increased more than that of hydrogen.

Synthetic Tank 101-SY Waste Studies (L. R. Pederson, Pacific Northwest Laboratory)

Results from several studies being performed by S. A. (Sam) Bryan and L. R. (Larry) Pederson with simulated Tank 101-SY wastes were described. Presentation materials are included in Appendix F.

Solubility of Nitrous Oxide. Larry and Sam have measured the solubility of N_2O in both distilled water and simulated waste at various temperatures. These tests were conducted to test the hypothesis that increased solubility of nitrous oxide relative to that of hydrogen would explain the difference in the observed ratio of these two gases both from Tank 101-SY and from thermal degradation tests with simulated wastes.

Larry's and Sam's results for the solubility of nitrous oxide in distilled water are in excellent agreement with the earlier (1980) literature values. The solubility of N_2O in simulated Tank 101-SY waste (not containing any organic complexants) at 40°C is in the range 0.003 to 0.01 g N_2O per kg waste per atmosphere N_2O. This latter solubility is greater than that of hydrogen, but too small to explain the differences between the observed N_2O/H_2 ratio in the gas evolved from Tank 101-SY and the ratio observed in the gases from experiments with simulated waste. In addition, the solubility of N_2O in waste solutions is sufficiently low that the inventory of dissolved N_2O that could be released is inconsequential.

Physical Properties of Simulated and Actual Tank 101-SY Waste. Larry and Sam are continuing to measure various physical properties, e.g., density; weight percent water; weight percent centrifuged solids; volume percent settled solids; and shear strength of simulated Tank SY-101 waste. The data suggest that the simulated waste slurries are physically comparable to the convecting layer in Tank 101-SY. Information concerning physical properties and their variation with dilution and temperature are expected to be useful in subsequent mitigation and remediation efforts.

Effect of Hydroxide Concentration on Gas Generation Rates and Stoichiometries. In early work, Delegard (1980) observed that the rate of gas generation from simulated Tank 101-SY waste was a function of its hydroxide ion concentration. Delegard reported that the maximum gas generation rate occurred at about 1.5 M NaOH.

Larry and Sam recently conducted experiments to extend Delegard's early work and to determine the effect of hydroxide ion concentration on the stoichiometry of gaseous products. These bench-scale studies were performed as part of a large program to investigate thermal oxidation of organic complexants at subcritical water temperature and pressure conditions.

In their experiments, Larry and Sam heated simulated Tank 101-SY solution containing either 0.3 M EDTA or 0.3 M HEDTA and 1 to 7 M NaOH for various periods at 90°C. Total moles of N_2, N_2O, and H_2 produced were determined. They noted that, under these conditions, small changes in hydroxide ion concentration corresponded to large changes in the rate of generation of gases, particularly nitrous oxide and nitrogen. For example, N_2O/H_2 mole ratios in the off gas from solutions containing HEDTA varied from 1 to as high as 10 as the hydroxide ion concentration changed from 0.5 to 6.5 M.

While the hydroxide ion concentration of the waste in the tank appears to have been nearly invariant with time, the importance of these results becomes apparent when one realizes that small errors in the analysis of the samples from the tank or in the make up of the simulated waste with respect to hydroxide can have a major impact on the gas composition.

Sub-Critical Oxidation of Organic Materials in Tank 101-SY. Larry and Sam reported on initial results obtained in an experimental approach aimed at determining if simple heating of the waste in Tank 101-SY to 200 to 300°C will oxidize contained organic materials to decomposition products that do not generate gases at tank temperatures.

The initial goal of this work is to identify organic decomposition products; assess the capacity of decomposition products, following heat pretreatment, to generate gases; and gain some knowledge of the kinetics of thermal degradation of selected organic materials.

The experimental approach followed involves heating a known amount, approximately 200 mL, of simulated Tank 101-SY waste containing various organic complexants and, in some cases, additional NaOH in Hastelloy C vessels to 200 to 250°C for about 2 h. The off gas from such heating is sampled and analyzed for ammonia and other constituents. Subsequently, portions of the thermally-treated waste are heated to 90°C and the amount and composition of gases evolved at this lower temperature are determined.

Highlights of results obtained to date include:

- Ammonia is a principal component of the off gas when simulated Tank 101-SY waste is heated at 200 to 250°C.
  - Simulated Tank 101-SY waste containing either HEDTA or EDTA generated particularly large amounts of ammonia when heated at 200 to 250°C.

- Ammonia is generated on a 1:1 mole basis from nitrogen-containing organics.

- Substantial amounts of ammonia were generated from simulated Tank 101-SY waste that did not contain any organic nitrogen.

- The effectiveness of thermal pretreatment at 200 to 250°C of simulated Tank 101-SY waste upon the amount and composition of gas subsequently generated at 90°C is highly dependent upon the concentration of NaOH in the waste.

  - When additional (i.e., 2 or 3 times the normal concentration) NaOH is present, thermal pretreatment at 200 to 250°C significantly reduces gas generation upon subsequent heating of the pretreated waste to 90°C.

  - Larry indicated that some of the pretreated wastes were being analyzed in the hope of determining identity and amount of organic degradation products.

  - Although the Science Panel is much impressed with these initial results for subcritical oxidation of organic complexants, it is not yet clear to what extent, if any, this technology can or will be used to mitigate or remediate gas generation in Tank 101-SY. However, the technology appears promising and appears to yield information about the mechanism by which the organics thermally decompose in Tank 101-SY. Therefore, the studies should continue.

Radiolytic Generation of Gases from Synthetic Wastes (D. Meisel, Argonne National Laboratory)

D. (Dani) Meisel described the latest results of the Argonne National Laboratory group to determine the amount and composition of gases generated when simulated Tank 101-SY wastes are irradiated (^{60}Co). Presentation materials are included in Appendix G. Dani stated that the Argonne group was currently interested in resolving three issues, namely:

1. How well do the experiments simulate conditions in Tank 101-SY, both radiolytically and chemically?

2. What are the radiolytic yields from slurries as opposed to homogeneous solutions?

3. How does the rate of thermal generation of gas from preirradiated simulated Tank 101-SY waste differ from that of waste that has not been preirradiated?

Concerning the first issue, Dani noted that the components in Tank 101-SY are subjected to both beta and alpha radiation where the dose rate is low and the cumulative dose is high. In contrast, in the laboratory radiations, components are irradiated by gamma radiation to low doses at high dose rates. But, Dani and coworkers stated that the dose contribution from alpha radiation is negligible and that, because of Compton Scattering effects, beta and gamma irradiation are equivalent. Thus, Dani and coworkers concluded that laboratory experiments using ^{60}Co radiation simulate very well the radiolytic conditions existing in Tank 101-SY. Dani noted, however, that the radiolytic chemistry results are only as good as the chemistry of Tank 101-SY is known; precise data for the type and concentration of organic materials in Tank 101-SY are still unavailable.

Dani also indicated that the rate at which simulated Tank 101-SY waste absorbs radiation has only minimal effect on the $G(H_2)$ but appears to have a much larger effect on the $G(N_2O)$. Data for N_2O has been extrapolated to low dose rates.

Dani noted that $G(H_2)$ generated in simulated Tank 101-SY waste slurries (solution plus sludge) irradiated at room temperature are about a factor of two lower than yields from homogeneous solutions. This result is accounted for on the basis of a lower water content of the slurry. Hydrogen yields increase when slurries are irradiated at higher temperatures because of the increased solubility of the sludge solids. In contrast to the results for H_2, radiolytic yields of N_2O from slurries are comparable to those from homogeneous solutions.

Dani also reported on studies of enhanced thermal generation of H_2 and N_2O from simulated Tank 101-SY waste solutions that have been preirradiated. (These additional studies were performed in response to a December 1991 request from the Science Panel.) In the latest tests, homogeneous simulated Tank 101-SY solutions containing (initially) only one organic compound, i.e., EDTA or HEDTA or citrate, were irradiated to total doses of about 40 Mrad. A simulated Tank 101-SY slurry containing HEDTA, EDTA, and citrate was also irradiated to a total dose of about 40 Mrad. Preirradiated solutions, after standing from 5 to 40 days at room temperature, were heated to 60°C and the amounts of H_2 and N_2O evolved were measured.

From data collected to date, Dani noted:

- Preirradiation substantially increases the rate of production of H_2 and N_2O from both homogeneous waste solutions and also from waste slurries.

- For homogeneous solution, the rate of production of H_2 increased in the order citrate<HEDTA<EDTA while for N_2O the production rate increased in the order citrate<EDTA<HEDTA.

- Slurry particles appear to catalyze the rate of production of hydrogen.

- Slurry particles appear to strongly retain both H_2 and N_2O gases, but H_2 is released more readily.

Overall radiolytic generation of gases from Tank 101-SY waste is small (approximately a half) compared to thermal generation rates. Also, as Dani's results affirm, thermal generation of gases from simulated Tank 101 SY solutions is much more sensitive to the exact experimental conditions than is radiolytic generation.

The data obtained for preirradiated solutions and slurries indicate that such preirradiation produces some unknown but highly reactive intermediate which promotes thermal generation of gas. Experimental work both at Argonne National Laboratory and the Georgia Institute of Technology needs to focus on identifying and characterizing the unknown intermediate.

Mechanistic Elucidation of Chemistry in Tank 101-SY (E. C. Ashby, Georgia Institute of Technology)

E. C. (Gene) Ashby and his group of collaborators at the Georgia Institute of Technology are actively investigating all facets of the thermal degradation of organic materials in Tank 101-SY. Gene described the current status of tests being conducted with simulated Tank 101-SY waste. Presentation materials are included in Appendix H.

Gene discussed recent results in five areas:

- kinetic studies
- isotopic labeling studies (^{13}C and ^{15}N)
- formaldehyde studies
- other model systems
- analytical development.

Kinetic Studies. Gene presented extensive data for an experiment in which so-called "Final Word Solution"[(a)] containing 0.0054 M glycolate as the only organic constituent was maintained at 120°C for 1582 h. The buildup in concentration of the principal aqueous-soluble glycolate decomposition products (formate, oxalate, and carbonate ions) was followed along with the decrease in concentration of nitrite and glycolate ions. A mathematical expression describing these results has not been derived.

A similar experiment was performed in which "Final Word Solution" containing 0.0053 M HEDTA as the only organic material was heated at 120°C for 500 h. Again, the buildup of formate ion concentration and the decrease in concentration of HEDTA and nitrite ion were followed.

In further studies, Gene and his colleagues also measured gas evolution rates when "Final Word Solution" containing one of the following organic compounds was heated at 120°C for times ranging from 400 to 1600 h:

- iminodiacetic acid
- N-methyliminodiacetic acid
- nitrilotriacetic acid
- symmetrical EDTA
- unsymmetrical EDTA.

No evolution of gas was observed from simulated waste solutions containing either nitrilotriacetic acid or unsymmetrical EDTA.

(a) 2.0 M NaOH
2.24 M $NaNO_2$
2.59 M $NaNO_3$
1.54 M $NaAlO_2$
0.42 M Na_2CO_3
0.21 M organic
(now known as SY1-SIM-91B)

Isotopic Labeling Studies. Simulated Tank 101-SY waste containing HEDTA labeled with ^{13}C was heated several weeks at 120°C. The ^{13}C NMR spectra of the heated solution was monitored to determine thermal fragmentation products. Pertinent observations included:

- Labeled formate and CO_2 (as carbonate ion) and oxalate were detectable after a few days heating.
- Labeled glycine, detectable after 34.5 days, was produced from the hydroxethyl labeled form of HEDTA.
- A doublet consistent with the presence of labeled iminodiacetic acid was present after six days heating of carboxylmethyl-labeled HEDTA.
- One quarter to one half of the HEDTA remained after 60.5 days heating.

Also used in their experiments was ^{13}C-labeled glycolate ($HO^{13}CH_2{}^{13}CO^{2-}$) ion in "Final Word Solution." Degradation products resulting from heating at 120°C for 25 days were determined. Thermal degradation products were monitored by ^{13}C NMR of heated waste samples. The disappearance of glycolate ion followed first order kinetics. They also obtained evidence of complexing of aluminum by glycolate ions. Thermal degradation products included formate, oxalate, and carbonate ions.

Formaldehyde System Studies. Gene and his coworkers earlier postulated a reaction mechanism to account for the gaseous products (e.g., H_2, N_2O, and N_2) evolved during chemical degradation of simulated Tank 101-SY wastes containing either glycolate or HEDTA. An important postulate of these mechanisms is that thermal degradation of glycolate and HEDTA produces formaldehyde. The formaldehyde produced reacts with base (OH^-) to form the so-called Cannizaro Intermediate ($CH_2O_2^-$). The Cannizaro Intermediate can then either react with formaldehyde to form methyl alcohol and HCO_2^- or with water to produce hydrogen gas, OH^-, and HCO_2^-.

Confirmation of the predicated reaction mechanism is provided by the presence of formate and oxalate ions among the thermal degradation products of Tank 101-SY wastes containing glycolate or HEDTA ions. Because of the importance of formaldehyde and its subsequent reactions in explaining thermal chemistry of Tank 101-SY waste, Gene and coworkers recently conducted extensive studies of the reaction of HCHO with OH^- to generate H_2. Important findings of these latter studies include:

- The ratio H_2:$HCOO^-$ is about 1:1 for the H_2-producing reaction indicating that water provides at least half of the hydrogen atoms in the H_2.
- The order in formaldehyde is about 1 at both 90°C and room temperature.
- The hydrogen yield increases as the HCHO concentration decreases indicating that the H_2-producing mechanism is first order formaldehyde and H_2O.
- The hydrogen yield increases with hydroxide ion concentration.
- The rate of hydrogen evolution decreases in the presence of p-hydroquinone indicating the presence of radical intermediates.

- Trace amounts of Cu(II) accelerate the hydrogen evolution rate, indicating that an electron transfer step could be involved.

- In the presence of hydrogen peroxide, hydrogen evolution is much faster, and the hydrogen yield is 100% based on the amount of peroxide added.

- Other aldehydes without alpha hydrogen also produced a significant amount of hydrogen in the presence of OH^-.

It is not possible at this time to say whether the reaction is polar or free radical in nature, however the nature of the reaction has no impact on the overall understanding of the chemical mechanism of gas generation in Tank 101-SY, but may have application for some basic scientific issue.

Other Model Systems. Gene and his group also conducted thermal degradation studies of "Final Word Solutions" each containing one of two model compounds, N, N-diethylethanolamine or N,N-dimethylglycine. The model systems are simplified versions of EDTA and HEDTA. These systems are much simpler than EDTA and HEDTA and facilitate mechanistic interpretation of the reaction of the $-CH_2CH_2OH$ and $-CH_2COOH$ groups. Important results were:

N, N-diethylethanolamine

- H_2, N_2O, and methane are observed as gaseous products.

- Formate and acetate ions are the most important products in the thermally degraded solution.

- Oxygen is absorbed by the test solution and only 20% of the original amount of oxygen is left after 300 h.

N, N-dimethylglycine

- Hydrogen is the most important gas observed in this reaction. Nitrous oxide and methane are produced only in trace amounts (<0.1%).

Analytical Development Studies. Quantitative analyses for EDTA and HEDTA have been accomplished at the Georgia Institute of Technology with the use of Dionex AS5 and AS 10 columns. A $CuCl_2$ or $NiCl_2$ solution was added to the EDTA or HEDTA solution before analysis.

Some effort was devoted to the analysis of the solids produced during the thermal reactions. When glycolate is the organic compound present in the thermal degradation of simulated Tank 101-SY waste, the insoluble solid generally contains a large amount of oxalate. When the simulated Tank 101-SY waste contains other organic compounds, the insoluble solids contain very little oxalate.

Ultraviolet spectrophotometric analyses failed to find direct evidence for a complex between Al(III) and nitrite ion. An Al(III)-NO_2^- complex has been postulated in the overall thermal degradation reaction mechanism scheme. Although this complex was not detected, this most likely means the concentration is very low, but sufficient to allow the nitrite to be added to the organic moiety.

Day 3, March 27, 1992

The morning of March 27 was concerned with presentations by Steve Agnew, Los Alamos National Laboratory, and Jim Colson, Pacific Northwest Laboratory. Jim's presentation materials are included in Appendix I, and Steve's in Appendix J.

Both presentations were concerned with experimental investigation of the potential application of sonic energy to agitate the contents of Tank 101-SY and thereby continuously release hydrogen and other gases. The principal result to emerge from both presentations is that sonic energy introduced into simulated Tank 101-SY waste is rapidly attenuated and, thus, is relatively ineffective in agitating either the liquid or solids present in the waste mixture.

Hanford Site Experimental Investigation of Ultrasonic Properties of Double-Shell Tank Waste Simulant (J. Colson, Pacific Northwest Laboratory)

According to Jim, acoustic attenuation

- is very high
- increases with frequency
- is not due to any void fraction
- decreases with pressure
- is not strongly temperature dependent
- decreases with dilution.

Mitigation of Bubble Nucleation in Tank 101-SY with Ultrasound (S. Agnew, Los Alamos National Laboratory)

Steve's studies with simulated wastes indicated the following:

- Attenuation of ultrasonic energy in simulated waste is not a straightforward phenomenon because of the occurrence of several non-linear effects in the waste slurry.

- The velocity of the sound wave is strongly dependent upon pressure, temperature, and distribution of gas bubbles.

Steve also stated that future studies by the group at Los Alamos National Laboratory will be aimed at

- use of higher power transducers to agitate Tank 101-SY waste in the model tank more completely

- determination of the slurry degassing threshold

- use of slurry standing waves to determine sound attenuation and speed.

The Science Panel members asked several pertinent questions and made several observations during and after Steve's presentation, namely:

- The attenuation problem appears to be with coupling. Most industrial applications involving sonic energy use cavitation to effect coupling. In the case of Tank 101-SY waste, the cavitation energy is very low because gas bubbles are already present. Therefore, we need to match impedance.

- The importance of gas bubbles cannot be over emphasized. Coupling to bubbles is not necessarily bad unless coupling does not act to release bubbles.

The Science Panel also speculated about the wisdom of continuing the work with sonification as a viable mitigation method. Resolution of formidable technical issues (e.g., attenuation) associated with large-scale application of sonic energy to near-term mitigation of Tank 101-SY appears to be very time consuming and expensive. Simpler mitigation methods, e.g., mechanical stirring, are already available.

Organic Methods Development and Preliminary Data on Composite Samples from Tank 101-SY (J. A. Campbell, Pacific Northwest Laboratory)

J.A. (Jim) Campbell provided the Science Panel an excellent summary and update of the status of identification and quantitation of organic constituents in composite samples of core segments taken from Tank 101-SY during Window C. Jim's presentation materials are included in Appendix K. Jim and his fellow workers obtained their data by derivatizing organic materials with boron trifluoride in methanol and analyzing the concentrated chloroform extract of the derivatized sample with GC-MS.

Jim presented data for one of the four composite samples from Tank 101-SY. Sample 961 was a composite of segments 14 through 18 from the top of the nonconvective layer. For this sample, Jim and his coworkers

- noted 41 peaks in the total ion chromatogram of the chloroform extract

- tentatively identified 25 of the 41 peaks

- estimated concentrations of the seven major components in Sample 961 as follows:

Peak Number	Component	Approximate Conc., micrograms/gram
1	butanedioic acid	80
10	nitrosoiminodiacetic acid	708
14	citric acid	45
18	nitrilotriacetic acid	185
23	ethylenediaminetriacetic acid	115
28	ethylenediaminetetraacetic acid	237
29	N(2-hydroxyethyl)ethylene-diaminetriacetic acid	25

- estimated that the seven major components account for only 10 to 20% of the total organic carbon (TOC) in Tank 101-SY.

Jim also stated that the complexants and complexant fragments identified thus far made up about 65% of the derivatizable material.

In continuing work, the plans are to

- apply ion chromatographic techniques and instrumentation to identify the remaining TOC. Much of the latter may be present as an oxalate.

- procure a high resolution mass spectrometer to confirm identification of compounds presently only tentatively identified

- investigate applicability of liquid chromatography to Tank 101-SY samples for quantitative analysis of organic constituents

- investigate other derivatization reagents for use with Tank 101-SY waste.

Finally, Jim and his associates also successfully applied GC-MS techniques to analyze for organic materials in some samples of preirradiated simulated Tank 101-SY waste obtained in studies by Dani Meisel at Argonne National Laboratory. Also, preliminary results obtained from ion chromatography studies showed the presence of significant concentration of formate ion in preirradiated solutions.

Non-Agenda Items

Several items not listed on the formal agenda were also addressed by the Science Panel in Denver.

Relevant Savannah River Experience (N. E. Bibler, Savannah River Laboratory)

N. E. (Ned) Bibler mentioned that several papers of possible interest to Tank Waste Science Panel members were presented by Savannah River Site authors at the recent Waste Management '92 meeting in Tucson, Arizona. He handed out copies of some of these papers. Ned went on to also point out the actual analyses of noble metals in Savannah River wastes agreed quite well with the values expected from ORIGIN code calculations.

Mitigation-Remediation Plans (D. M. Strachan, Pacific Northwest Laboratory)

D. M. (Denis) Strachan very briefly summarized for the Panel highlights of a soon-to-be issued report detailing plans for mitigation of Tank 101-SY by stirring methods. Denis' remarks occasioned considerable comments and discussion by Panel members. The gist of these comments will be summarized in a letter from the Panel to J. L. Deichman. [Note added in proof: This letter was never issued.]

Executive Sessions

The Tank Waste Science Panel held Executive Sessions at the end of Day 1 and Day 3. These sessions resulted in a number of action items by various Panel members. One action item was to write a "white paper" on organic wastes at Hanford.

Experimental Plan

The Tank 101-SY mitigation Project Experimental Plan was presented to the External Advisory Committee on March 20, 1992. The presentation materials are included here in Appendix L.

Acknowledgement

These meetings and reports would be impossible without the support of several people whose names do not appear elsewhere in this report. The continuing support of John L. Deichman, Gerald D. Johnson, and Robert J. Cash is recognized. Their fiscal support and encouraging participation at these meetings is appreciated. Also providing encouragement to their staff are John G. Propson and Nicholas W. Kirch. Arrangements for the meeting is always a time consuming and often diplomatic assignment. Judith E. Gelhaus performed this assignment well. Finally, David K. Hilliard is gratefully acknowledged for editing the visible product of this effort.

Appendix A

Attendees

TANK WASTE SCIENCE PANEL
ATTENDEES

March 25-27, 1992
Red Lion Hotel
Denver, Colorado

Steve F. Agnew	Los Alamos National Laboratory
E. C. Ashby	Georgia Institute of Technology
Roger M. Bean	Pacific Northwest Laboratory
Ned E. Bibler	Westinghouse Savannah River Co.
Jim A. Campbell	Pacific Northwest Laboratory
Jim B. Colson	Pacific Northwest Laboratory
Thom H. Dunning, Jr.	Pacific Northwest Laboratory
G. Gerton	Department Of Energy
R. T. Hallen	Pacific Northwest Laboratory
Dan L. Herting	Westinghouse Hanford Co.
E. Phil Horwitz	Argonne National Laboratory
Dan Meisel	Argonne National Laboratory
George B. Mellinger	Pacific Northwest Laboratory
Larry R. Pederson	Pacific Northwest Laboratory
Dan A. Reynolds	Westinghouse Hanford Co.
Wally Schulz	Consultant
Duane D. Siemer	WINCO
Denis M. Strachan	Pacific Northwest Laboratory
W. J. Thomson	Washington State University
Ed Tuthill	Brookhaven National Laboratory

Appendix B

Agenda

AGENDA FOR THE

TANK WASTE SCIENCE PANEL MEETING

DENVER, COLORADO

MARCH 25 - 27, 1992

Wednesday, March 25

Ferrocyanide Program
Chemical Mechanisms and Analyses

1:00	Introductory Remarks	WW Schulz
1:30	Results from the Chemical Mechanisms of Ferrocyanide Reactions and Precipitation	GF Schiefelbein
2:30	Results from the Development of Analytical Techniques for Ferrocyanide	SA Bryan
3:15	Break	
3:30	Discussion	
4:30	Executive Session	

Thursday, March 26, 1992

Hydorgen Program
Chemical Mechanisms

8:00	Breakfast - at the meeting room	
8:30	Introductry Remarks	TH Dunning, Jr
8:40	Results from the December 4, 1991 Gas Release Event	DA Reynolds
9:15	Summary of Results from the Tank 101-SY Core Sample Anlayses	DL Herting
10:00	Break	
10:15	Results from the Gas Generation Experiments at Westinghouse Hanford Co.	DL Herting
11:00	Results from the Studies at Pacific Northwest Laboratory	LR Pederson
12:00	Lunch - at the meeting room	
12:30	Results from the Radiolysis Experiments at Argonne National Laboratory	D Meisel
1:30	Results form the Experiments at Georgia Institute of Technology	EC Ashby
2:30	Results from the Development of Analytical Methods of Organic Analyses	JA Campbell
3:30	Break	
3:45	Discussion of the Chemical Mechanisms	

Friday, March 27, 1992

Hydrogen Program

Physical Mechanisms and Mitigation Concepts

8:00	Breakfast - in the meeting room	
8:30	Results from Ultrasound Testing at Pacific Northwest Laboratory	JE Colson
9:30	Results from the Development of Ultrasound Mitigation at Los Alamos National Lab	SF Agnew
10:30	Executive Session	

Appendix C

Solubilization of Ferrocyanides in Aqueous Base

Ferrocyanide Safety Project

"Predecisional Information"

SOLUBILIZATION OF FERROCYANIDES IN AQUEOUS BASE

Richard T. Hallen
Gary F. Schiefelbein
Michael A. Lilga
Robert J. Romine
William F. Riemath
John L. Cox

Pacific Northwest Laboratory
P. O. Box 999
Richland, WA 99352

Tank Waste Science Panel Meeting
Denver, Colorado
March 25-27, 1992

C.2

$$Na_2NiFe(CN)_6 + 2\ NaOH \rightarrow Na_4Fe(CN)_6 + Ni(OH)_2$$

Results of Initial Ferrocyanide Solubility Scoping Experiments

	Exp. 1	Exp. 2
[NaOH]	0.1*N*	1.0*N*
initial pH	12.9	13.8
final pH	10.5	13.0
$Na_2NiFe(CN)_6 \cdot Na_2SO_4 \cdot 4.5\ H_2O$ (g)	1.0005	1.0041
moles $Fe(CN)_6^{4-}$ or Ni^{2+}	1.85×10^{-3}	1.86×10^{-3}
weight of recovered solids (g)	0.3316	0.5113
solution [Fe] (mg/L)	2030	1600
moles Fe in solution	1.82×10^{-3}	1.43×10^{-3}
fraction total Fe in solution	98%	77%
solution [Ni] (mg/L)	39	3.3
moles Ni in solution	3.32×10^{-5}	2.81×10^{-6}
fraction total Ni in solution	1.8%	0.15%
$[NH_3]$ in gas (ppm)	30	375
approx. moles NH_3 produced	8.04×10^{-8}	2.34×10^{-6}
approx. %-yield NH_3	0.0007	0.02

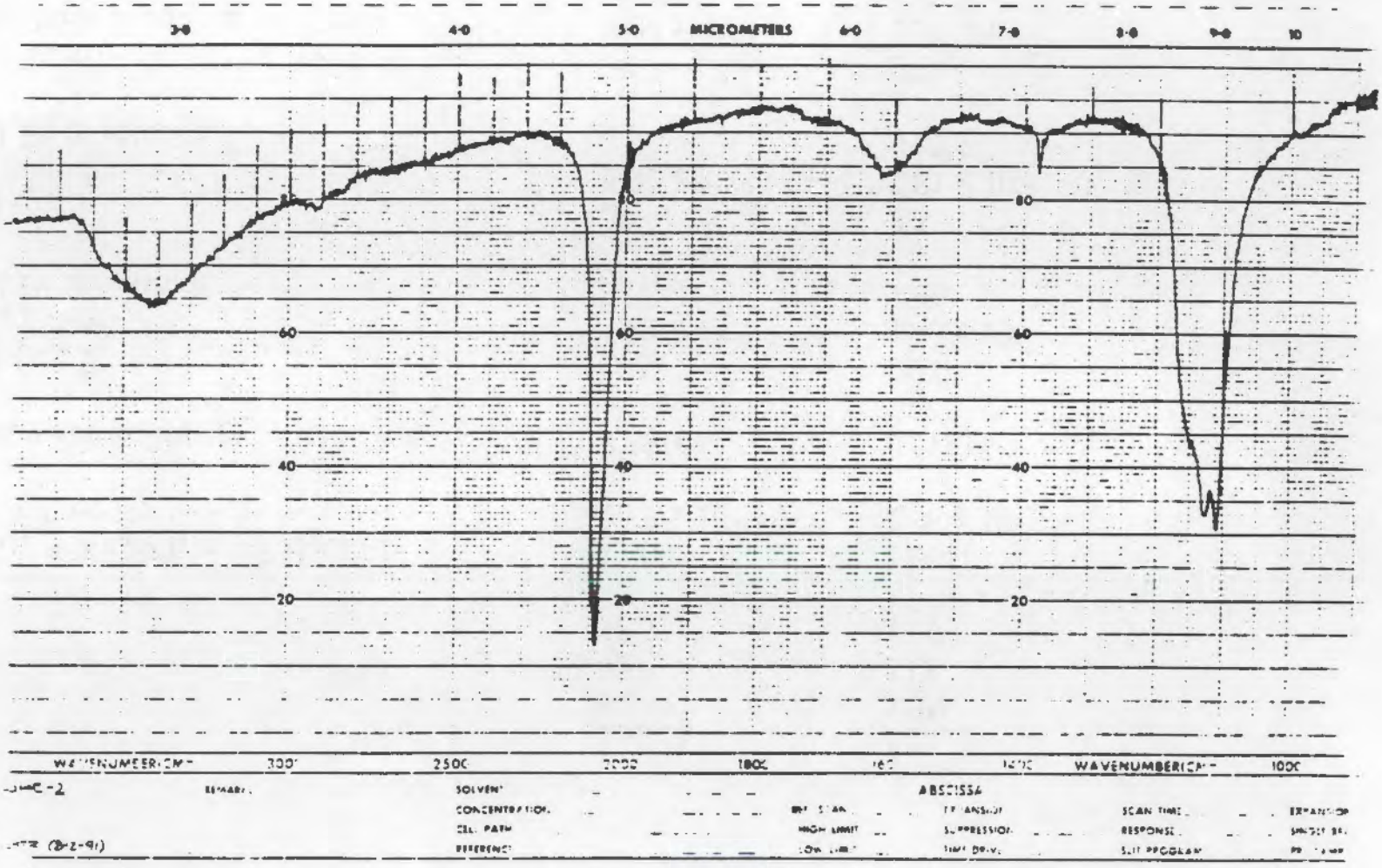
3·0
4·0
5·0
MICROMETERS
6·0
7·0
8·0
9·0
10
80
60
40
20
WAVENUMBERICM⁻
3000
2500
2000
1800
1600
1400
WAVENUMBERICM⁻
1000
WHC-2
SOLVENT
CONCENTRATION
CELL PATH
REFERENCE
ABSCISSA
SCAN TIME
RESPONSE
SLIT PROGRAM

WHC-2

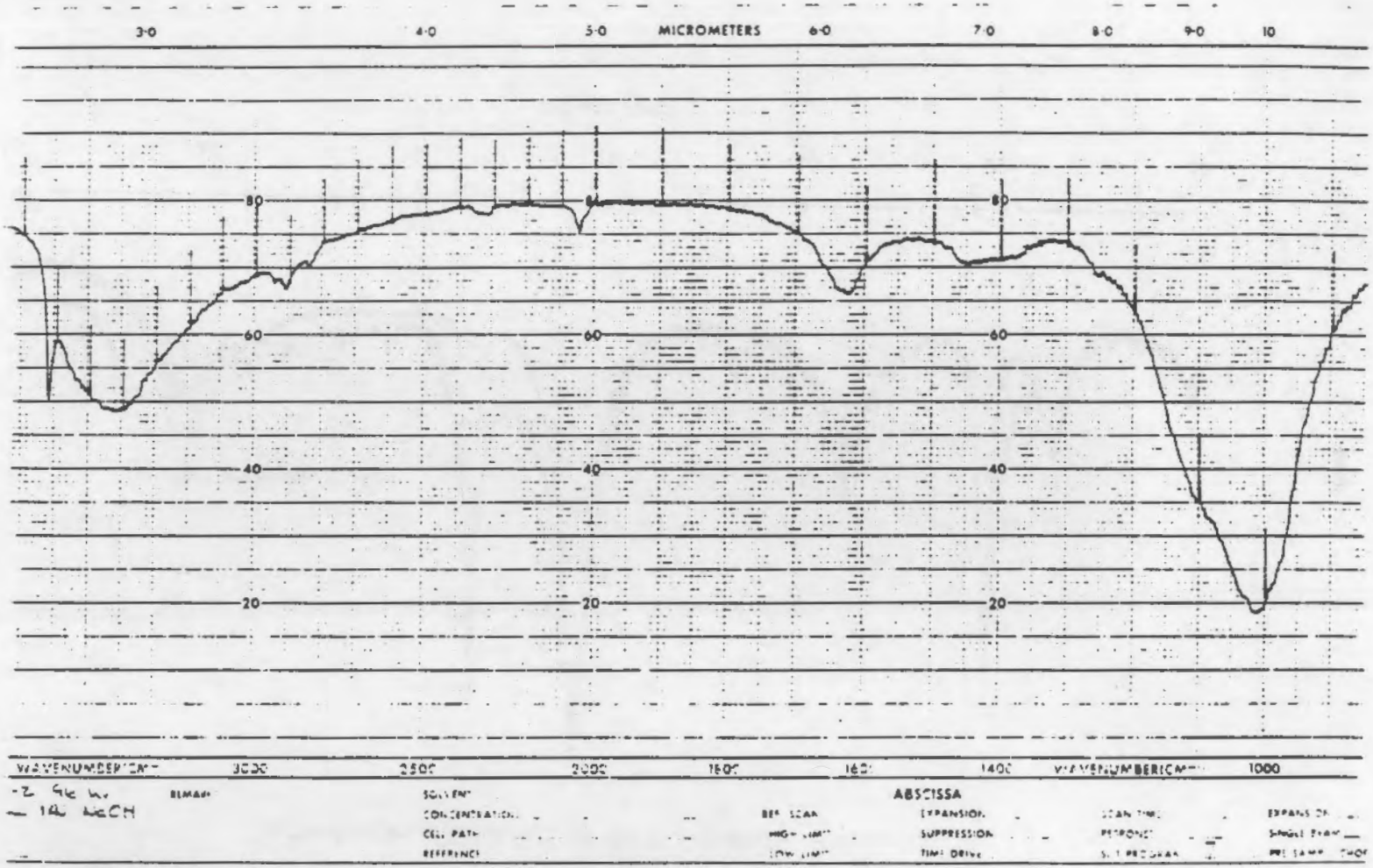

WHC-2
96 hr
1.0 N NaOH

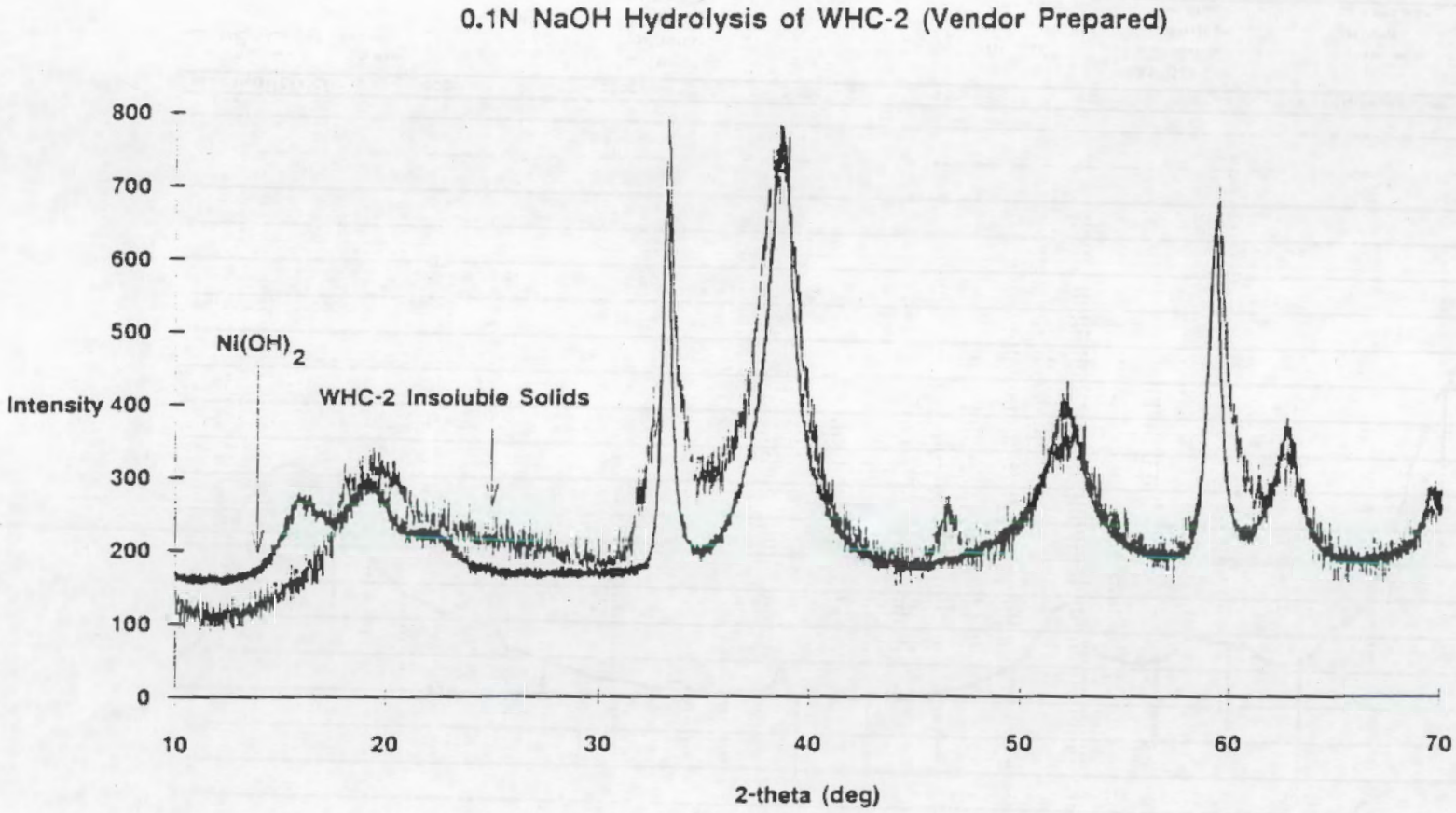
0.1N NaOH Hydrolysis of WHC-2 (Vendor Prepared)
Intensity
800
700
600
500
400
300
200
100
0
Ni(OH)2
WHC-2 Insoluble Solids
10
20
30
40
50
60
70
2-theta (deg)

FERROCYANIDE SOLUBILITY EXPERIMENTS

Studies with Vendor-Prepared Material
$Na_2NiFe(CN)_6 \cdot Na_2SO_4 \cdot 4.5\ H_2O$

I. pH Variation: pH = 12, 13, 14
- monitor solution [Fe]
- determine composition of soluble and insoluble species

II. pH Variation at Constant $[Na^+]$
- pH 12, 1*M* $[Na^+]$
- pH 13, 1*M*, 2*M*, 6*M* $[Na^+]$
- pH 14, 1*M* $[Na^+]$

III. pH 13 at 1*M* $[Na^+]$ With Added Salts
- Na salts of NO_3^-, NO_2^-, PO_4^{3-}, SO_4^{2-}, CO_3^{2-}, OH^-

IV. Temperature Variation at pH 13 and 1*M* $[Na^+]$
- 25, 50, 75°C

V. Static Solubility Test
- pH 13, 1*M* $[Na^+]$, 25°C

Studies with Flowsheet-Prepared Materials

VI. In-Farm 1, Rev. 8 (EB Supernate from BX-110)
VII. In-Farm 1, Rev. 9
VIII. In-Farm 2, Rev. 11 (C Farm TBP Waste)
IX. In-Farm 2, Rev. 12

- pH 13, 1*M* $[Na^+]$, 25°C

Vendor-1 : 1 gram

NaOH : 50ml

magnetically stirred in teflon flasks

144h reaction time

Reactions solutions sampled and analyzed for Fe by AA and/or ICP

Free CN^- by IC

Transmission IR of KBr pellets

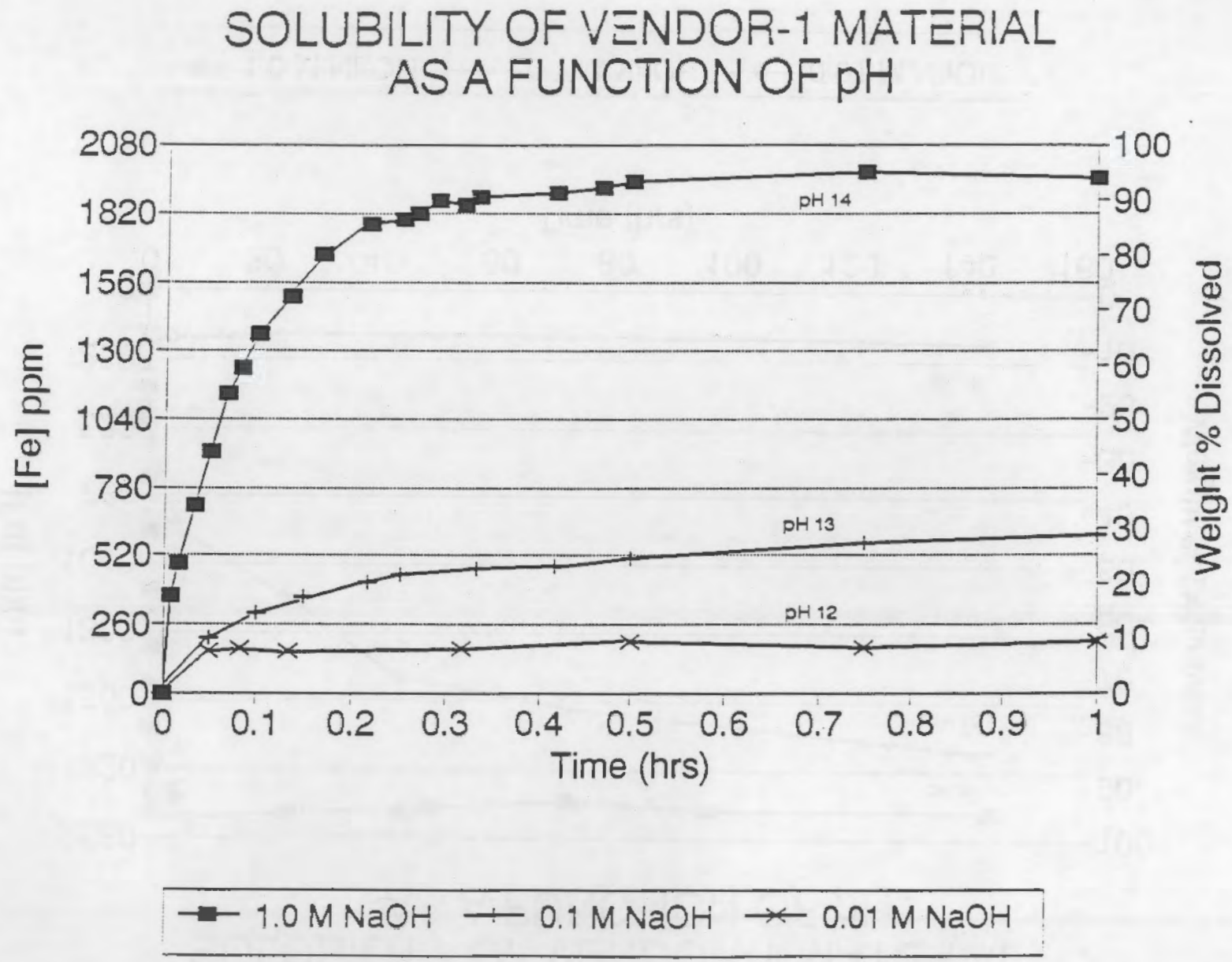
SOLUBILITY OF VENDOR-1 MATERIAL
AS A FUNCTION OF pH
[Fe] ppm
Weight % Dissolved
Time (hrs)
2080
1820
1560
1300
1040
780
520
260
0
100
90
80
70
60
50
40
30
20
10
0
0
0.1
0.2
0.3
0.4
0.5
0.6
0.7
0.8
0.9
1
pH 14
pH 13
pH 12
1.0 M NaOH
0.1 M NaOH
0.01 M NaOH

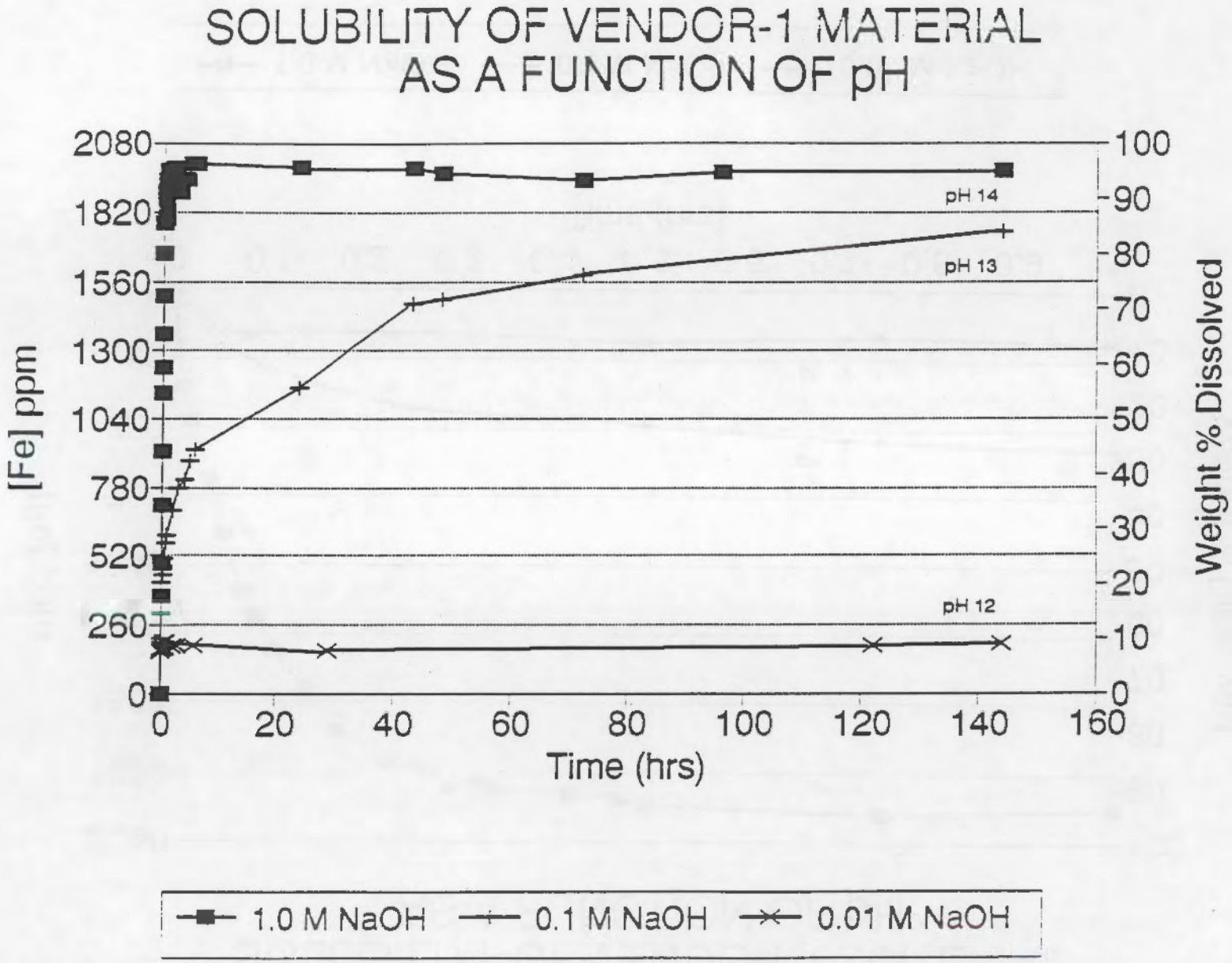
SOLUBILITY OF VENDOR-1 MATERIAL
AS A FUNCTION OF pH
[Fe] ppm
Weight % Dissolved
Time (hrs)
2080
1820
1560
1300
1040
780
520
260
0
100
90
80
70
60
50
40
30
20
10
0
0
20
40
60
80
100
120
140
160
pH 14
pH 13
pH 12
1.0 M NaOH
0.1 M NaOH
0.01 M NaOH

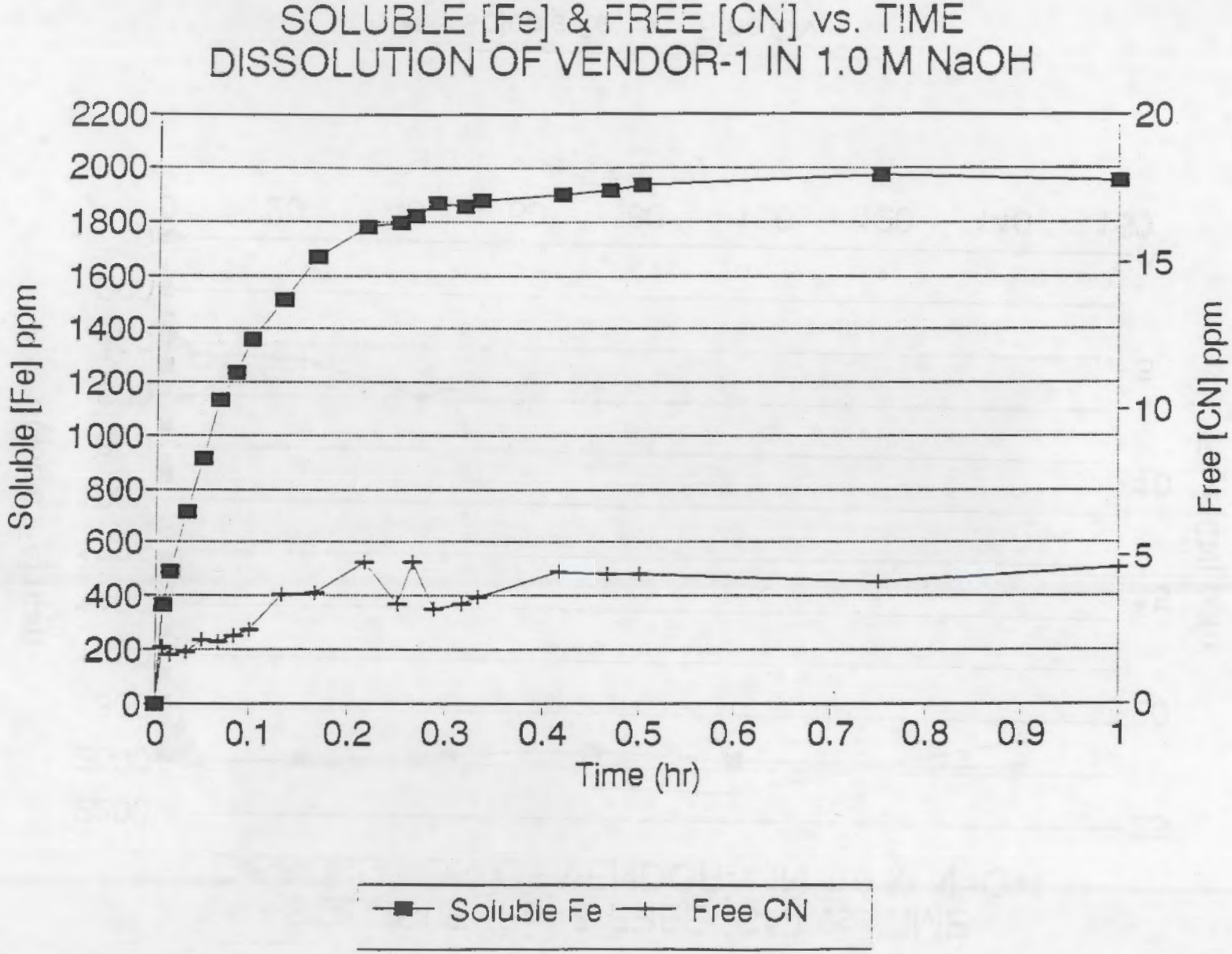
SOLUBLE [Fe] & FREE [CN] vs. TIME
DISSOLUTION OF VENDOR-1 IN 1.0 M NaOH
Soluble [Fe] ppm
Free [CN] ppm
Time (hr)
2200
2000
1800
1600
1400
1200
1000
800
600
400
200
0
20
15
10
5
0
0
0.1
0.2
0.3
0.4
0.5
0.6
0.7
0.8
0.9
1
Soluble Fe
Free CN

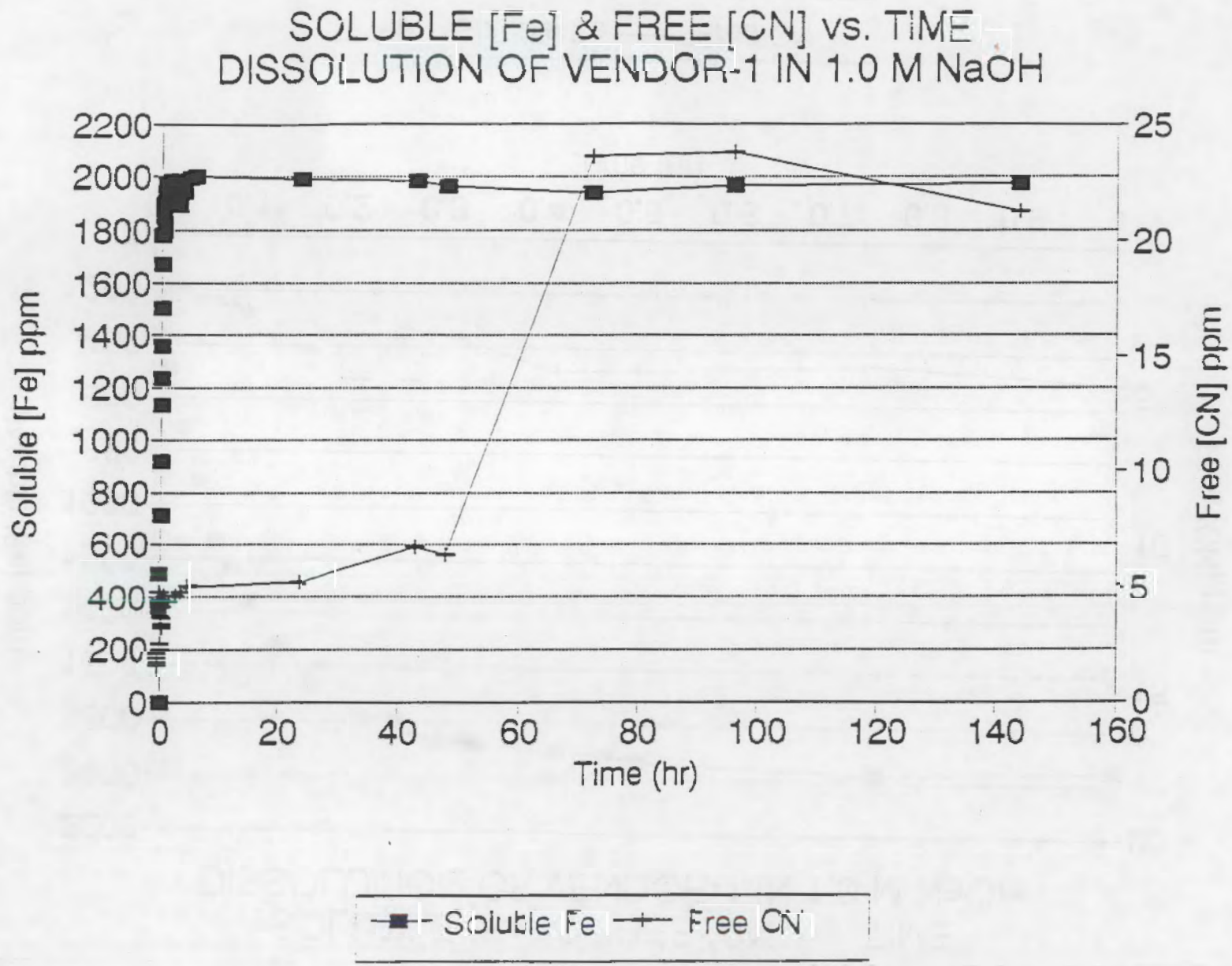
SOLUBLE [Fe] & FREE [CN] vs. TIME
DISSOLUTION OF VENDOR-1 IN 1.0 M NaOH
Soluble [Fe] ppm
Free [CN] ppm
Time (hr)
2200
2000
1800
1600
1400
1200
1000
800
600
400
200
0
25
20
15
10
5
0
0
20
40
60
80
100
120
140
160
Soluble Fe
Free CN

PLOT OF FREE [CN] vs. SOLUBLE [Fe]
DISSOLUTION OF VENDOR-1 IN 1.0 M NaOH

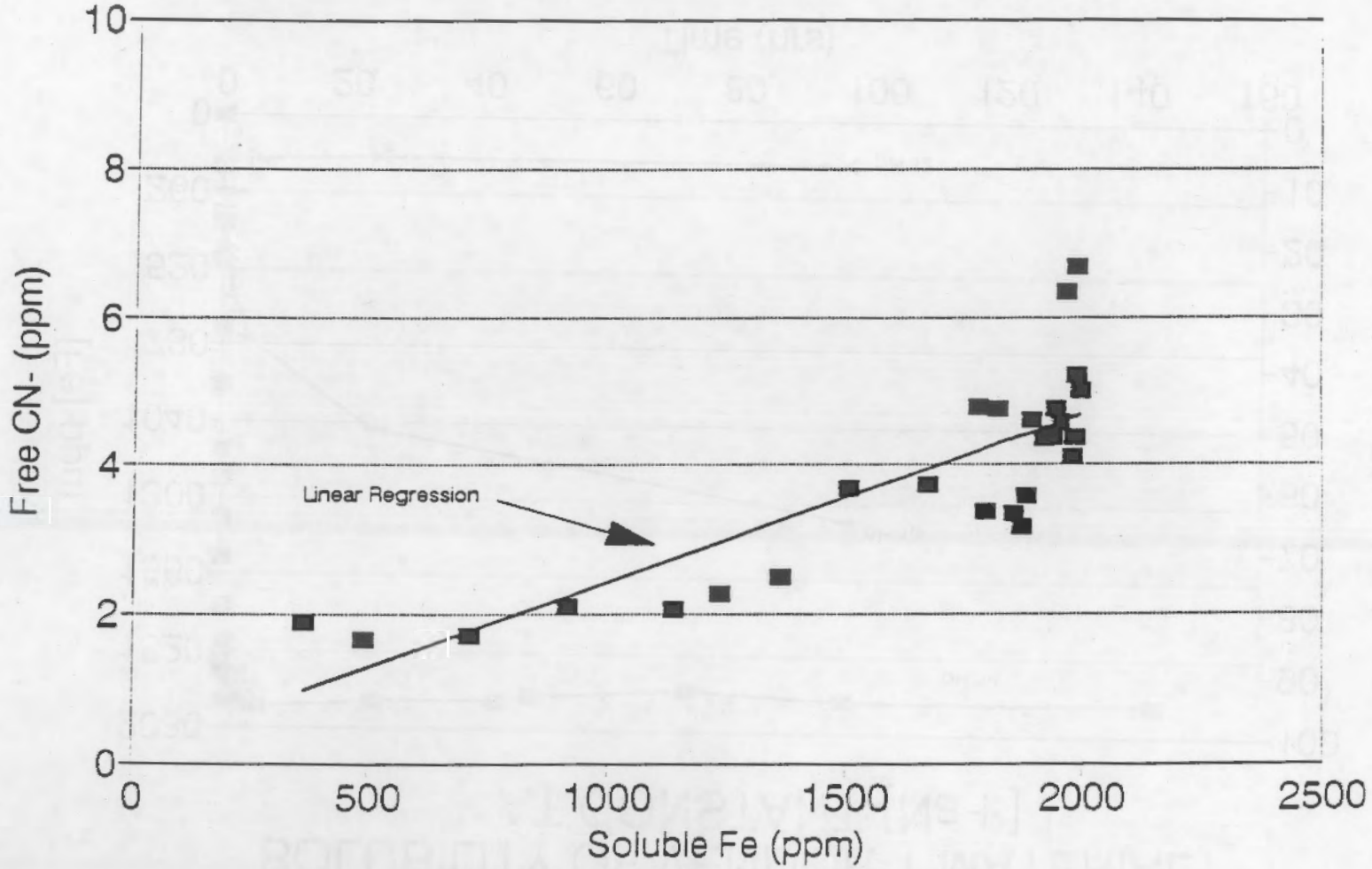

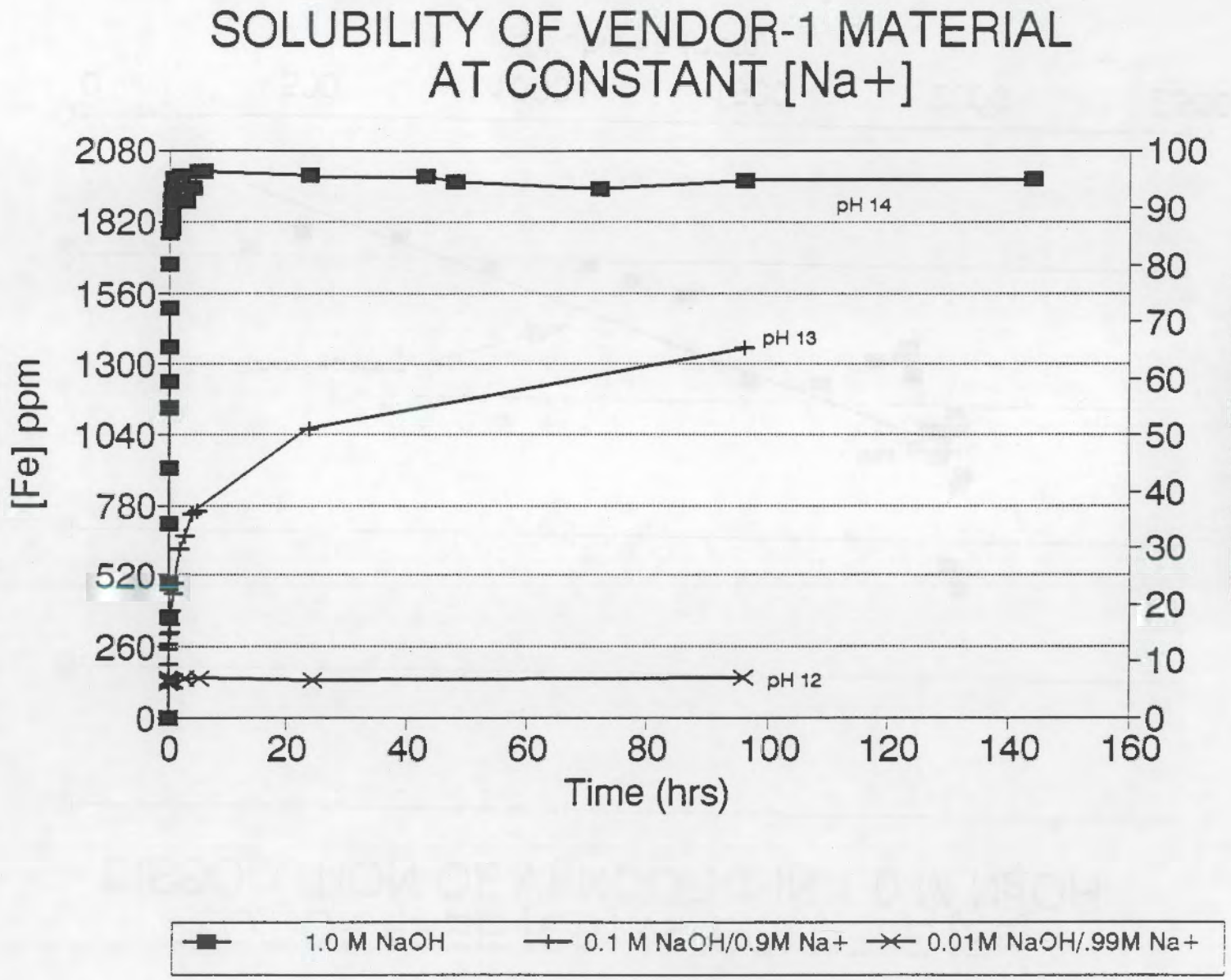
SOLUBILITY OF VENDOR-1 MATERIAL
AT CONSTANT [Na+]
[Fe] ppm
Weight % Dissolved
Time (hrs)
2080
1820
1560
1300
1040
780
520
260
0
100
90
80
70
60
50
40
30
20
10
0
0
20
40
60
80
100
120
140
160
pH 14
pH 13
pH 12
1.0 M NaOH
0.1 M NaOH/0.9M Na+
0.01M NaOH/.99M Na+

AFFECT OF SODIUM ON SOLUBILITY OF VENDOR-1 IN 0.1 M NaOH

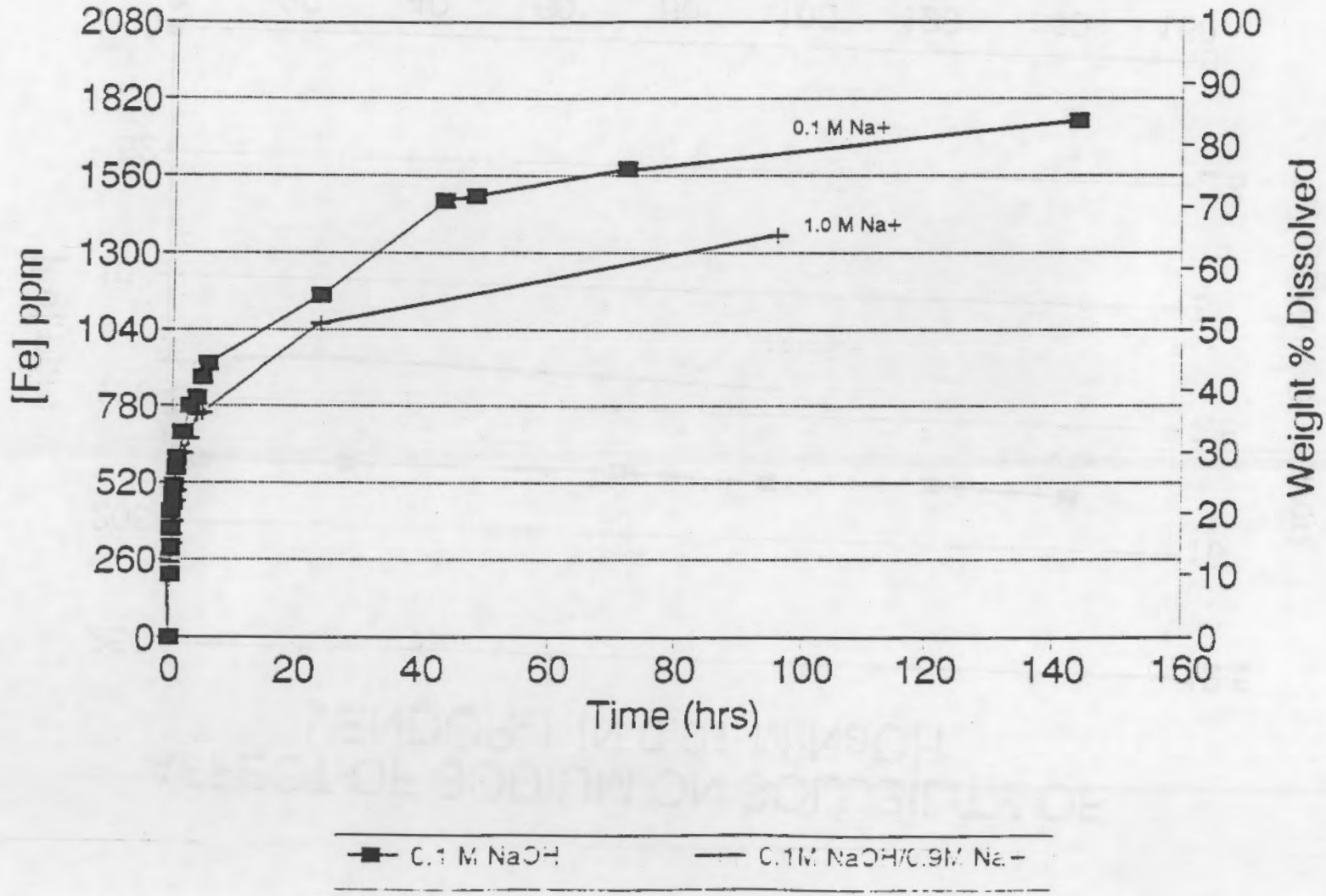

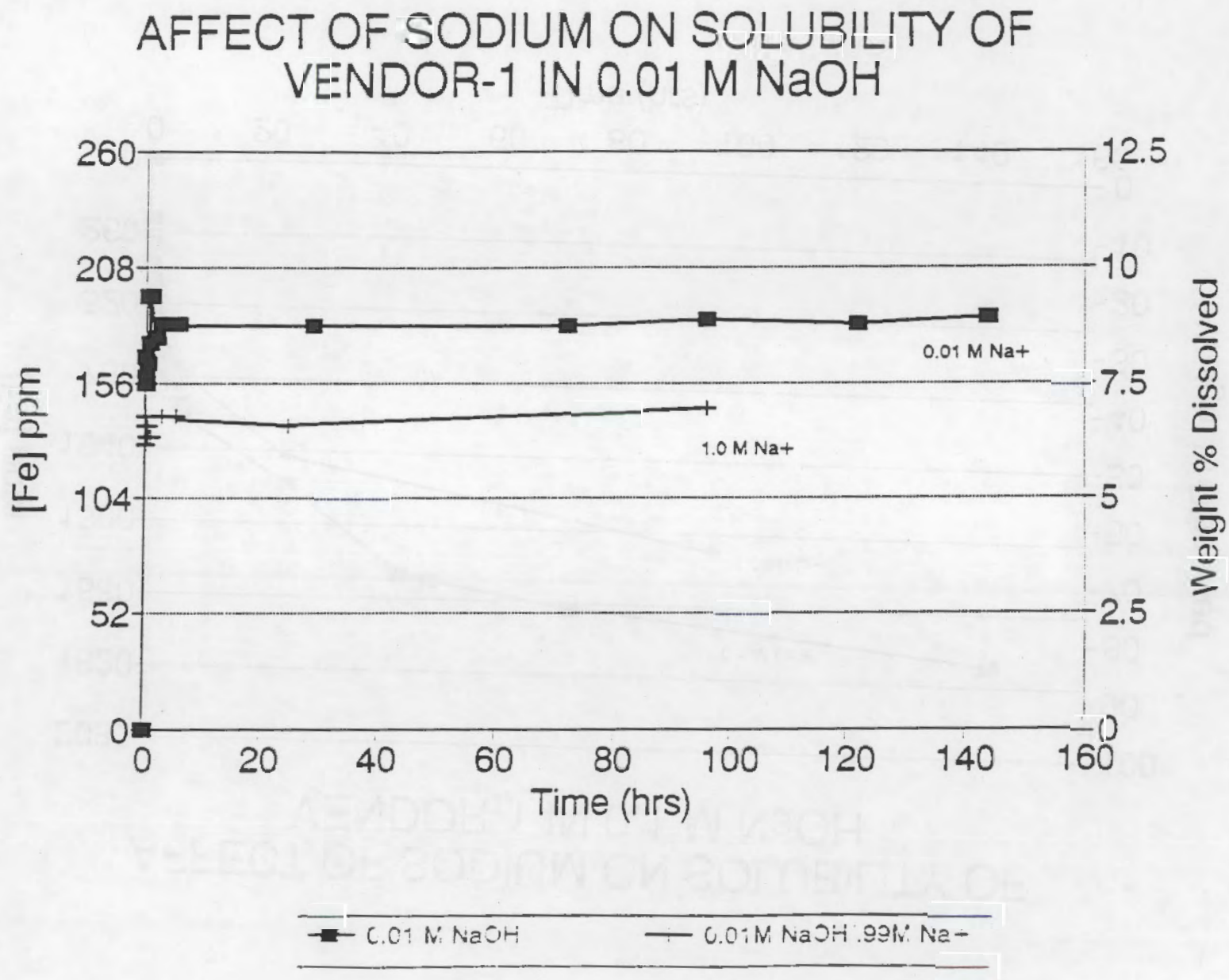
AFFECT OF SODIUM ON SOLUBILITY OF VENDOR-1 IN 0.01 M NaOH
260
208
156
104
52
0
[Fe] ppm
12.5
10
7.5
5
2.5
0
Weight % Dissolved
0.01 M Na+
1.0 M Na+
0
20
40
60
80
100
120
140
160
Time (hrs)
0.01 M NaOH
0.01M NaOH .99M Na+

AFFECT OF SODIUM ON SOLUBILITY OF VENDOR-1 IN 0.01 M NaOH

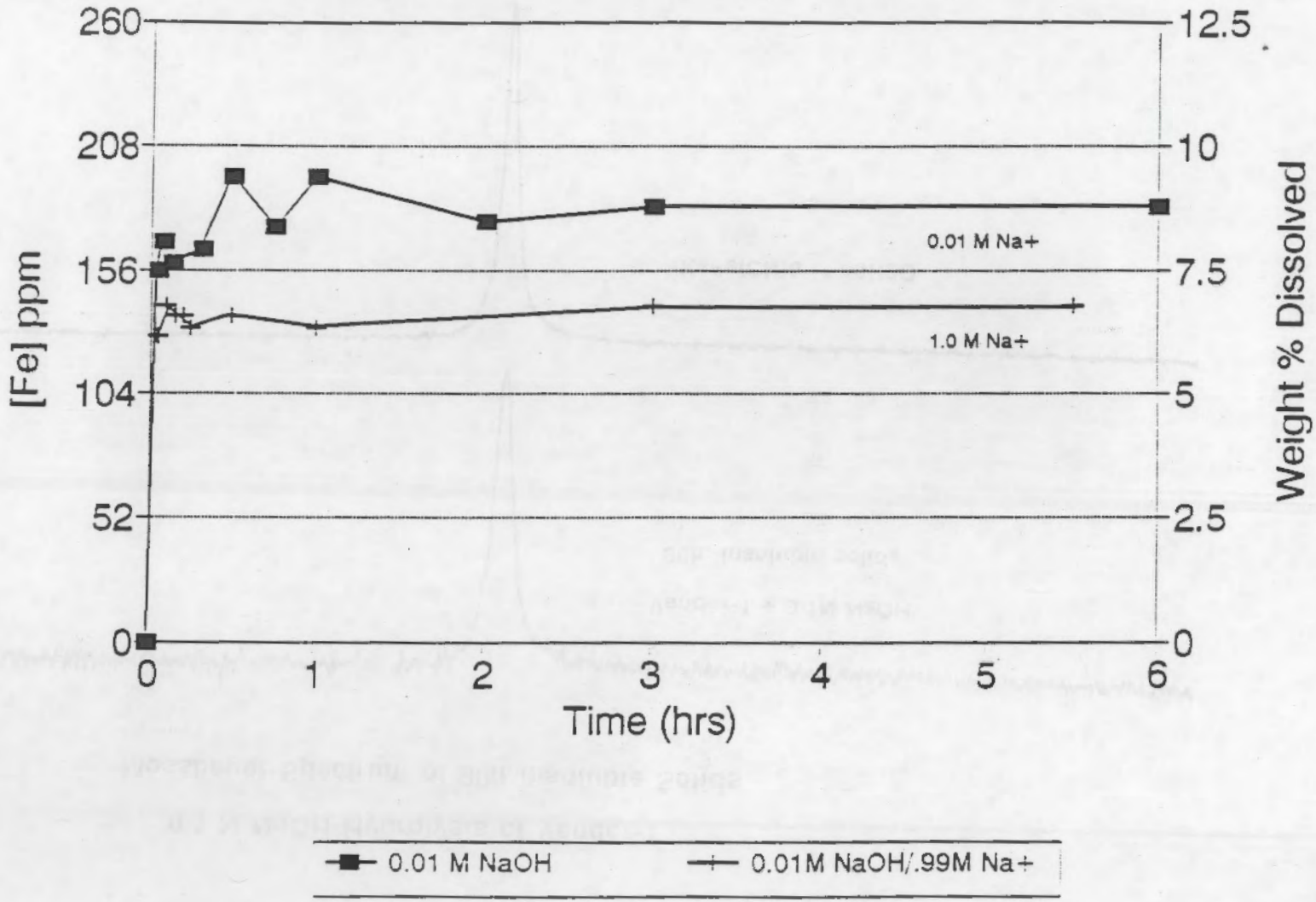

0.1 N NaOH Hydrolysis of Vendor-1

Mossbauer Spectrum of 80h Insoluble Solids

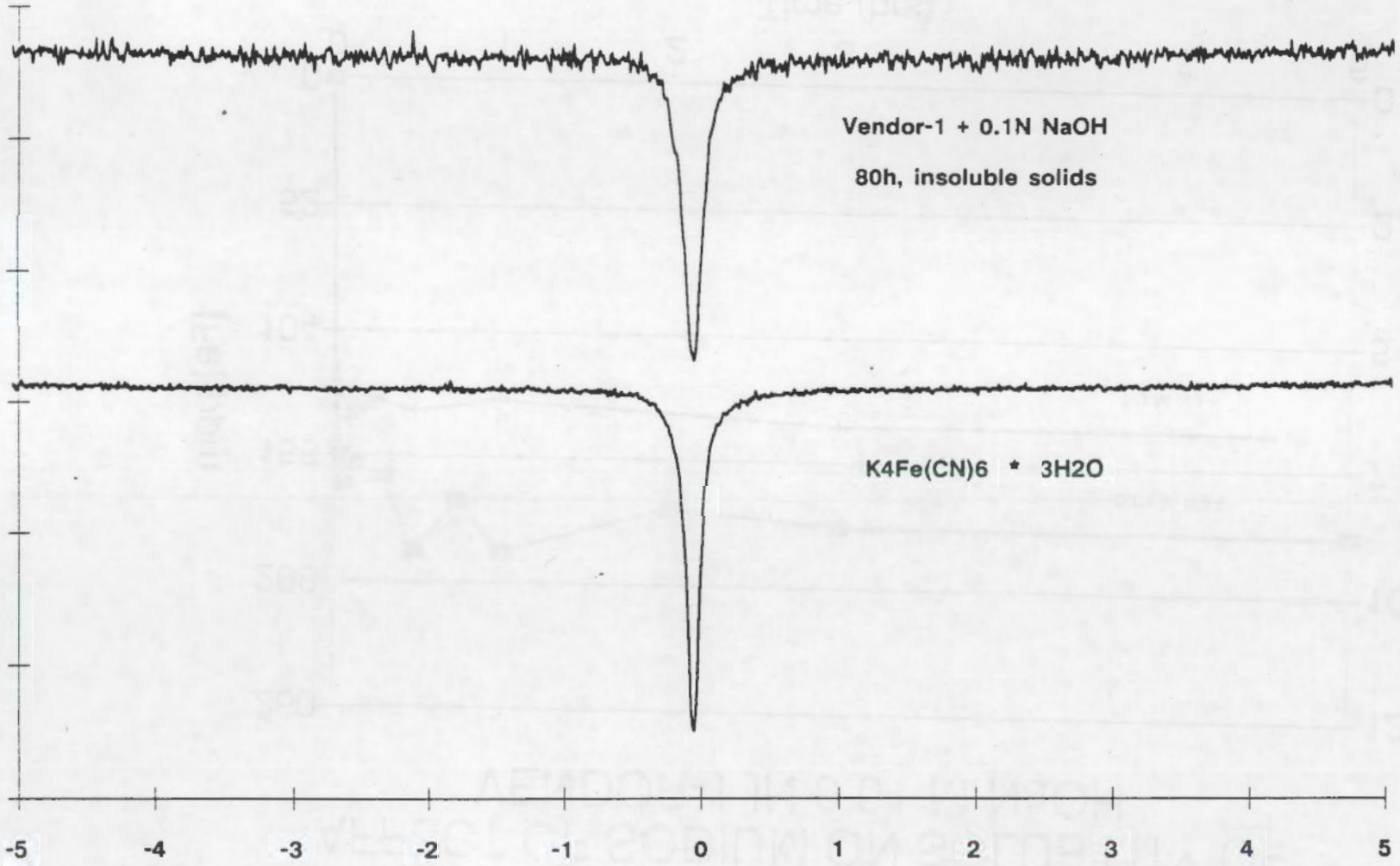

IR ANALYSIS OF REACTION PRODUCTS IN THE REGION OF 4000 - 3000 cm^{-1}

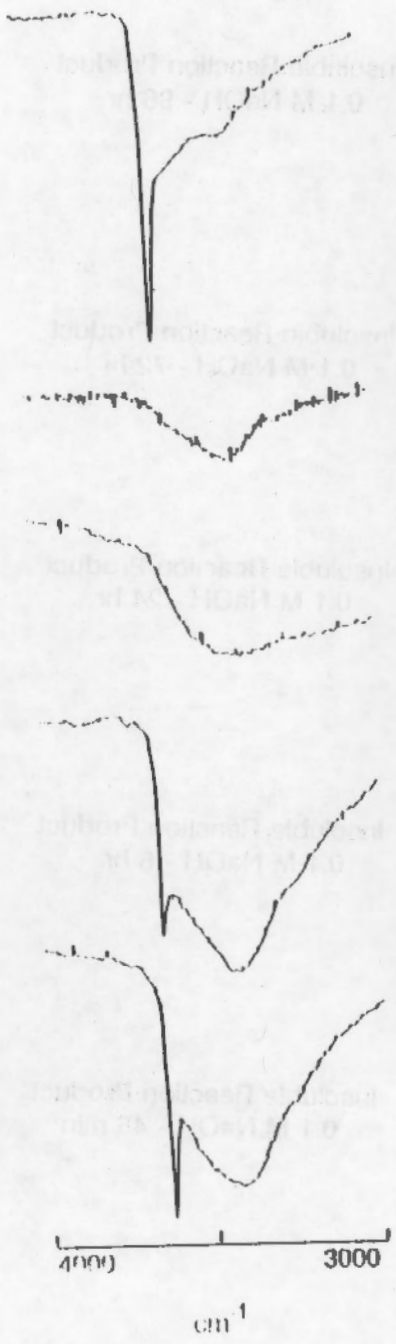

$Ni(OH)_2$

0.1 M Soluble Reaction Product

1.0 M Soluble Reaction Product

0.1 M Insoluble Reaction Product

1.0 M Insoluble Reaction Product

IR ANALYSIS OF REACTION PRODUCTS IN THE REGION OF 4000 - 3000 cm^{-1}

Insoluble Reaction Product
0.1 M NaOH - 96 hr

Insoluble Reaction Product
0.1 M NaOH - 72 hr

Insoluble Reaction Product
0.1 M NaOH - 24 hr

Insoluble Reaction Product
0.1 M NaOH - 6 hr

Insoluble Reaction Product
0.1 M NaOH - 45 min

IR ANALYSIS OF REACTION PRODUCTS IN THE REGION OF CN^- ABSORBANCE

Vendor-1
(max abs. 2085 cm^{-1})

0.1 M Insoluble Reaction Product
(max abs. 2085 cm^{-1})

0.1 M Soluble Reaction Products
(max abs. 2060 cm^{-1})

Appendix D

Gaseous Products from the Thermal Decomposition of Ferrocyanides

Ferrocyanide Safety Project

"Predecisional Information"

GASEOUS PRODUCTS FROM THE THERMAL DECOMPOSITION OF FERROCYANIDES

Richard T. Hallen
William F. Riemath

Pacific Northwest Laboratory
P. O. Box 999
Richland, WA 99352

Tank Waste Science Panel Meeting
Denver, Colorado
March 25-27, 1992

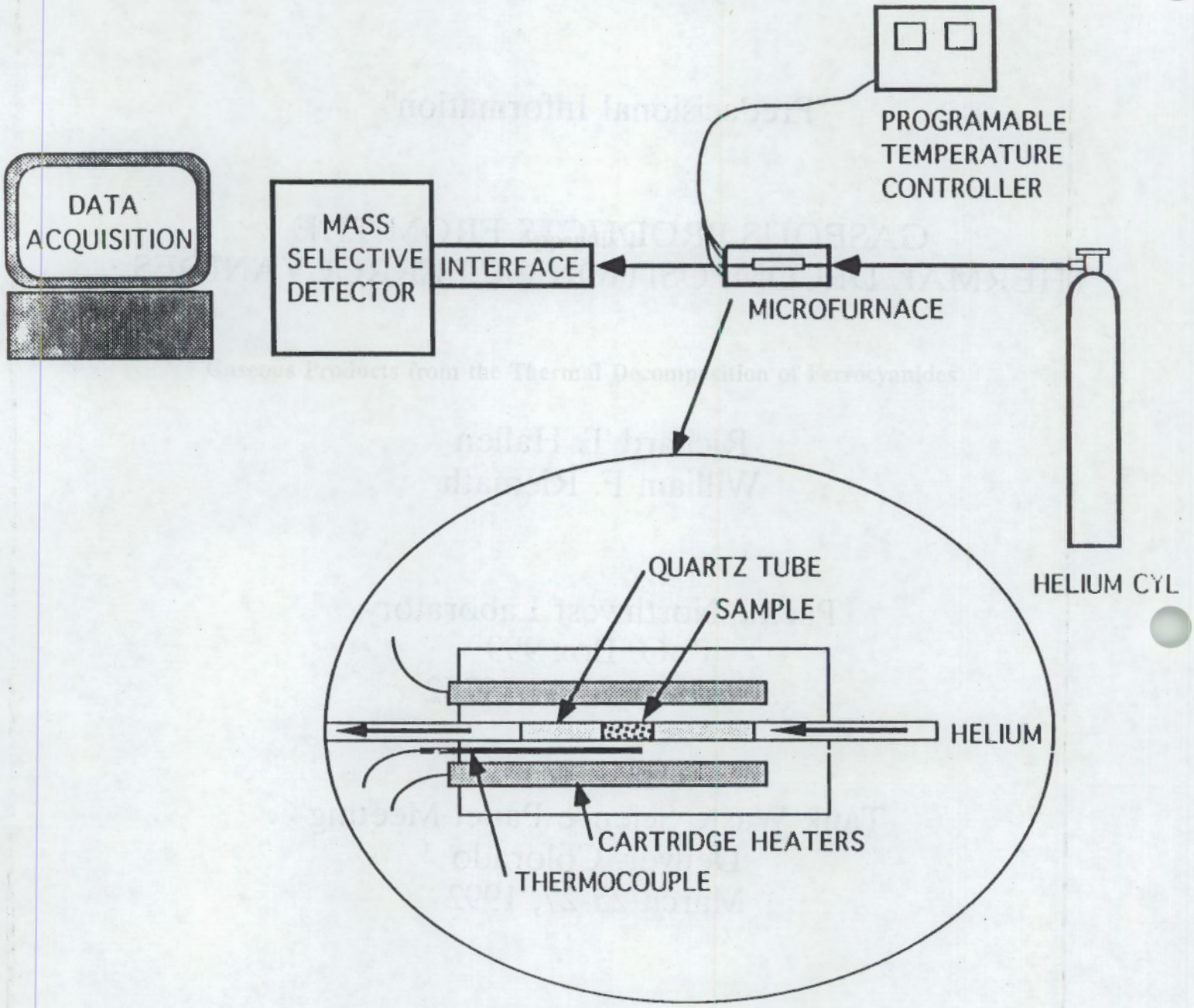

FIGURE 14. Illustration of instrumentation used in TG analysis and microfurnace sample holder.

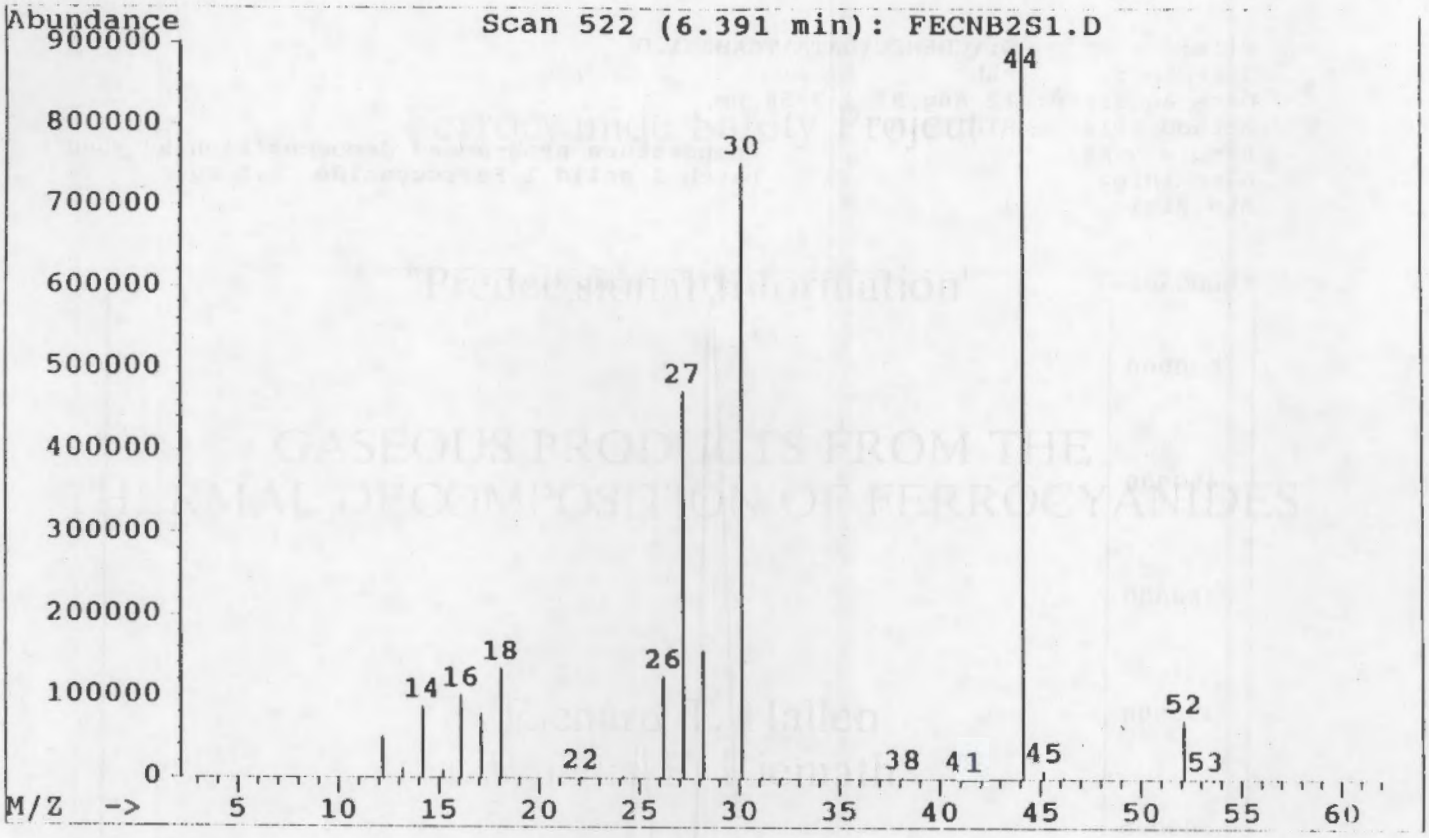

Scan 522 (6.391 min): FECNB2S1.D

m/z	abund.	m/z	abund.
12.20	50272	28.20	157760
13.20	12191	30.15	755136
14.20	88128	31.15	3614
15.20	9932	32.15	2803
16.10	102296	38.15	2628
17.10	78856	41.15	1531
18.10	135232	44.15	902912
22.10	2237	45.15	11701
24.20	3361	46.15	3972
26.20	125352	52.10	73288
27.20	473984	53.20	2512

FIGURE 2. The mass spectrum and relative abundance of gaseous components from the decomposition of flowsheet ferrocyanide at 350 C.

File: G:\CHEMPC\DATA\TGAB2S1.D
Operator: rth
Date Acquired: 12 Aug 91 3:54 pm
Method File: RTHTGA.M
Sample Name: temperature programmed decomposition 50 -500
Misc Info: batch 2 solid 1 Ferrocyanide 4.5 mg
ALS vial: 1

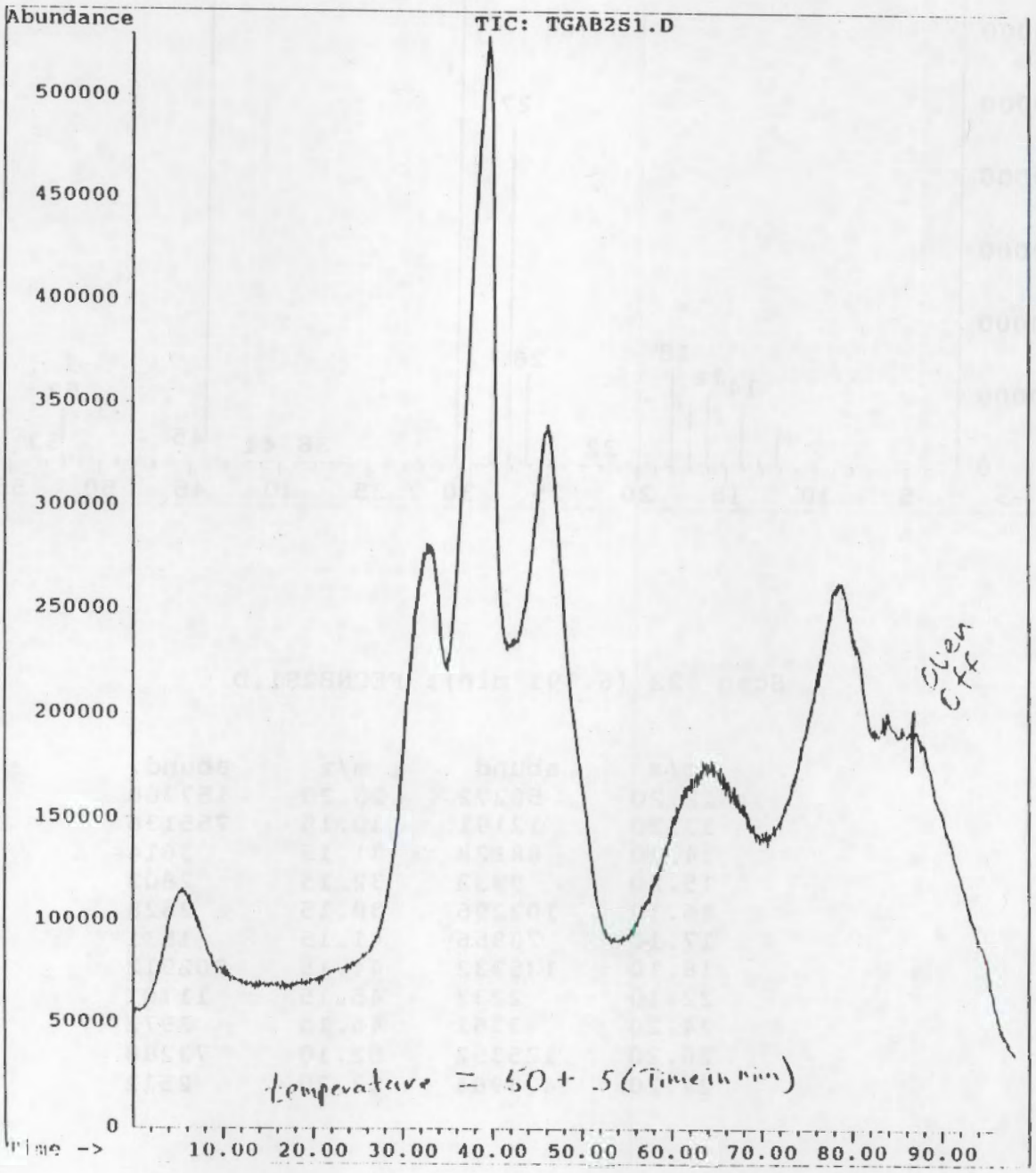

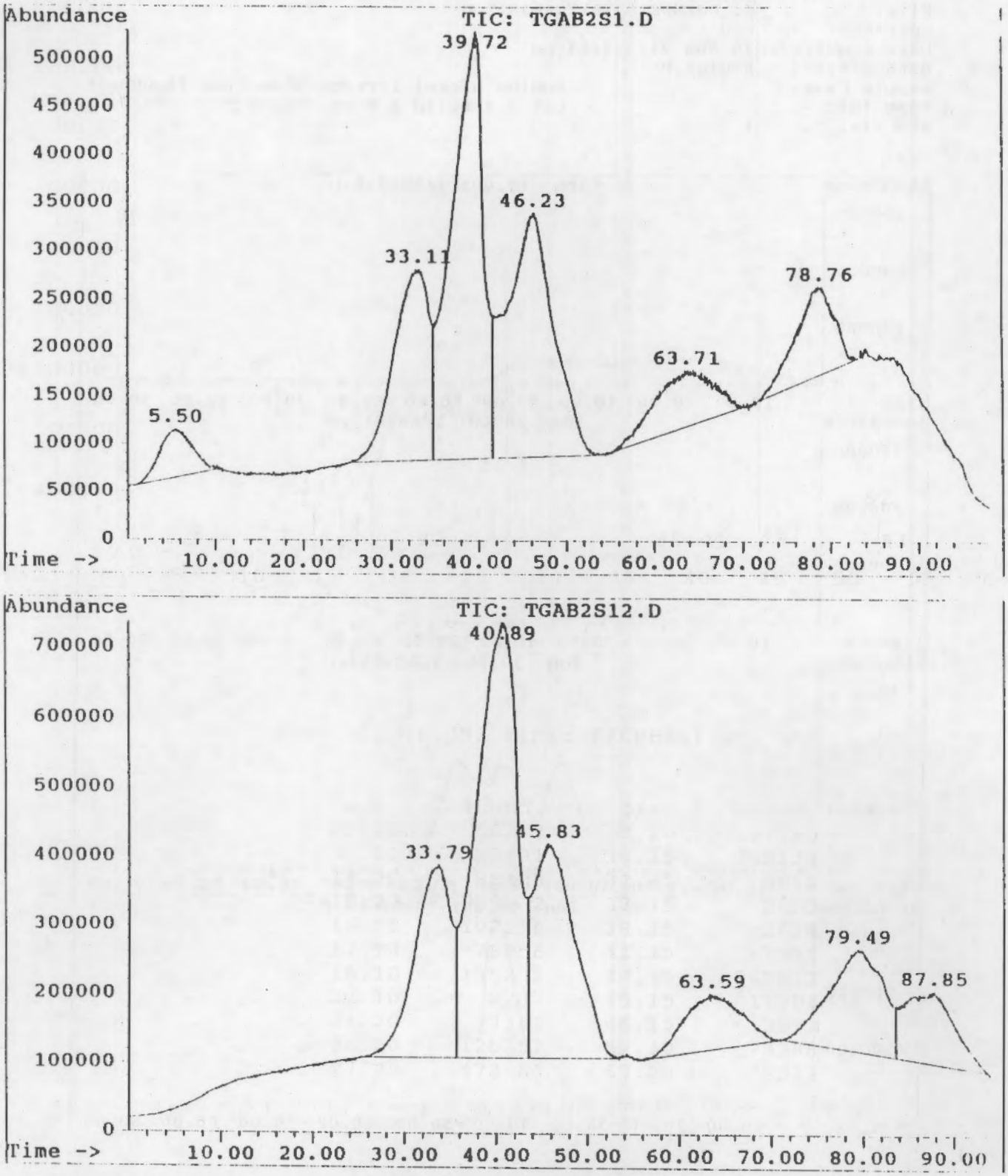

FIGURE 16. Duplicate experiments of different sample size showing total ion traces for the thermal decomposition of PNL flowsheet ferrocyanide (Batch 2 Solid 1).

File: G:\CHEMPC\DATA\TGAB2S12.D
Operator: RTH
Date Acquired: 30 Aug 91 2:03 pm
Method File: RTHTGA.M
Sample Name: sodium nickel ferrocyanide from flowsheet
Misc Info: batch 2 solid 1 8 mg sample 50 - 500 C, 5/mi
ALS vial: 1

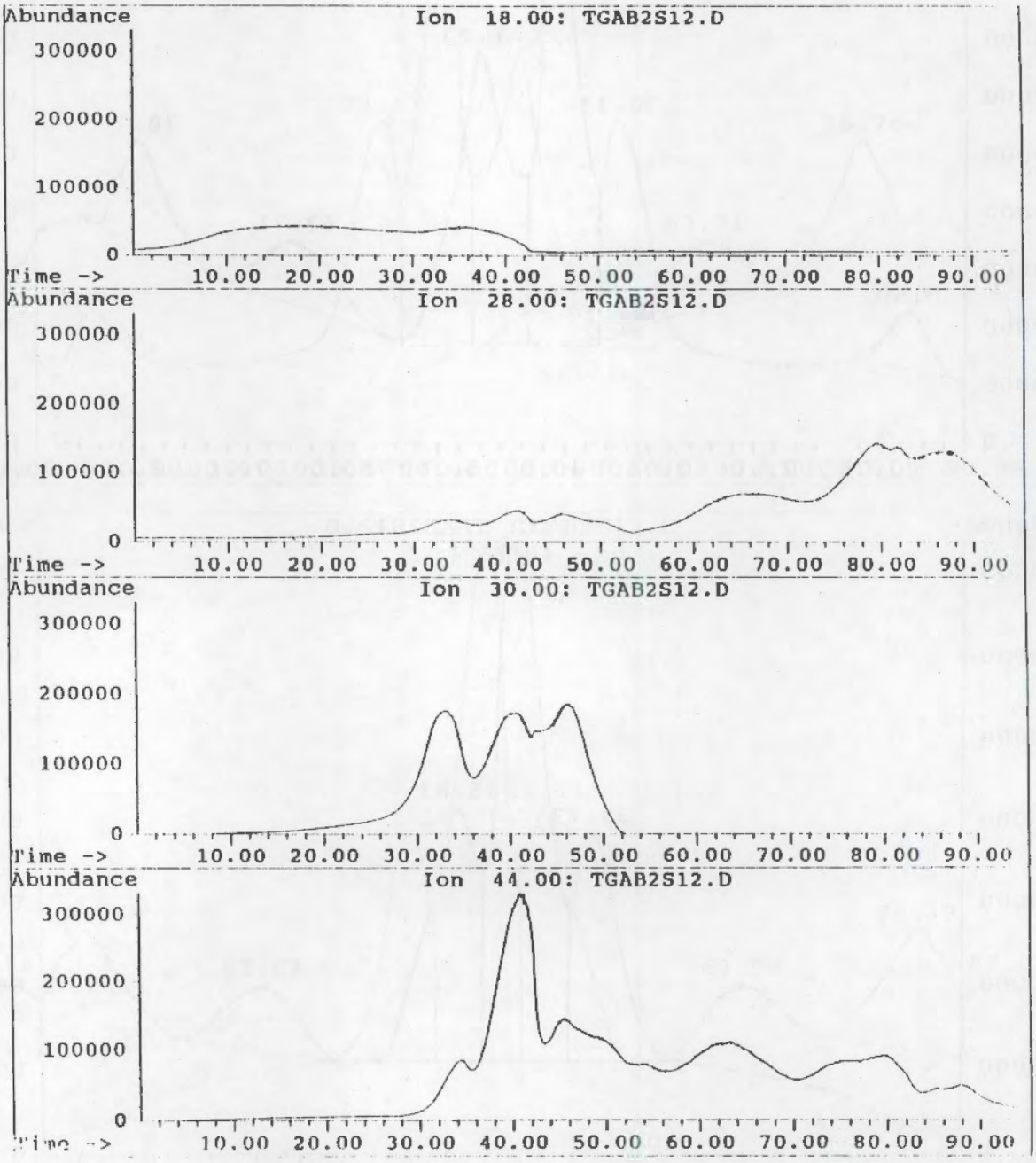

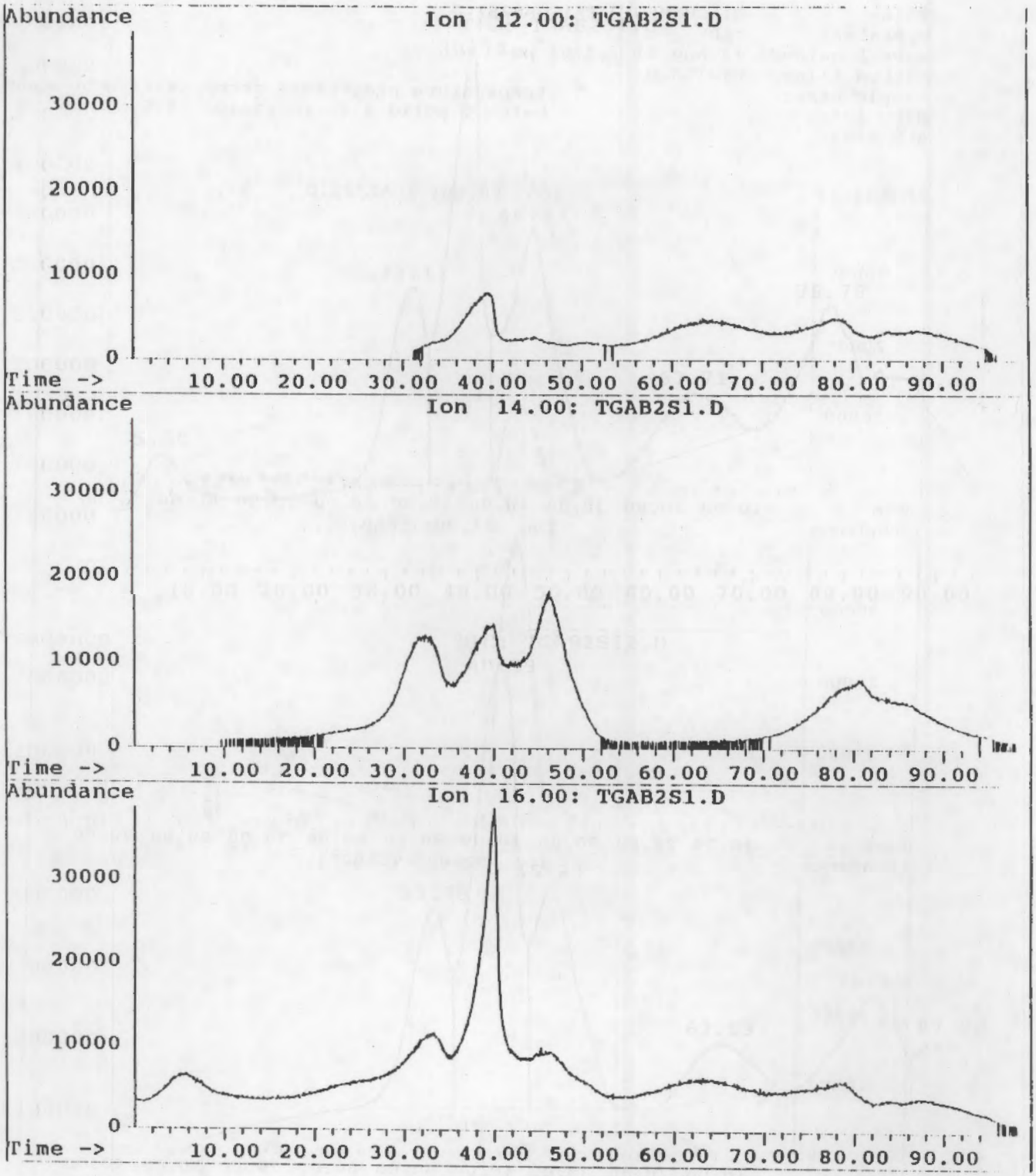

Figure 18. Extracted ion traces for carbon (mass 12), nitrogen (mass 14) an oxygen (mass 16) from the thermal decomposition of PNL flowsheet ferrocyanide.

File: G:\CHEMPC\DATA\TGAB2S1.D
Operator: rth
Date Acquired: 12 Aug 91 3:54 pm
Method File: RTHTGA.M
Sample Name: temperature programmed decomposition 50 -500
Misc Info: batch 2 solid 1 Ferrocyanide 4.5 mg
ALS vial: 1

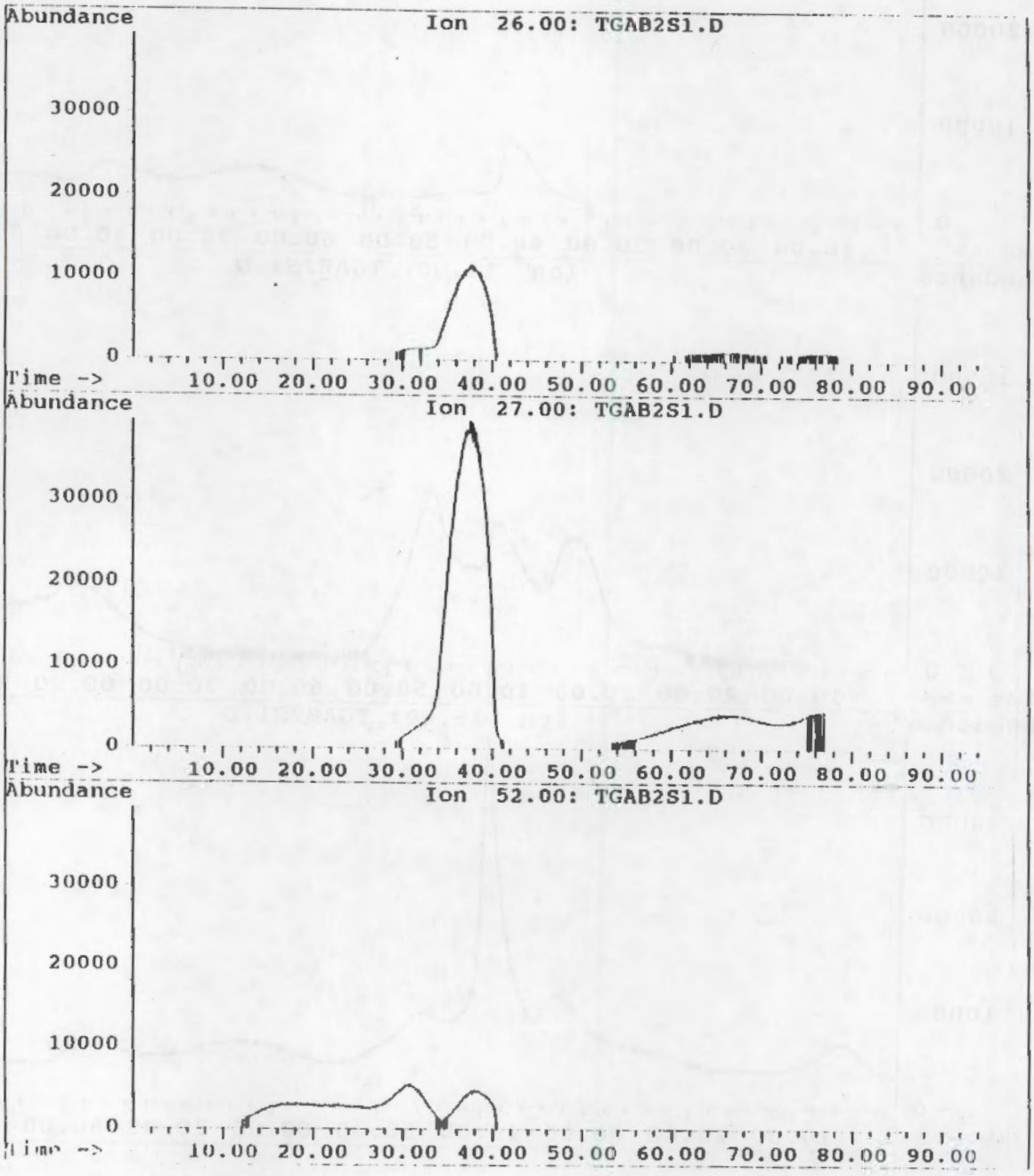

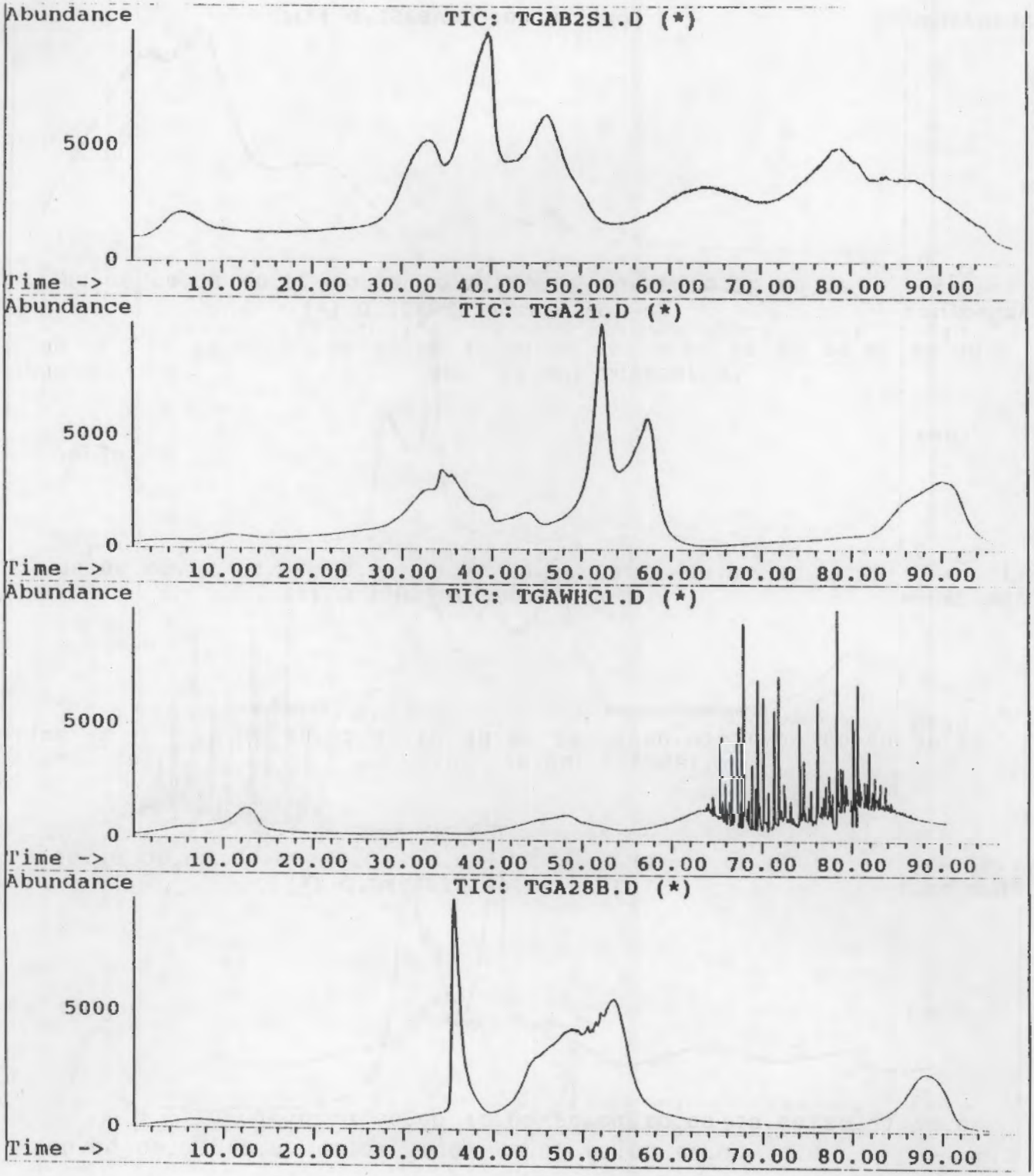

FIGURE 20. Total ion traces for the thermal decomposition of flowsheet materials: Batch 2 Solid 1, FECN-21, WHC-1 and FECN-28b plus nitrate/nitrite.

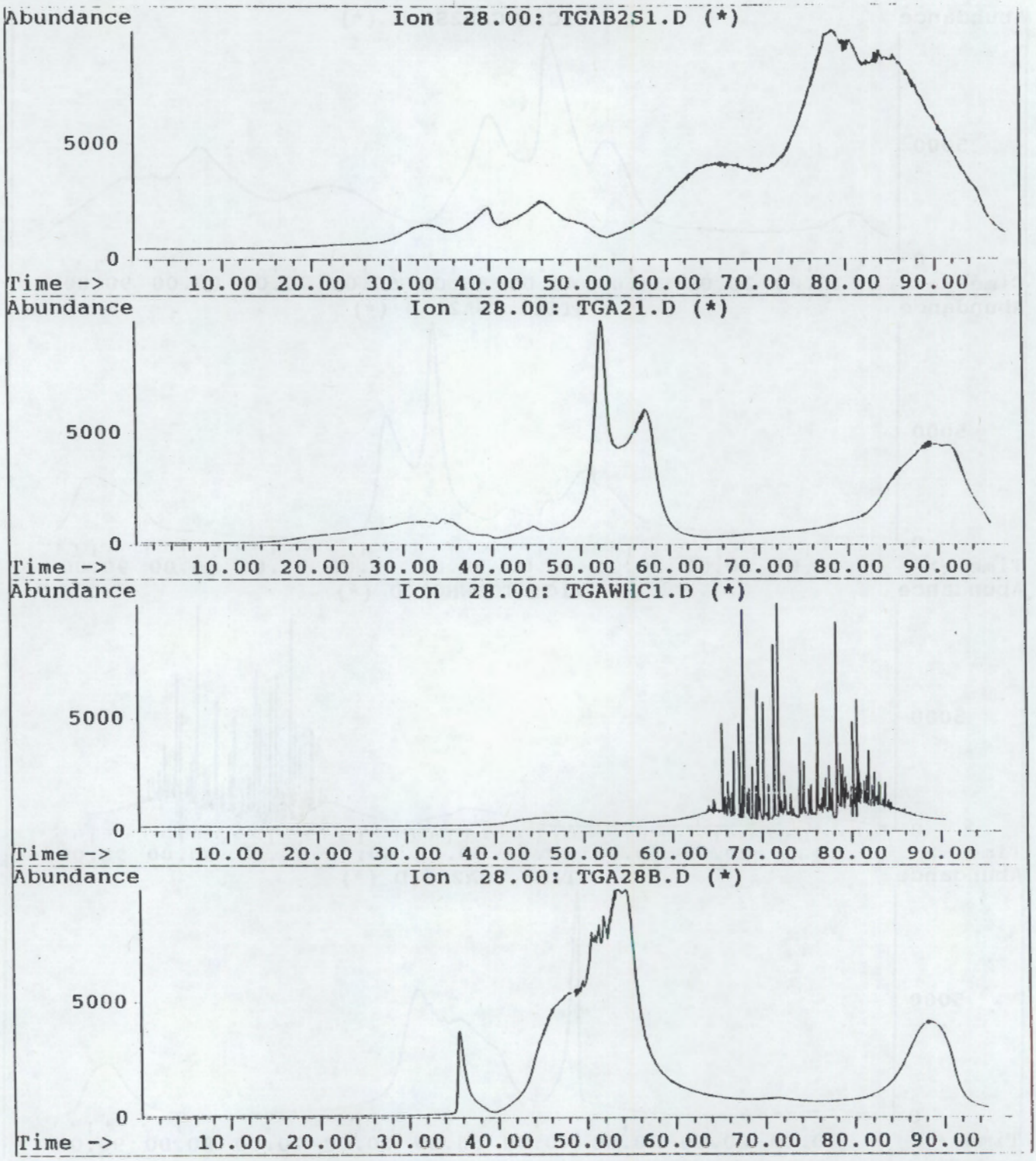

FIGURE 21. Extracted ion traces for mass ion 28 for the thermal decomposition of flowsheet materials: Batch 2 Solid 1, FECN-21, WHC-1 and FECN-28b.

File: G:\CHEMPC\DATA\TGA21.D
Operator: RTH
Date Acquired: 6 Sep 91 7:53 am
Method File: RTHTGA.M
Sample Name: FECN 21 no additional NO3 or NO@
Misc Info: Temperature Programmed 5 C/minute 50-500 C
ALS vial: 1

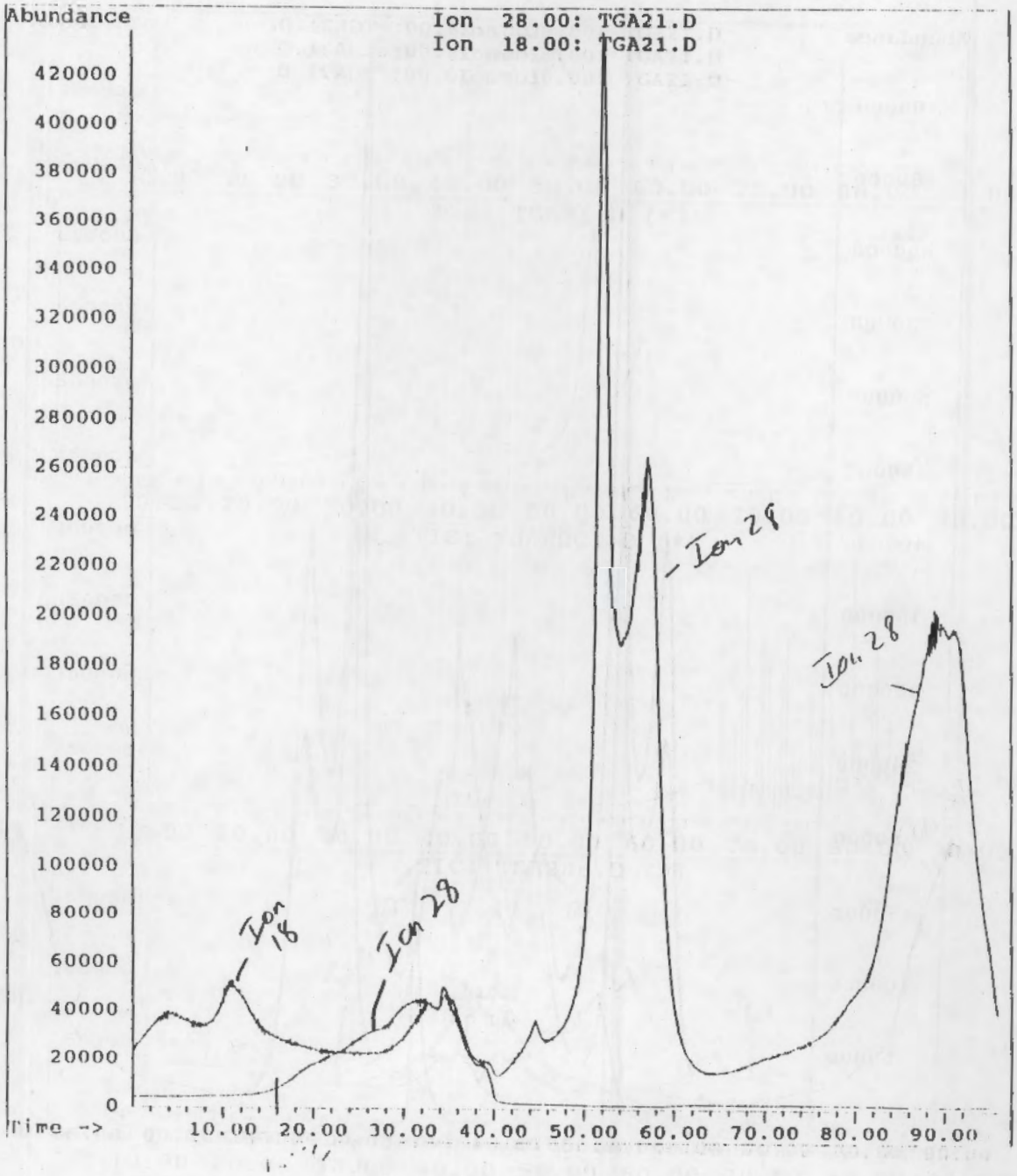

File: G:\CHEMPC\DATA\TGA21.D
Operator: RTH
Date Acquired: 6 Sep 91 7:53 am
Method File: RTHTGA.M
Sample Name: FECN 21 no additional NO3 or NO@
Misc Info: Temperature Programmed 5 C/minute 50-500 C
ALS vial: 1

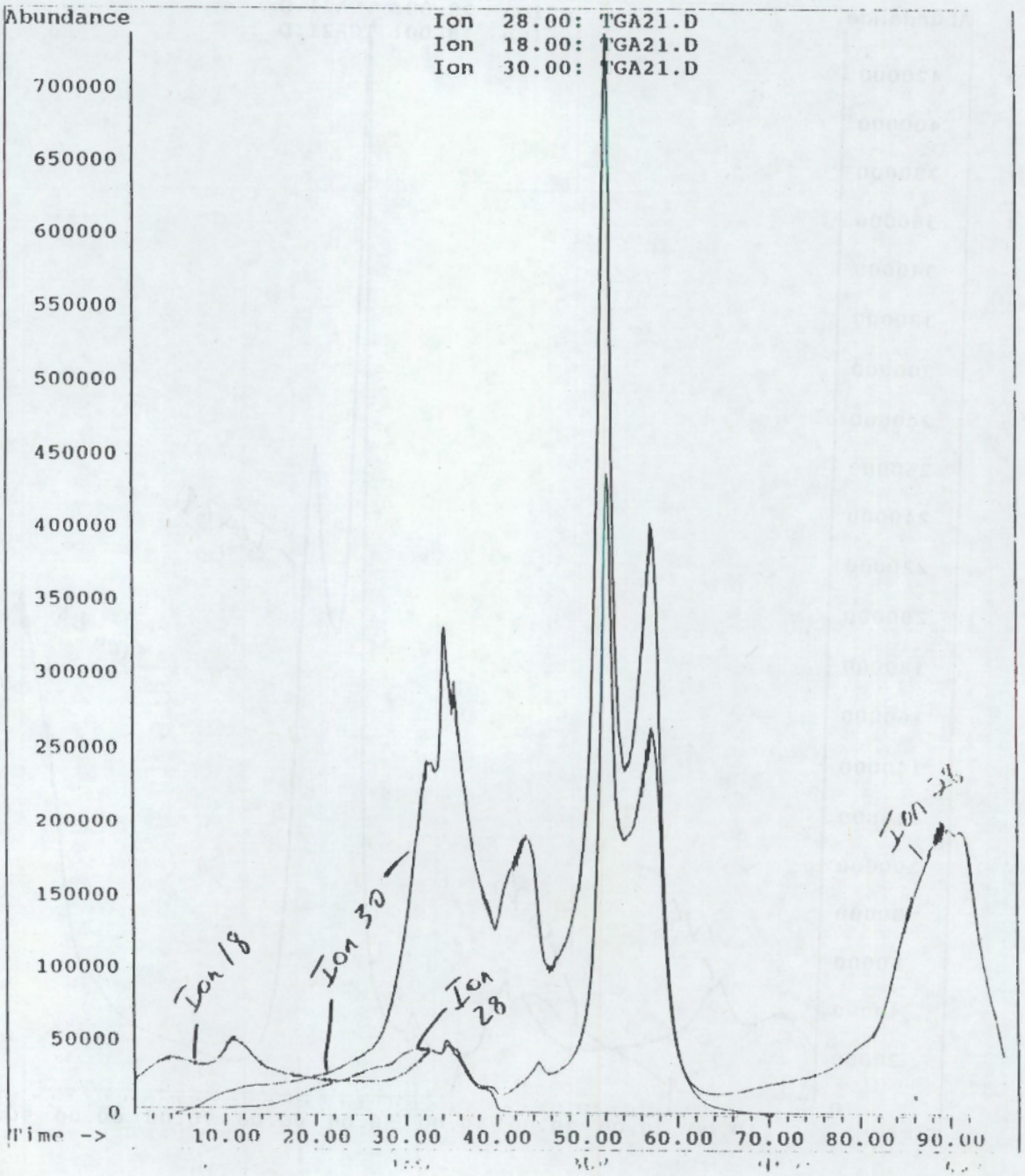

File: G:\CHEMPC\DATA\TGA21.D
Operator: RTH
Date Acquired: 6 Sep 91 7:53 am
Method File: RTHTGA.M
Sample Name: FECN 21 no additional NO3 or NO@
Misc Info: Temperature Programmed 5 C/minute 50-500 C
ALS vial: 1

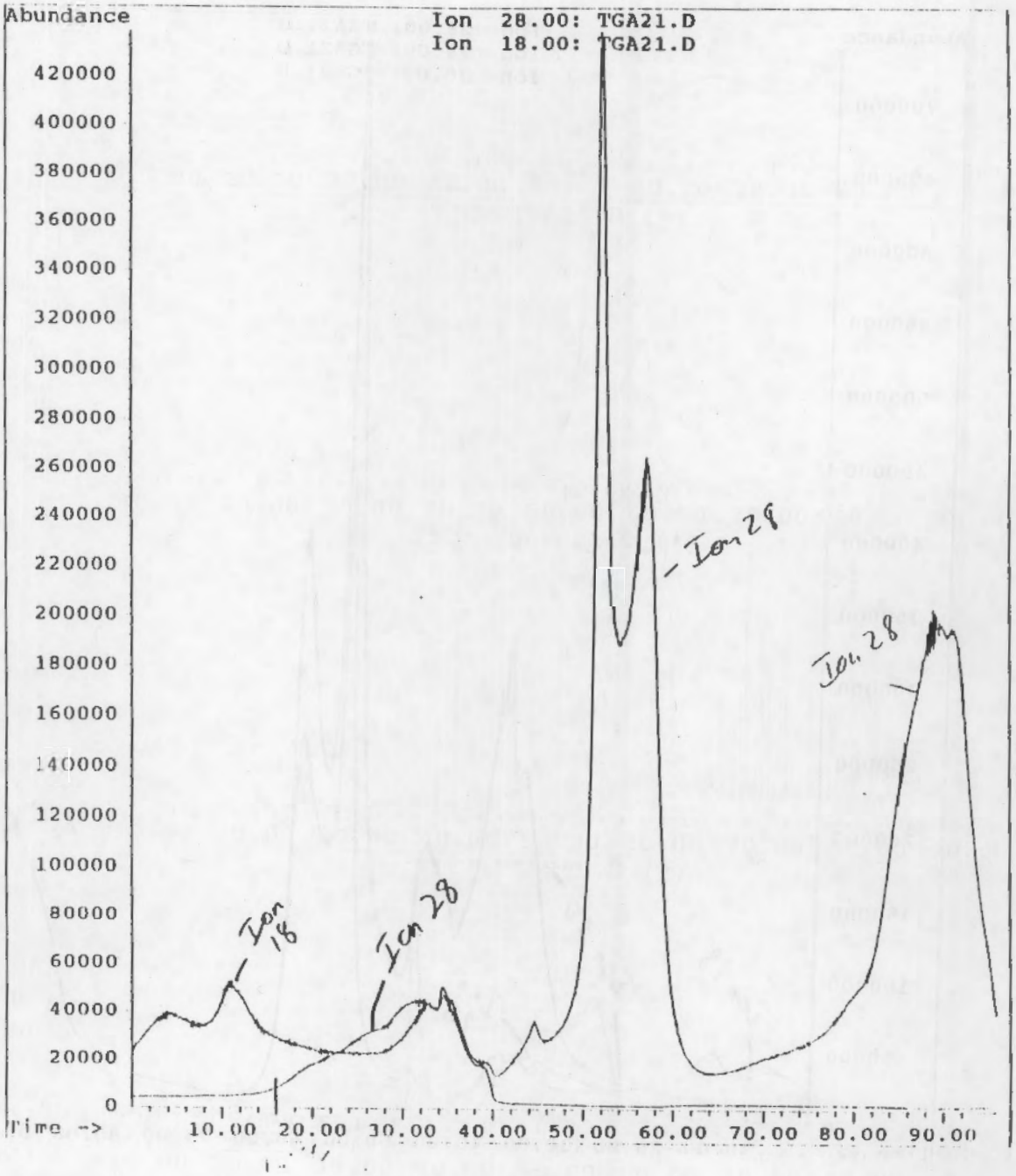

File: G:\CHEMPC\DATA\TGA21.D
Operator: RTH
Date Acquired: 6 Sep 91 7:53 am
Method File: RTHTGA.M
Sample Name: FECN 21 no additional NO3 or NO@
Misc Info: Temperature Programmed 5 C/minute 50-500 C
ALS vial: 1

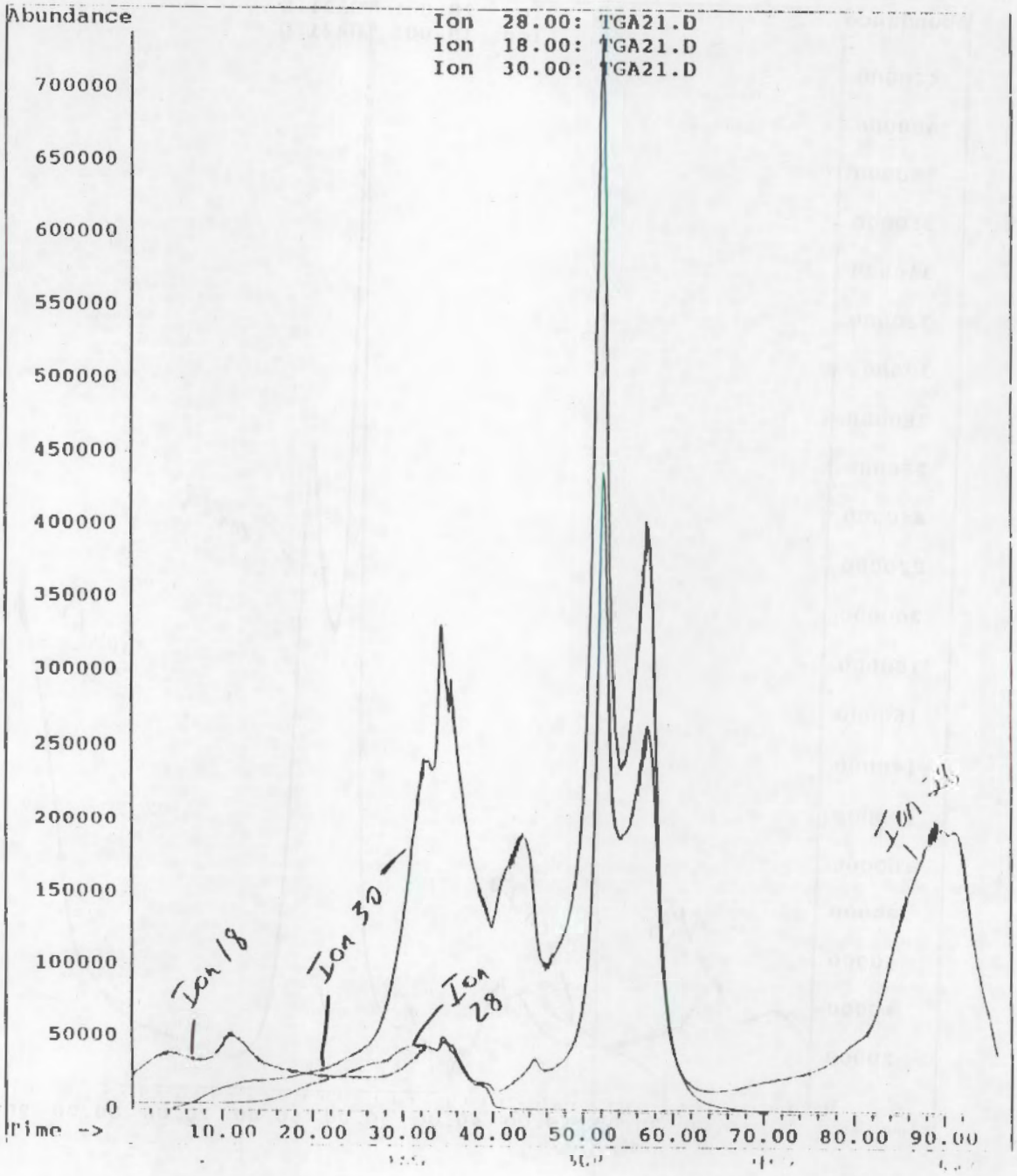

File: G:\CHEMPC\DATA\TGA21.D
Operator: RTH
Date Acquired: 6 Sep 91 7:53 am
Method File: RTHTGA.M
Sample Name: FECN 21 no additional NO3 or NO@
Misc Info: Temperature Programmed 5 C/minute 50-500 C
ALS vial: 1

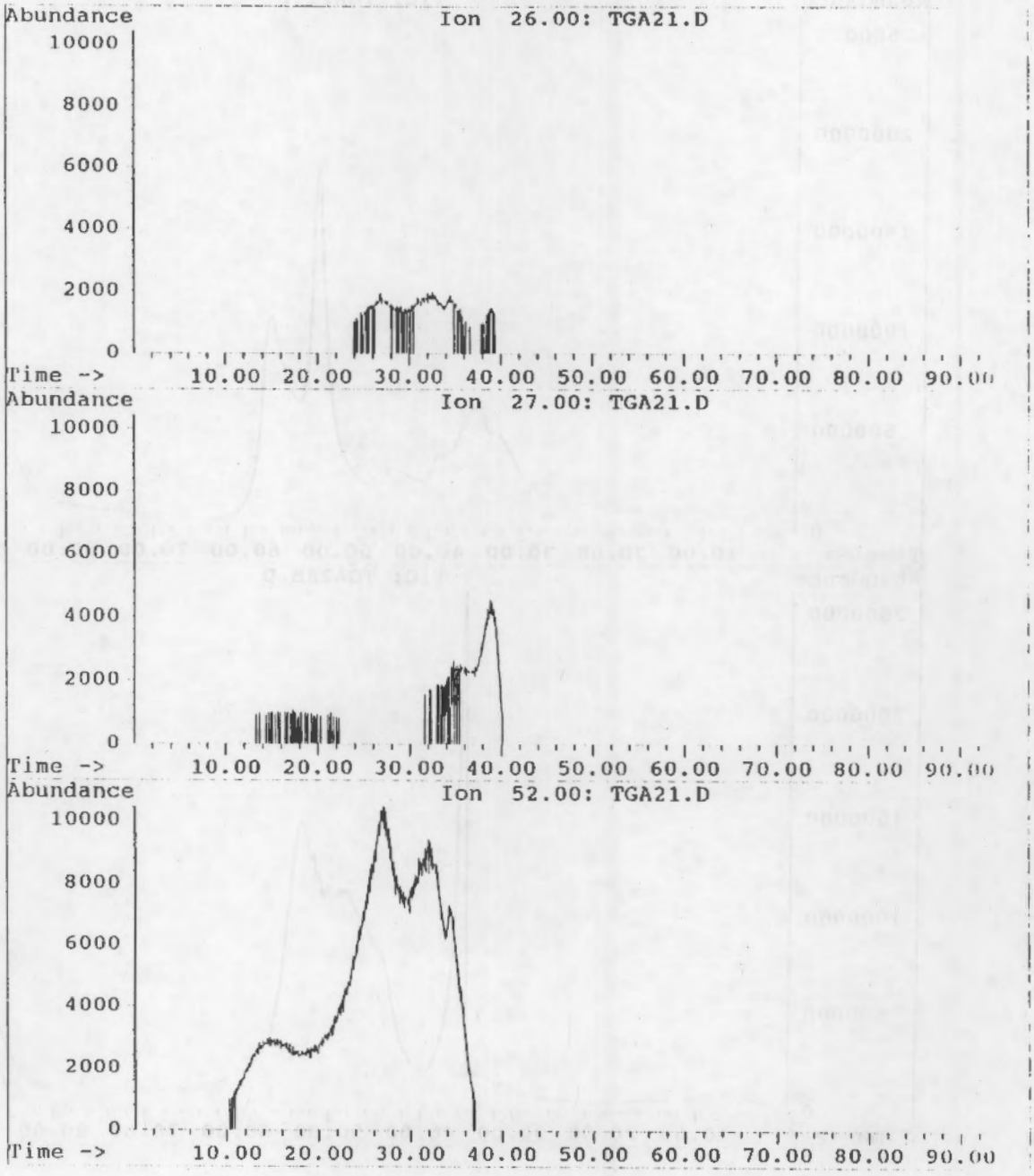

File: G:\CHEMPC\DATA\TGA28B.D
Operator: RTH
Date Acquired: 4 Sep 91 4:00 pm
Method File: RTHTGA.M
Sample Name: FECN 28b and 50% NO3/NO2 mix
Misc Info: Temperature Programmed 5 C/minute 50-500 C
ALS vial: 1

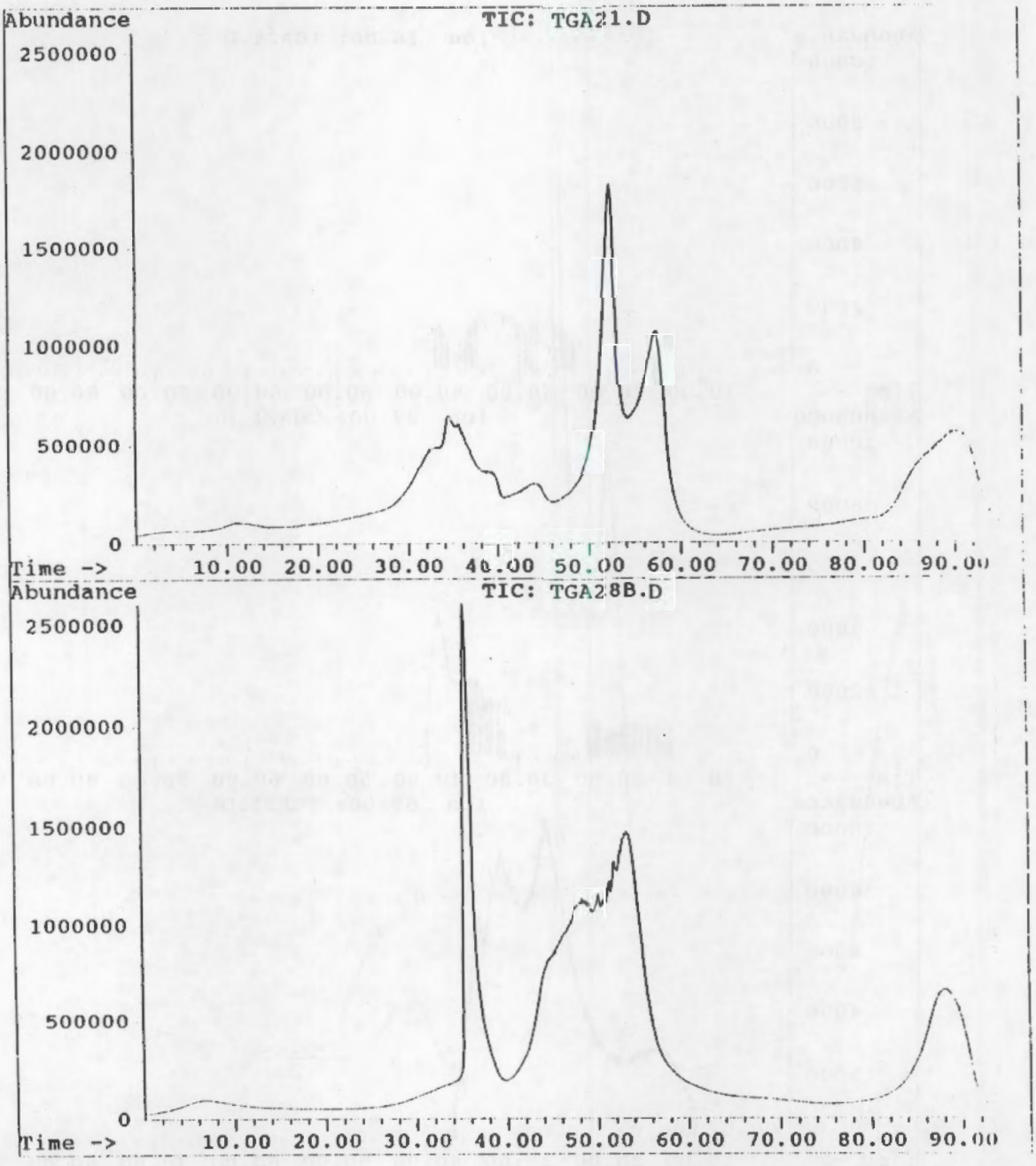

File: G:\CHEMPC\DATA\TGA28B.D
Operator: RTH
Date Acquired: 4 Sep 91 4:00 pm
Method File: RTHTGA.M
Sample Name: FECN 28b and 50% NO3/NO2 mix
Misc Info: Temperature Programmed 5 C/minute 50-500 C
ALS vial: 1

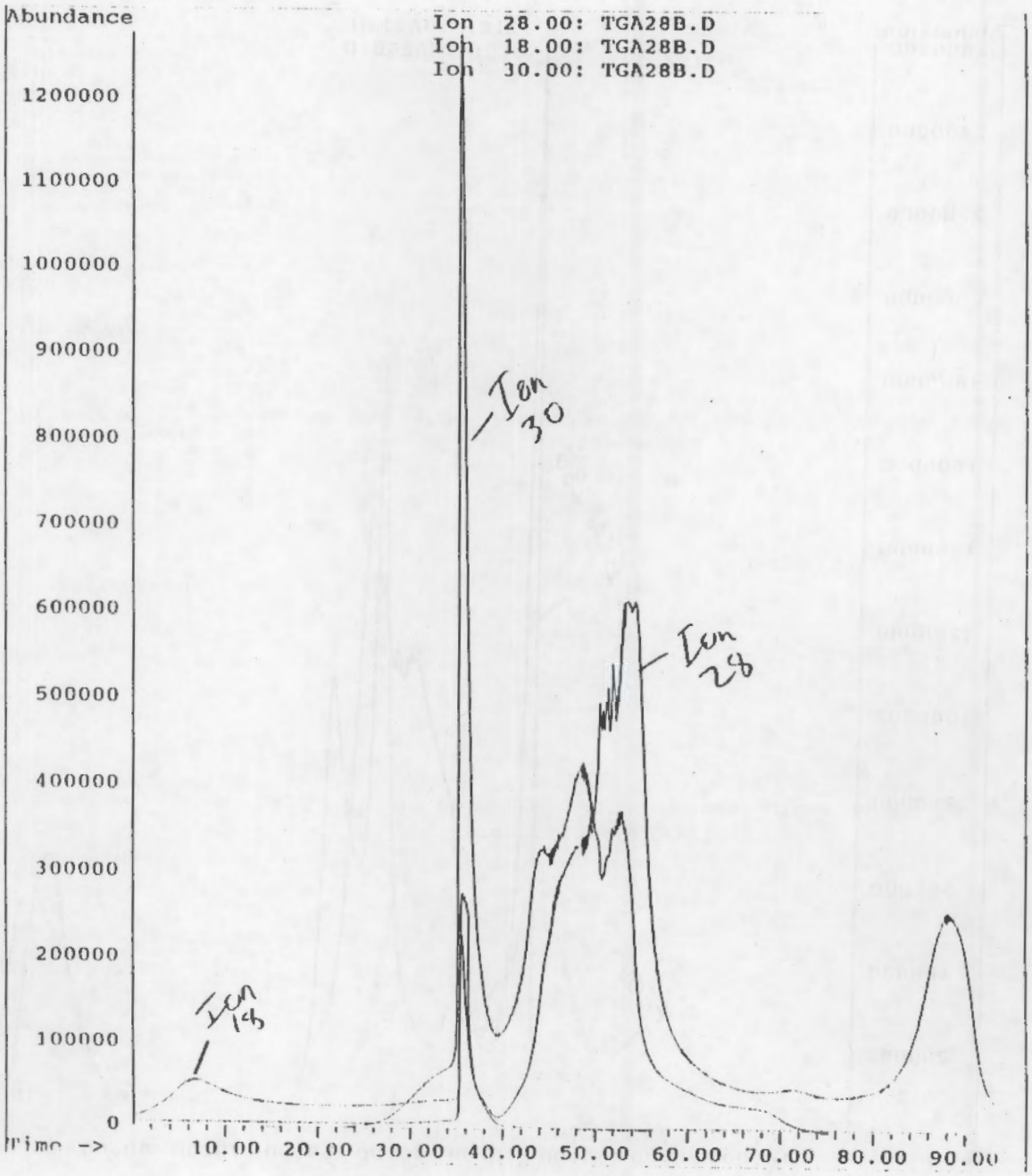

File: G:\CHEMPC\DATA\TGA28B.D
Operator: RTH
Date Acquired: 4 Sep 91 4:00 pm
Method File: RTHTGA.M
Sample Name: FECN 28b and 50% NO3/NO2 mix
Misc Info: Temperature Programmed 5 C/minute 50-500 C
ALS vial: 1

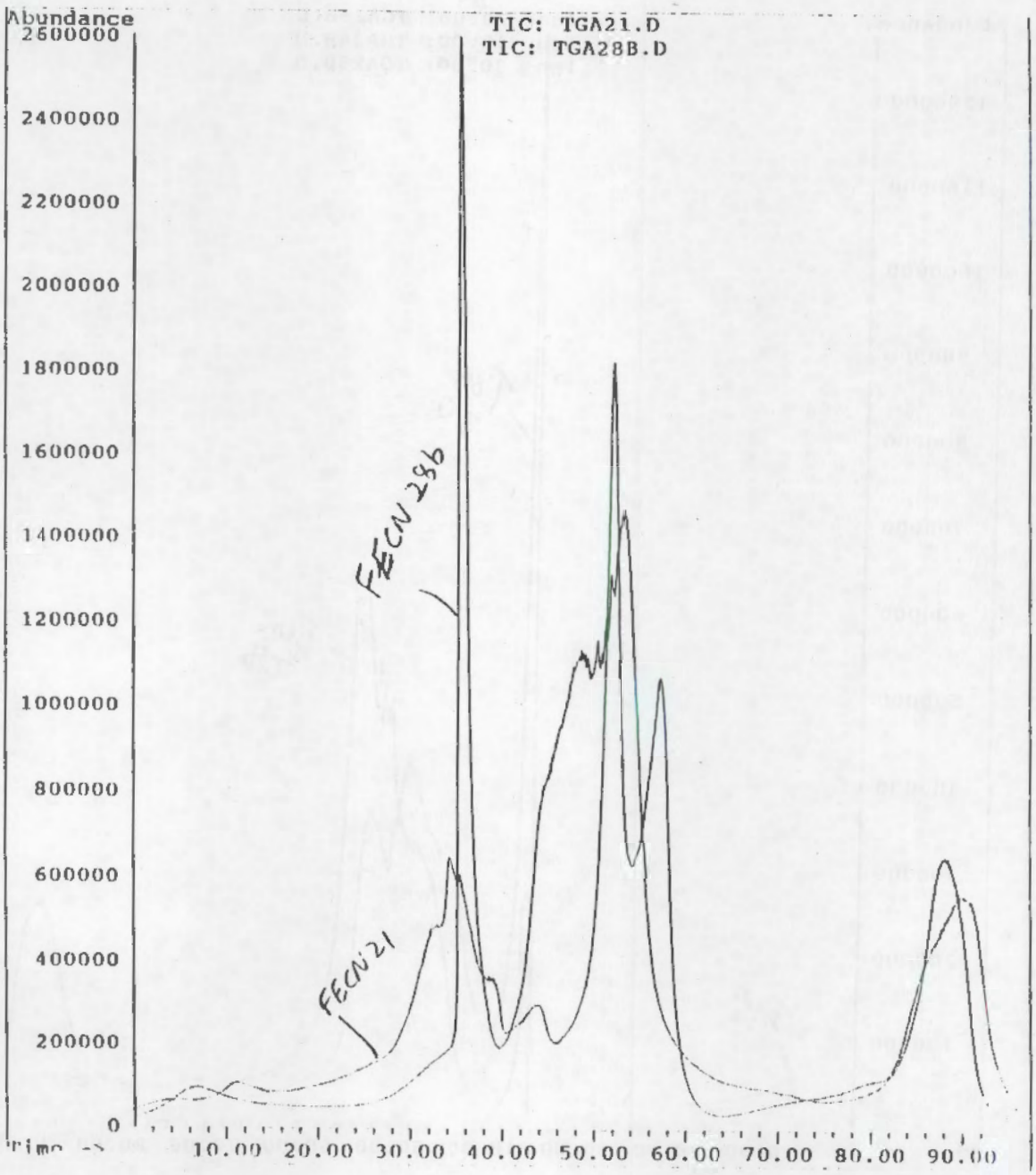

File: G:\CHEMPC\DATA\TGA21.D
Operator: RTH
Date Acquired: 6 Sep 91 7:53 am
Method File: RTHTGA.M
Sample Name: FECN 21 no additional NO3 or NO@
Misc Info: Temperature Programmed 5 C/minute 50-500 C
ALS vial: 1

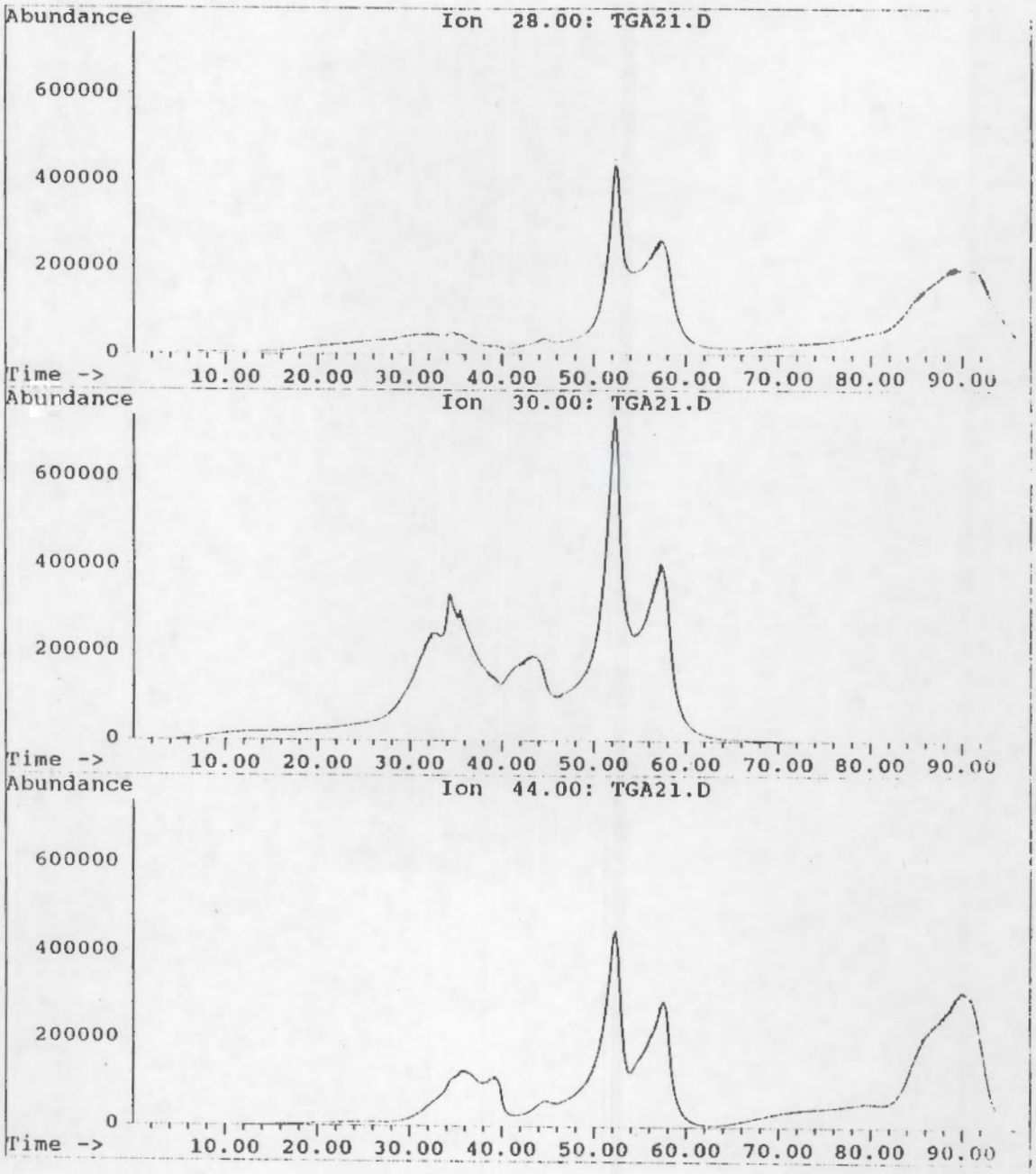

Appendix E

Evaluation of Window C Core

EVALUATION OF WINDOW C CORE

Presented to

Tank Science Panel

By

D. A. Reynolds

Westinghouse Hanford Company

March 26, 1992

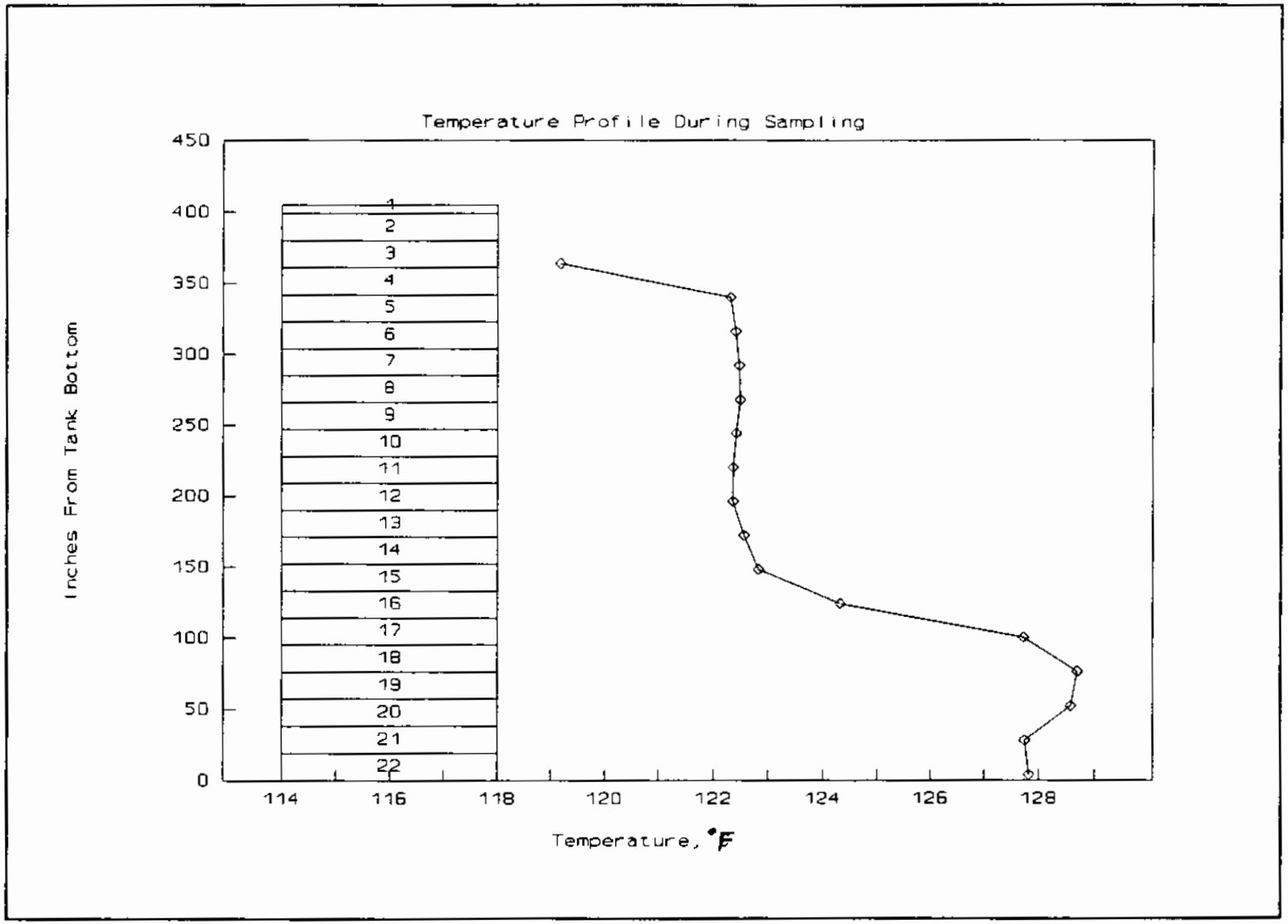
Temperature Profile During Sampling
Inches From Tank Bottom
450
400
350
300
250
200
150
100
50
0
1
2
3
4
5
6
7
8
9
10
11
12
13
14
15
16
17
18
19
20
21
22
114
116
118
120
122
124
126
128
Temperature, °F

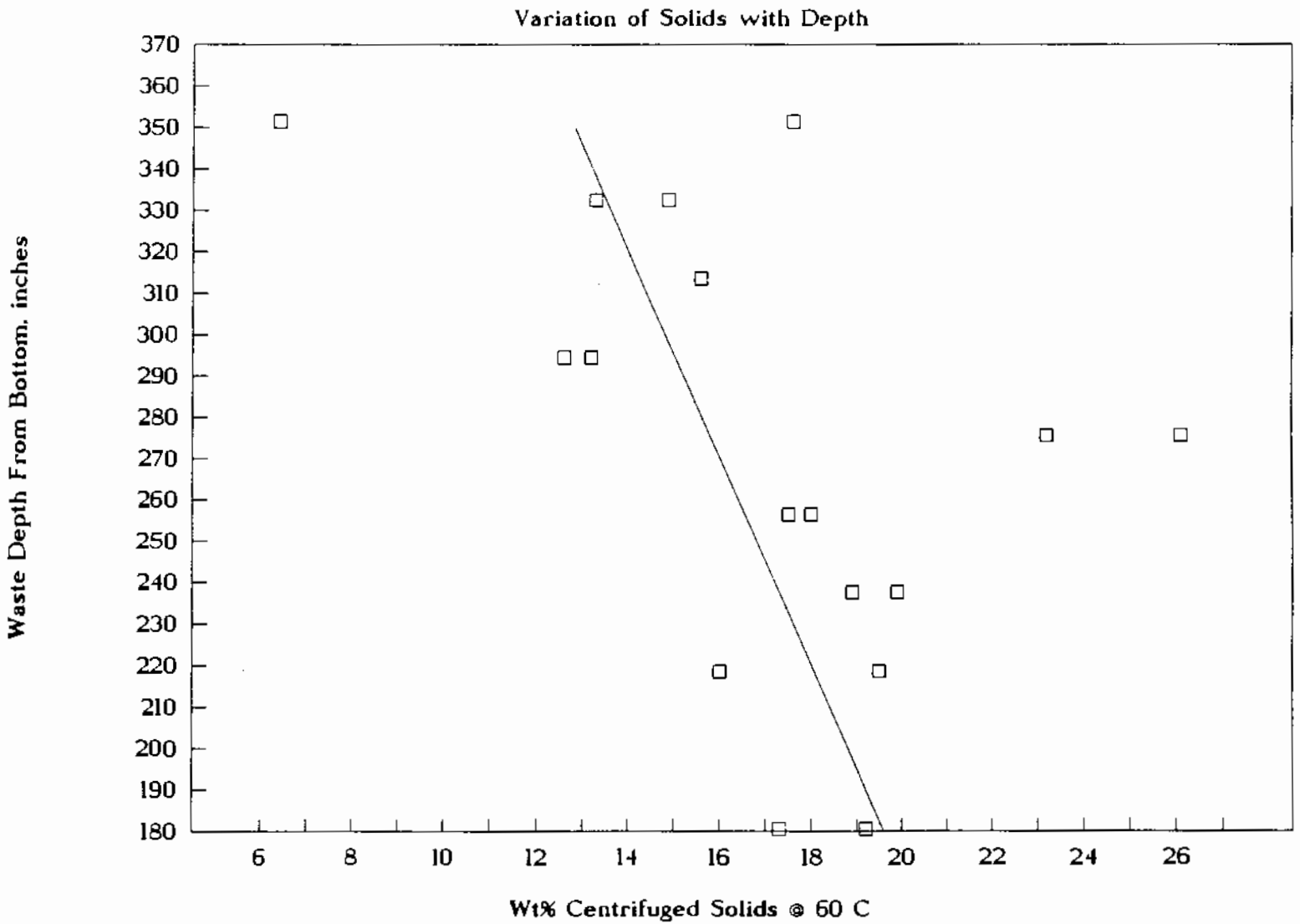
Variation of Solids with Depth
Waste Depth From Bottom, inches
370
360
350
340
330
320
310
300
290
280
270
260
250
240
230
220
210
200
190
180
6
8
10
12
14
16
18
20
22
24
26
Wt% Centrifuged Solids @ 60 C

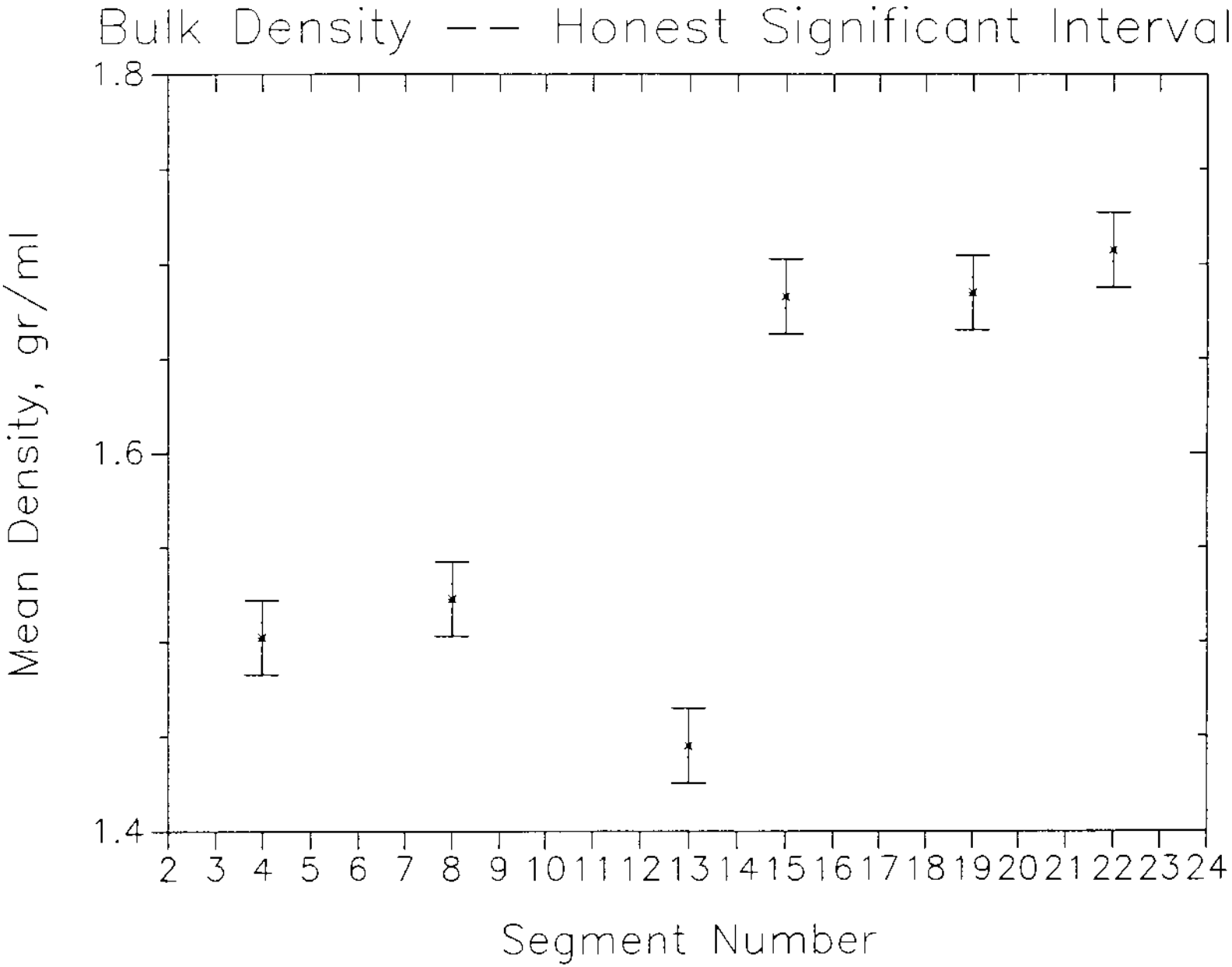
Bulk Density -- Honest Significant Interval
Mean Density, gr/ml
1.8
1.6
1.4
2 3 4 5 6 7 8 9 10 11 12 13 14 15 16 17 18 19 20 21 22 23 24
Segment Number

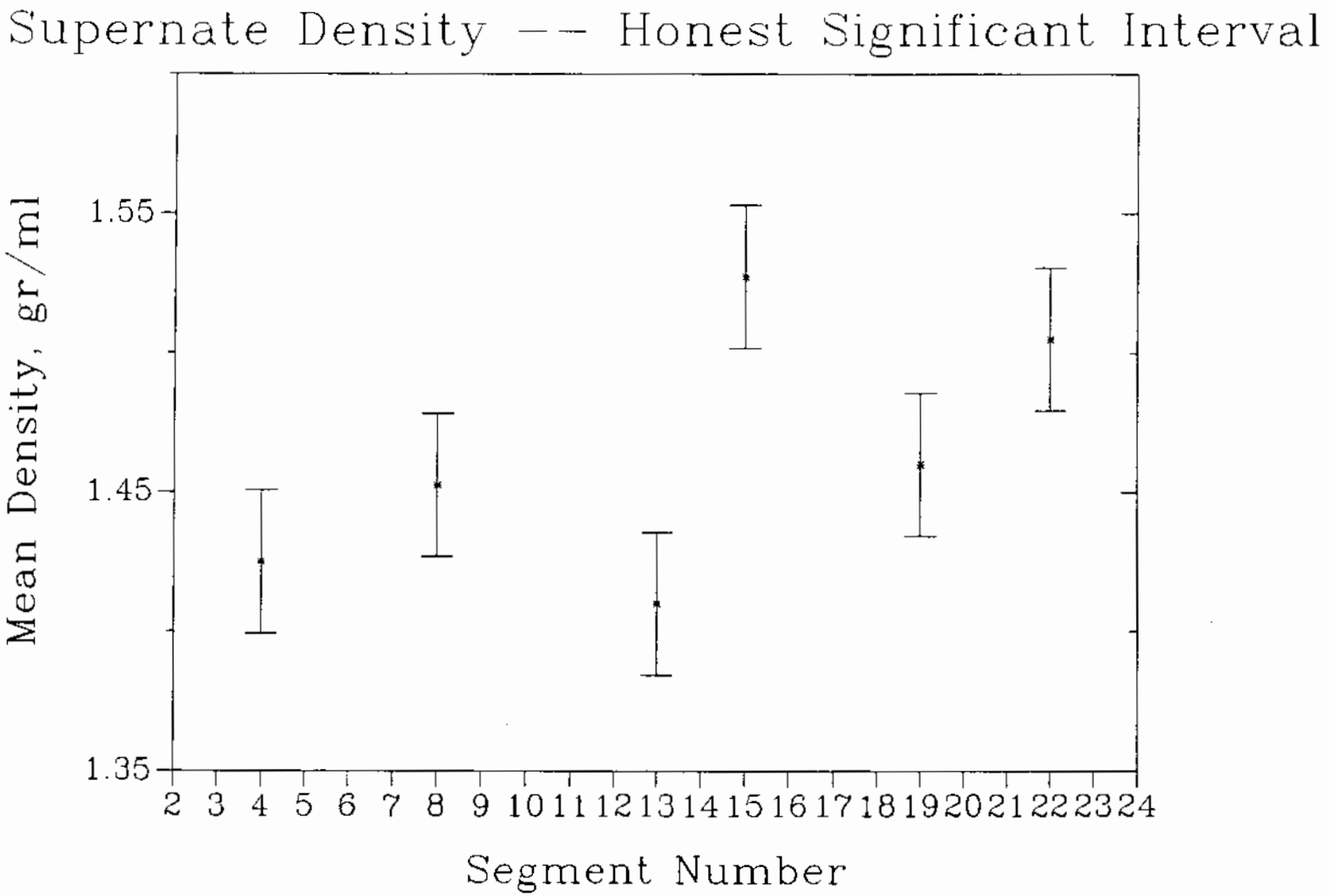
Supernate Density -- Honest Significant Interval
Mean Density, gr/ml
1.55
1.45
1.35
2 3 4 5 6 7 8 9 10 11 12 13 14 15 16 17 18 19 20 21 22 23 24
Segment Number

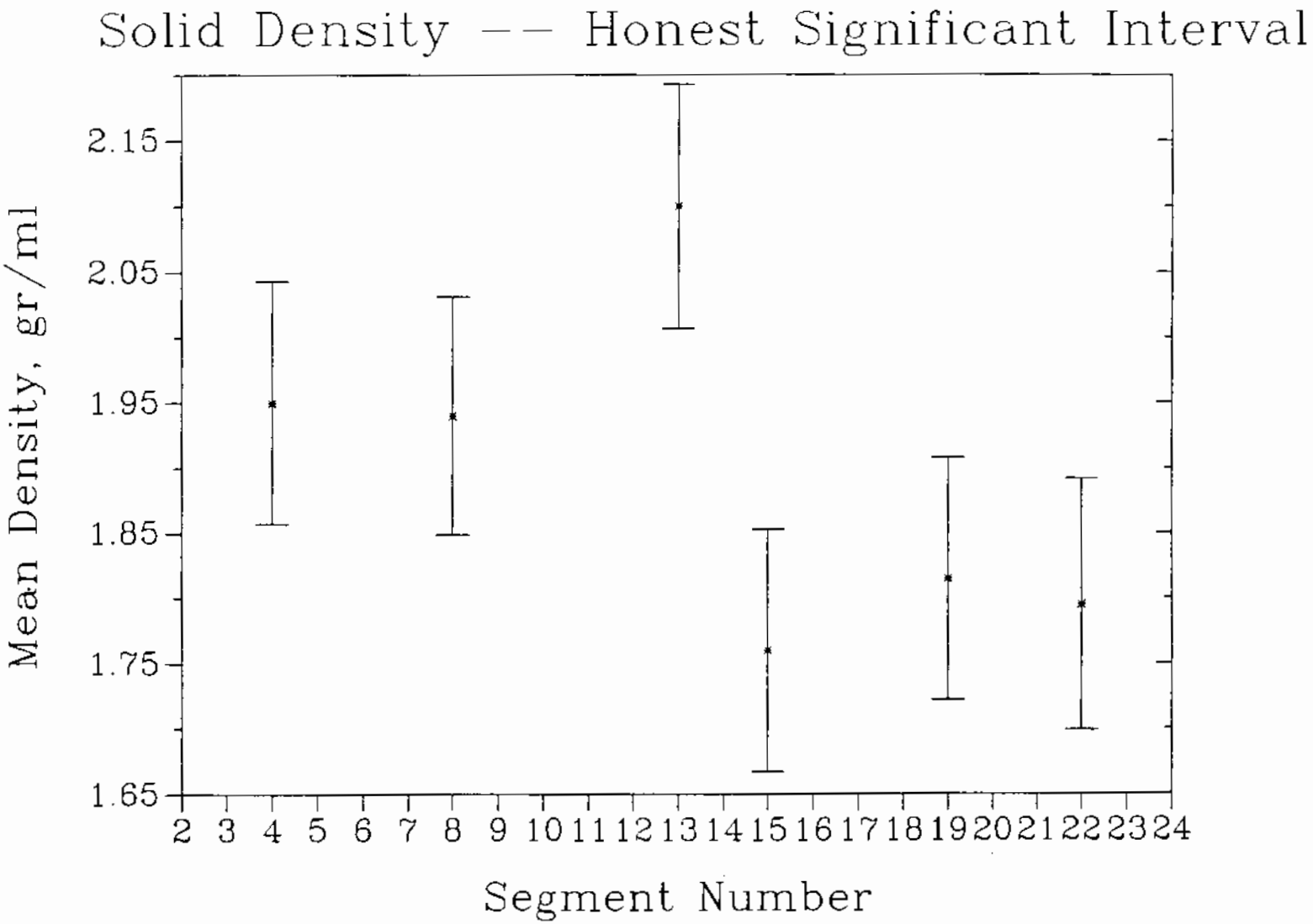
Solid Density -- Honest Significant Interval
Mean Density, gr/ml
2.15
2.05
1.95
1.85
1.75
1.65
2 3 4 5 6 7 8 9 10 11 12 13 14 15 16 17 18 19 20 21 22 23 24
Segment Number

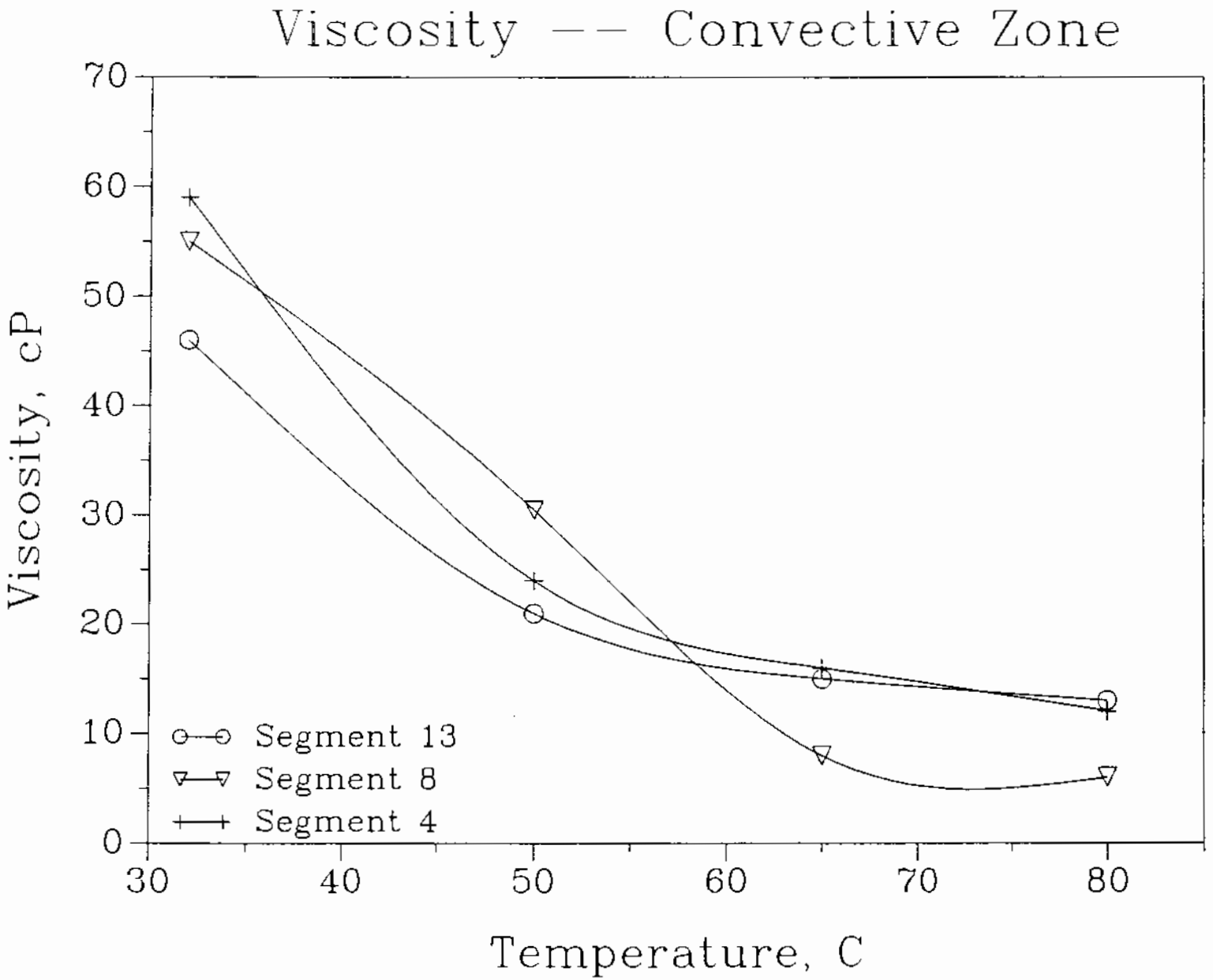
Viscosity -- Convective Zone
Viscosity, cP
Temperature, C
Segment 13
Segment 8
Segment 4
0
10
20
30
40
50
60
70
30
40
50
60
70
80

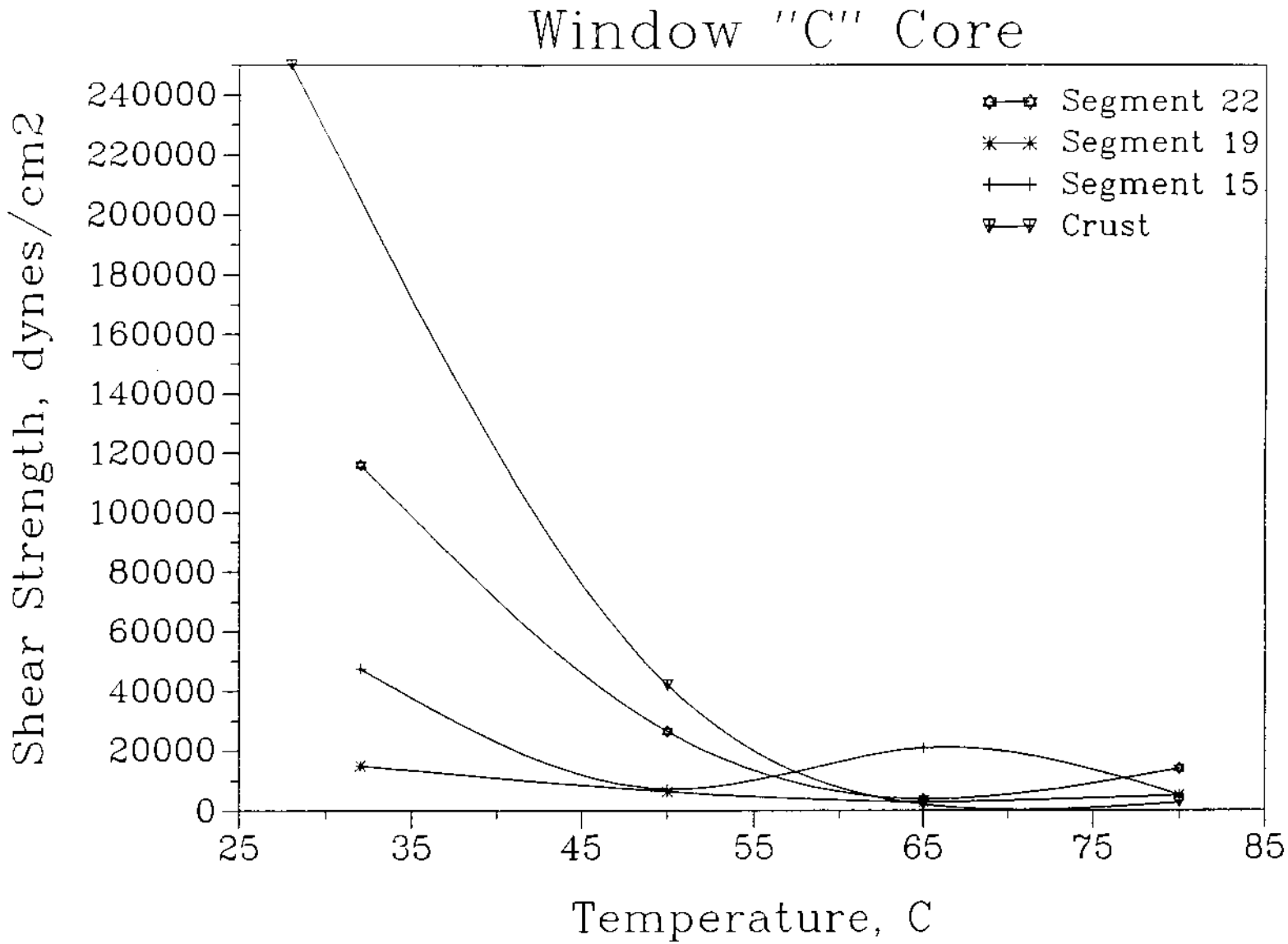
Window "C" Core
Shear Strength, dynes/cm2
240000
220000
200000
180000
160000
140000
120000
100000
80000
60000
40000
20000
0
25
35
45
55
65
75
85
Temperature, C
Segment 22
Segment 19
Segment 15
Crust

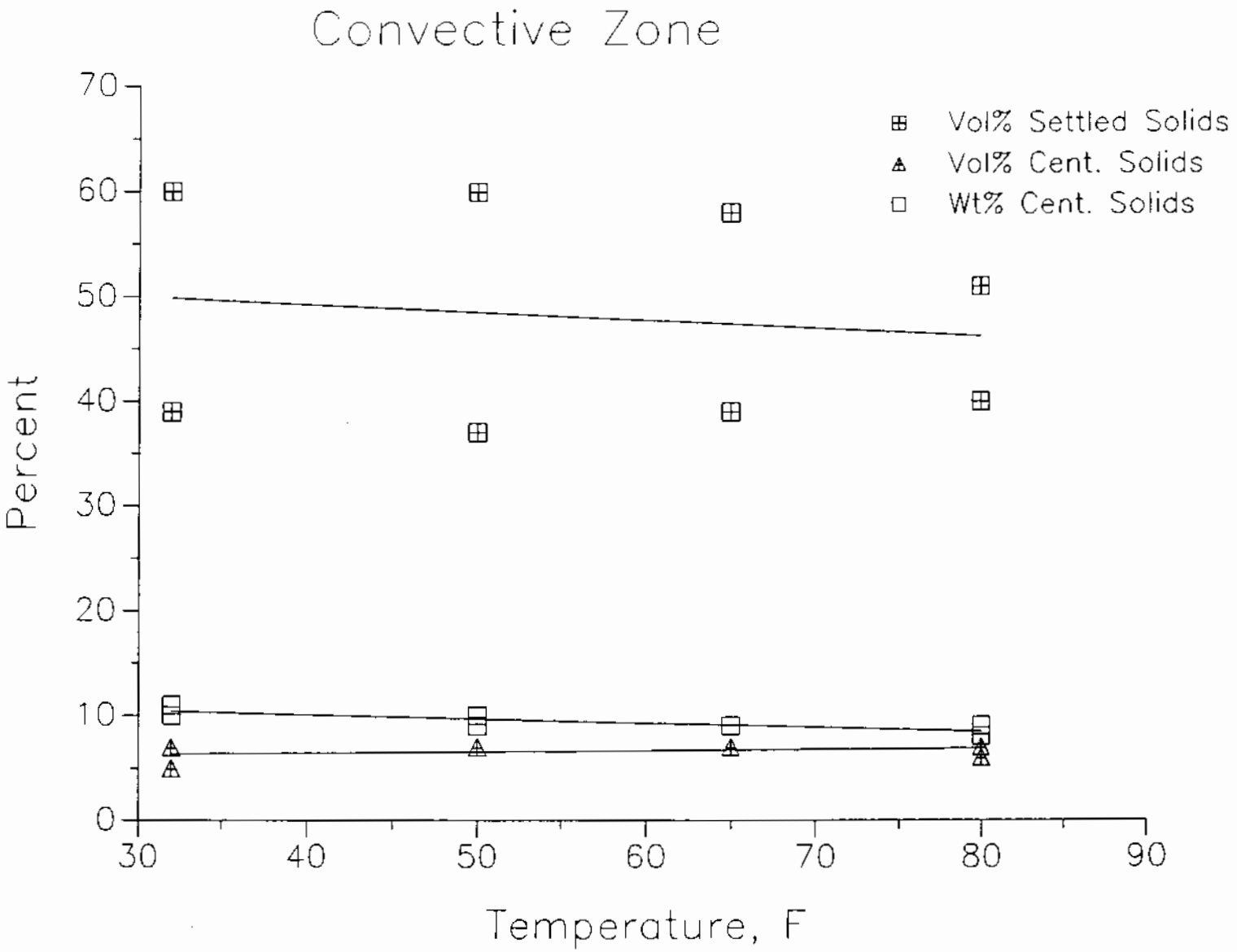
Convective Zone
Vol% Settled Solids
Vol% Cent. Solids
Wt% Cent. Solids
Percent
70
60
50
40
30
20
10
0
30
40
50
60
70
80
90
Temperature, F

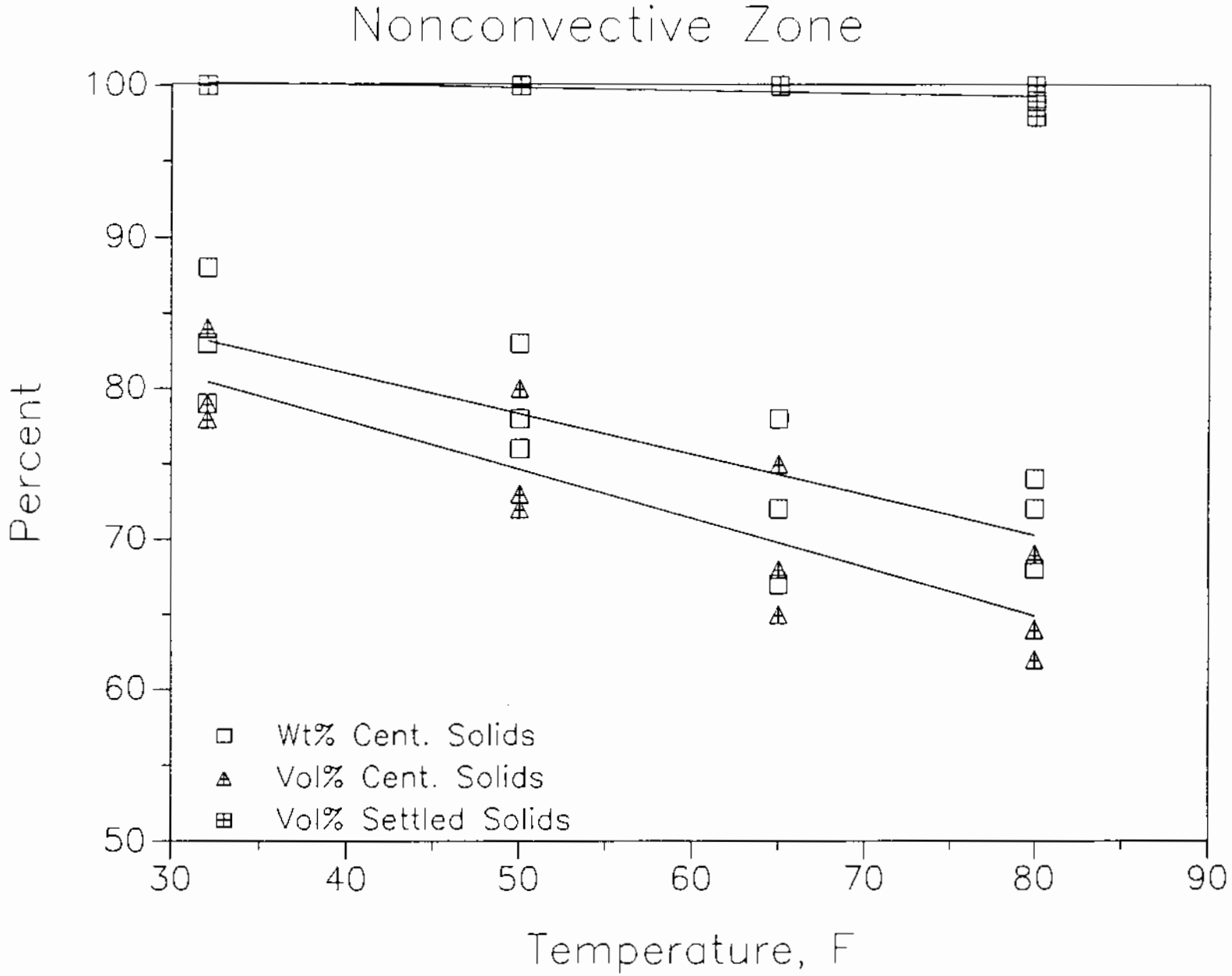
Nonconvective Zone
100
90
80
70
60
50
Percent
30
40
50
60
70
80
90
Temperature, F
Wt% Cent. Solids
Vol% Cent. Solids
Vol% Settled Solids

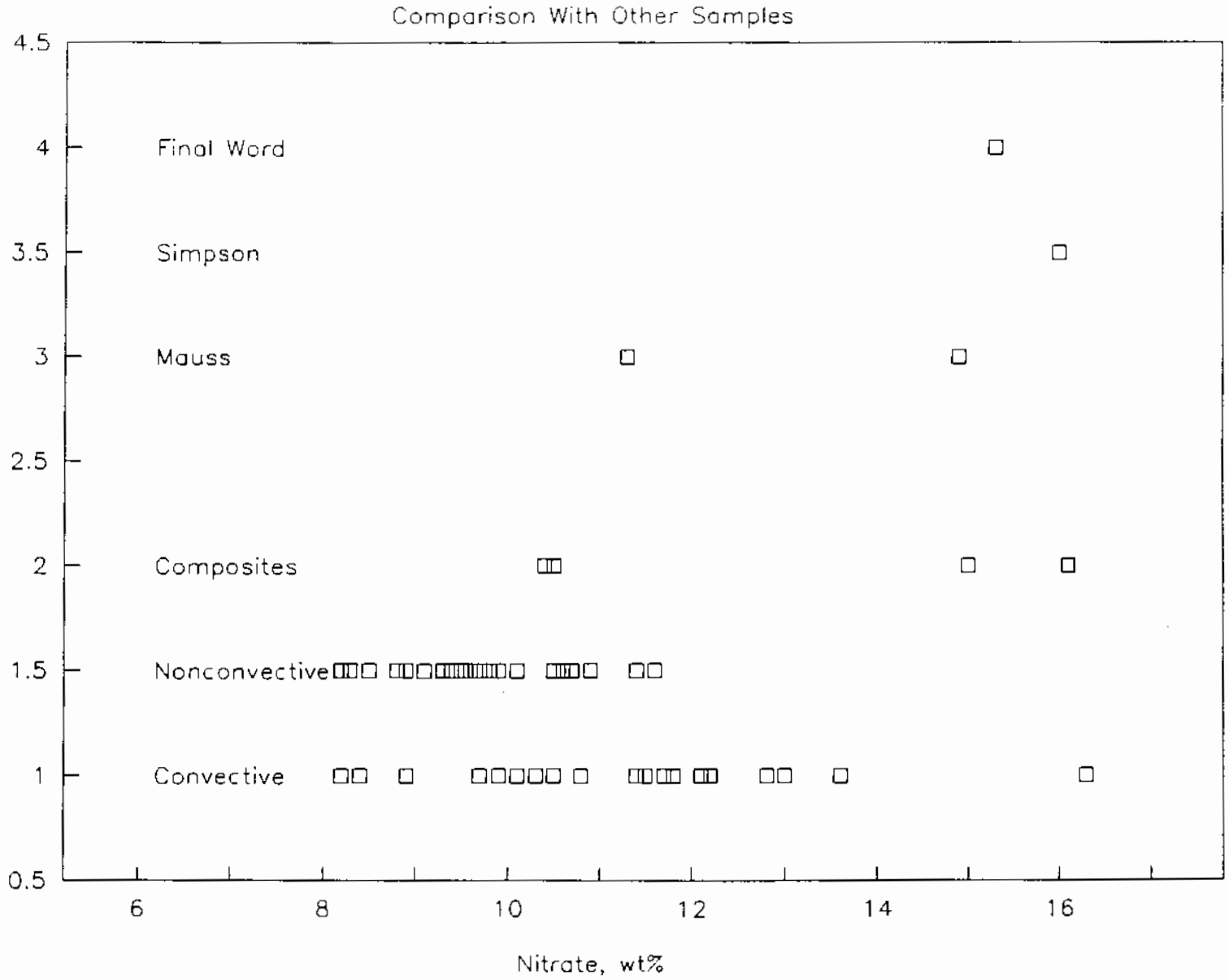
Comparison With Other Samples
4.5
4
3.5
3
2.5
2
1.5
1
0.5
Final Word
Simpson
Mauss
Composites
Nonconvective
Convective
6
8
10
12
14
16
Nitrate, wt%

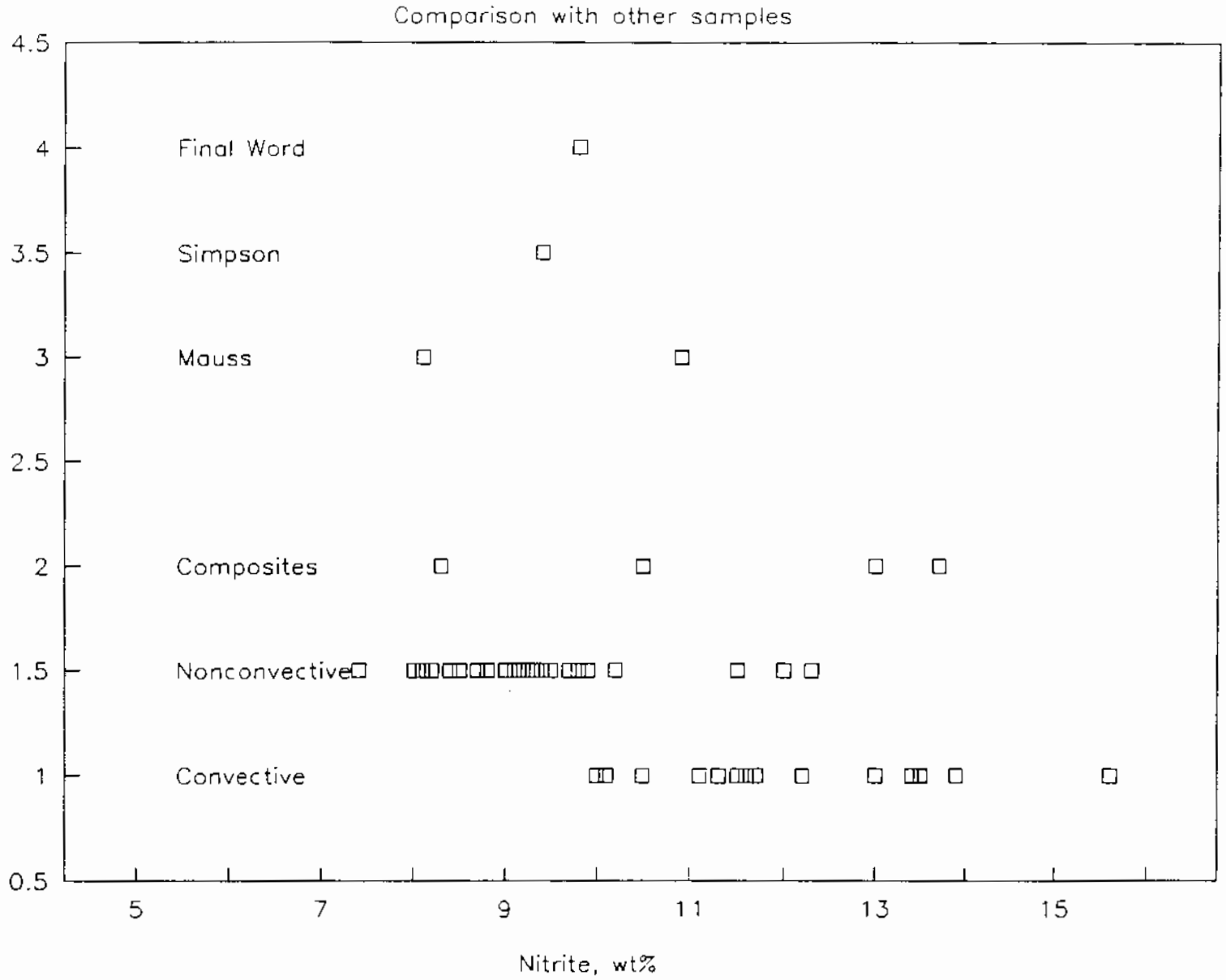
Comparison with other samples
4.5
4
3.5
3
2.5
2
1.5
1
0.5
Final Word
Simpson
Mauss
Composites
Nonconvective
Convective
5
7
9
11
13
15
Nitrite, wt%

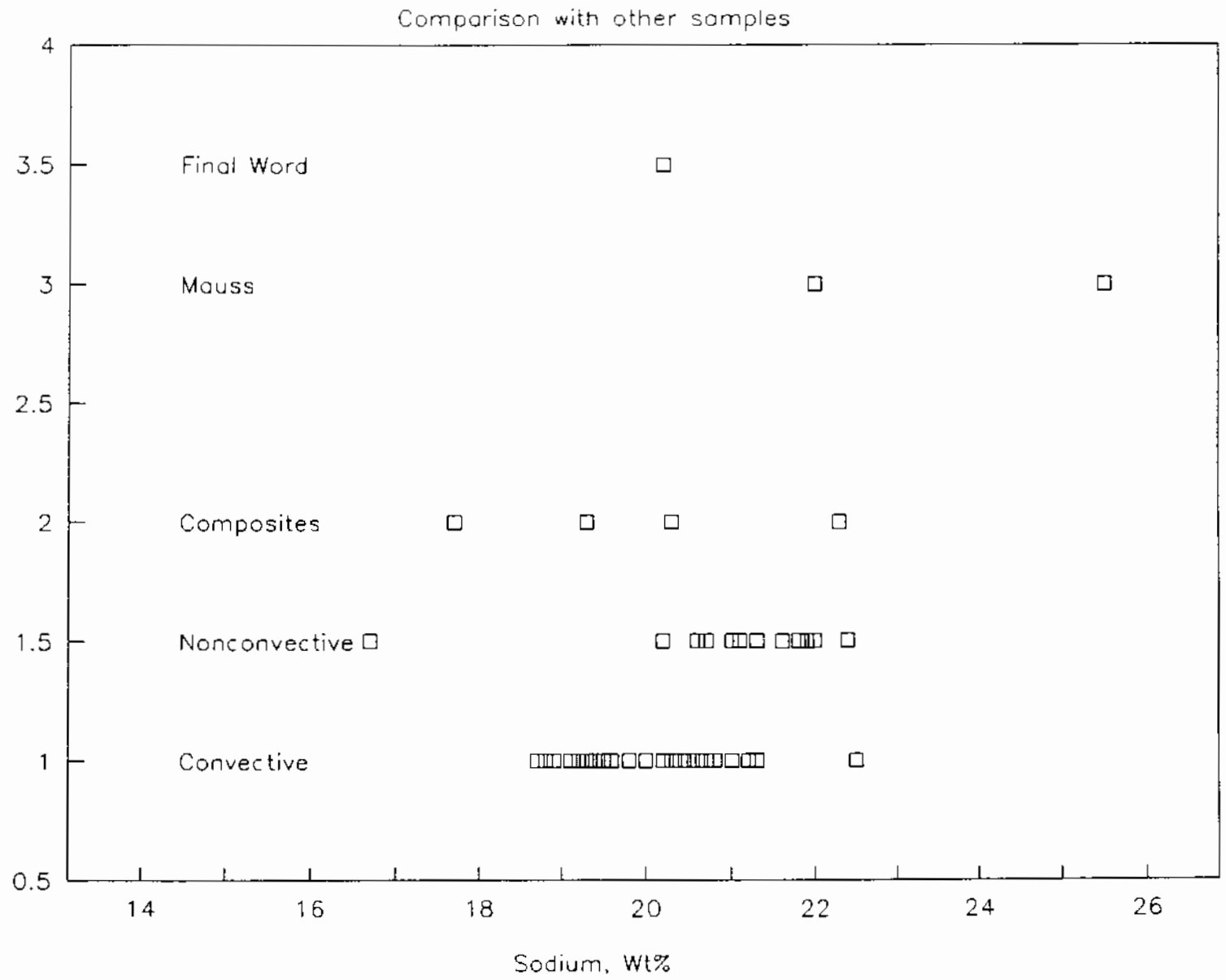
Comparison with other samples
4
3.5
3
2.5
2
1.5
1
0.5
Final Word
Mauss
Composites
Nonconvective
Convective
14
16
18
20
22
24
26
Sodium, Wt%

Table 2-1. Summary of Analyses of Core Sample Facies Samples.
[All values in weight percent except DSC total exotherms (cal/g) and ^{137}Cs ($\mu Ci/g$).] (2 sheets)

Analysis	Segment												
	1[a]	2[b]	3[a]	4	5	6	7	8	9	10	11	13	14 Top
%H2O grav	60.0	57.8	--	34.3	35.0	--	40.3	32.6	36.5	36.0	36.5	32.9	--
%H2O TGA	--	--	--	45.8	46.3	--	41.9	38.6	43.5	43.4	40.5	26.8	36.1
DSC-tot exo	--	--	--	-65	-75	--	-77	-86	-76	-80	-77	-130	-86
TOC - PNL	--	--	--	--	--	--	--	--	--	--	--	--	--
TOC - wd	0.81	0.69	--	1.20	1.27	1.22	1.06	1.22	1.33	1.26	1.31	1.26	1.36
NO_3^- - wd	7.38	8.01	--	12.8	12.0	13.3	10.1	11.9	10.7	9.0	8.6	9.7	10.6
NO_2^- - wd	7.40	6.63	--	13.8	12.4	13.9	10.6	12.2	11.0	10.3	10.7	11.3	10.5
^{137}Cs wd	327	315	10	461	505	524	546	391	508	532	490	412	387
^{137}CS ad	--	--	--	514	319	345	463	367	406	441	471	396	425
Na - ad	--	--	--	20.7	20.1	20.9	19.8	20.3	19.5	19.9	19.7	20.2	21.3
Al - ad	--	--	--	2.7	3.4	3.4	3.8	2.3	3.3	3.6	3.8	3.6	3.2
Fe - ad	--	--	--	0.004	0.005	--	0.005	0.011	0.007	--	0.006	0.008	--
Cr - ad	--	--	--	0.041	0.052	0.049	0.050	0.084	0.088	0.089	0.079	0.079	0.271
Ca - ad	--	--	--	0.014	0.007	0.008	0.009	0.007	0.017	0.009	0.010	0.008	0.034
Other[c]	--	--	--	6.9	6.9	6.9	6.9	6.9	6.9	6.9	6.9	6.9	6.9
Mass Balance =				98.1	97.7	--	99.4	92.7	96.0	93.8	94.8	92.8	96.9
Ion Balance =				0.99	0.98	0.96	1.03	1.04	1.01	1.07	1.04	1.04	1.12

Table 2-1. Summary of Analyses of Core Sample Facies Samples. [All values in weight percent except DSC total exotherms (cal/g) and ^{137}Cs (μCi/g).] (2 sheets)

Analysis	Segment												
	14 Bot	15	16	16R	17	18	19	20	21	22	20A	21A	22A
%H2O grav	39.0	27.0	30.7	26.7	31.8	33.6	31.6	35.0	31.9	32.4	23.2	18.1	19.9
%H2O TGA	38.3	38.5	36.5	35.1	36.1	34.4	33.8	34.4	30.7	31.2	34.8	31.8	31.2
DSC - tot exo	-104	-99	-89	-93	-69	-125	-83	-53	-84	-59	-68	-57	-80
TOC - PNL	1.36	1.58	1.49	1.62	1.25	1.50	1.53	1.32	1.46	1.49	1.69	1.62	1.65
TOC - wd	1.70	1.93	1.92	1.92	2.02	2.06	1.88	2.02	1.91	1.91	1.85	1.87	1.87
NO_3^- - wd	9.3	11.2	10.5	11.1	10.8	9.5	10.2	9.2	10.0	10.6	8.6	8.8	8.6
NO_2^- - wd	9.1	8.4	9.9	9.3	9.4	8.9	10.4	9.0	8.2	8.8	8.8	10.6	9.3
^{137}Cs - wd	329	364	364	357	375	386	374	384	375	376	322	351	318
^{137}Cs - ad	402	374	426	375	319	366	353	387	351	310	387	375	406
Na - ad	20.7	18.9	20.2	21.8	21.3	21.9	21.6	21.1	22.4	21.8	20.2	20.6	20.9
Al - ad	3.7	2.9	3.6	3.4	3.3	3.7	3.5	3.7	3.6	3.8	3.8	3.7	3.8
Fe - ad	0.035	0.051	0.0389	0.042	0.043	0.042	0.046	0.048	0.047	0.062	0.090	0.119	0.070
Cr - ad	0.547	0.565	0.696	0.736	0.721	0.704	0.761	0.736	0.729	0.790	0.649	0.649	0.706
Ca - ad	0.063	0.026	0.021	0.025	0.024	0.031	0.030	0.042	0.036	0.055	0.053	0.056	0.050
Other [c]	11.0	11.0	11.0	11.0	11.0	11.0	11.0	11.0	11.0	11.0	11.0	11.0	11.0
Mass Balance =	98.9	85.2	92.6	89.8	94.3	95.8	94.8	90.3	88.2	89.7	76.8	73.9	86.0
Ion Balance =	1.12	1.03	1.04	1.14	1.12	1.17	1.11	1.21	1.30	1.22	1.18	1.15	1.20

(a) sample compromised by water dilution
(b) sample compromised by water dilution; solid fraction of sample designated Composite #5
(c) "Other" represents estimated contribution from all other sources -- see Table 2-2.

ad = acid digest preparation
DSC = differential scanning calorimetry
grav = gravimetric method
PNL = Pacific Northwest Laboratory
TGA = thermogravimetric analysis
TOC = total organic carbon, WHC thermal combustion method
tot exo = total integrated exotherms in cal/g
wd = water digest preparation

Table 2-2. Estimated Weight Percents of Components Not Analyzed ("Other" in Table 2-1).

Component	Convective Layer	Non-Convective Layer
Cl^-	0.9	0.8
PO_4^{3-}	0.5	0.9
SO_4^{2-}	0.1	0.7
TIC	0.5	1.1
NH_3	0.0	0.3
OH^-	2.6	2.5
K^+	0.3	0.3

TIC = total inorganic carbon

Table 2-3 shows a comparison between the segment average values and the two dip samples from 101-SY analyzed in 1986 (see Appendix H). Also shown in the table is the composition of the synthetic waste recipe used for a variety of laboratory studies over the past year. In general, these comparisons show that modeling studies and chemical studies done over the past year based on historical (1986) sample results and on synthetic waste compositions are valid, because the core sample results confirm what was already known about the composition of the waste. Of course, the core samples provided significant information that was unknown concerning waste homogeneity and physical properties, and gave a more accurate picture of the waste composition.

Compared to the 1986 values, the current nitrate values are lower and the nitrite values are higher. This could be explained by radiolytic reduction of nitrate to nitrite. The synthetic recipe is high in nitrate (relative to the core sample results), but the nitrite is on target.

The TOC values for the convective layer segments are lower than the 1986 samples, while the values for the non-convective layer are higher than the 1986 values. This could indicate a change to less soluble organic compounds as a result of chemical decomposition of the organics over the five year period. The overall average TOC content of the tank is remarkably close to the 1986 sample results. The synthetic recipe was intentionally set to a conservatively high level of TOC.

Sodium and aluminum are both slightly lower in the core samples than the 1986 samples. This may not be a statistically significant difference. The synthetic values are on target. Calcium values are comparable, but the chromium is much higher in the core samples. There was no calcium or chromium in the synthetic waste.

Table 2-3. Comparison of Segment Averages with Historical Samples (All Values in Weight Percent).

	Convective layer	"Middle slurry"*	Non-convective layer	"Bottom slurry"*	Synthetic recipe
NO_3^-	10.3	14.9	10.2	11.3	15.3
NO_2^-	11.7	10.9	9.1	8.1	9.8
TOC	1.25	1.5	1.9	1.5	2.4
Na	20.1	25.5	21.2	22.0	20.2
Al	3.4	4.4	3.5	3.6	3.96
Ca	0.012	0.016	0.036	0.017	0.0
Cr	0.088	0.004	0.70	0.002	0.0

*See Appendix H.

2.4 COMPOSITE SAMPLES

Five composite samples representing the convective layer (composites 1 and 2), the nonconvective layer (3 and 4), and the crust (5) underwent more extensive analyses than the individual segment samples. Results of the composite sample analyses are presented in Appendix B and are discussed in detail in Section 8. Tables 8-1 and 8-2 summarize the analytical results. Some of the analyses done only on composite samples include the major anions carbonate and hydroxide, the complete list of ICP metals, and the major radionuclides.

The metal ions present in the waste occurred in the following order of abundance: Na > Al > K, Cr > Ca > Fe > Ni > Mo, Zn. All other ICP metals were present at concentrations of less than 50 ppm. The Na, K, and Al were found about equally distributed among all waste fractions (liquid, bulk sample, centrifuged solids), while the remaining metals were clearly much more concentrated in the solid phase than in the liquid phase.

The major alpha-emitting isotope was found to be ^{241}Am, which is present at activities of about 200 nCi/g of waste in the nonconvective layer, and much lower in the convective layer. The liquid fraction of the convective layer contained less than 1 nCi ^{241}Am/g of liquid, while the centrifuged solids (representing about 20% by weight of the convective layer) contained about 50 nCi/g of solids. The activity of $^{239/240}Pu$ was consistently about one-tenth the activity of ^{241}Am. Therefore, the convective layer could be considered a non-TRU waste, while the nonconvective layer is a TRU waste.

The amount of hydroxide in the waste averaged about 2.5 weight percent OH^-, corresponding to a concentration of about 2.4 M NaOH. This is

Table 3-4. Summary of Centrifuged Solid/Liquid Phase Separations at 60°C.

	Weight % liquid			Weight % solids*		
Segment	Cone #1	Cone #2	Average	Cone #1	Cone #2	Average
4	82.4	93.6	88.0	17.6	6.4	12.0
5	85.1	86.7	85.9	14.9	13.3	14.1
6	84.4	--	84.4	15.6	--	15.6
7	87.4	86.8	87.1	12.6	13.2	12.9
8	76.8	73.9	75.3	23.2	26.1	24.7
9	82.5	82.0	82.2	17.5	18.0	17.8
10	81.1	80.1	80.6	18.9	19.9	19.4
11	80.5	84.0	82.3	19.5	16.0	17.7
13	80.8	82.7	81.8	19.2	17.3	18.2
14	49.8	--	49.8	50.2	--	50.2
Average	Segments 4-13		83.1	Segments 4-13		16.9

* - Keep in mind that "centrifuged solids" contain a substantial fraction of interstitial liquid, generally more than half, by weight.

WHC-SD-WM-DTR-024 REV 0

Table 3-6. Weight Percent Centrifuged Solids and Liquids at 60°C.

Composite	Weight % liquid			Weight % solids		
	Cone #1	Cone #2	Average	Cone #1	Cone #2	Average
1	61.4	66.9	64.2	38.6	33.1	35.8
2	62.0	52.6	57.3	47.4	38.0	42.7
3	21.0	23.4	22.2	79.0	76.6	77.8
4	18.8	----*	18.8	81.2	----	81.2

* Due to limited sample amount only one cone was processed for composite number 4.

Table 6-1. Summary of Analytical Results for Window C Crust Samples. (2 sheets)

Treatment/ analysis	Auger samples by riser number					Sludge weight samples				Units
	22A Top	22A Bot	13A	11A	16A	22A	13A	11A	16A	
Direct										
$\%H_2O$, grav	20.2	20.6	29.1	34.8	23.1	(a)	(a)	(a)	(a)	wt %
$\%H_2O$, TGA	18.9	19.9	31.6	40.8	23.4	16.2	31.7	17.0	16.3	wt %
pH	13.3	12.9	--	--	--	--	--	--	--	--
TOC-PNL	1.55	1.45	1.55	0.95	--	--	--	--	--	wt %
DSC	-42	-60	-66	-28	-37	-62	-46	-44	-43	cal/g
Water digest										
TOC	2.10	1.86	1.92	1.61	1.54	--	1.82	1.84	2.31	wt %
TIC	1.67	1.18	1.00	1.58	1.05	--	0.83	2.43	2.26	wt %
NH_3/NH_4^+	<0.04	<0.04	<0.04	0.05	0.04	--	--	--	--	wt %
^{137}Cs	430	340	310	320	350	--	365	470	670	µCi/g
F^-	<0.10	<0.04	<0.04	<0.10	<0.10	--	<0.01	--	--	wt %
Cl^-	0.90	2.13	1.27	0.66	0.90	--	0.96	(b)	--	wt %
NO_3^-	14.40	17.10	14.05	12.40	16.00	--	15.30	12.80	18.60	wt %
PO_4^{3-}	0.90	0.49	0.90	1.28	0.85	--	<1.40	--	--	wt %
SO_4^{2-}	1.06	1.56	1.25	1.47	1.21	--	0.96	(b)	--	wt %
NO_2^-	13.90	14.75	10.43	8.05	12.10	--	11.70	15.20	15.00	wt %
Acid digest										
^{137}Cs	470	400	350	--	370	--	--	--	--	µCi/g
^{237}Np	<0.1	<0.12	<0.11	<1.1	--	--	<0.7	--	--	µCi/g
Na	24.1	24.6	22.5	19.5	23.2	--	23.2	25.60	I.S.	wt %
Al	4.04	4.31	3.11	2.93	3.80	--	3.66	4.62	I.S.	wt %
Ca	0.02	0.02	0.03	0.04	0.02	--	0.05	0.06	I.S.	wt %
Cr	0.47	0.40	0.58	0.51	0.35	--	0.58	0.36	I.S.	wt %
Fe	0.07	0.03	0.05	0.14	0.03	--	0.04	0.15	I.S.	wt %
Mass balance	101.6	104.7	99.8	100.1	98.0	--	105.1	103.5	--	wt %
Ion balance(c)	0.86	0.86	0.98	0.84	0.93	--	1.01	0.83	--	--

Mass Balance = wt % H_2O grav + 3*TOC + 5*TIC + Cl^- + NO_3^- + PO_4^{3-} + SO_4^{2-} + NO_2^- + Na + 2.2*Al + Ca + Cr + Fe + 2.1

Table 6-1. Summary of Analytical Results for Window C Crust Samples. (2 sheets)

Treatment/ analysis	Auger samples by riser number					Sludge weight samples				Units
	22A Top	22A Bot	13A	11A	16A	22A	13A	11A	16A	
Fusion										
TB	670	530	580	570	690	--	1700	--	--	µCi/g
AT	0.18	2.05	0.4	<0.15	0.02	--	0.42	--	--	µCi/g
^{137}Cs	435	375	310	310	500	--	955	--	--	µCi/g
U	60	86	123	75	72	--	230	--	--	µg/g
$^{239,240}Pu$	0.012	0.010	0.024	0.012	0.007	--	0.028	--	--	µCi/g
^{241}Am	0.115	0.102	0.198	0.137	0.12	--	0.228	--	--	µCi/g
^{237}Np	<0.5	<0.66	<0.7	<0.5	<0.5	--	<0.6	--	--	µCi/g
^{99}Tc	0.4	0.42	0.3	0.26	0.42	--	0.0002	--	--	µCi/g
^{129}I	<0.015	<1.6	<0.07	<0.01	<0.04	--	<0.02	inc	inc	µCi/g
^{90}Sr	20.9	22.9	34.2	26.8	25.2	--	71.2	inc	inc	µCi/g

DSC = differential scanning calorimetry
grav = gravimetric
I.S. = insufficient sample
TIC = total inorganic carbon
TOC = total organic carbon, Westinghouse Hanford Company thermal combustion method
TOC-PNL = total organic carbon, Pacific Northwest Laboratory chemical oxidation method
(a)Used % H_2O, TGA values for mass balance where gravimetric values not determined.
(b)Used average values of all other crust samples to calculate mass and ion balance.
(c)See text, Section 6.0.

Ion balance is the ratio of cation equivalents to anion equivalents, and should equal 1.00. Sodium represents the only significant source of cations, because potassium, the second most abundant cation, contributes about 1% as much as sodium. Therefore the total equivalents of cation is calculated by dividing the weight percent sodium by its atomic weight:

Cation Equivalents = Na/23

The calculation for the total equivalents of anions is more complex:

$$\text{Anion Equivalents} = TOC/36 + TIC/6 + Cl/35.45 + NO_3/62 + 3*PO_4/95 + 2*SO_4/96 + NO_2/46 + Al/27 + 2.1/17$$

The factor of 1/36 for TOC accounts for an average of one negative charge for every three carbon atoms in typical 101-SY organic compounds such as Na_3HEDTA. The factor of 1/6 for TIC accounts for two negative charges per carbon atom in carbonate. The factor 2.1/17 accounts for the estimated hydroxide contribution as discussed above.

The mass balance results in Table 6-1 are generally well within the range acceptable for these kinds of analyses, though they are consistently high. The ion balance results are, conversely, consistently low. This indicates that one or more of the anion values may be consistently overstated by a small amount. The ion balance is particularly sensitive to errors in TIC, because the equivalent weight for carbon is only 6 g, compared to 62 g for NO_3^- and 46 g for NO_2^-. For example, changing the TIC for sludge weight sample 11A from 2.43% to 1.37% (which is the average of the other crust samples) would lower the mass balance from 103.5 to 98.2 and would raise the ion balance from 0.83 to 0.96, which is much more reasonable.

6.1 DIRECT SAMPLE ANALYSES

Weight percent water was determined by oven drying at 120°C (see "Percent Water" in Appendix D) and/or by TGA as discussed in Section 5.0. In one case, it was also determined by Karl Fischer titration. Agreement among the methods was very good in most cases (Table 6-1.) One exception was Auger 11A, where the TGA value is six weight percent higher than the gravimetric (oven drying) method. The mass balance calculation at the bottom of Table 6-1 uses the gravimetric value for percent water, unless there is only a TGA value. Thus, the mass balance for sample Auger 11A could be higher than that shown in the table if the TGA percent water is correct. The mass balance of 100.1 implies that the gravimetric value is more likely correct for this particular sample.

The pH values shown in the table are lower than one would expect for a sample as high in caustic as these are thought to be. However, Appendix D points out the uncertainty in the pH values near either end of the pH scale, especially for very high ionic strength, high sodium samples.

Table 7-9. Weight Percent Total Organic Carbon (Westinghouse Hanford values) in Segment Samples.

Segment	Sample		Duplicate		Liquid phase average	Solid phase	Weighted combined average
	Trial 1	Trial 2	Trial 1	Trial 2			
4	1.08	1.06	1.18	1.20	1.13	1.74	1.20
5	1.22	1.24	1.20	--	1.22	1.59	1.27
6	1.12	1.17	--	--	1.14	1.63	1.22
7	0.73	--	1.15	1.18	0.94	1.88	1.06
8	1.03	1.06	1.15	--	1.09	1.60	1.22
9	1.29	1.26	1.13	--	1.20	1.93	1.33
10	1.05	--	1.17	1.22	1.12	1.87	1.26
11	1.09	--	1.27	--	1.18	1.94	1.31
13	1.16	--	1.11	1.13	1.14	1.80	1.26
14t	0.81	0.82	--	--	0.82	1.90	1.36
Convective layer averages:					1.10	1.79	1.25

Segment	Sample		Duplicate		Bulk sample average		
	Trial 1	Trial 2	Trial 1	Trial 2			
14b	1.67	1.69	1.72	--		1.70	
15	1.91	--	2.01	1.88		1.93	
16	1.92	--	--	--		1.92	
16R	1.97	1.94	1.87	1.91		1.92	
17	2.04	--	2.00	--		2.02	
18	2.11	--	2.09	1.94		2.06	
19	1.92	1.76	1.91	--		1.88	
20	1.96	--	2.08	--		2.02	
21	2.01	1.93	1.88	1.83		1.91	
22	1.89	--	1.92	--		1.91	
20A	1.88	1.80	1.85	--		1.85	
21A	1.88	--	1.85	--		1.87	
22A	1.91	1.90	1.83	--		1.87	
Nonconvective layer average:						1.91	

Figure 7-3. Distribution of Total Organic Carbon.

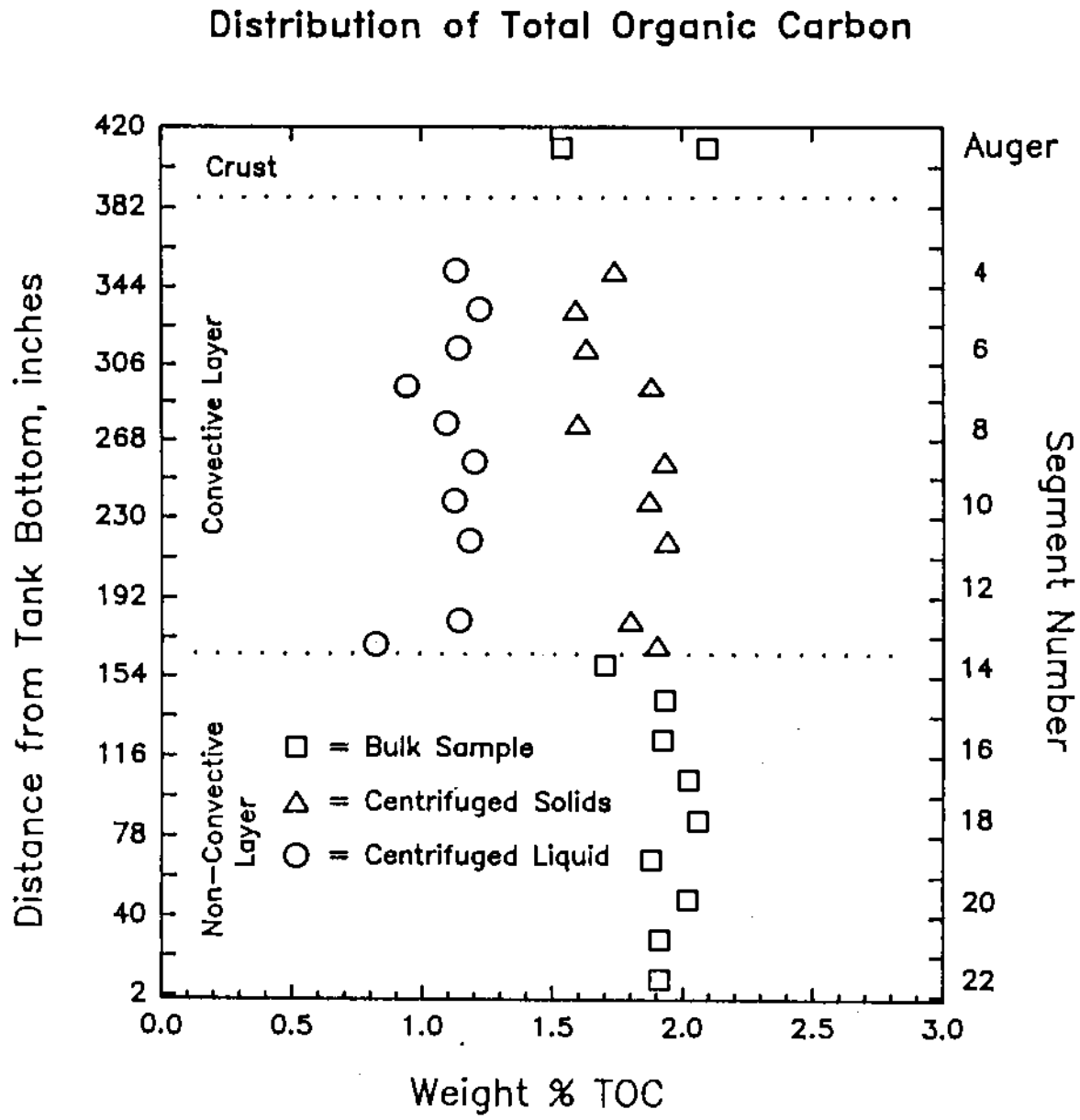

8.0 CHEMICAL AND RADIOCHEMICAL ANALYSES OF CORE COMPOSITE SAMPLES

Composite samples were made by blending together portions of individual facies samples in the same proportion, by weight, as the facies were found in the core sample. A full complement of chemical and radionuclide analyses was performed on each of the composite samples.

Five composite samples were prepared from the one full, 22-segment core sample taken in Window C. The facies that were used to prepare each composite are shown in Table 3-5. Briefly, they are: composite 1, segments 4 - 8; composite 2, segments 9 - 14 Top; composite 3, segments 14 Bottom - 18; composite 4, segments 19 - 22; and composite 5, solid fraction of segment 2. Thus, composites 1 and 2 represent the convective layer, while 3 and 4 represent the nonconvective layer, and composite 5 represents the crust.

Composite samples 1 - 4 were prepared for analysis in the same way as the convective layer segment samples, by heating the samples to 60 °C and centrifuging. Appendix E shows logic diagrams for the sample breakdown procedures used. In addition, bulk samples from composites 3 and 4 were analyzed to provide direct comparison to the individual segment analyses. For the nonconvective layer segments, the decision was made not to analyze the centrifuged solid phase. Because there were about 80% centrifuged solids at 60 °C, there was essentially no difference in composition between the centrifuged solids and the bulk sample (see Table 3-6).

Tables 8-1a and 8-1b show a summary of the liquid phase analytical results (chemical and radionuclide, respectively) for the composite samples. The results for the centrifuged solids and bulk samples are shown in Tables 8-2a and 8-2b. These tables give the averages of replicate analyses of duplicate samples. In some cases, additional samples were prepared and analyzed due to discrepancies in the initial results. Results of all the individual analytical determinations are in Appendix B. Mass balance and ion balance in Tables 8-1a and 8-2a were calculated in the same way as described in Section 6.0.

Some of the analyses performed on individual segment samples were not repeated on the composite samples. They include thermal analysis (DCS/TGA), weight percent water, and TOC. However, several species were analyzed in both segment and composite samples, including nitrate, nitrite, ^{137}Cs, and five ICP metals. These analytes provide a comparison between the composite samples and the average of the segments used to form each composite. Some of these comparisons are shown in Table 8-3. The last column in this table is the standard deviation determined from the segment analyses, and is taken from Tables 10-5 and 10-6.

Overall, the agreement between segments and composites is reasonably good, but there are some exceptions. The concentration of nitrate in the liquid phase was much higher for the composite samples than the corresponding segment samples. The amount of nitrate in the centrifuged solids was too variable to assign an average value for composites 1 and 2. For example, values reported for composite 1 centrifuged solids were: 26.3, 26.9, 7.8, 33.7, 8.3, 7.2, 15.2, and 14.6% NO_3^- by weight (as shown in Appendix B). Some

Table 8-1a. Chemical Analysis of Composite Sample Liquid Phase (Weight Percent Except Cyanide).

Analysis	Composite number			
	1	2	3	4
NO_3^-	16.1	15.0[c]	11.9	12.2
NO_2^-	13.7	13.0[c]	9.9	8.7
Cl^-	0.89	1.02[c]	0.92	0.70
F^-	--	--	0.07	0.04
PO_4^{3-}	0.53	0.56[c]	0.91	0.91[a]
SO_4^{2-}	0.13	0.05[c]	0.08	0.28
TIC	0.26	0.66[c]	1.60[c]	1.60[a]
TOC	0.94	0.94[a]	1.14	0.94
NH_3/NH_4^+	0.01	0.01	0.02	--
OH^-	2.82	2.82[a]	3.08	1.98
CN^- (ppm)	90	91	90	394
Na	19.3	17.7	21.1	17.9
Al	3.07	2.75	3.38	2.96
Cr	0.006	0.005	0.013	0.022
Fe	--	0.003	0.006	--
Ca	0.046	0.058	0.052	0.119
K	0.361	0.312	0.380	0.338
Mo	0.011	0.009	0.012	0.009
Ni	0.004	0.003	0.010	0.006
Zn	0.009	0.005	0.009	0.022
H_2O (b)	36.53	35.73	36.13	36.13
Mass Bal	101.4	96.4	103.5	96.6
Ion Bal	0.89	0.85	0.87	0.82

[a]Value not determined; assumed to be same as composite from same layer (in order to calculate mass and charge balance).

[b]Value not determined; assumed average of segment samples for convective layer (assumed nonconvective liquid equal to convective layer liquid average).

[c]One or more duplicate sample results discarded.

Table 8-2a. Chemical Analysis of Composite Bulk Samples and Centrifuged Solids (Weight Percent Except Cyanide).

Analysis	Centrifuged solids		Bulk samples		
	#1	#2	#3	#4	#5
NO_3^-	8.7[c]	8.7[c]	10.5	10.4	12.8
NO_2^-	11.1	13.9	10.5	8.3	8.5
Cl^-	0.73	0.68	0.76	0.93	0.65[e]
F^-	0.03	--	--	--	0.17[e]
PO_4^{3-}	0.50	0.44	0.81	0.90	1.08[e]
SO_4^{2-}	0.20	0.24	0.67	0.71	0.89[e]
TIC	1.02	1.18	0.99	1.15	1.38
TOC (b)	1.70	1.89	1.97	1.93	1.96
NH_3/NH_4^+	0.19[e]	0.26[e]	0.31	0.37	<0.09
OH^-	2.12[e]	1.58	2.52	2.42	1.69
CN^- (ppm)	152[d]	117[d]	389	409	469
Na	22.0	22.5	20.3	22.3	20.1
Al	2.52	2.71	3.57	3.7	3.86
Cr	0.20	0.22	0.58	0.71[e]	0.76
Fe	0.015	0.029	0.054	0.061	0.116
Ca	0.128	0.127	0.066	0.044[e]	0.054
K	0.267	0.508	0.310	0.301	0.241
Mo	--	--	0.009	0.009	--
Ni	0.011	--	0.039	0.026[e]	0.027
Zn	0.005	--	0.007	0.007	0.005
H_2O (a)	35.03	35.03	34.04	32.52	33.65
Mass Bal	97.0	101.7	100.2	99.5	101.9
Ion Bal	1.13	1.07	0.93	1.04	0.89

[a]Wt. % H_2O for Composites 1 and 2 taken from segment data in Table 7-7b; for Composites 3 and 4 taken from segment averages (see Appendix B); Composite 5 determined directly.

[b]TOC values for Composites 1 and 5 determined directly; other values taken from segment averages (Table 7-9).

[c]Average of values from corresponding segments.

[d]Bulk sample, not centrifuged solids.

[e]One or more duplicate sample results discarded.

Table 8-3. Comparison of Composite Sample Analytical Results with Averages of Corresponding Segment Sample Results. Values are in weight percent except for ^{137}Cs, which is in uCi/g.

Analysis	Phase	Composite #	Composite sample	Segment average	σ^b
NO_3^-	Liquid	1	16.1	12.3	0.65
		2	15.0	10.1	
	Solid	1	[a]	8.7	0.67
		2	[a]	8.7	
	Bulk	3	10.5	10.4	0.67
		4	10.4	10.0	
NO_2^-	Liquid	1	13.7	12.8	1.12
		2	13.0	11.2	
	Solid	1	11.1	10.5	0.74
		2	13.9	9.6	
	Bulk	3	10.5	9.2	0.74
		4	8.3	9.1	
Na	Liquid	1	19.3	20.3	1.24
		2	17.7	19.9	
	Solid	1	22.0	20.9	0.93
		2	22.5	20.6	
	Bulk	3	20.3	20.8	0.93
		4	22.3	21.7	
^{137}Cs[c]	Liquid	1	403	469	118
		2	427	458	
	Solid	1	328	382	44
		2	329	407	
	Bulk	3	360	370	44
		4	319	364	

[a]Duplicate sample results varied too much to assign an average value.
[b]Aanalytical standard deviation for segment samples, from Tables 10-5 and 10-6.
[c]Average of water digest, acid digest, and fusion values.

Appendix F

Synthetic Tank 101-SY Waste Studies

Synthetic Tank 101-SY Waste Studies

Larry Pederson and Sam Bryan

Pacific Northwest Laboratory

Tank Waste Science Panel

03/26/92

Outline

Nitrous oxide solubility measurements

Physical properties of synthetic vs. actual waste; effect of heating and dilution

Nitrous oxide/hydrogen product ratios as a function of hydroxide ion concentrations

Sub-critical oxidation of organic compounds in synthetic wastes

Gas Solubilities in Synthetic Tank 101-SY Wastes

Relative solubilities of nitrous oxide, nitrogen, and hydrogen may be an important factor in determining the ratios of gases released during rollover events

Nitrous oxide at least 10 times more soluble in water than either nitrogen or hydrogen (DA Reynolds memo to GD Johnson dated 01/02/92, quoting from CL Young, 1982)

Solubility of nitrous oxide in solutions of high ionic strength are not well understood; data are limited with regard to temperature and salt concentration; solubility is expected to decrease substantially with increasing ionic strength.

(note: 1 gram nitrous oxide dissolved per liter, the solubility at 25°C in water, corresponds to roughly 70,000 cubic feet of gas at STP in a million gallon tank.)

APPARATUS FOR MEASURING GAS SOLUBILITIES IN SYNTHETIC WASTE

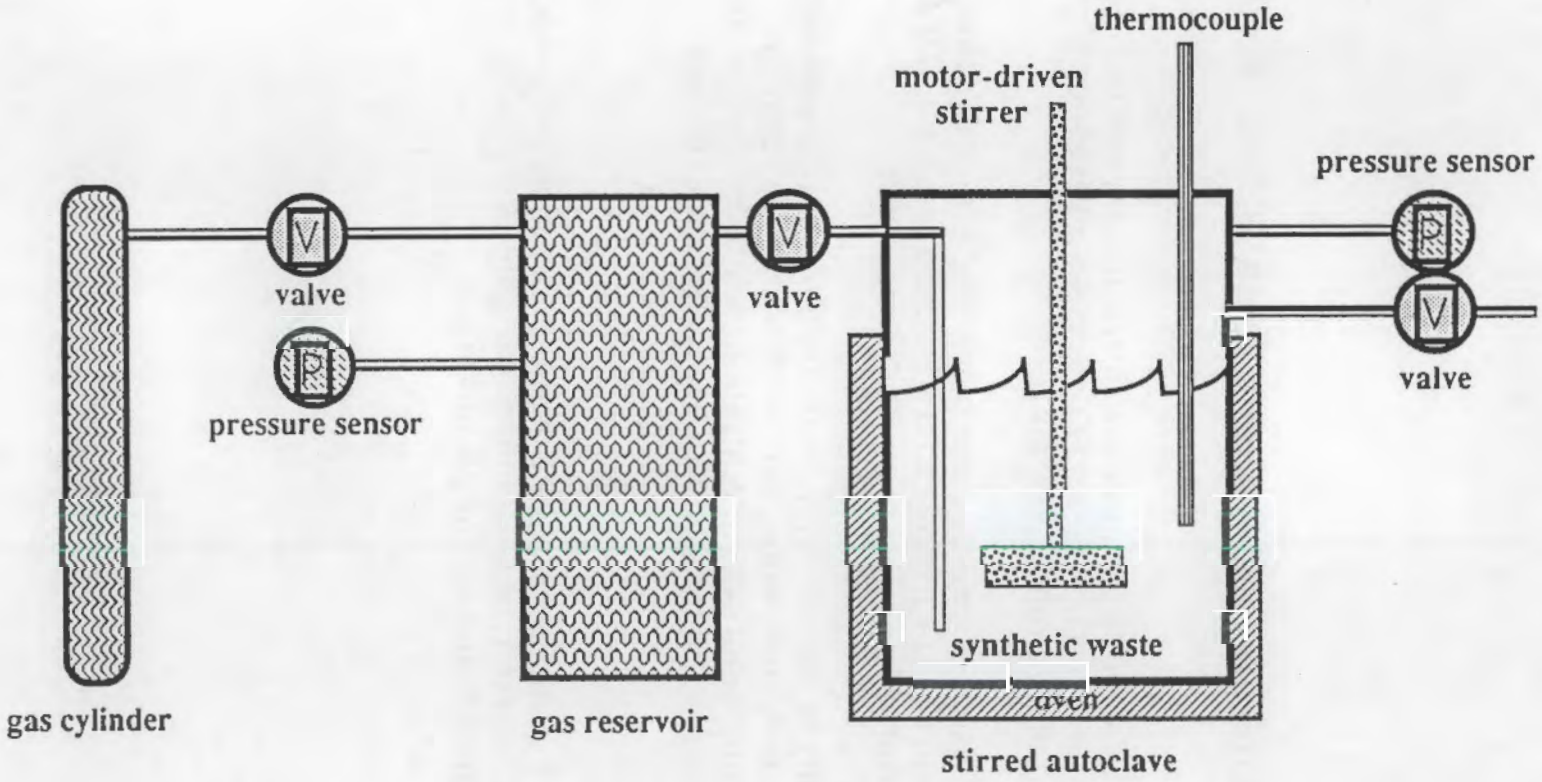

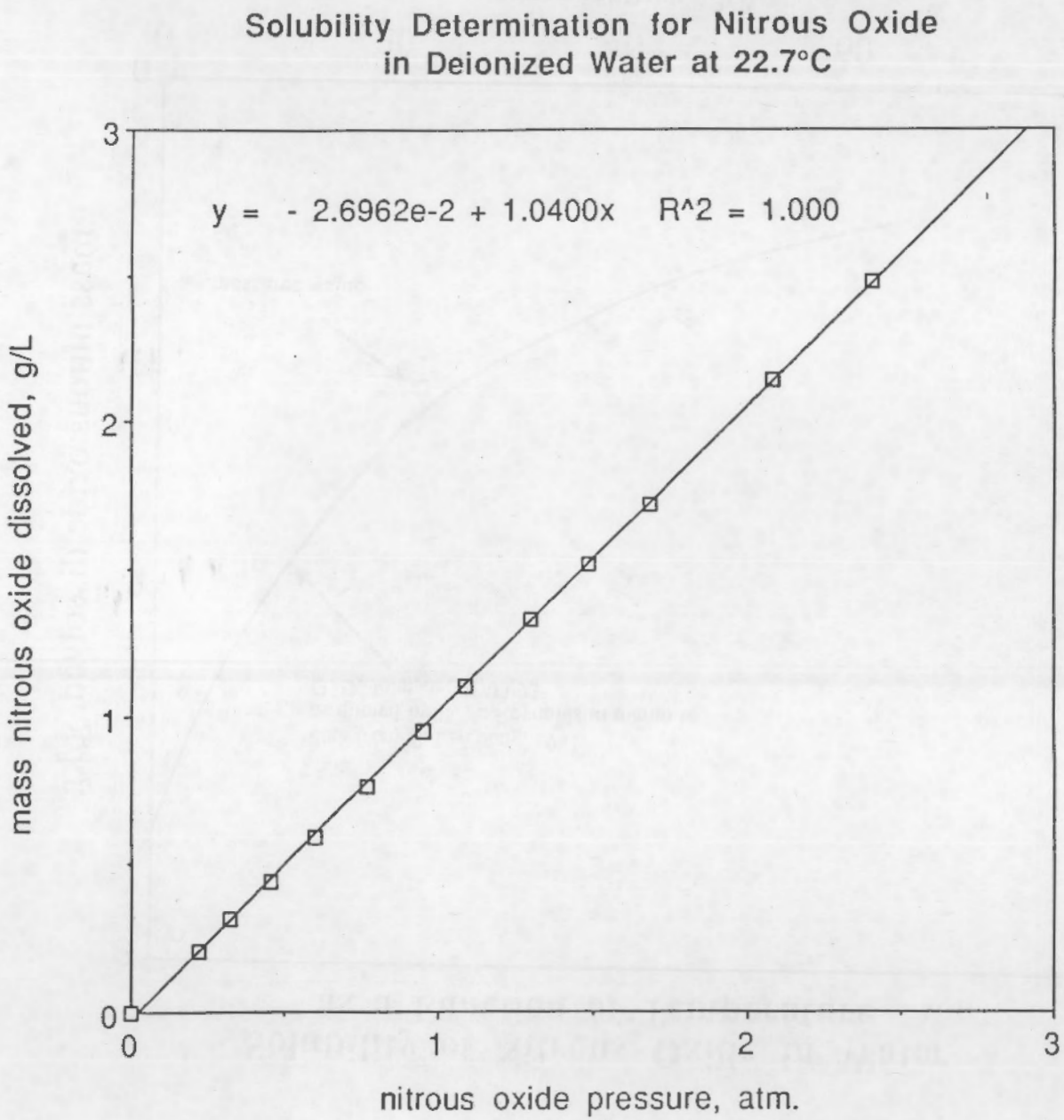
Solubility Determination for Nitrous Oxide
in Deionized Water at 22.7°C
y = - 2.6962e-2 + 1.0400x R^2 = 1.000
mass nitrous oxide dissolved, g/L
nitrous oxide pressure, atm.
0
1
2
3

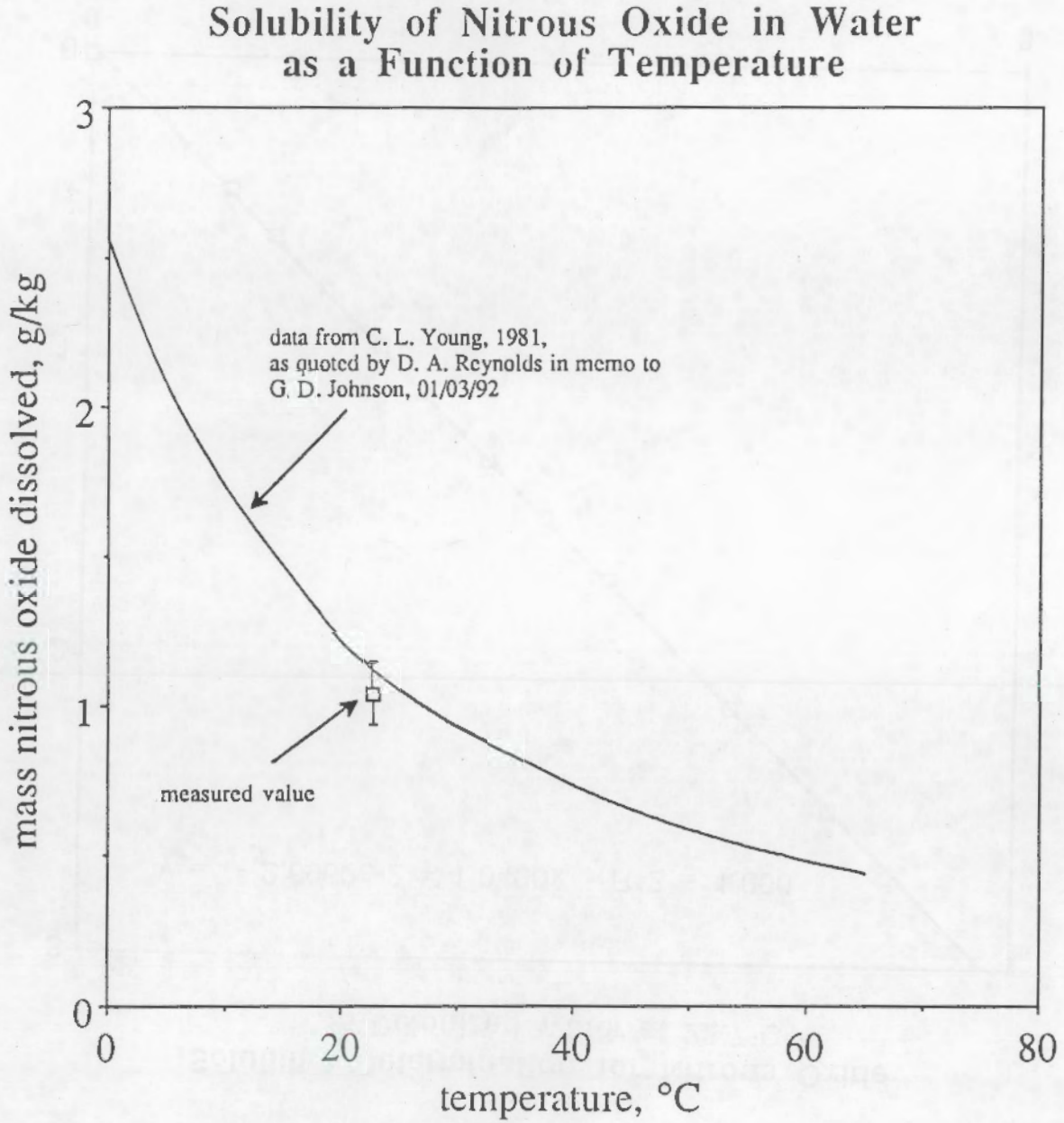
Solubility of Nitrous Oxide in Water
as a Function of Temperature
mass nitrous oxide dissolved, g/kg
temperature, °C
0
1
2
3
0
20
40
60
80
data from C. L. Young, 1981,
as quoted by D. A. Reynolds in memo to
G. D. Johnson, 01/03/92
measured value

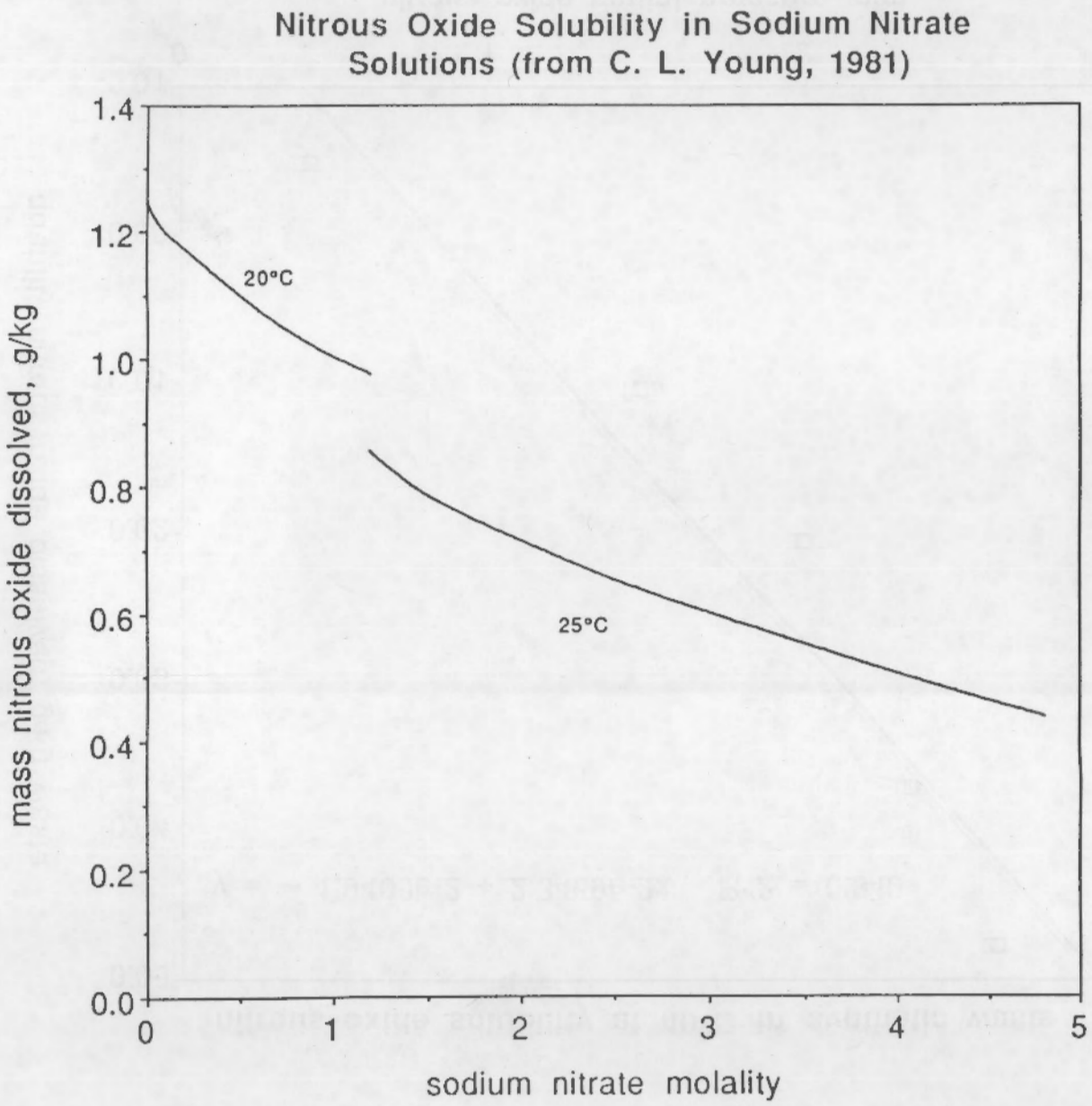
Nitrous Oxide Solubility in Sodium Nitrate Solutions (from C. L. Young, 1981)
mass nitrous oxide dissolved, g/kg
1.4
1.2
1.0
0.8
0.6
0.4
0.2
0.0
20°C
25°C
0
1
2
3
4
5
sodium nitrate molality

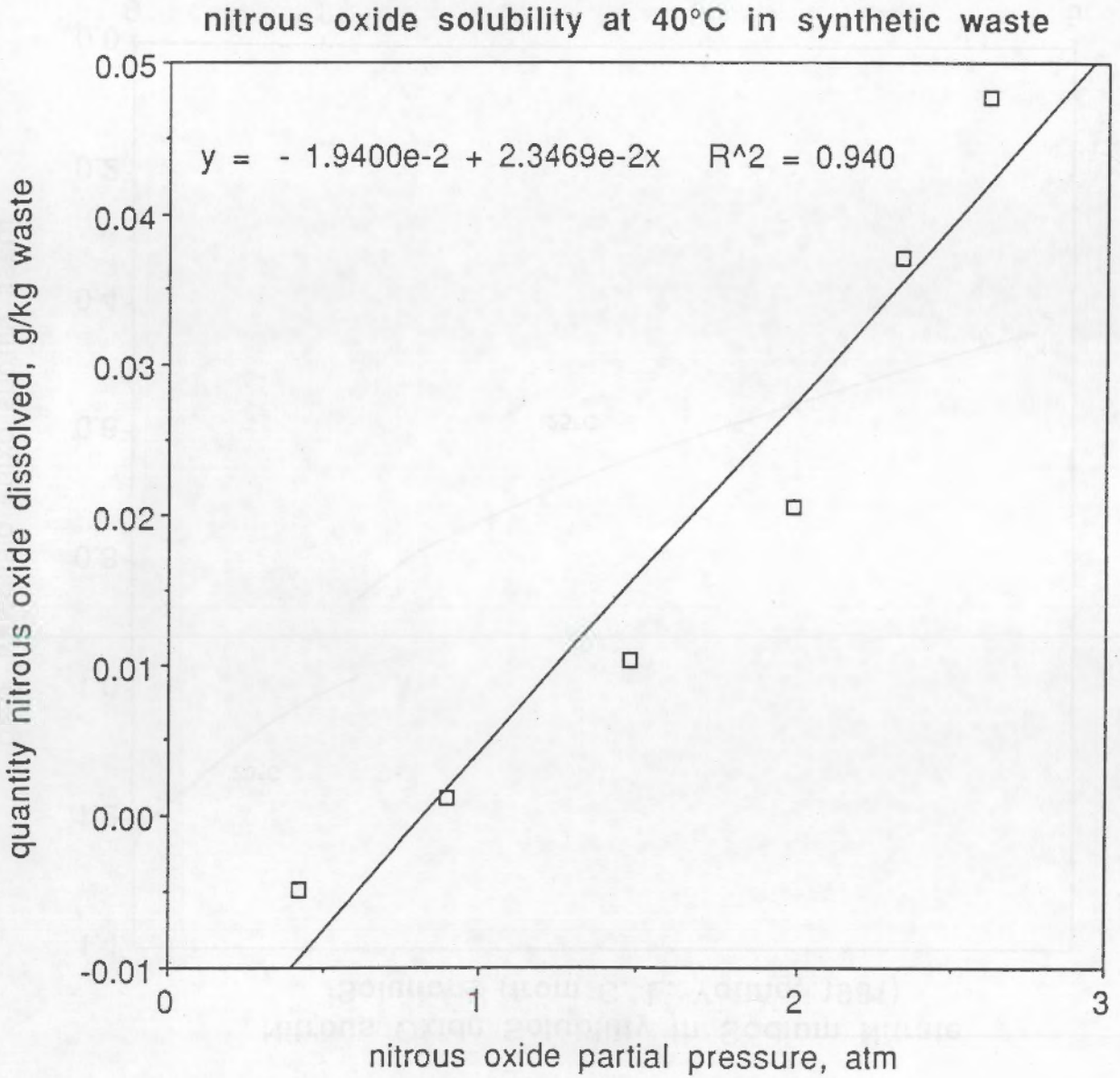
nitrous oxide solubility at 40°C in synthetic waste
y = - 1.9400e-2 + 2.3469e-2x R^2 = 0.940
quantity nitrous oxide dissolved, g/kg waste
0.05
0.04
0.03
0.02
0.01
0.00
-0.01
0
1
2
3
nitrous oxide partial pressure, atm

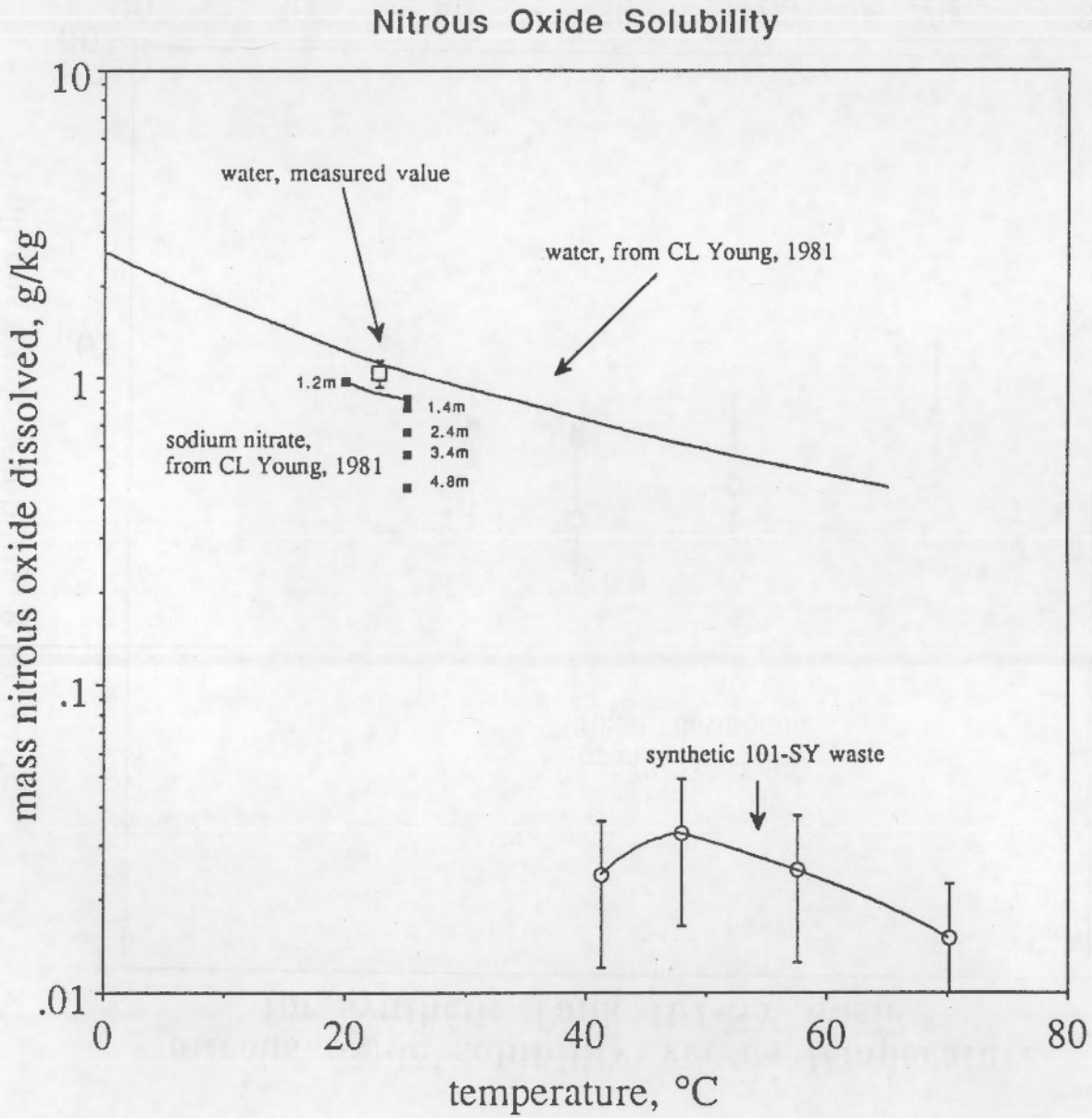
Nitrous Oxide Solubility
10
1
.1
.01
mass nitrous oxide dissolved, g/kg
water, measured value
water, from CL Young, 1981
1.2m
1.4m
2.4m
3.4m
4.8m
sodium nitrate,
from CL Young, 1981
synthetic 101-SY waste
0
20
40
60
80
temperature, °C

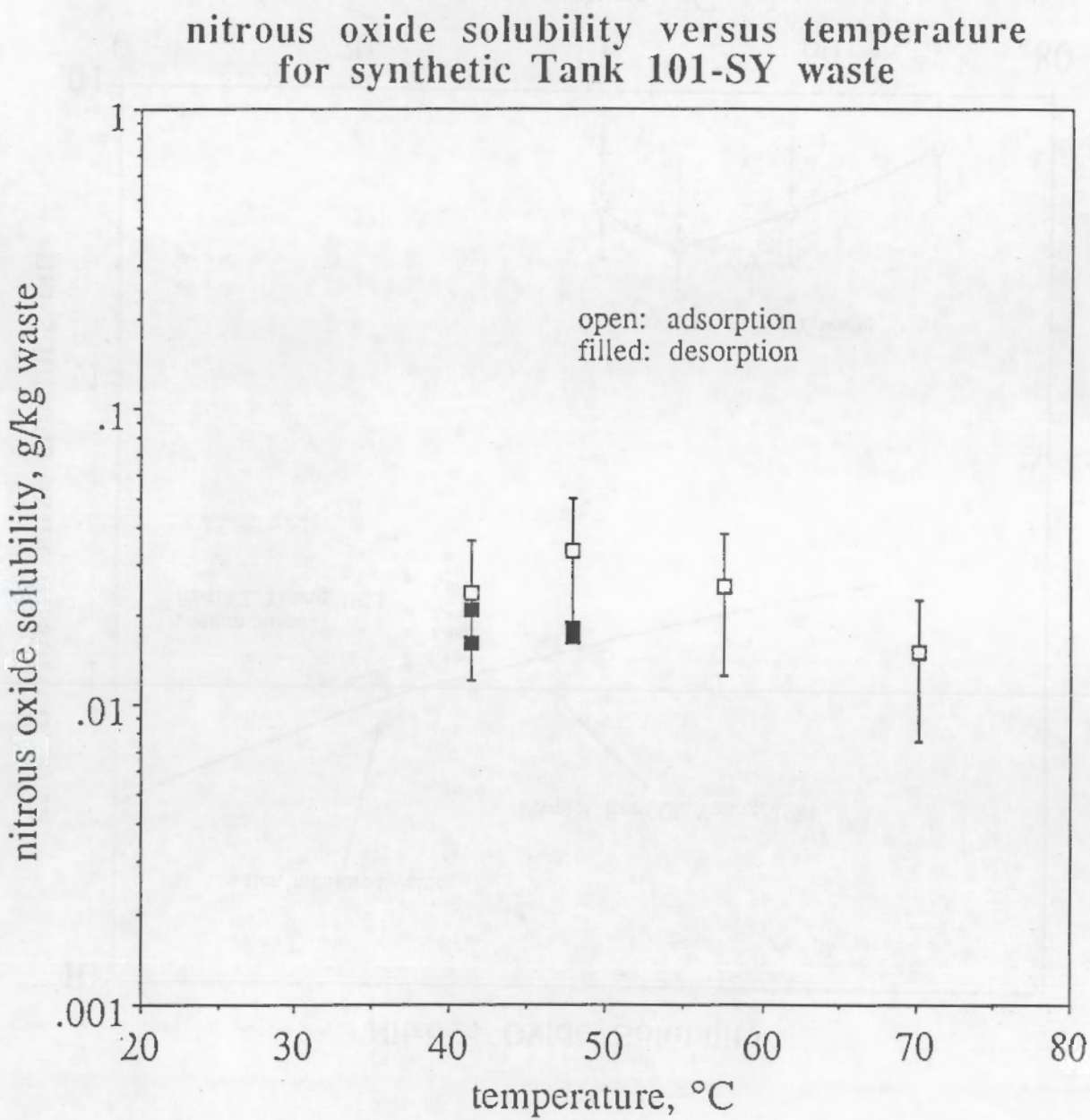
nitrous oxide solubility versus temperature
for synthetic Tank 101-SY waste
nitrous oxide solubility, g/kg waste
1
.1
.01
.001
open: adsorption
filled: desorption
20
30
40
50
60
70
80
temperature, °C

F.10

Nitrous Oxide Solubility in Synthetic Wastes

solubility determination for distilled water is in good agreement with literature

results for synthetic wastes (organics not included) indicate solubilities of 0.01-0.03 g nitrous oxide per kg waste per atmosphere nitrous oxide

low temperature (<40°C) solubility measurements in progress

Comparison of Physical Properties of Synthetic and Actual Wastes

Synthetic waste composition based on most recent waste analysis data

Comparisons made of:

- density
- weight percent water
- weight percent centrifuged solids
- volume percent settled solids
- shear strength

Effect of heating and dilution on weight percent centrifuged solids assessed for synthetic wastes (identical measurements will be made for actual wastes later by Tingey and Jones)

Component	Synthetic Formulation	Calculated from 101-SY Data[1]
	Wt%	
TOC	1.52[2]	1.58
Na	19.6	20.5
Al	3.6	3.5
Cl^{-1}	1.5	1.5
PO_4^{-3}	1.1	1.1
NO_2^{-1}	10.8	11.5
NO_3^{-1}	9.5	10
CO_3^{-2}	1.5	1.6
F^{-1}	0.12	0.1
OH^{-1}	3.1	3.1
SO_4^{-2}	0.19	0.19
Cr	0.35	0.37
Cu	$8x10^{-4}$	---
Fe	0.026	0.028
Ni	0.0078	0.008
Ca	0.02	0.021
K	0.36	0.37
H_2O	40.4	38
Total	100.0	100.9

1. Calculated by RT Allemann
2. Total TOC from Na_4EDTA and Na_3HEDTA

Comparison of Properties of Several 101-SY Core Segments and Synthetic Waste

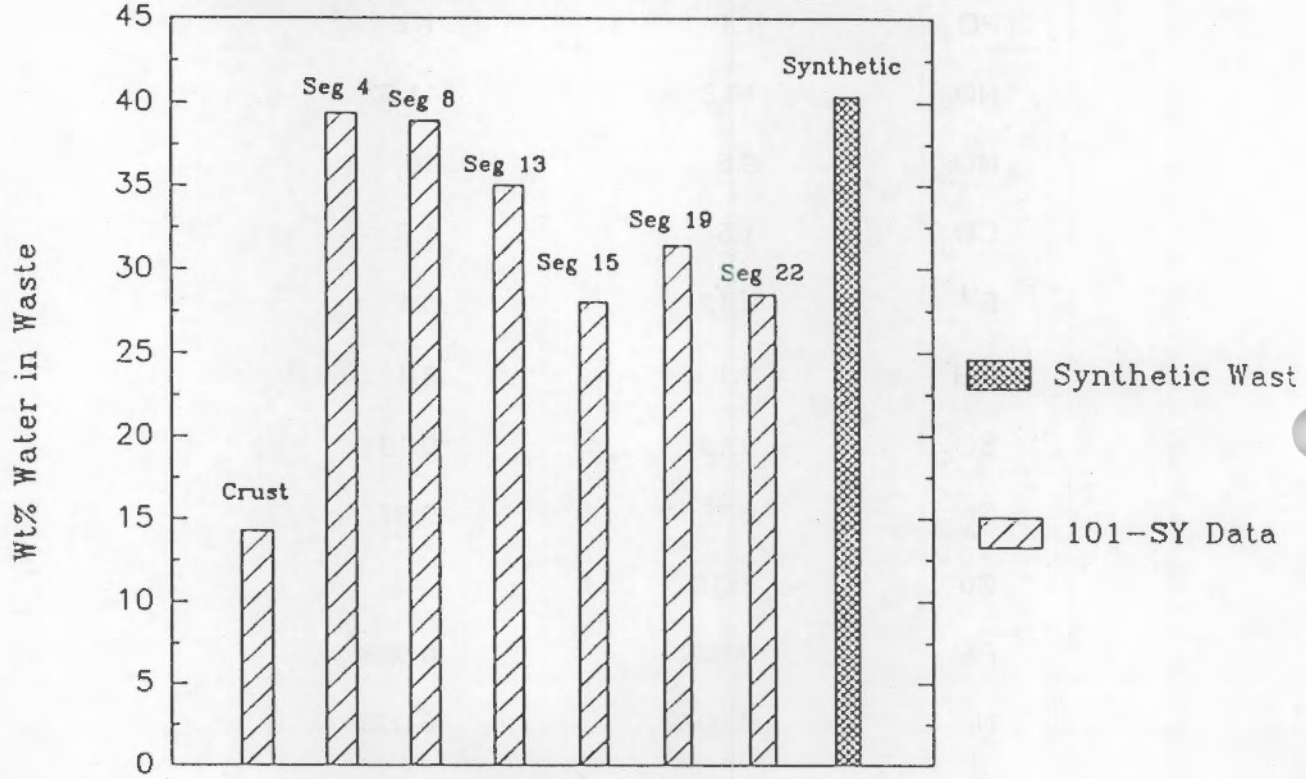

Comparison of 101-SY Properties with Synthetic Waste Properties

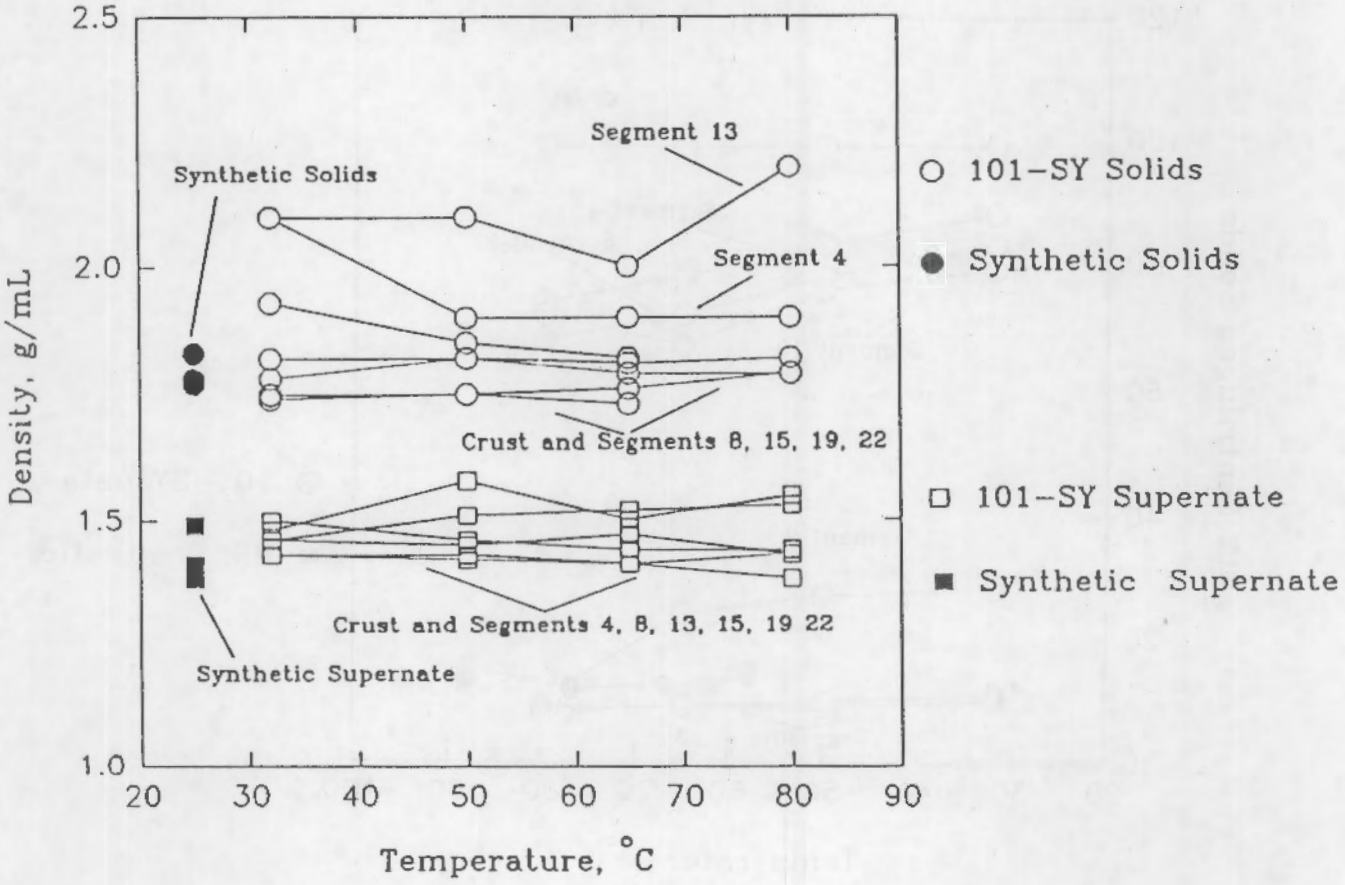

Comparison of 101-SY Physical Properties with Synthetic Waste Properties

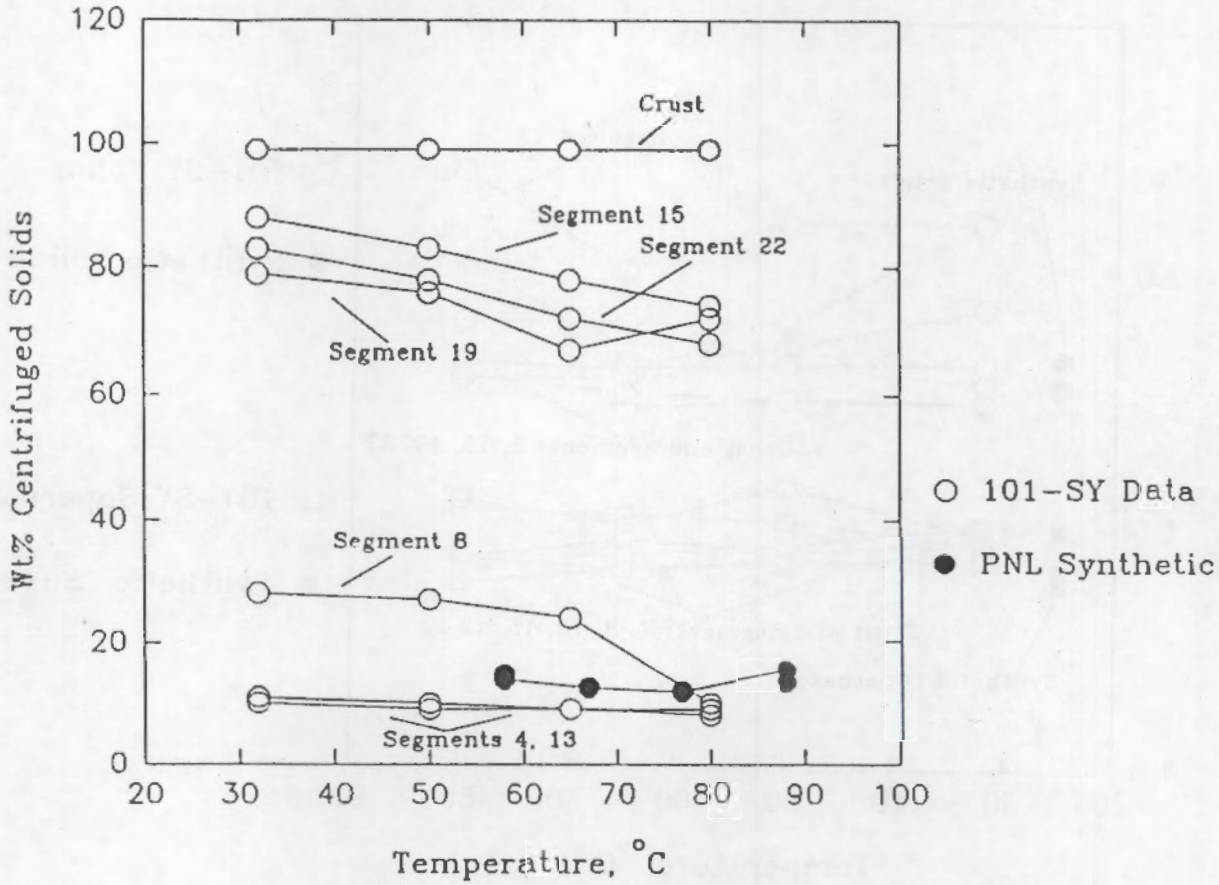

Comparison of 101-SY Physical Properties with Synthetic Waste Properties

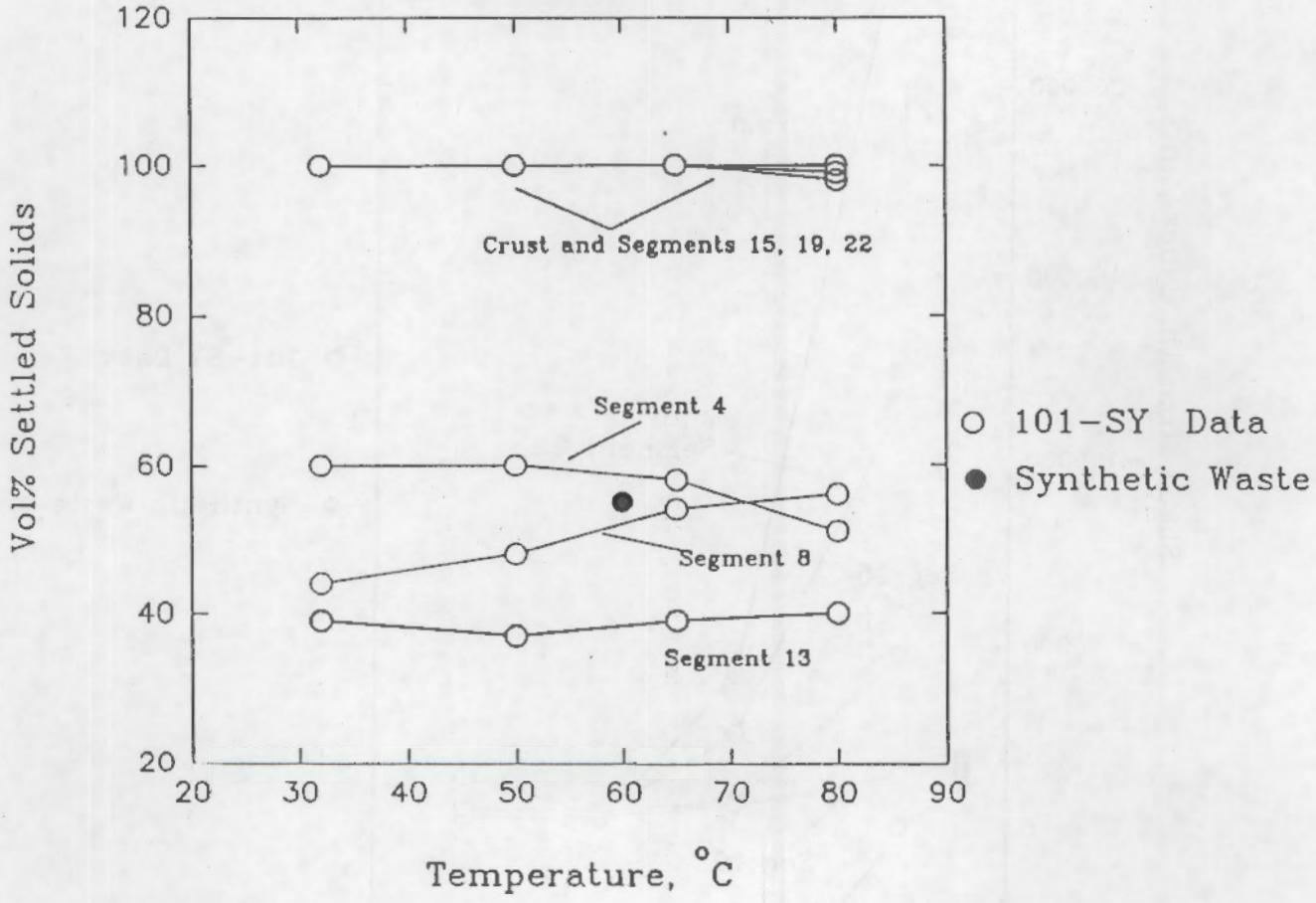

Comparison of 101-SY Physical Properties with Synthetic Waste Properties

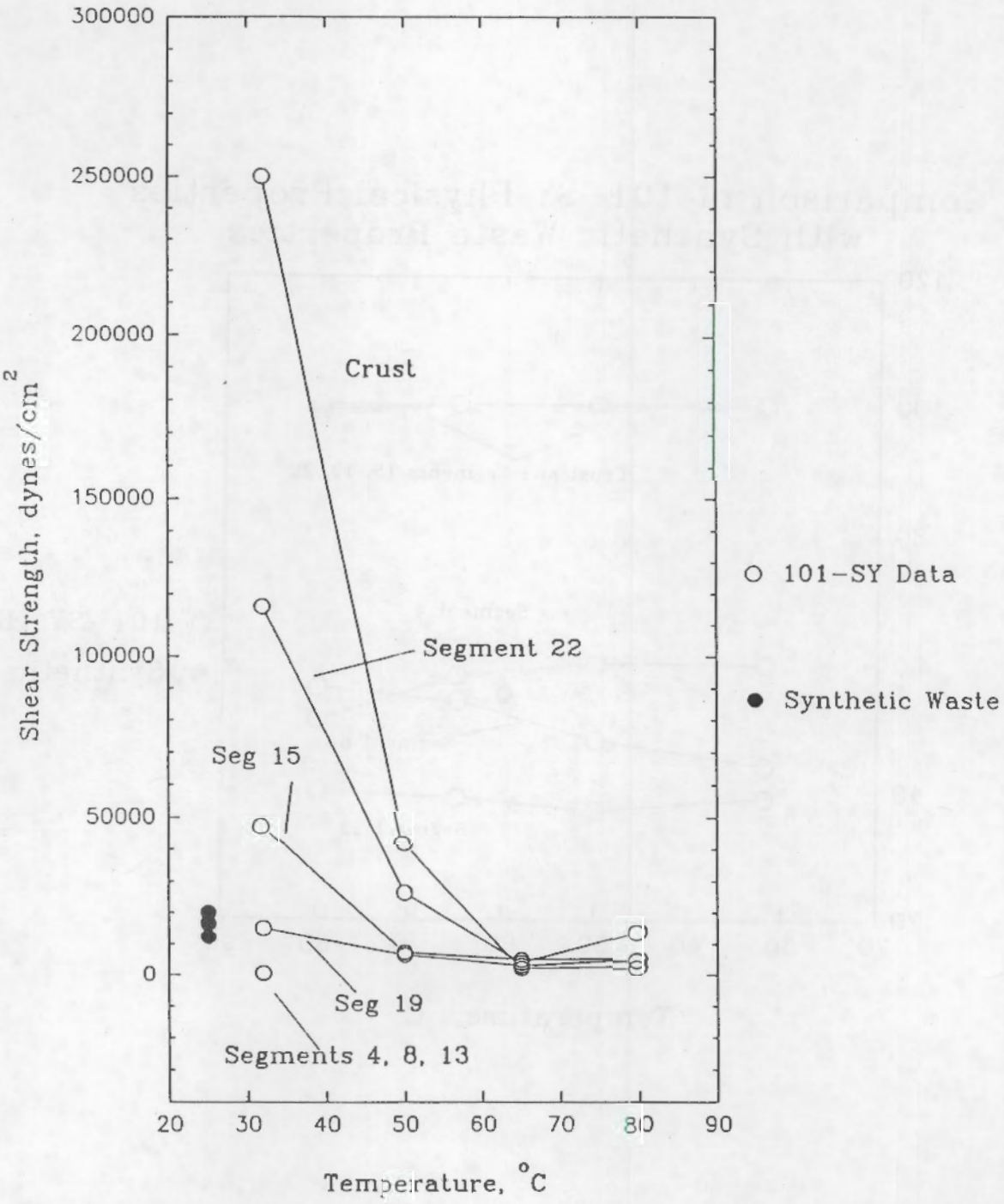

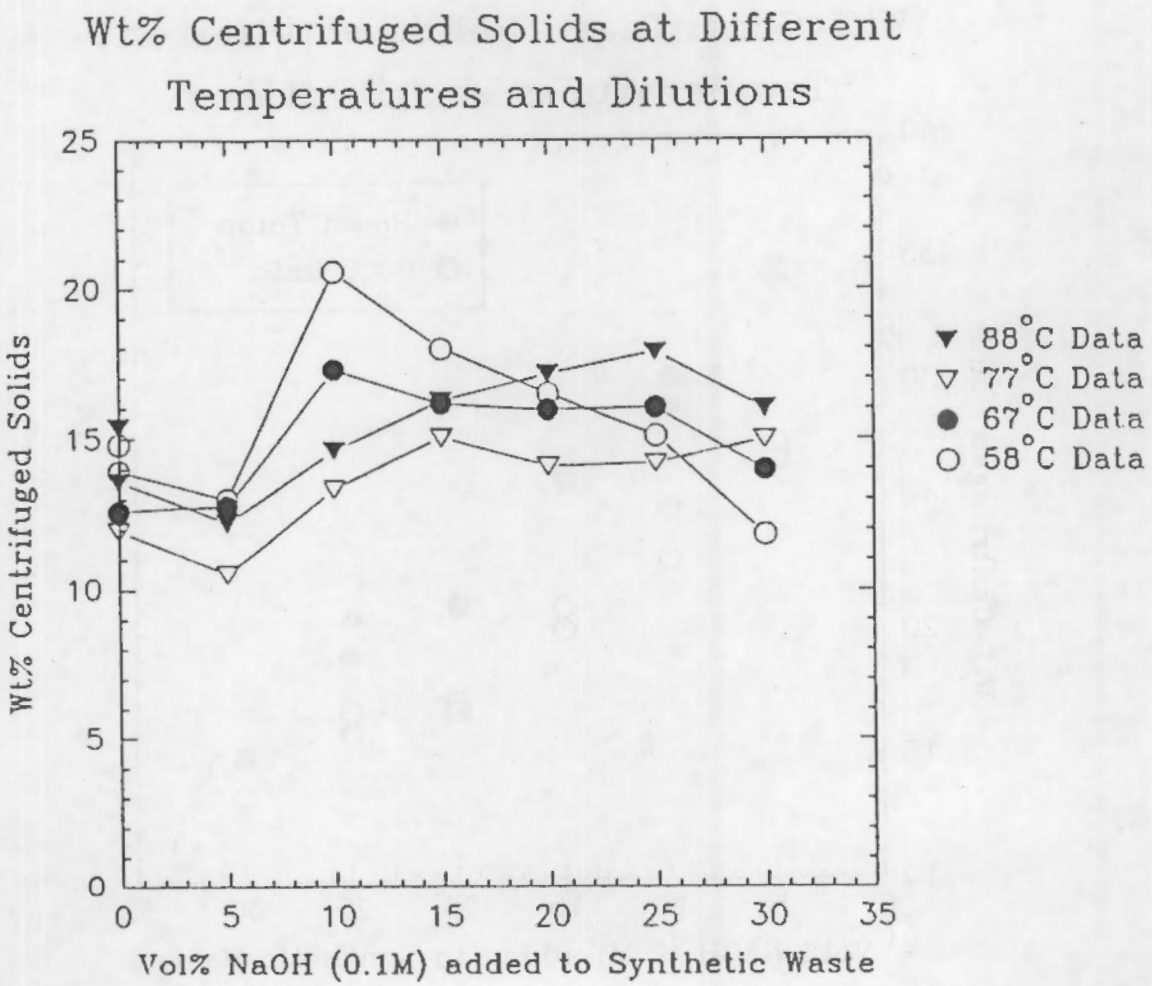

(waste contains 0.3 molar HEDTA)

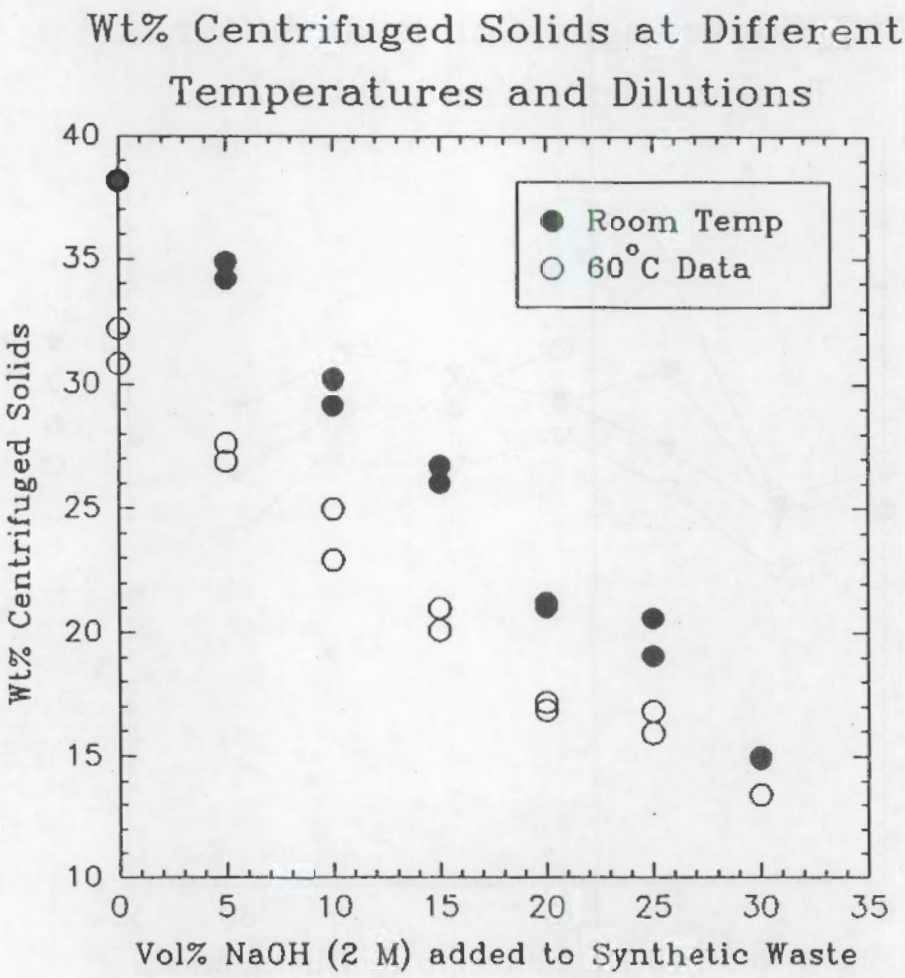

(waste contains no organic constituents)

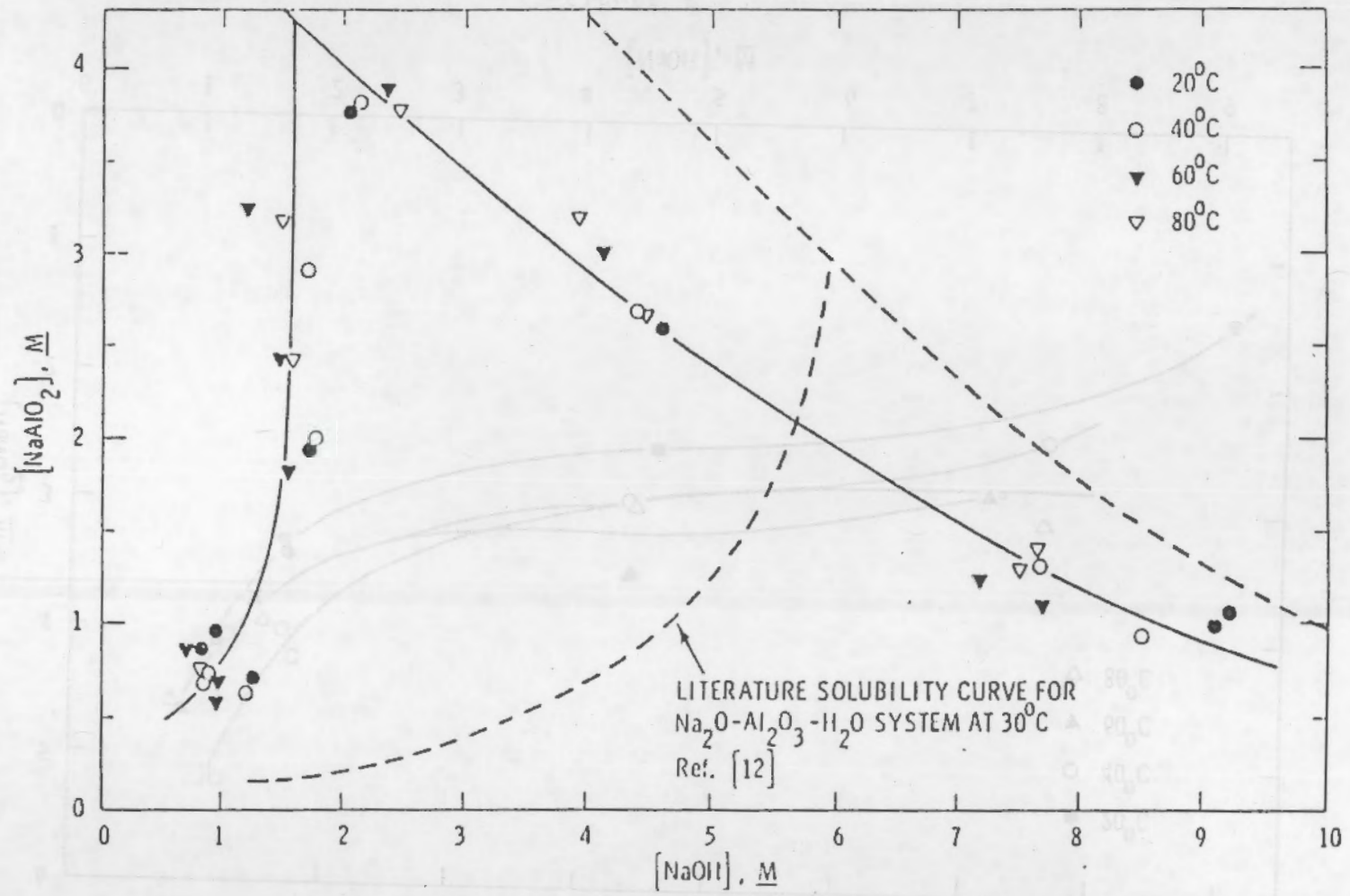

FIGURE 3

SOLUBILITY OF SODIUM ALUMINATE IN SYNTHETIC WASTE SOLUTIONS
(SATURATED WITH $NaNO_3$, $NaNO_2$, Na_2SO_4, AND Na_2CO_3)

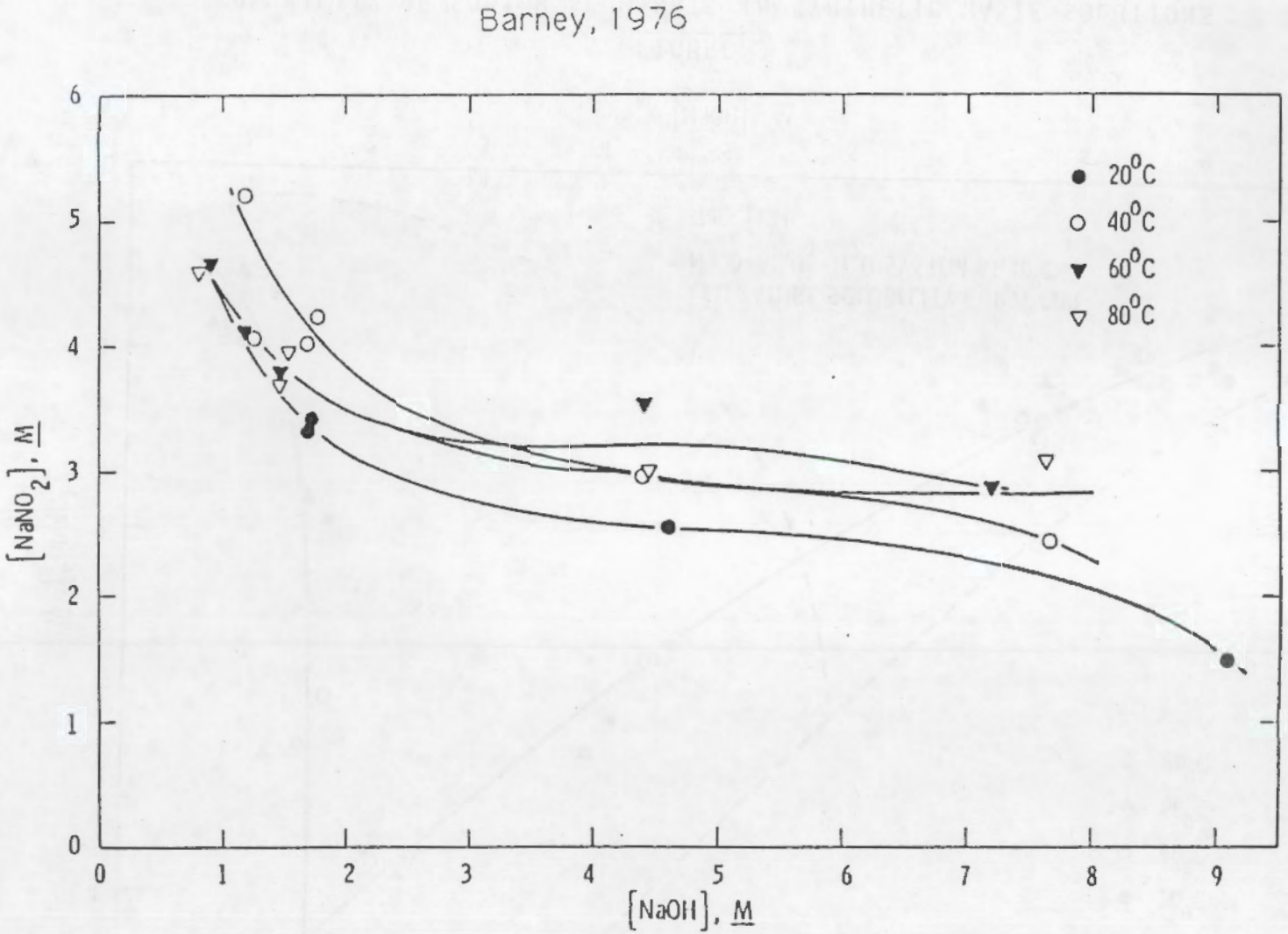

FIGURE 5

SOLUBILITY OF SODIUM NITRITE IN SYNTHETIC WASTE SOLUTIONS (SATURATED)

Infrared Spectra of Inorganic Phases Present in Tank 101-SY
(absorbance scale)

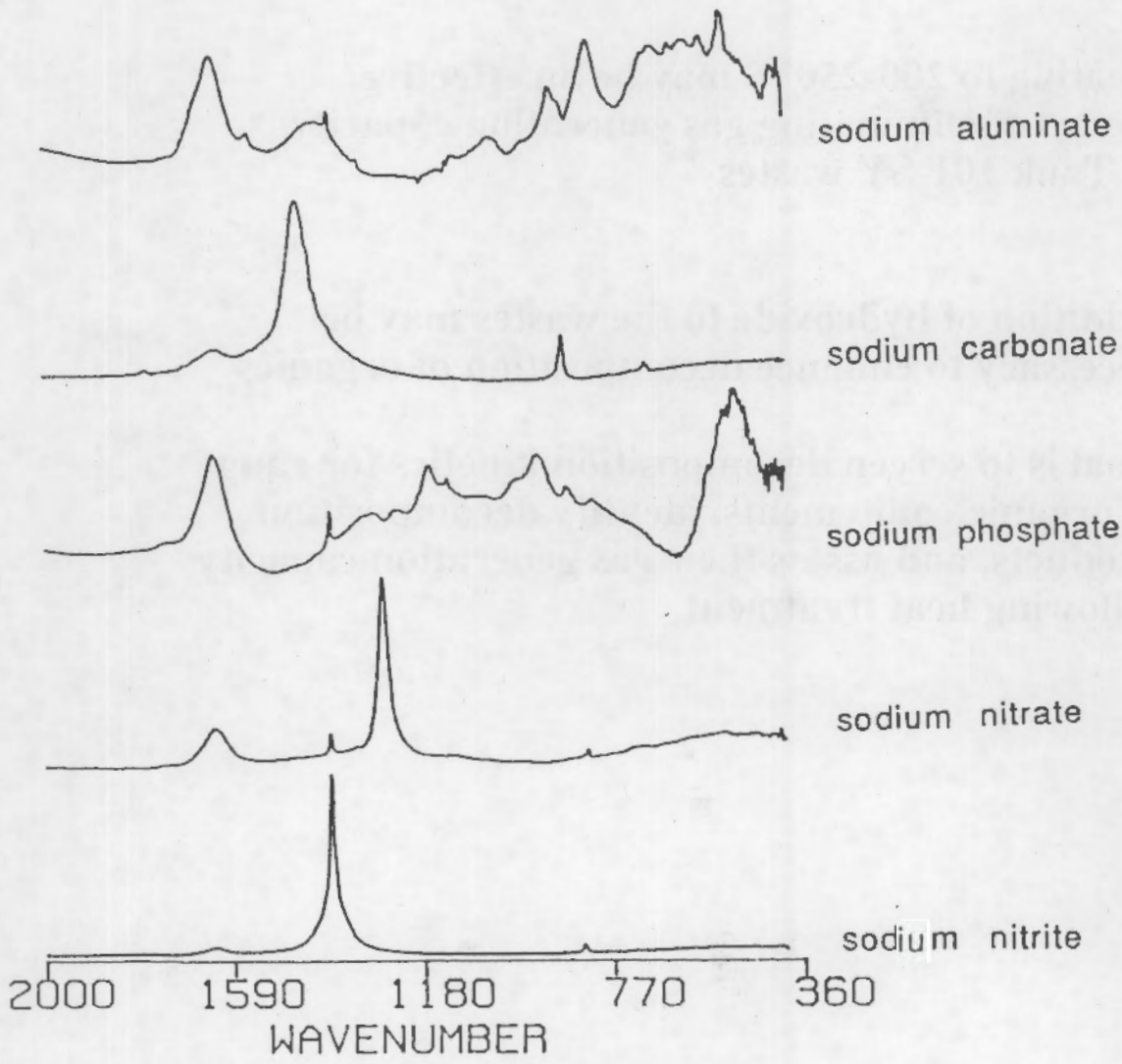

Sub-Critical Oxidation of Organics in Synthetic Wastes

Heating to 200-250°C may be an effective means of eliminating gas generation capacity of Tank 101-SY wastes

Addition of hydroxide to the wastes may be necessary to enhance decomposition of organics

Goal is to screen decomposition kinetics for range of organic components, identify decomposition products, and assess their gas generation capacity following heat treatment

Sub-Critical Oxidation of Organics in Synthetic Waste

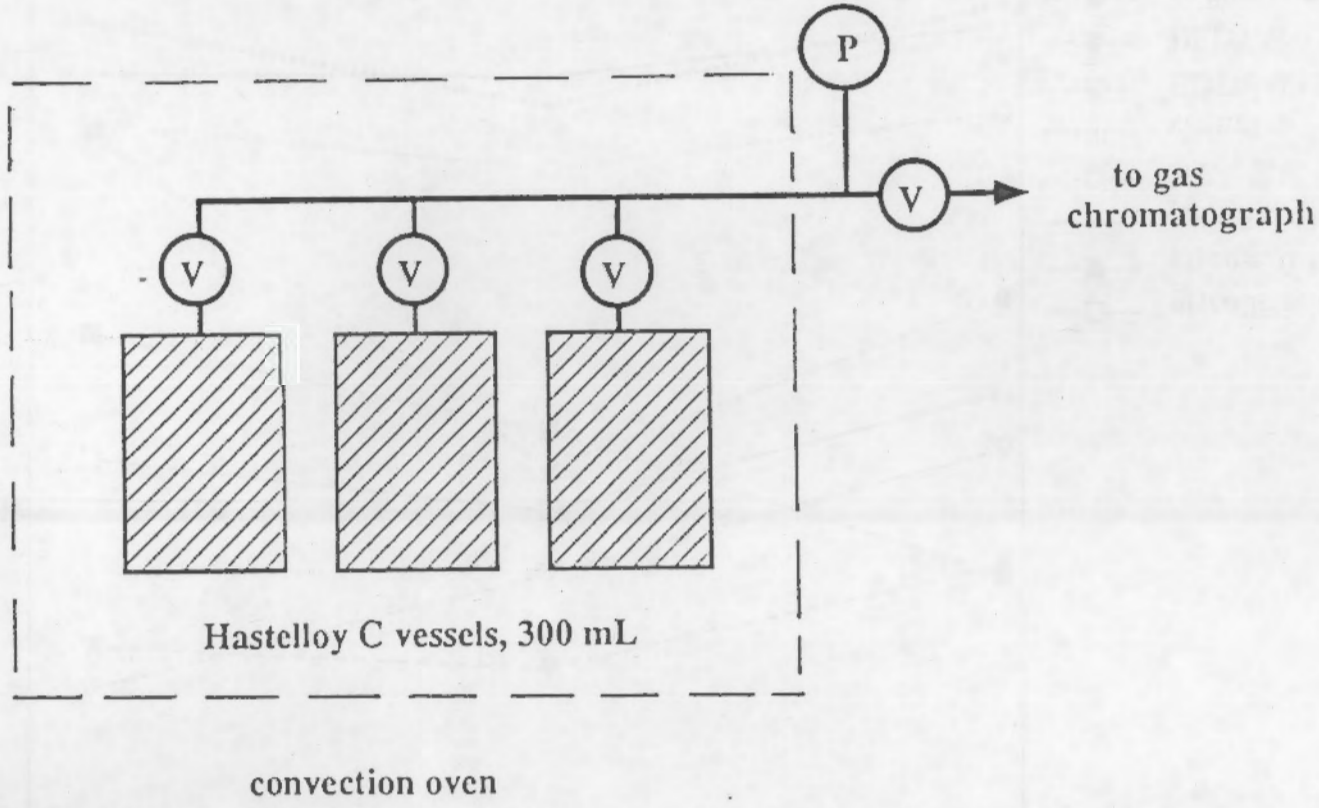

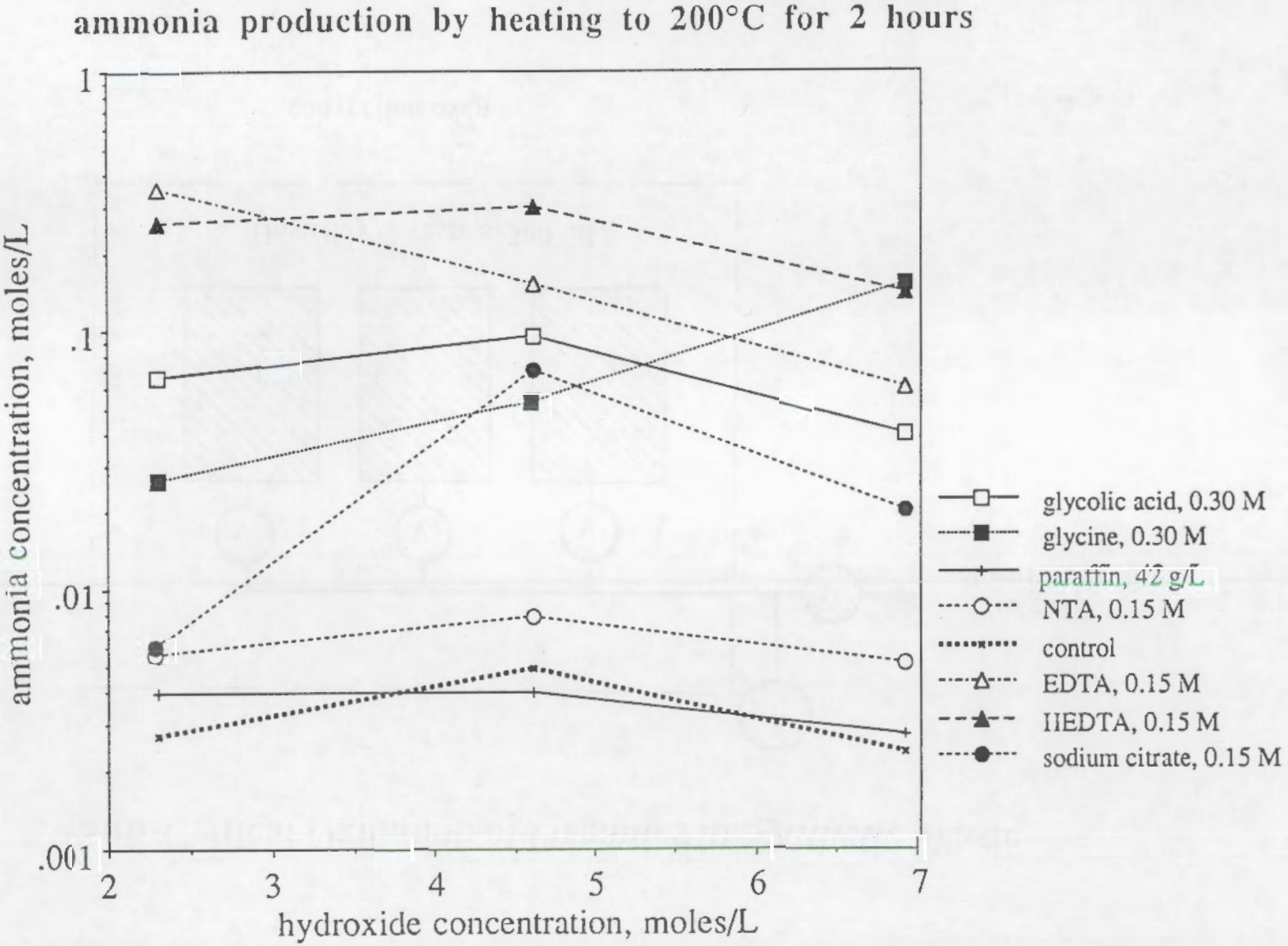
ammonia production by heating to 200°C for 2 hours
ammonia concentration, moles/L
1
.1
.01
.001
2
3
4
5
6
7
hydroxide concentration, moles/L
glycolic acid, 0.30 M
glycine, 0.30 M
paraffin, 42 g/L
NTA, 0.15 M
control
EDTA, 0.15 M
HEDTA, 0.15 M
sodium citrate, 0.15 M

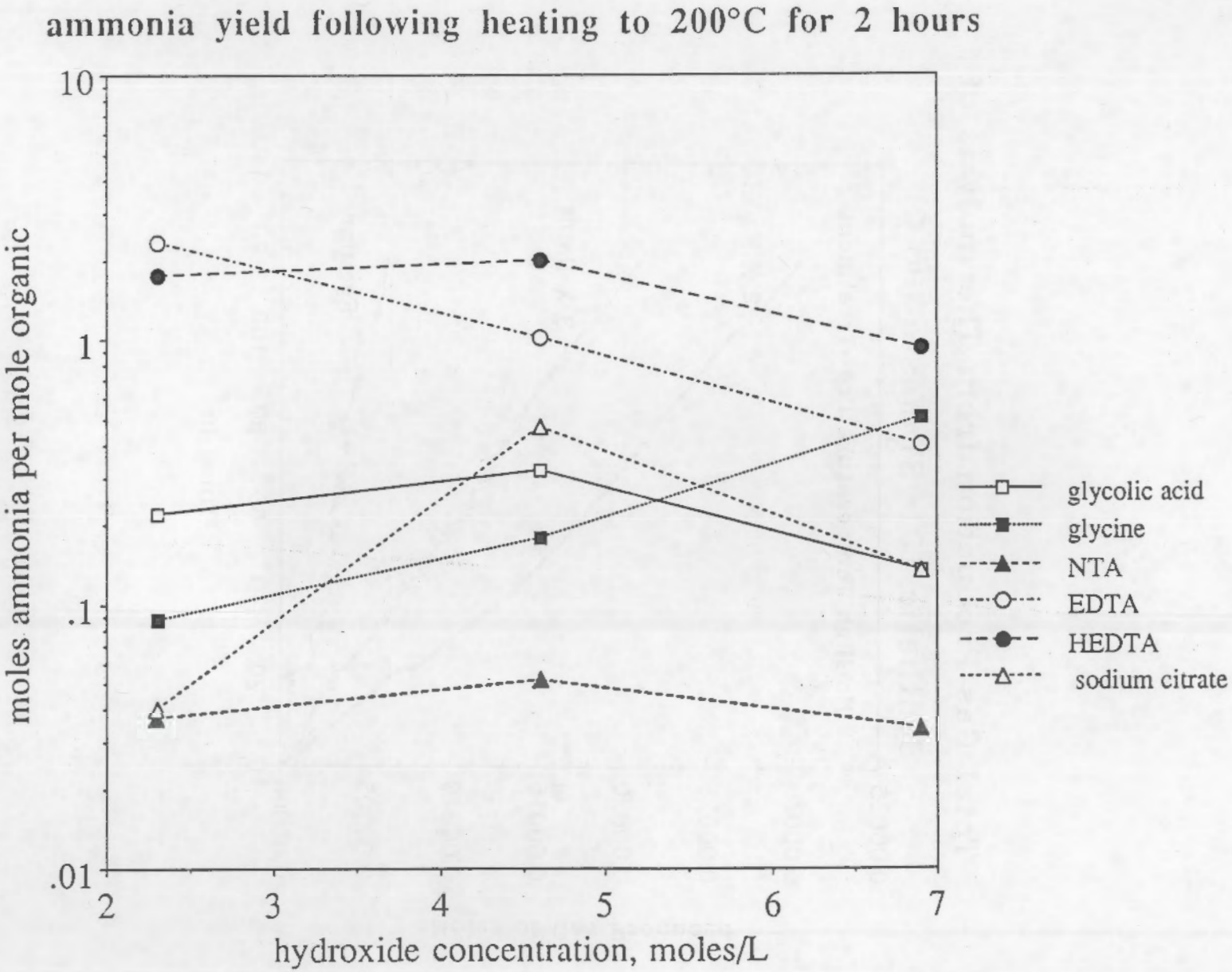
ammonia yield following heating to 200°C for 2 hours
10
1
.1
.01
moles ammonia per mole organic
2
3
4
5
6
7
hydroxide concentration, moles/L
glycolic acid
glycine
NTA
EDTA
HEDTA
sodium citrate

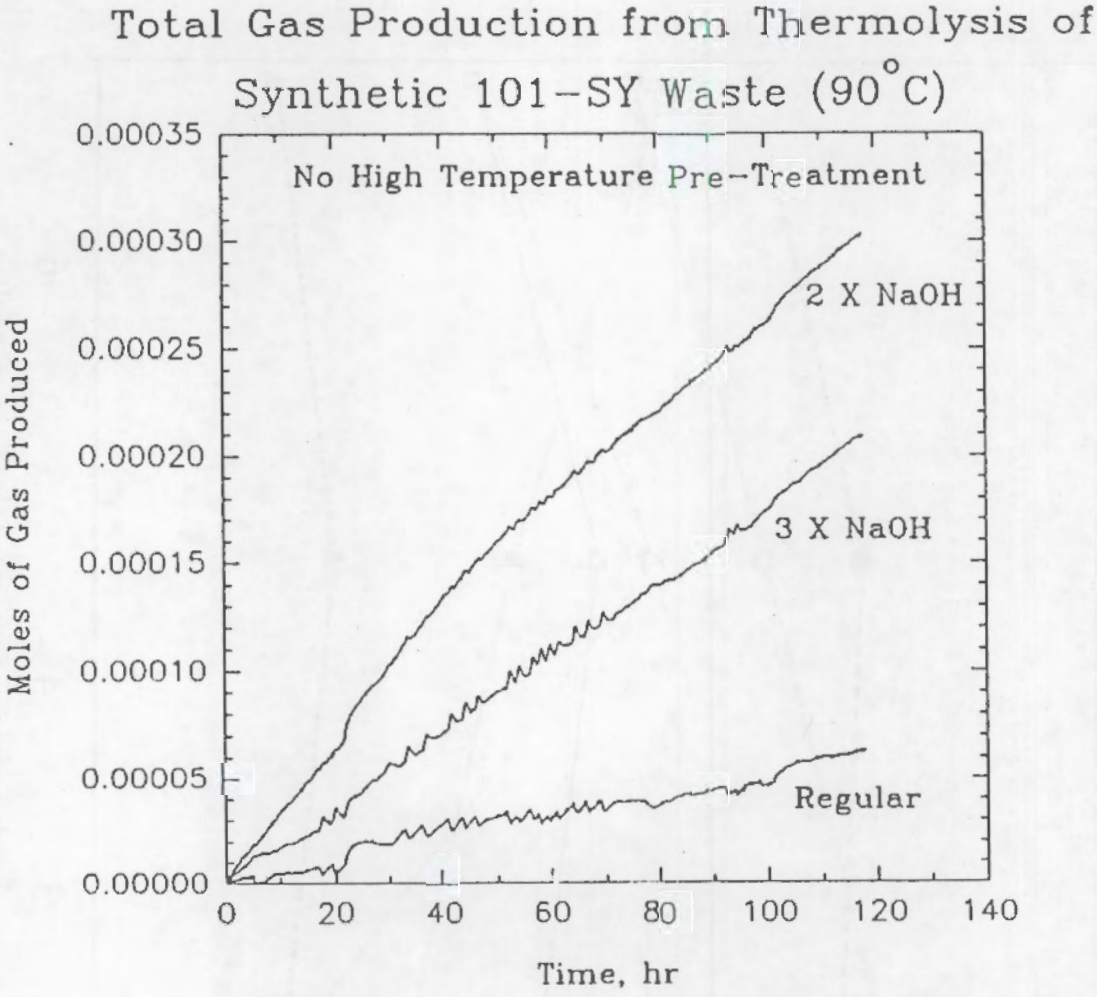
Total Gas Production from Thermolysis of
Synthetic 101-SY Waste (90°C)
No High Temperature Pre-Treatment
2 X NaOH
3 X NaOH
Regular
Moles of Gas Produced
0.00035
0.00030
0.00025
0.00020
0.00015
0.00010
0.00005
0.00000
0
20
40
60
80
100
120
140
Time, hr

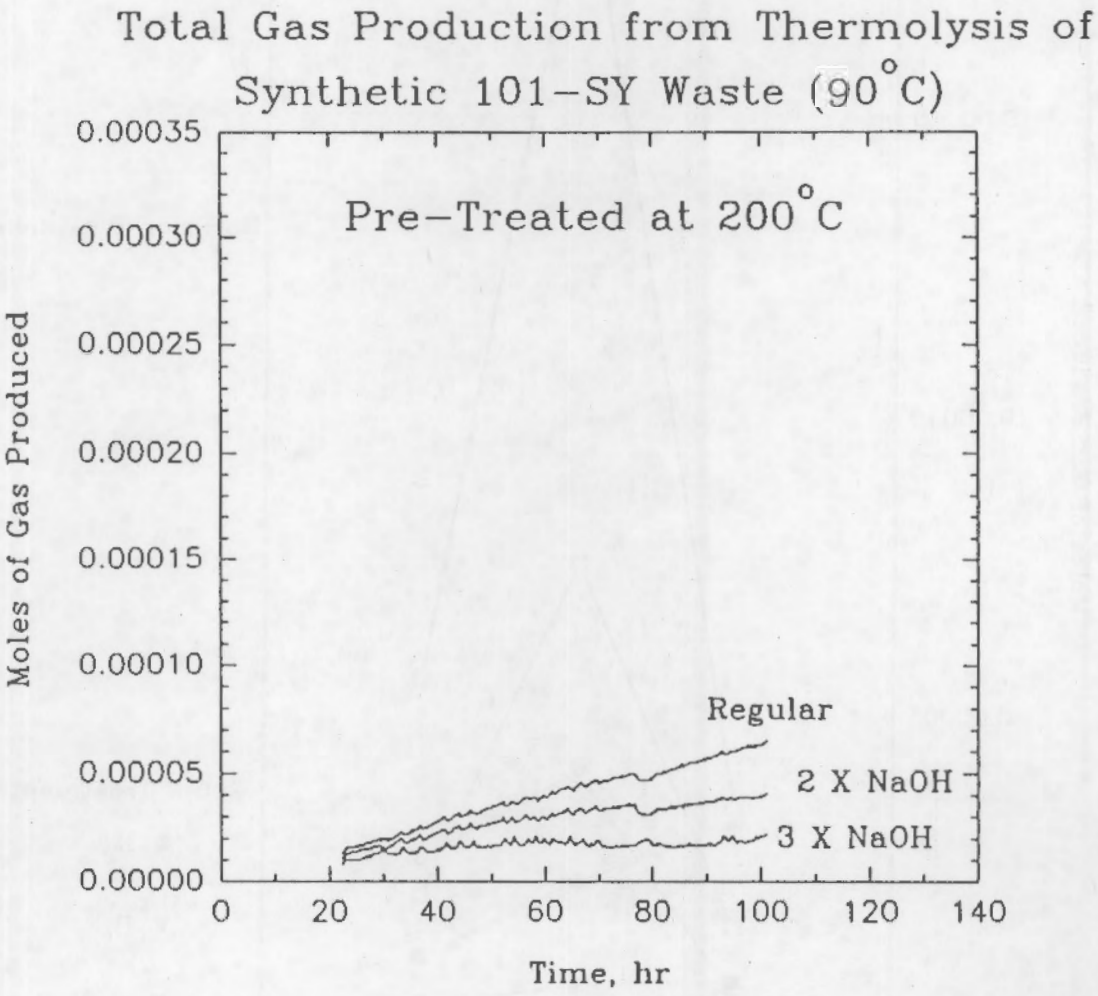
Total Gas Production from Thermolysis of
Synthetic 101-SY Waste (90°C)
Pre-Treated at 200°C
Moles of Gas Produced
0.00035
0.00030
0.00025
0.00020
0.00015
0.00010
0.00005
0.00000
0
20
40
60
80
100
120
140
Time, hr
Regular
2 X NaOH
3 X NaOH

(waste contains 0.15 molar HEDTA)

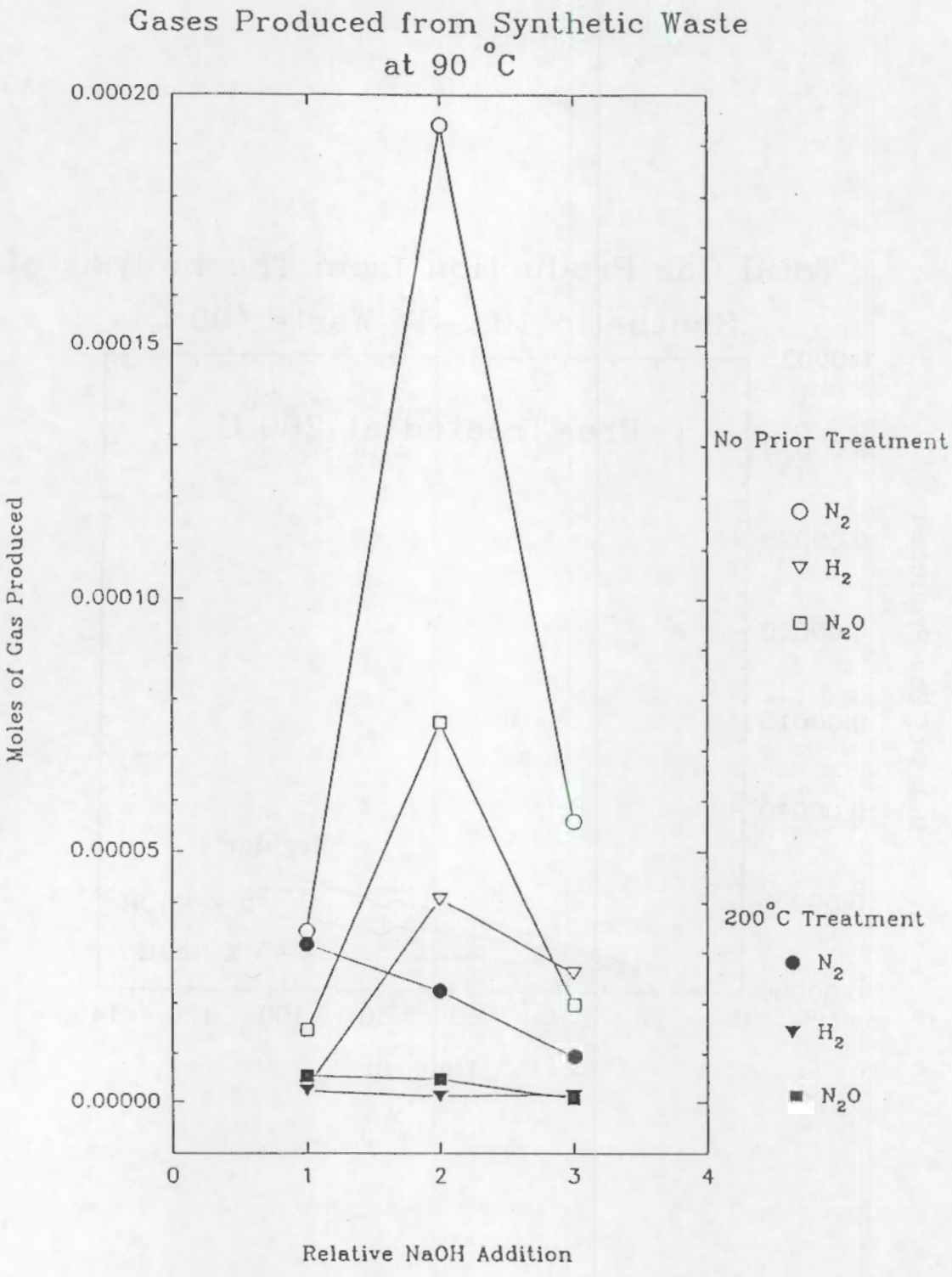

Subcritical Oxidation of Organics

Ammonia a principal degradation product

HEDTA, EDTA, glycine yield largest amounts

substantial amounts for some compounds that contain no organic nitrogen

Gas generation capacity (at tank temperature) much reduced by heat treatment to 200°C when additional base is present; heat treatment not effective in reducing without additional base

Gas compositions show a strong hydroxide ion dependence

Analysis of degradation products for representative samples being performed by J. Campbell; TOC being determined for all

Role of Hydroxide Ion on Rates and Stoichiometries of Gases Generated in Synthetic Wastes

Delegard (1980) showed a maxima in the initial reaction rate in synthetic wastes as a function of hydroxide ion concentration

Recent data suggests that hydroxide ion concentrations also affects the stoichiometry of gaseous products (hydroxide ion additions were suggested by H Babad as necessary for effective sub-critical oxidation of organics in synthetic wastes)

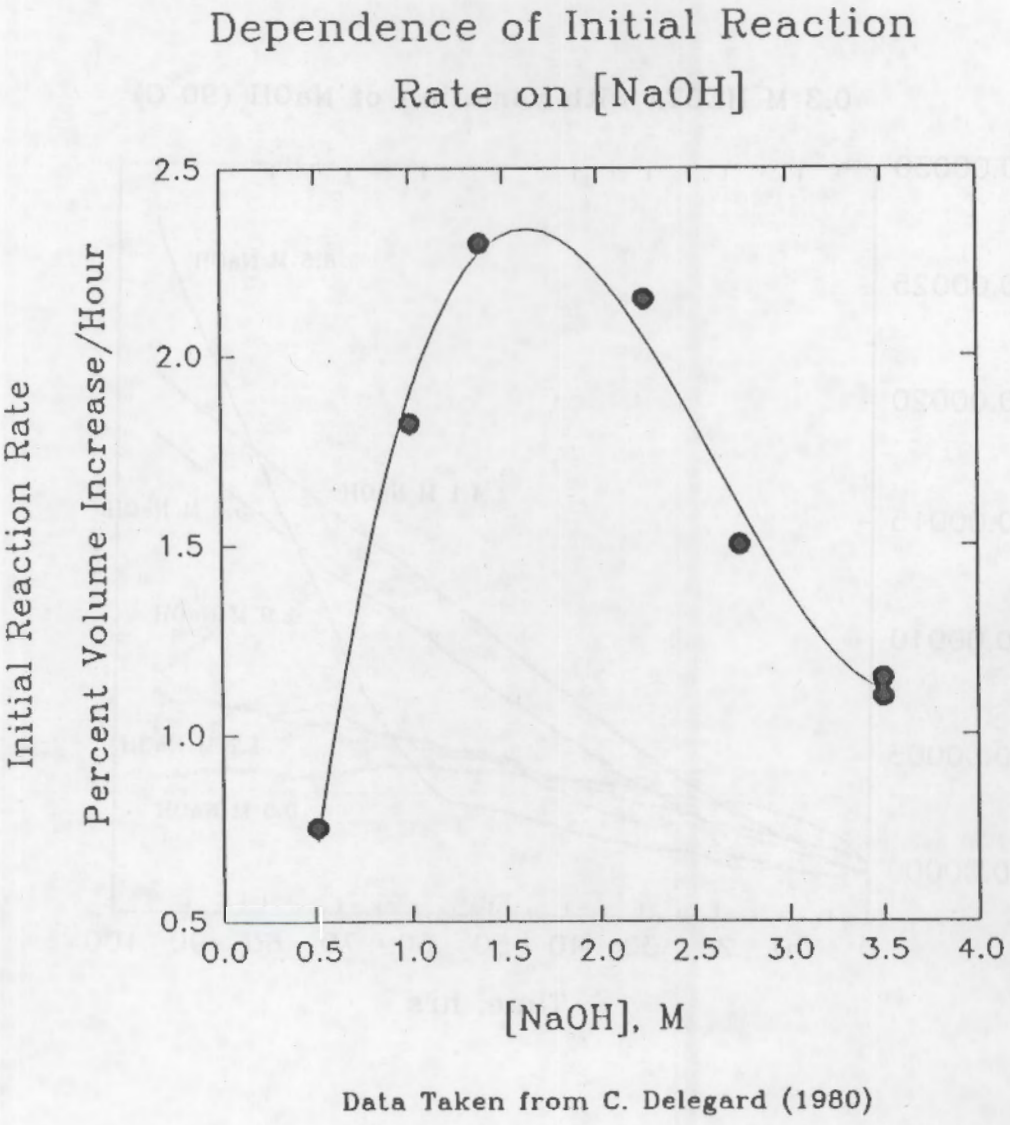

Data Taken from C. Delegard (1980)

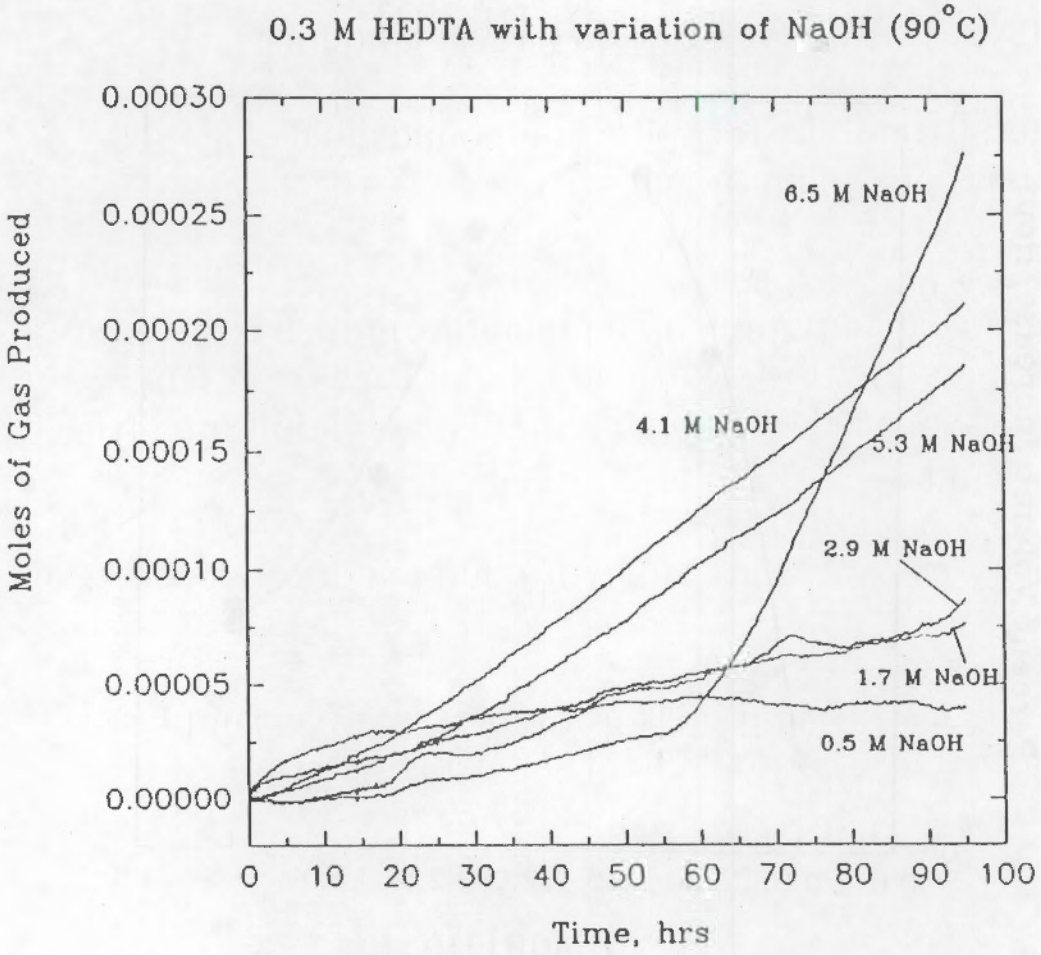
0.3 M HEDTA with variation of NaOH (90°C)
Moles of Gas Produced
0.00030
0.00025
0.00020
0.00015
0.00010
0.00005
0.00000
0
10
20
30
40
50
60
70
80
90
100
Time, hrs
6.5 M NaOH
4.1 M NaOH
5.3 M NaOH
2.9 M NaOH
1.7 M NaOH
0.5 M NaOH

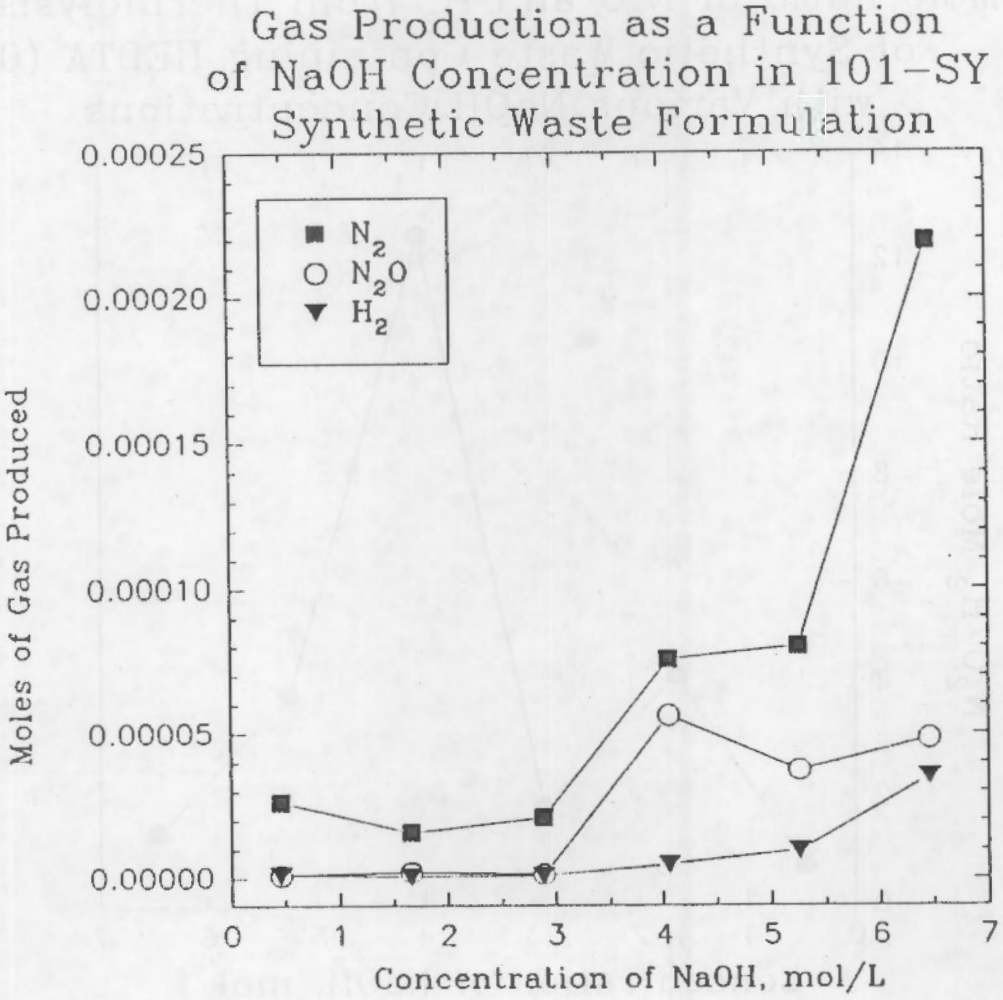
Gas Production as a Function
of NaOH Concentration in 101-SY
Synthetic Waste Formulation
Moles of Gas Produced
0.00025
0.00020
0.00015
0.00010
0.00005
0.00000
N2
N2O
H2
0
1
2
3
4
5
6
7
Concentration of NaOH, mol/L

Mole Ratio of N_2O and H_2 from Thermolysis (90°C) of Synthetic Waste Containing HEDTA (0.3M) with Various NaOH Concentrations

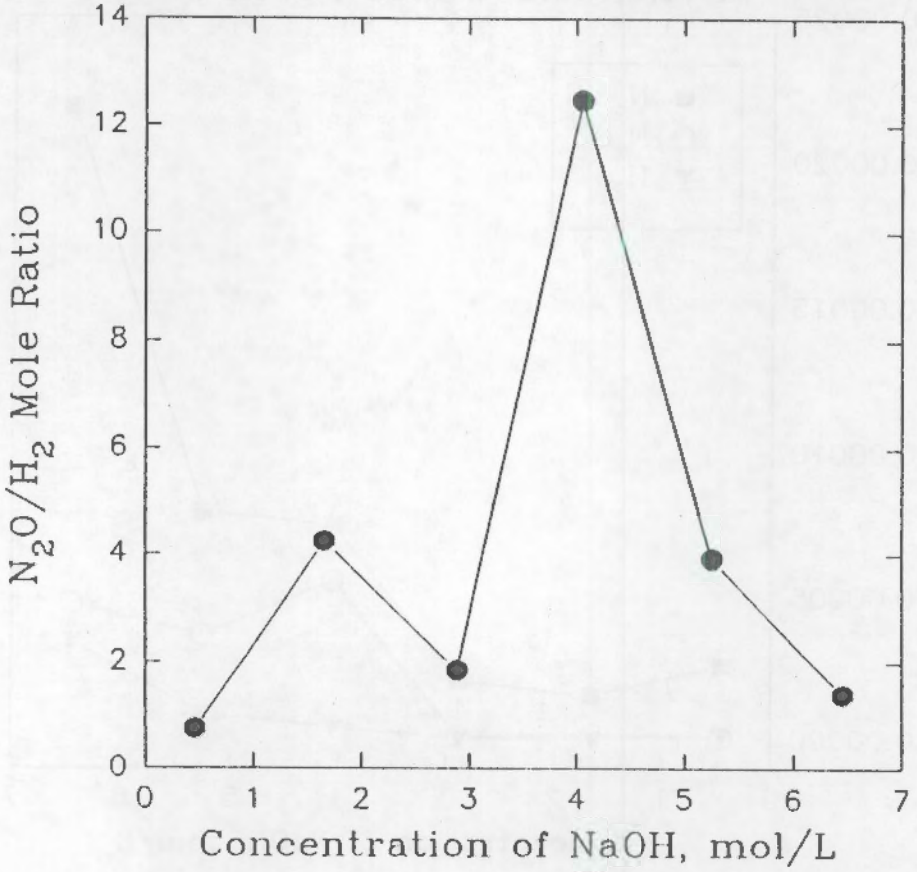

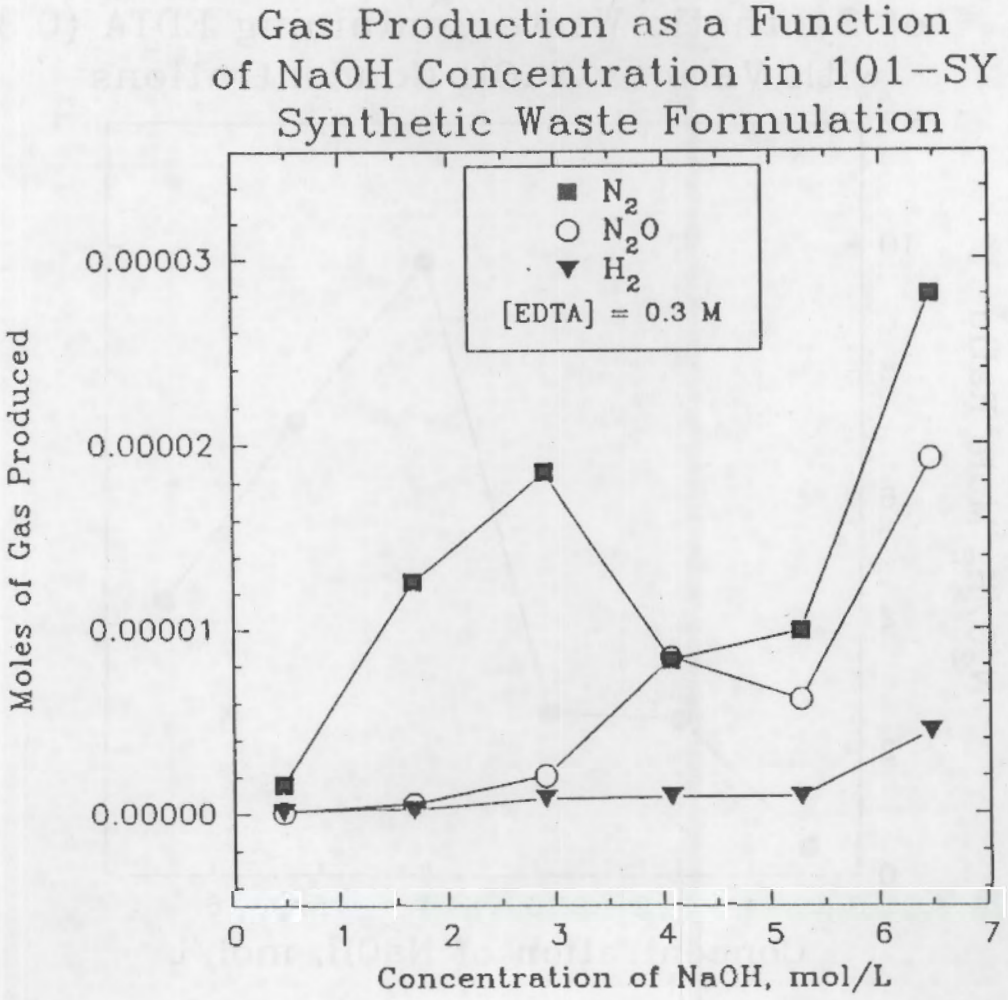
Gas Production as a Function
of NaOH Concentration in 101-SY
Synthetic Waste Formulation
N2
N2O
H2
[EDTA] = 0.3 M
Moles of Gas Produced
0.00003
0.00002
0.00001
0.00000
0
1
2
3
4
5
6
7
Concentration of NaOH, mol/L

Mole Ratio of N_2O and H_2 from Thermolysis (90°C) of Synthetic Waste Containing EDTA (0.3M) with Various NaOH Concentrations

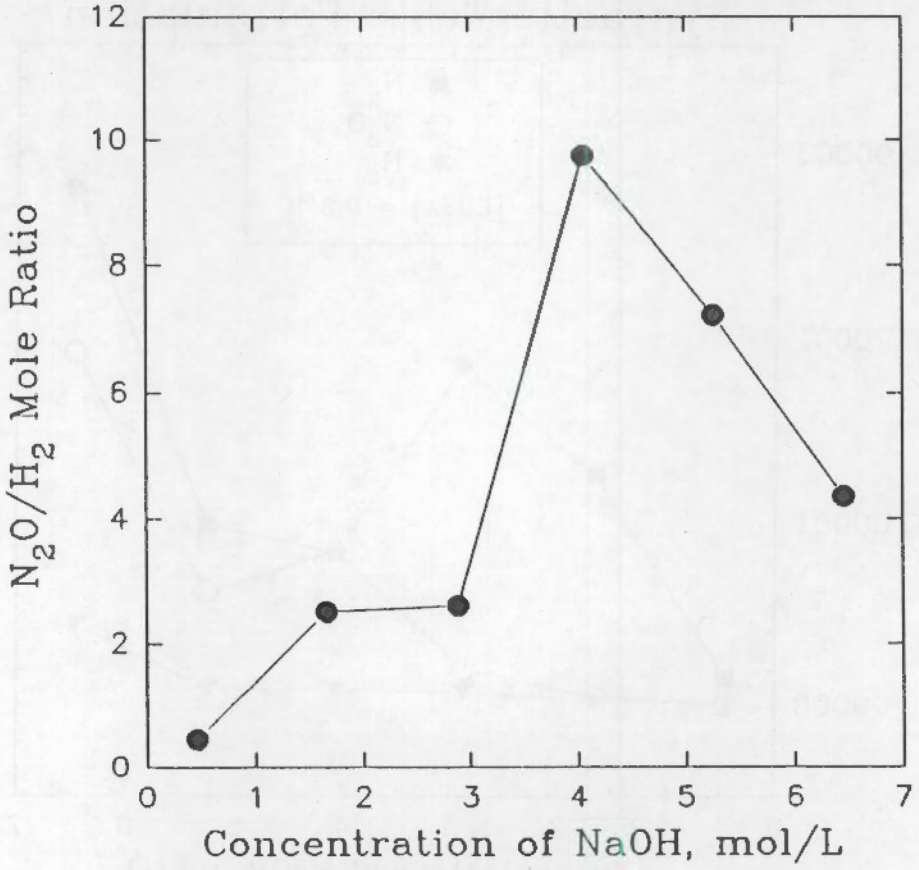

Role of Hydroxide Ion Concentration on Gas Product Stoichiometry

nitrous oxide/hydrogen ratios varied from 1-12 for wastes containing HEDTA, depending on the hydroxide ion concentration; similar results for EDTA (thermally-driven)

small change in hydroxide concentration corresponded to large changes in gas product stoichiometries

Appendix G

Radiolytic Generation of Gases from Synthetic Waste

Science Panel Meeting, March 25-27, 1992, Denver, CO

RADIOLYTIC GENERATION OF GASES FROM SYNTHETIC WASTE

Presented by:

Dan Meisel
Chemistry Division
Argonne National Laboratory
9700 S. Cass Av.
Argonne, IL 60439-4831
Tel. (708) 252 3472
Fax (708) 252 4992
MEISEL@ANLCHM

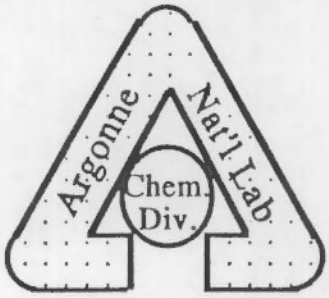

Issues to Discuss:

* How Well Do We Simulate the Tank (Radiolytically and Chemically)?
* Radiolytic Yields from Slurries
* Thermal Generation Rates from Preirradiated and Control Systems

Issue 1:

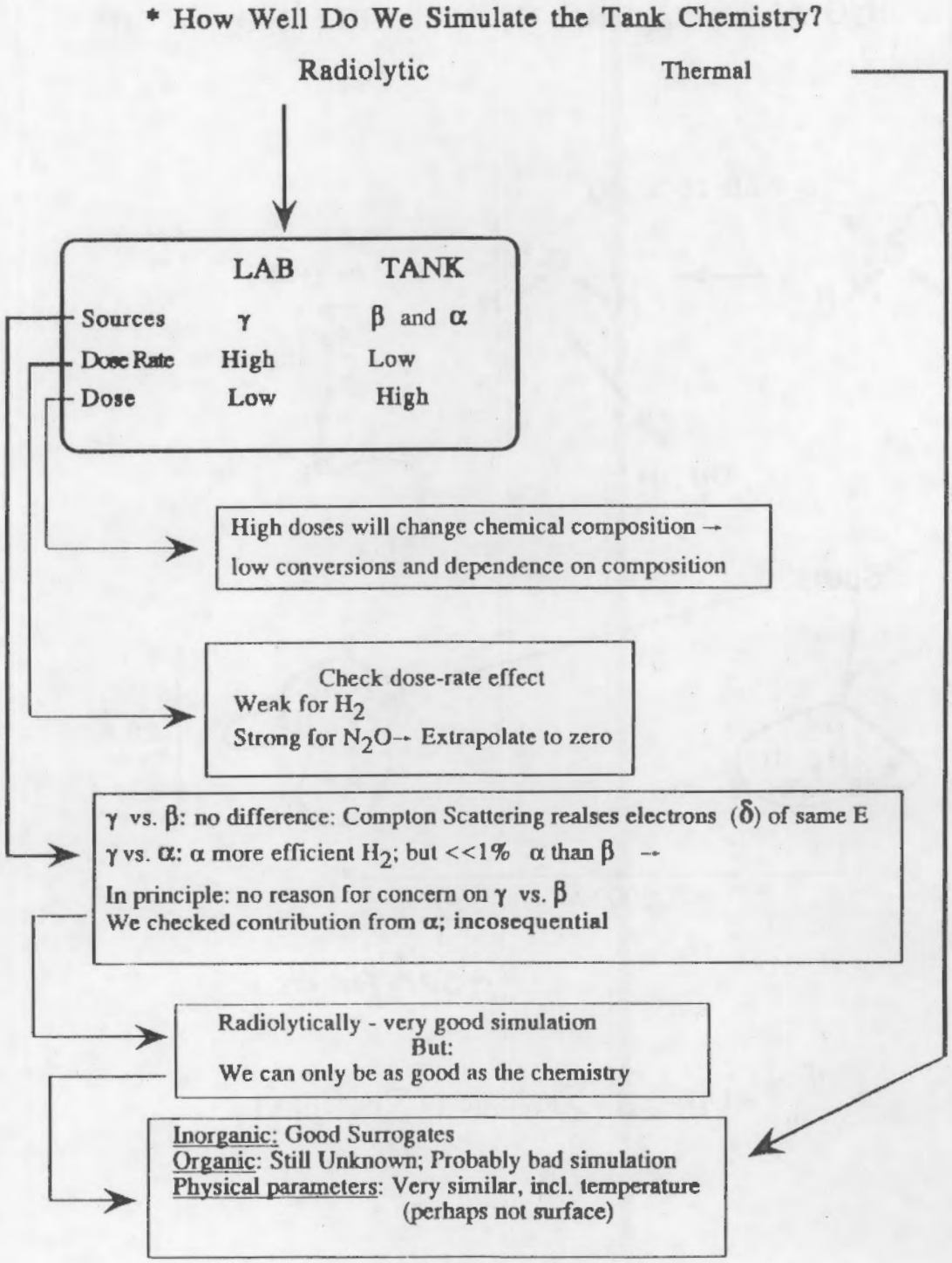
* How Well Do We Simulate the Tank Chemistry?
Radiolytic
Thermal
LAB
TANK
Sources
γ
β and α
Dose Rate
High
Low
Dose
Low
High
High doses will change chemical composition →
low conversions and dependence on composition
Check dose-rate effect
Weak for H_2
Strong for N_2O→ Extrapolate to zero
γ vs. β: no difference: Compton Scattering realses electrons (δ) of same E
γ vs. α: α more efficient H_2; but <<1% α than β →
In principle: no reason for concern on γ vs. β
We checked contribution from α; incosequential
Radiolytically - very good simulation
But:
We can only be as good as the chemistry
Inorganic: Good Surrogates
Organic: Still Unknown; Probably bad simulation
Physical parameters: Very similar, incl. temperature
(perhaps not surface)

(γ or β Radiation)

$$H_2O \wedge\!\!\!\rightarrow e^-_{aq} ; H^\bullet ; \underline{\underline{H_2}} \qquad OH ; H_2O_2; \qquad H^+$$

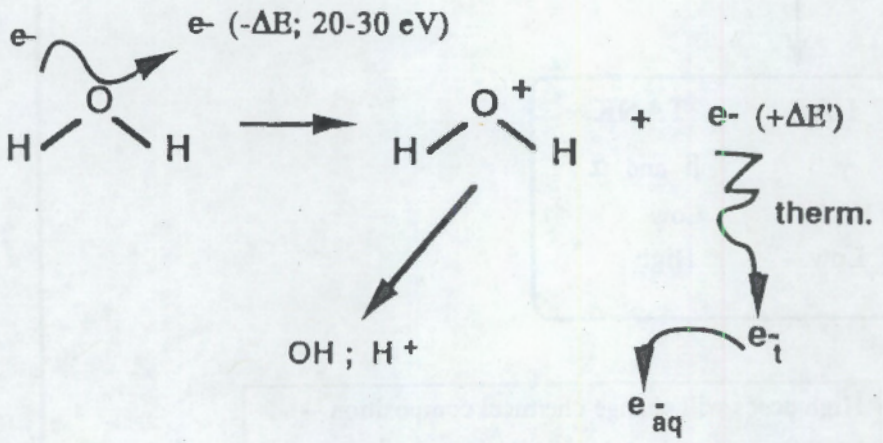

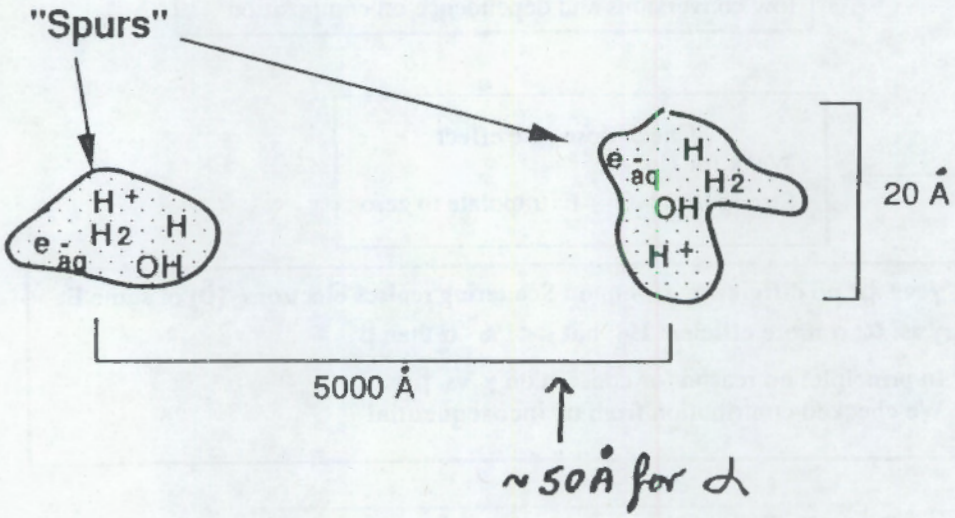

$$\frac{\partial[c_i]}{\partial t} = D_i\nabla^2[c_i] - \sum_j k_{ij}[c_i][c_j] + \sum_{j,k} k_{jk}[c_j][c_k]$$

Table C-1. Conversion table for radiation sources in tank 101-SY (from $\frac{\mu Ci}{l}$[a] to $\frac{krad}{min}$).

		Top Sample		Middle Sample		Bottom
		Slurry	Supernate	Slurry	Supernate	Slurry
		Transuranics				
^{241}Am	$\frac{\mu Ci}{l}$	< 16.5	<4.51	<15.1	<5.87	<14.8
	$\frac{krad}{min}$	$< 3.3 \times 10^{-6}$	$<0.9 \times 10^{-6}$	$<3.0 \times 10^{-6}$	$<1.2 \times 10^{-6}$	$<3.0 \times 10^{-6}$
^{239}Pu	$\frac{\mu Ci}{l}$	8.65	8.30	16.7	22.9	18.9
	$\frac{krad}{min}$	1.61×10^{-6}	1.55×10^{-6}	3.11×10^{-6}	4.26×10^{-6}	3.52×10^{-6}
^{235}U	$\frac{\mu Ci}{l}$	$< 4.0 \times 10^{-3}$		$<4.0 \times 10^{-6}$		$<7.1 \times 10^{-3}$
	$\frac{krad}{min}$	$<6.6 \times 10^{-10}$		--		11.2×10^{-10}
Total α[b]	$\frac{krad}{min}$	4.91×10^{-6}	2.45×10^{-6}	6.11×10^{-6}	5.46×10^{-6}	6.52×10^{-6}
		β & γ				
^{137}Cs	$\frac{\mu Ci}{l}$	2.88×10^{5}	3.08×10^{5}	6.95×10^{5}	7.24×10^{5}	6.66×10^{5}
	$\frac{krad}{min}$	0.87×10^{-2}	0.92×10^{-2}	2.09×10^{-2}	2.18×10^{-2}	2.01×10^{-2}
$^{89/90}Sr$	$\frac{\mu Ci}{l}$	$<6.05 \times 10^{3}$	6.81×10^{3}	7.20×10^{3}	3.24×10^{3}	1.35×10^{4}
	$\frac{krad}{min}$	0.44×10^{-4}	0.49×10^{-4}	0.52×10^{-4}	0.24×10^{-4}	0.98×10^{-2}
^{90}Y	$\frac{\mu Ci}{l}$	6.05×10^{3}	6.81×10^{3}	7.2×10^{3}	3.24×10^{3}	1.35×10^{4}
	$\frac{krad}{min}$	1.99×10^{-4}	2.24×10^{-4}	2.35×10^{-4}	1.07×10^{-4}	4.45×10^{-4}
^{99}Tc	$\frac{\mu Ci}{l}$	91.0	--	195	--	209
	$\frac{krad}{min}$	9.37×10^{-7}	--	2.01×10^{-6}		2.1×10^{-6}
Total $\beta + \gamma$[c]	$\frac{krad}{min}$	0.89×10^{-2}	0.951×10^{-2}	2.13×10^{-2}	2.19×10^{-2}	2.06×10^{-2}
Ratio $\frac{\alpha}{\beta+\gamma}$		5.5×10^{-4}	2.58×10^{-4}	2.88×10^{-4}	2.49×10^{-4}	3.16×10^{-4}

[a] Values in $\frac{\mu Ci}{l}$ were taken from Table 1, p. 9 in document 86431-91-008.

[b] Sum of the above α sources.

[c] Sum of the above $\beta + \gamma$ sources.

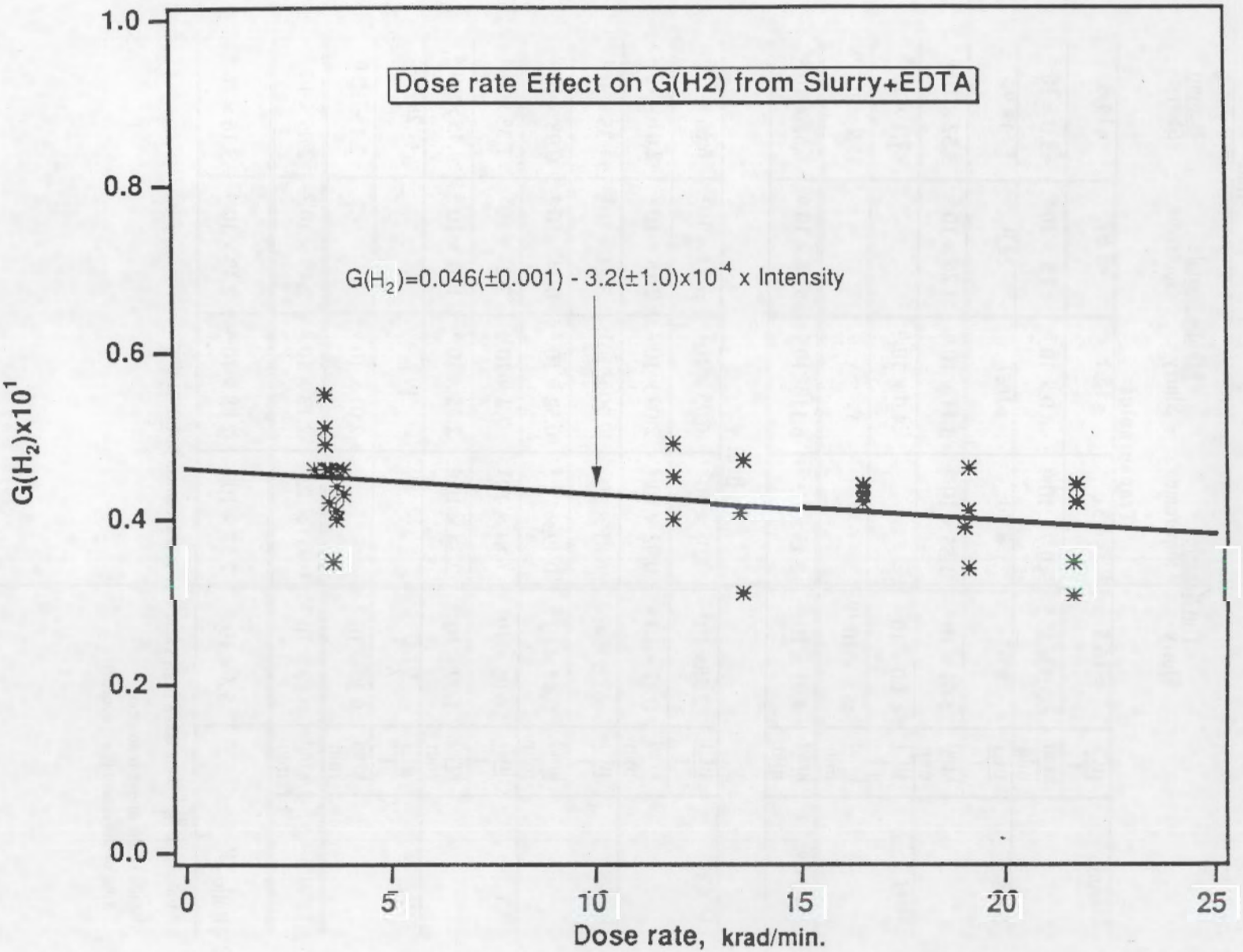
Dose rate Effect on G(H2) from Slurry+EDTA
G(H2)=0.046(±0.001) - 3.2(±1.0)x10^-4 x Intensity
G(H2)x10^1
1.0
0.8
0.6
0.4
0.2
0.0
0
5
10
15
20
25
Dose rate, krad/min.

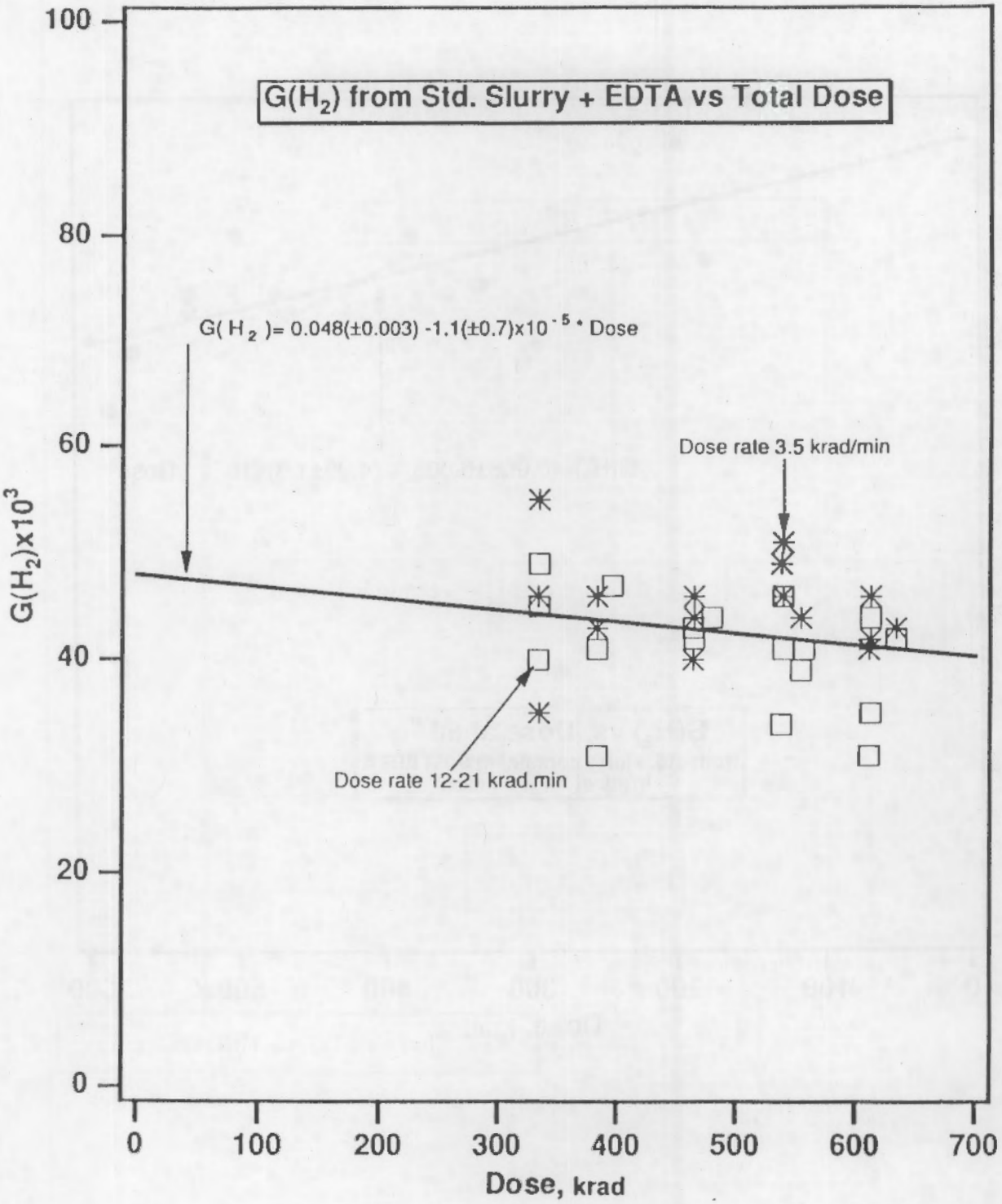
G(H2) from Std. Slurry + EDTA vs Total Dose
G(H 2)= 0.048(±0.003) -1.1(±0.7)x10 -5 * Dose
Dose rate 3.5 krad/min
Dose rate 12-21 krad.min
G(H2)x10^3
Dose, krad
100
80
60
40
20
0
0
100
200
300
400
500
600
700

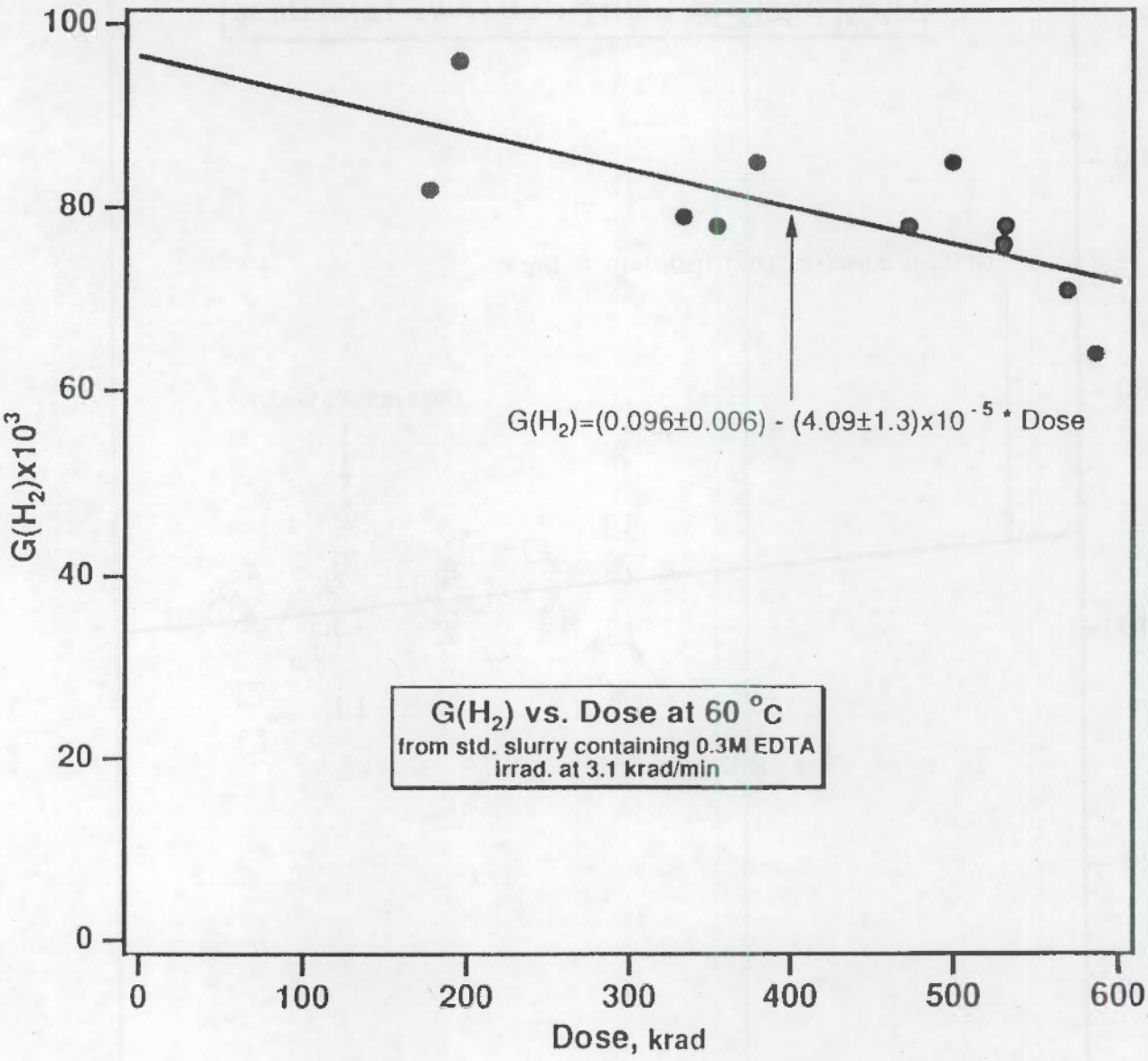
100
80
60
40
20
0
G(H2)x10^3
0
100
200
300
400
500
600
Dose, krad
G(H2)=(0.096±0.006) - (4.09±1.3)x10^-5 * Dose
G(H2) vs. Dose at 60 °C
from std. slurry containing 0.3M EDTA
irrad. at 3.1 krad/min

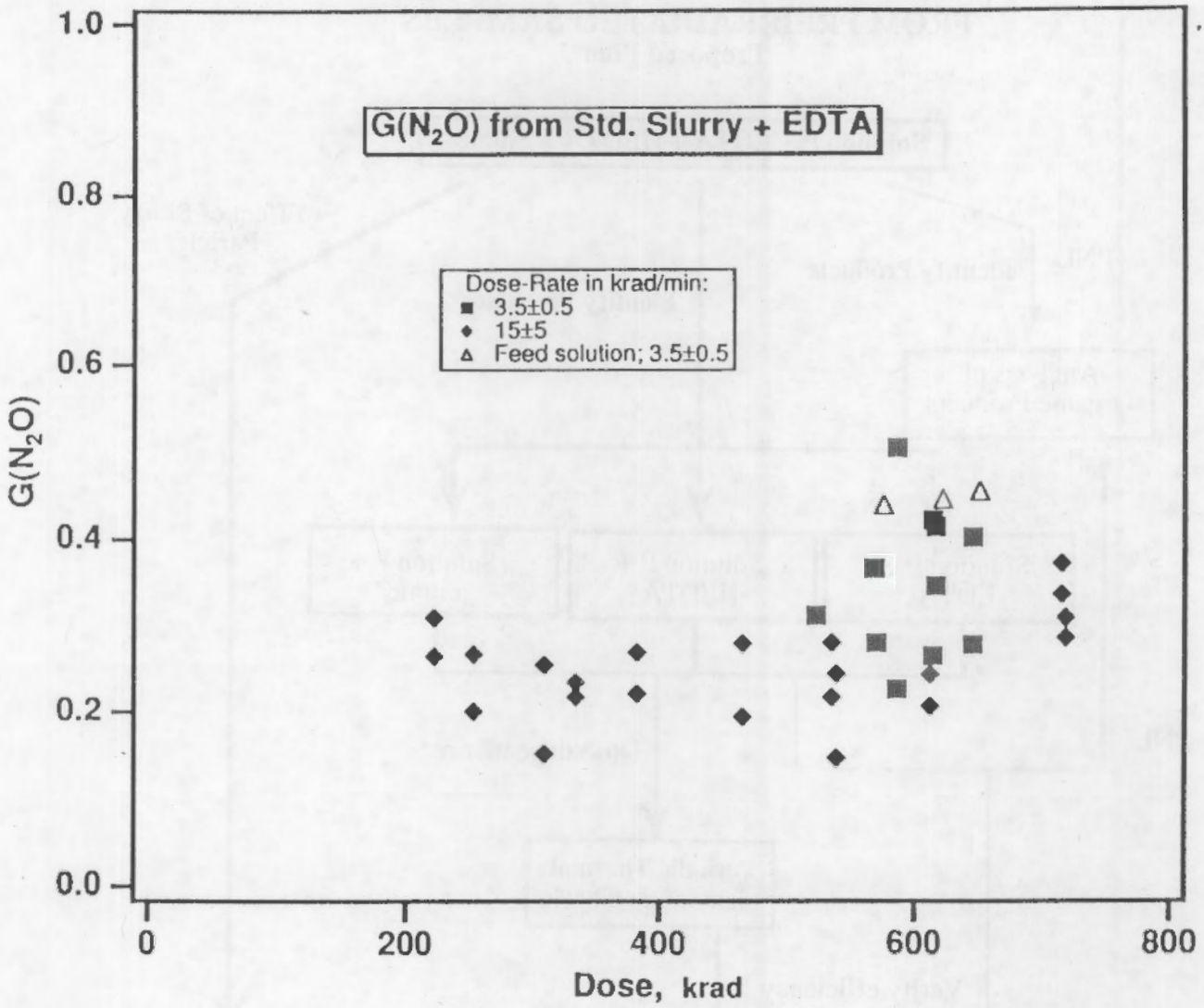
G(N2O) from Std. Slurry + EDTA
Dose-Rate in krad/min:
3.5±0.5
15±5
Feed solution; 3.5±0.5
G(N2O)
1.0
0.8
0.6
0.4
0.2
0.0
0
200
400
600
800
Dose, krad

ENHANCED THERMAL GENERATION FROM PREIRRADIATED SAMPLES

Proposed Plan

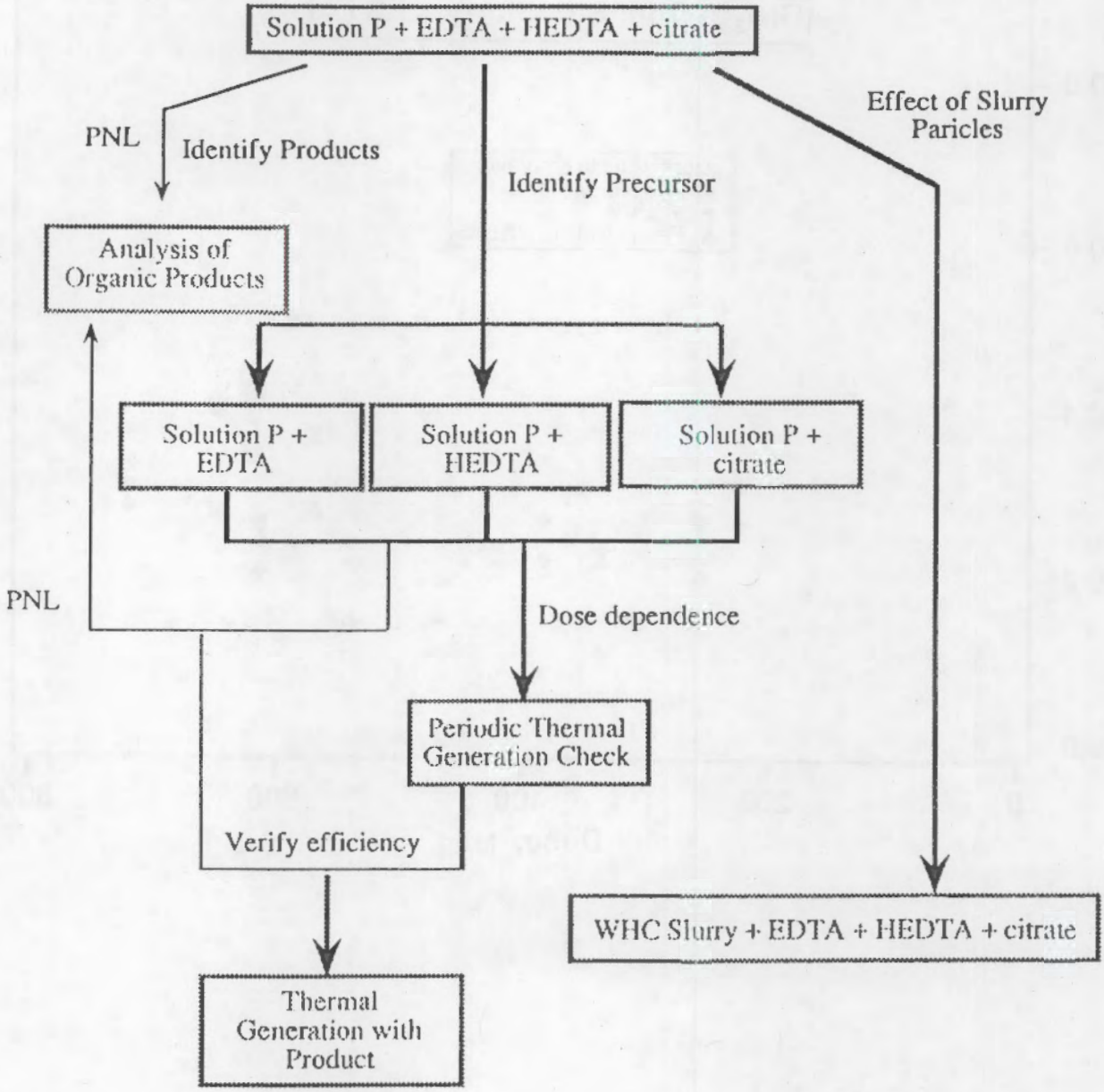

ENHANCED THERMAL GENERATION FROM PREIRRADIATED SAMPLES

Results To Date 3/20/92

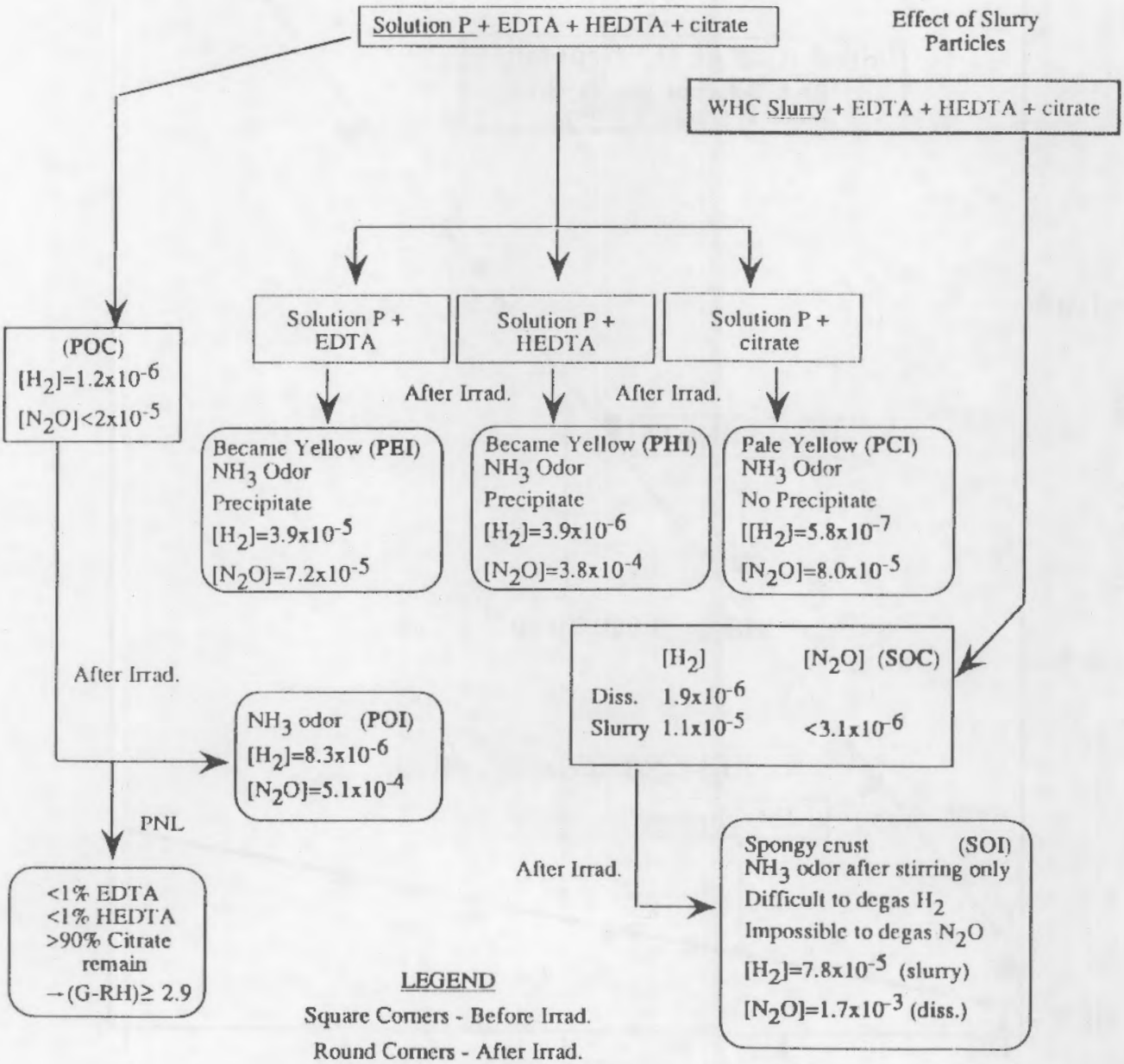

LEGEND

Square Corners - Before Irrad.

Round Corners - After Irrad.

Initial Rates are in mM/min • L)

@ 60°C

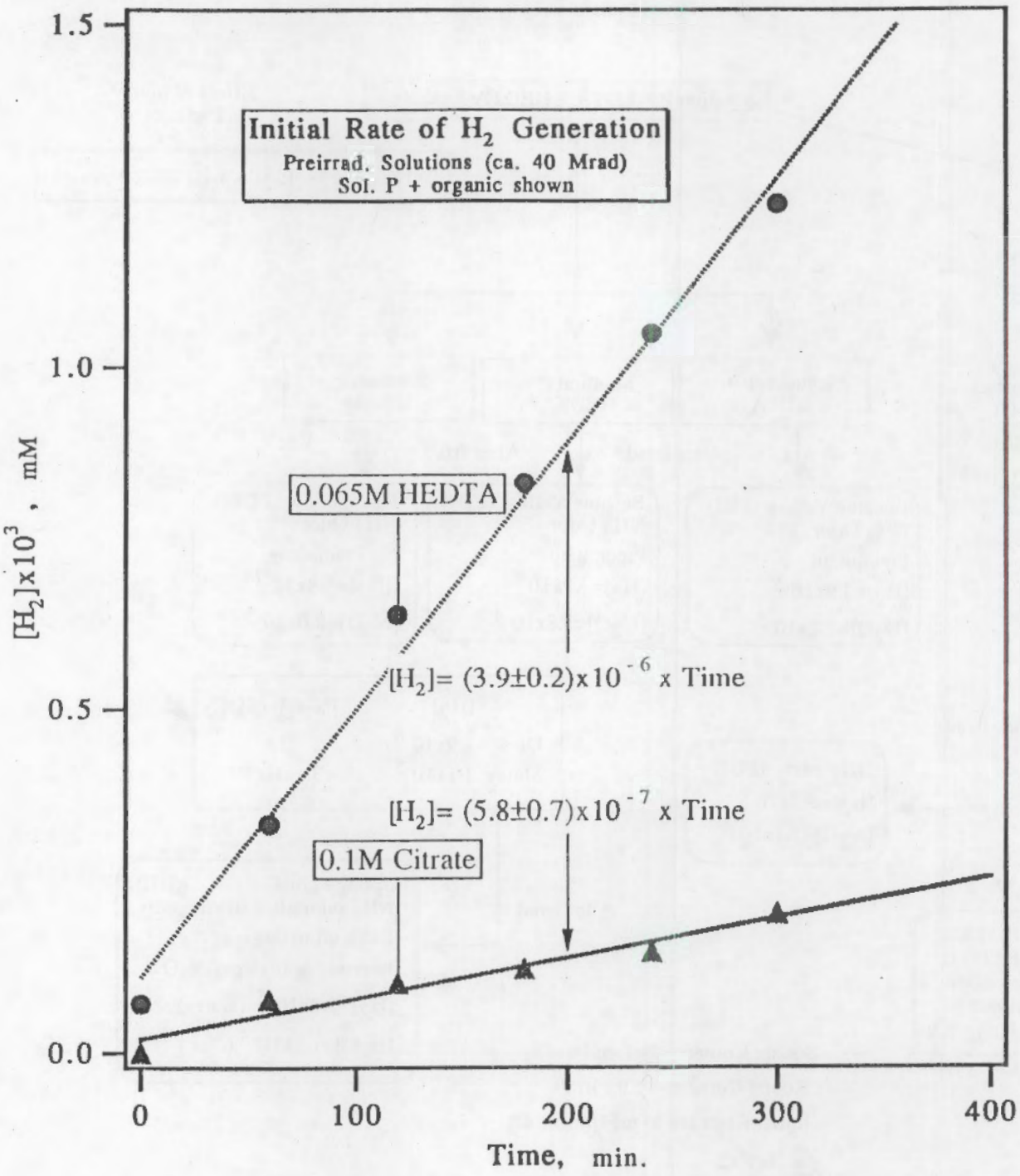
Initial Rate of H_2 Generation
Preirrad. Solutions (ca. 40 Mrad)
Sol. P + organic shown
0.065M HEDTA
$[H_2]= (3.9\pm0.2)\times10^{-6}$ x Time
$[H_2]= (5.8\pm0.7)\times10^{-7}$ x Time
0.1M Citrate
$[H_2]\times10^3$, mM
1.5
1.0
0.5
0.0
0
100
200
300
400
Time, min.

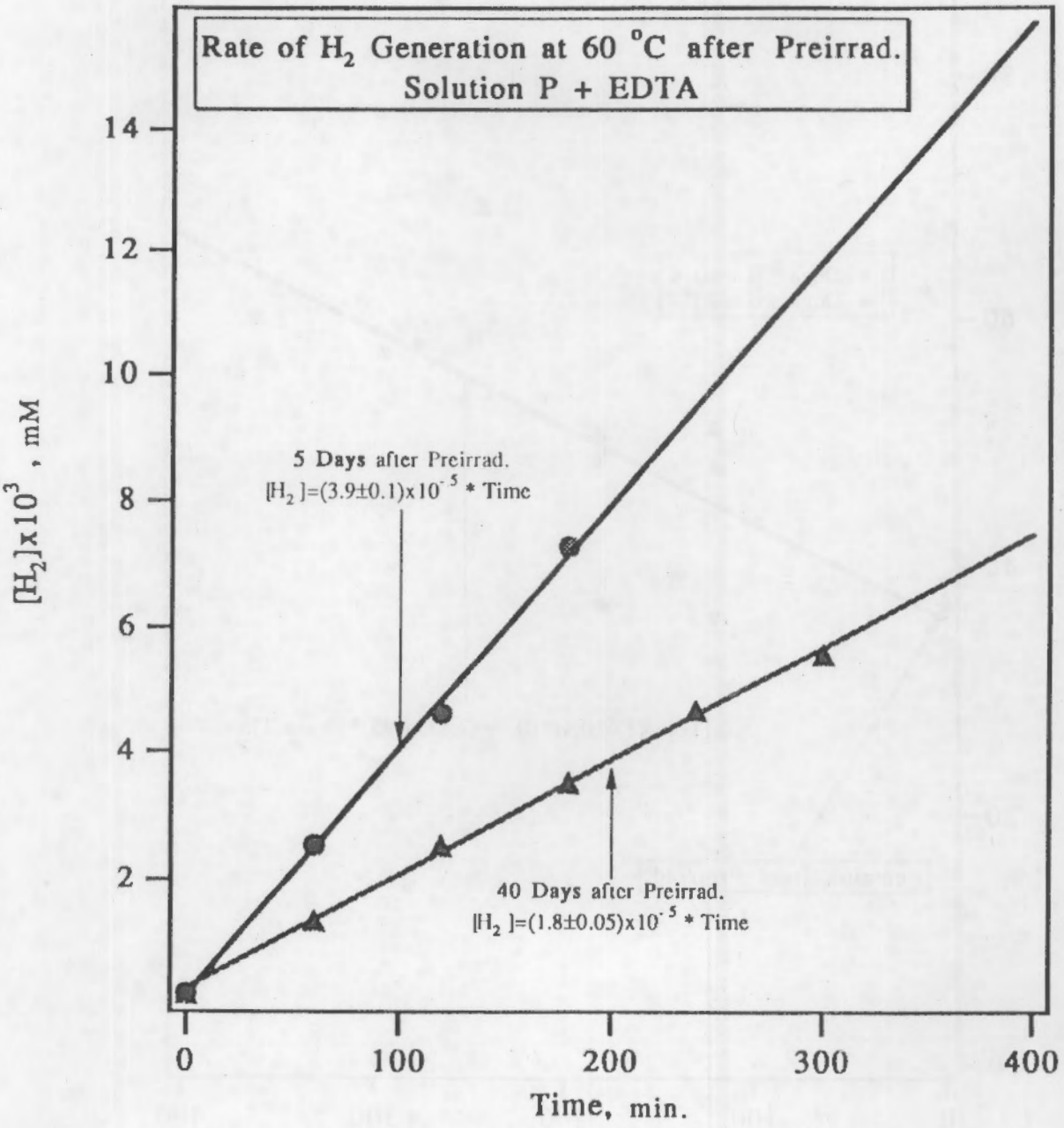
Rate of H_2 Generation at 60 °C after Preirrad.
Solution P + EDTA
14
12
10
8
6
4
2
$[H_2]x10^3$, mM
5 Days after Preirrad.
$[H_2]=(3.9\pm0.1)x10^{-5}$ * Time
40 Days after Preirrad.
$[H_2]=(1.8\pm0.05)x10^{-5}$ * Time
0
100
200
300
400
Time, min.

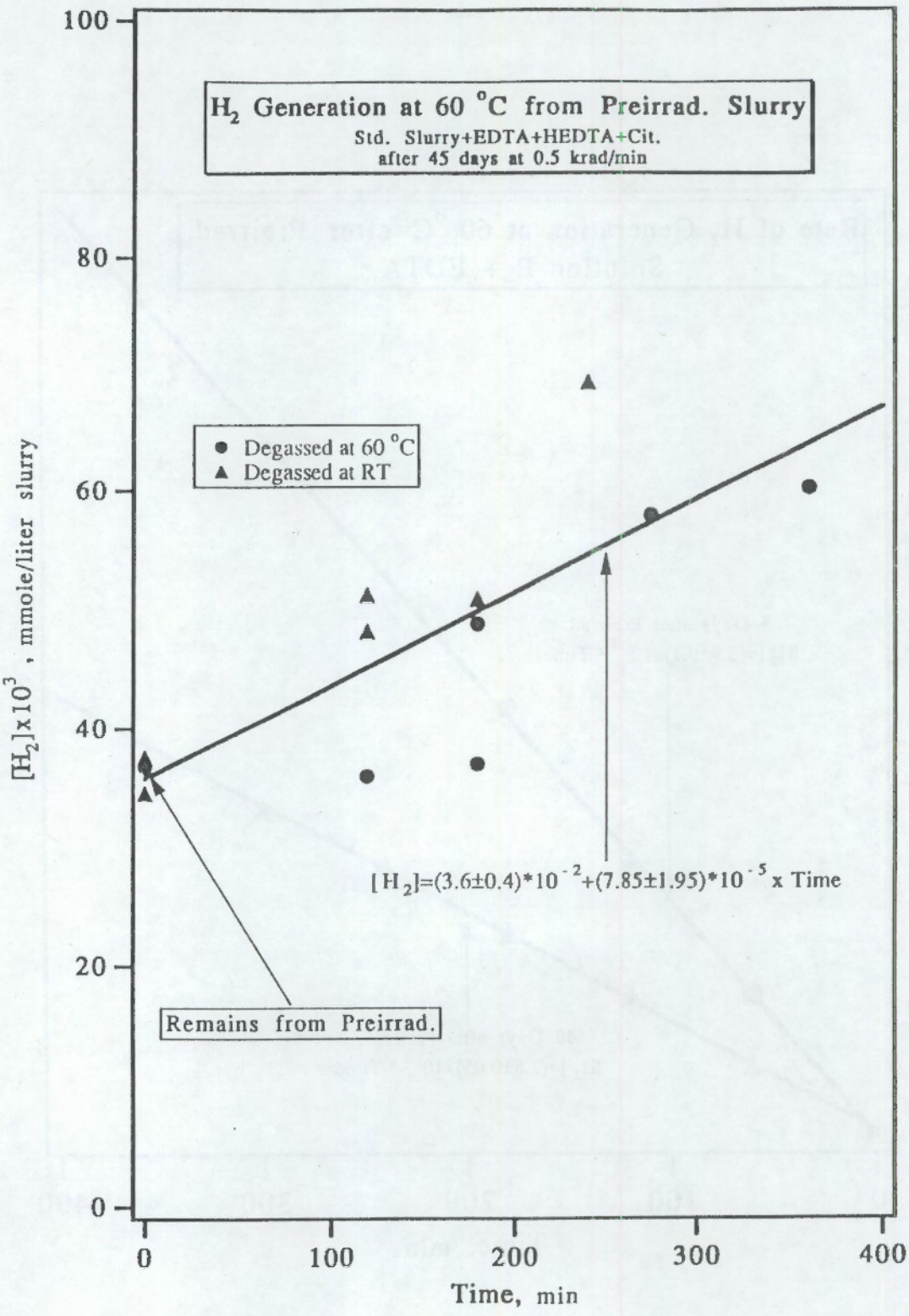
H_2 Generation at 60 °C from Preirrad. Slurry
Std. Slurry+EDTA+HEDTA+Cit.
after 45 days at 0.5 krad/min
Degassed at 60 °C
Degassed at RT
$[H_2]=(3.6\pm0.4)*10^{-2}+(7.85\pm1.95)*10^{-5}$ x Time
Remains from Preirrad.
$[H_2]x10^3$, mmole/liter slurry
Time, min
0
20
40
60
80
100
0
100
200
300
400

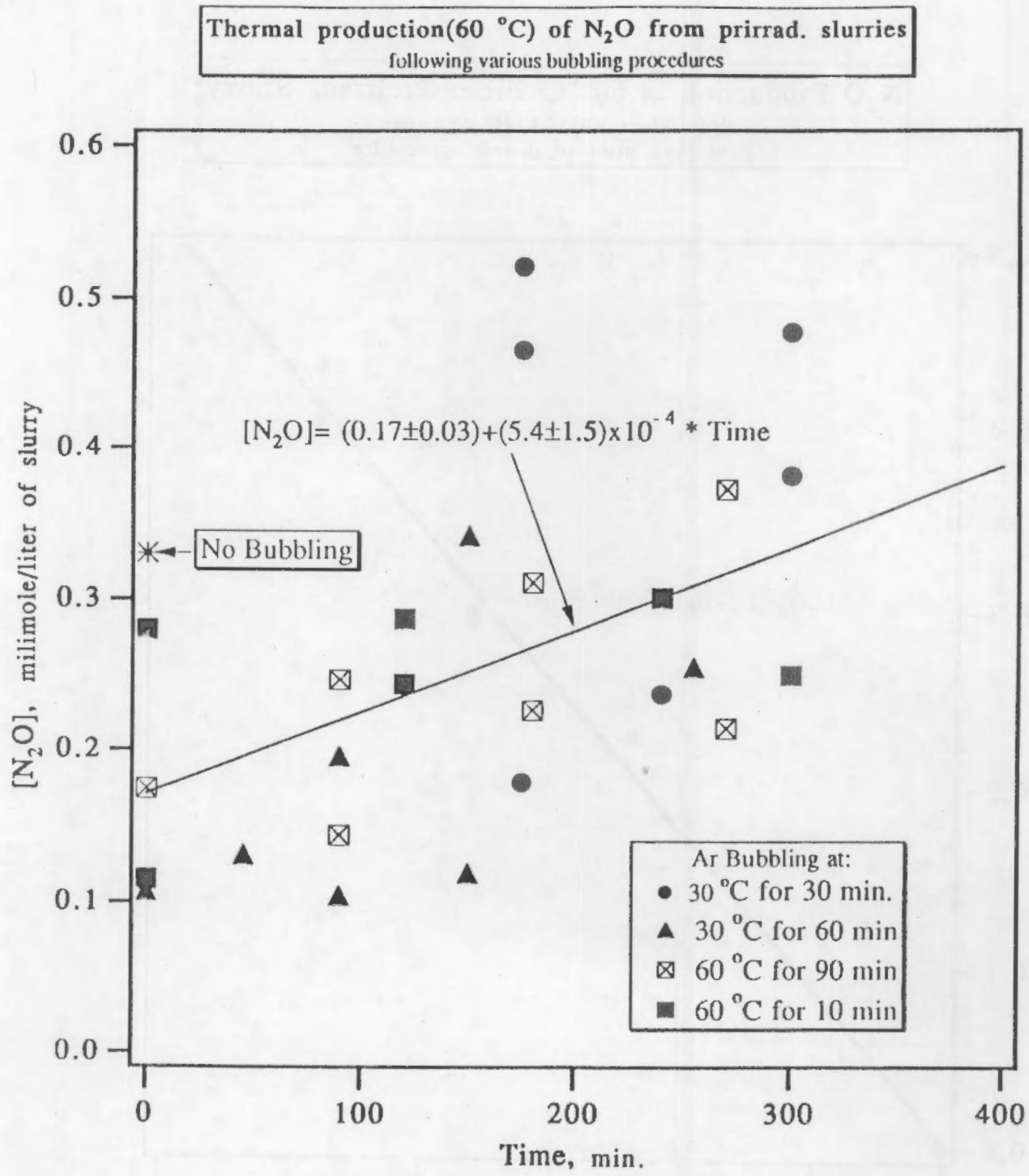
Thermal production(60 °C) of N_2O from prirrad. slurries
following various bubbling procedures
$[N_2O]= (0.17\pm0.03)+(5.4\pm1.5)x10^{-4}$ * Time
No Bubbling
Ar Bubbling at:
30 °C for 30 min.
30 °C for 60 min
60 °C for 90 min
60 °C for 10 min
$[N_2O]$, milimole/liter of slurry
Time, min.
0.0
0.1
0.2
0.3
0.4
0.5
0.6
0
100
200
300
400

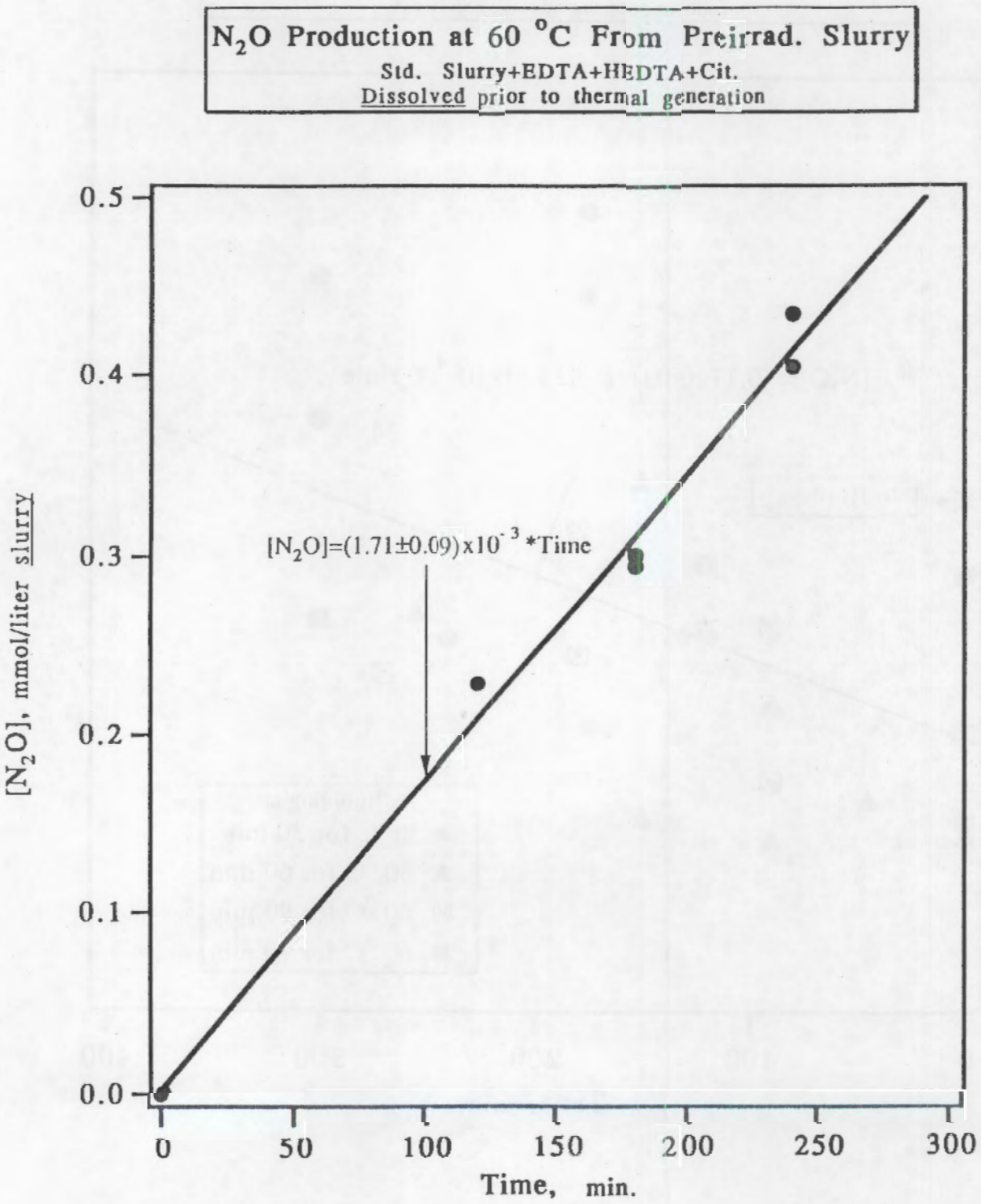
N_2O Production at 60 °C From Preirrad. Slurry
Std. Slurry+EDTA+HEDTA+Cit.
Dissolved prior to thermal generation
$[N_2O]=(1.71\pm0.09)\times10^{-3}$ *Time
$[N_2O]$, mmol/liter slurry
0.0
0.1
0.2
0.3
0.4
0.5
0
50
100
150
200
250
300
Time, min.

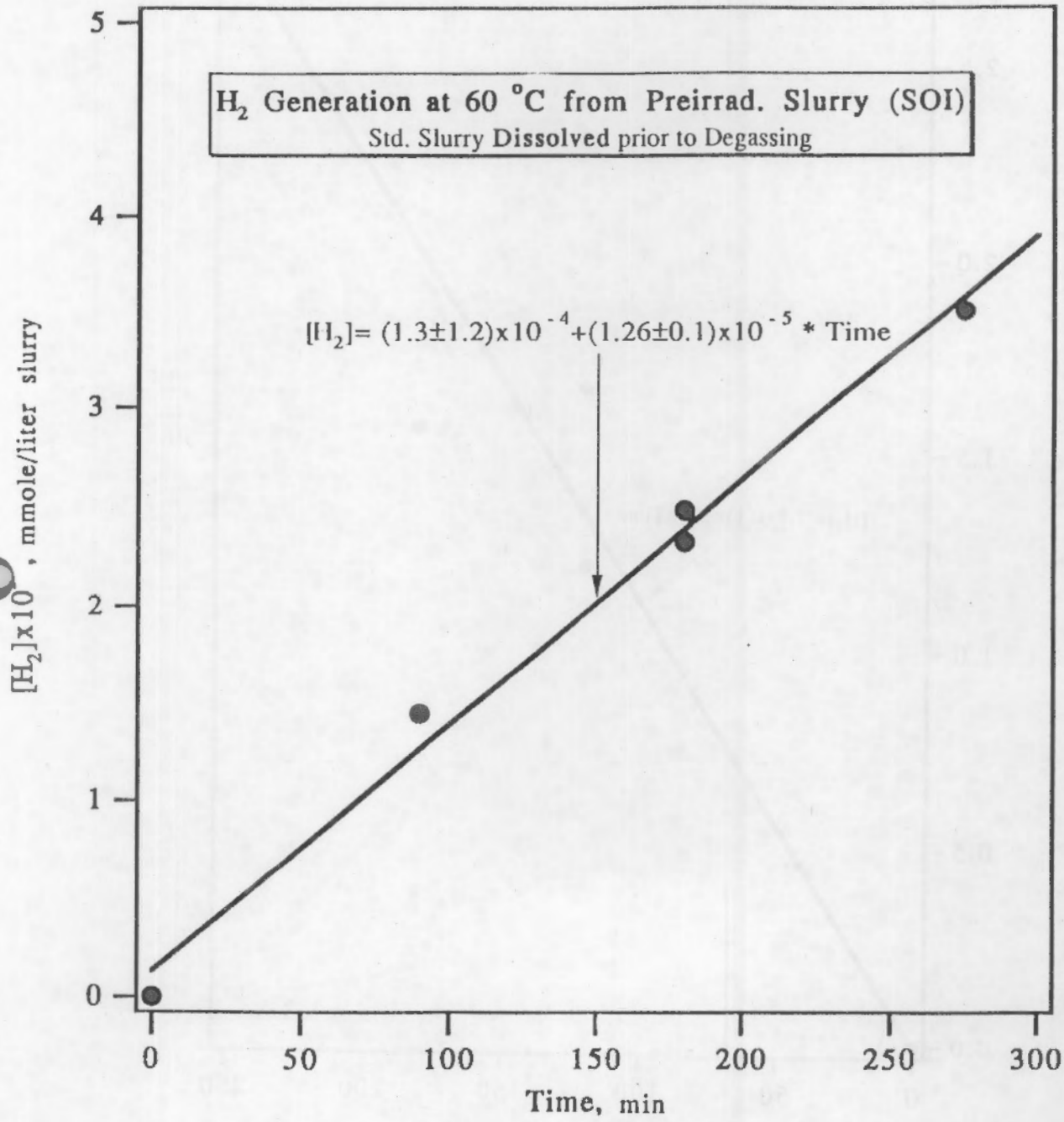
H_2 Generation at 60 °C from Preirrad. Slurry (SOI)
Std. Slurry Dissolved prior to Degassing
$[H_2]= (1.3\pm1.2)\times10^{-4}+(1.26\pm0.1)\times10^{-5}$ * Time
$[H_2]\times10$, mmole/liter slurry
Time, min
0
1
2
3
4
5
0
50
100
150
200
250
300

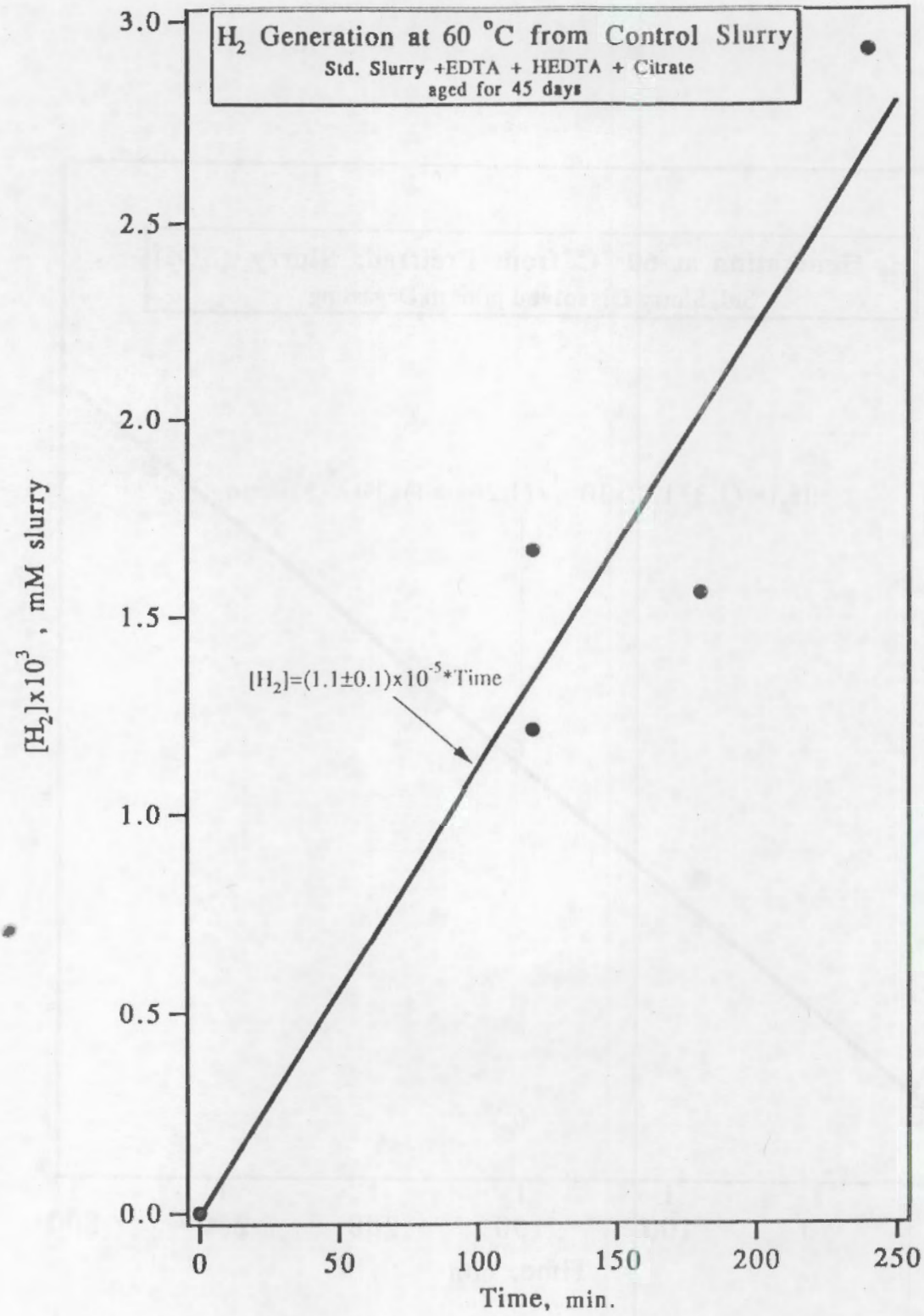
H2 Generation at 60 °C from Control Slurry
Std. Slurry +EDTA + HEDTA + Citrate
aged for 45 days
[H2]=(1.1±0.1)x10-5*Time
[H2]x10^3 , mM slurry
Time, min.
3.0
2.5
2.0
1.5
1.0
0.5
0.0
0
50
100
150
200
250

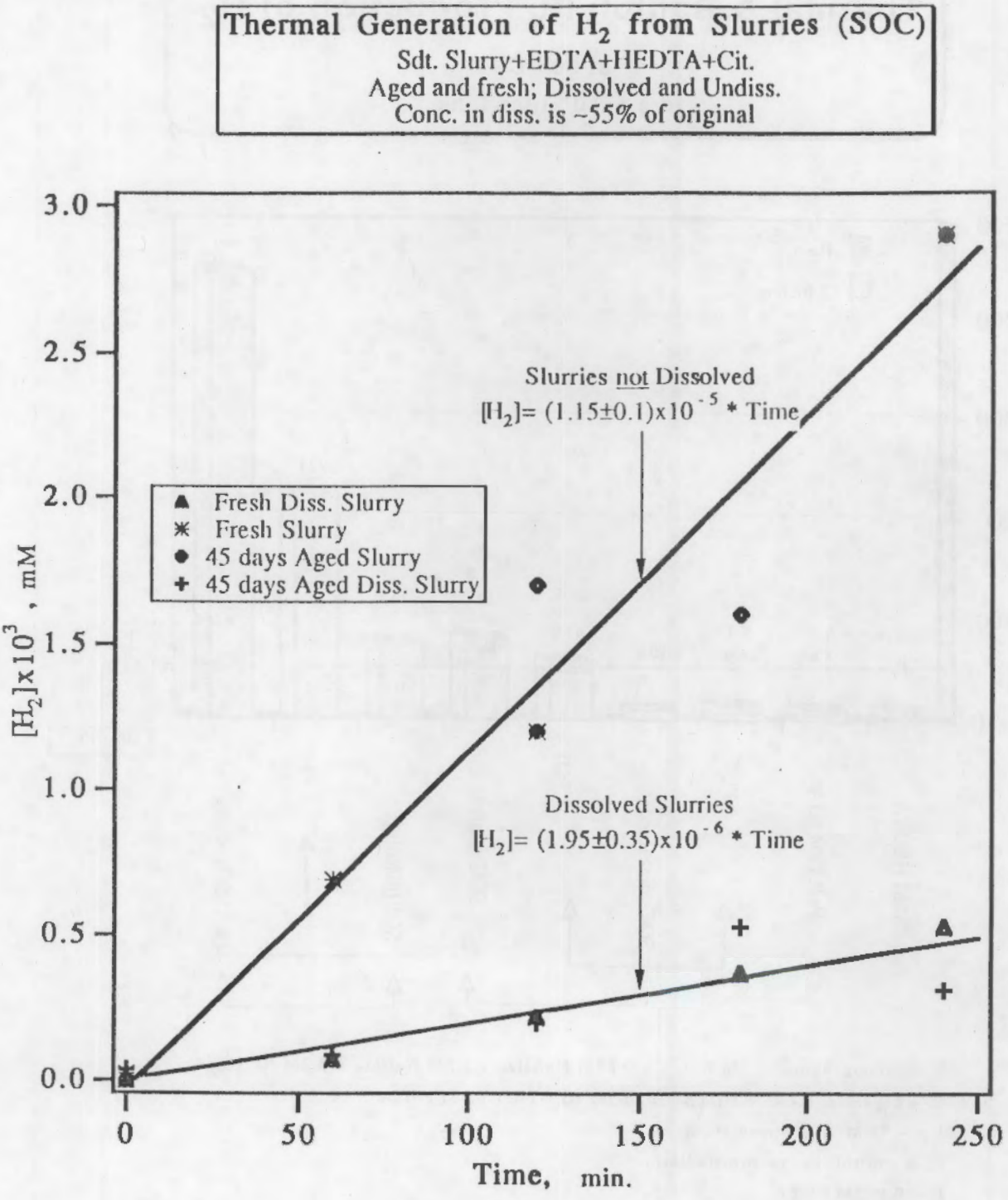
Thermal Generation of H_2 from Slurries (SOC)
Sdt. Slurry+EDTA+HEDTA+Cit.
Aged and fresh; Dissolved and Undiss.
Conc. in diss. is ~55% of original
Slurries not Dissolved
$[H_2]= (1.15\pm0.1)x10^{-5}$ * Time
Dissolved Slurries
$[H_2]= (1.95\pm0.35)x10^{-6}$ * Time
Fresh Diss. Slurry
Fresh Slurry
45 days Aged Slurry
45 days Aged Diss. Slurry
$[H_2]x10^3$, mM
Time, min.
0.0
0.5
1.0
1.5
2.0
2.5
3.0
0
50
100
150
200
250

Thermal & Radiolytic Production of H_2

at 60 °C

in a 4×10^6 liter tank

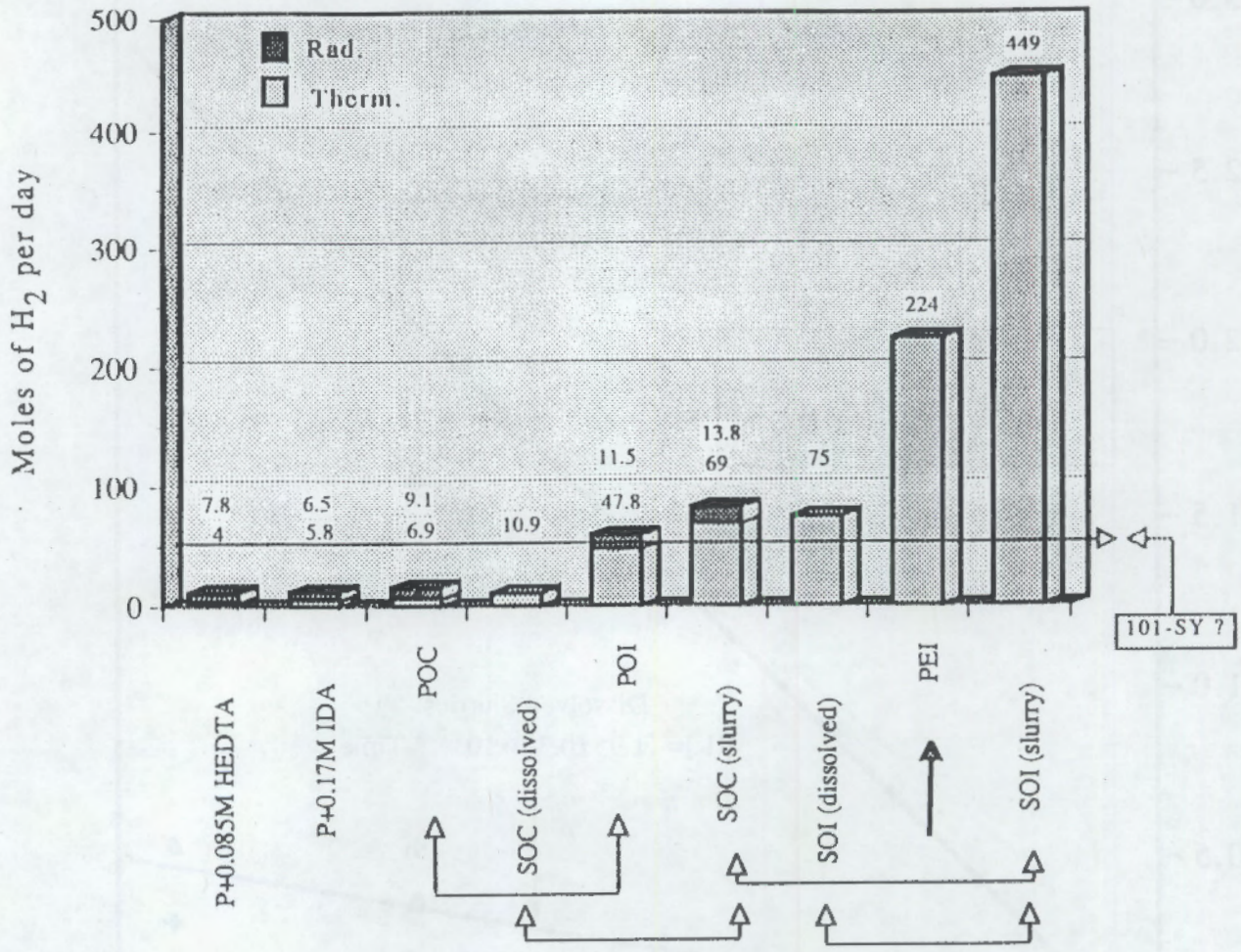

P = Homogeneous; 2.3M NaOH + 0.86M $NaAlO_2$ + 2.8M $NaNO_3$ + 2.2M $NaNO_2$

O = organics; 0.065M EDTA + 0.065M HEDTA + 0.1M citrate

I = ~ 33 Mrad preirradiation

C = control, i.e. no preirradiation

E = 0.065M EDTA

S = slurry; 2.3M NaOH + 2.2M $NaAlO_2$ + 3.7M$NaNO_3$ + 3.2M $NaNO_2$ + 0.6M Na_2CO_3

Conclusions

ISSUE 1 - Simulation quality:

* Very good simulation of the radiation; not so good for the chemistry.

ISSUE 2 - Radiolytic yields from slurries:

* H_2 yields in the slurry significantly lower than from homogeneous at RT (because of lower H_2O content and higher NO_x).
* Yield significantly increase with temp. (probably because increased solubility).
* Little changes in N_2O yields and in observations from homogeneous.

ISSUE 3 - Preirrad., Thermal Generation, Retention etc.

* Particles retain H_2 and N_2O very strongly.
* Slurry particles catalyze H_2 production.
* Preirrad. increases rate of H_2 and N_2O production. For H_2 EDTA > HEDTA > Citrate. For N_2O HEDTA>EDTA>Citrate.
* Ratio of H_2/N_2O will depend on preirrad. dose.

FUTURE:

* See plan.

Appendix H

Mechanistic Elucidation of Chemistry in Tank 101-SY

Mechanistic Elucidation of Chemistry in Tank 101-SY

Tank Waste Science Panel Meeting

Denver, Colorado

March 26, 1992

Professors: **E.C. Ashby**
E. Kent Barefield
Charles L. Liotta
Henry M. Neumann

Post Doctoral Assistants:

Fabio Doctorovich
Ashok Konda
Kai Zhang

M.S. Chemist: **Jeff Hurley**

Technicians: **D. Allen Annis**
M. Juliao
G. Pansino

Contents

$HOCH_2COO^-$ + Final word solution --------> $HCOO^-$ + $C_2O_4^=$ + CO_2 ($CO_3^=$)

Glycolate **Formate Oxalate Carbonate**

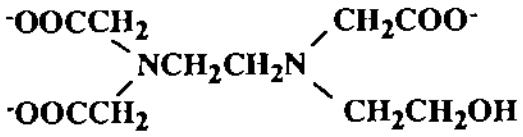

+ Final word solution -------> $HCOO^-$ + $C_2O_4^=$ + CO_2 ($CO_3^=$)

HEDTA

Final word solution

NaOH - 2.0 M
$NaAlO_2$ - 1.54 M
$NaNO_3$ - 2.59 M
$NaNO_2$ - 2.24 M
Na_2CO_3 - 0.42 M
Organics - 0.21 M

Table 1 Glycolate

TIME (hours)	NITRITE (moles) 10^2	NITRATE (moles) 10^2	OXALATE (moles) 10^4	FORMATE (moles) 10^4	GLYCOLATE (moles) 10^3
0	5.60	6.48	0	0	5.41
77	5.50	6.63	<0.5	1.22	4.78
197	5.38	6.58	5.89	4.03	3.95
310	5.35	6.30	4.93	5.22	3.37
406	5.33	6.55	8.76	5.99	2.93
514	5.30	6.50	10.5	6.77	2.66
672	5.30	6.37	15.2	7.16	1.96
981	5.05	6.37	22.1	8.25	0.459
1250	5.03	6.47	26.5	8.85	0.243
1474	5.00	6.33	27.7	9.23	0.269
1582	4.92	6.65	31.1	9.26	0.111

Figure 1

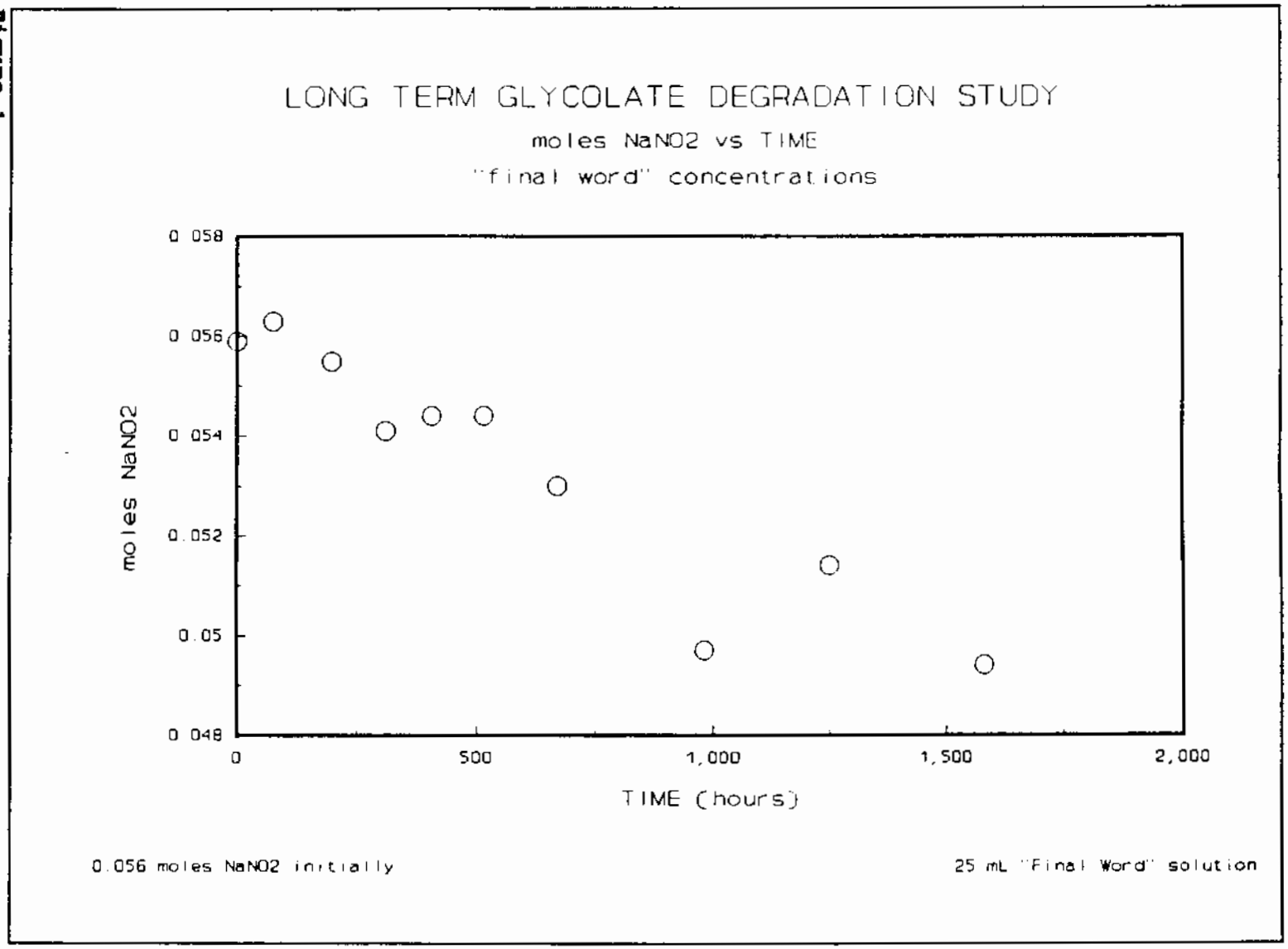
LONG TERM GLYCOLATE DEGRADATION STUDY
moles NaNO2 vs TIME
"final word" concentrations
moles NaNO2
0.058
0.056
0.054
0.052
0.05
0.048
0
500
1,000
1,500
2,000
TIME (hours)
0.056 moles NaNO2 initially
25 mL "Final Word" solution

H.S

Figure 2

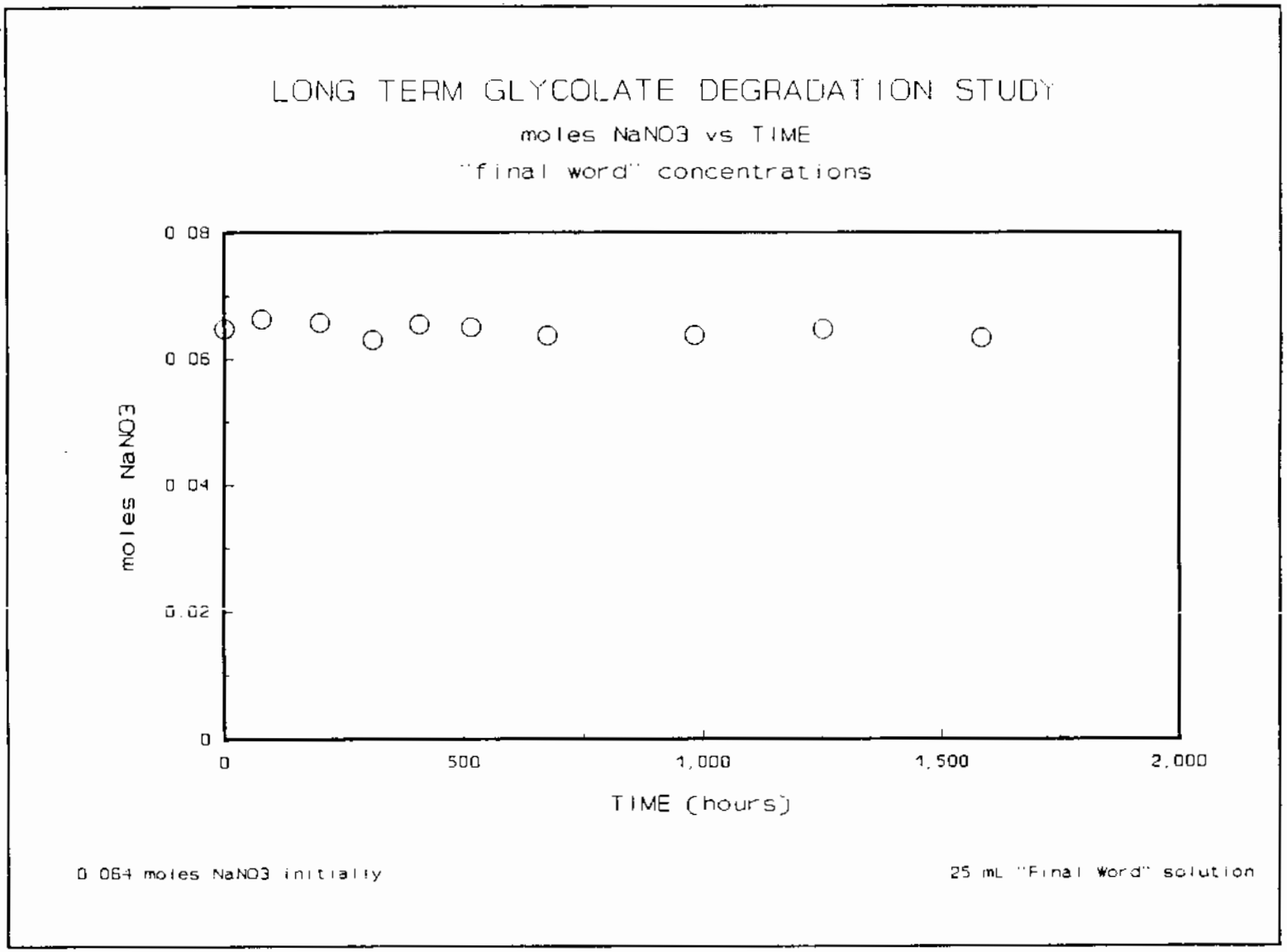
LONG TERM GLYCOLATE DEGRADATION STUDY
moles NaNO3 vs TIME
"final word" concentrations
0.08
0.06
0.04
0.02
0
moles NaNO3
0
500
1,000
1,500
2,000
TIME (hours)
0.064 moles NaNO3 initially
25 mL "Final Word" solution

Figure 3

LONG TERM GLYCOLATE DEGRADATION STUDY
moles Oxalate vs Time
"final word" concentrations
0.005
0.004
0.003
0.002
0.001
0
moles oxalate
0
500
1,000
1,500
2,000
TIME (hours)
no oxalate initially
25 mL "Final Word" solution

Figure 4

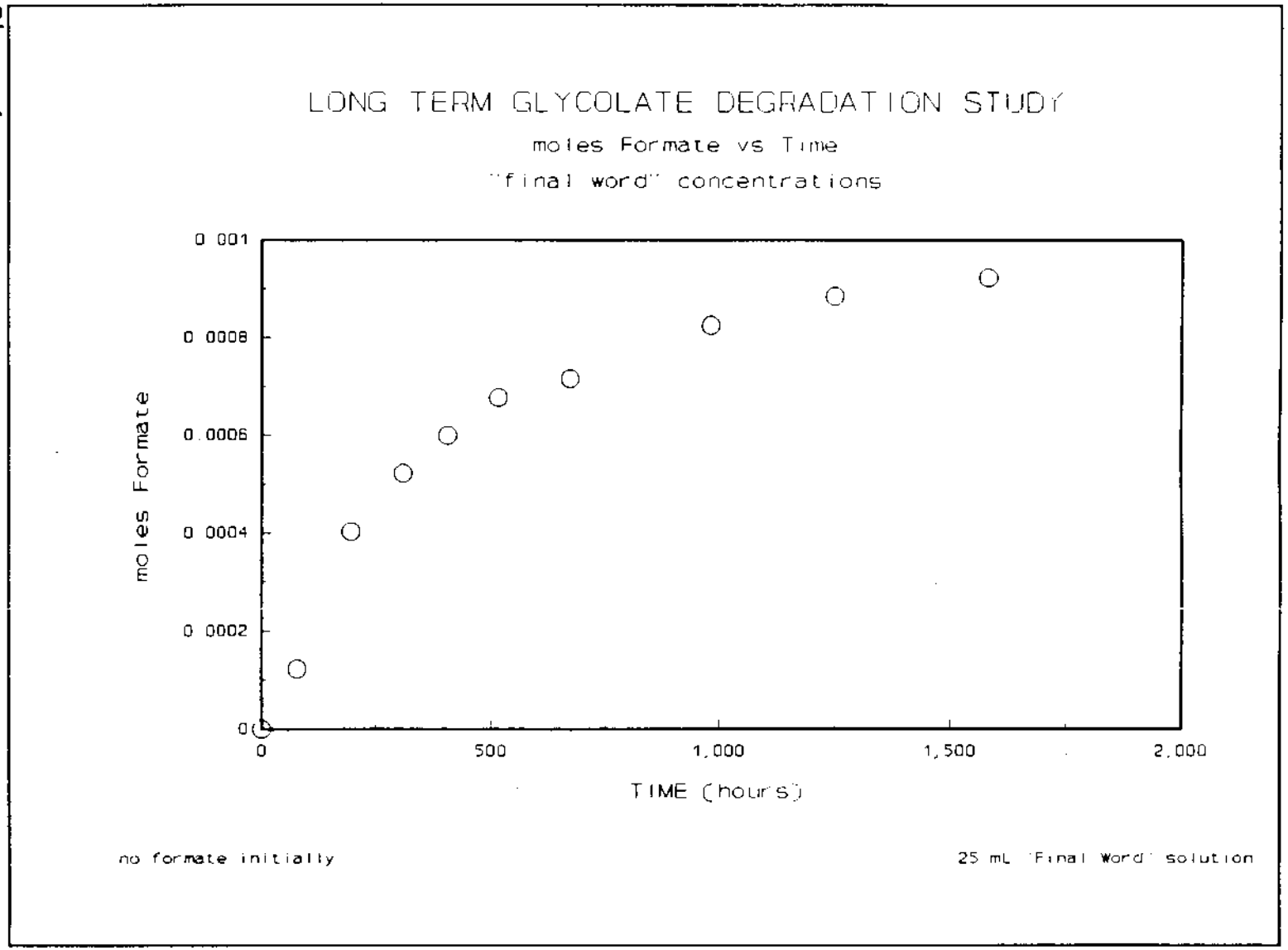
LONG TERM GLYCOLATE DEGRADATION STUDY
moles Formate vs Time
"final word" concentrations
moles Formate
0.001
0.0008
0.0006
0.0004
0.0002
0
0
500
1,000
1,500
2,000
TIME (hours)
no formate initially
25 mL 'Final Word' solution

Figure 5

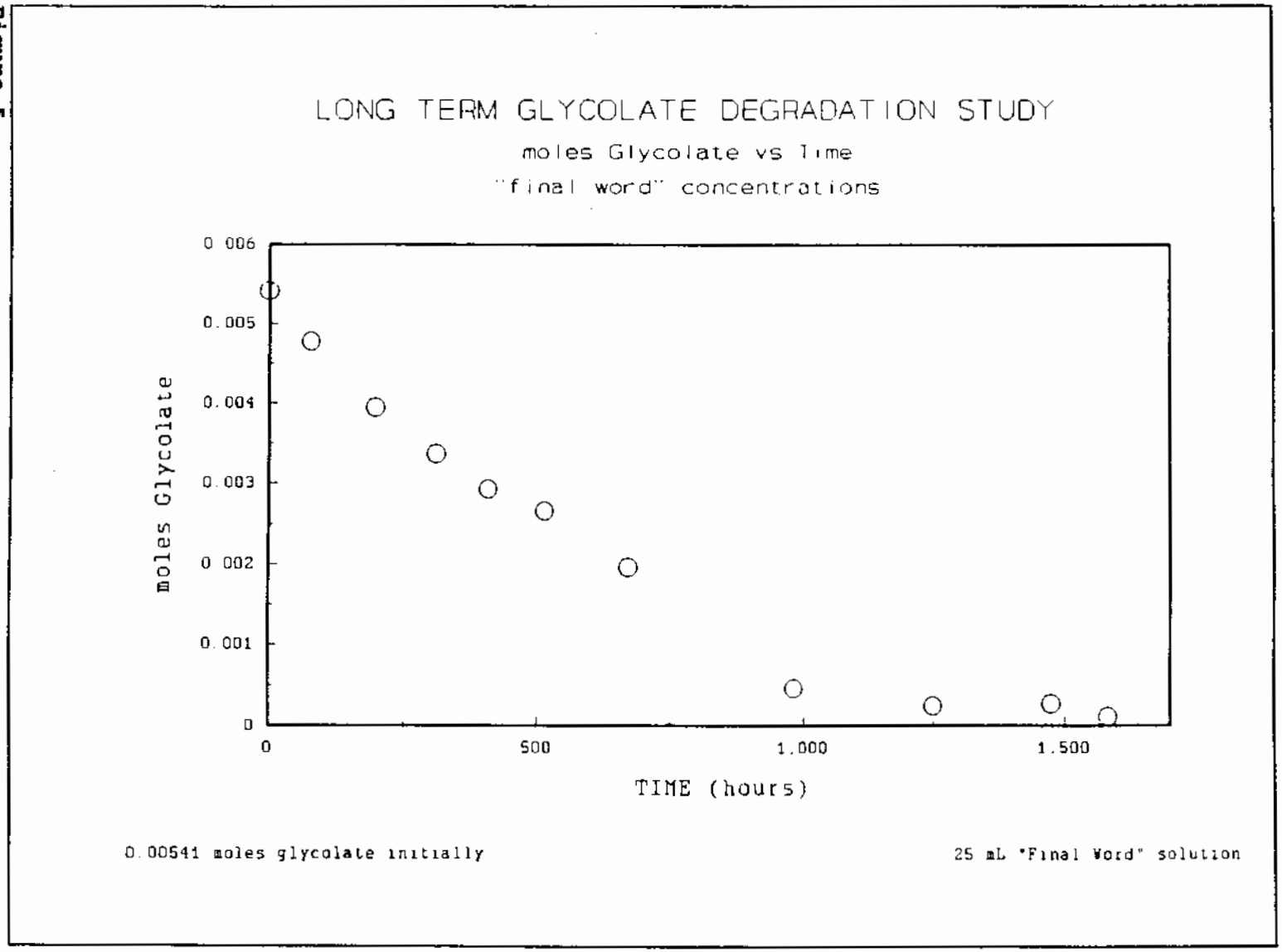
LONG TERM GLYCOLATE DEGRADATION STUDY
moles Glycolate vs Time
"final word" concentrations
moles Glycolate
0.006
0.005
0.004
0.003
0.002
0.001
0
0
500
1,000
1,500
TIME (hours)
0.00541 moles glycolate initially
25 mL "Final Word" solution

Figure 5b

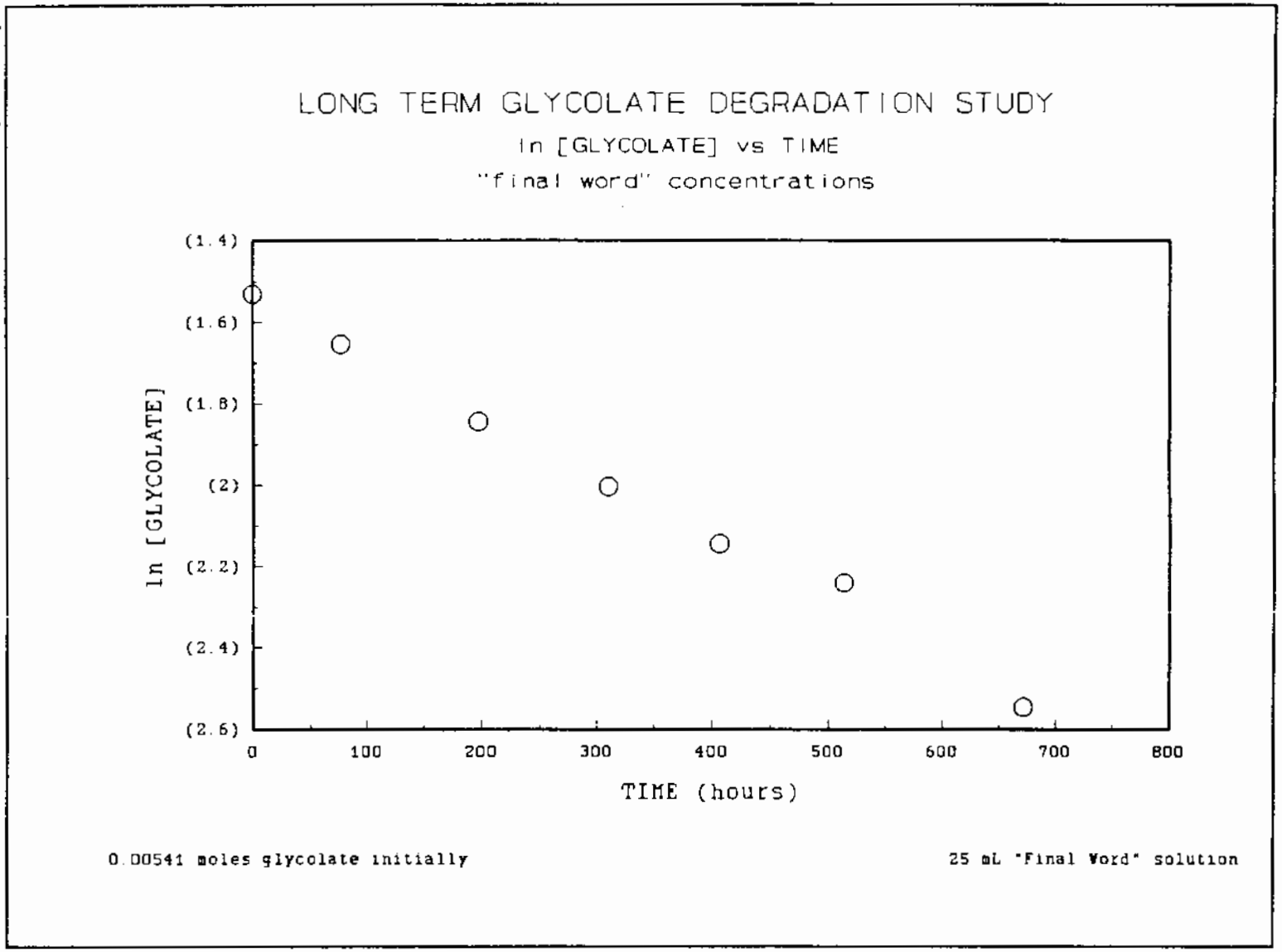
LONG TERM GLYCOLATE DEGRADATION STUDY
ln [GLYCOLATE] vs TIME
"final word" concentrations
ln [GLYCOLATE]
(1.4)
(1.6)
(1.8)
(2)
(2.2)
(2.4)
(2.6)
0
100
200
300
400
500
600
700
800
TIME (hours)
0.00541 moles glycolate initially
25 mL "Final Word" solution

Table 2 HEDTA

TIME (hours)	NITRITE (moles) 10^2	NITRATE (moles) 10^2	FORMATE (moles) 10^3	HEDTA (moles) 10^3
0	5.60	6.65	0	5.30
112.5	5.48	6.55	0.48	5.08
191	5.43	6.57	1.01	4.84
303	5.40	6.50	1.02	4.47
408.5	5.38	6.74	1.30	4.03
500.5	5.33	6.64	1.89	3.60

Figure 6

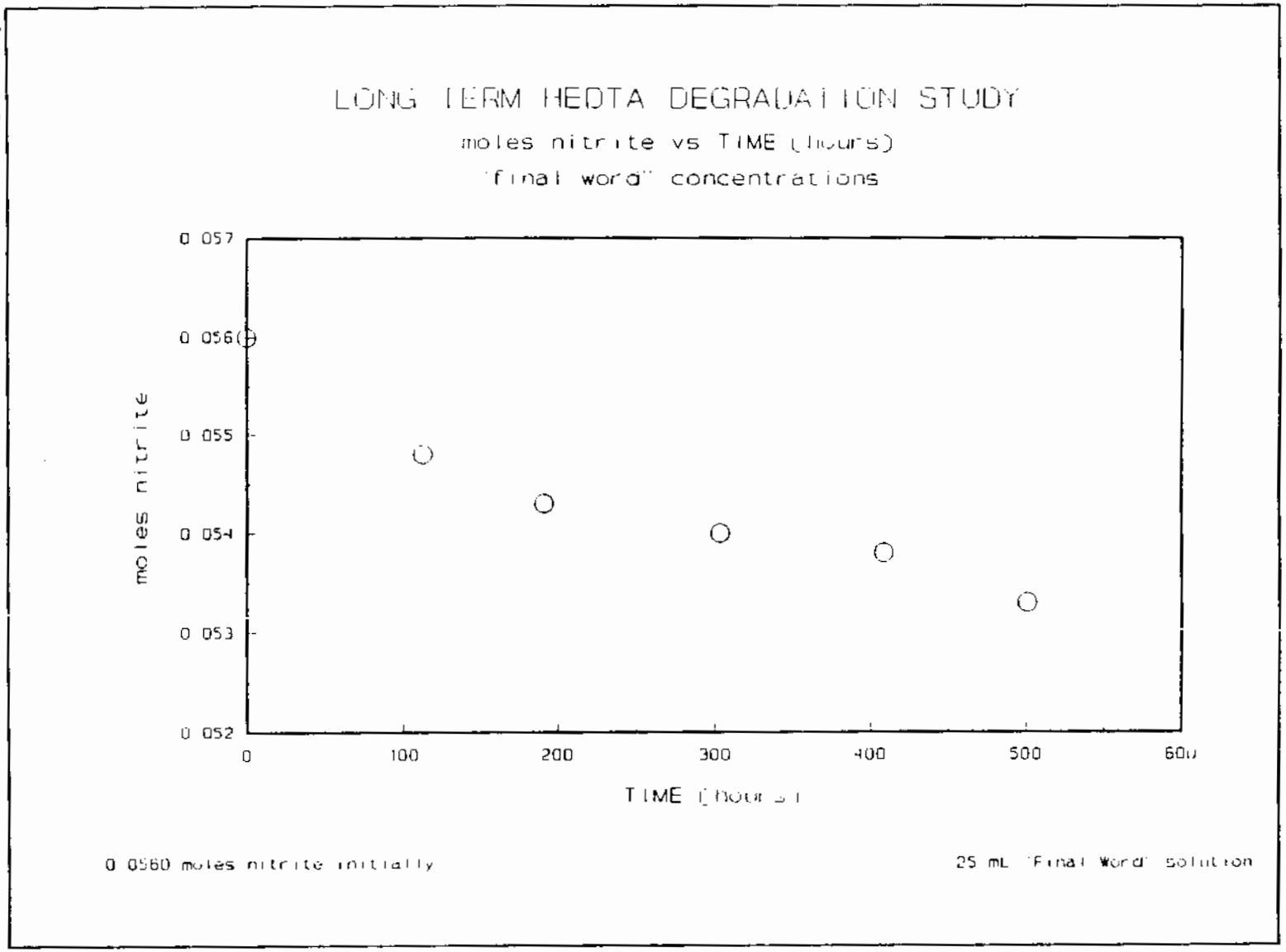
LONG TERM HEDTA DEGRADATION STUDY
moles nitrite vs TIME (hours)
"final word" concentrations
moles nitrite
0.057
0.056
0.055
0.054
0.053
0.052
0
100
200
300
400
500
600
TIME (hours)
0.0560 moles nitrite initially
25 mL "Final Word" solution

Figure 7

LONG TERM HEDTA DEGRADATION STUDY
moles nitrate vs TIME (hours)
"final word" concentrations
moles nitrate
0.1
0.08
0.06
0.04
0.02
0
0
100
200
300
400
500
600
TIME (hours)
0.0665 moles nitrate initially
25 mL "Final Word" solution

Figure 8

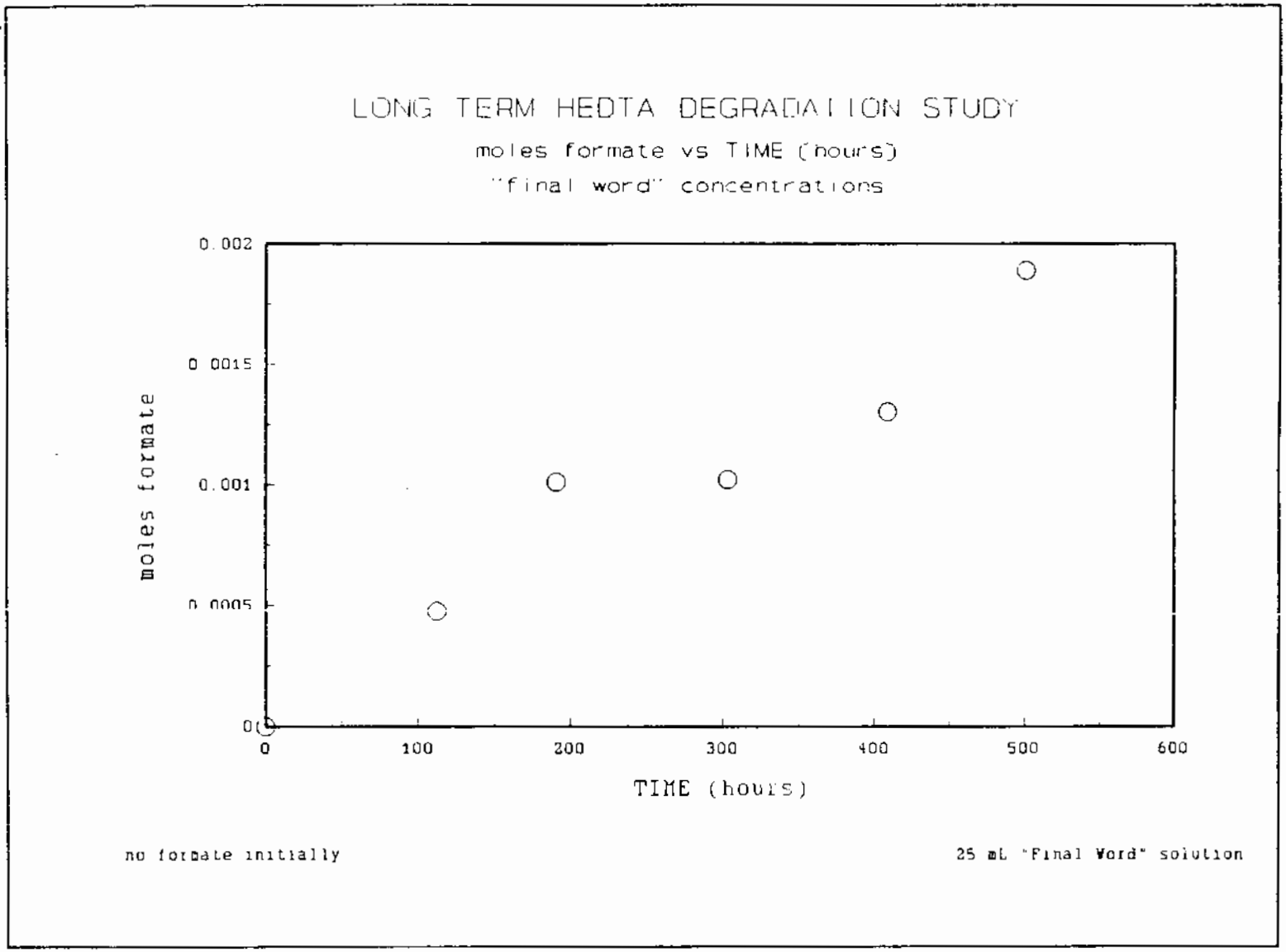
LONG TERM HEDTA DEGRADATION STUDY
moles formate vs TIME (hours)
"final word" concentrations
moles formate
0.002
0.0015
0.001
0.0005
0
0
100
200
300
400
500
600
TIME (hours)
no formate initially
25 mL "Final Word" solution

Figure 9

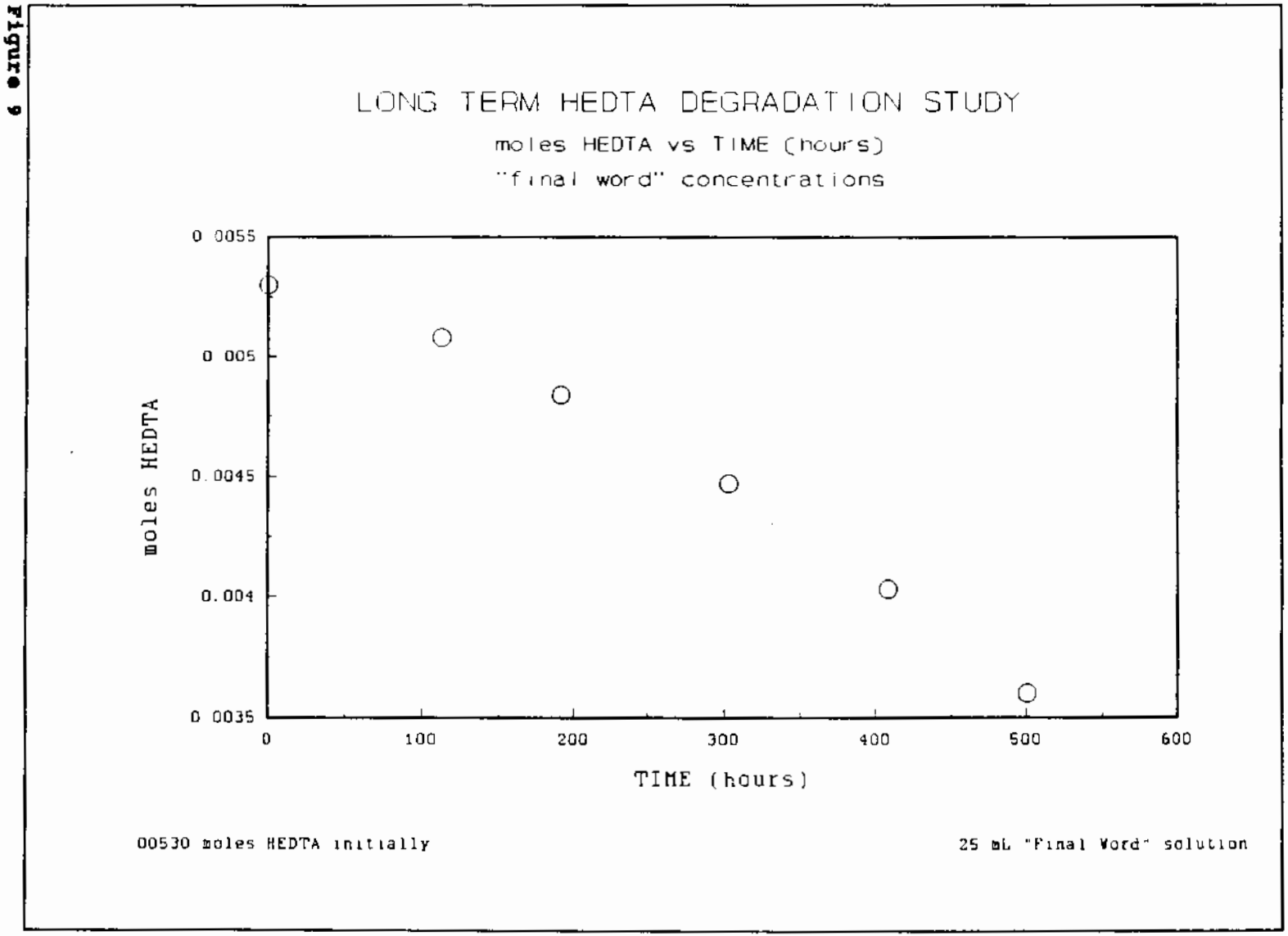
LONG TERM HEDTA DEGRADATION STUDY
moles HEDTA vs TIME (hours)
"final word" concentrations
moles HEDTA
0.0055
0.005
0.0045
0.004
0.0035
0
100
200
300
400
500
600
TIME (hours)
00530 moles HEDTA initially
25 mL "Final Word" solution

Figure 9b

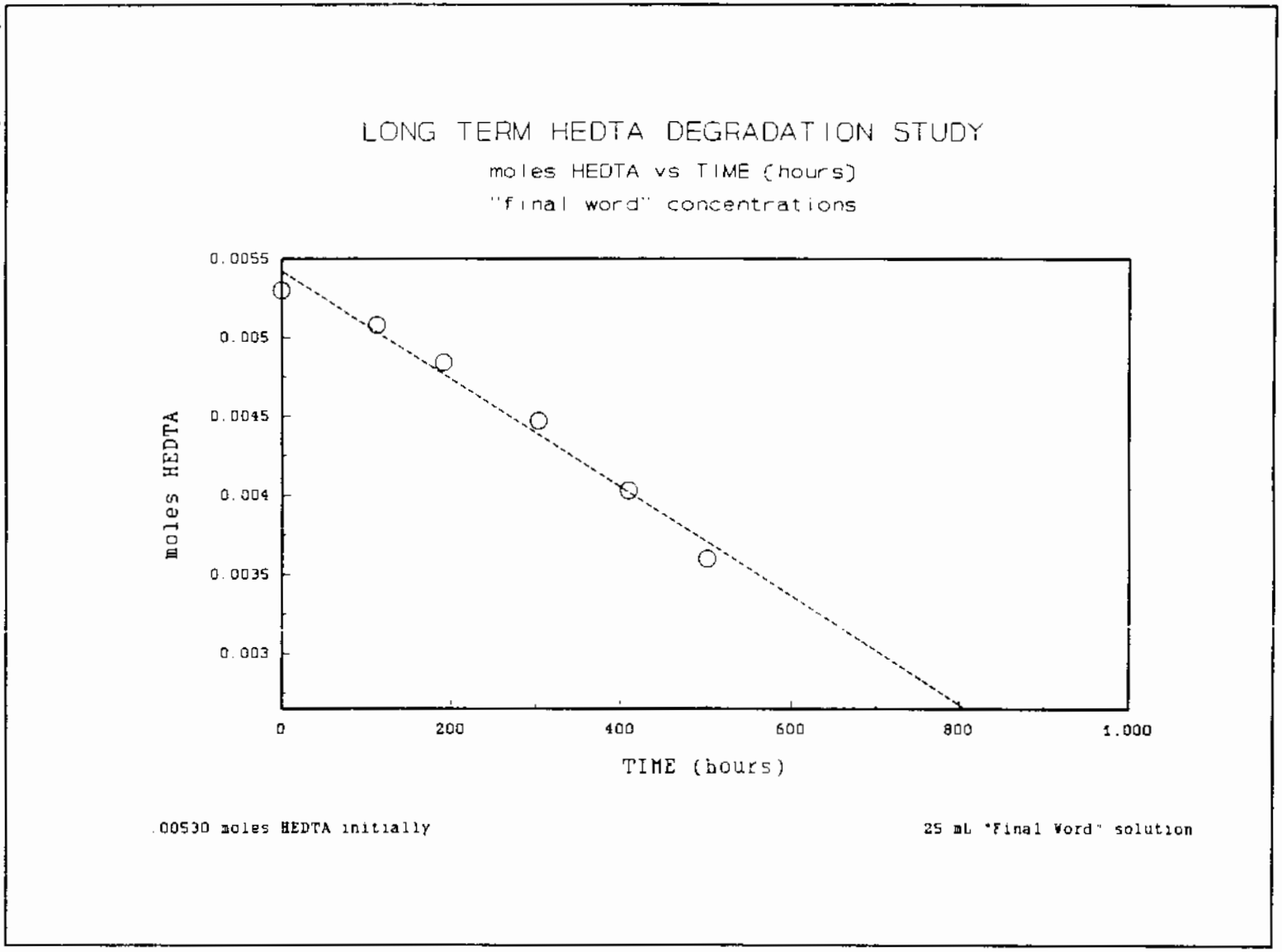
LONG TERM HEDTA DEGRADATION STUDY
moles HEDTA vs TIME (hours)
"final word" concentrations
0.0055
0.005
0.0045
0.004
0.0035
0.003
moles HEDTA
0
200
400
600
800
1.000
TIME (hours)
.00530 moles HEDTA initially
25 mL "Final Word" solution

Figure 9c

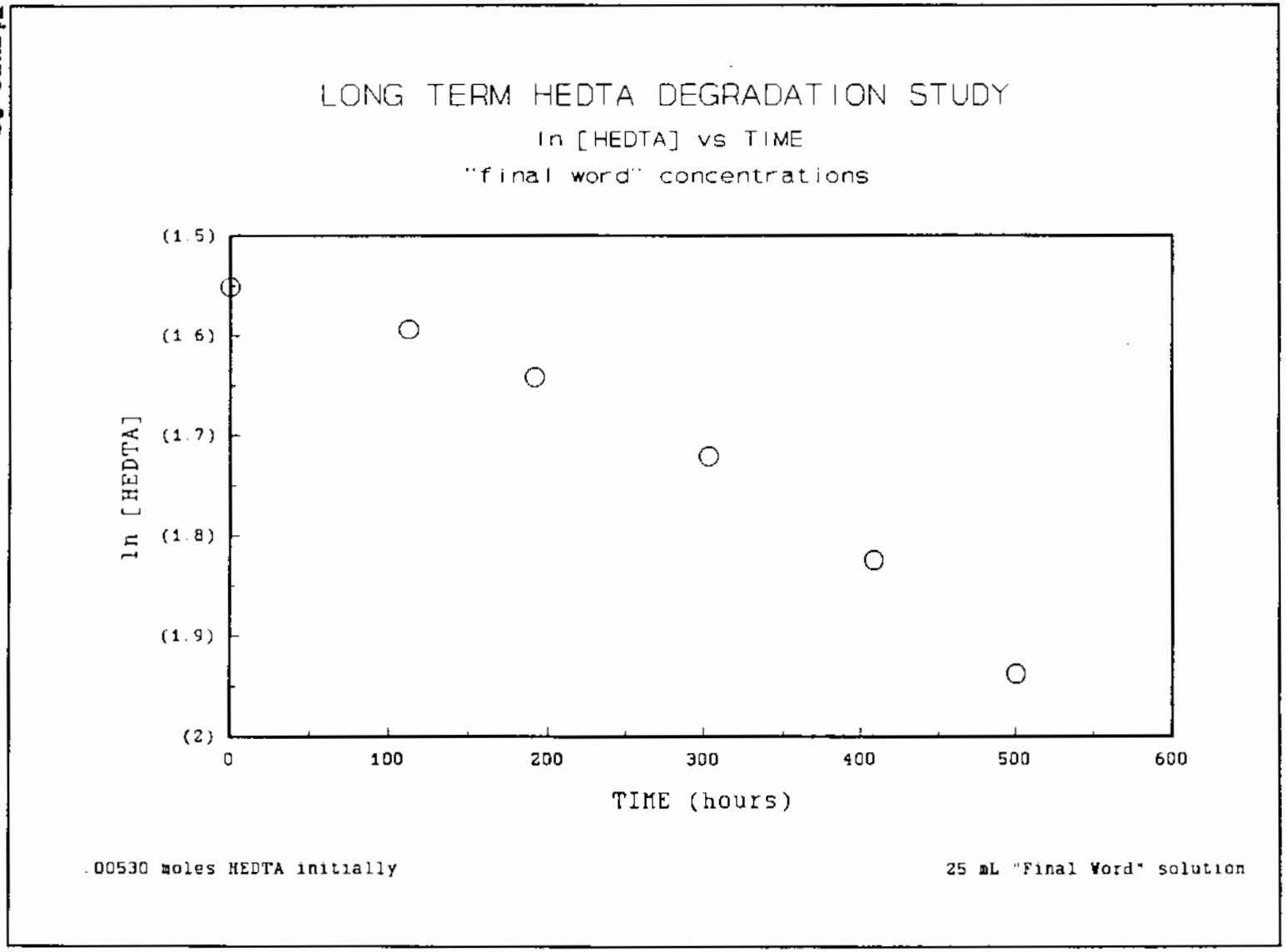
LONG TERM HEDTA DEGRADATION STUDY
ln [HEDTA] vs TIME
"final word" concentrations
ln [HEDTA]
(1.5)
(1.6)
(1.7)
(1.8)
(1.9)
(2)
0
100
200
300
400
500
600
TIME (hours)
.00530 moles HEDTA initially
25 mL "Final Word" solution

Table 3 Organic Components

ORGANIC COMPONENT	GAS EVOLUTION (mL/hour)
iminodiacetic acid[1]	0.20
symmetrical ethylenediaminediacetic acid[2]	0.23*
glycine	0.18*
sarcosine[3]	0.17
N-methyliminodiacetic acid[4]	0.14
nitrilotriacetic acid[5]	0[7]
unsymmetrical ethylenediaminediacetic acid[6]	0[8]
glycolate	0.34
HEDTA	0.39

[1] IDA
[2] S-EDDA
[3] N-methylglycine
[4] NMIDA
[5] NTA
[6] U-EDDA
[7] Experiment run for 357.5 hours
[8] Experiment run for 403 hours

* experiment still in progress

Figure 10

GAS EVOLUTION EXPERIMENT B69
HOMOGENEOUS CONDITIONS
IDA UNDER AIR ATMOSPHERE
GAS EVOLVED (mL)
350
300
250
200
150
100
50
0
200
400
600
800
1,000
1,200
TIME (hours)
EXPERIMENT
B69
reaction apparatus 1

Figure 11

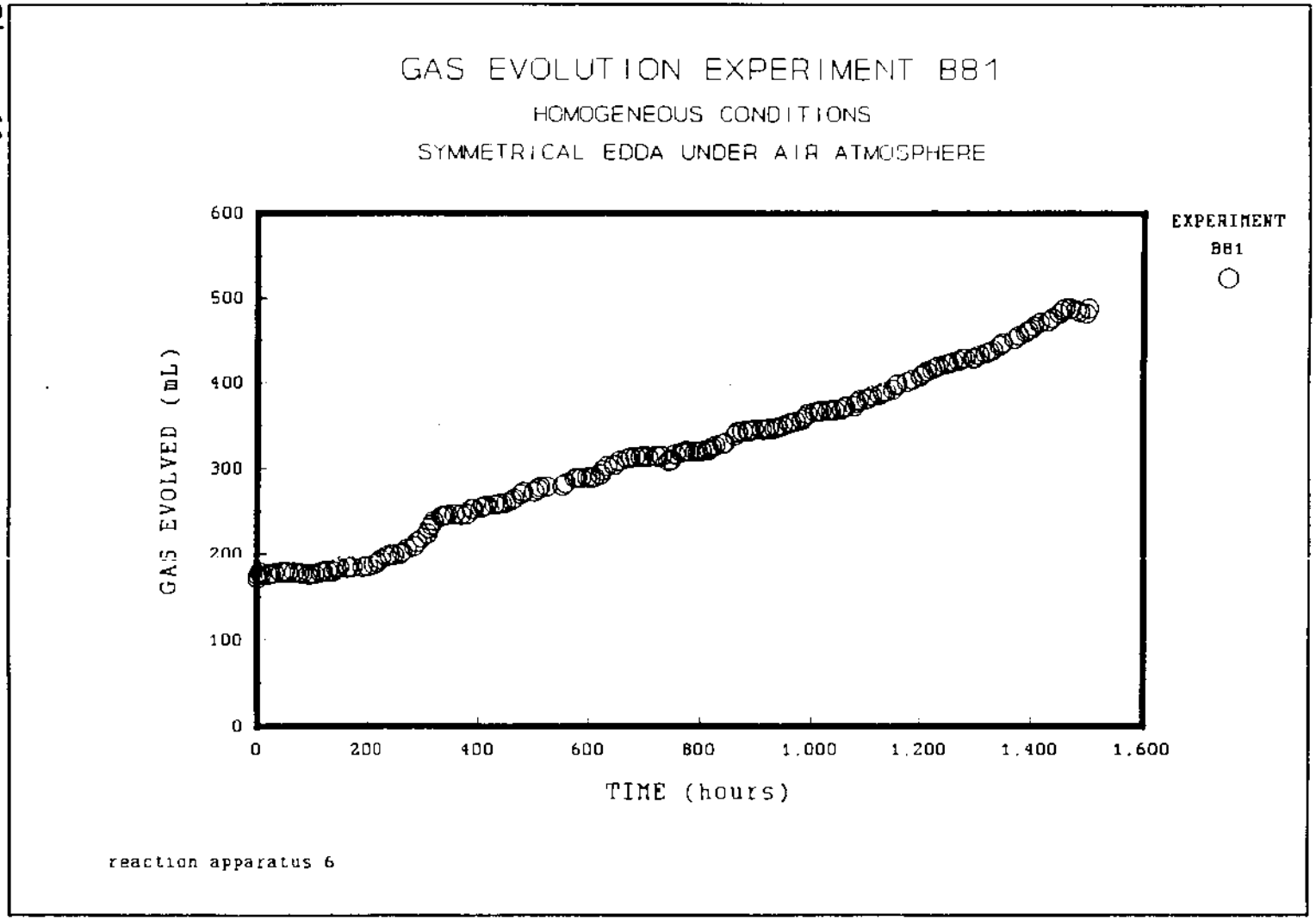
GAS EVOLUTION EXPERIMENT B81
HOMOGENEOUS CONDITIONS
SYMMETRICAL EDDA UNDER AIR ATMOSPHERE
GAS EVOLVED (mL)
600
500
400
300
200
100
0
0
200
400
600
800
1,000
1,200
1,400
1,600
TIME (hours)
EXPERIMENT
B81
reaction apparatus 6

Figure 12

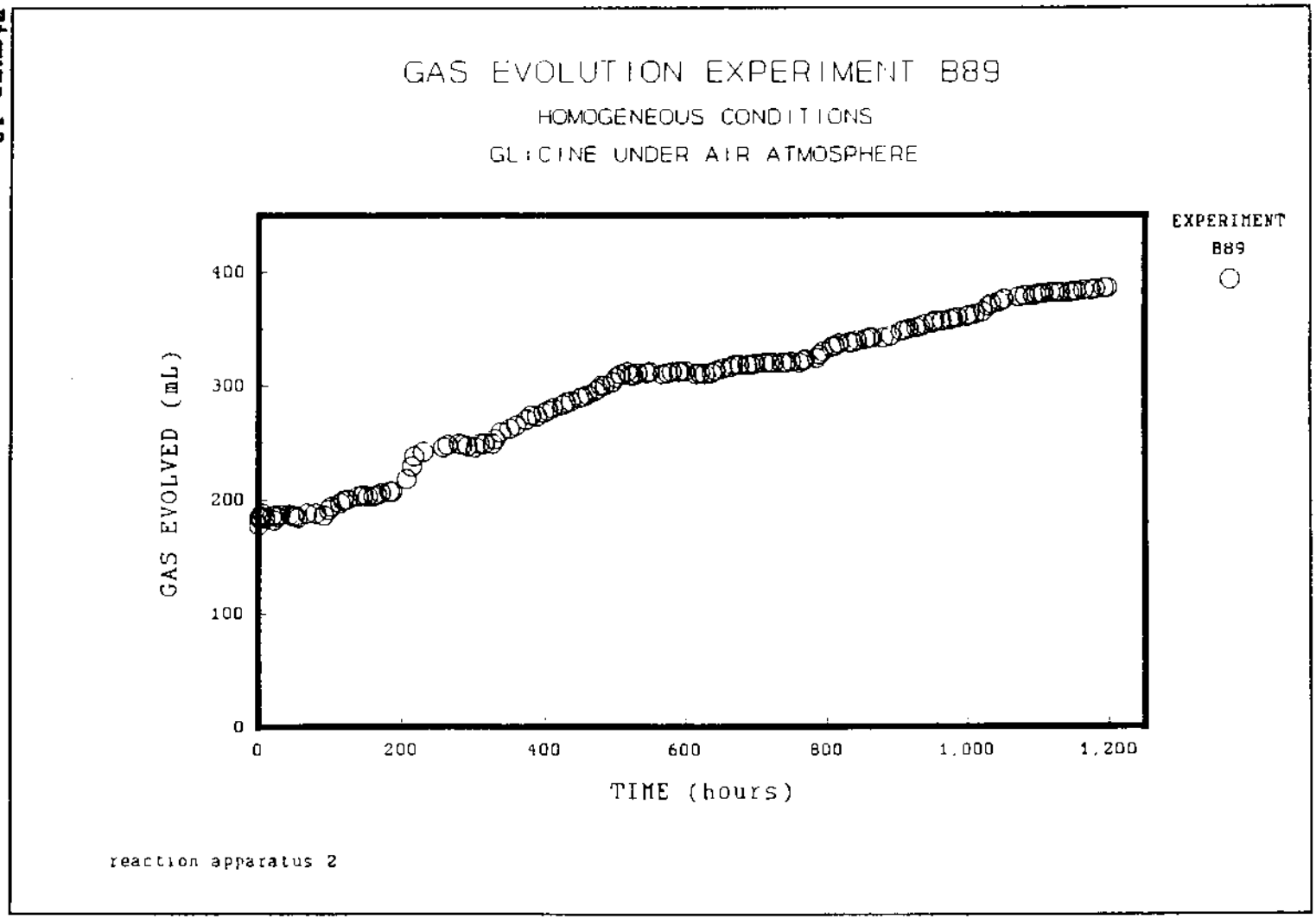
GAS EVOLUTION EXPERIMENT B89
HOMOGENEOUS CONDITIONS
GLYCINE UNDER AIR ATMOSPHERE
EXPERIMENT
B89
GAS EVOLVED (mL)
0
100
200
300
400
0
200
400
600
800
1,000
1,200
TIME (hours)
reaction apparatus 2

Figure 13

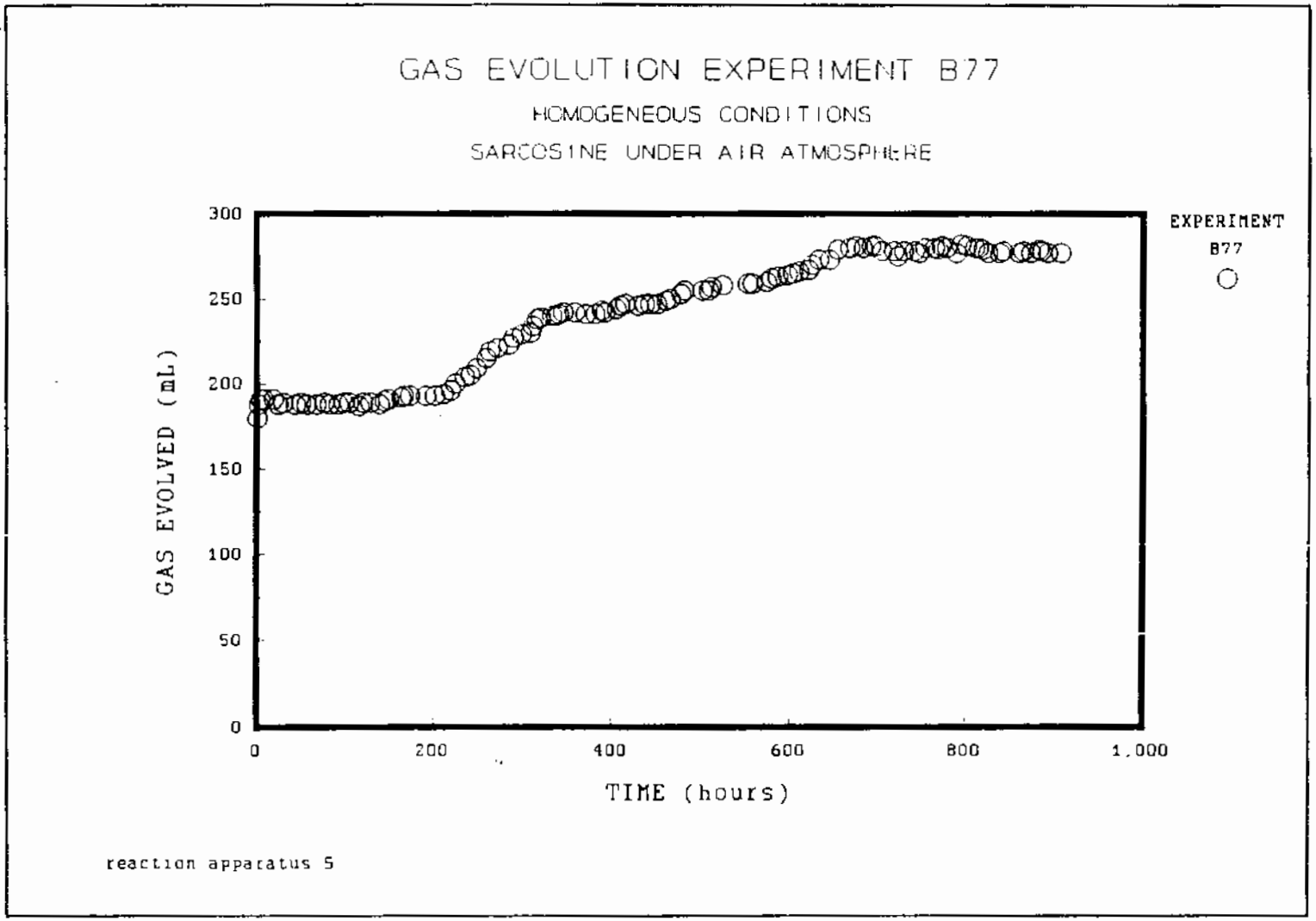
GAS EVOLUTION EXPERIMENT B77
HOMOGENEOUS CONDITIONS
SARCOSINE UNDER AIR ATMOSPHERE
GAS EVOLVED (mL)
300
250
200
150
100
50
0
0
200
400
600
800
1,000
TIME (hours)
EXPERIMENT
B77
reaction apparatus 5

Figure 14

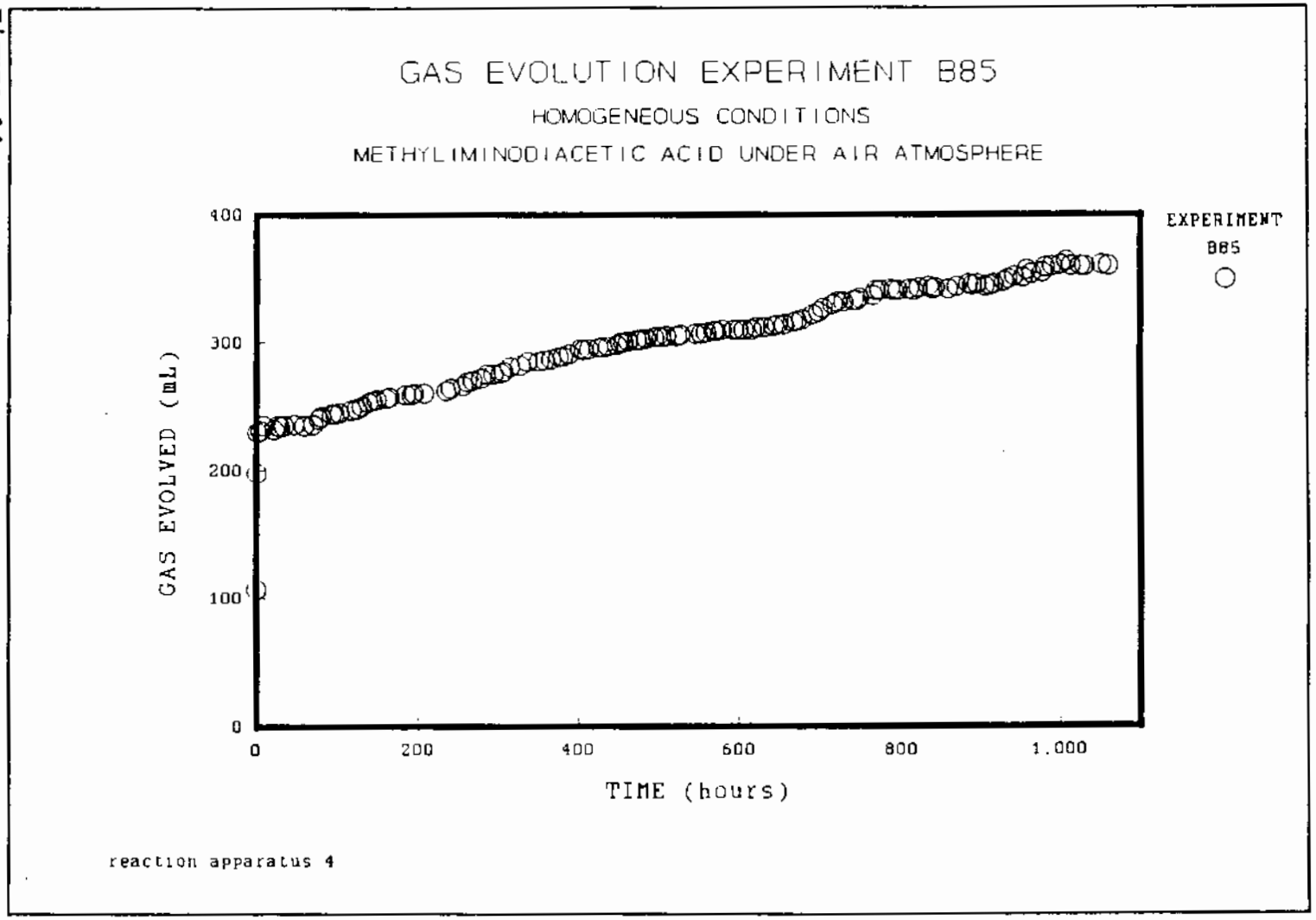
GAS EVOLUTION EXPERIMENT B85
HOMOGENEOUS CONDITIONS
METHYLIMINODIACETIC ACID UNDER AIR ATMOSPHERE
GAS EVOLVED (mL)
400
300
200
100
0
0
200
400
600
800
1,000
TIME (hours)
EXPERIMENT
B85
reaction apparatus 4

Figure 15

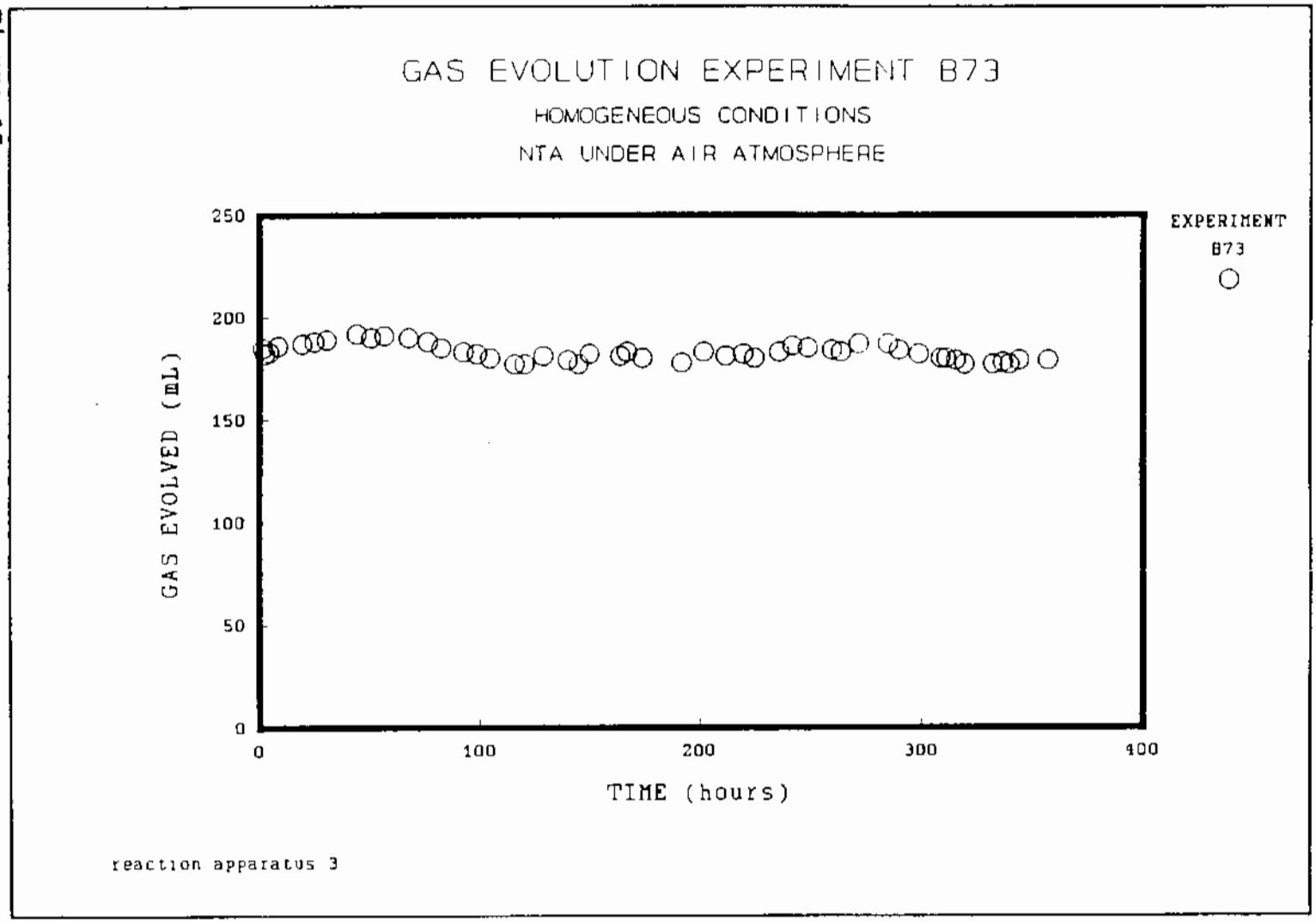
GAS EVOLUTION EXPERIMENT B73
HOMOGENEOUS CONDITIONS
NTA UNDER AIR ATMOSPHERE
GAS EVOLVED (mL)
250
200
150
100
50
0
0
100
200
300
400
TIME (hours)
EXPERIMENT
B73
reaction apparatus 3

Figure 16

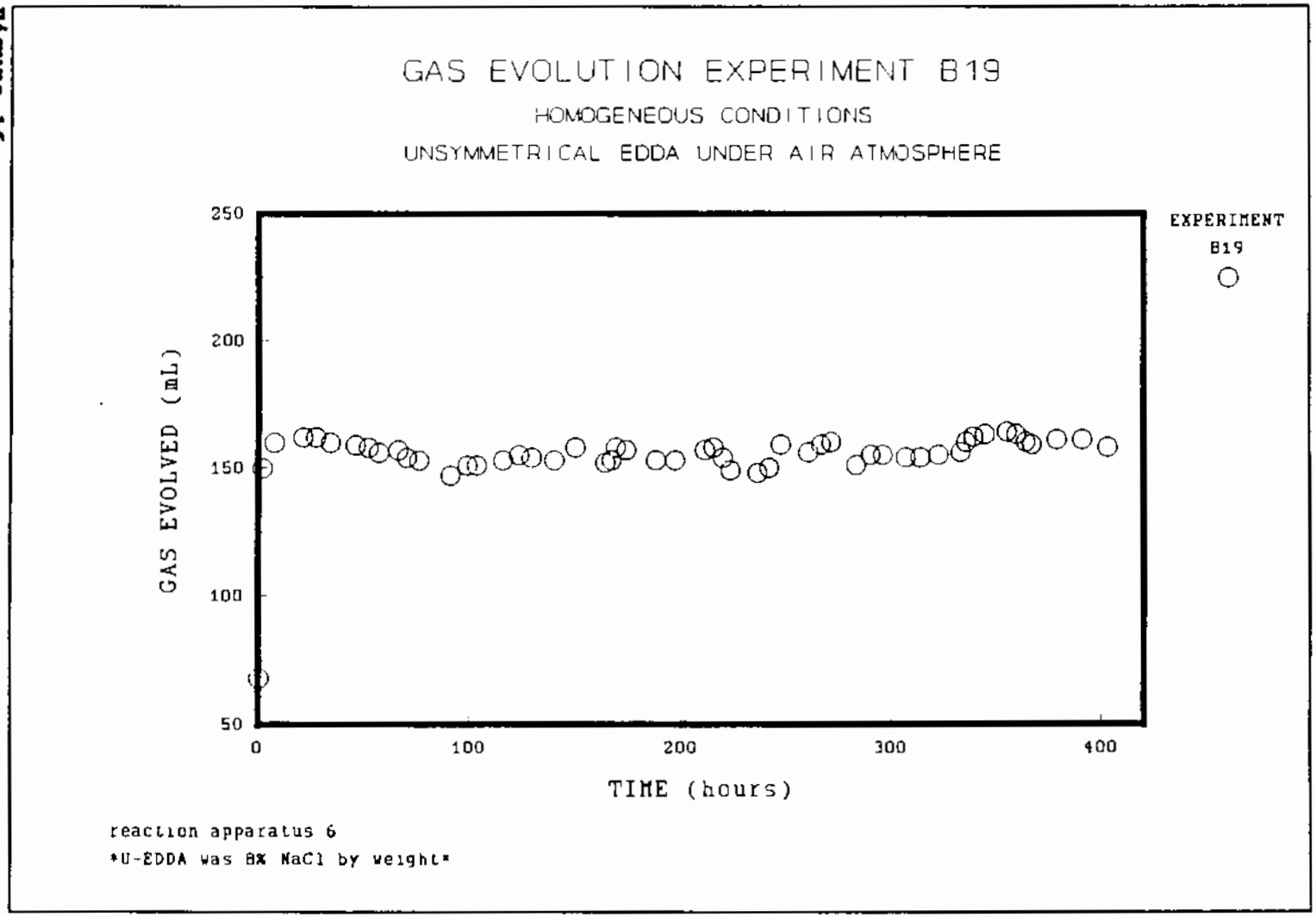
GAS EVOLUTION EXPERIMENT B19
HOMOGENEOUS CONDITIONS
UNSYMMETRICAL EDDA UNDER AIR ATMOSPHERE
GAS EVOLVED (mL)
250
200
150
100
50
0
100
200
300
400
TIME (hours)
EXPERIMENT
B19
reaction apparatus 6
U-EDDA was 8% NaCl by weight

PROPOSED MECHANISM OF THERMAL DEGRADATION OF GLYCOLATE

1) $Al(OH)_4^- + NO_2^- \rightleftarrows Al(OH)_3\text{-}O\text{-}N{=}O^- + OH^-$

2) $Al(OH)_3\text{-}O\text{-}N{=}O + HO\text{-}CH_2\text{-}CO_2^- \rightleftarrows Al(OH)_4^- + O{=}N\text{-}O\text{-}CH_2\text{-}CO_2^-$

3) $O{=}N\text{-}O\text{-}CH_2\text{-}CO_2^- \rightarrow NO^- + O{=}CH_2 + CO_2$

4) $O{=}N\text{-}O\text{-}CH_2\text{-}CO_2^- + OH^- \rightarrow NO^- + H\text{-}(CO)\text{-}CO_2^- + H_2O$

5) $2NO^- \rightleftarrows N_2O_2^{-2}$

6) $N_2O_2^{-2} + H_2O \rightleftarrows HN_2O_2^- + OH^-$

7) $HN_2O_2^- \rightarrow N_2O + OH^-$

8) $N_2O + Al(OH)_3\text{-}O\text{-}N{=}O^- \rightarrow N_2 + Al(OH)_3\text{-}O\text{-}NO_2$

9) $N_2O + NO_2^- \rightarrow N_2 + NO_3^-$

10) $CH_2{=}O + OH^- \rightleftarrows HO\text{-}CH_2\text{-}O^-$

11) $HO\text{-}CH_2\text{-}O^- + OH^- \rightleftarrows {}^-O\text{-}CH_2\text{-}O^- + H_2O$

12) $^-O\text{-}CH_2\text{-}O^- + H_2O \rightarrow H_2 + H\text{-}COO^- + OH^-$

13) $H\text{-}(CO)\text{-}CO_2^- + OH^- \rightleftarrows {}^-O\text{-}CH(OH)\text{-}CO_2^- \rightleftarrows (^-O)_2\text{-}CH\text{-}CO_2^-$

14) $(^-O)_2\text{-}CH\text{-}CO_2^- + H_2O \rightarrow H_2 + {}^-O_2C\text{-}CO_2^- + OH^-$

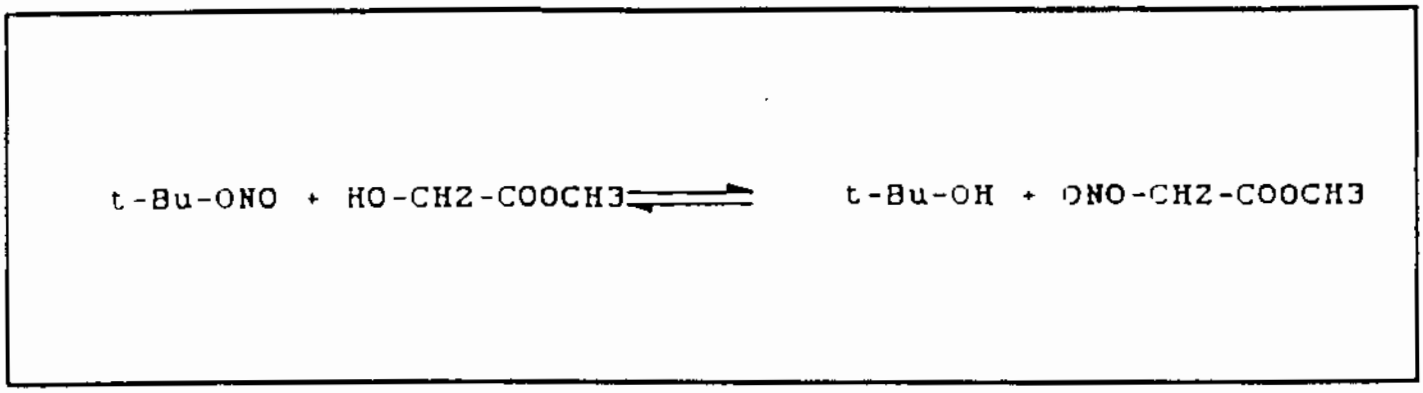

Figure 17

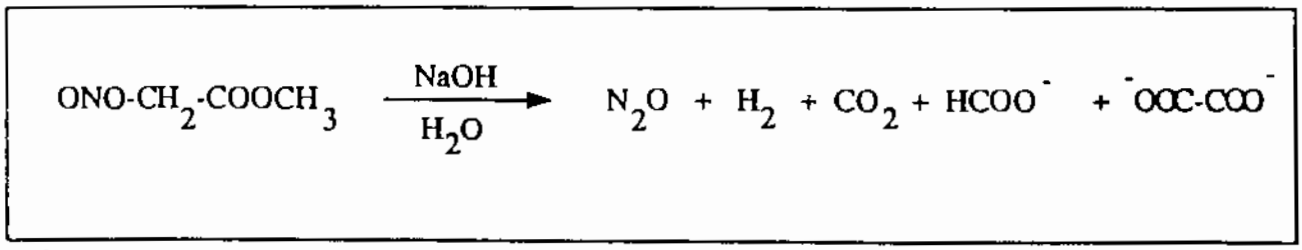

Figure 18

Decomposition of C-13 Labeled HEDTA

Objective:

To determine thermal fragmentation products.

Synthesis of labeled compounds:

Alkylation of labeled $H_2NCH_2CH_2NH^{13}CH_2{}^{13}CH_2OH$ (from 1,2-diaminoethane and labeled ethylene oxide) with $BrCH_2CO_2H$.

Alkylation of $H_2NCH_2CH_2NHCH_2CH_2OH$ with $Br^{13}CH_2{}^{13}CO_2H$.

Experiment:

Heat simulated waste mixtures prepared with labeled HEDTA's and monitor ^{13}C NMR spectra. Intensities measured relative to external benzene-d_6.

Observations:

Labeled formate and CO_2 (as carbonate) and oxalate were detectable from both labeled forms after a few days.

Labeled glycine was detectable after 34.5 days from the hydroxyethyl labeled form; its concentration continued to increase.

> At 60.5 days unlabeled glycine was also detectable. The ratio of unlabeled glycine to labeled glycine was estimated to be 6:1 at this time.
>
> One quarter to one half of the HEDTA remained after 60.5 days (estimated from ion chromatography and NMR, respectively)

A doublet consistent with the presence of labeled IDA was after about six days in the carboxymethyl labeled form.

Thermal Decomposition Products from C-13 Labeled HEDTA

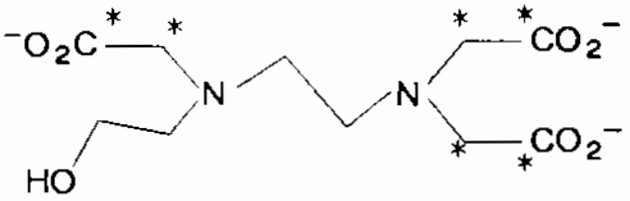

Formate, Carbon Dioxide
Oxalate
IDA

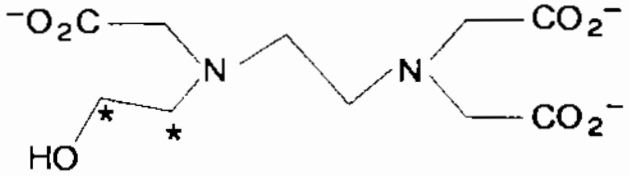

Formate, Carbon Dioxide
Oxalate
Glycine

*denotes C-13 enrichment; NMR detection of products

Formate	-	$HCOO^-$
Carbon Dioxide	-	CO_2
Oxalate	-	$C_2O_4^{2-}$
IDA	-	$HN(CH_2COOH)_2$
Glycine	-	H_2NCH_2COOH

Figure 1

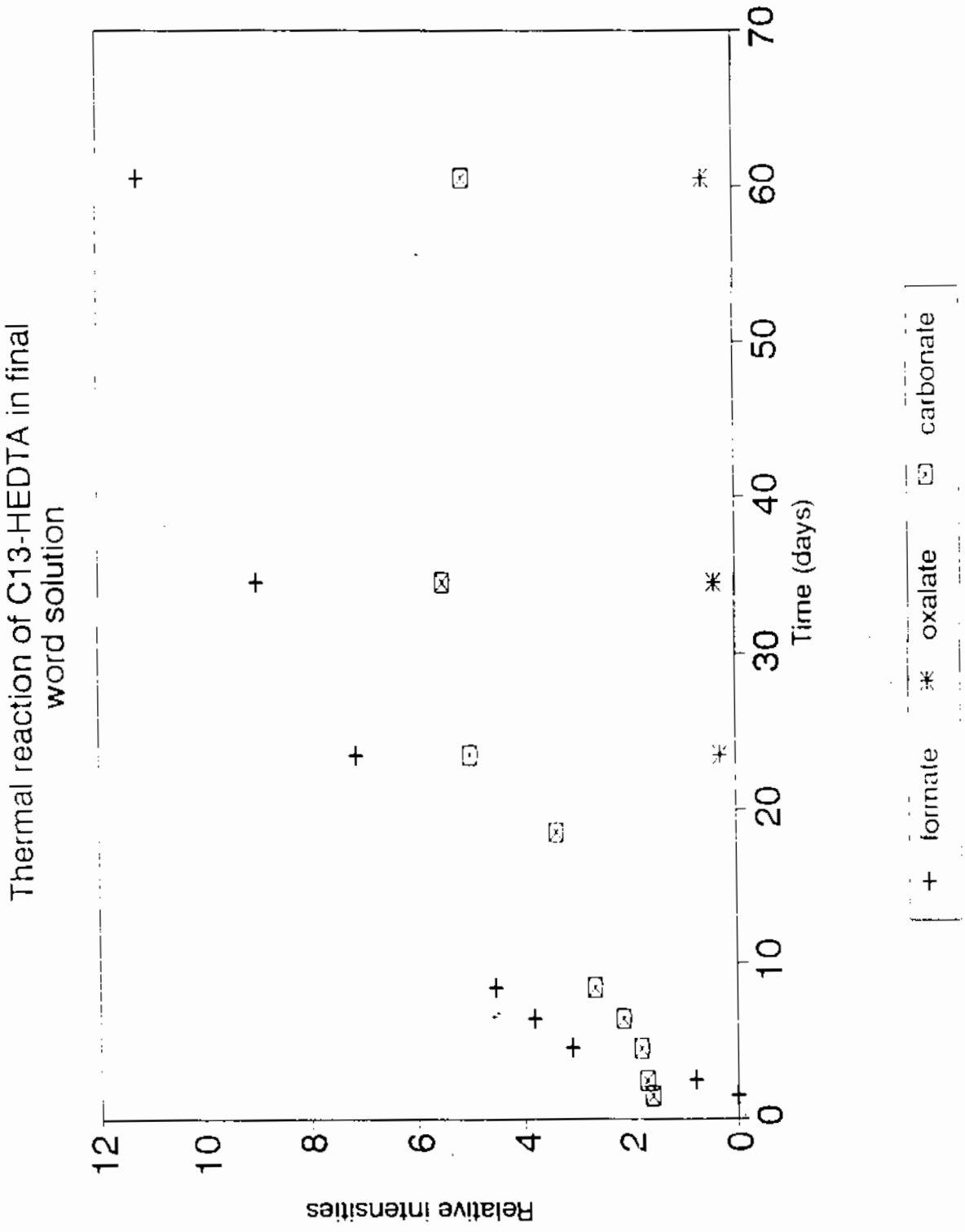
Thermal reaction of C13-HEDTA in final word solution
Relative intensities
0
2
4
6
8
10
12
0
10
20
30
40
50
60
70
Time (days)
formate
oxalate
carbonate

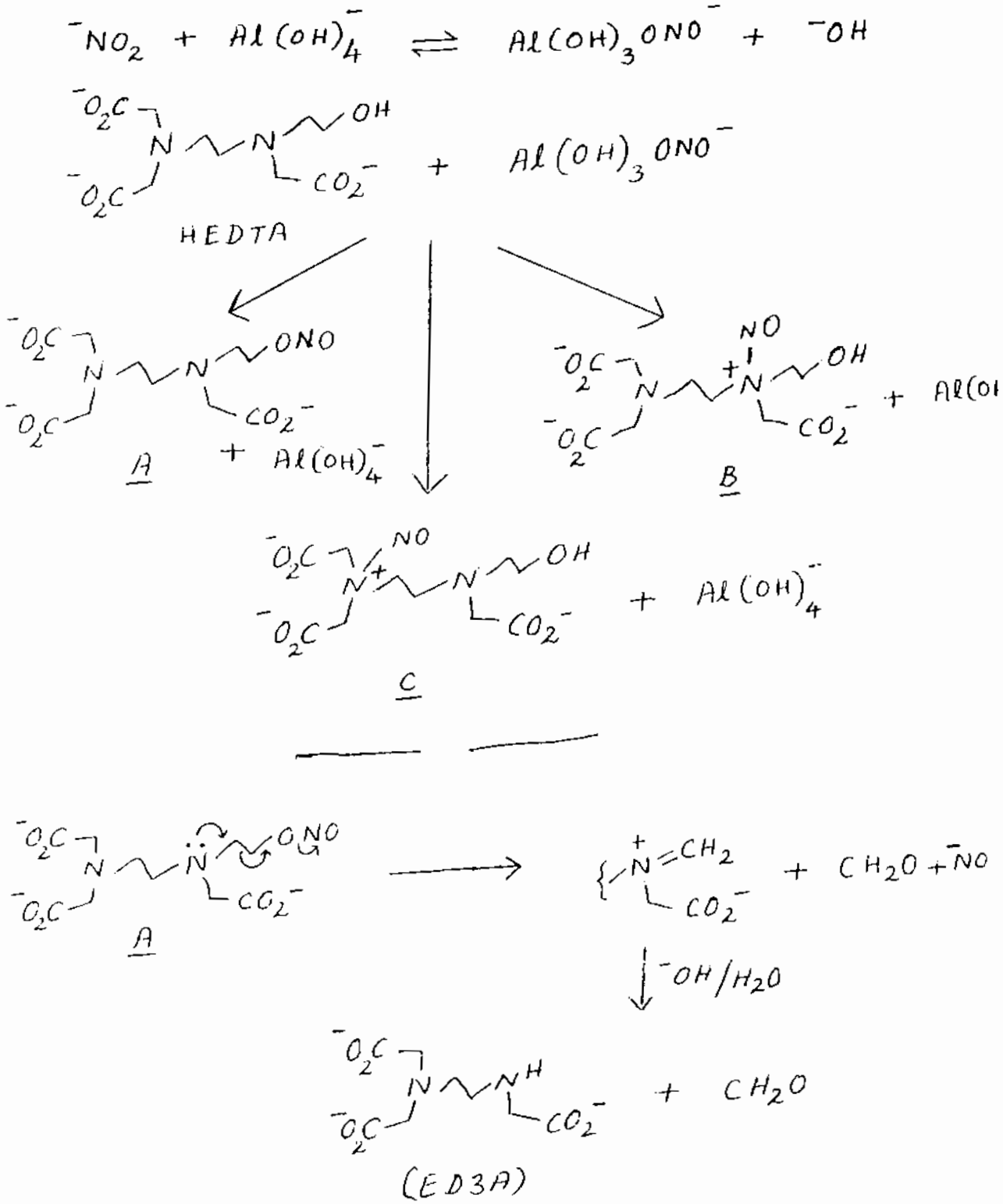
$^-NO_2 + Al(OH)_4^- \rightleftharpoons Al(OH)_3ONO^- + {}^-OH$
HEDTA
$Al(OH)_3ONO^-$
A
$+ Al(OH)_4^-$
B
+ Al(OI
C
$+ Al(OH)_4^-$

A
$+ CH_2O + {}^-NO$
$^-OH/H_2O$
(ED3A)
$+ CH_2O$

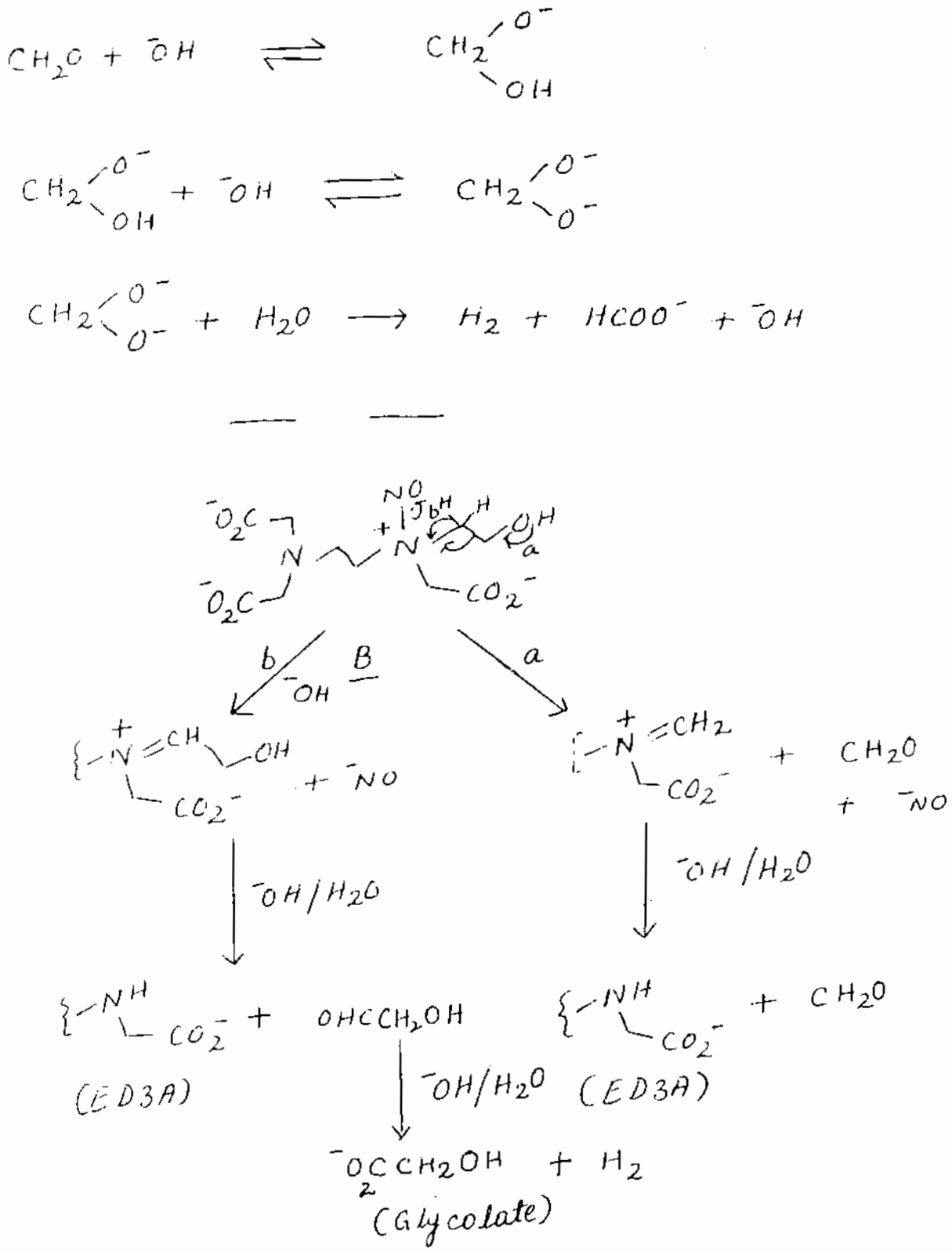
b
B
a
(EDTA)
(EDTA)
(Glycolate)

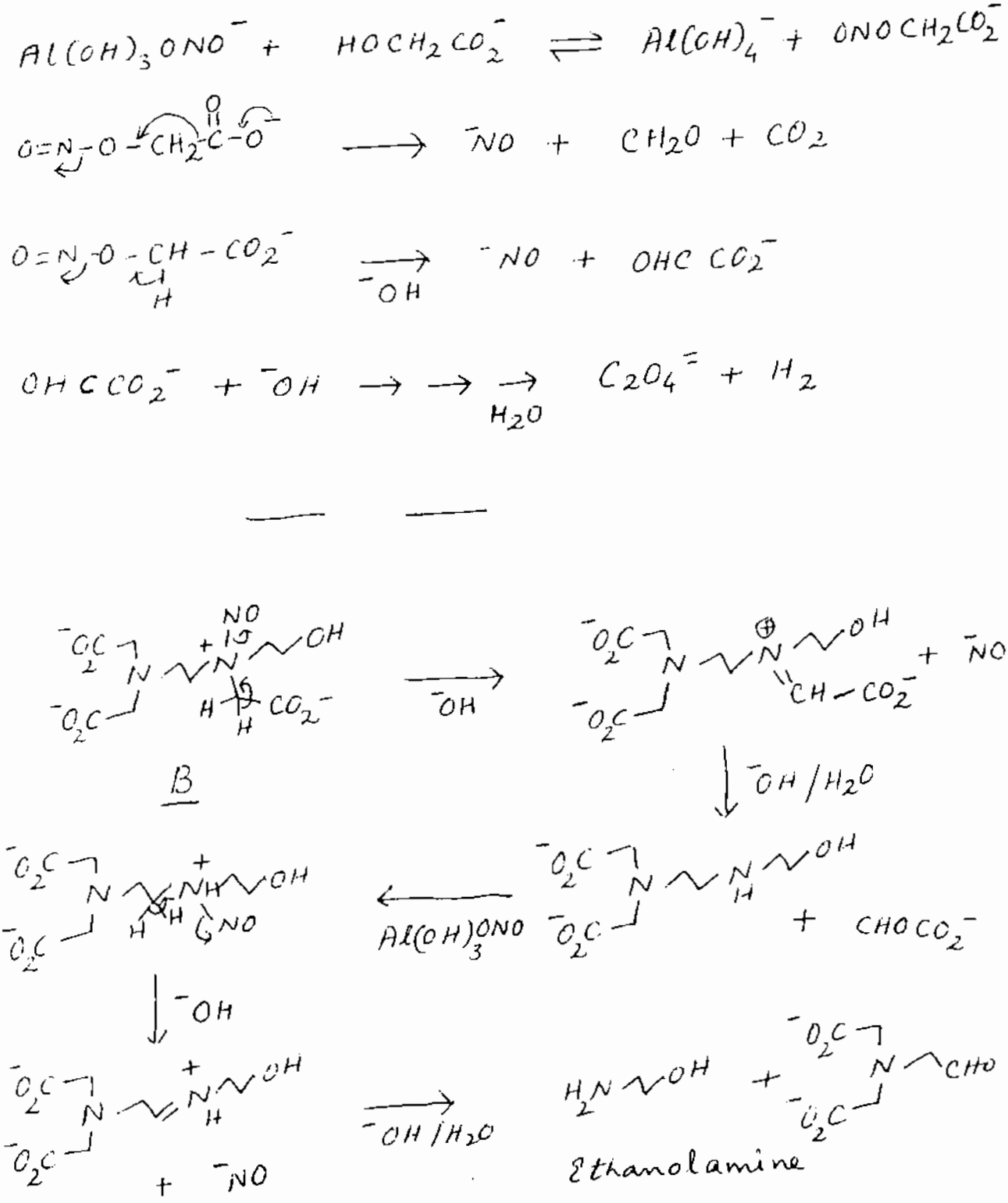

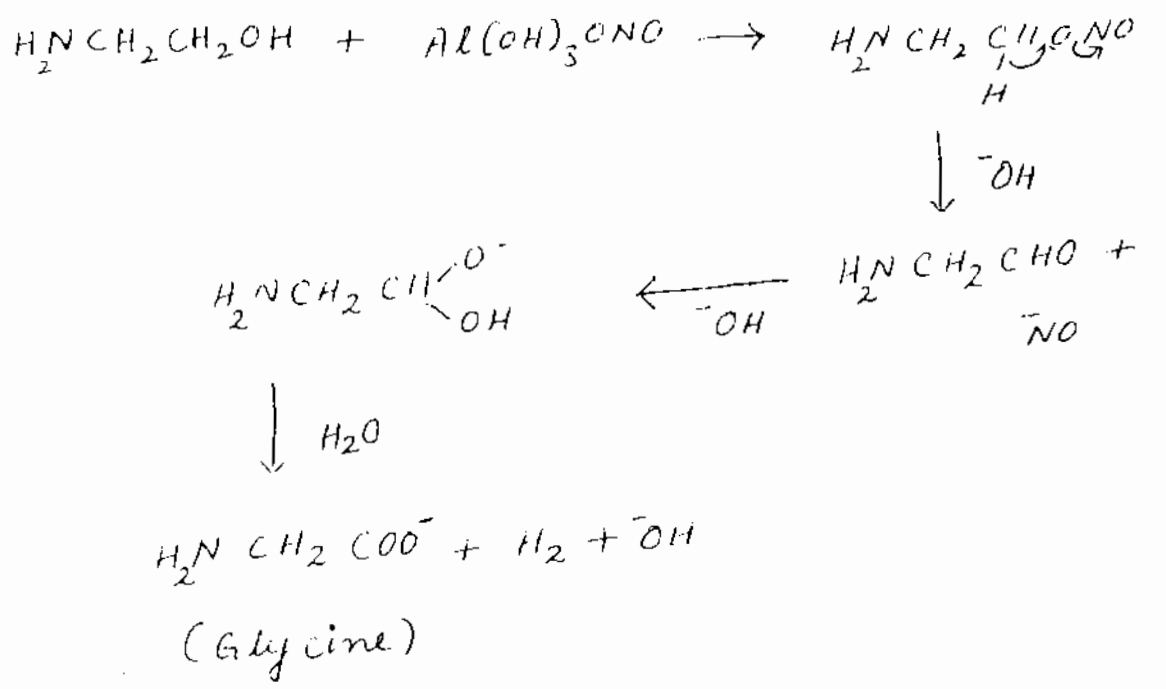

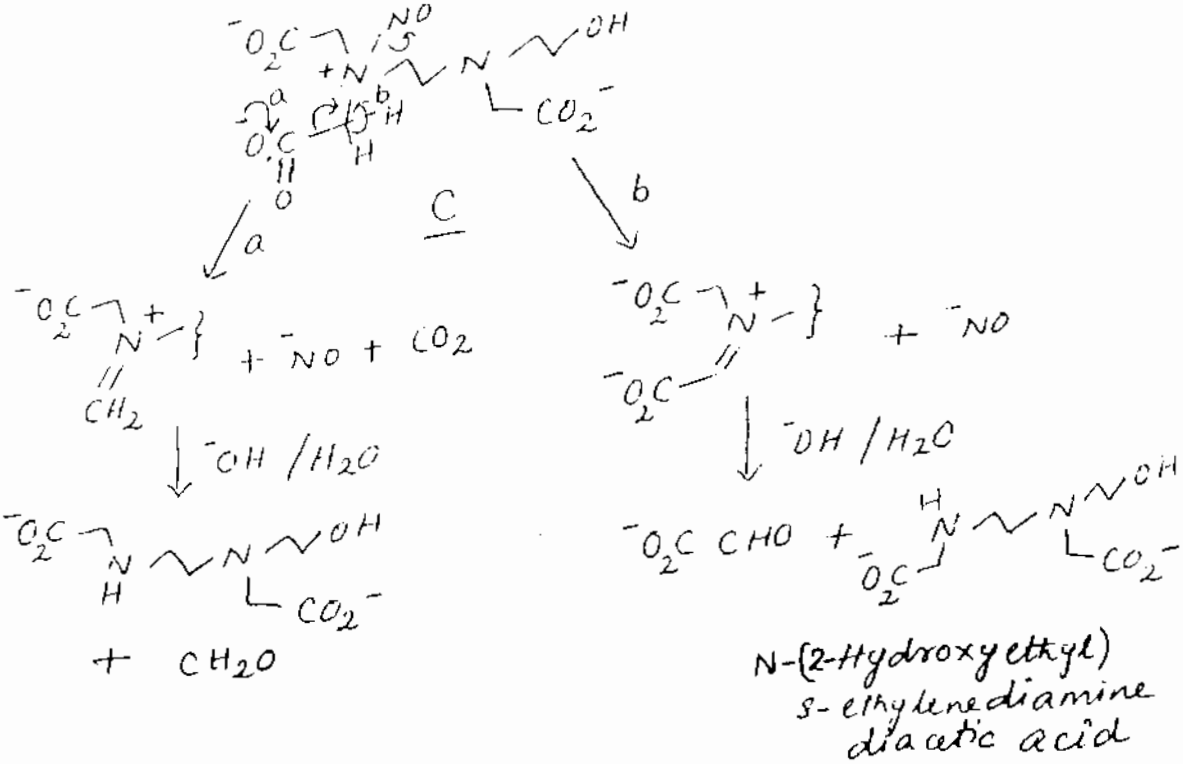

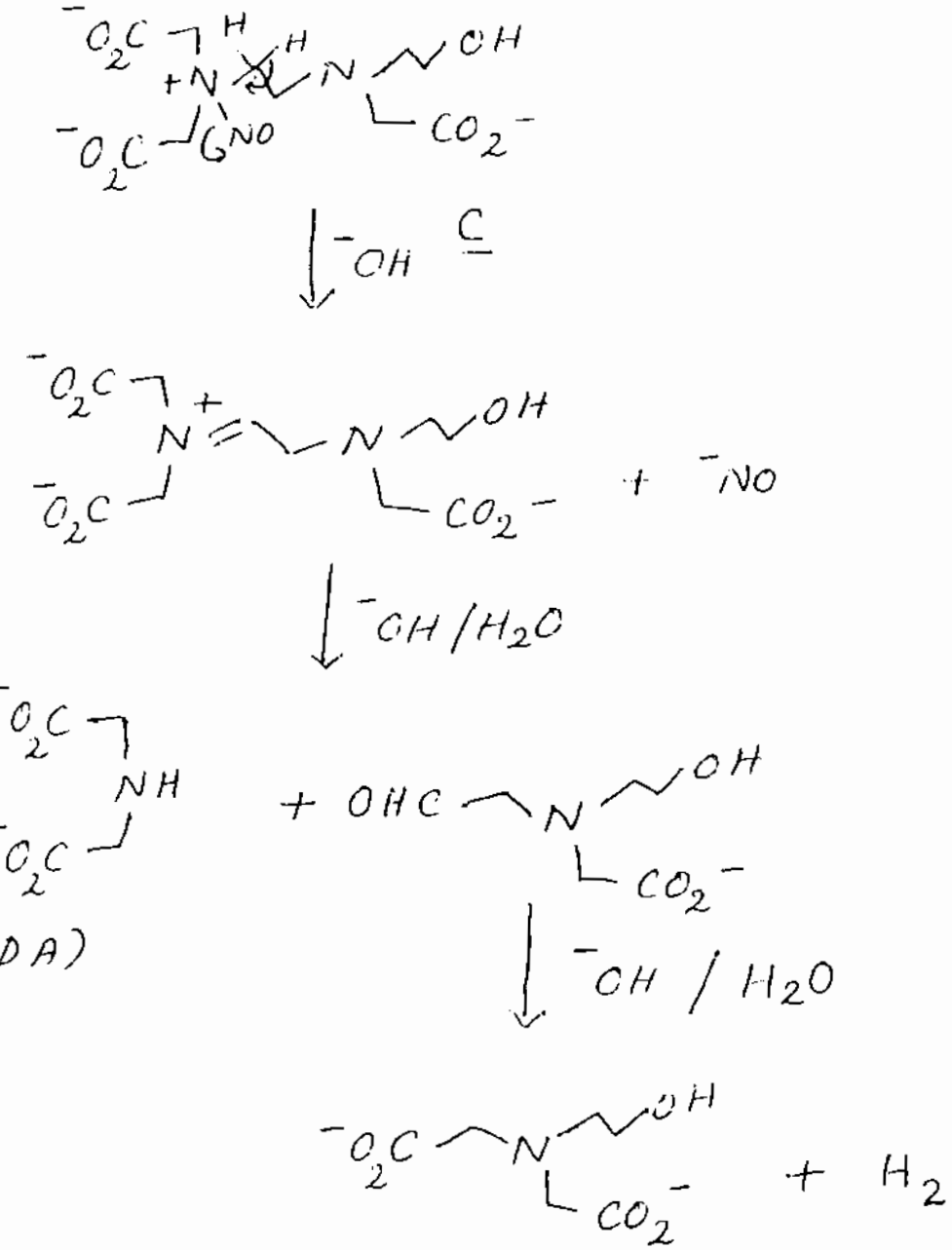
(IDA)
N-(2-Hydroxyethyl)
iminodiacetic acid

CARBON-13 CHEMICAL SHIFTS (ppm) IN FINAL WORD SOLUTION WITH C_6D_6 AS AN EXTERNAL STANDARD

EDTA	51.95	59.13	59.26	180.81				
HEDTA	51.47	52.09	56.75	58.45	59.11	59.39	180.71	180.99
*ED3A	45.71	52.50	54.99	59.92	180.62	180.99		
NTA	59.16	59.37	59.59	180.48				
IDA	52.19	180.61						
*s-EDDA	47.63	52.43	180.62					
u-EDDA	37.81	58.20	59.74	59.77	59.92	180.50	180.60	
*N-ME s-EDDA	42.31	45.63	52.57	56.26	56.31	61.89	179.56	180.56
*N-ME ED3A	42.60	52.65	54.43	59.88	62.15	180.53	180.80	
HIDA	57.43	57.49	57.54	57.61	58.34	59.89	180.64	
*DMG	44.66	44.73	63.31	179.48				
*GLY	45.05	182.68						
GLY. ACID	61.86	183.07						
*N-ME GLY	34.83	54.29	180.65					
*N-ME IDA	42.86	61.79	180.23					
ED	43.49							
N-ME ED	34.90	39.93	53.03					
HED	40.28	50.79	50.96	60.23				
*EDMA	40.06	50.73	52.30	180.56				
*N-ME u-EDDA	34.99	40.18	44.34	53.03	175.50			

*Chemical shifts for these compounds are measured with respect to sodium carbonate of the final word solution; chemical shift of sod. carbonate in final word solution is obtained with C_6D_6 as an external standard

Table 1

EDTA - Ethylenediaminetetraacetic acid
HEDTA - N-(hydroxyethyl)ethylenediamine-N,N'-triacetic acid
ED3A - Ethylenediaminetriacetic acid
NTA - Nitrilotriacetic acid
IDA - Iminodiacetic acid
s-EDDA - Ethylenediamine-N,N'-diacetic acid
u-EDDA - Ethylenediamine-N,N-diacetic acid
N-ME s-EDDA - N-(methyl)ethylenediamine-N,N'-diacetic acid
N-ME ED3A - N-(methyl)ethylenediaminetriacetic acid
HIDA - N-(hydroxyethyl)iminodiacetic acid
DMG - N,N-(dimethyl)glycine
GLY - Glycine
GLY ACID - Glycolic acid
N-ME GLY - N-(methyl)glycine
N-ME IDA - N-(methyl)iminodiacetic acid
ED - Ethylenediamine
N-ME ED - N-(methyl)ethylenediamine
HED - N-(hydroxyethyl)ethylenediamine
EDMA - Ethylenediamine-N-monoacetic acid
N-ME u-EDDA - N-(methyl)ethylenediamine-N,N-diacetic acid

Thermal Decomposition of ED3A-ED3A Lactam

Objective:

To examine products derived from thermal decomposition of ED3A and its rate of decomposition relative to HEDTA.

Experiment:

Simulated tank mixture including ED3A-lactam heated at 120 °C.

Observations:

After 18 days the evolution of hydrogen appeared to have ceased.

NMR (C-13) indicated that no ED3A-lactam (or ED3A) remained.

Formate, glycine and oxalate were identified as products.

From IC analysis 0.33 equiv. of formate and 0.2 equiv. of oxalate were present in the solution.

Decomposition of C-13 Labeled Glycolate $HO^{13}CH_2{}^{13}CO_2^-$

Objective:

To determine products derived from glycolate *in situ*.

Experiment:

Heat simulated waste mixture prepared with labeled acid and monitor ^{13}C NMR spectrum. Intensities measured relative to external benzene-d_6.

Observations:

Evidence for complexation of glycolate by aluminum; necessity of aluminum for decomposition not yet determined.

Formate, oxalate and carbonate are observed as products.

Disappearance of glycolate is first order.

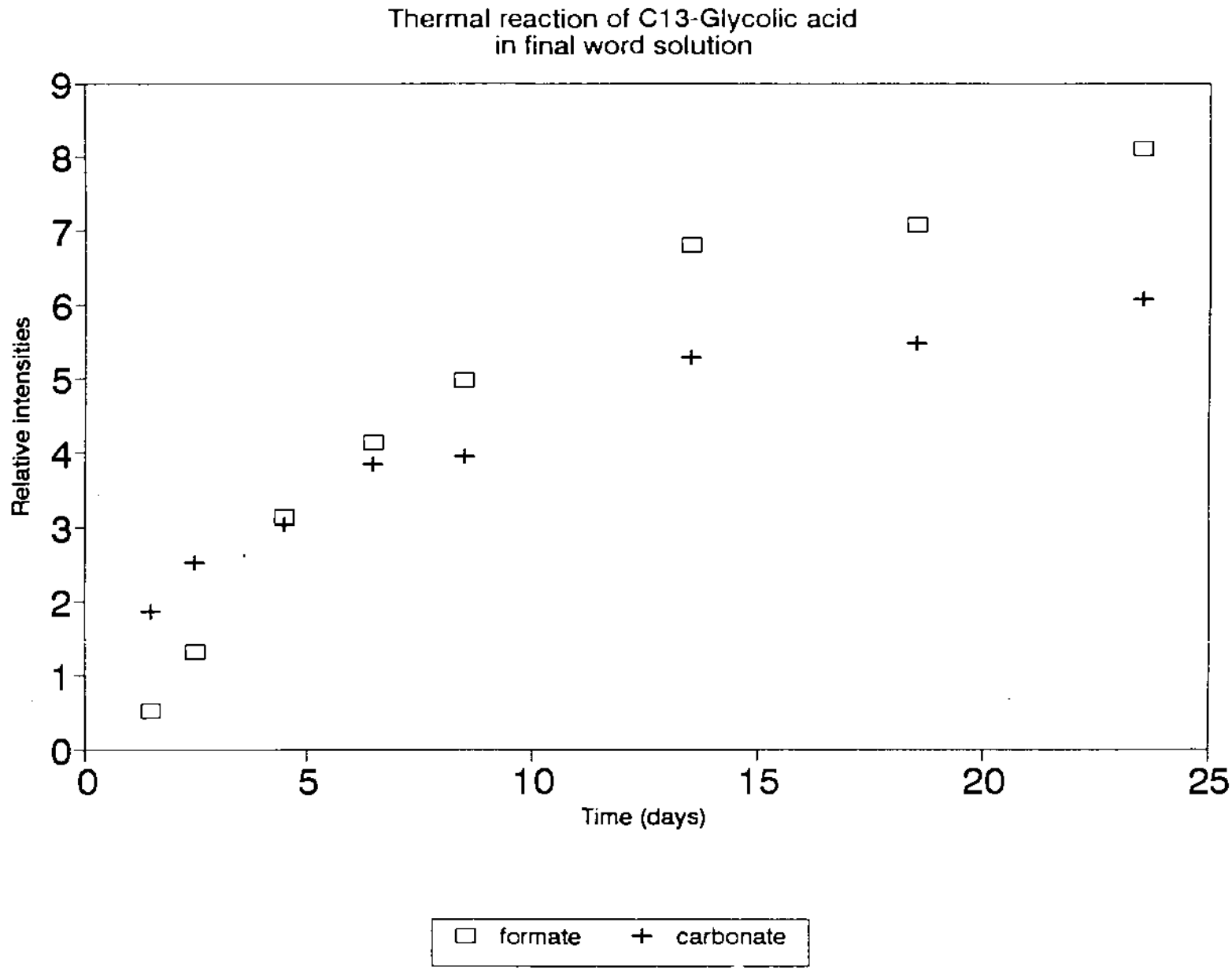
Thermal reaction of C13-Glycolic acid
in final word solution
Relative intensities
0
1
2
3
4
5
6
7
8
9
0
5
10
15
20
25
Time (days)
formate
carbonate

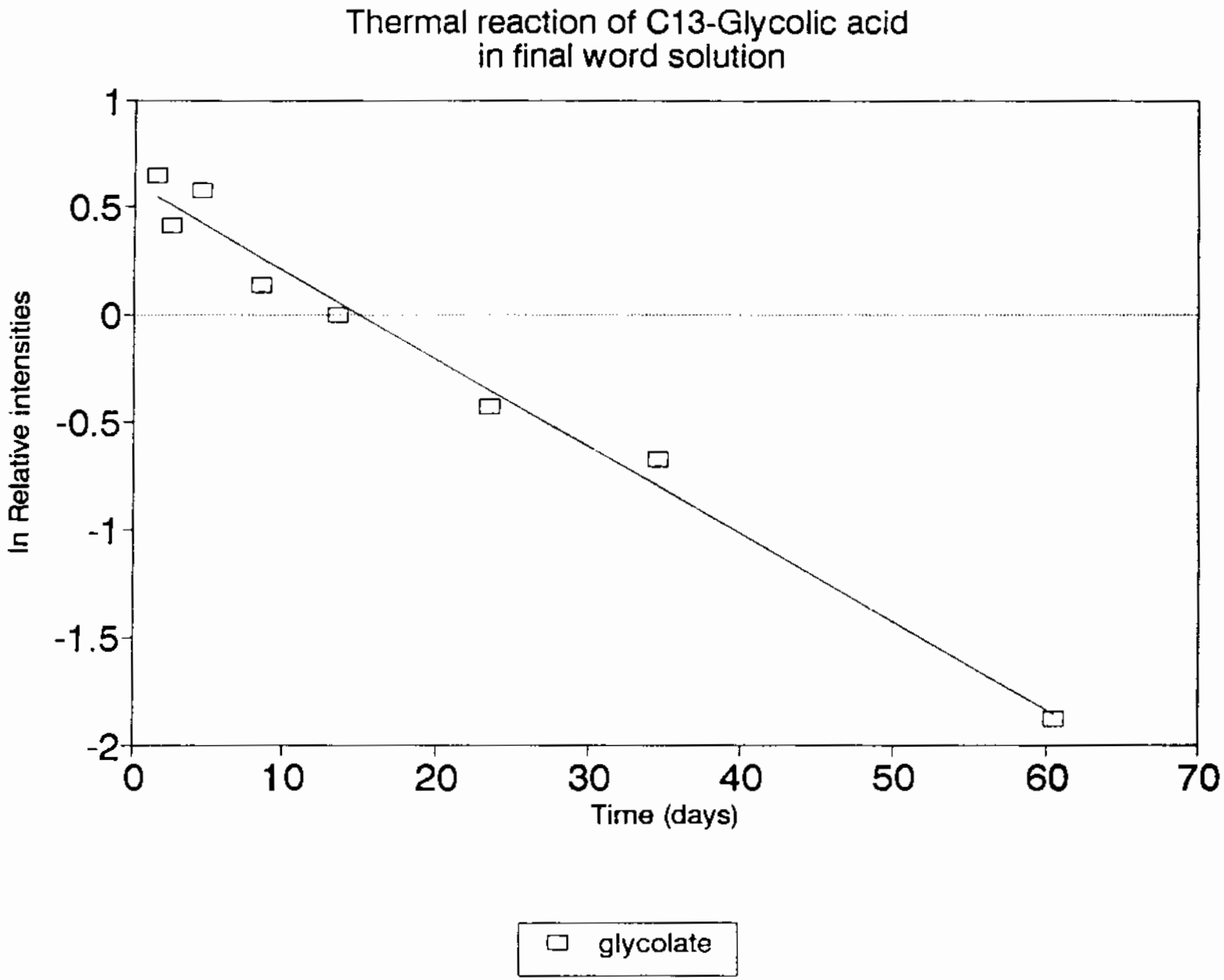
Thermal reaction of C13-Glycolic acid
in final word solution
ln Relative intensities
1
0.5
0
-0.5
-1
-1.5
-2
0
10
20
30
40
50
60
70
Time (days)
glycolate

Origin of Nitrous Oxide and Ammonia In Thermal Decompositions of HEDTA and Derived Organics

Experiment:

Simulated tank mixtures prepared with 1) 99% labeled $^{15}NO_2^-$ and $^{15}NO_3^-$ 2) 99% $^{15}NO_2^-$, and 3) 99% $^{15}NO_3^-$ heated at 120°

Experiment 1) was performed under air and under helium; 2) and 3) under helium only

Headspace gases analyzed by mass spectroscopy

Dissolved gases passed through $(CH_3)_2CHC(O)Cl$ to trap NH_3 as the imide

Conclusions:

Fully labeled N_2 and N_2O constitute the majority of the nitrogen containing products that are detectable by mass spectrometry in all reactions involving $^{15}NO_2^-$.

No label is incorporated in N_2 or N_2O when only $^{15}NO_3^-$ is used.

Peaks at m/e 45 and 29 are present in the mass spectra of gases under all conditions; these are consistent with $^{15}N^{14}NO$ or $^{14}N^{15}NO$, and $^{14}N^{15}N$. However, the relative intensities of the m/e 45 and 29 peaks and their intensities relative to the peaks from the fully labeled gases are not the same under all conditions which raises doubts as to their assignment.

No ^{15}N incorporation into the imide was detectable under air. No imide was detected from the experiment done under helium.

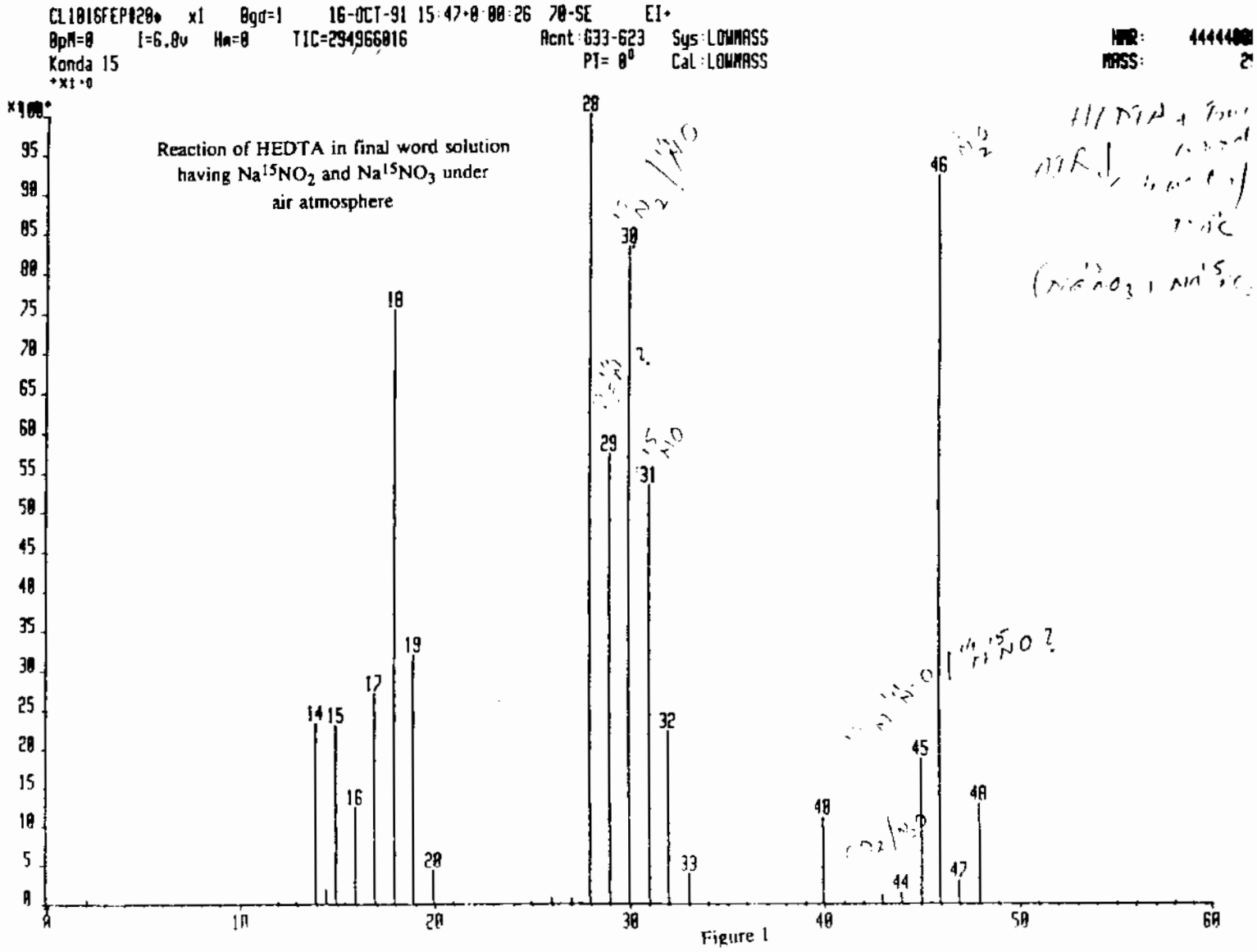
CL1016FEP#20◆ x1 Bgd=1 16-OCT-91 15:47:0:00:26 70-SE EI+
BpM=0 I=6.8v Ha=0 TIC=294966016 Acnt:633-623 Sys:LOWMASS
Konda 15 PT= 0° Cal:LOWMASS
Reaction of HEDTA in final word solution
having $Na^{15}NO_2$ and $Na^{15}NO_3$ under
air atmosphere
14 15 16 17 18 19 20 28 29 30 31 32 33 44 45 46 47 48 48
0 10 20 30 40 50 60

Figure 1

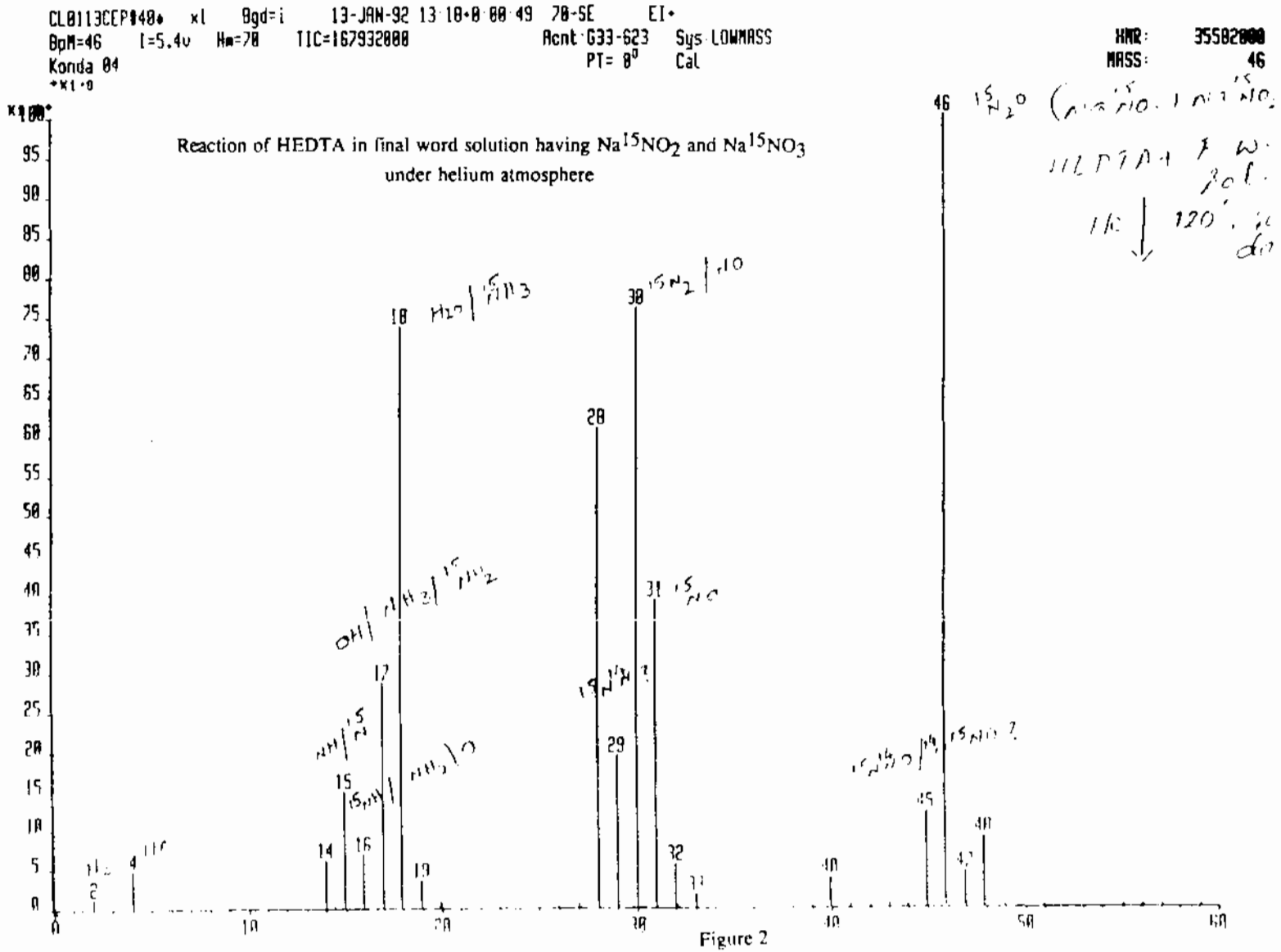
CL0113CEP#48♦ xl Bgd=i 13-JAN-92 13:10:8.00 49 70-SE EI+
BpM=46 I=5.4v Hm=70 TIC=167932000 Acnt G33-623 Sys LOWMASS
Konda 04 PT= 0° Cal
HMR: 35582000
MASS: 46
Reaction of HEDTA in final word solution having $Na^{15}NO_2$ and $Na^{15}NO_3$
under helium atmosphere

Figure 2

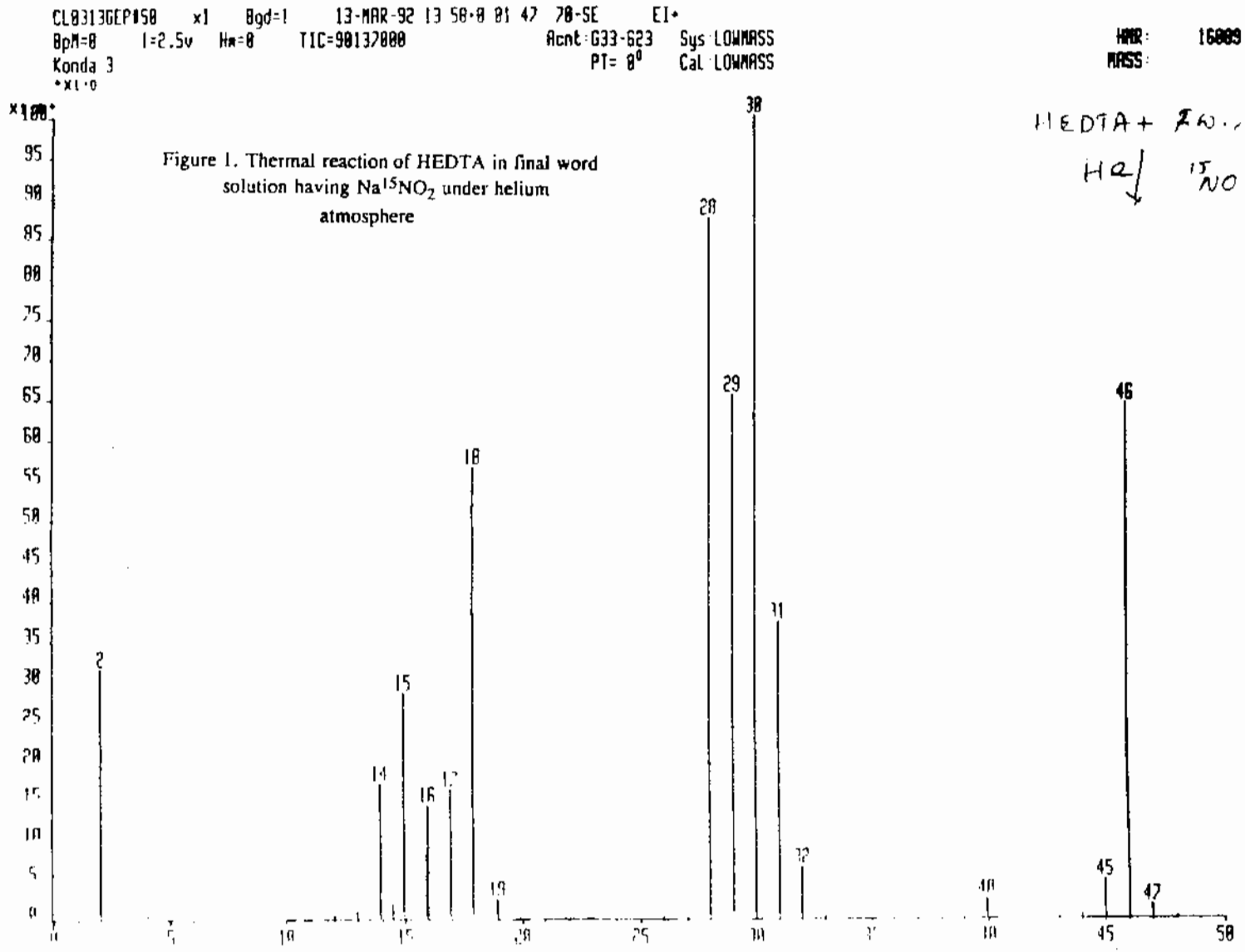
CL8313GEP#50 x1 Bgd=1 13-MAR-92 13 58·8 81 47 70-SE EI+
BpM=8 I=2.5v Hm=8 TIC=90137000 Acnt:G33-623 Sys:LOWMASS
Konda 3 PT= 8° Cal:LOWMASS
HMR: 16009
MASS:
HEDTA + Fe..
Ha
15NO
Figure 1. Thermal reaction of HEDTA in final word solution having Na15NO2 under helium atmosphere

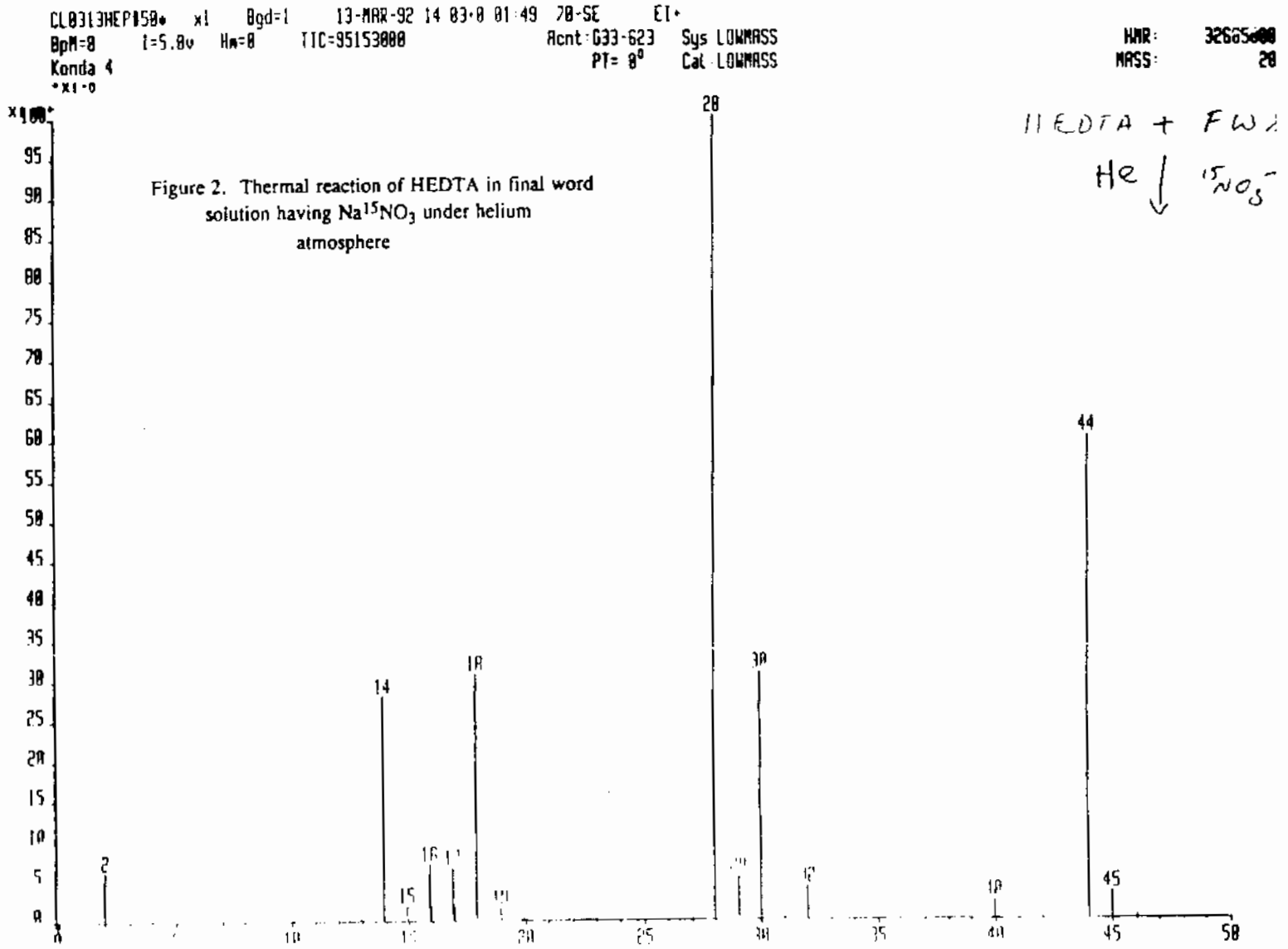

Figure 2. Thermal reaction of HEDTA in final word solution having $Na^{15}NO_3$ under helium atmosphere

11 EDTA + FW2

He ↓ $^{15}NO_3^-$

FORMALDEHYDE

- STOICHIOMETRY OF THE REACTION.

The ratio H_2:$HCOO^-$ is approximately 1:1 for the hydrogen-producing reaction. This indicates that the hydrogen molecule does not originate from formaldehyde only (for the ratio should be 0.5:1), but that water provides *at least* half of the hydrogen atoms necessary to produce H_2.

- ORDER IN FORMALDEHYDE AT DIFFERENT TEMPERATURES.

The order in formaldehyde is approximately 1 at r.t. and 90°C, indicating that one formaldehyde molecule is involved in the rate-determining step.

- RATE OF HYDROGEN EVOLUTION (CH_2O vs. CD_2O).

An important isotopic effect (>4) was observed, clearly indicating that the hydrogen-carbon bond is involved in the determining step of the reaction.

- YIELD OF HYDROGEN AT DIFFERENT CONCENTRATIONS OF CH_2O.

The hydrogen yield increases as the formaldehyde concentration decreases, both at r.t. and 60°C, indicating that the hydrogen-producing reaction is unimolecular respect to formaldehyde, and competes favorably at low [CH_2O] with the Cannizzaro (bimolecular) mechanism.

- EFFECT OF BASE CONCENTRATION ON THE HYDROGEN YIELD.

As the concentration of base increases, the hydrogen yield increases. This is due to the fact tbat when [OH^-] increases, the concentration of free aldehyde (which is necessary for the Cannizzaro reaction) decreases, thus allowing the hydrogen-producing reaction to predominate.

- REACTION IN THE PRESENCE OF p-HYDROQUINONE.

The rate of hydrogen evolution decreases in the presence of p-hydroquinone, indicating the presence of radical intermediates.

- EFFECT OF CUPRIC ION.

Trace amounts of cupric ion accelerate the hydrogen evolution, indicating that an electron transfer step could be involved.

- REACTION IN THE PRESENCE OF HYDROGEN PEROXIDE.

In the presence of hydrogen peroxide, the hydrogen evolution is much faster, and the hydrogen yield is 100% based on the amount of hydrogen peroxide added. Several mechanisms have been proposed in the literature in order to explain these results.

- **HYDROGEN YIELDS FROM ALDEHYDES IN THE PRESENCE OF BASE.**
  All investigated aldehydes without alfa hydrogens produced a significant amount of hydrogen in the presence of base, while propanaldehyde (which has two alfa hydrogens) produced only trace amounts of hydrogen.

- **PROPOSED MECHANISM.**
  Polar or electron transfer mechanisms could be involved. The second one could be either an initial electron transfer from the Cannizzaro intermediate to water followed by a hydrogen atom abstraction, or a chain reaction initiated by small amounts of hydrogen atoms produced by the thermally induced decomposition of formaldehyde.

- **DEUTERIUM TRACER EXPERIMENTS.**
  Though initially the deuterium labelling seemed to be an easy way to determine the mechanism of this reaction, its usefulness was seriously compromised because of an exchange reaction between hydrogen an deuterium oxide. At 90°C D_2 was the major gas observed when the reaction was carried out in the presence of D_2O/OD^-. Though H_2 was intitially the most important gas observed at r.t., this result could not be reproduced, and HD and D_2 where observed as the major products in later experiments. All these results can be explained taking into account the H_2/D_2O exchange, which produces HD and D_2.

REACTION OF FORMALDEHYDE IN THE PRESENCE OF BASE

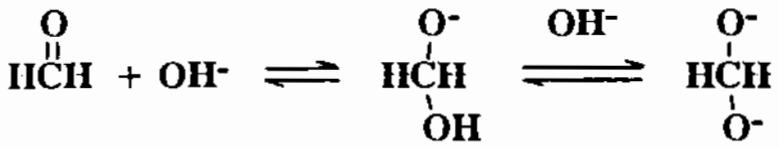

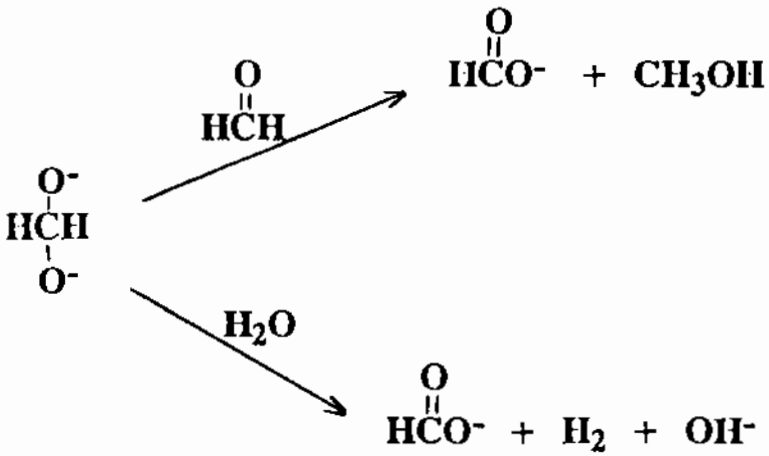

STOICHIOMETRY OF THE REACTION

T	$[CH_2O]_i$	[NaOH]	$\%H_2$	$\%HCOO^-$	$\%CH_3OH$
rt	4.10^{-4}	19	102.4	97.0	
90°C	2.10^{-2}	17	41.1	71.3	27.0

$$\%HCOO^- - \%CH_3OH = 71.3 - 27.0 = 44.3 \approx 41.1 = \%H_2$$

Table. Order in Formaldehyde at Different Temperatures

$[NaOH]_i M$	$[CH_2O]_i M$	T, °C	order[a]
18	0.02 to 1	28 ± 1	1.09
7	0.02 to 0.1	90 ± 1	0.91

[a] Calculated by measuring the initial rates of H_2 evolution at different $[CH_2O]$, and then taking the slope from the plot ln (initial rate) vs. $\ln([CH_2O])$.

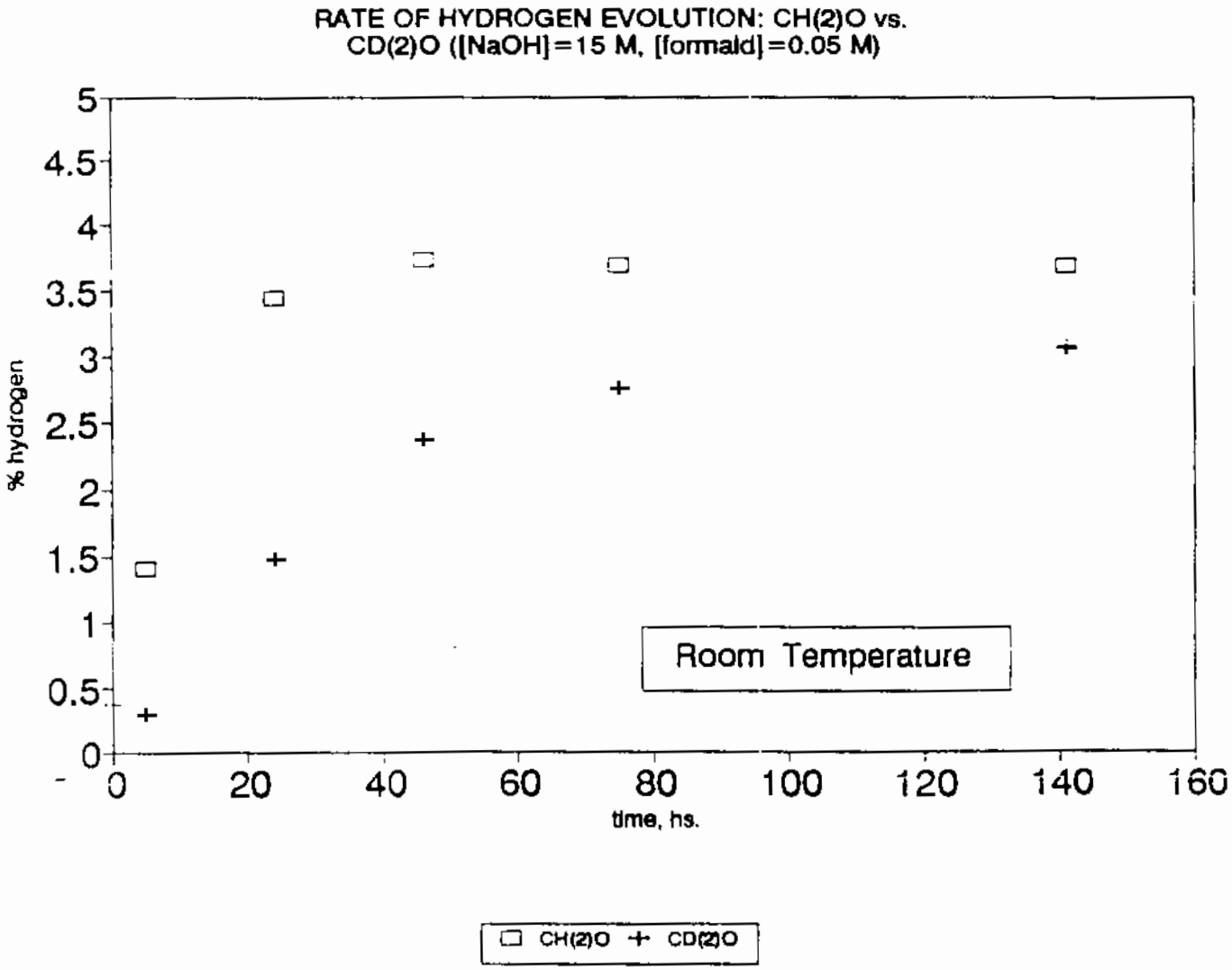
RATE OF HYDROGEN EVOLUTION: CH(2)O vs.
CD(2)O ([NaOH]=15 M, [formald]=0.05 M)
% hydrogen
time, hs.
Room Temperature
CH(2)O
CD(2)O

Yield of Hydrogen at Different Concentrations of Formaldehyde.

$[CH_2O]$	2.10^{-1}	2.10^{-2}	2.10^{-3}	4.10^{-4}	4.10^{-5}
$\%H_2$[a]	1.4	8.2	34.5	61.1	103.8
$\%H_2$[b]	6.5	30.8	75.7	102.4	99.0

[a]T = 60°C, [NaOH] = 11 M.
[b]T = r.t., [NaOH] = 19 M.

Effect of Base Concentration on the Hydrogen Yield.

T, °C	$[CH_2O]$, M	[NaOH], M	$\%H_2$
60	0.2	3	0.1
60	0.2	15	14.2

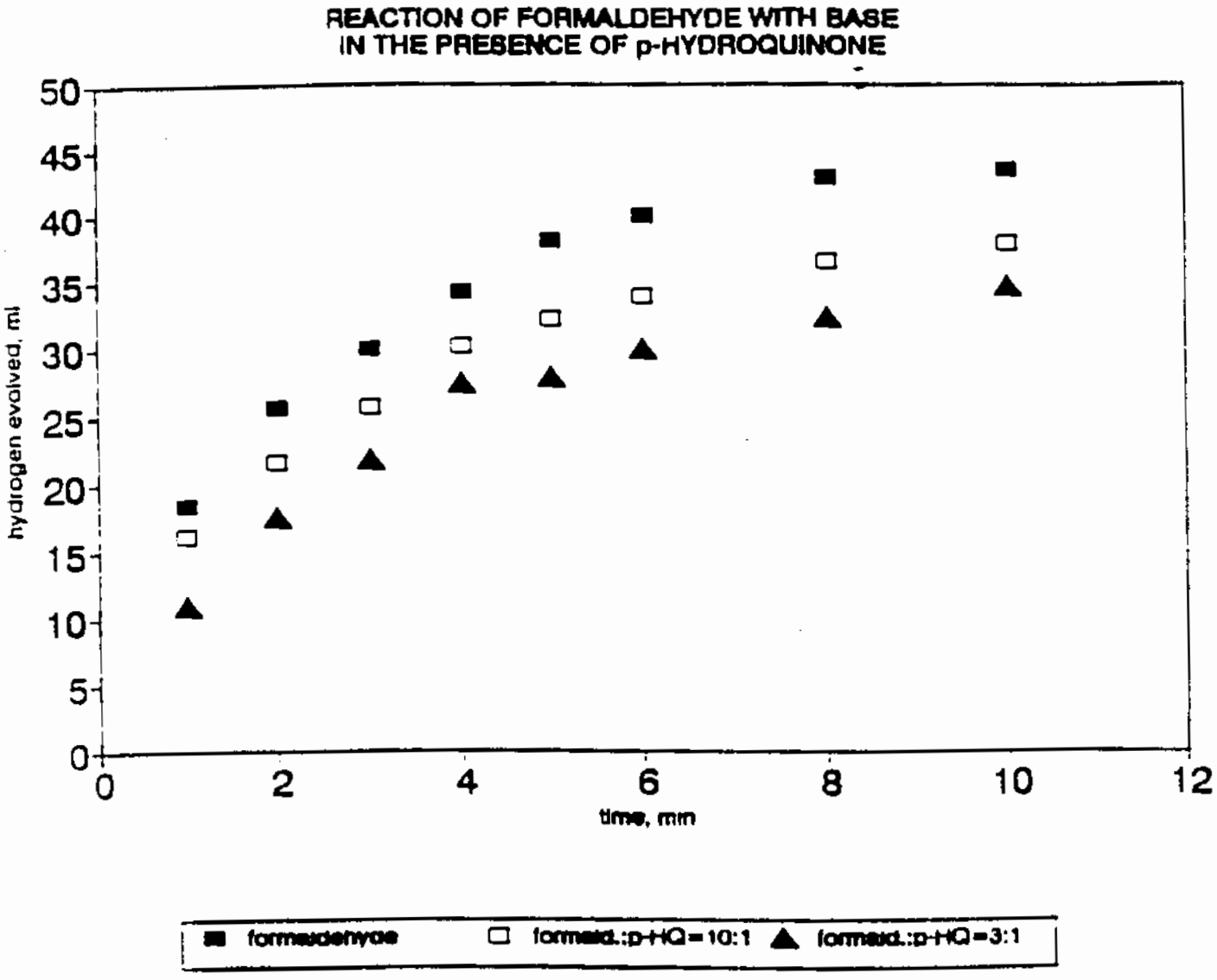
REACTION OF FORMALDEHYDE WITH BASE
IN THE PRESENCE OF p-HYDROQUINONE
hydrogen evolved, ml
50
45
40
35
30
25
20
15
10
5
0
0
2
4
6
8
10
12
time, mm
formaldehyde
formald.:p-HQ=10:1
formald.:p-HQ=3:1

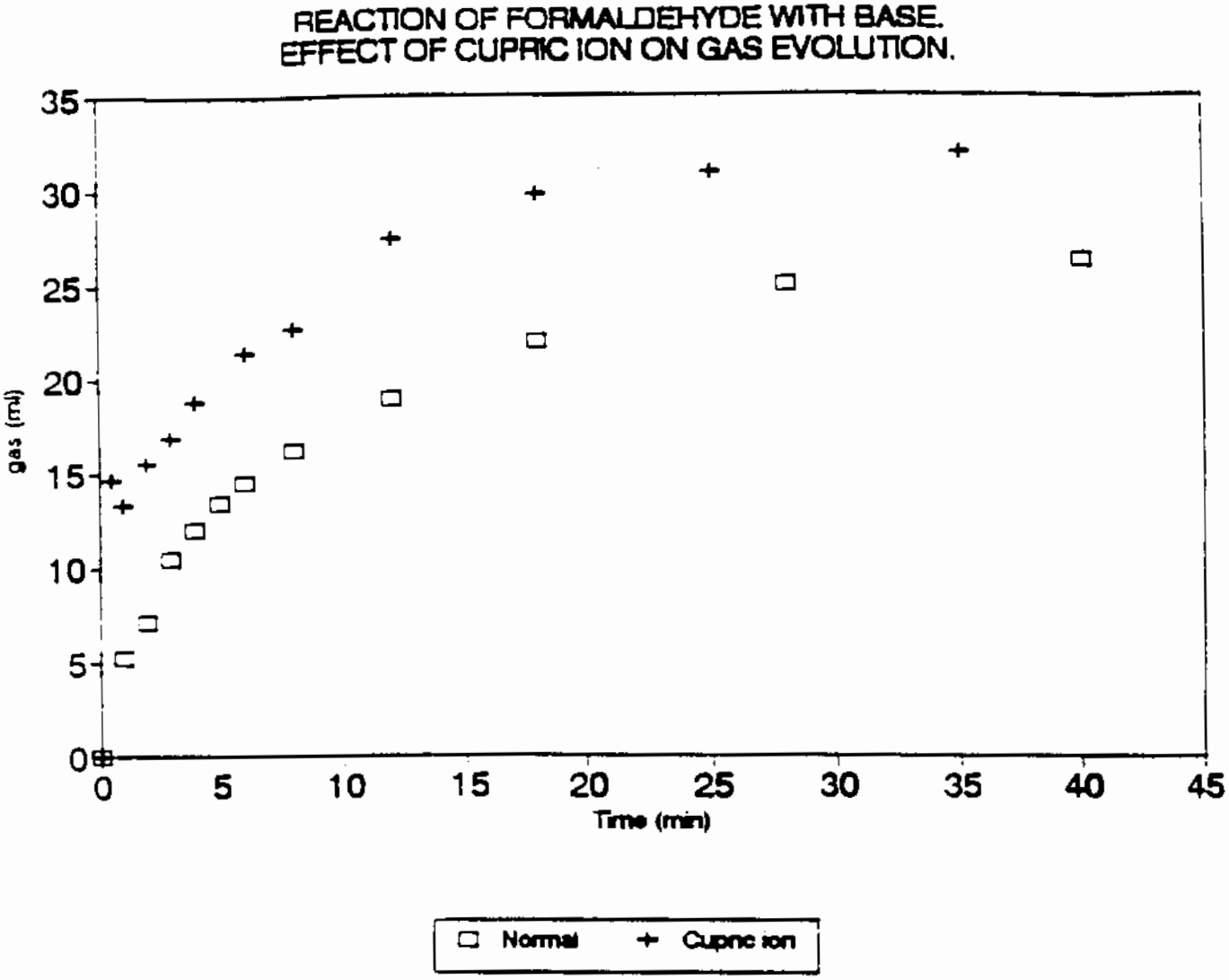

$$CuCl_2 + 2\ CH_2O + 4NaOH \rightarrow Cu + H_2 + 2\ HCOONa + 2H_2O + 2\ NaCl$$

REACTION IN THE PRESENCE OF HYDROGEN PEROXIDE

$$2\ CH_2O + H_2O_2 + 2NaOH \rightarrow 2\ HCOONa + 2H_2O + H_2$$

[NaOH]	$[CH_2O]$	$[H_2O_2]$	%$HCOO^-$	%CH_3OH	%H_2 [a]
2	0.20	0.11	96	0	99.5
2	0.20	0.02	21[b]	traces[b]	21.4[b]

[a] Yield based on formaldehyde.
[b] Results after 30 minutes of reaction.

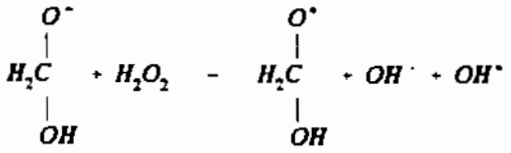

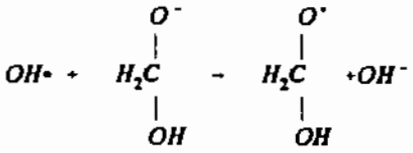

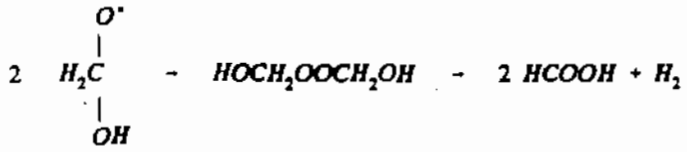

Wirtz, K; Bonhoeffer, K. F.; Z. *Physik Chem.*, 328, 108-112 (1936).

Hydrogen yields from aldehydes in the presence of base.[a]

aldehyde	$\%H_2$
benzaldehyde	16.9
glyoxalate	29.0
pivalaldehyde	30.1
formaldehyde	41.1
propanaldehyde	1.6

[a] T = 90°C, [NaOH] = 17 M, [RCHO] = 0.017 M in all cases.

PhCHO	CHO-COONa	$(CH_3)_3CCHO$	CH_3CH_2CHO
benzaldehyde	glyoxalate	pivalaldehyde	propanaldehyde

DEUTERIUM TRACER EXPERIMENTS

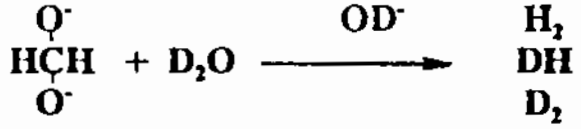

90°C: $D_2 > > HD, H_2$

rt : $(H_2 > > HD, D_2)$
$HD, D_2 > > H_2$

PROPOSED MECHANISM FOR HYDROGEN GENERATION FROM FORMALDEHYDE IN THE PRESENCE OF BASE

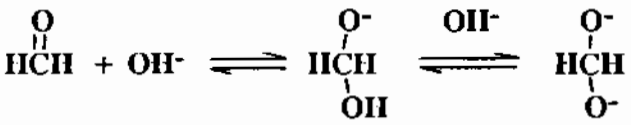

Polar

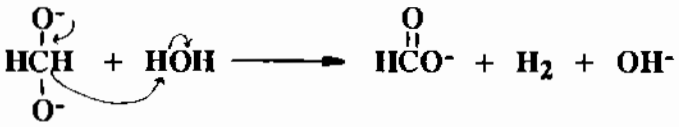

Electron Transfer

A-

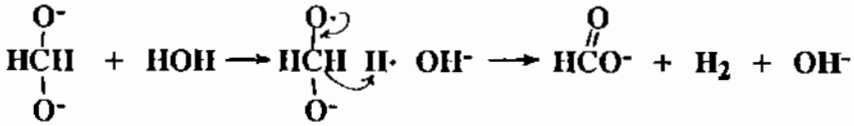

B-

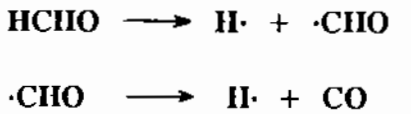

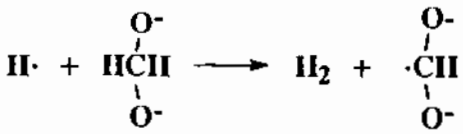

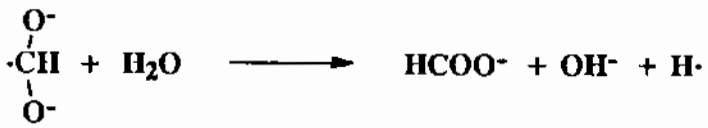

SUMMARY

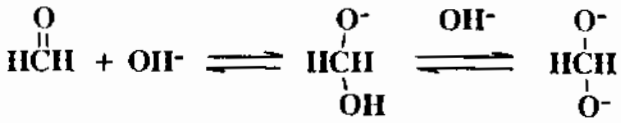

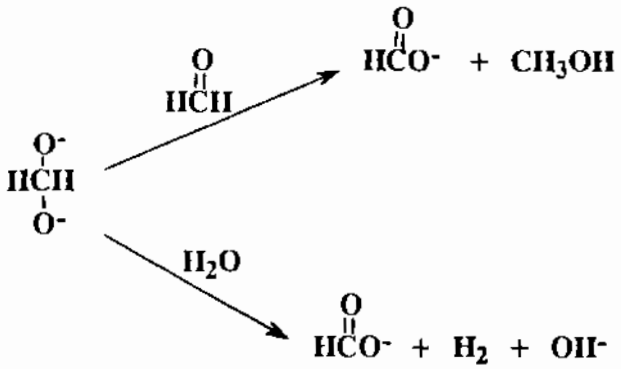

MECHANISM: Polar
Free Radical

STUDIES:
- Isotopic Labeling
- Concentration of base
- Concentration of formaldehyde
- Kinetics
- Stoichiometry
- Radical Traps
- Effect of Transition Metal Ions
- Effect of Hydrogen Peroxide

MODEL SYSTEMS

- MODEL SYSTEMS.

The model systems are simplified versions of EDTA and HEDTA. These systems are much simpler than EDTA and HEDTA and should allow one to determine the reactions of the $-CH_2CH_2OH$ and $-CH_2COOH$ groups without being affected by the others groups found in EDTA and HEDTA which complicate the mechanistic interpretation of the results.

N,N-DIETHYLETHANOLAMINE IN FINAL WORD SOLUTION.

- GAS EVOLUTION MEASUREMENTS.

Gas absorption is observed until approximately 400 hs. After that period, the gas evolution starts.

- OXYGEN ABSORPTION.

Oxygen is absorbed by the solution and only 20% of the original amount of oxygen present is left after 300 hs. Though the oxygen evolution could not be followed after tbat time, an extrapolation predicts that all the oxygen should be consumed at approximately 400 hs.

- HYDROGEN, NITROUS OXIDE, AND METHANE PRODUCTION.

Hydrogen, nitrous oxide, and methane are observed as gaseous products. Though hydrogen is initially produced at a faster rate than nitrous oxide, its production slows down at approximately 300 hs. while nitrous oxide doesn't diminish its production rate even after 1000 hs.

- FORMATE AND ACETATE PRODUCTION.

Formate and acetate are the most important products observed by ^{1}H-NMR. A small amount of formate is observed since the beginning of the reaction due to impurities present in the final word solution (presumably due to carbonate).

N,N-DIMETHYLGLYCINE.

- HYDROGEN EVOLUTION.

Hydrogen is tbe most important gas observed in this reaction. Nitrous oxide and methane are produced only in trace amounts (< 0.1%).

- PRODUCT YIELDS AT 956 hrs.

The quantities of starting material and oxygen consumed, and hydrogen and

MODEL SYSTEMS

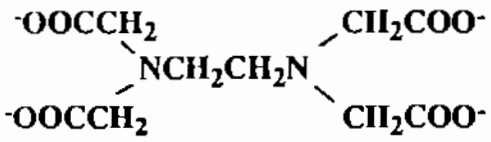

EDTA

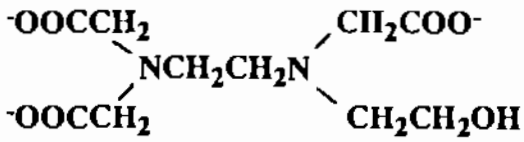

HEDTA

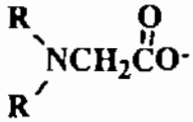

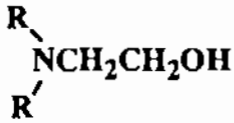

(R = alkyl)

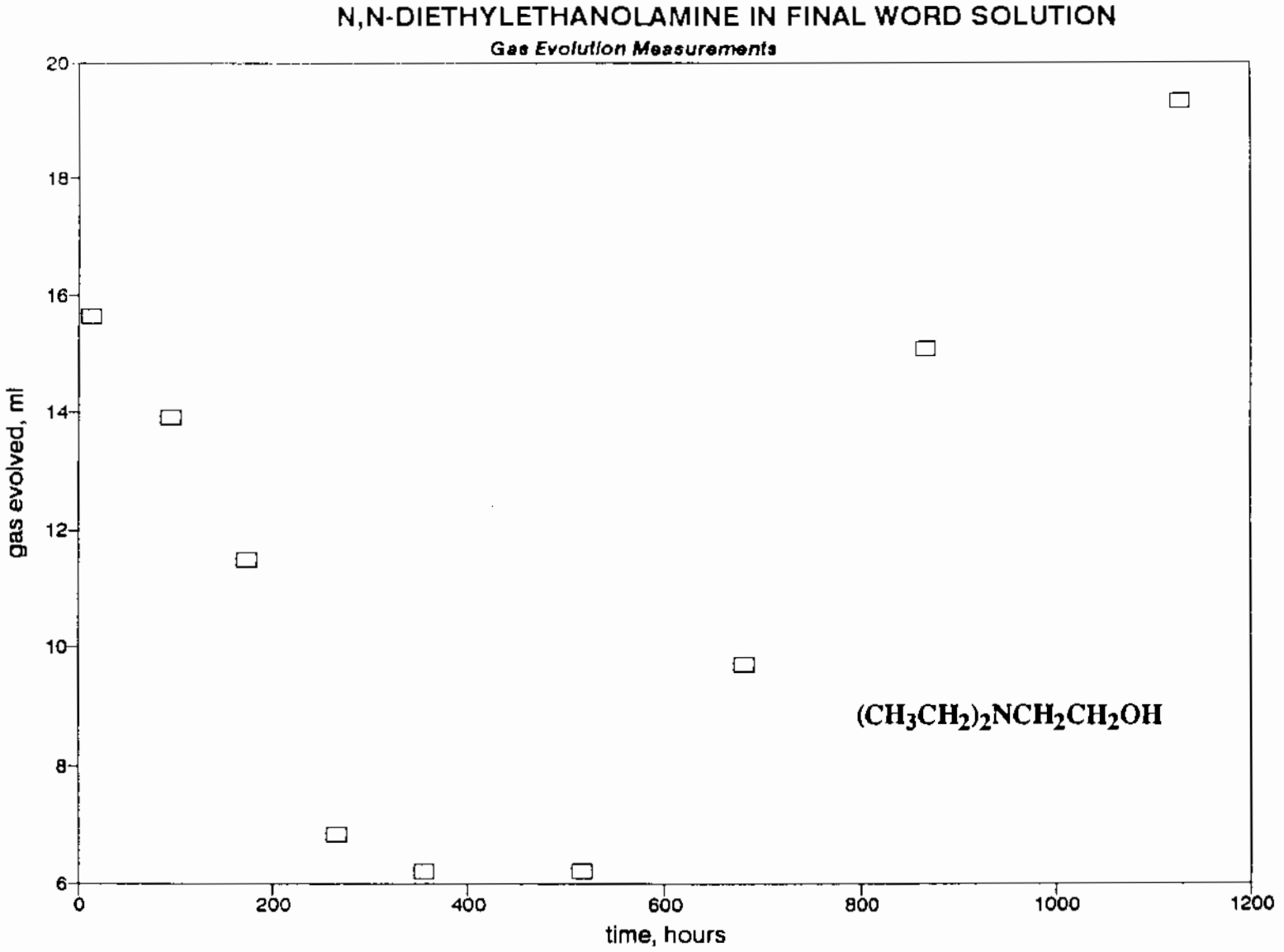
N,N-DIETHYLETHANOLAMINE IN FINAL WORD SOLUTION
Gas Evolution Measurements
gas evolved, ml
time, hours
20
18
16
14
12
10
8
6
0
200
400
600
800
1000
1200
(CH3CH2)2NCH2CH2OH

DEA-1

N,N-DIETHYLETHANOLAMINE IN FINAL WORD SOLUTION

Oxygen absorption

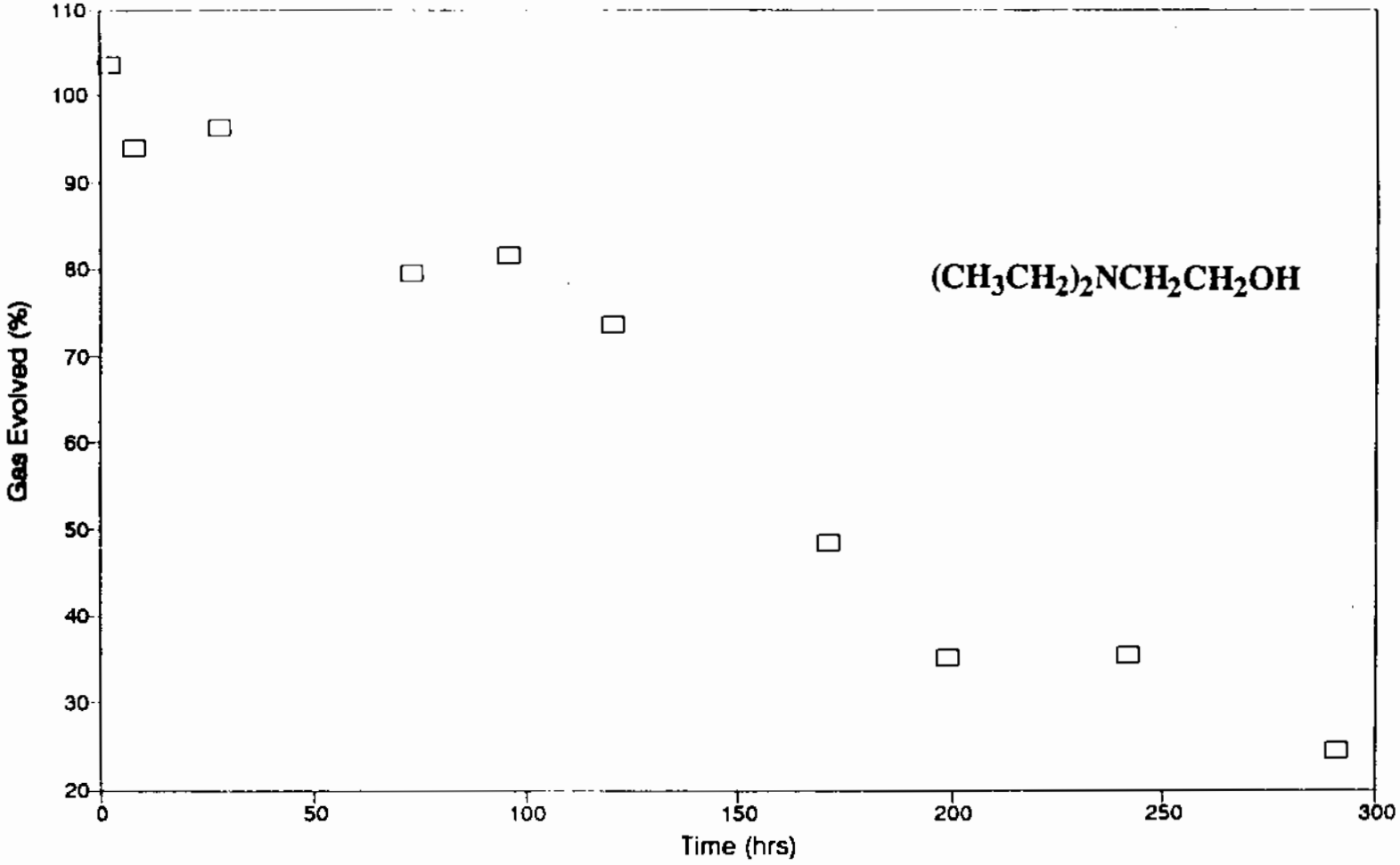

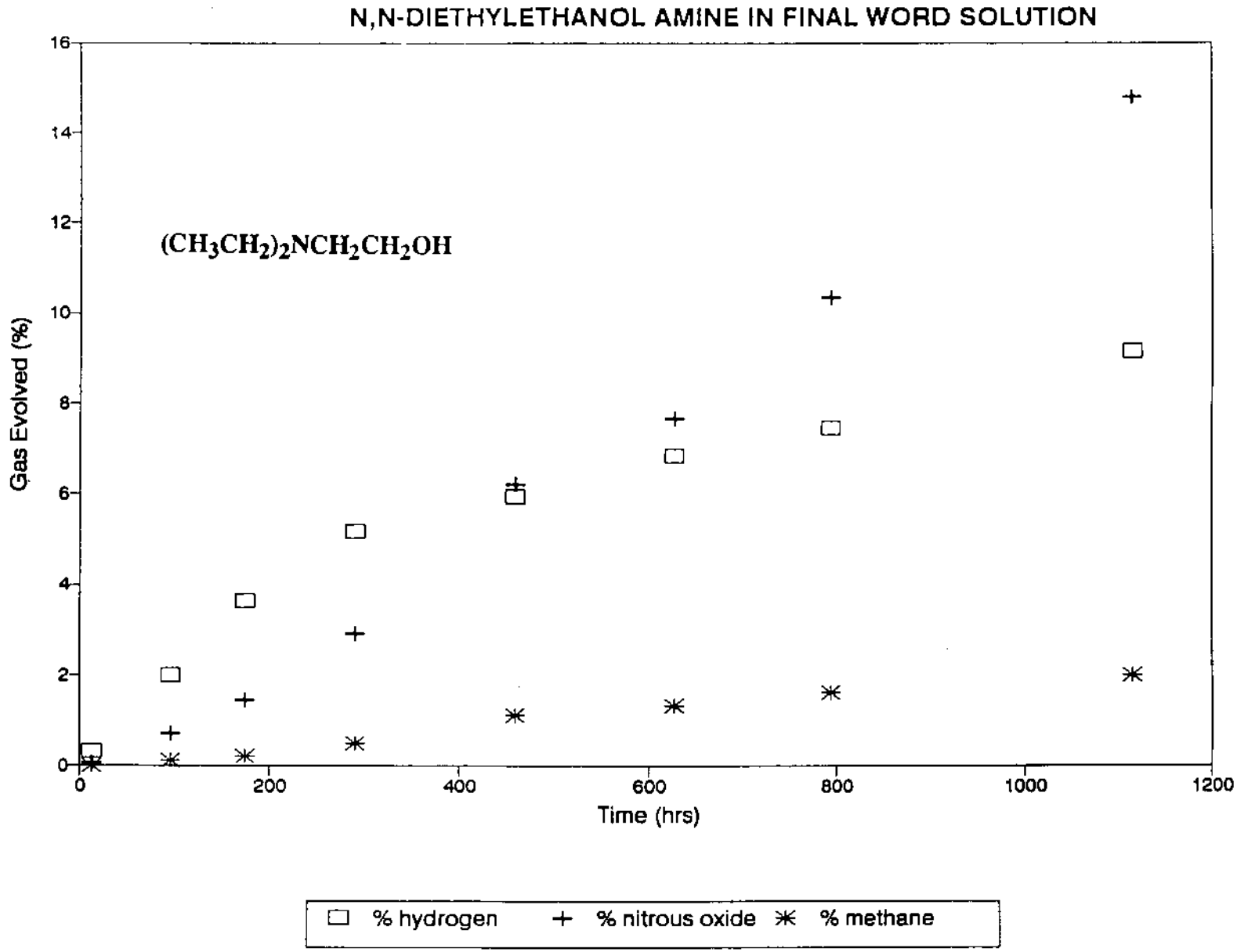
N,N-DIETHYLETHANOL AMINE IN FINAL WORD SOLUTION
$(CH_3CH_2)_2NCH_2CH_2OH$
Gas Evolved (%)
Time (hrs)
0
2
4
6
8
10
12
14
16
0
200
400
600
800
1000
1200
% hydrogen
% nitrous oxide
% methane

DEA-1

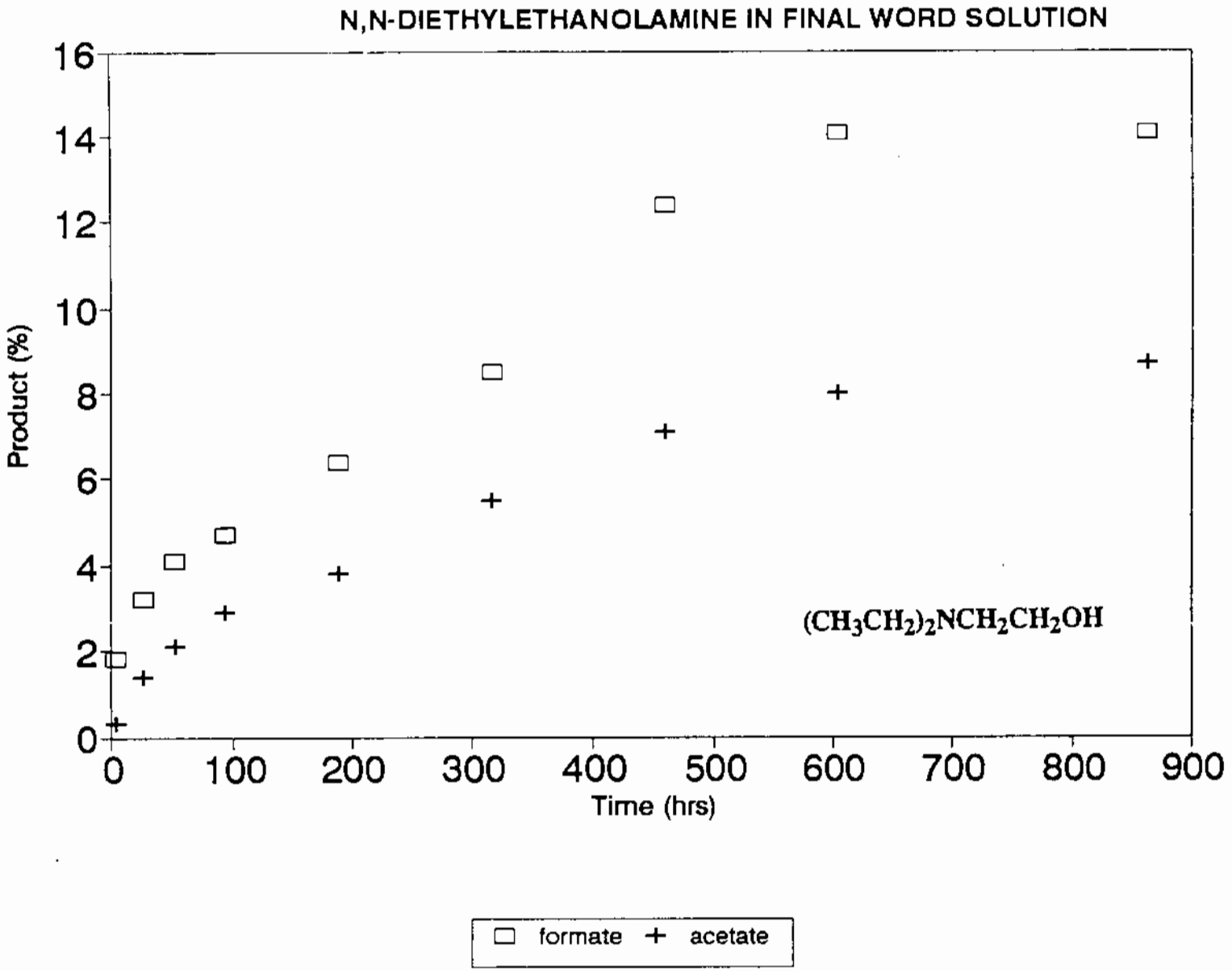
N,N-DIETHYLETHANOLAMINE IN FINAL WORD SOLUTION
Product (%)
16
14
12
10
8
6
4
2
0
0
100
200
300
400
500
600
700
800
900
Time (hrs)
(CH3CH2)2NCH2CH2OH
formate
acetate

DEA-2

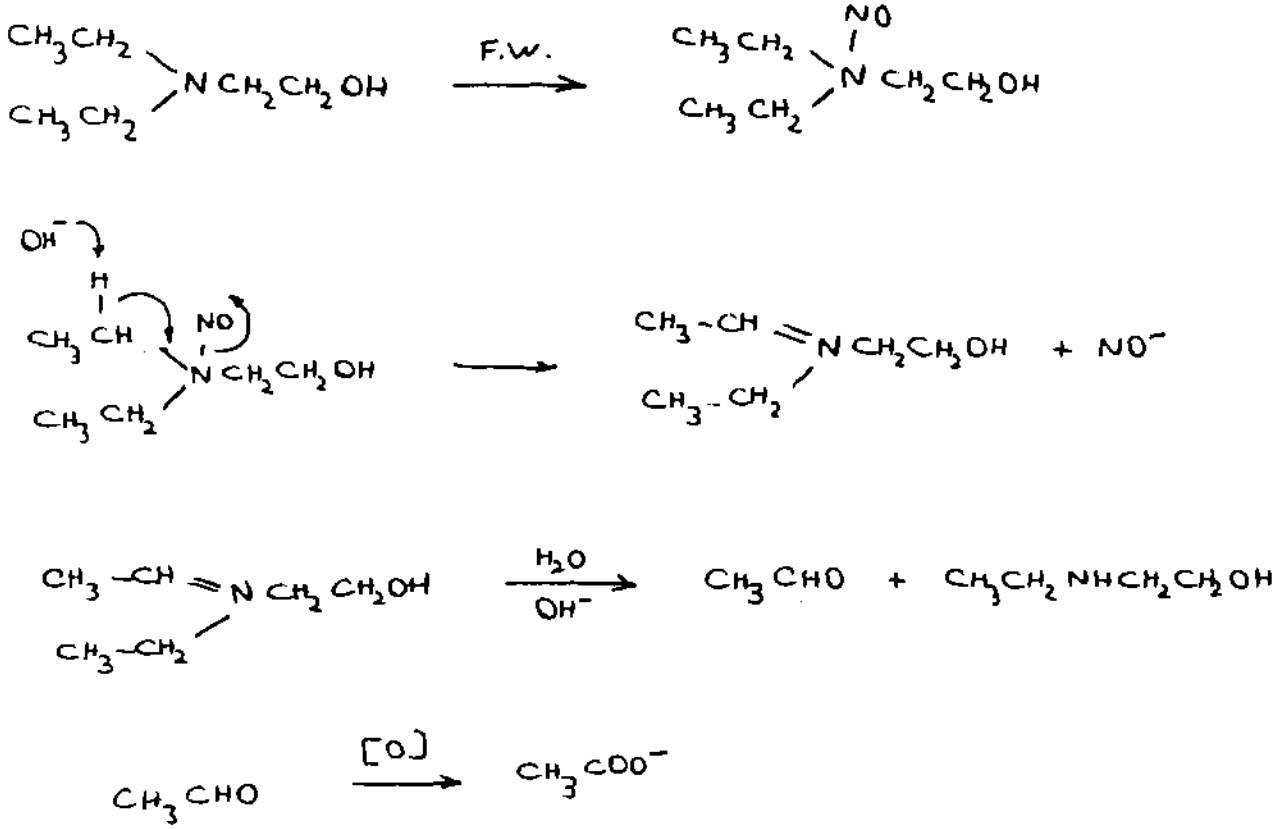

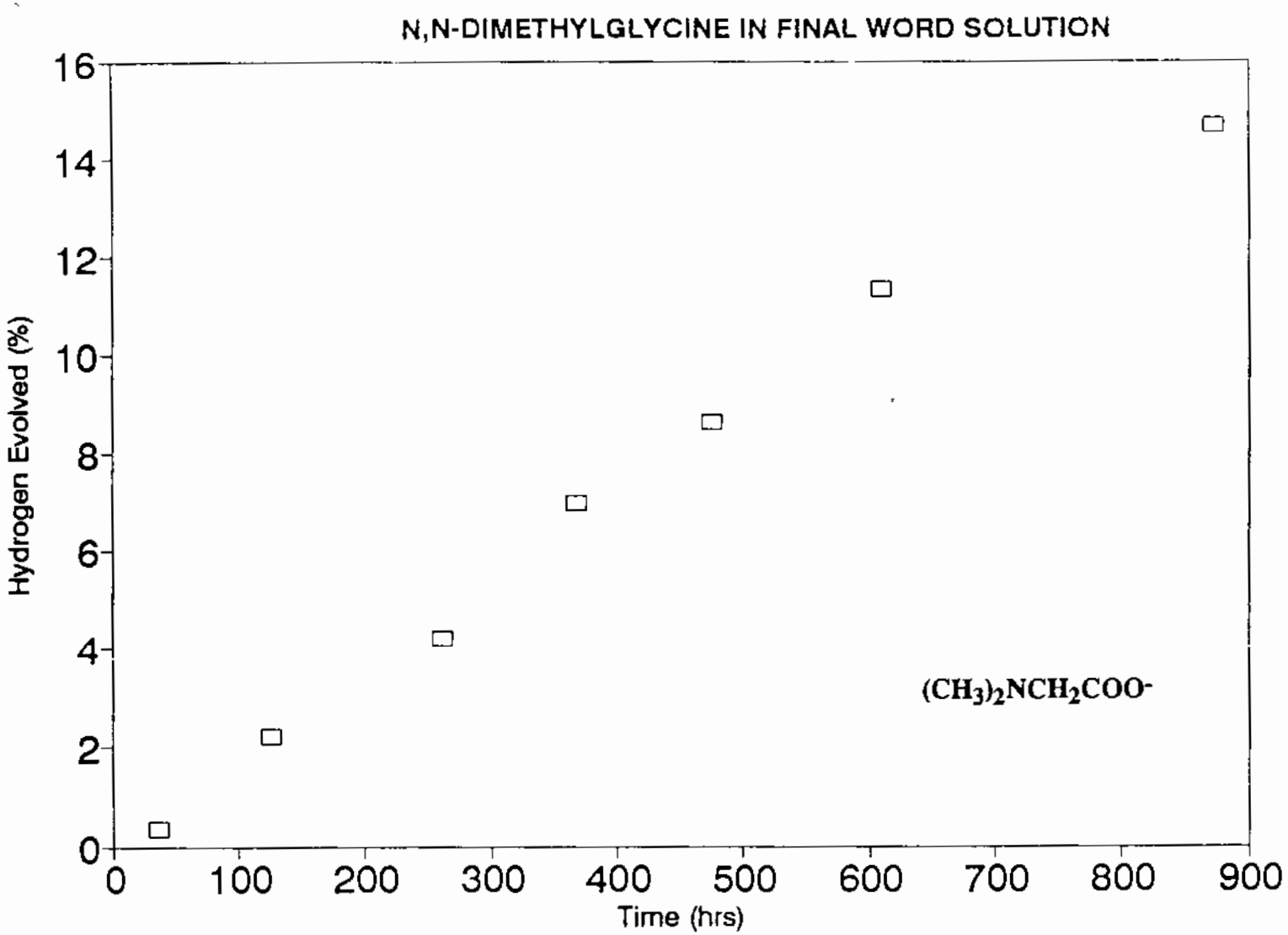
N,N-DIMETHYLGLYCINE IN FINAL WORD SOLUTION
Hydrogen Evolved (%)
0
2
4
6
8
10
12
14
16
0
100
200
300
400
500
600
700
800
900
Time (hrs)
$(CH_3)_2NCH_2COO^-$

DMG-1

N,N-DIMETHYLGLYCINE IN FINAL WORD SOLUTION

Compound	$(CH_3)_2NCH_2COO^-$	$HCOO^-$	H_2	O_2 (absorbed)
% (956 hs)	86.6	16.3	14.0	17.1

RELATIVE INTENSITIES N_2:Ar IN DIFFERENT SAMPLES.

SAMPLE	N_2:Ar in sample	N_2:Ar in background
$N_2O:H_2$=1:1	36:1	67:1
$N_2O:H_2$=1:5	18:1	67:1
$N_2O:H_2$=1:10	18:1	67:1
HEDTA/air	42:1	67:1
DIMETHYLGLYCINE/air	8:1	63:1
GLYCOLATE/air	32:1	67:1

Mass spectral analyses of N_2O and H_2 mixtures

$N_2O:H_2$	Relative intensities $N_2O:H_2$	Response factor
1:1	23.8:1	23.8
1:5	4.00:1	20.0
1:10	2.10:1	21.0

Search for Complex Formation between Al(III) and NO_2^-

An attempt was made to find direct evidence for a complex between Al(III) and nitrite ion, utilizing UV spectrophotometry in the region in which NO_2^- absorbs. Nitrite has an absorption maximum at 354 nm, and concentration conditions were chosen for measurements at this maximum.

In sample solution, the concentration of nitrite was kept constant(0.03M) and the concentration of aluminate changed from 0; 0.03; 0.1; 0.5 to 0.96M.

The spectra of the five solutions were identical within experimental error for wavelength between 320 and 400 nm. there were slightly differences in the region 255 - 320 nm, where absorption by blank solution is significant.

Thus, no direct evidence for complex formation was found in these experiments.

IC Analysis of Solid from Thermal Reactions

Analysis of the insoluble solid formed in a thermal reaction was done as part of the measurements to obtain mass balance in the reaction. The amounts of substances in the solid make only a small contribution to the overall mass balance, but the composition of the solid could be of importance in determining the behavior of the system.

When glycolate is the organic component in the thermal reaction, the insoluble solid generally contains a high percentage of oxalate. The unusual behavior in the Gly-300 run (with short reaction time) might be accounted for if the concentration of oxalate in solution had not yet become great enough to form solid.

Formulas are given for two compounds, reported in the literature as formed in basic solutions containing Al(III) and $C_2O_4^{2-}$. Our conditions are much more concentrated in NaOH and in Al(III) than the literature conditions, however. Analyses for Al and Na, and use of powder diffraction should help characterize these solids.

When other compounds are the organic components, the percentage of oxalate in the solid is zero or very low. Oxalate was found in the liquid phase of some of these runs, but the amount was always low.

IC Analysis of Solid from Thermal Reactions

Kinetic Run		Weight (grams)	Oxalate (%)	Nitrate (%)
B - 26 Gly/Air	726.5 hours	0.496	54	trace
B - 11 Gly/He/Cr	1540 hours	2.6	34	5
B - 4 Gly/Air/Cr	1434 hours	0.54	1	2
A - 126 Gly/Air	1060 hours	0.88	52	4
Gly - 300 Gly/Air	310 hours	0.051	0	14
Gly - 400 Gly/Air	406 hours	0.083	39	4
Gly - 500 Gly/Air	514 hours	0.081	42	6
Gly - 600 Gly/Air	672 hours	0.17	42	5
Gly - 800 Gly/Air	981 hours	0.36	27	8
Gly - 900 Gly/Air	1250 hours	0.43	30	4
Gly -1000 Gly/Air	1474 hours	0.50	30	6

Two known aluminum oxalate compounds are shown as following:

$Al_3(OH)_7(C_2O_4)\cdot 3H_2O$ $C_2O_4^{2-}$: 25.7%

$NaAl(OH)_2(C_2O_4)\cdot 3H_2O$ $C_2O_4^{2-}$: 38.9%

IC analysis of Solid from Thermal Reactions

Kinetic Run		Weight (grams)	Oxalate (%)	Nitrate (%)
A - 50 HEDTA/Air	1770 hours	0.86	2	26
A - 55 HEDTA/He	540 hours	0.24	0	10
B - 19 U-EDDA/Air	403 hours	0.104	0	8
B - 33 U-EDDA/Air	203 hours	0.446	0	5
B - 60 IDA/He	281 hours	0.171	0	8
B - 95 DMG/Air	304 hours	0.102	0	10
B - 73 NTA/Air	357.5 hours	0.091	0	9
B - 77 Sarcosine/Air	908 hours	0.935	0	14
B - 69 IDA/Air	1139 hours	0.33	1	10
B - 85 MIDA/Air	1060 hours	1.24	1.2	7
H - 1 HEDTA/Air	200 hours	0.11	0	11
H - 3 HEDTA/Air	300 hours	0.05	0	13
H - 4 HEDTA/Air	400 hours	0.10	0	9
H - 5 HEDTA/Air	500 hours	0.15	0	8

Quantitative analyses for EDTA and HEDTA have been accomplished with the use of Dionex AS5 and AS10 columns. Before analysis a $CuCl_2$ or $NiCl_2$ solution was added to the EDTA or HEDTA solution, with the metal cation and $EDTA^{4-}$ (or $HEDTA^{3-}$) in a 1.2:1 ratio, based on the initial starting material concentration. The pH of the solution was adjusted to about 11.

Two chromatograms are shown.

A-55 HEDTA/He (AS10 column)

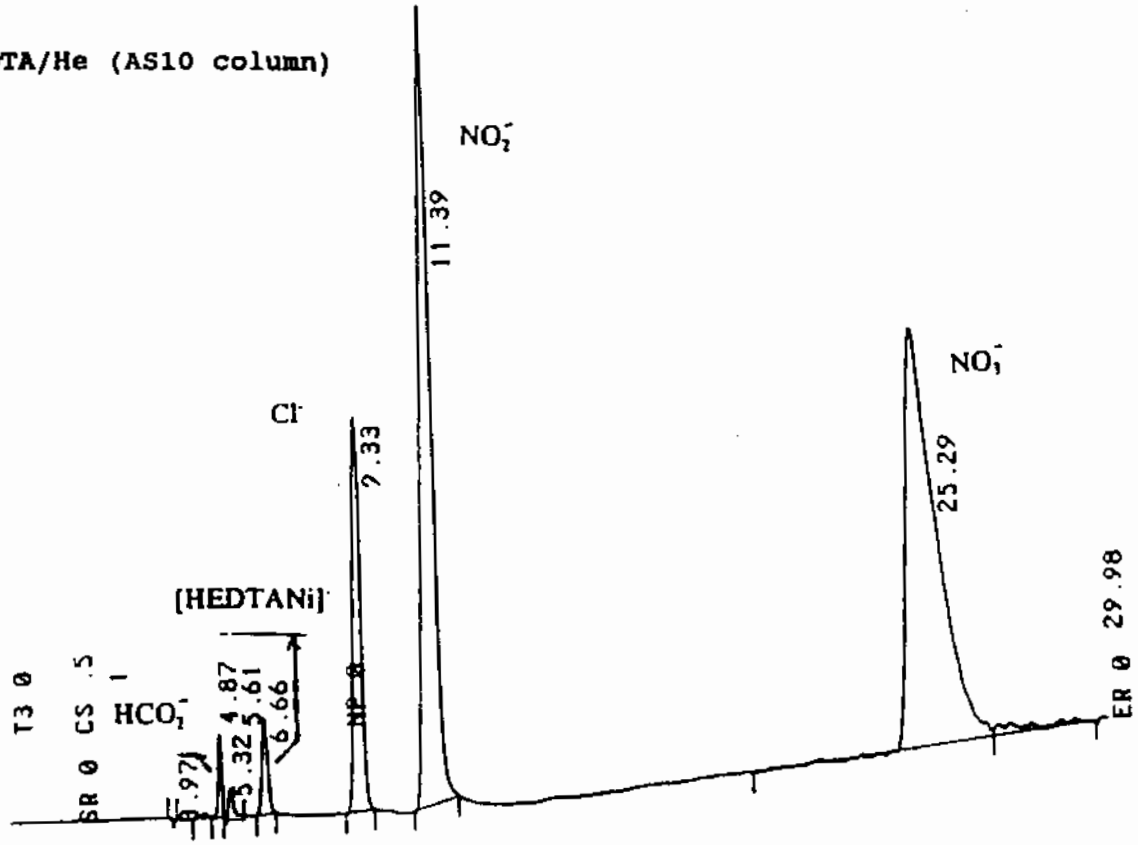

B-45 EDTA/Air (AS5 column)

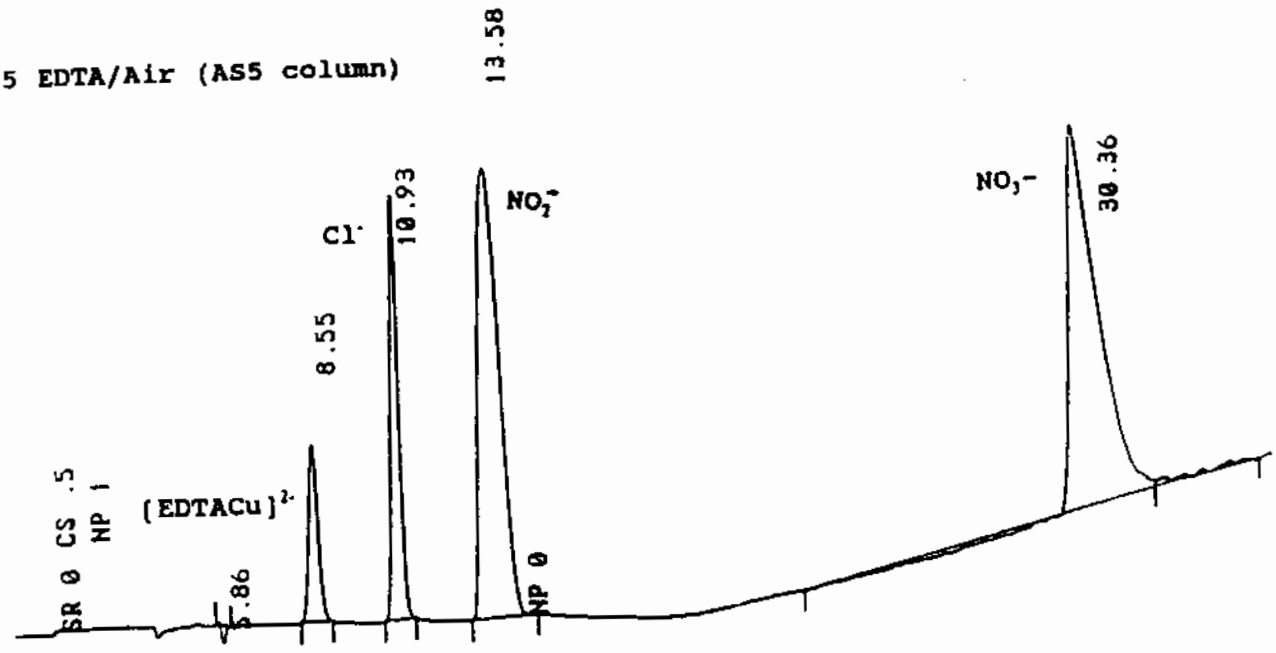

Appendix I

Hanford Site Experimental Investigations of Ultrasonic Properties of DST Waste Simulant

Hanford Site Experimental Investigations of Ultrasonic Properties of DST Waste Simulant

presented to

Waste Tank Science Panel

by

J. B. (James) Colson
Pacific Northwest Laboratory
March 27, 1992

Contributors: B. P. Hildebrand and C. L. Shepard, PNL

Pacific Northwest
Laboratory

OUTLINE

- Experimental measurements of acoustic properties
  - Effects of voids on attenuation
  - Variation of attenuation with temperature
  - Variation of attenuation with pressure
  - Effects of dilution on attenuation
  - Measurements of acoustic velocity
  - Pressure effects on acoustic coupling
- Progress on liquid waveguide concept
  - Design
  - Performance
- Summary

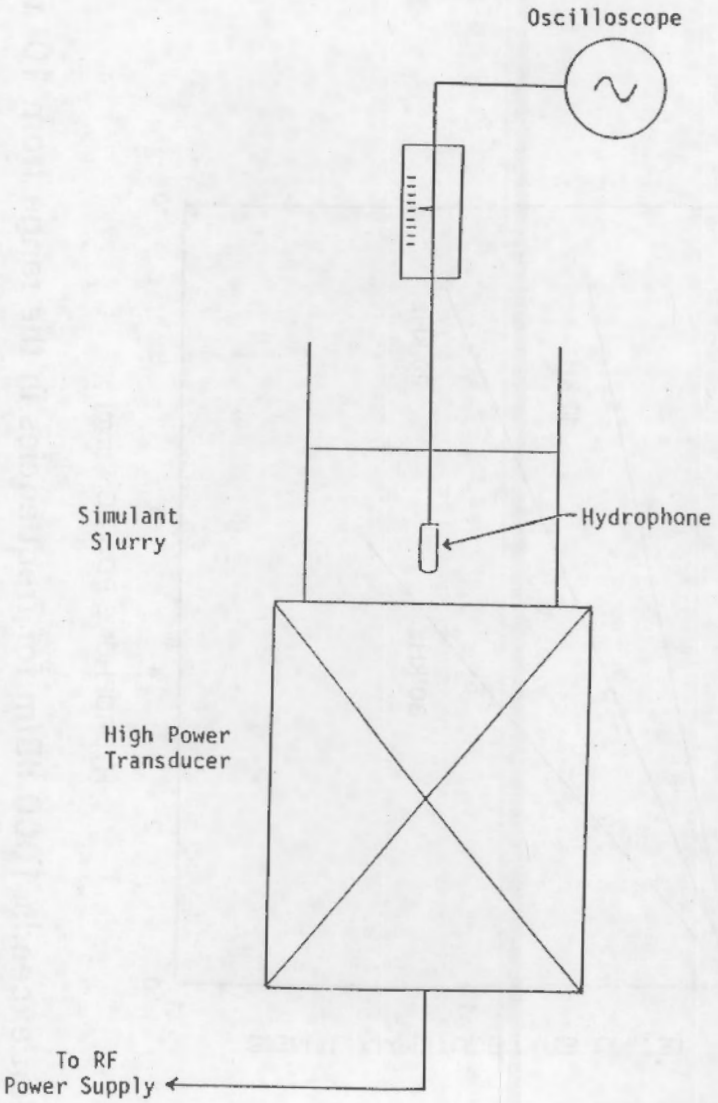

Experimental Arrangement for Attenuation Measurements

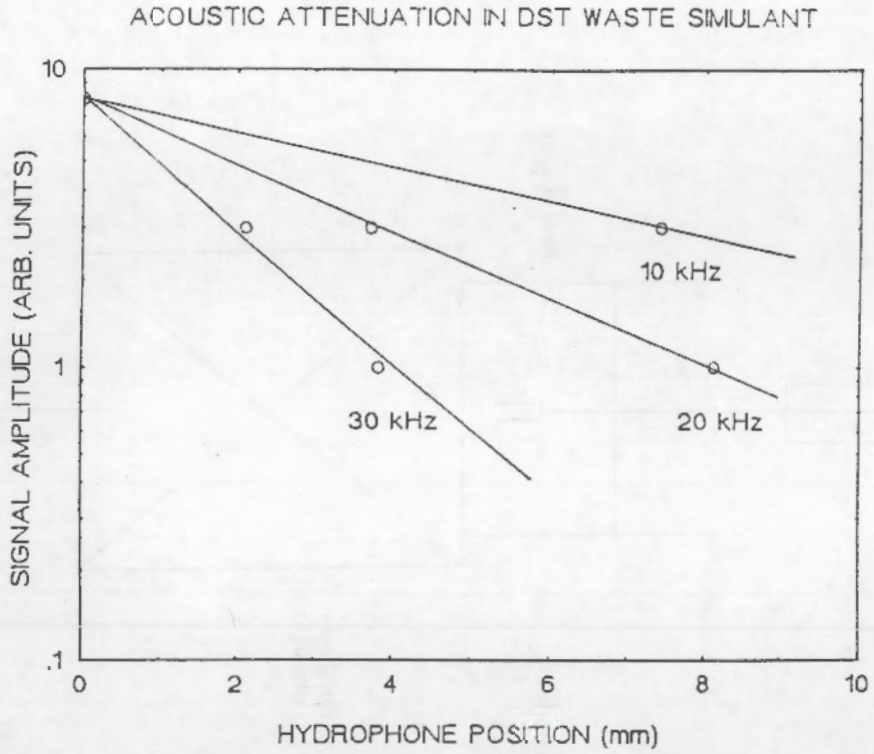

Attenuation exceeds 1000 dB/m for frequencies in the range from 10- to 30-kHz.

Acoustic Attenuation at Various Frequencies

- Attenuation increases with decreasing void fraction
- Attenuation is probably not due to bubbles within the simulant

Simulant Condition	Frequency (kHz)	Attenuation (Np/cm)	Attenuation (dB/m)
As Is	10	1.3	1100
	20	2.6	2200
	30	5.5	4800
Void Fraction 0.13%	10	3.2	2780
	20	4.9	4300
	30	4.9	4300
Void Fraction 0.07%	10	4.6	4000
	20	6.2	5400
	30	---	----

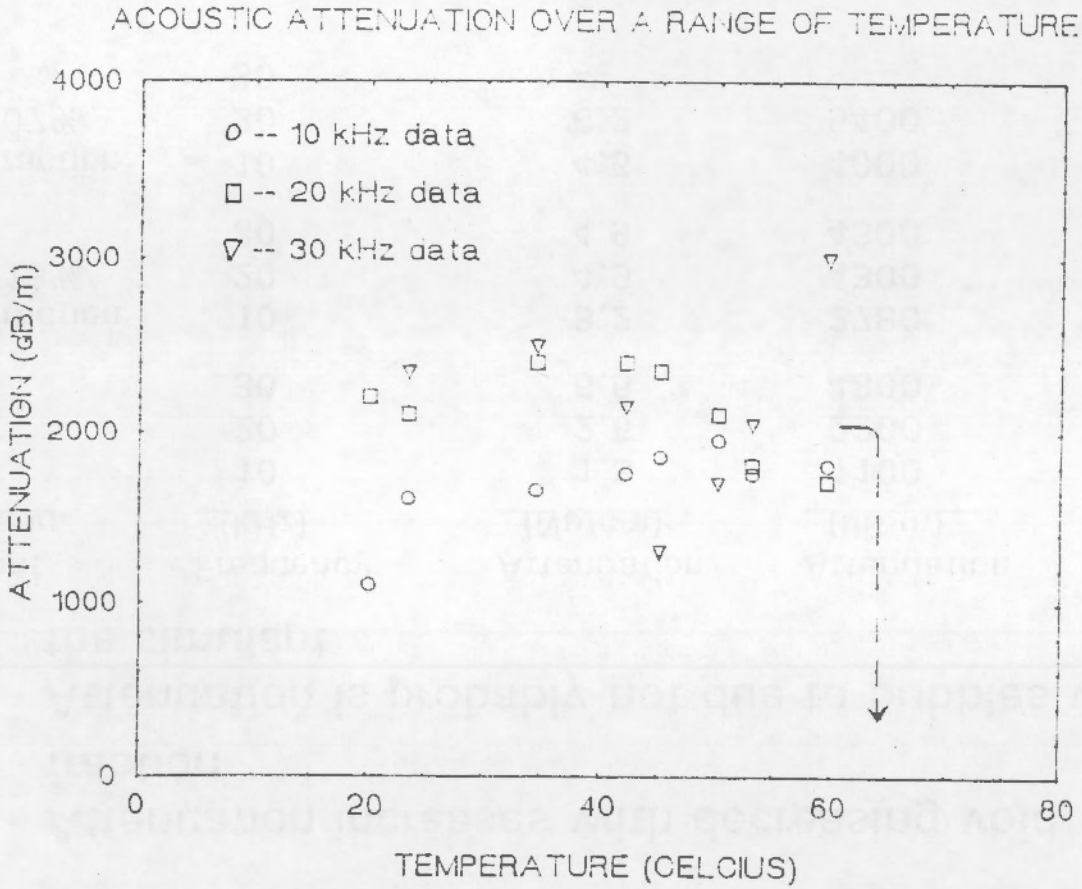

Attenuation is constant and high until a transition temperature is reached.

Pacific Northwest Laboratory

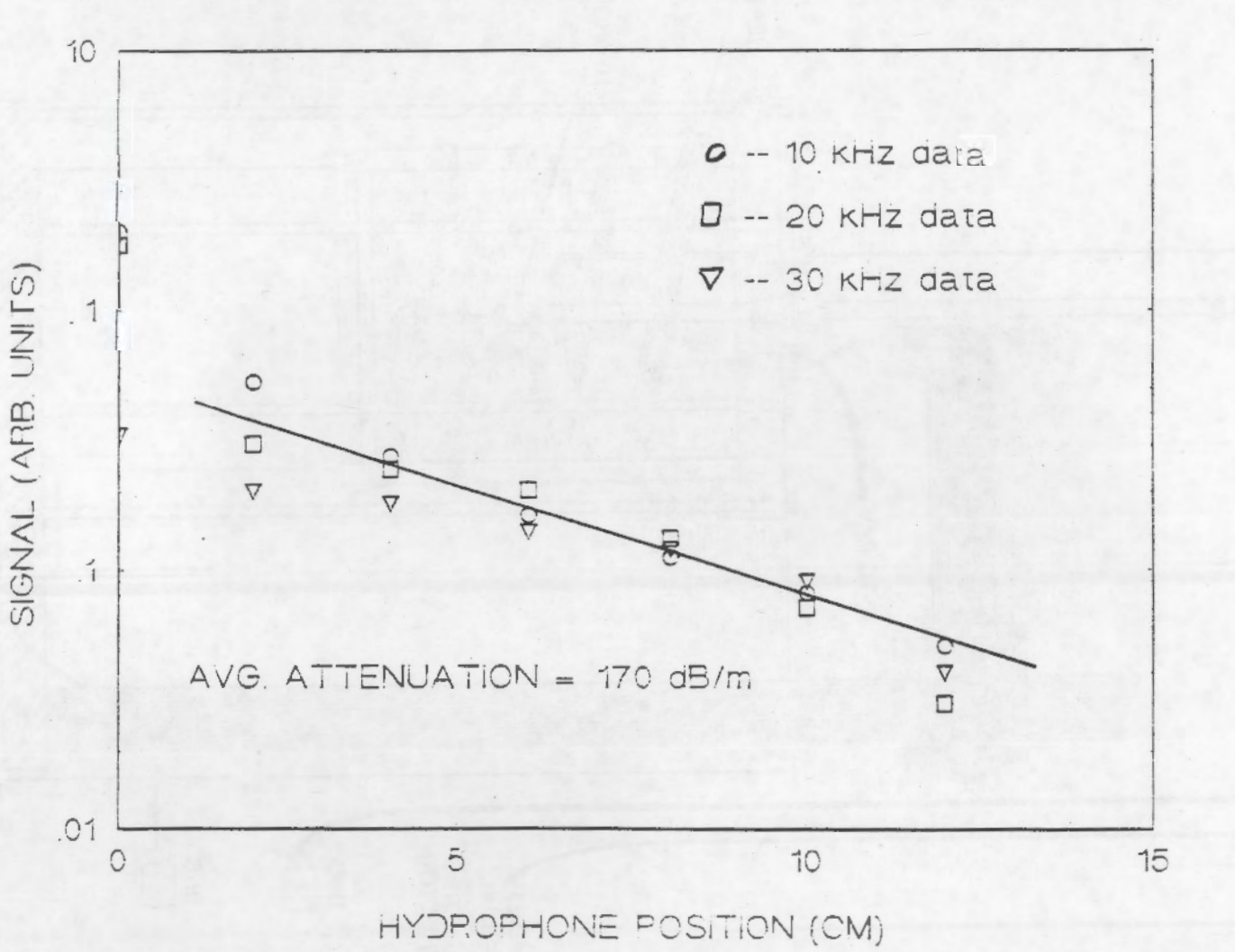
ACOUSTIC ATTENUATION OF DST SIMULANT PREHEATED TO 70 C
10
.1
.01
SIGNAL (ARB. UNITS)
o -- 10 kHz data
□ -- 20 kHz data
▽ -- 30 kHz data
AVG. ATTENUATION = 170 dB/m
0
5
10
15
HYDROPHONE POSITION (CM)

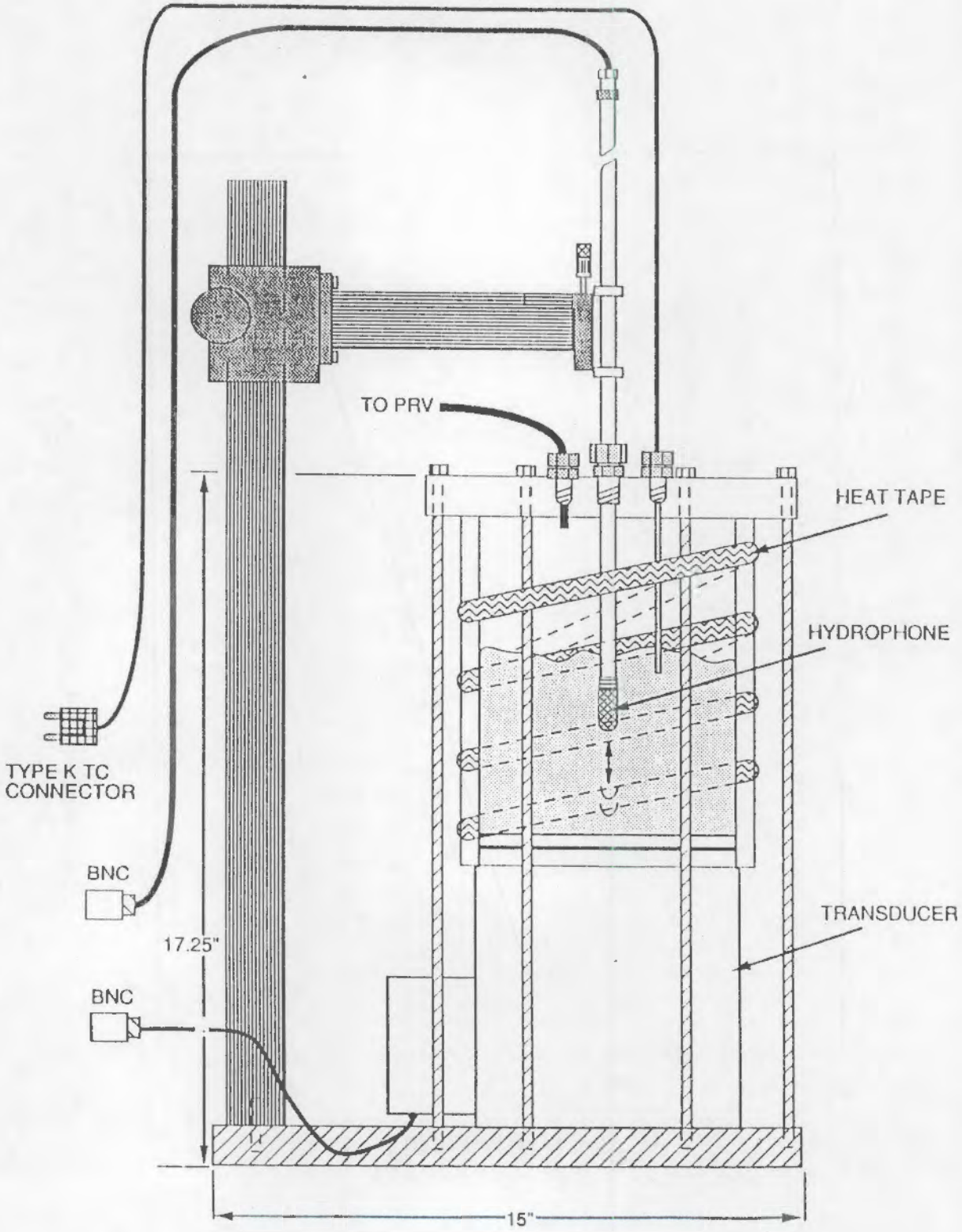
TO PRV
HEAT TAPE
HYDROPHONE
TYPE K TC
CONNECTOR
BNC
17.25"
BNC
TRANSDUCER
15"

SIMULANT SLURRY ATTENUATION AT LOW TEMPERATURE AND TWO PRESSURES

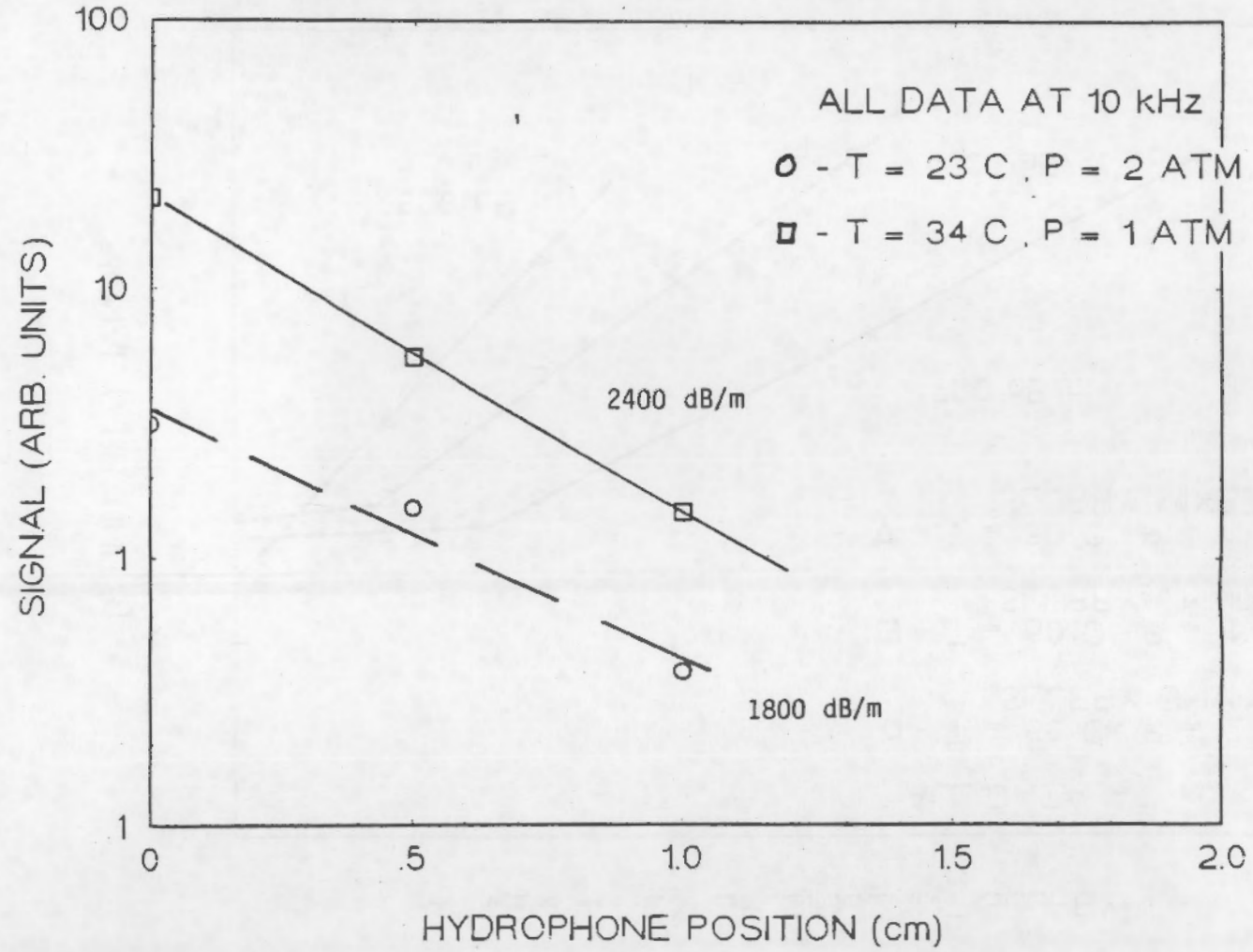

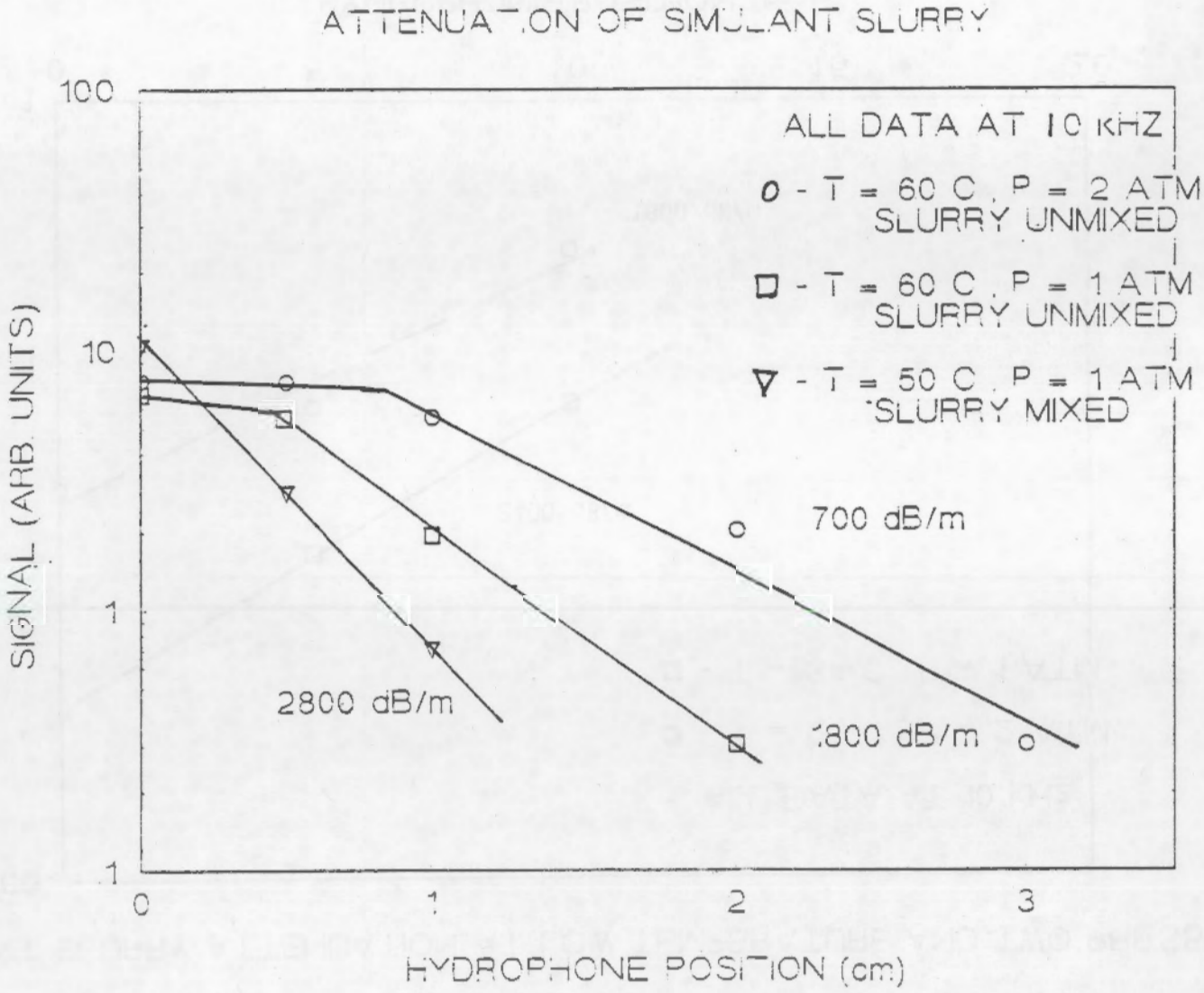
ATTENUATION OF SIMULANT SLURRY
ALL DATA AT 10 KHZ
O - T = 60 C , P = 2 ATM
SLURRY UNMIXED
□ - T = 60 C , P = 1 ATM
SLURRY UNMIXED
▽ - T = 50 C , P = 1 ATM
SLURRY MIXED
700 dB/m
1800 dB/m
2800 dB/m
SIGNAL (ARB. UNITS)
100
10
1
.1
0
1
2
3
HYDROPHONE POSITION (cm)

SIMULANT SLURRY ATTENUATION AT HIGH TEMPERATURES AND TWO PRESSURES

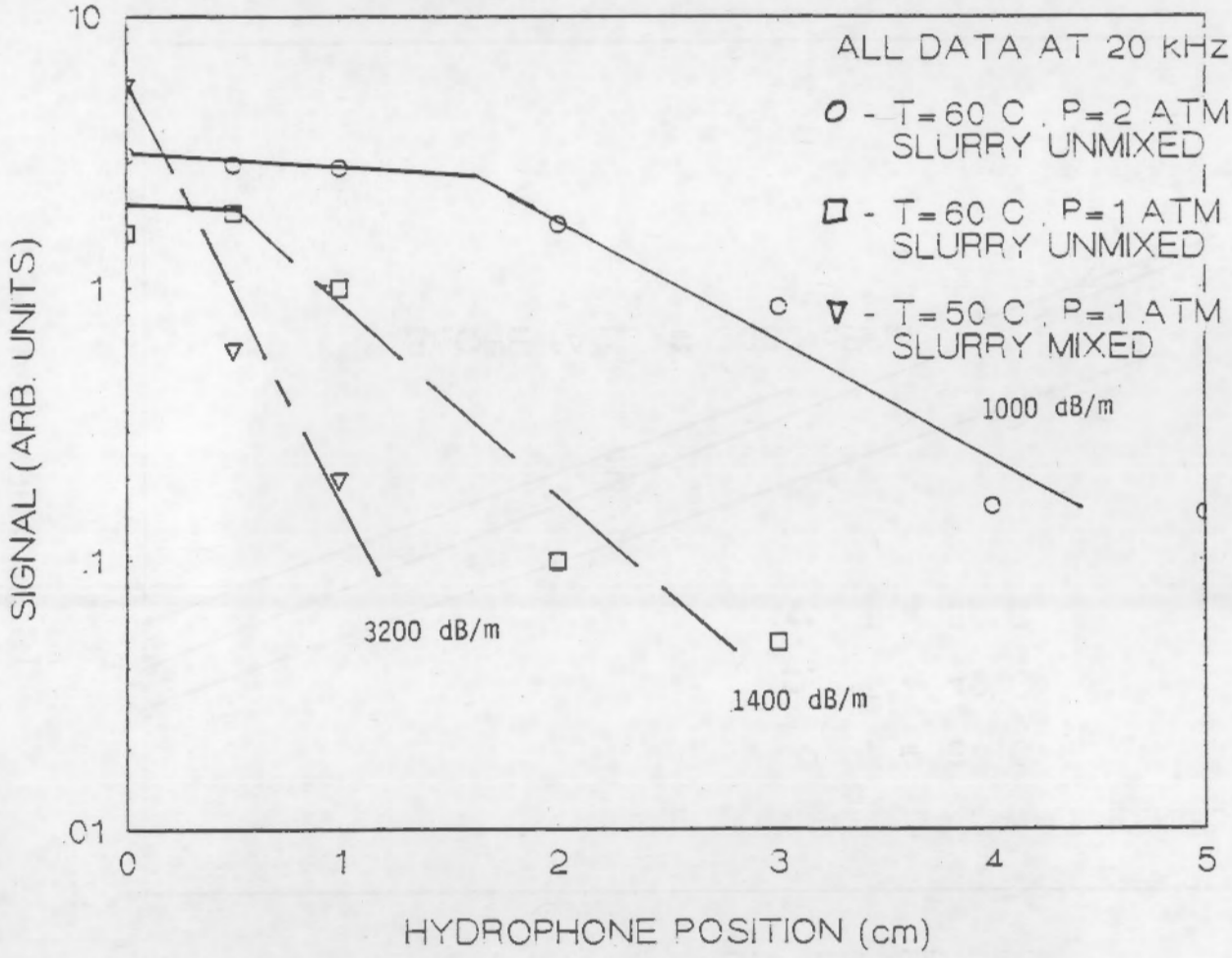

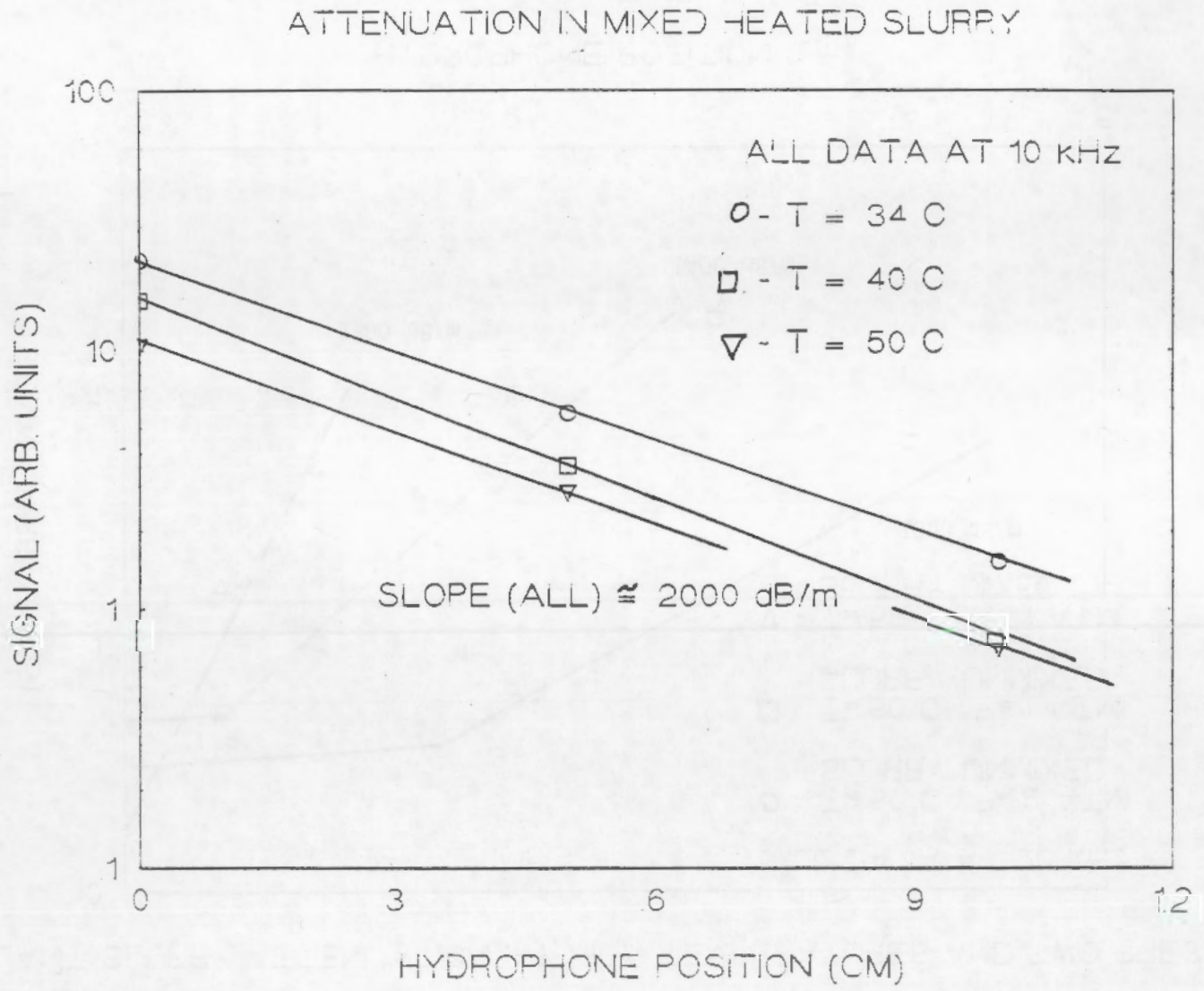
ATTENUATION IN MIXED HEATED SLURRY
ALL DATA AT 10 kHz
O - T = 34 C
□ - T = 40 C
▽ - T = 50 C
SLOPE (ALL) ≅ 2000 dB/m
SIGNAL (ARB. UNITS)
100
10
1
0
3
6
9
12
HYDROPHONE POSITION (CM)

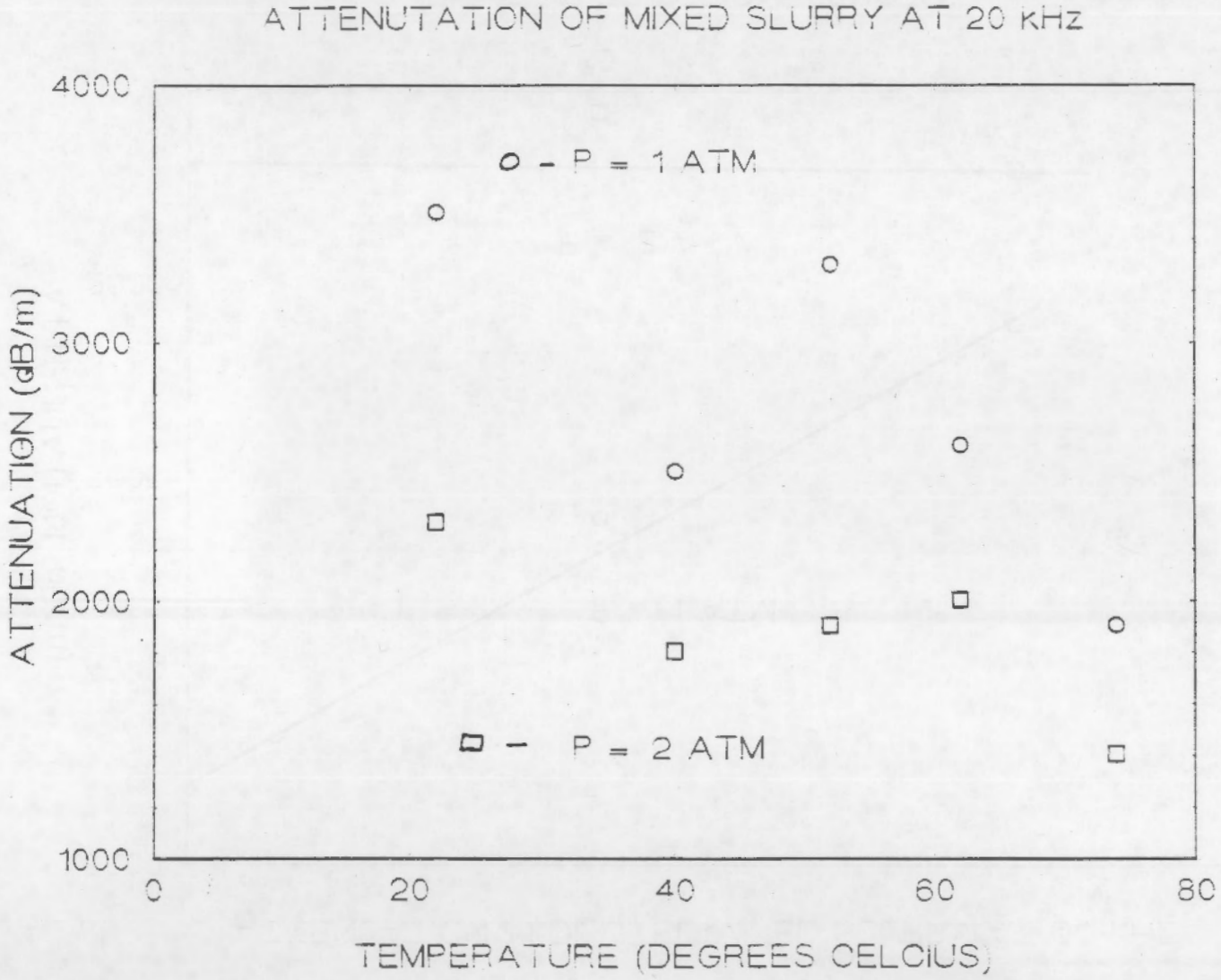
ATTENUTATION OF MIXED SLURRY AT 20 kHz
4000
3000
2000
1000
ATTENUATION (dB/m)
o - P = 1 ATM
□ - P = 2 ATM
0
20
40
60
80
TEMPERATURE (DEGREES CELCIUS)

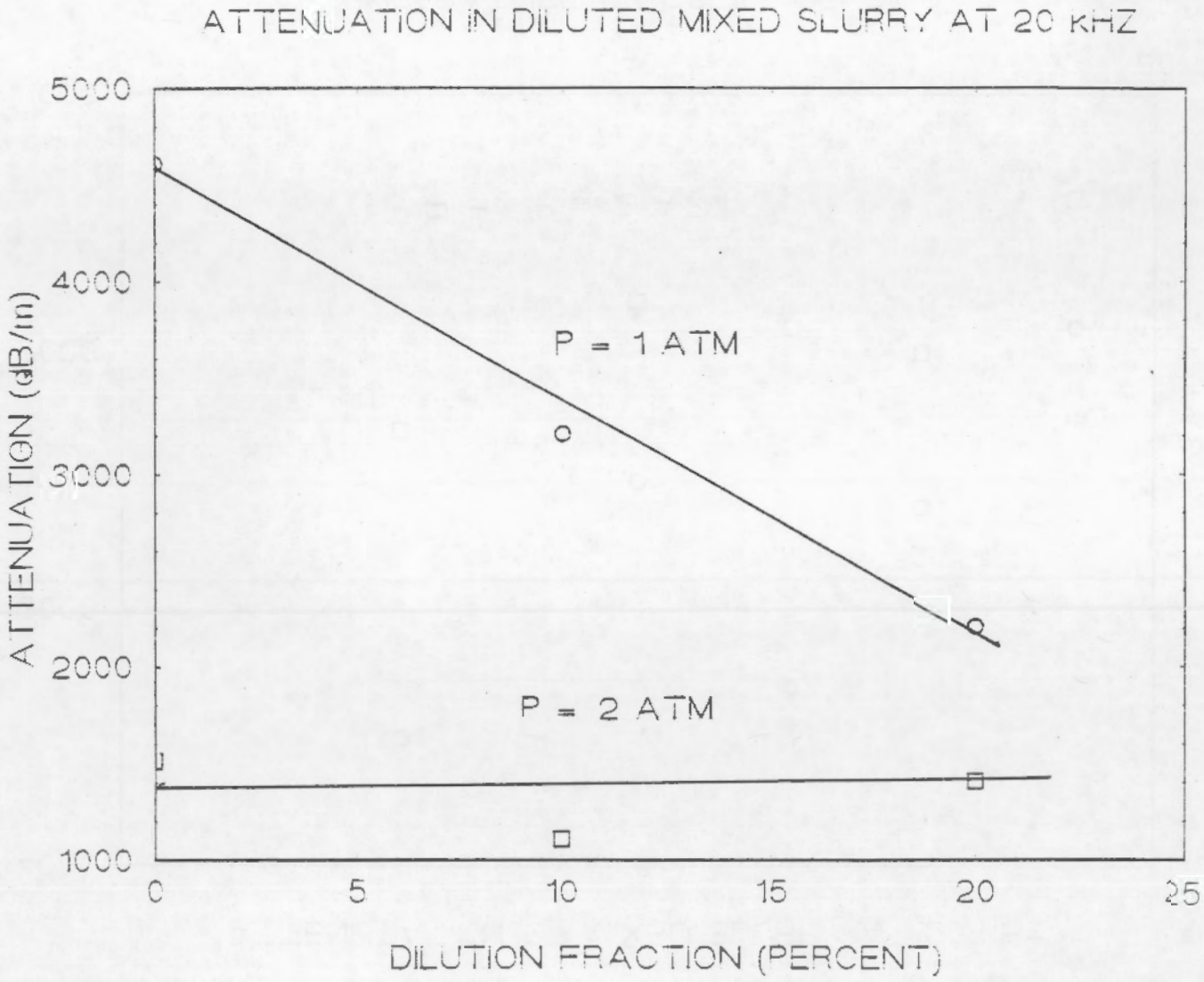
ATTENUATION IN DILUTED MIXED SLURRY AT 20 KHZ
ATTENUATION (dB/m)
5000
4000
3000
2000
1000
P = 1 ATM
P = 2 ATM
0
5
10
15
20
25
DILUTION FRACTION (PERCENT)

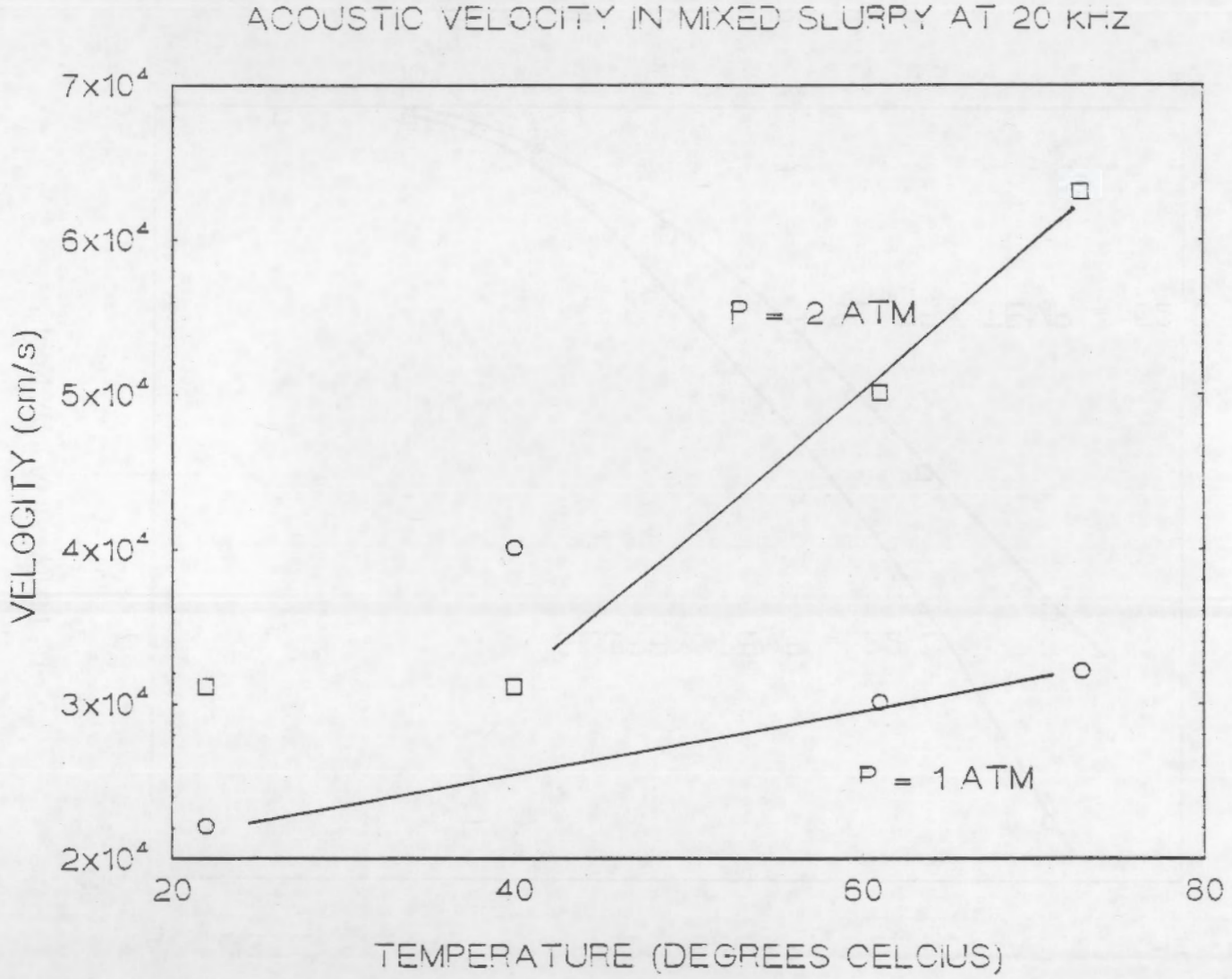
ACOUSTIC VELOCITY IN MIXED SLURRY AT 20 KHZ
7x10⁴
6x10⁴
5x10⁴
4x10⁴
3x10⁴
2x10⁴
VELOCITY (cm/s)
P = 2 ATM
P = 1 ATM
20
40
60
80
TEMPERATURE (DEGREES CELCIUS)

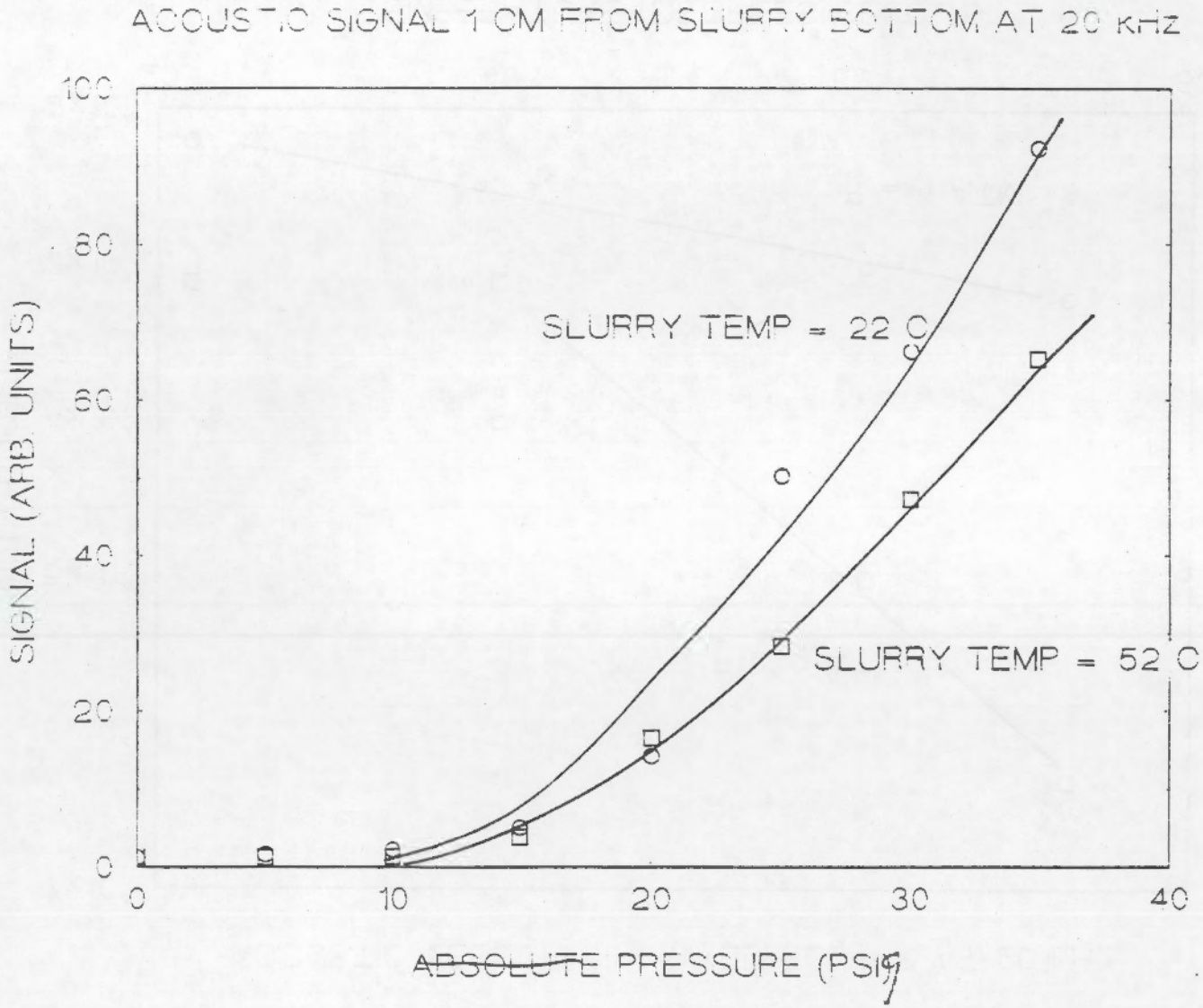
ACOUSTIC SIGNAL 1 CM FROM SLURRY BOTTOM AT 20 KHZ
SIGNAL (ARB. UNITS)
100
80
60
40
20
0
0
10
20
30
40
ABSOLUTE PRESSURE (PSIG)
SLURRY TEMP = 22 C
SLURRY TEMP = 52 C

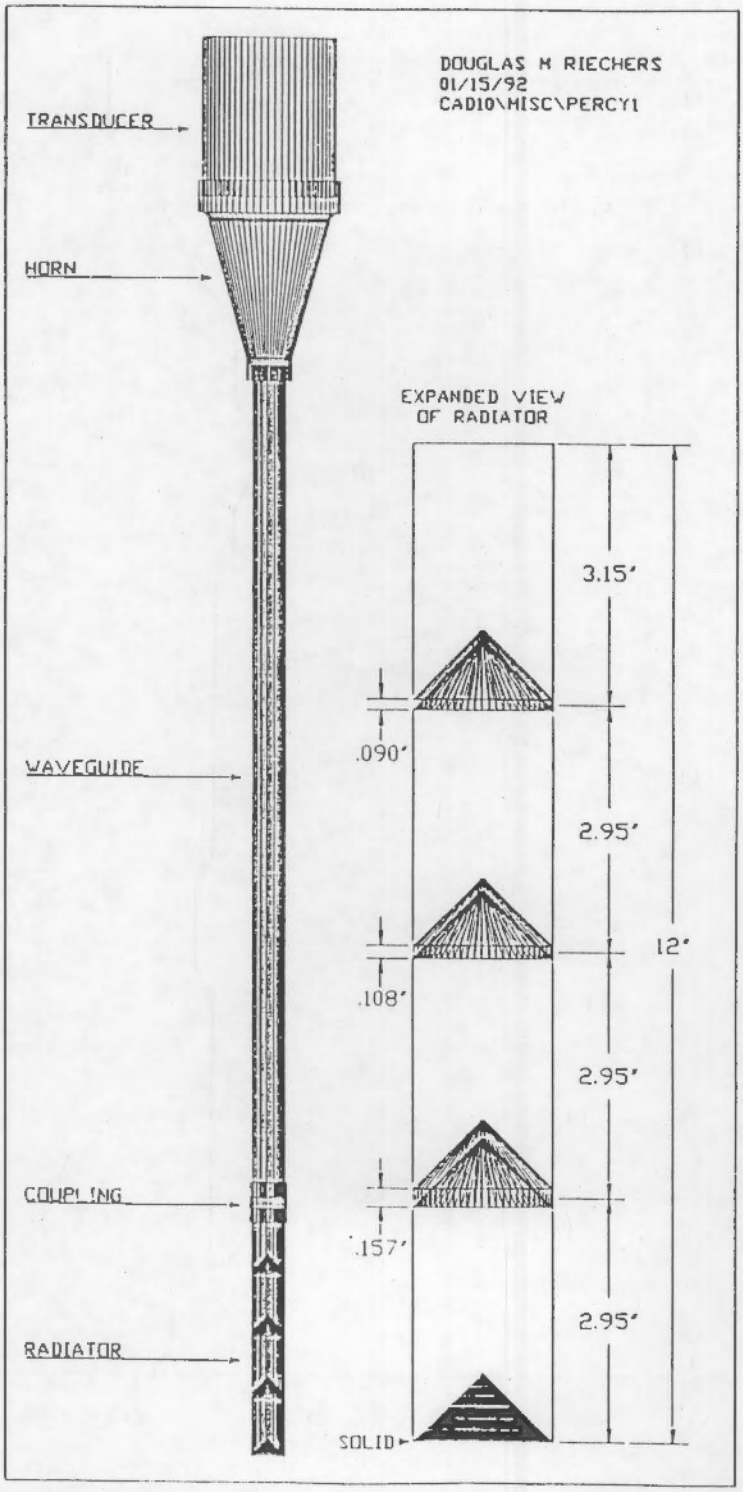

A prototype liquid-filled waveguide has been constructed.

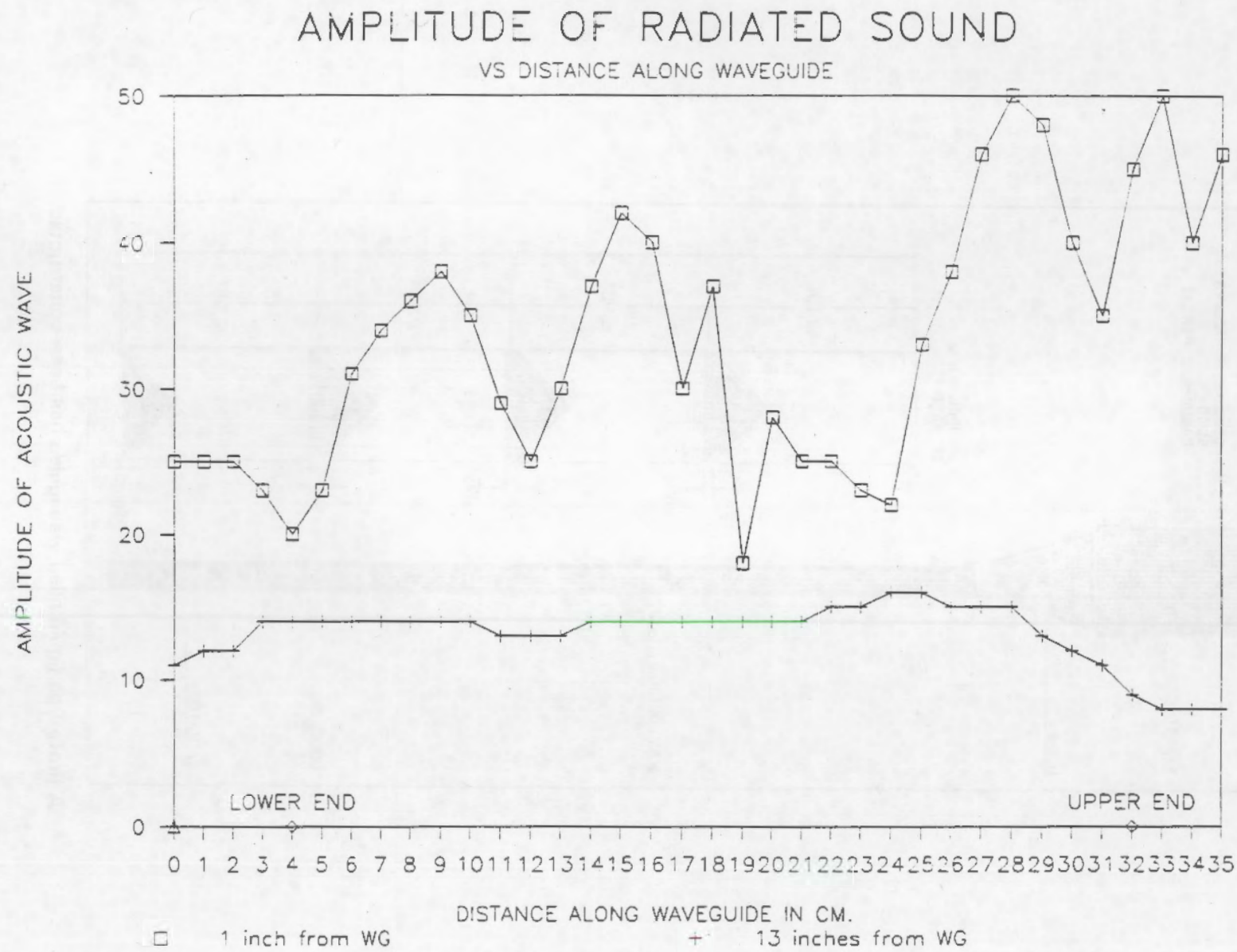
AMPLITUDE OF RADIATED SOUND
VS DISTANCE ALONG WAVEGUIDE
AMPLITUDE OF ACOUSTIC WAVE
50
40
30
20
10
0
LOWER END
UPPER END
0 1 2 3 4 5 6 7 8 9 10 11 12 13 14 15 16 17 18 19 20 21 22 23 24 25 26 27 28 29 30 31 32 33 34 35
DISTANCE ALONG WAVEGUIDE IN CM.
1 inch from WG
13 inches from WG

SUMMARY

- Acoustic Attenuation
  - Very high
  - Increases with frequency
  - Not due to void fraction
  - Decreases with pressure
  - Not strongly temperature dependent
  - Low near radiator for unmixed slurry
  - Decreases with dilution

SUMMARY (continued)

- Acoustic Velocity

  - Increases with temperature
  - Increases with pressure

- Acoustic Coupling

  - Increases with pressure
  - No significant effect below about 1.5 ATM absolute
  - Temperature dependent

Appendix J

Mitigation of Bubble Nucleation in High-Level Waste Tank 101-Sy with Application of Ultrasound

Mitigation of Bubble Nucleation in High-Level Waste Tank 101SY with Application of Ultrasound

Presentation, March 27, 1992
PNL Sciene Panel Meeting
Denver, CO

All information is predecisional

Principle Investigator:
Stephen F. Agnew, Isotope and Structural Chemistry
Group INC-4, MS C346, (505) 665-1764

Harold Sullivan, Engineering and Safety Analysis, N-6

Steve Eisenhawer, Engineering and Safety Analysis, N-6

Dipen N. Sinha, Electronics Research
Group MEE-11, MS D429, (505) 667-0062

Bill Ward, Advanced Engineering Technology
Group MEE-13, MS J576, (505) 665-1844

Los Alamos National Laboratory
Los Alamos, NM 87545

Overview

1) Update on model and experiment.

2) Discussion of coupling and attenuation problems.

3) Functional design criteria.

4) Next to do...

Status

Tank is completed

Instrumentation in place.
—heater at 1.8" depth, 500 watts.
—TC readout as function of depth, per inch.
—fast time response pressure transducer (0.5 sec).
—acoustic level monitor (±1 mm).
—all data to computer station.
—waveguide/radiator for 20 kHz ultrasound.
—calibrated hydrophone
—spectrum analyzer

Instrumentation now being installed.
—higher power transducer (475 watt)

Tank constituents are:

species	total amount	est. in supernate
$NaNO_3$	2.7 M	2.1 M
$NaNO_2$	3.9 M	3.6 M
NaOH	3.3 M	3.3 M
$NaAlO_2$	2.2 M	2.0 M
Na_2CO_3	0.53 M	0.15 M
Na_4EDTA	0.12 M (50 g/L)	0.06? M
Na_3HEDTA	0.13 M (50 g/L)	0.06? M
total Na	14.0 M	11.7 M
NH_3	due to aluminum reaction	

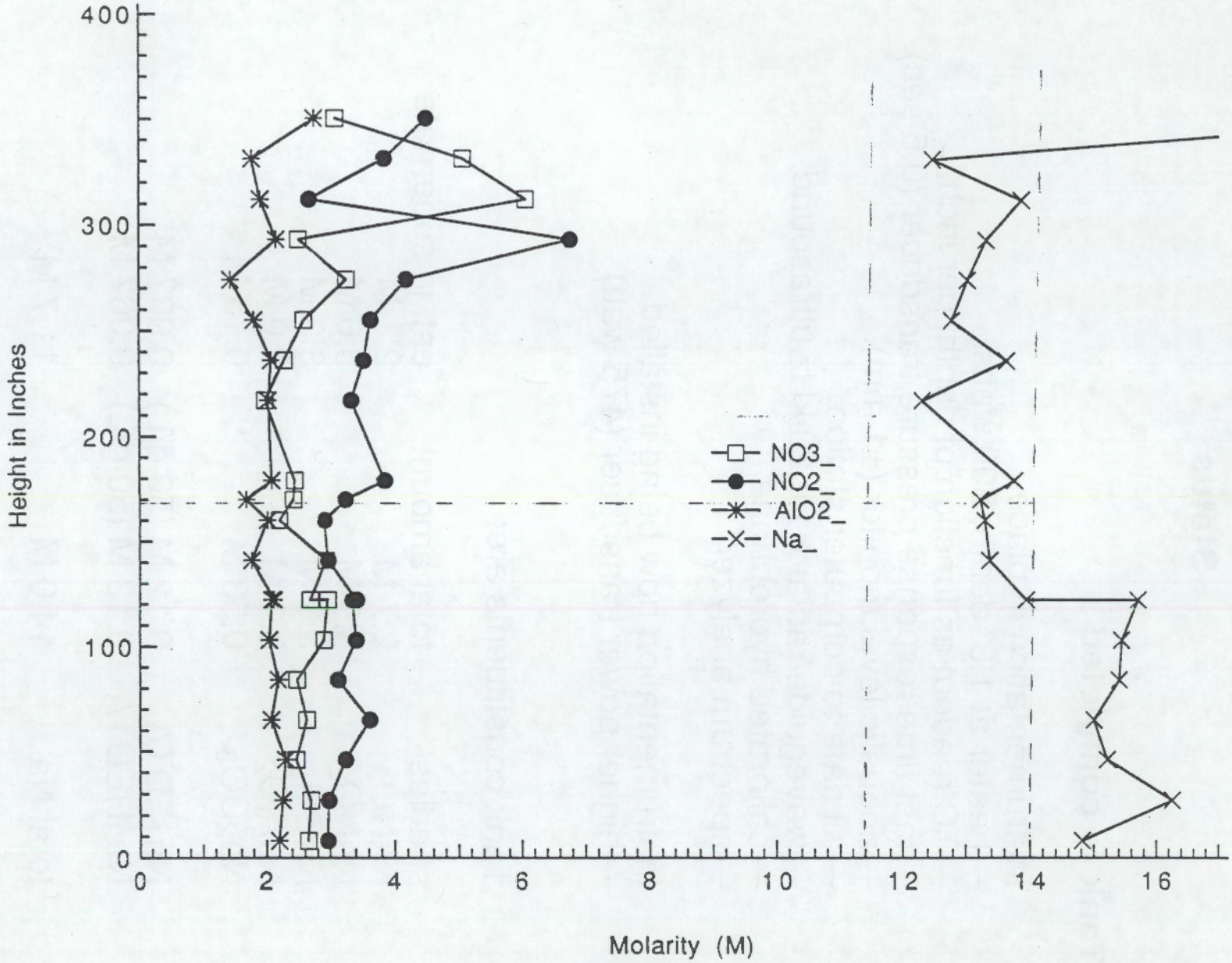
400
300
200
100
0
Height in Inches
0
2
4
6
8
10
12
14
16
Molarity (M)
NO3_
NO2_
AlO2_
Na_

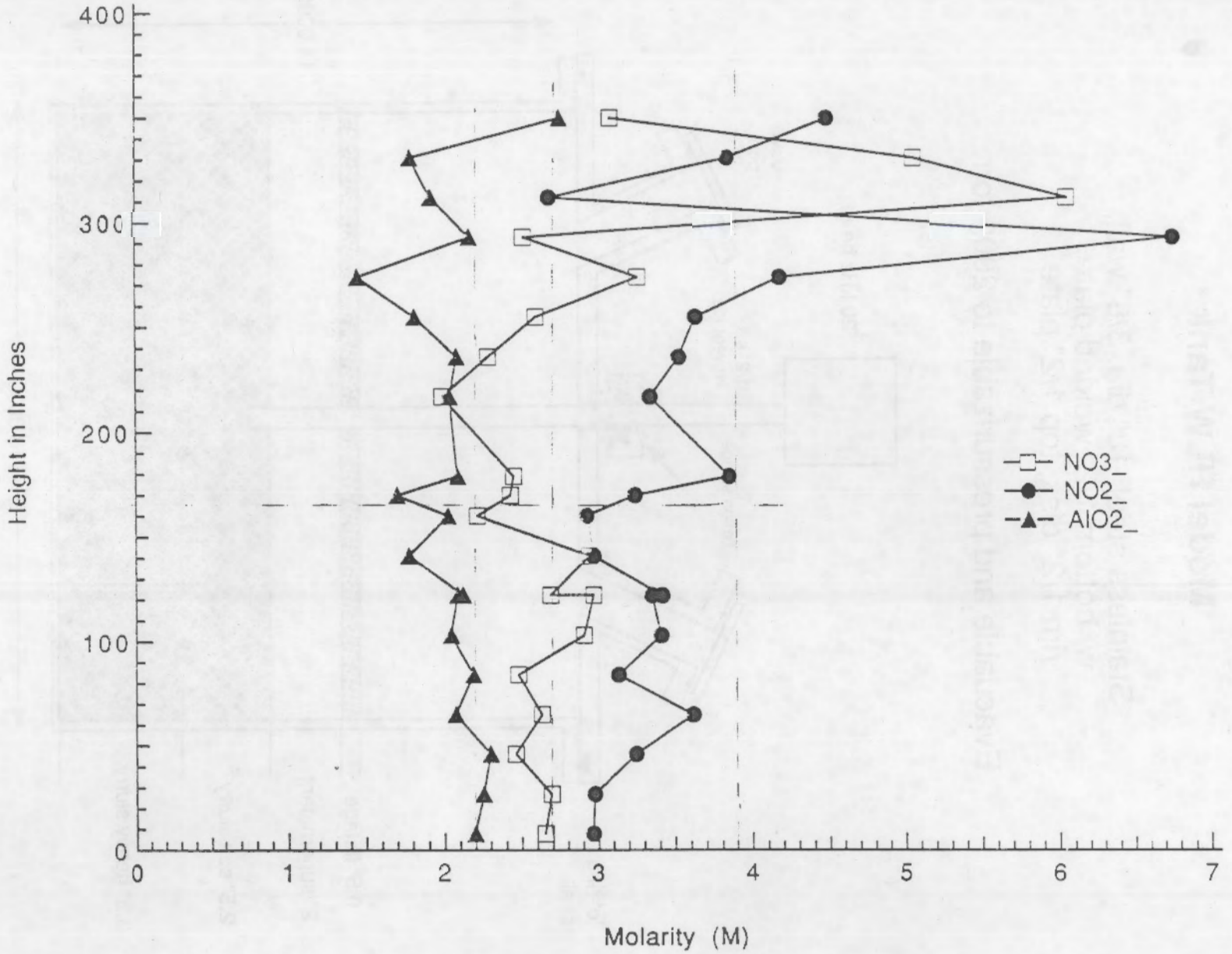
400
300
200
100
0
Height in Inches
0
1
2
3
4
5
6
7
Molarity (M)
NO3_
NO2_
AlO2_

Model HLW Tank

Stainless steel, 18" dia. 3/8" wall,
w/ bottom 1/2" welded plate,
rim 1/2" disk, top 1/2" plate.

Evacuable and pressurizable to 2000 torr.

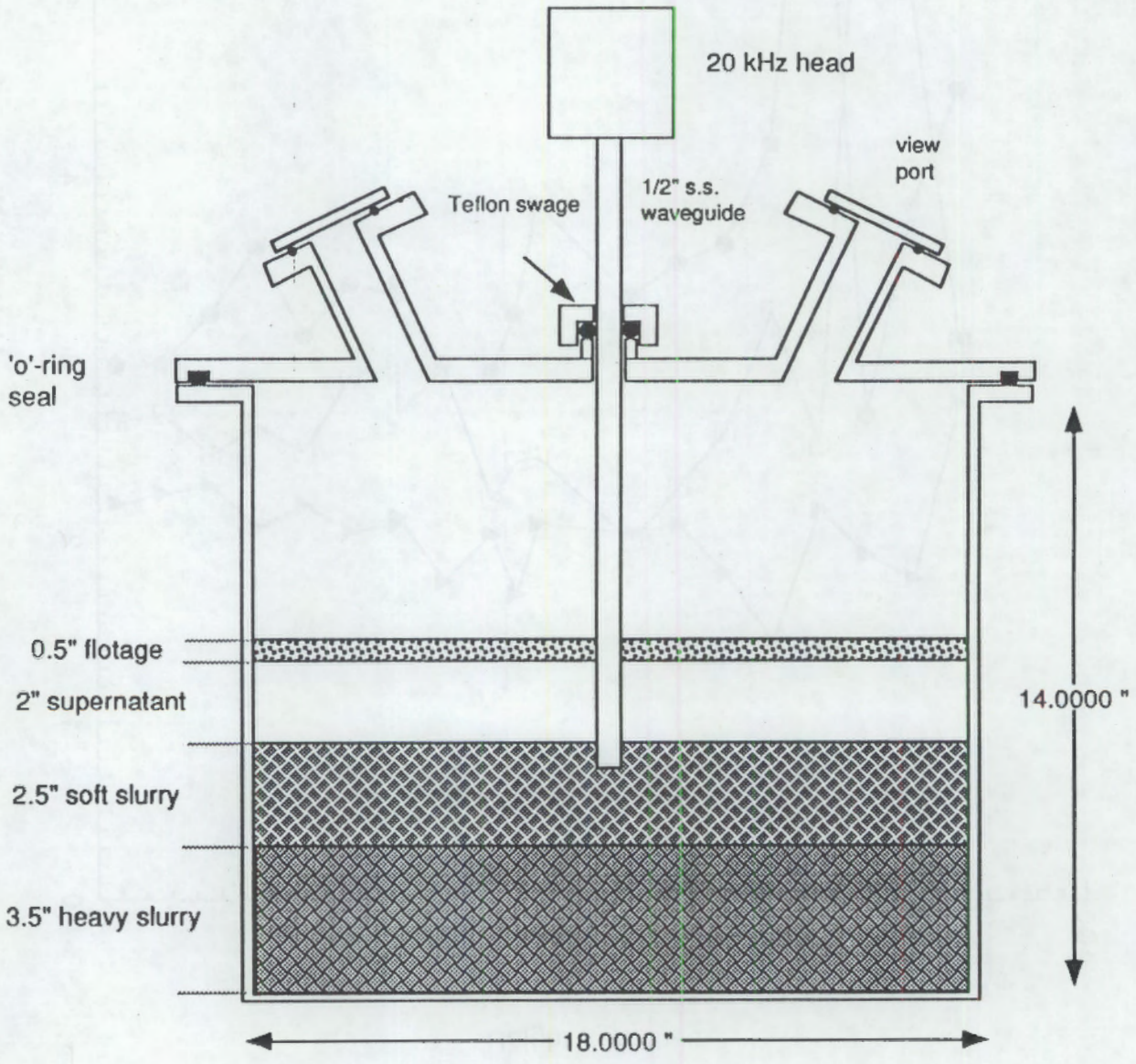

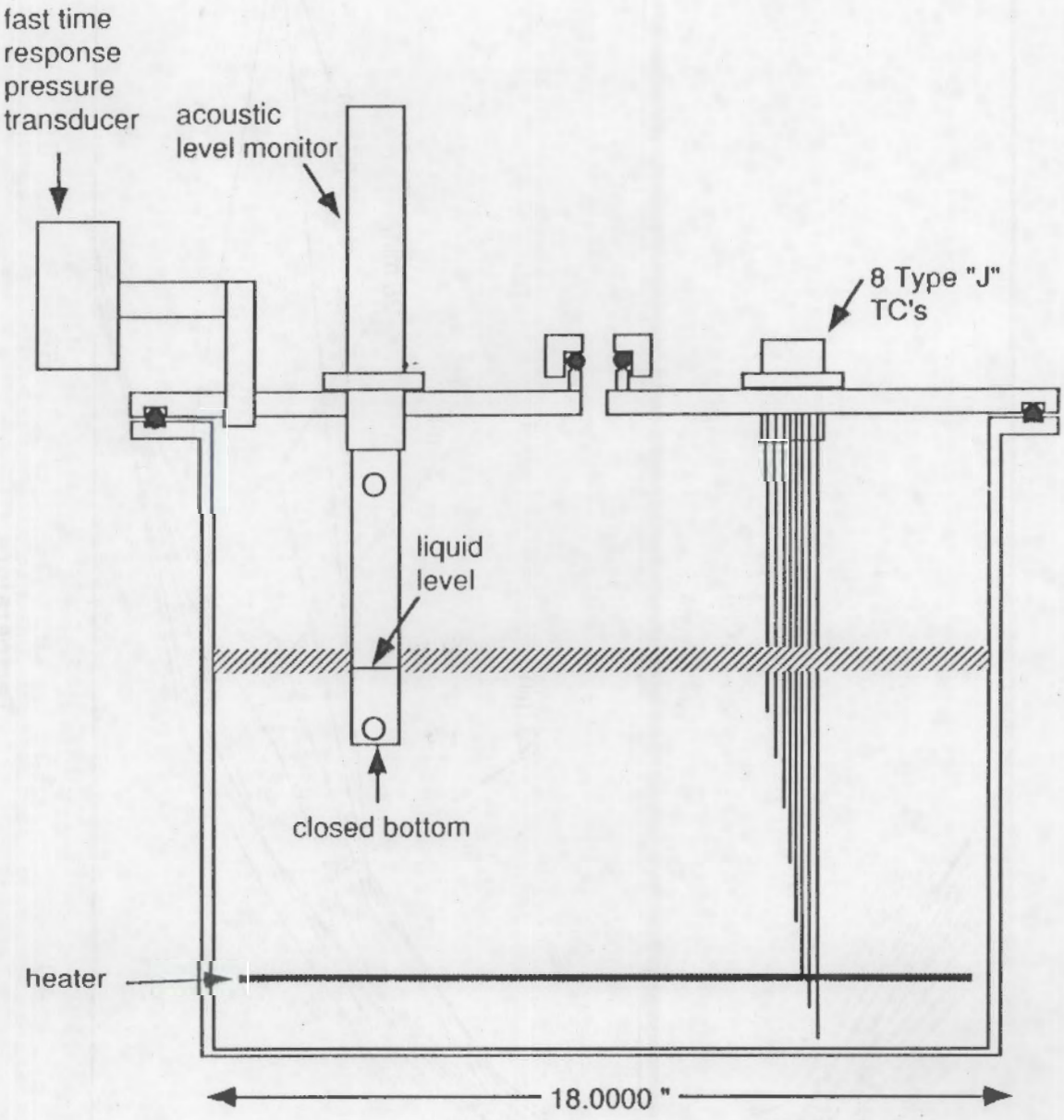
fast time
response
pressure
transducer
acoustic
level monitor
8 Type "J"
TC's
liquid
level
closed bottom
heater
18.0000 "

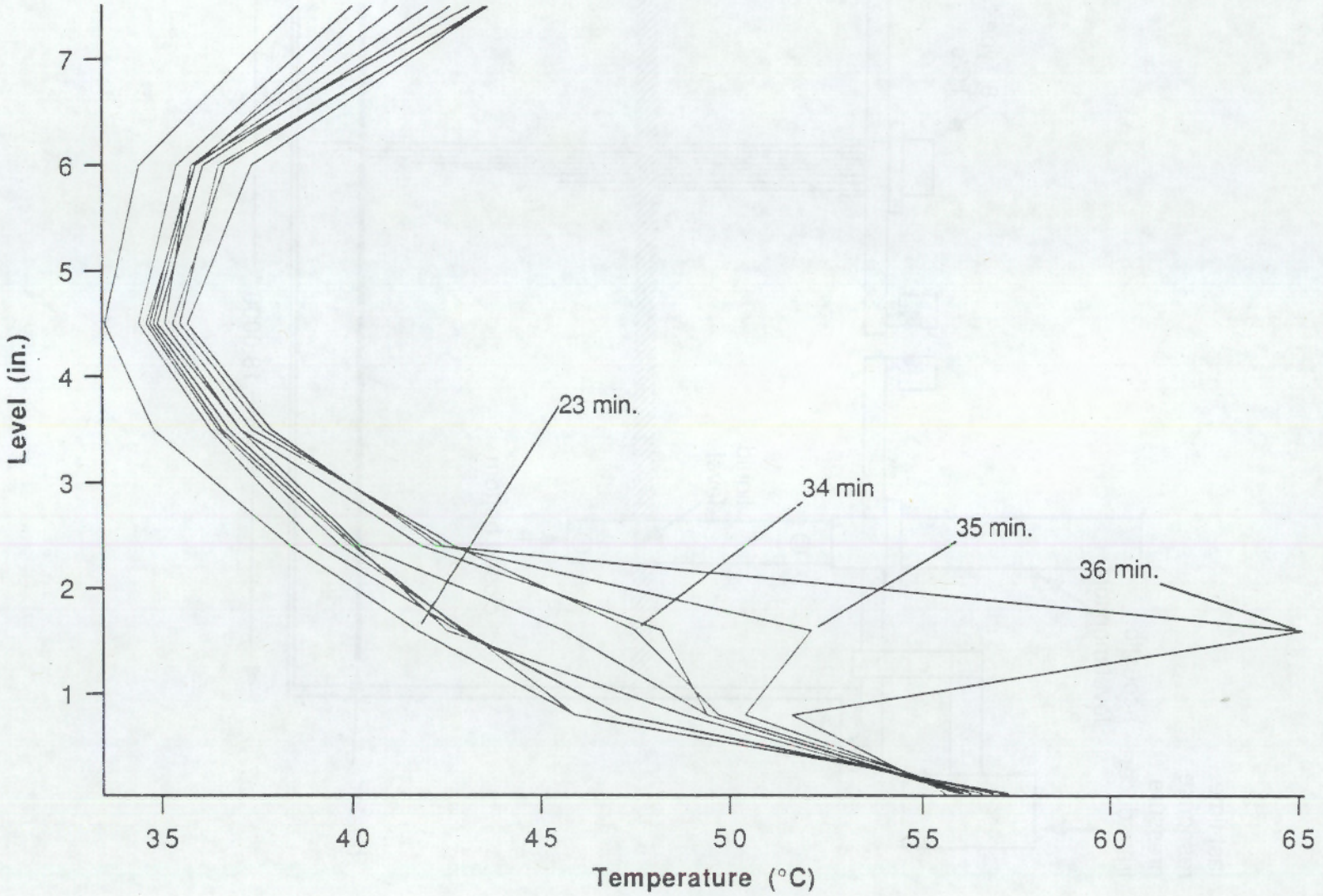
Level (in.)
7
6
5
4
3
2
1
23 min.
34 min
35 min.
36 min.
35
40
45
50
55
60
65
Temperature (°C)

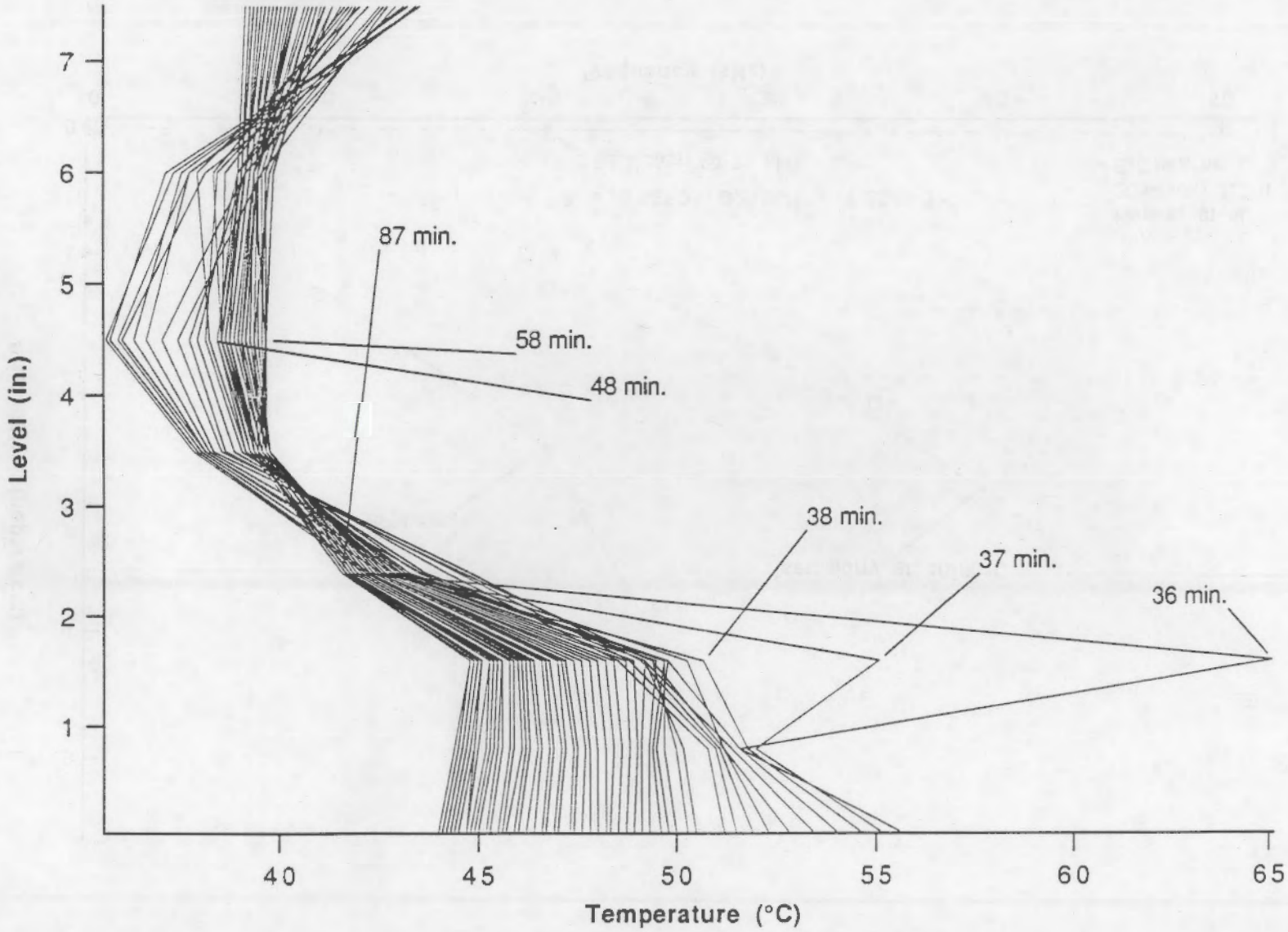
Level (in.)
7
6
5
4
3
2
1
87 min.
58 min.
48 min.
38 min.
37 min.
36 min.
40
45
50
55
60
65
Temperature (°C)

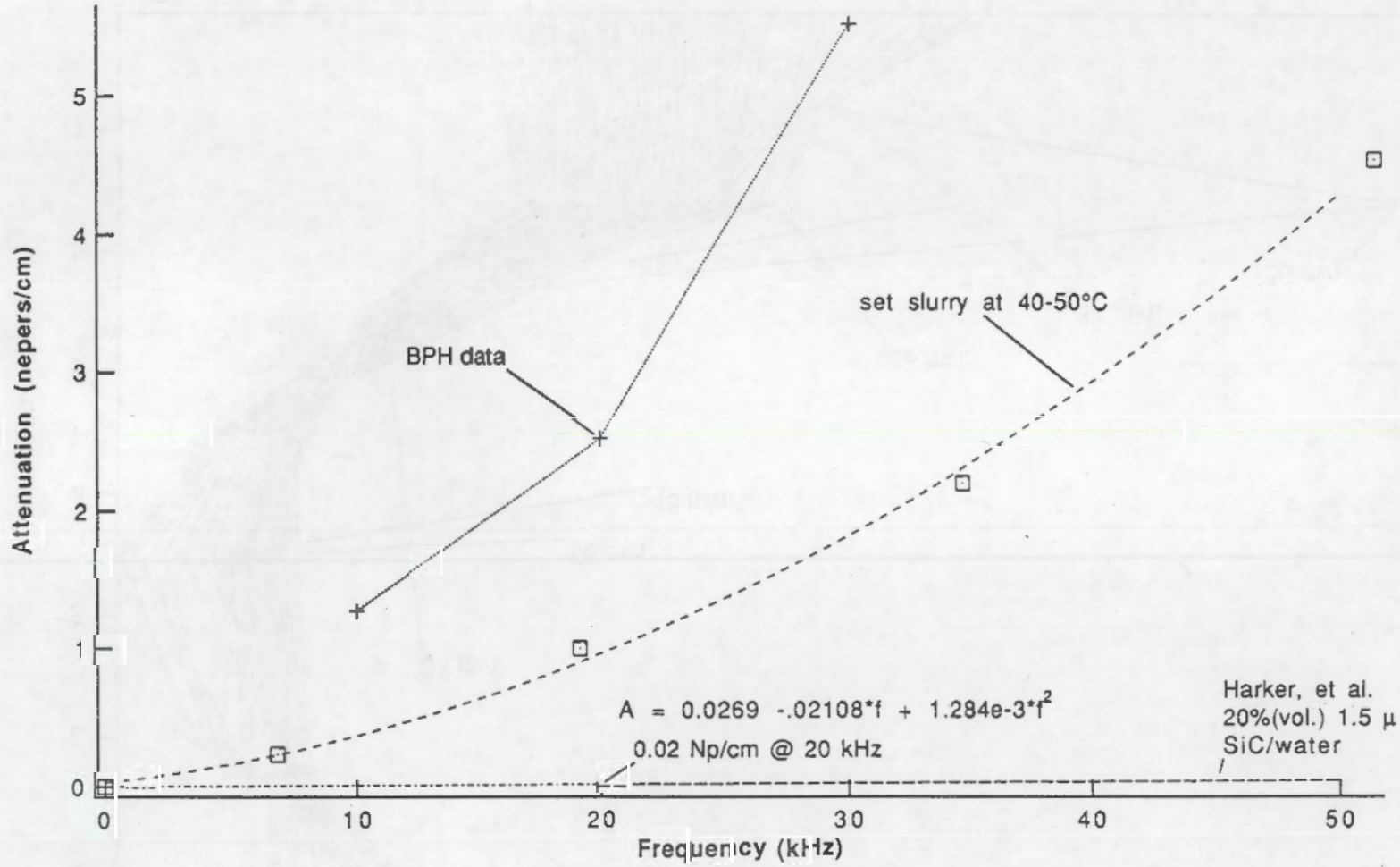
Attenuation (nepers/cm)
5
4
3
2
1
0
0
10
20
30
40
50
Frequency (kHz)
BPH data
set slurry at 40-50°C
A = 0.0269 -.02108*f + 1.284e-3*f²
0.02 Np/cm @ 20 kHz
Harker, et al.
20%(vol.) 1.5 μ
SiC/water

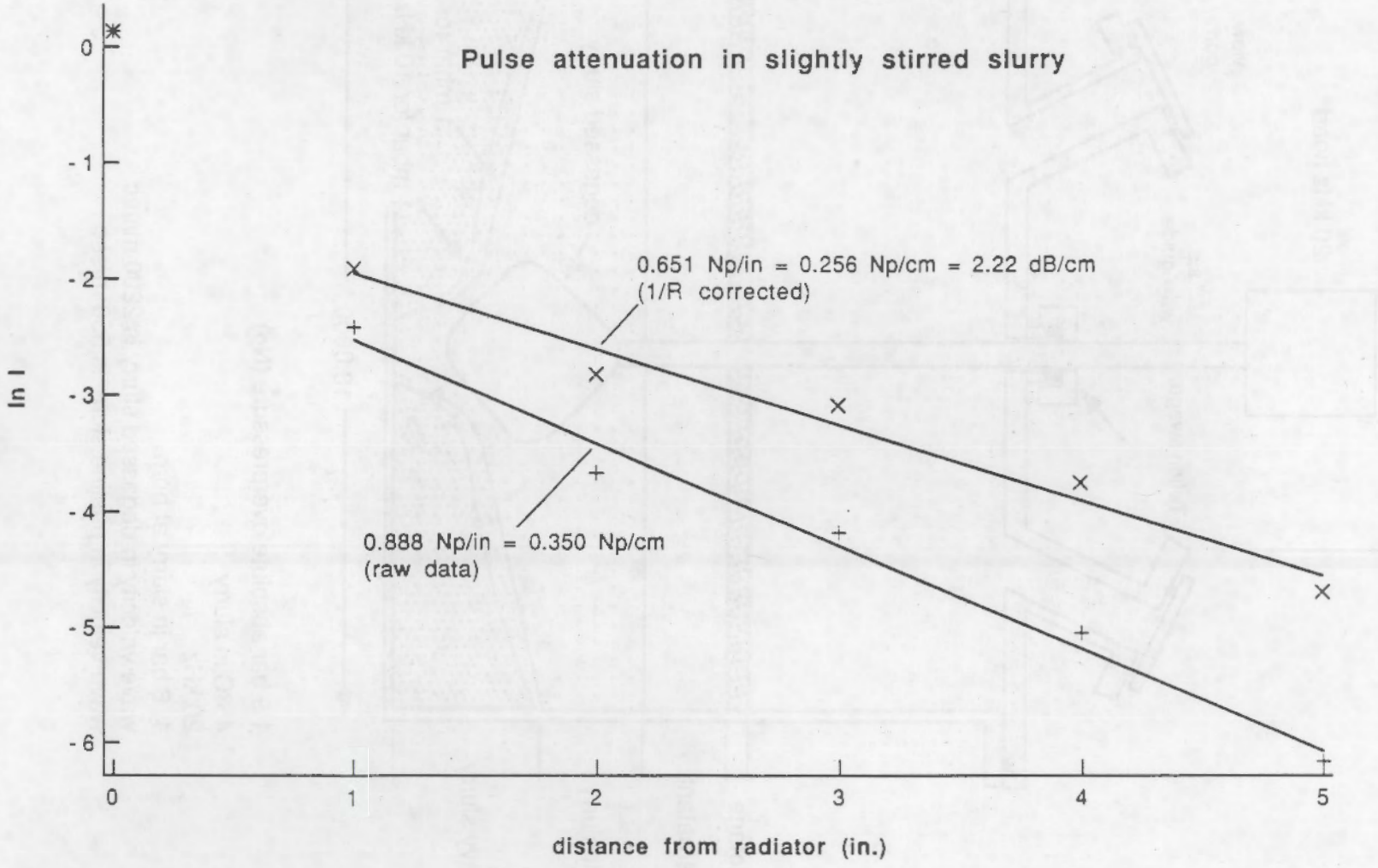
Pulse attenuation in slightly stirred slurry
0.651 Np/in = 0.256 Np/cm = 2.22 dB/cm
(1/R corrected)
0.888 Np/in = 0.350 Np/cm
(raw data)
ln I
0
-1
-2
-3
-4
-5
-6
0
1
2
3
4
5
distance from radiator (in.)

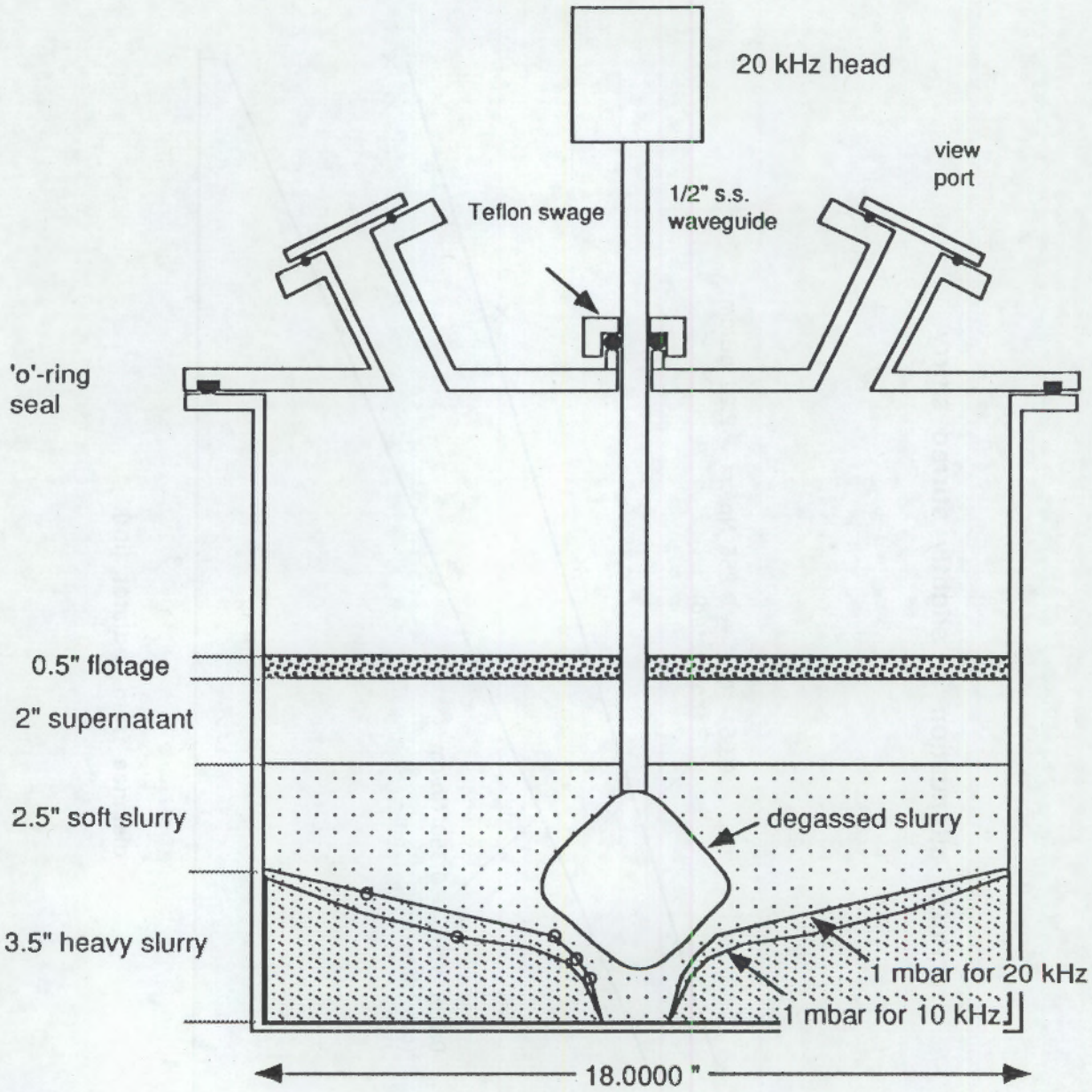

1.9 bar absolute overpressure (N_2)
45°C in slurry
20 kHz
1. 6 bar in slurry at horn
wave velocity in degassed slurry is 2200 m/sec
wave velocity in pristine slurry is 550 m/sec

Problems with Coupling

—functional design criteria established for transducer, coupler, and waveguide (three possible vendors).

—but, standard horn only allows 350 watts into slurry (7% of available).

—need improved radiator design.

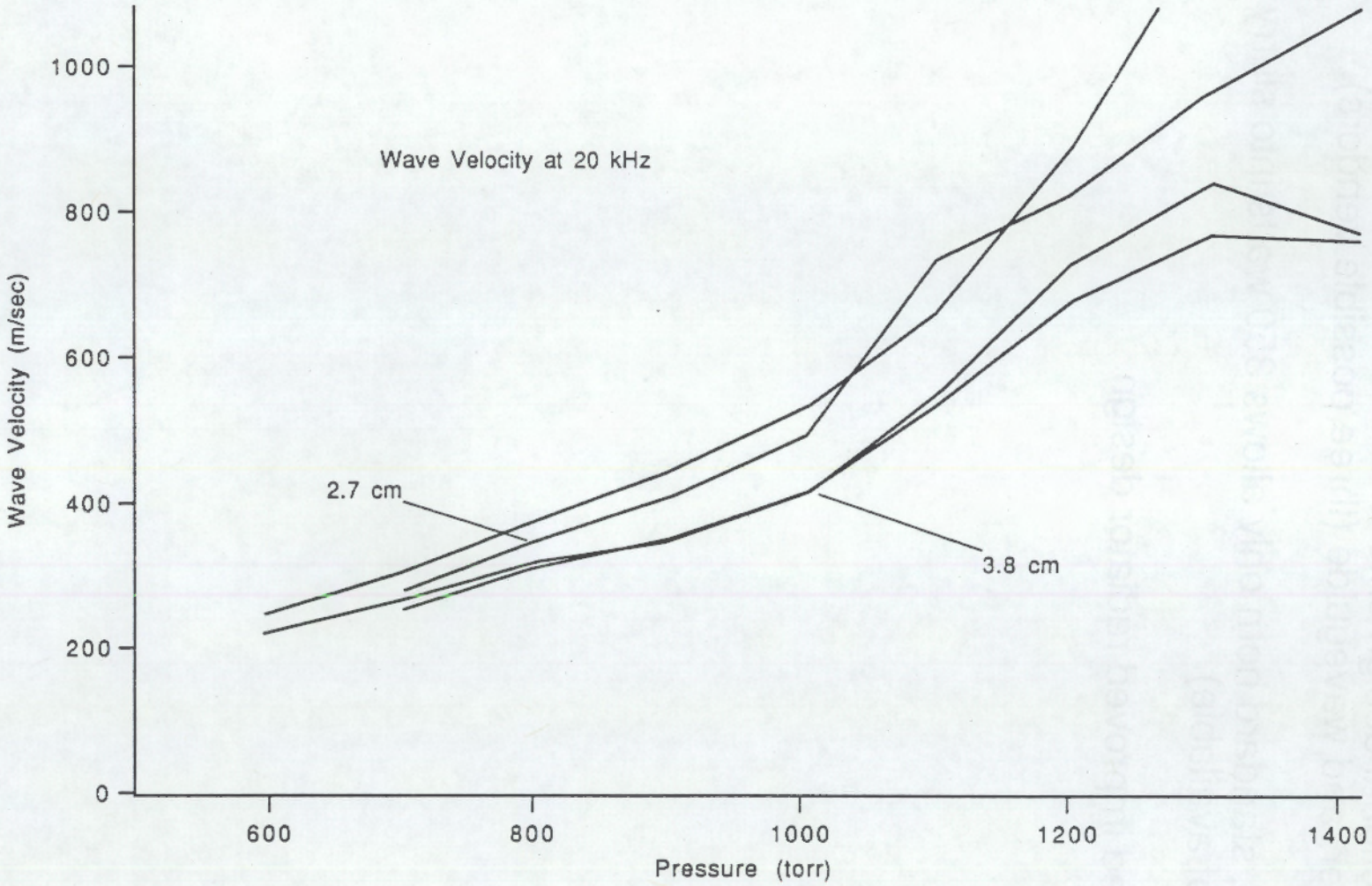
Wave Velocity at 20 kHz
Wave Velocity (m/sec)
1000
800
600
400
200
0
2.7 cm
3.8 cm
600
800
1000
1200
1400
Pressure (torr)

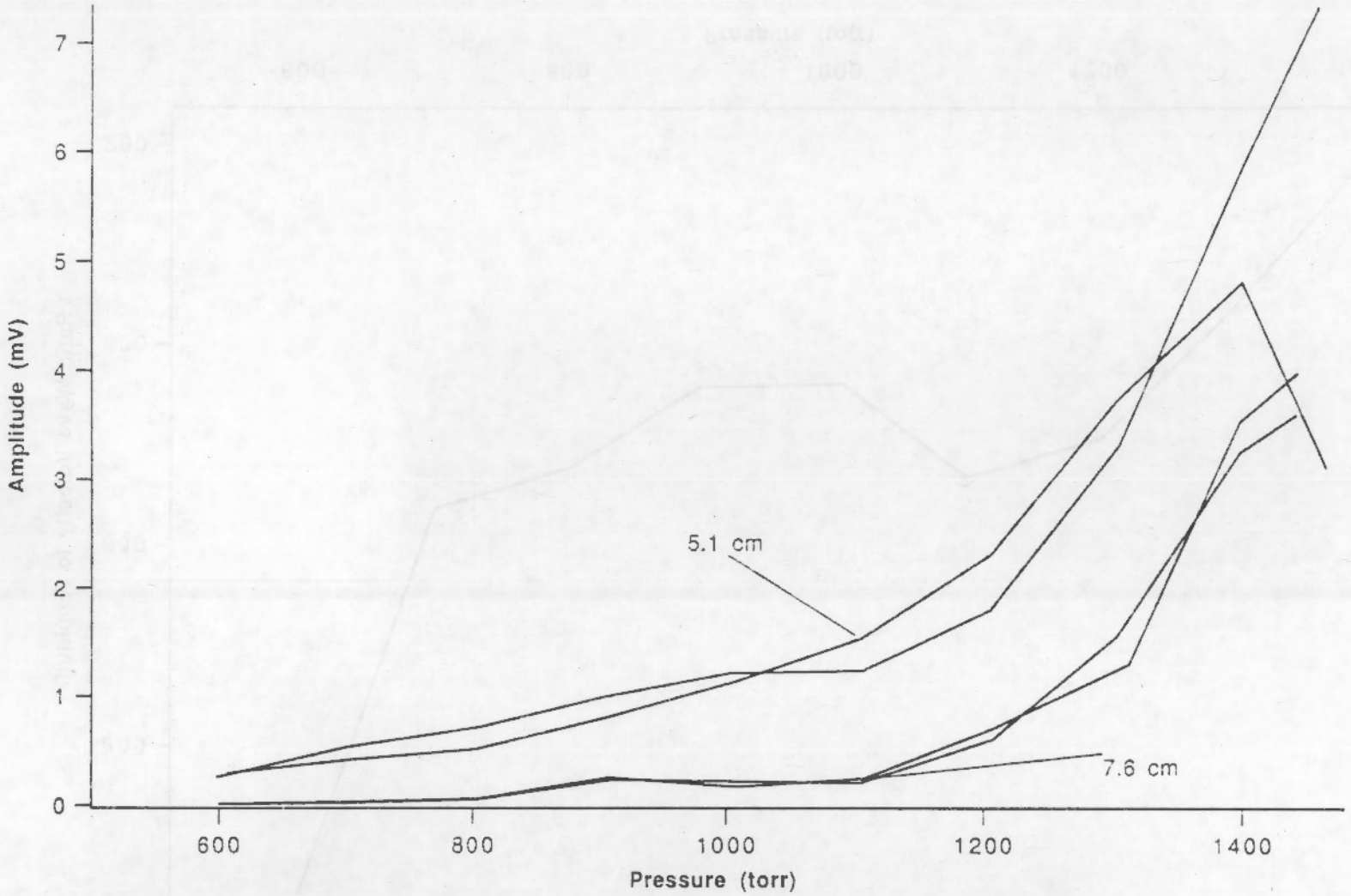
Amplitude (mV)
0
1
2
3
4
5
6
7
600
800
1000
1200
1400
Pressure (torr)
5.1 cm
7.6 cm


Ratio Wave Velocity to Amplitude
800
600
400
200
600
800
1000
1200
1400
Pressure (torr)

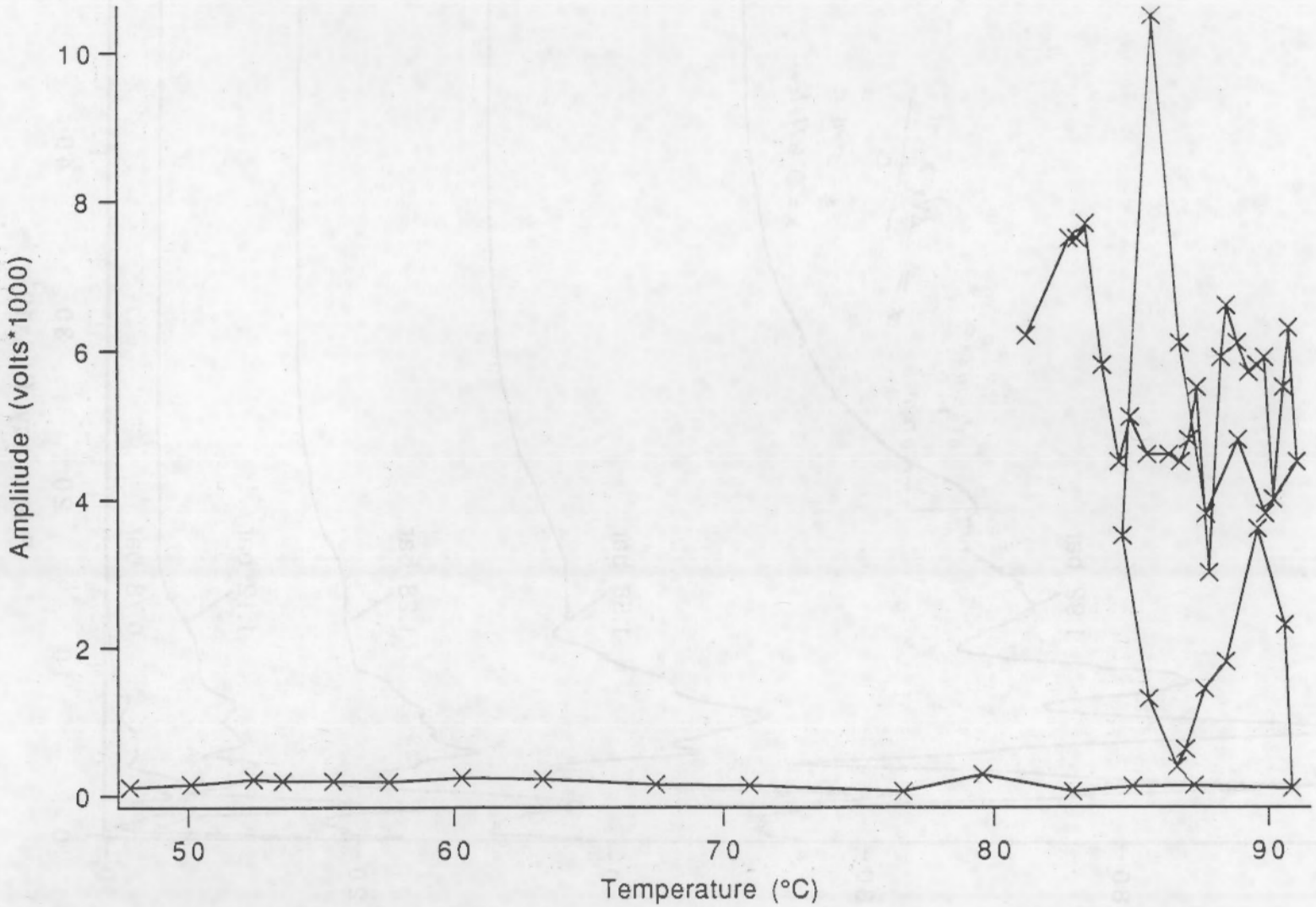
Amplitude (volts*1000)
10
8
6
4
2
0
50
60
70
80
90
Temperature (°C)

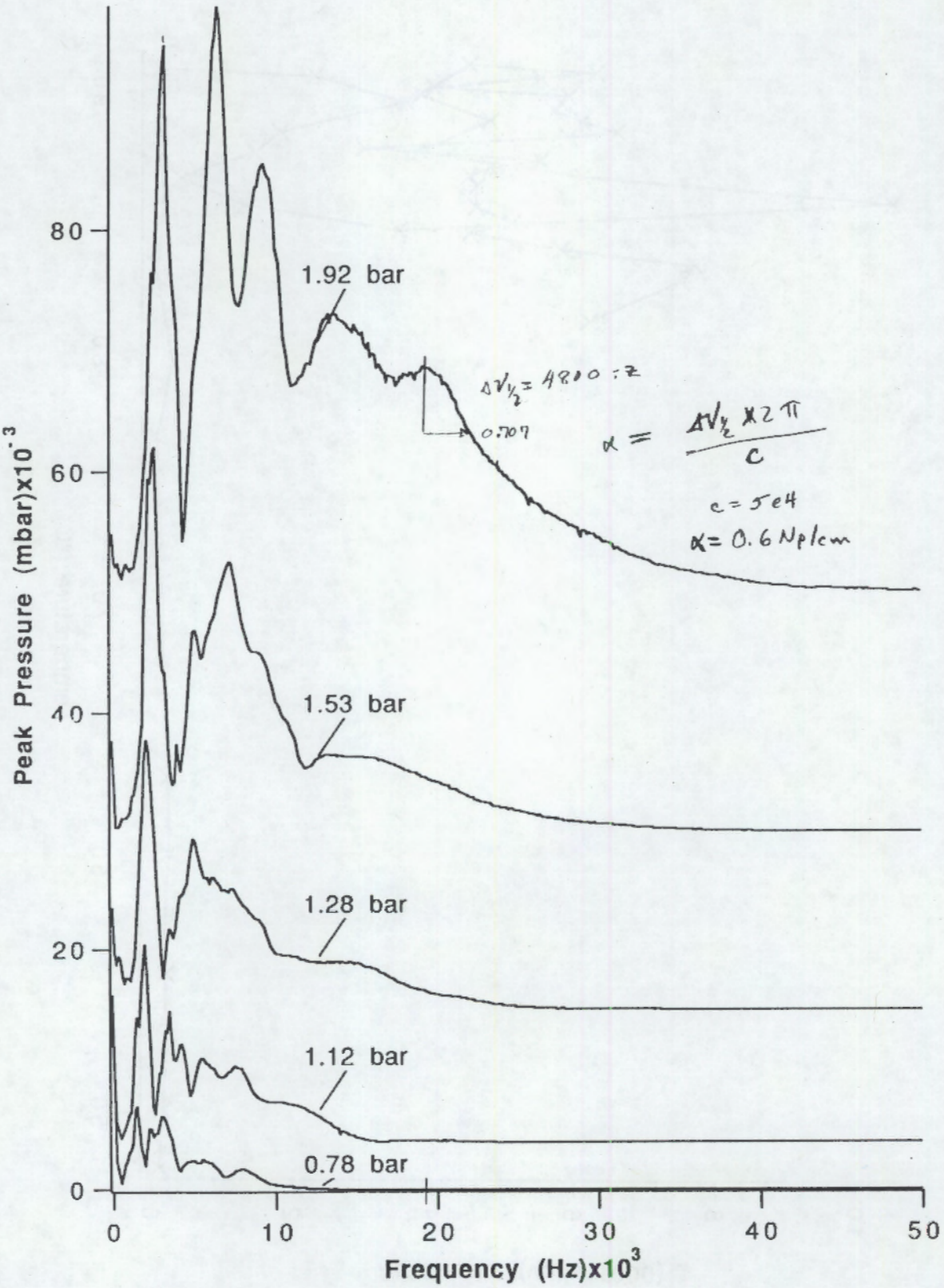
80
60
40
20
0
Peak Pressure (mbar)x10^{-3}
1.92 bar
1.53 bar
1.28 bar
1.12 bar
0.78 bar
$\Delta\nu_{1/2}$ = 4800 Hz
0.707
$\alpha = \frac{\Delta\nu_{1/2} \times 2\pi}{c}$
c = 5e4
α = 0.6 Np/cm
0
10
20
30
40
50
Frequency (Hz)x10^3

Next step...

1) Use higher power transducer to agitate slurry in model tank more completely.

2) Find slurry degassing threshold (in mbar).

3) Use slurry standing waves to determine attenuation and sound speed.

4) Finish radiator.

Summary

—ultrasonic attenuation is not straightforward due to multitude of non-linear effects in slurry. Ranges from 1.0 Np/cm to 0.04 Np/cm at 20 kHz (8.69 dB/Np).

—wave velocity strongly dependent on pressure, temperature, and gas bubble distribution.

—demonstrated slurry agitation with small as 1 mbar pressure wave.

Mitigation of Bubble Nucleation in High-Level Waste Tank 101SY with Application of Ultrasound

Presentation, March 26, 1992
Task Force Advisory Panel
Mitigation Project sub-Group Meeting
Salt Lake City, UT

All information is predecisional

Principle Investigator:
Stephen F. Agnew, Isotope and Structural Chemistry
Group INC-4, MS C346, (505) 665-1764

Harold Sullivan, Engineering and Safety Analysis, N-6

Steve Eisenhawer, Engineering and Safety Analysis, N-6

Dipen N. Sinha, Electronics Research
Group MEE-11, MS D429, (505) 667-0062

Bill Ward, Advanced Engineering Technology
Group MEE-13, MS J576, (505) 665-1844

Los Alamos National Laboratory
Los Alamos, NM 87545

---Draft---Predecisional---

Functional design criteria for ultrasonic mitigation system...

The system will consist of a converter and power supply on top of the tank, a shrouded waveguide through the riser, air space, and convecting layer, with a radiator attached to the end of the waveguide within the non-convecting layer. The radiator will be positioned approximately 40" from the bottom of the tank, and will be 48" in length. It will attach to the 2" titanium waveguide at the waveguide's free surface.

The wave guide will be shrouded in a 1/8" wall 4" diameter s.s. 304 pipe, and sealed at the lower end. It must attach to the waveguide at a node point, which occur every 5.5" along the waveguide, and 2.25" from the free surface. The waveguide must be shrouded to prevent losses in the convecting layer. This shroud will be an 1/8" s.s. 304 pipe, sealed at the ends and bolted between two segments of the waveguide at a node point that is close the the radiator (see Figs. 1 and 2).

The converter and power supply are manufactured by Sonics and Materials, Danbury, CT, (203) 744-4400 and are model VC-3000 (see Figure). This power supply is capable of providing 3000 watts continuous energy to the converter at 20±0.05 kHz, which will drive a 2" titanium diameter free surface to 0.8 mil (peak to peak). This corresponds to a peak pressure in the titanium of 310 bar and an energy density in the titanium of 1740 watts/cm^2. A 2" titanium waveguide at 310 bar peak pressure has an energy density is 1740 w/cm^2, but in practice, only a small fraction of that is actually delivered because of limitations associated with the transducer and radiator. In particular, a 3.0 kW unit will only support an energy transmission of 150 w/cm^2. Higher powers are possible for short periods of time.

Sonics and Materials will fabricate the 2" titanium waveguide, which will be made in 8' segments that will screw together. The waveguide length will need to be adjusted on site in a vertical geometry to bring it into tune with the converter and power supply.

The radiator design is not yet complete, but will conform to the general dimensions shown in Fig. 2. It will be a thin wall s.s. 304 hollow can (~1/8"), 6" in diameter and 48" long. It will be impedance matched to the 2" titanium waveguide, to which it will be attached. The bottom plate of the radiator will be a thicker plate to dampen the end motion.

Hydrophones

Four pairs of hydrophones will be needed in an array around the radiator. Each pair will measure the attenuation and sound speed, as well as the absolute sound pressure at that point in the slurry. Two pairs will be located at 12" from the bottom at right angles, and two pairs at 36" from bottom at right angles. Each pair will be in-line, with the near phone at 2", and the second at 4"

from the surface of the radiator. The second phone pair will be at 6" and 8", and the bottom four phones will be similarly placed at that height.

Temperature

Increasing temperature in the layer adjacent to radiator allows the radiator to couple more effectively with the slurry, and a heater design that allowed the heating of the volume immediately surrounding the radiator would be advantageous. This is shown in Fig. 3. Ideally, the heated layer would be at least one half of a wavelength at 20 kHz, or 2.2".

Description of Operation

The ultimate effectiveness of ultrasound to degas the slurry depends critically on two phenomena. First, the sonic energy must couple into the slurry from the radiator fairly efficiently. The radiator design that we have chosen will be strongly coupled to the slurry because of the thickness of the walls, which makes the fundamental mode's phase velocity supersonic in the slurry.

Second, the sonic energy must propagate fairly well in the degassed or agitated slurry. When the absorption of the sound waves within the degassed slurry adjacent to the radiator reduces the pressure of the wave below the yield point of the slurry, no further slurry agitation will occur. This limit will determine the total affected volume, and further excitation beyond this limit will only heat the already agitated and degassed slurry.

We know from our tests on the model tank that the initial attenuation of set slurry is ~0.6 Np/cm at 50°C at 20 kHz, and a sound speed of 550 m/sec at 1.9 bar absolute pressure. This attenuation is a factor of ten every ln(10)/.6 = 3.8 cm or 1.5". The set slurry has a very low threshold for stability, however, and acoustic pressure in the range 1-10 mBar is sufficient to disrupt, agitate, and degas the slurry. Once agitated, the slurry's sound speed increases to 2200 m/sec, while its attenuation drops to 0.1 Np/cm or lower. Thus, although the use of 20 kHz initially produces a localized effect, the propagation of the ultrasound is dependent on the nature of the slurry and its degree of agitation and gas content.

The strength of the slurry has been measured to be on the order of 1,000 to 4,000 dynes/cm^2 (1-4 mBar) at 50-60°C, with increasing strength attributed to increasing depth. When the sound amplitude exceeds the slurry strength, however, it breaks it up and allows the bubbles to rise.

Using the design threshold of 1 bar for the surface of the radiator, the effective diameter action for slurry breakup will be 25-50". This assumes that the degassed slurry reverts to 0.10-0.05 Np/cm attenuation at 20 kHz, which is what we observe in agitated slurry at 50°C.

If the attenuation in this region should drop any further, the effective diameter of the degassed slurry will correspondingly increase. We have seen large reductions in the attenuation with increasing temperature, although we do not understand this effect very well. There is also a large change in attenuation

with progressive sonic disruption of the slurry. The surface of degassed slurry progresses with sonication more slowly as the cylinder expands and the pressure at the surface of the degassed layer is reduced. A 48" long 6" diameter radiator that is delivering 3000 watts to the slurry would penetrate to 9" in about one day. Degassing progresses at an exponentially decreasing rate as a function of distance from the radiator. For example, if it takes 2.4 hours for disruption up to the 100 mBar point, it will take 1 day to get to the 10 mBar point, and 10 days for the 1 mBar point.

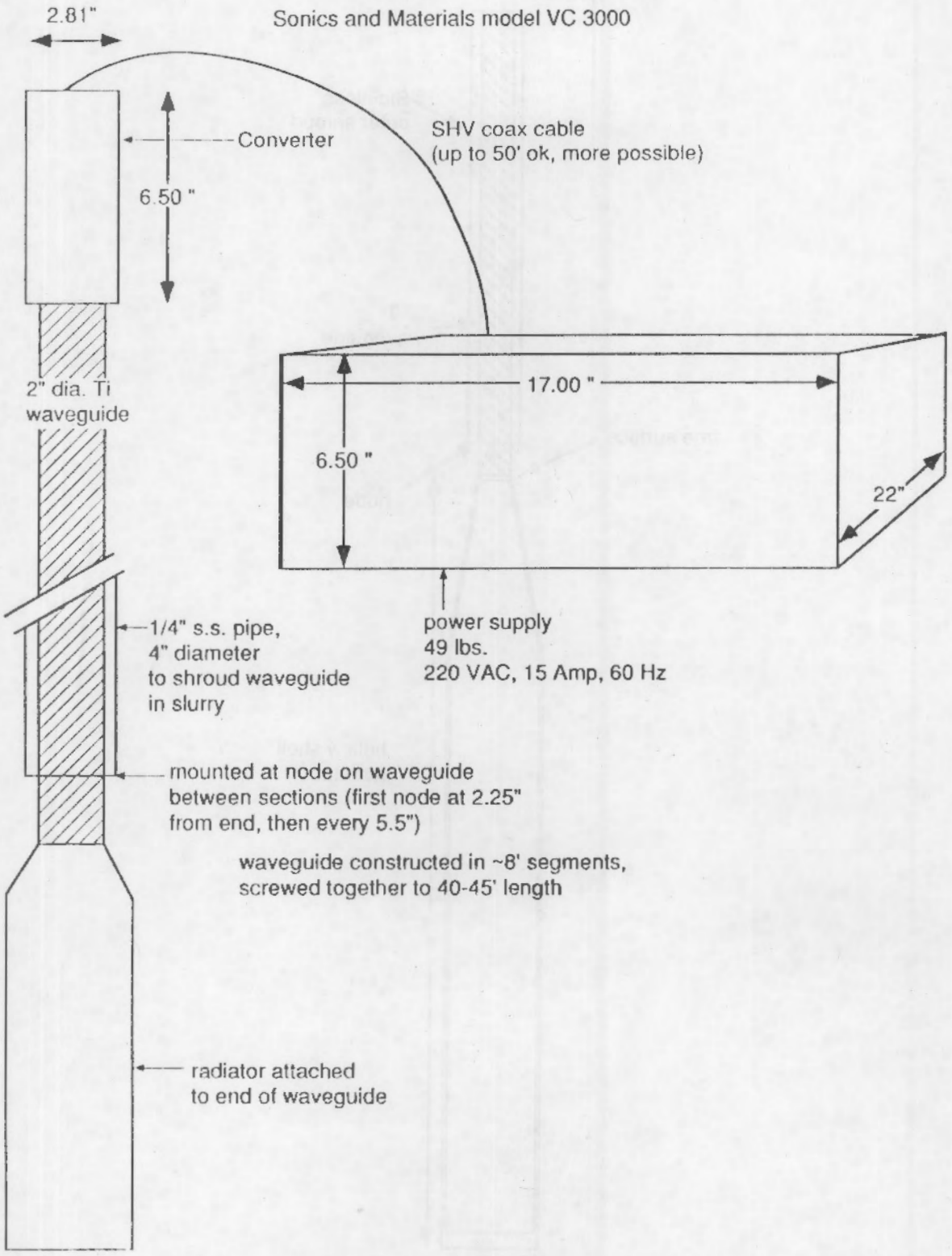
2.81"
Sonics and Materials model VC 3000
Converter
6.50 "
SHV coax cable
(up to 50' ok, more possible)
2" dia. Ti
waveguide
17.00 "
6.50 "
22"
power supply
49 lbs.
220 VAC, 15 Amp, 60 Hz
1/4" s.s. pipe,
4" diameter
to shroud waveguide
in slurry
mounted at node on waveguide
between sections (first node at 2.25"
from end, then every 5.5")
waveguide constructed in ~8' segments,
screwed together to 40-45' length
radiator attached
to end of waveguide

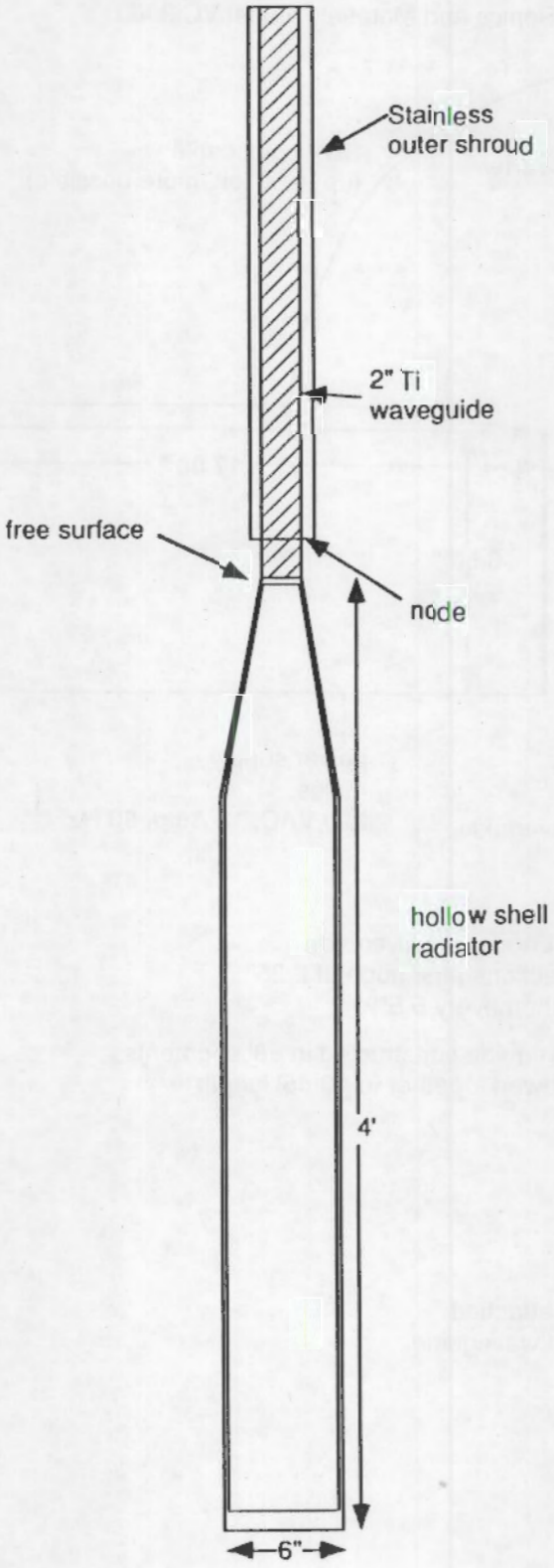
Stainless
outer shroud
2" Ti
waveguide
free surface
node
hollow shell
radiator
4'
6"

2" Ti wave guide
310 bar (0-peak) in Ti
1.0 bar in slurry
1750 watts total power in slurry
3000 watts available

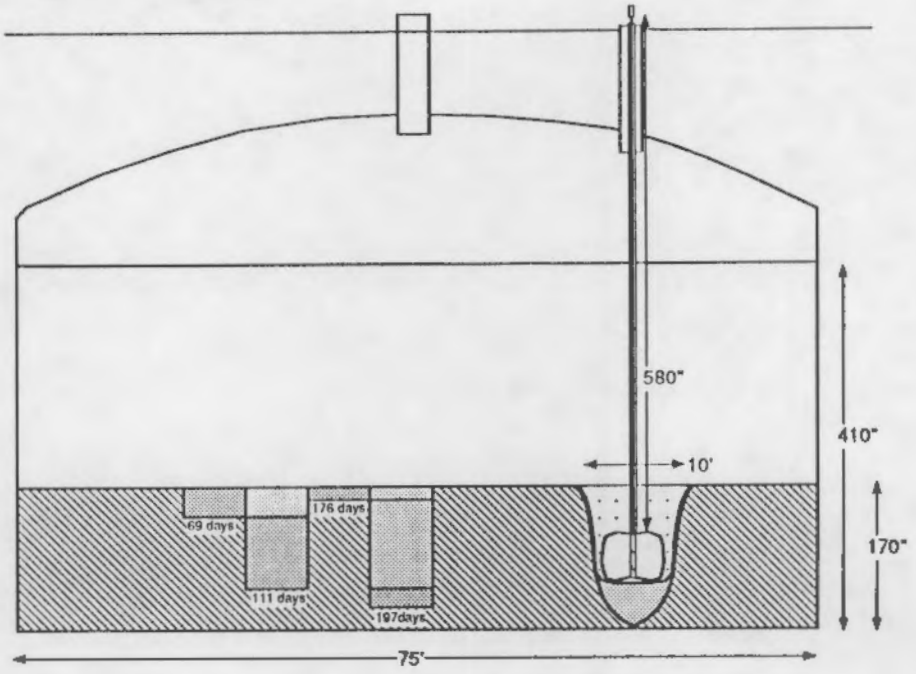

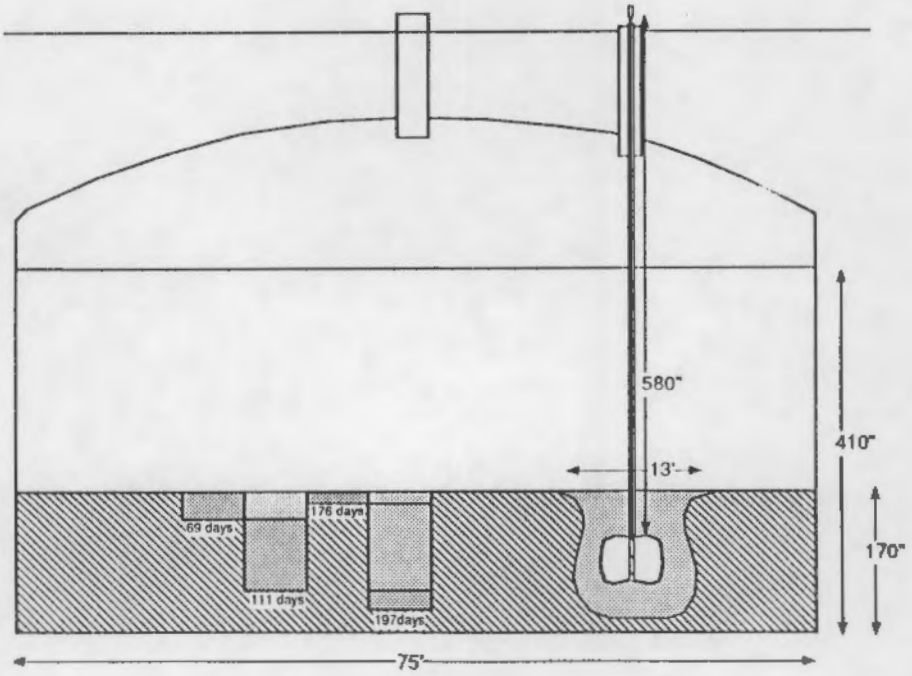

Appendix K

Organic Methods Development and Preliminary Data on Composite Samples and Simulated Waste Samples

ORGANIC METHODS DEVELOPMENT AND PRELIMINARY DATA ON COMPOSITE SAMPLES AND SIMULATED WASTE SAMPLES

DR. J.A. CAMPBELL

OUTLINE

- COMPOSITE SAMPLES

  PRELIMINARY RESULTS
  - DERIVATIZATION GC/MS
  - ION CHROMATOGRAPHY

  FURTHER STUDIES

- ARGONNE SAMPLES

  PRELIMINARY RESULTS
  - DERIVATIZATION GC/MS
  - ION CHROMATOGRAPHY

  FURTHER STUDIES

- METHODS DEVELOPMENT STATUS

- FURTHER METHODS DEVELOPMENT

PRELIMINARY

Table 1. List of Samples and Corresponding Segment Locations

Sample #	Segments & Location
1073	Composite of segments 4-8, top of convective layer
1091	Composite of segments 9-14, bottom of convective layer
961	Composite of segments 14-18, top of nonconvective layer
1078	Composite of segments 19-22, bottom of nonconvective layer

IMPORTANT ITEMS TO REMEMBER

- GC/MS METHOD HAS NOT BEEN VALIDATED

- STANDARDS NOT AVAILABLE FOR SOME OF COMPONENTS, SO CONCENTRATIONS ARE APPROXIMATE AND I.D. ARE TENTATIVE

PRELIMINARY

FIGURE 1. Total ion chromatogram of the concentrated extract of the BF3/methanol derivatized tank 101-SY composite sample.

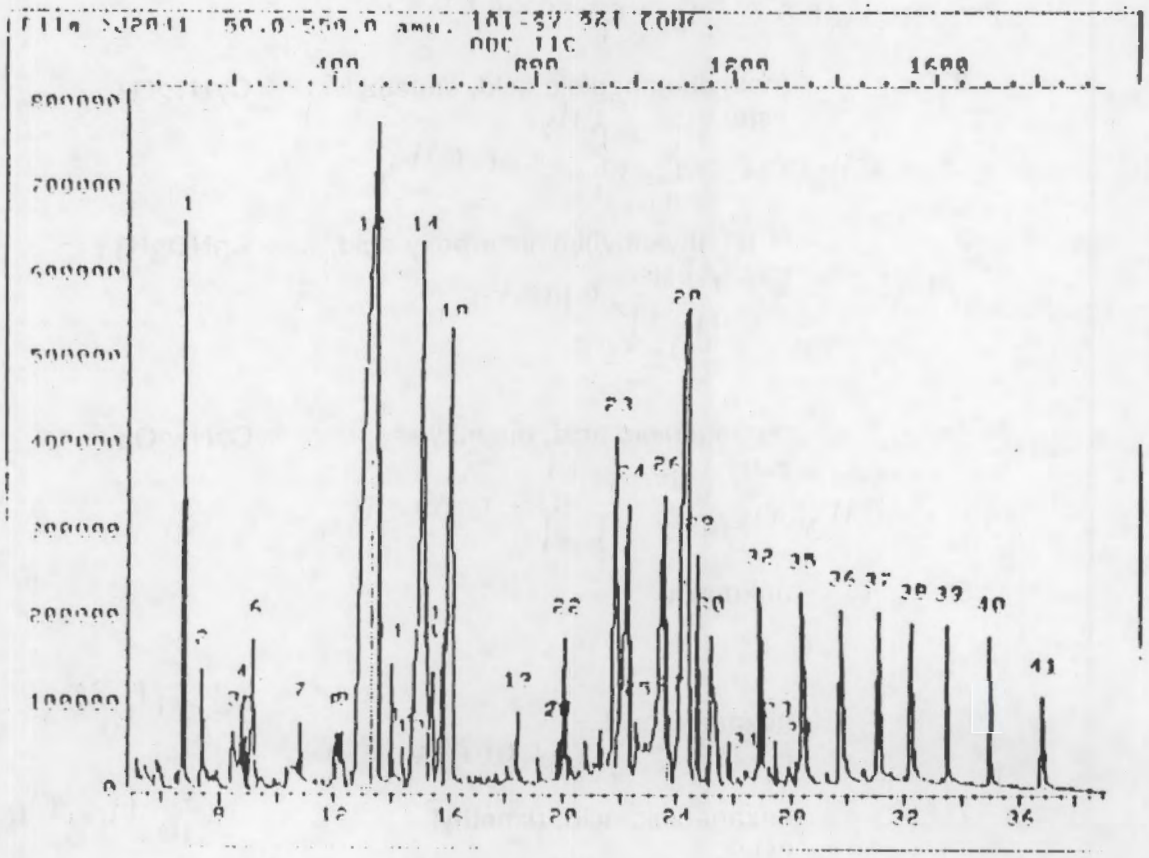

SAMPLE # 961
41 of the peaks > 1%

PRELIMINARY

Table 1. Tenatively identified Components from Figure 1.

Component #	Tentative I.D.	Molecular Form.
1	butanediooic acid, dimethylester 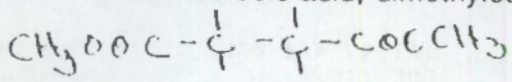	$C_6H_{10}O_4$
2	methylbutanedioic acid, dimethyl ester 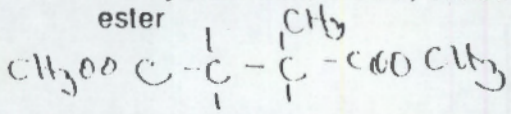	$C_7H_{12}O_4$
3	N-(methylethyl)iminocarboxy acid, methyl ester (a) 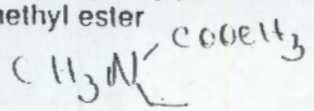	$C_5NO_2H_{11}$
4	pentanedioic acid, dimethyl ester 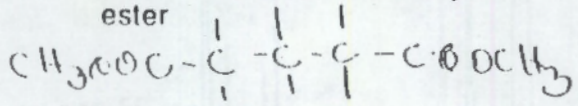	$C_7H_{12}O_4$
5	unknown	
6	hexanoic acid 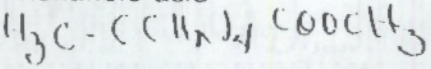	$C_7H_{14}O_2$
7	hexanedioic acid, dimethyl ester 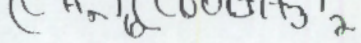	$C_{10}H_{18}O_4$
8	N-(ethylene)iminocarboxyacetic acid, dimethyl ester (b) 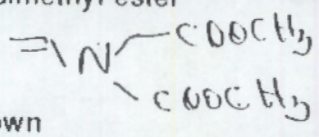	$C_9NO_4H_{11}$
9	unknown Carboxylic Acid	

10 N-(nitroso)minodiacetic acid, dimethyl ester $C_6N_2O_5H_{10}$

(a)

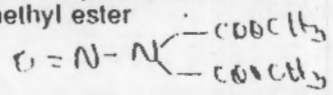

11 N-(methylimonocarboxy)ethylenediamine -N-acetic acid $C_7N_3O_3H_{13}$

(b)

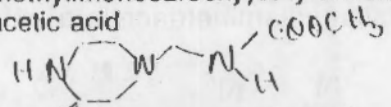

12 unknown CHELATOR FRAGMENT

(b)

13 1,2-benzenedicarboxylic acid, dimethyl ester $C_{10}O_4H_{10}$

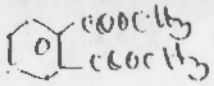

14 citric acid, trimethyl ester $C_9O_7H_{14}$

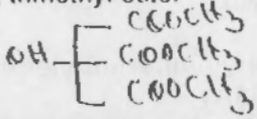

15 N-(2-hydroxyethyl)iminodiacetic acid (HEIDA) $C_6O_4NH_{11}$

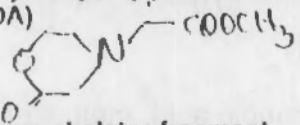

16 unknown chelator fragment

(b)

17 unknown chelator fragment

(b)

18 nitriloacetic acid, trimethyl ester $C_9NO_6H_{15}$

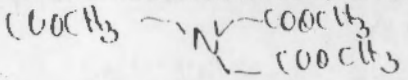

19 unknown CHELATOR FRAGMENT

20 unknown

21 unknown

22 N-(2-hydroxyethyl)-N'-(methyl) ethylenediamine-N-N'-diacetic acid or N-(Carobxy)ethylediamine-N-N'-diacetic acid $C_{10}N_2O_4H_{18}$

(b)

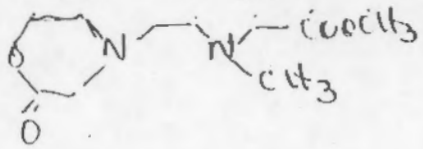

OR

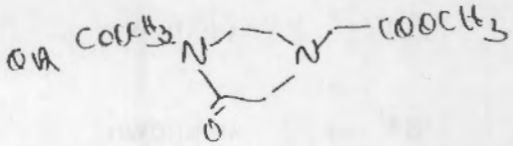

23 ethylenediaminetriacetic acid (EDTA) $C_{10}O_5N_2H_{16}$

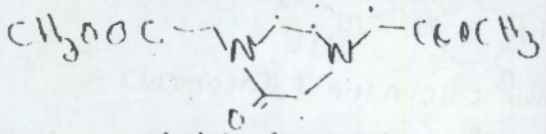

24 chelator fragment

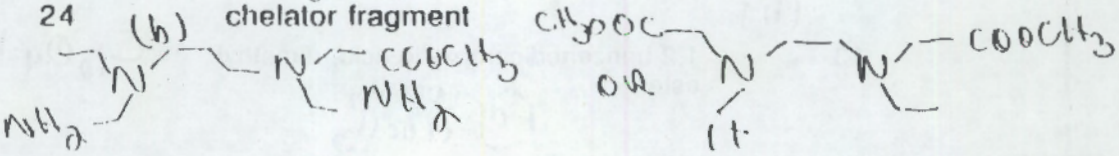

25 unknown

26 N-(methylamine)ethylenediaminetriacetic acid (MAED3A) $C_{12}O_6N_3H_{23}$

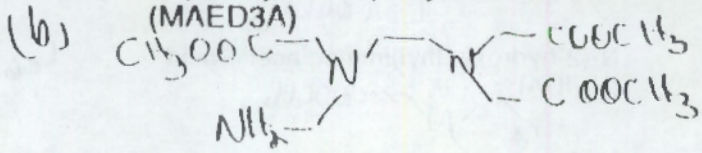

27 octadecanoic acid, methyl ester $C_{19}H_{38}O_2$

28 ethylenediaminetetracetic acid, tetramethyl ester (EDTA) $C_{14}O_8N_2H_{24}$

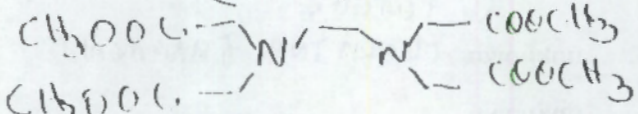

29 N-(2hydroxyethyl)ethylenediaminetriacetic acid (HEDTA) $C_{13}O_7N_2H_{24}$

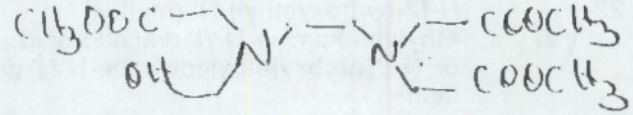

30 unknown

31 unknown

PRELIMINARY

32	uinknown	
33	unknown	
34	1,2-benzenedicarboxylic acid, bis(2-ethyl hexyl) ester	$C_{24}H_{38}O_4$
35-41	unknown	

phthalate

(a) confirmed by high-resolution mass spectrometry.
(b) need HRMS for accurate mass (elemental composition)

PRELIMINARY

Table 3. Approximate Concentrations (µg/g) of Major Components in Sample 961by GC/MS

Component		Approximate Concentration (µg/g)
1	butanedioic acid	80
10	nitrosoiminodiacetic acid	708
14	citric acid (CA)	45
18	nitrilotriacetic acid (NTA)	185
23	ethylenediaminetriacetic acid (ED3A)	115
28	ethylenediaminetetracetic acid (EDTA)	237
29	N-(2hydroxyethyl)ethylenediamine triacetic acid (HEDTA)	25

Accounts for 10-20% of the TOC

PRELIMINARY

Figure 2. Ion Chromatogram of Sample 1091.

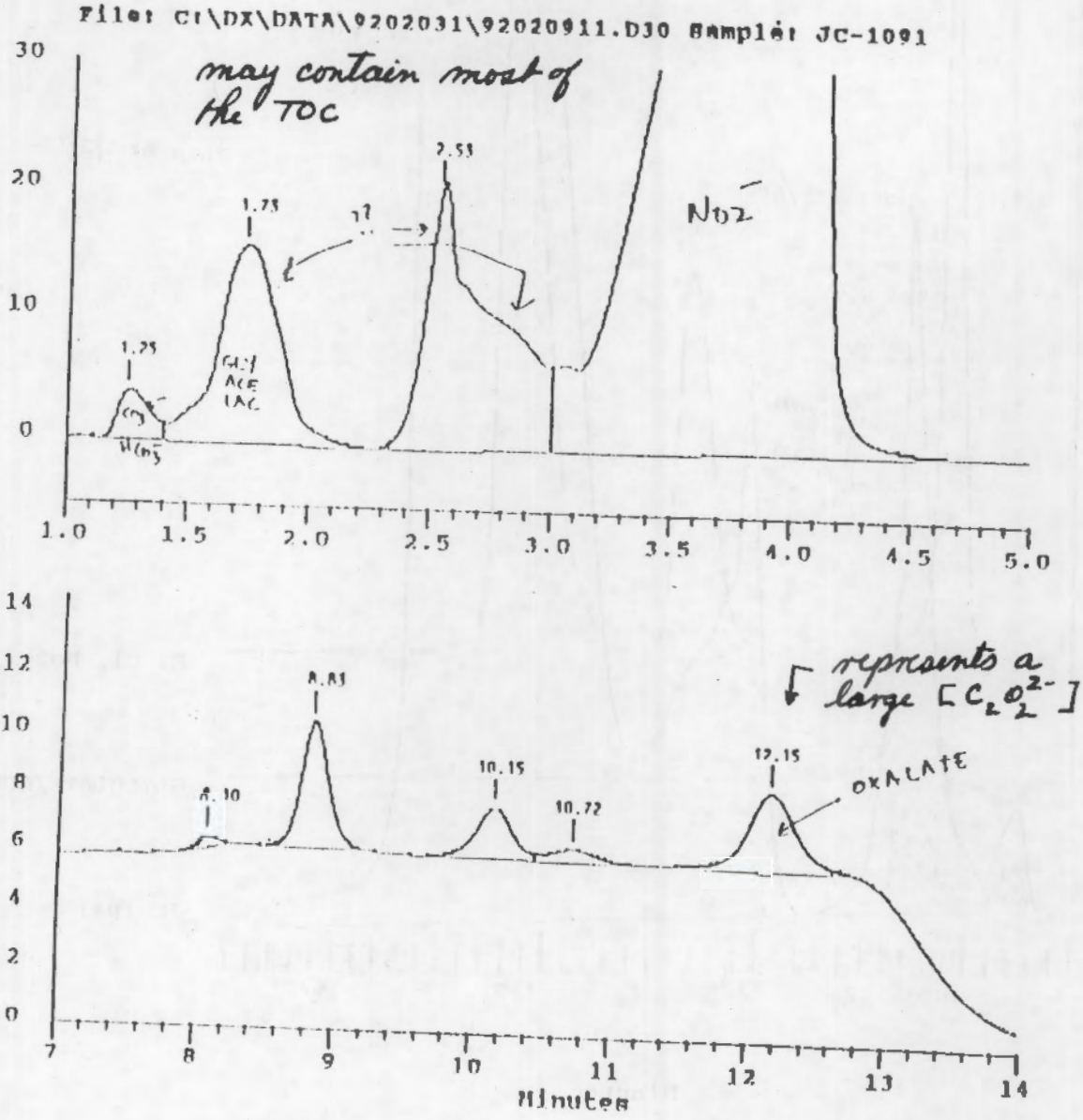

Figure 3. (a) Ion Chromatogram of Sample 1091 and (b) Standards (------)

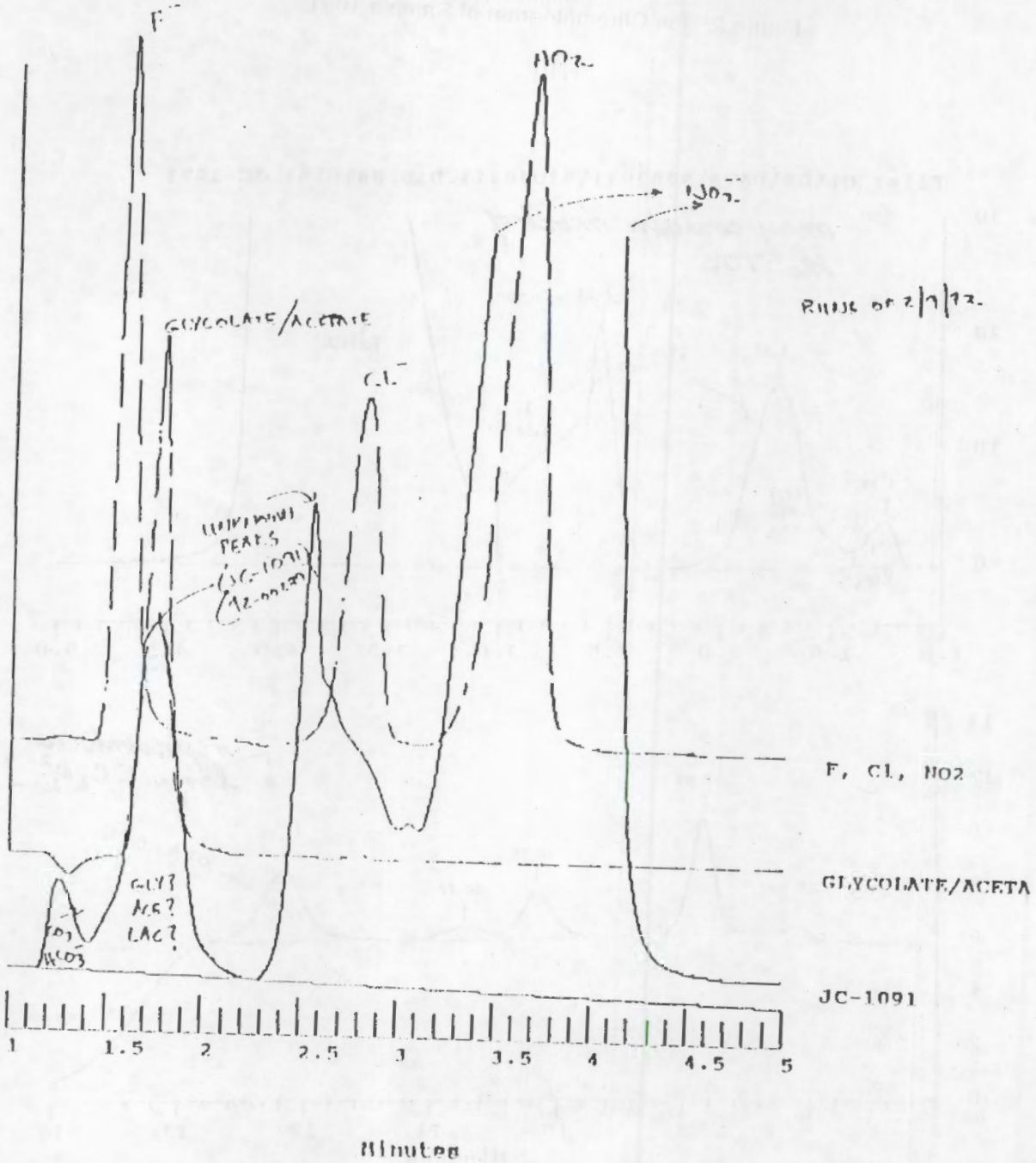

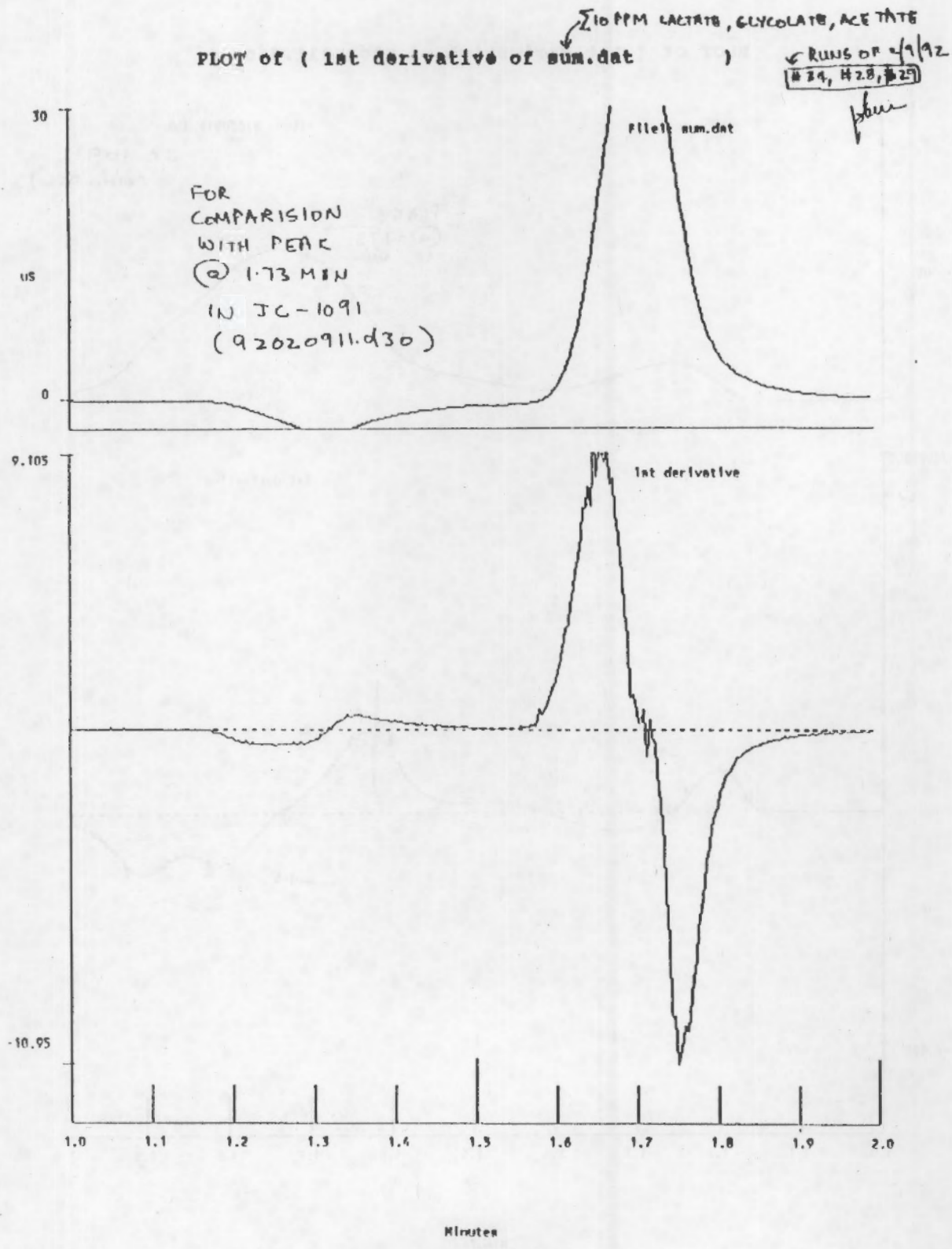
∑ 10 PPM LACTATE, GLYCOLATE, ACETATE
PLOT of (1st derivative of sum.dat)
RUNS OF 4/9/92
#24, #28, #29
30
uS
0
File: sum.dat
FOR
COMPARISION
WITH PEAK
@ 1.73 MIN
IN JC-1091
(92020911.d30)
9.105
-10.95
1st derivative
1.0
1.1
1.2
1.3
1.4
1.5
1.6
1.7
1.8
1.9
2.0
Minutes

PLOT of (1st derivative of 92020911.d30)

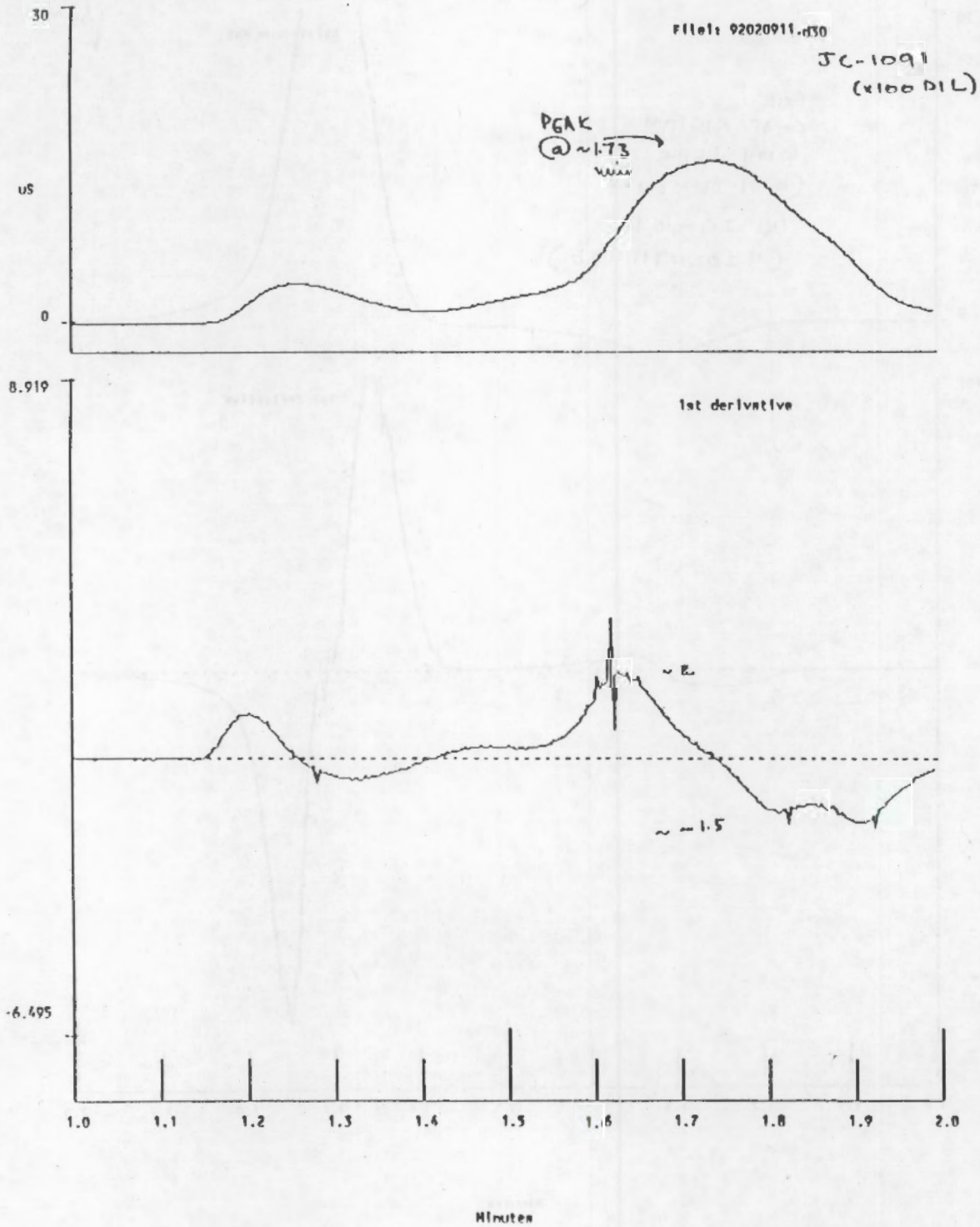

SUMMARY FOR COMPOSITE SAMPLES

- 5 CHELATORS AND FRAGMENTS IDENTIFIED AND COMPARED WITH STANDARD FOR RETENTION TIMES AND MS

- 10 CHELATOR AND FRAGMENTS THAT NEED HRMS TO CONFIRM STRUCTURE

- APPROXIMATELY 25 COMPONENTS TENTATIVELY I.D.

- APPROXIMATE CONCENTRATIONS FOR MAJOR COMPONENTS

- CHELATORS AND FRAGMENTS MAKE UP 10-20% OF TOC

- CHELATORS AND CHELATOR FRAGMENTS CONSTITUTE 65% OF ANALYZED, DERIVATIZABLE MATERIAL

- REMAINING TOC BY IC

FUTURE STUDIES ON COMPOSITES

- QUANTIFY BY GC
- HRMS ON TENTATIVELY ID COMPONENTS
- CONTINUE WITH IC
- DERIVATIZE WITH ANOTHER REAGENT TO ANSWER QUESTION OF NITROSOIDA

- APPLY LC METHOD

SIMULATED WASTE SAMPLES FROM DAN MEISEL AT ARGONNE NATIONAL LABS

PRELIMINARY

Figure 5. Total Ion Chromatogram of the Derivatized Control Sample from Meisels

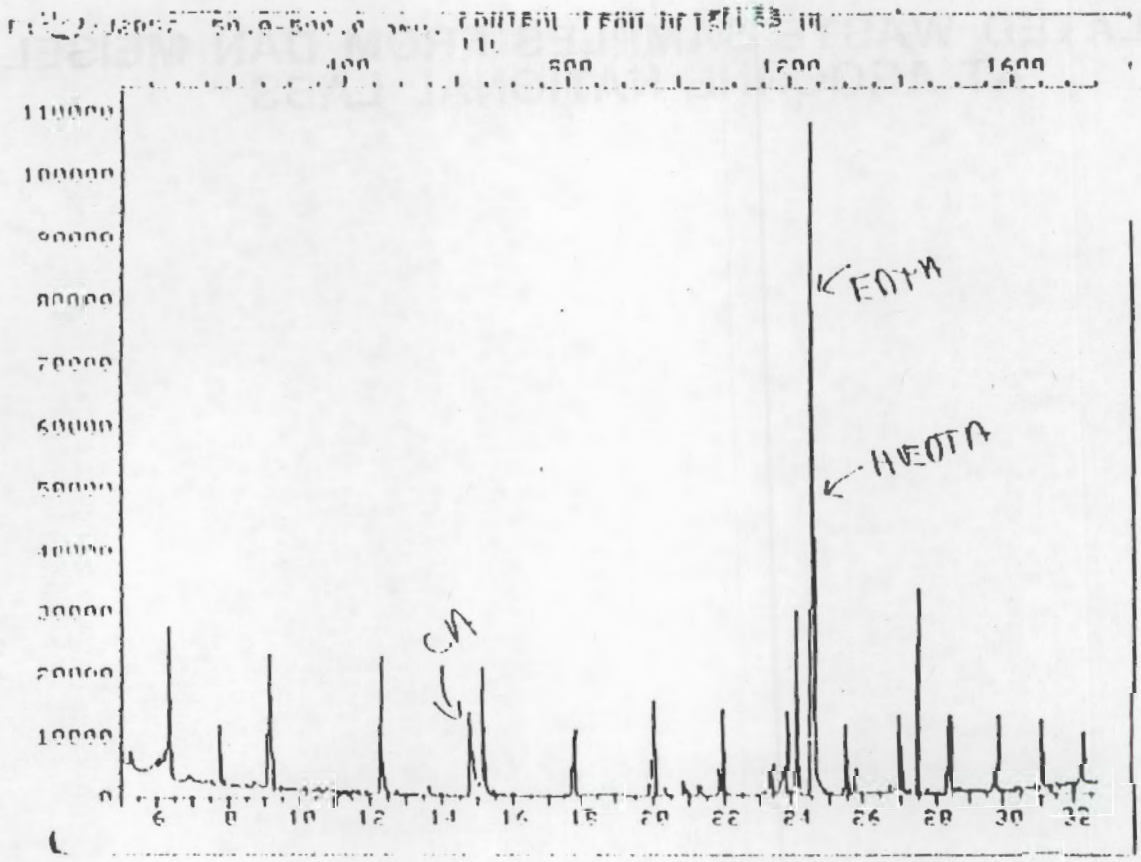

PRELIMINARY

Figure 6. Total Ion Chromatogram of Derivatized, Irradiated Sample from Meisels.

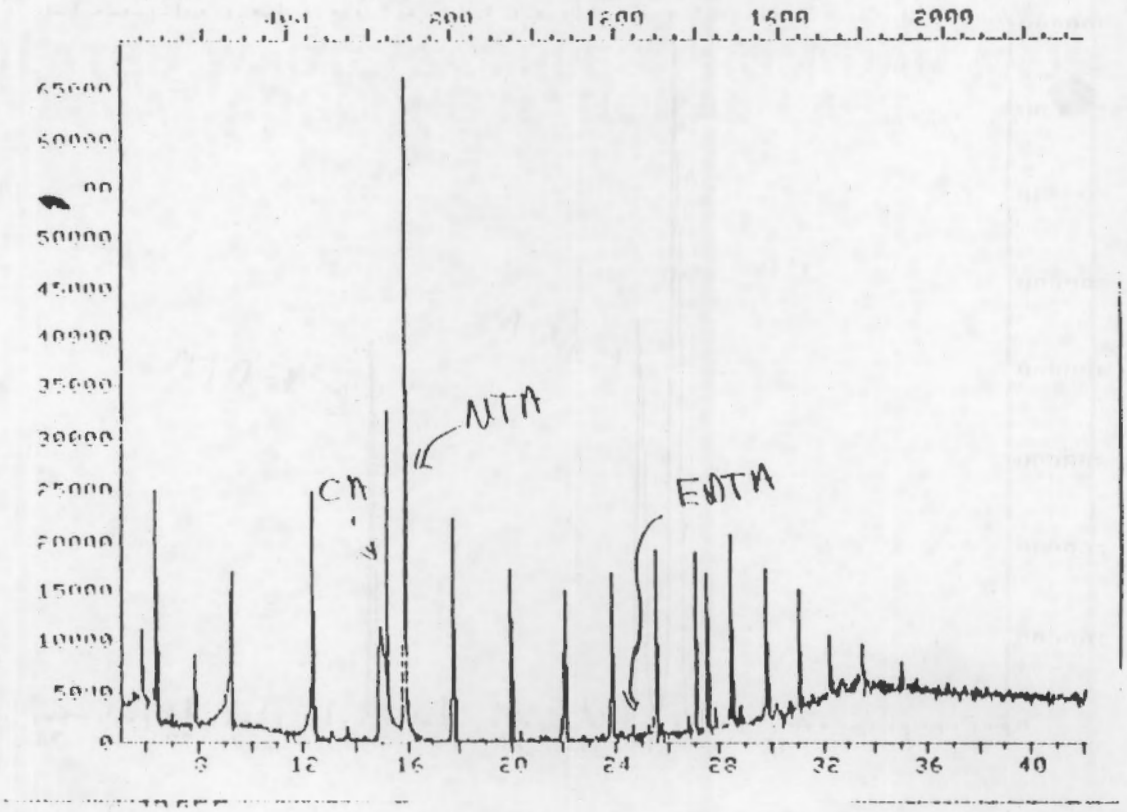

Figure 4. Total Ion Chromatogram of Derivalized NTA, EDTA, and CA.

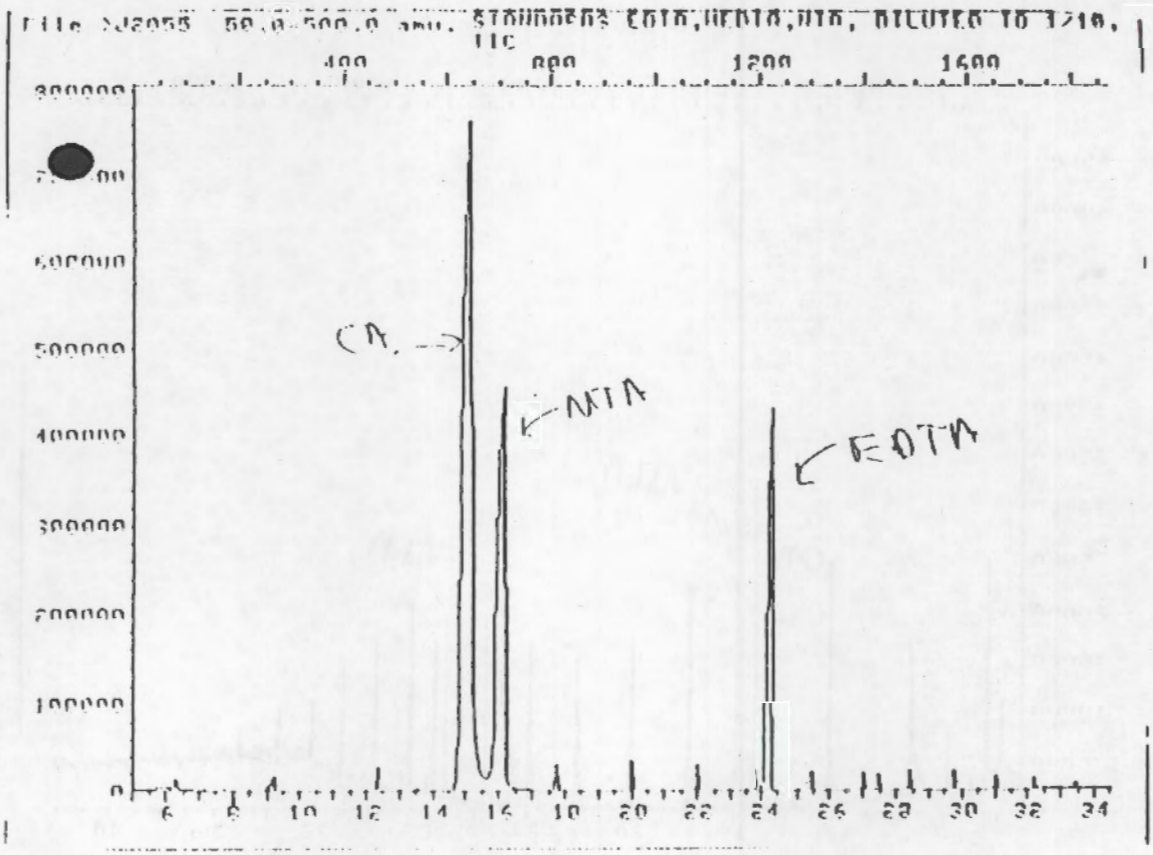

PRELIMINARY

Table 4. Estimates of Concentration (PPM) for Major Components in Samples from Meisels by Ion Chromatography

	Sample C	Sample I
Formate	107	960
Glycolate	10	93
Glyoxalate	N.D.	N.D.

ACKNOWLEDGMENTS

RICH LUCKE
KAREN GRANT
P.K. MELETHIL
KARL POOL
RICK STEELE
JOHN RAU
BILL ROBINS
MSU

REVIEW OF METHODS DEVELOPMENT

STATUS

- GC/MS about ready
- LC almost ready
- LC/MS
- other techniques
  microcol. LC and capil. zone electrophor. allow use of small samples of the aqueous wash of the sample.

Issues

- NO MECHANISM FOR TRANSFER OF TECHNIQUES
- MS ENGINE WITH 325 PERSONNEL

FUTURE WORK

- CONTINUE TO RESOLVE TOC BALANCE IN COMPOSITES AND SIMULATED WASTES

- DETERMINE ACCURATE MASS FOR COMPONENTS IN COMPOSITE

- CONTINUE IC DEVELOPMENT

- CONTINUE PROCUREMENT PROCEDURE FOR HRMS

- EVALUATE MICROCOLUMN TECHNOLOGIES

- PUT MECHANISM INTO PLACE FOR TRANSFERRING METHODS TO 325 PERSONNEL

PRELIMINARY REPORT

PRELIMINARY

Analysis of Crust,Composite Samples (Window C) from tank 101-SY, and Samples from Dan Meisel at Argonne Laboratories by Derivatization GC/MS and Ion Chromatography

J.A. CAMPBELL, K.H. POOL, AND P.K. MELETHIL

INTRODUCTION

Ethylenediaminetetraacetic acid (EDTA) and hydroxyethylenediaminetriacetic acid (HEDTA) were added to tank 101-SY and are reportedly the major organic components. A knowledge of the organic constituents present in the waste tank 101-SY is necessary to the understanding of the chemical mechanism(s) responsible for the production of hydrogen.

The object of this task is to develop analytical methods to analyze simulated and actual waste samples for chelators, chelator fragments, and other organic constituents. Liquid chromatography (LC), derivatization gas chromatography/mass spectrometry (GC/MS), and liquid chromatography/mass spectrometry (LC/MS) are the three techniques we have focused on for the analysis of chelators and chelator fragments (1-3). We are also developing other techniques such as ion chromatography/mass spectrometry and derivatization gas chromatography/mass spectrometry to identify smaller degradation products such as oxalate and glycolate. These techniques should be considered complementary. In addition, these techniques can be applied to waste samples to identify components other than chelators. As these and other techniques are developed, they will be transferred to the personnel in the 325 Building to be implemented for routine analysis of various samples. At this point in time, the developed techniques have not been validated. As a result, the data discussed here should be evaluated accordingly.

Dan Meisel of Argonne Laboratories sent us several samples for analysis. Sample C (control) contained the following constituents: sodium nitrate, sodium nitrite, sodium hydroxide, sodium aluminate, sodium citrate, sodium EDTA, and sodium HEDTA in water. Sample I (irradiated) contained the same constituents but had been irradiated. Meisel found that when he heated irradiated sample, approximately three times as much hydrogen was produced as the non-irradiated sample. Samples have been analyzed for chelator and chelator fragments.

We are attempting to gain insight into the mechanism(s) responsible for the production of hydrogen in tank 101-SY by characterizing both actual waste samples and simulated wastes. Our attention has primarily focused on applying the developed methods to the analysis of the composite samples provided by Westinghouse. Preliminary results of those analyses by derivatization GC/MS are presented here as

well as the results from initial studies by ion chromatography on both the composite samples and simulated waste samples.

EXPERIMENTAL

The composite samples from tank 101-SY are fairly radioactive, >300mR. As a result, the extractions and derivatizations had to be carried out in the hot cell facilities in the 325 building. The aqueous extract is also slightly radioactive; however, we have developed derivatization and extraction procedures which remove a portion of the organics and leave the radioactivity associated with the solid material.

Analysis of composite core samples and samples from Dan Meisel by derivatization GC/MS.

Derivatization of tank 101-SY composite samples.

Samples designated 961, 1073, 1078, and 1091, composited by Westinghouse personnel, were received into the hot cell facilities in building 325. Approximately 2 g of solid composite sample was weighed and placed in an Erlenmeyer flask with 20 mL of MilliQ water. The solution was stirred for 24 hours and then filtered with a 0.45µm filter to remove any remaining undissolved solid material. The water solution was concentrated to dryness with nitrogen blow down techniques. The remaining residue was then derivatized with boron trifluoride/methanol in the following manner. Two milliliters of boron trifluoride/methanol solution (Aldrich) was added to the residue and heated at 100° C for 1 hour in a sealed reactivial. After cooling, 1 mL of chloroform was added to the reaction mixture and vortexed. The reaction mixture was added to a test tube containing 5 mL of 0.1M KH_2PO_4 adjusted to pH 7.0 with NaOH. After vortexing this mixture, the top layer was removed and the bottom layer containing the methyl esters of the chelators was collected. The chloroform solution was removed from the hot cell, monitored for radioactivity levels, prior to concentration and preparation for subsequent GC/MS analysis.

Ion Chromatography

A Dionex 4000L ion chromatograph equipped with an AI-450 data reduction software package was utilized. An AG4A was used as a guard column and an AS4A column was the analytical column. The eluant was a mixture of 1.8 mM Na_2CO_3 and 1.7 mM $NaHCO_3$ and distilled water. A gradient elution was employed with a flow rate of 1.5 ml/min.

Derivatization of control and irradiated samples from Dan Meisel.

Three milliliters of the control and irradiated samples were placed in separate reactivials and lyophilized (freeze-dried) to remove the water. One mL of BF_3/methanol was added to each vial and the mixtures were heated to 100° C for 1 hour. After cooling, 1 mL of chloroform was added to the mixture and vortexed. This mixture was then added to a test tube containing 5 mL of 0.1M KH_2PO_4 which had previously been adjusted to pH 7.0 with NaOH. After vortexing this mixture, the top layer was removed and the bottom layer containing the methyl esters of the chelators was retained. This chloroform solution was concentrated to 1 mL and analyzed by GC/MS.

Ion Chromatography

A Dionex 4000i system equipped with a HPIC AS5A-5µ column was utilized for the ion chromatographic studies of the simulated waste samples from Meisel. The eluent was 0.75 mM NaOH at a flow rate of 1 mL/min.

GC/MS Conditions.

A J&W Scientific fused silica DB-5, 30m X 0.25 mm i.d. (0.25µm film thickness) column was used in the splitless injection mode. The oven program usually consisted of the following: 50° C for 1 min., 50-300° C at 8° C/min, and then 300° C for 5 min. The mass spectrometer was a 5988A GC/MS operated in the electron impact mode (70 eV), tuned daily with perfluorobutylamine, and scanned from 50-500 amu. The injection port was 250° and the mass spectrometry interfaces were also at 250° C. The source of the mass spectrometer was at 200° C.

RESULTS and DISCUSSION

Table 1 is a list of the composite samples and locations from tank 101-SY. The discussion will be divided into two areas: (a) analysis of tank 101-SY samples and (b) samples from Dan Meisel.

Tank 101-SY Samples.

Figure 1 is a total ion chromatogram of the concentrated extract of the BF_3/methanol derivatized tank 101-SY composite sample for qualitative analysis. Table 2 is a list of the tentatively identified components and their corresponding structures for sample 961. Table 3 is a list of the major components and their approximate concentrations (µg/g sample) obtained by GC/MS. The components will also be quantified by GC. Standards of many of these compounds are not available; as a result, the identifications of many of the components are tentative and the concentrations are approximate.

The components listed in Table 1 are typical of the chemicals present in all four composite samples. However, there are concentration differences between composite samples.

The chelators and chelator fragments make up approximately 65% of the derivatizable material in this extract. At most, the derivatizable fraction only accounts for approximately 10-20% of the total organic carbon.

Compound 10 (See Table 2 and Figure 1)had been identified as MAIDA in previous studies (4). However, we were able to measure the accurate mass (elemental composition) of this particular component by high resolution mass spectrometry. Since we do not have this capability at PNL, the cold sample was sent to Montana State University and the results were obtained in one month. If a high resolution mass spectrometer were accessible, those studies would have been completed in several days. Accurate mass measurements indicated this component is N2C6O5H10. The correct structure is (A) rather than MAIDA.

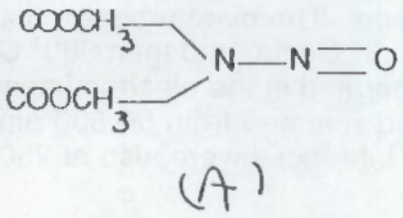

(A)

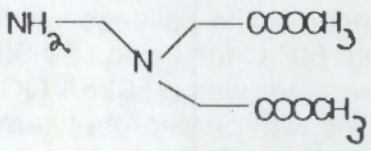

MAIDA

These results give us the first indication of a possible interaction between the inorganic components (high nitrate and nitrite composition) and the organics. It is interesting to note that this particular component was not produced as a result of derivatization with boron trifluoride/methanol on Meisel's samples that contain high nitrate and nitrite. Further studies are needed to prove conclusively that this component is actually in the tank and not a byproduct of the derivatization procedure.

In order to identify or account for the rest of the total organic carbon, one of the composite samples was analyzed by ion chromatography to look for the smaller degradation products such as oxalate, acetate, formate, glyoxalate, and glycolate. Figure 2 is an ion chromatogram of a composite sample. Figure 3 is a chromatogram of the composite sample with the ion chromatogram of several of the standards. Preliminary results indicate the presence of oxalate. The two peaks that we believe

contain organic carbon need to be separated and isolated for identification. We are currently in the process of doing that, but not all of the results are available at this time.

Analysis of Dan Meisel Samples

Figure 4 is a total ion chromatogram of a standard containing 1.77 mg/mL EDTA, 3.17 mg/mL of NTA, and 2.48 mg/mL of citric acid derivatized with boron trifluoride/methanol to form the methyl esters. Figure 5 is a total ion chromatogram of derivatized control sample, and Figure 6 is a total ion chromatogram of the derivatized, irradiated sample. Preliminary total organic carbon(TOC) values are 1.63% (gC/g solution)-control and 1.52% - solution I.

The data from the control sample show the presence of citric acid, HEDTA, and EDTA. The GC/MS results from the irradiated sample indicate the presence of citric acid, nitrilotriacetic acid (NTA), and very little EDTA or HEDTA.

Preliminary results obtained from ion chromatography studies show both formate and glycolate in the control samples, but approximately 10 times those concentrations in the irradiated samples. These results are presented in Table 4. Even in the control sample there is some evidence of chemical degradation. However, the disappearance of EDTA and HEDTA in the irradiated sample indicates radiolytical degradation as well.

CONCLUSIONS

We have been able to provide tentative identifications on approximately 25 components in the derivatized fraction from composite samples from tank 101-SY. Approximate concentrations have also been obtained on the major components in that fraction. Since many of the standards are not available; the identifications have been labelled tentative and the concentrations approximate.

Chelators account for approximately 65% of the derivatizable fraction but only approximately 10-20% of the total organic carbon. Progress is being made in accounting for the remaining TOC by ion chromatography, but further work is needed.

REFERENCES

1. R.B. Lucke, J.A. Campbell, K.L. McKeeta, and S.A. Clauss. Analysis of Chelators and Chelator Fragments by Derivatization GC/MS. In: Proceedings of the 39th ASMS Conference on Mass Spectrometry and Allied Topics., May 19-24, 1991, Knoxville, Tennessee, p. 720-721.

2. J.A. Campbell, R.B. Lucke, and S.A. Clauss. Application of LC/MS to the Study of Chelators in Mixed Hazardous Wastes. In: Proceedings of the 39th ASMS

Conference on Mass Spectrometry and Allied Topics., May 19-24, 1991, Knoxville, Tennessee, p. 1334-1335.

3. J.A. Campbell, R.B. Lucke, and H.Udseth. Analysis of Chelators and Chelator Fragments by Electrospray Mass Spectrometry. To be presented at the 40th ASMS Conference on Mass Spectrometry and Allied Topics, May 19-24, 1992, Washington, D.C.,

4. A.P. Toste and T.J. Lechner-Fish. 1989. Organic Diagenisis in Commercial, Low-level Nuclear Wastes. Radioactive Waste Management and the Nuclear Fuel Cycle, 12, 291-301.

PRELIMINARY

Table 1. List of Samples and Corresponding Segment Locations

Sample #	Segments & Location
1073	Composite of segments 4-8, top of convective layer
1091	Composite of segments 9-14, bottom of convective layer
961	Composite of segments 14-18, top of nonconvective layer
1078	Composite of segments 19-22, bottom of nonconvective layer

PRELIMINARY

Table 1. Tenatively identified Components from Figure 1.

Component #	Tentative I.D.	Molecular Form.
1	butanediooic acid, dimethylester 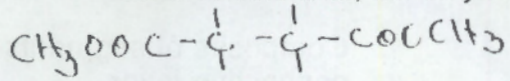	$C_6H_{10}O_4$
2	methylbutanedioic acid, dimethyl ester 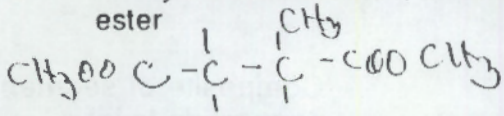	$C_7H_{12}O_4$
3	N-(methylethyl)iminocarboxy acid, methyl ester (a) 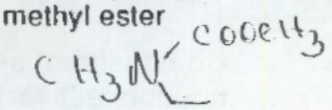	$C_5NO_2H_{11}$
4	pentanedioic acid, dimethyl ester 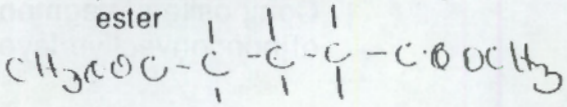	$C_7H_{12}O_4$
5	unknown	
6	hexanoic acid 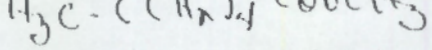	$C_7H_{14}O_2$
7	hexanedioic acid, dimethyl ester 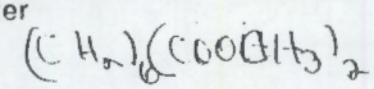	$C_{10}H_{18}O_4$
8	N-(ethylene)iminocarboxyacetic acid, dimethyl ester (b) 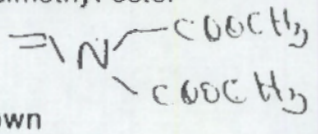	$C_9NO_4H_{11}$
9	unknown CARBOXYLIC ACID	

10 N-(nitroso)minodiacetic acid, dimethyl ester $C_6N_2O_5H_{10}$

(a)

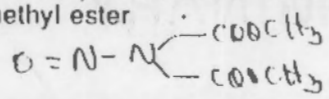

11 N-(methylimonocarboxy)ethylenediamine -N-acetic acid $C_7N_3O_3H_{13}$

(b)

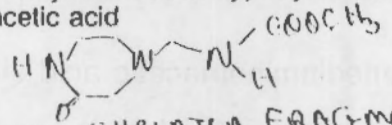

12 unknown CHELATOR FRAGMENT

(b)

13 1,2-benzenedicarboxylic acid, dimethyl ester $C_{10}O_4H_{10}$

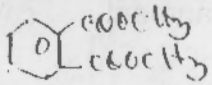

14 citric acid, trimethyl ester $C_9O_7H_{14}$

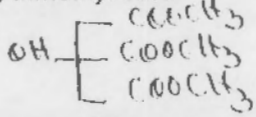

15 N-(2-hydroxyethyl)iminodiacetic acid (HEIDA) $C_6O_4NH_{11}$

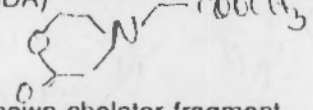

16 unknown chelator fragment

(b)

17 unknown chelator fragment

(b)

18 nitriloacetic acid, trimethyl ester $C_9NO_6H_{15}$

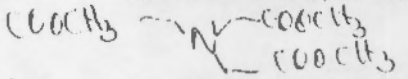

19 unknown CHELATOR FRAGMENT

20 unknown

21 unknown

22 N-(2-hydroxyethyl)-N'-(methyl) ethylenediamine-N-N'-diacetic acid or N-(Carobxy)ethylediamine-N-N'-diacetic acid $C_{10}N_2O_4H_{18}$

(b)

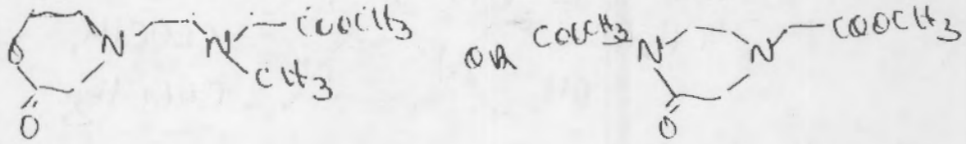

23 ethylenediaminetriacetic acid (ED3A) $C_{10}O_5N_2H_{16}$

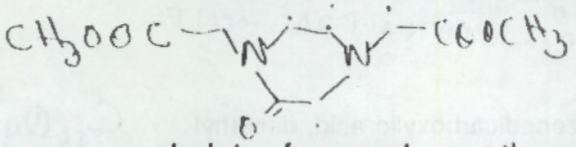

24 chelator fragment

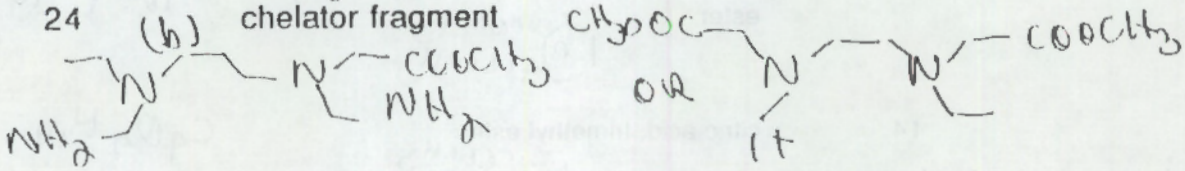

25 unknown

26 N-(methylamine)ethylenediaminetriacetic acid (MAED3A) $C_{12}O_6N_3H_{23}$

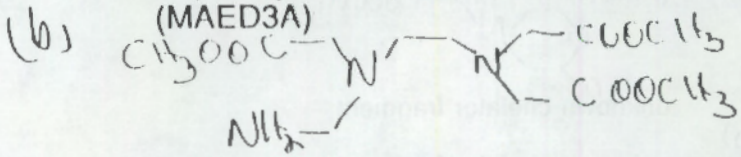

27 octadecanoic acid, methyl ester $C_{19}H_{38}O_2$

28 ethylenediaminetetracetic acid, tetramethyl ester (EDTA) $C_{14}O_8N_2H_{24}$

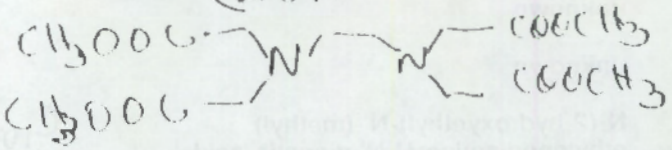

29 N-(2hydroxyethyl)ethylenediaminetriacetic acid (HEDTA) $C_{13}O_7N_2H_{24}$

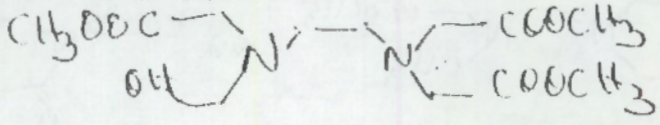

30 unknown

31 unknown

PRELIMINARY

32	uinknown	
33	unknown	
34	1,2-benzenedicarboxylic acid, bis(2-ethyl hexyl) ester	$C_{24}H_{38}O_4$
35-41	unknown	

phthalate

(a) confirmed by high resolution mass spectrometry.
(b) need HRMS for accurate mass (elemental composition)

PRELIMINARY

Table 3. Approximate Concentrations (µg/g) of Major Components in Sample 961by GC/MS

Component		Approximate Concentration (µg/g)
1	butanedioic acid	80
10	nitrosoiminodiacetic acid	708
14	citric acid (CA)	45
18	nitrilotriacetic acid (NTA)	185
23	ethylenediaminetriacetic acid (ED3A)	115
28	ethylenediaminetetracetic acid (EDTA)	237
29	N-(2hydroxyethyl)ethylenediamine triacetic acid (HEDTA)	25

PRELIMINARY

Table 4. Estimates of Concentration (PPM) for Major Components in Samples from Meisels by Ion Chromatography

	Sample C	Sample I
Formate	107	960
Glycolate	10	93
Glyoxalate	N.D.	N.D.

PRELIMINARY

FIGURE 1. Total ion chromatogram of the concentrated extract of the BF_3/methanol derivatized tank 101-SY composite sample.

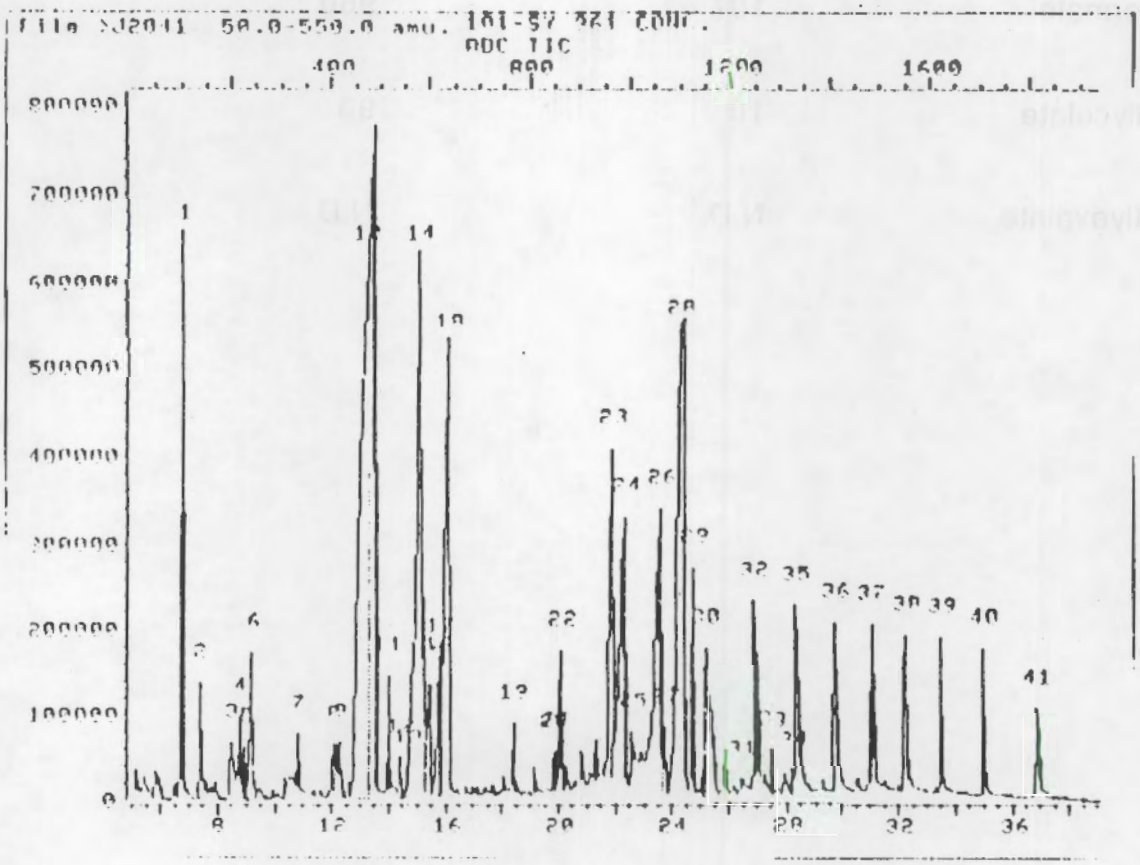

PRELIMINARY

Figure 2. Ion Chromatogram of Sample 1091.

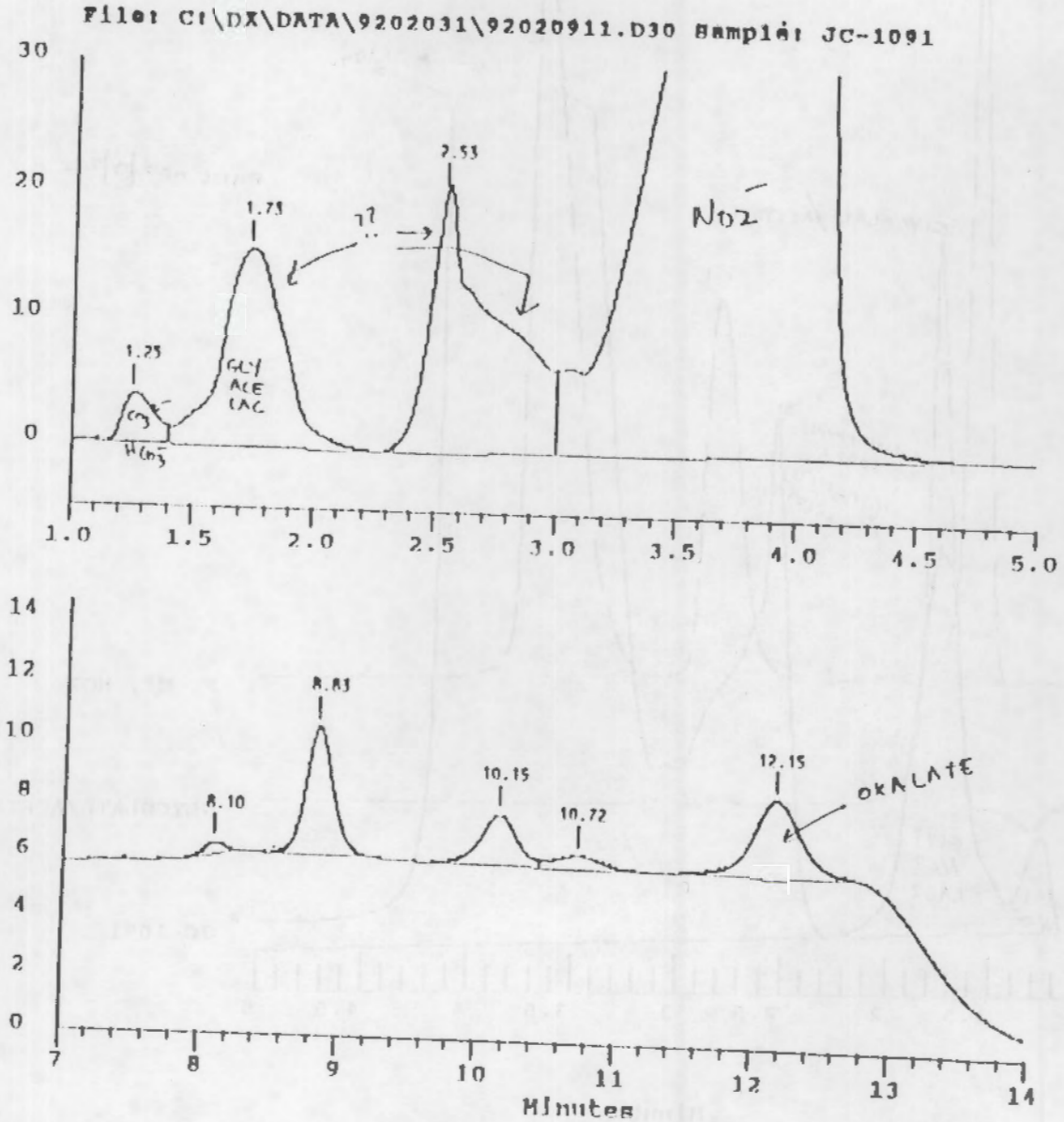

Figure 3. (a) Ion Chromatogram of Sample 1091 and (b) Standards (------)

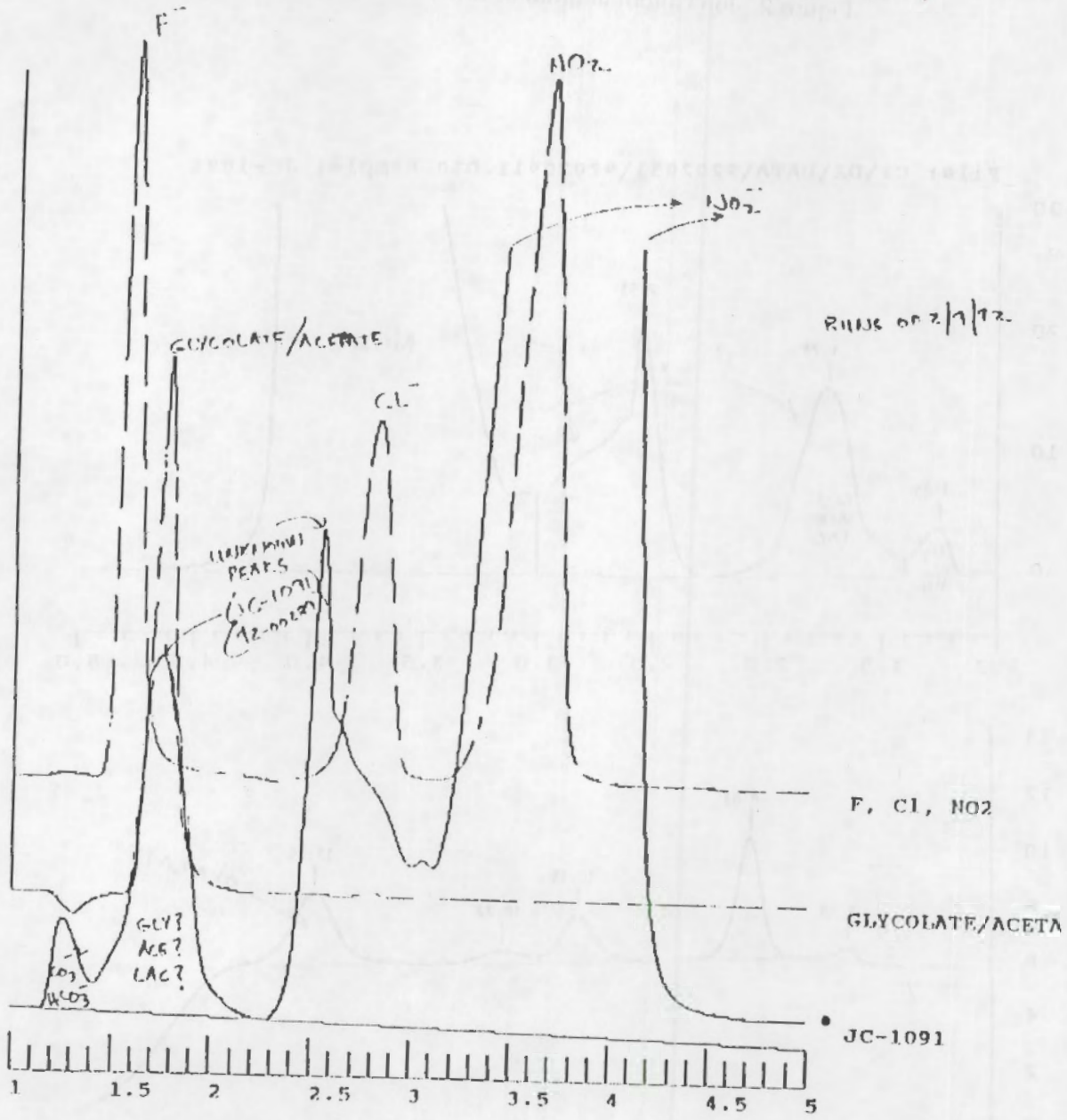

PRELIMINARY

Figure 4. Total Ion Chromatogram of Derivatized NTA, EDTA, and CA.

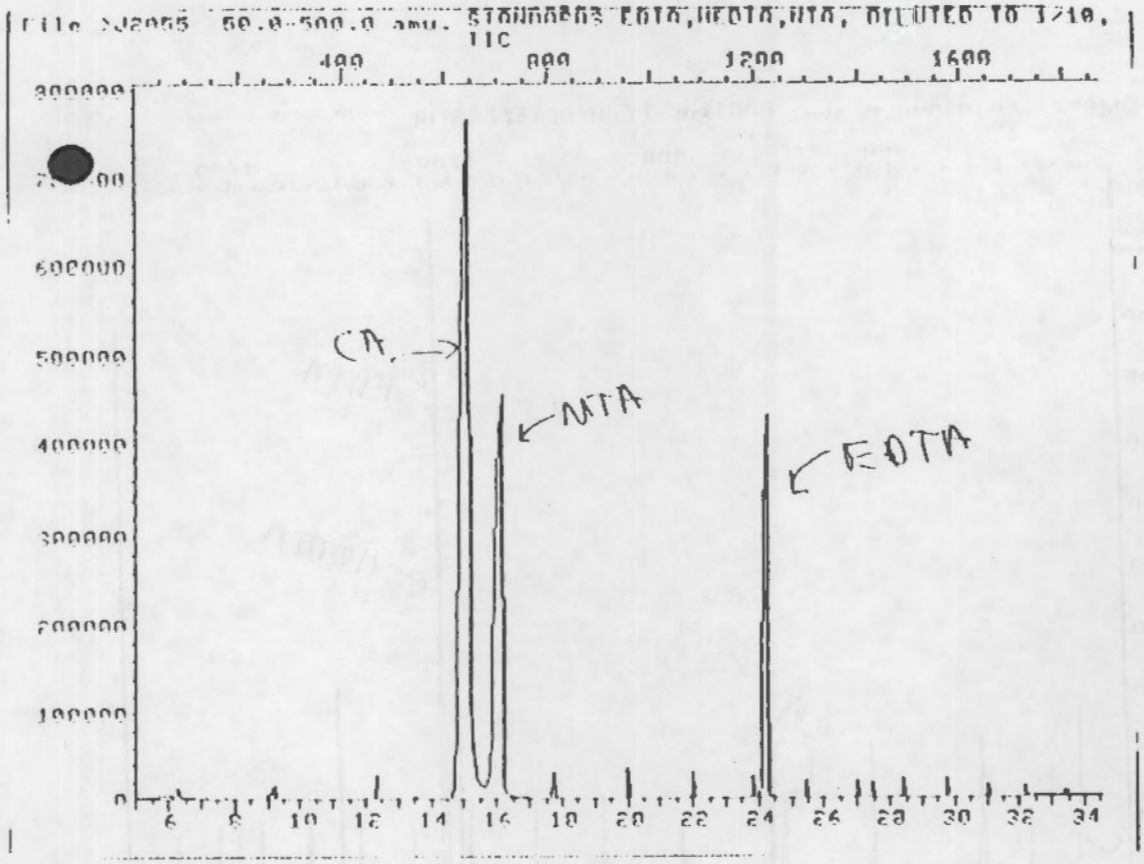

PRELIMINARY

Figure 5. Total Ion Chromatogram of the Derivatized Control Sample from Meisels

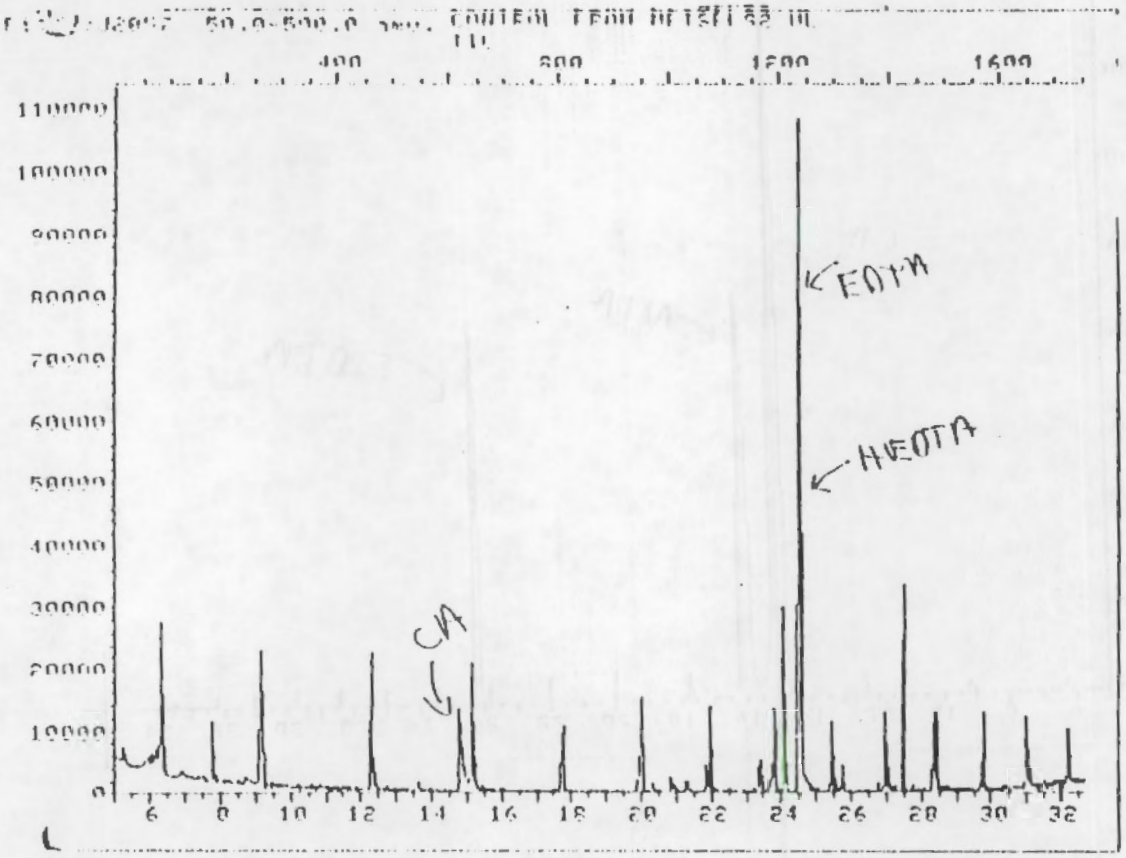

PRELIMINARY

Figure 6. Total Ion Chromatogram of Derivatized, Irradiated Sample from Meisels.

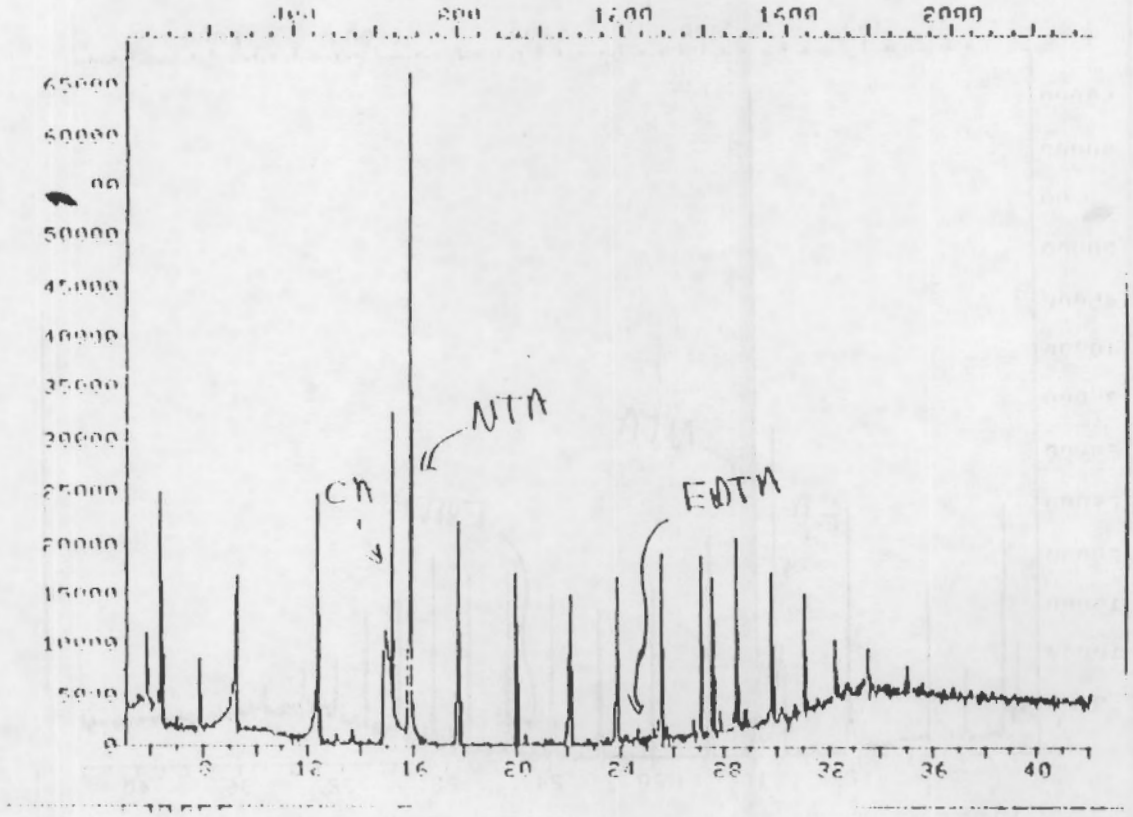

PRELIMINARY

Figure 6. Total Ion Chromatogram of Derivatized, Irradiated Sample from Meisels.

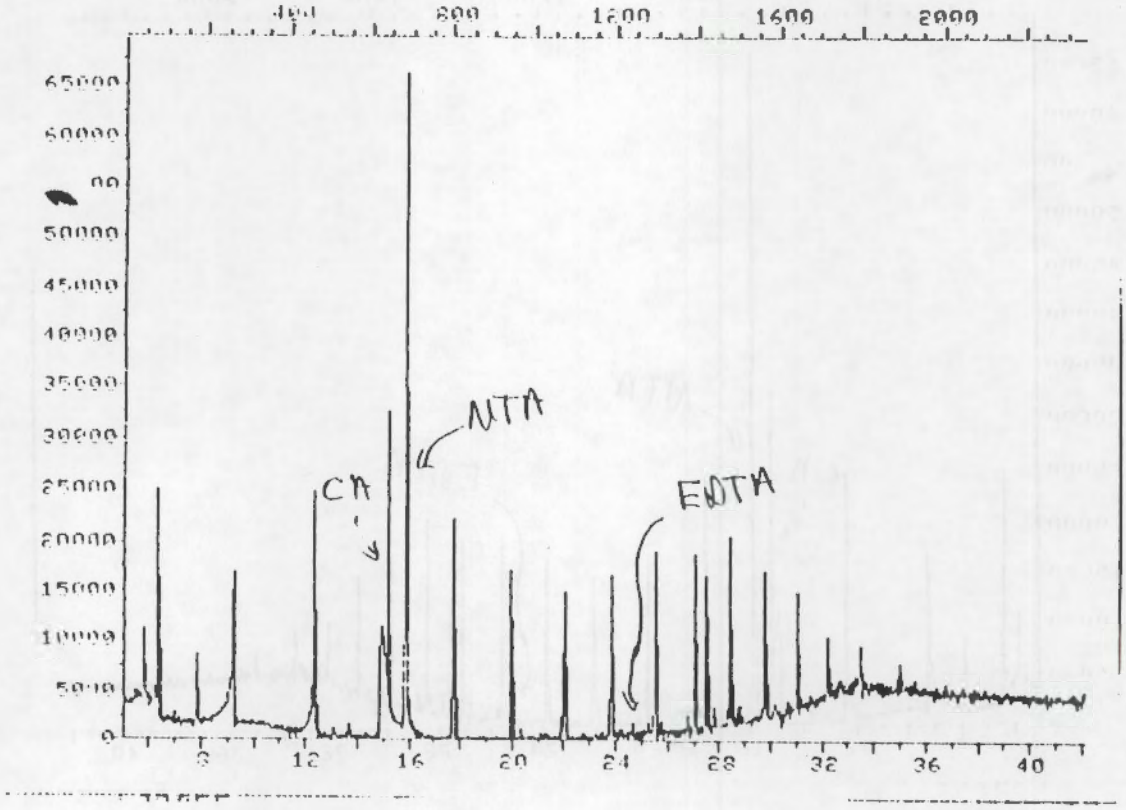

REVIEW OF METHODS DEVELOPMENT

METHODS OF ANALYSIS FOR CHELATORS

- DERIVATIZATION GC/MS
- LC
- LC/MS
- ELECTROSPRAY/MS

DERIVATIZATION GC/MS

- BORON TRIFLUORIDE/METHANOL
- SILYLATION
- DIAZOMETHANE
- BUTANOL/HCL
- CHLOROETHANOL/HCL

DERIVATIZATION METHODS

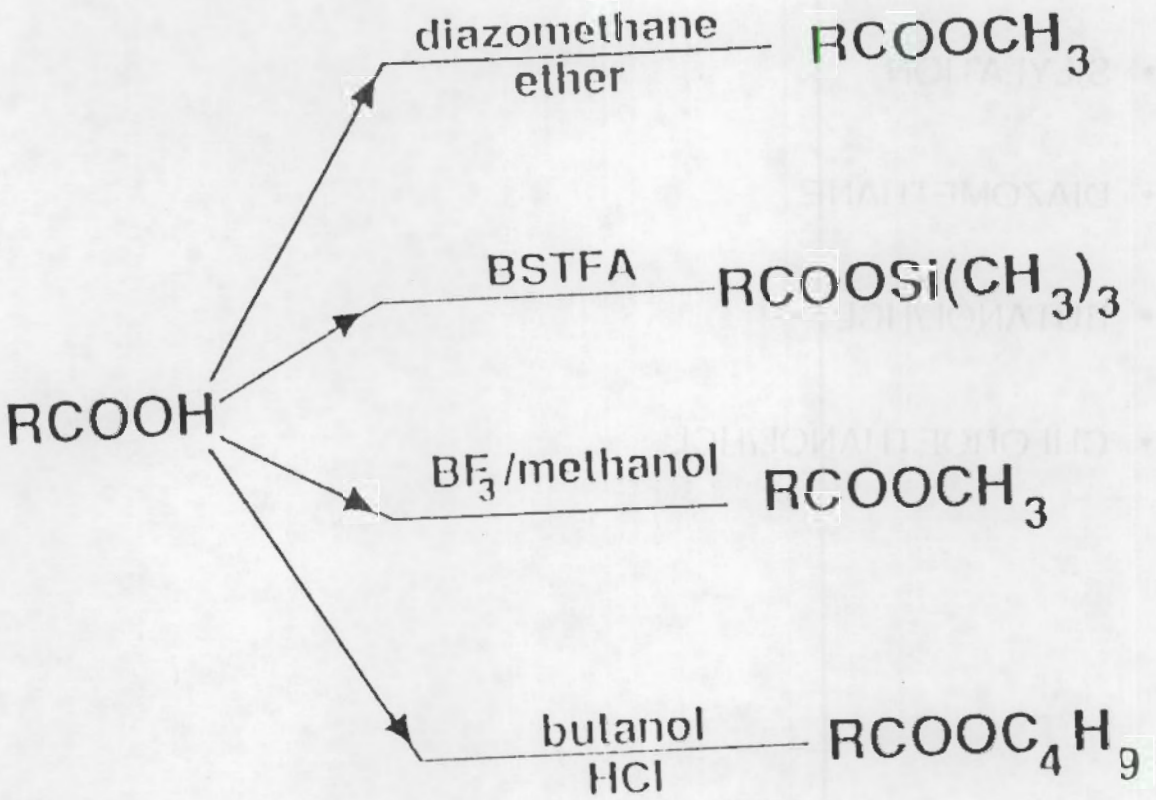

Mass Spectrum of Derivatized HEDTA

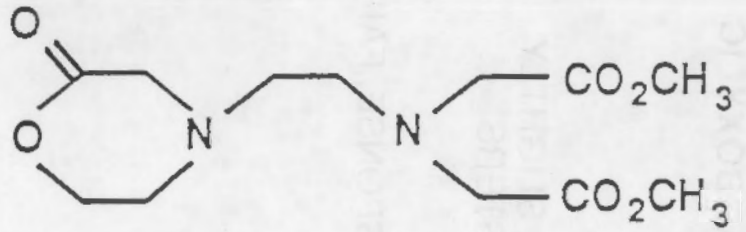

MW=288 (lactone)

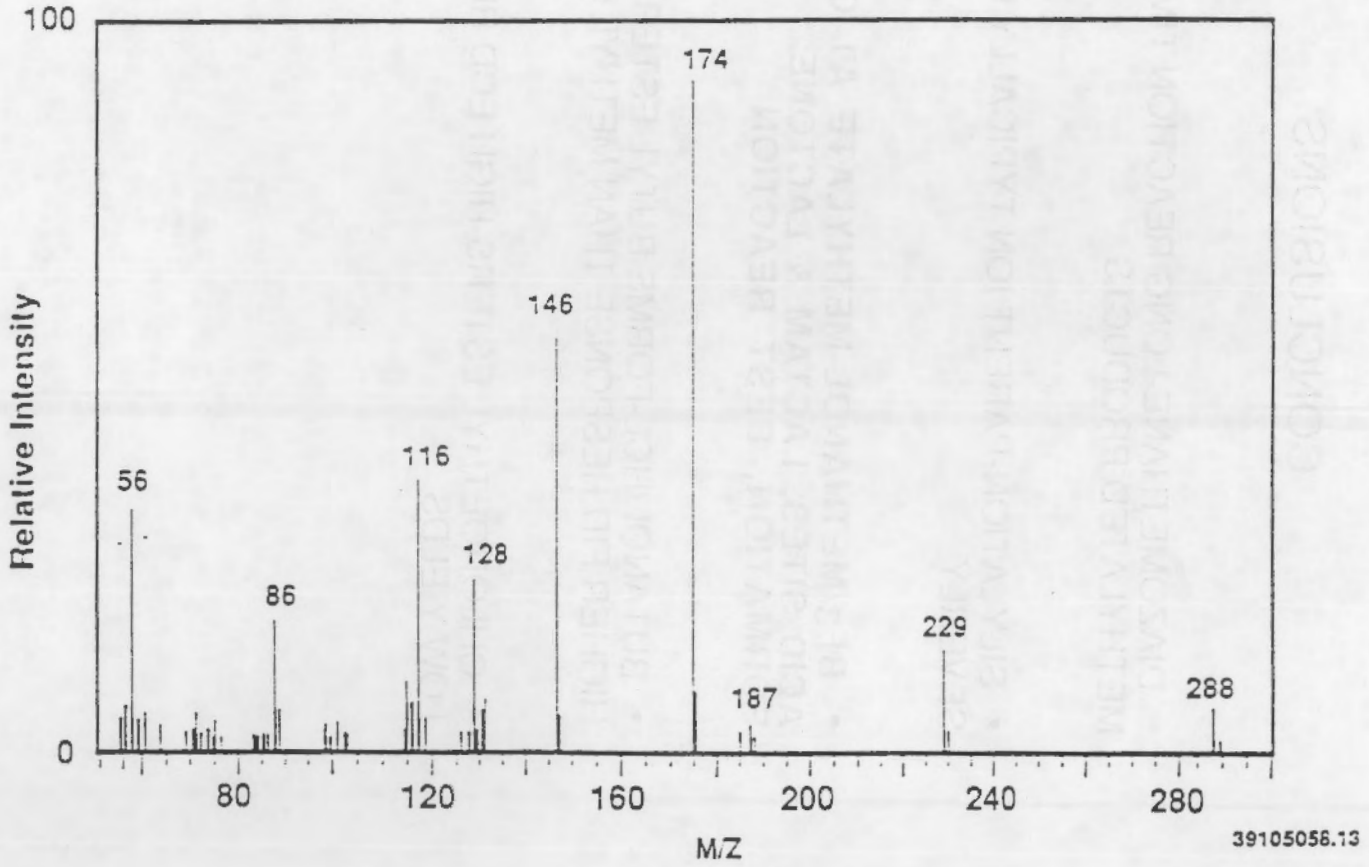

CONCLUSIONS

- DIAZOMETHANE-LONG REACTION TIME, MULTIPLY METHYLATED PRODUCTS

- SILYLATION-PARENT ION TYPICALLY FRAGMENTS SEVERLY

- **BF_3/METHANOL-METHYLATE AT CARBOXYLIC ACID SITES, LACTAM & LACTONE FORMATION, BEST REACTION**

- BUTANOL/HCL-FORMS BUTYL ESTERS, SLIGHTLY HIGHER FID RESPONSE THAN METHYL ESTERS

- CHLOROETHYL ESTERS-HIGH ECD RESPONSE, FAIRLY LOW YIELDS

DISADVANTAGES OF DERIVATIZATION

- MAY REQUIRE ADDITIONAL SAMPLING HANDLING
- MAY GIVE LOW OR VARIABLE RECOVERIES
- OFTEN REQUIRES THE USE OF HAZARDOUS REAGENTS
- DOESN'T ALLOW TO ANALYZE AQEOUS PHASE-ONLY DERIVATIZABLE AND EXTRACTABLE

HPLC

- W.R. GRACE METHOD
- CU OR FE
- OUR METHOD HAS NO CU IN MOBILE PHASE

Sample: [illegible] Channel: Model 4[illegible] Filename: 91-16-5
Acquired: 16 JAN 91 10:01 Method: C:\[illegible] Operator:
Inj Vol: 20.00
Comments: Grace mobile phase; 2[illegible] nm

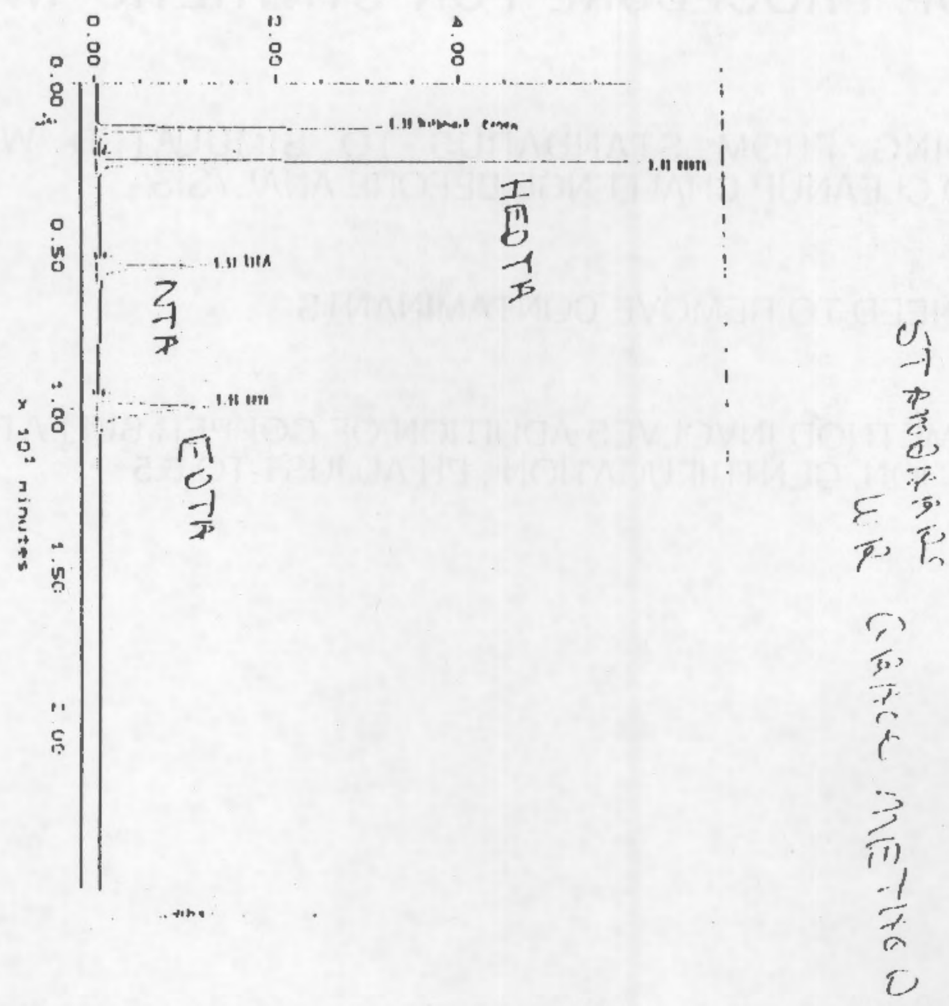

WATERS [illegible] Division of Millipore

MAXIMA 820 PEAK INTEGRATION REPORT

Printed: 16-JAN-1991 15:00:19

SAMPLE: [illegible]

LC Sy Method: Grace method
Acquired: 16 JAN 1991 10:01
Rate: 2.0 points/sec
Duration: 25.330 minutes
Operator:

Type: UNKN
Instrument: Waters HPLC
Filename: 91-16-5
Inj#: 1
Injection Volume: 20.0

DETECTOR: [illegible]

PK#	ID#	Peak Start (minutes)	Peak End (minutes)	Retention (minutes)	Type	Peak Area (microvolt-secs)	Peak Height (microvolts)	Area Percent	Hght Percent	Component Name
1		0.033	2.517	1.192	BV	3041792.8	391301.16	13.91	20.10	[illegible] contr.
2	1	2.161	5.267	3.030	VV	9001361.1	590119.43	38.19	51.38	HEDTA
3		5.307	8.529	5.511	VV	1632695.2	134391.32	11.91	8.51	NTA
4	2	8.535	21.113	9.900	VB	1591507.5	196627.18	38.30	9.74	EDTA
TOTAL						15160190	1000011.3			

CLEANUP PROCEDURE FOR SYNTHETIC WASTE

- GOING FROM STANDARDS TO SIMULATED WASTES PRODUCED CLEANUP CHALLENGE BEFORE ANALYSIS

- NEED TO REMOVE CONTAMINANTS

- METHOD INVOLVES ADDITION OF COPPER SULFATE, ACID PRECIPITATION, CENTRIFUGATION , PH ADJUST TO 6.5

LC/MS

- MOBILE PHASES COMPATIBLE WITH LC NOT FOR MS
- REVERSE PHASE C2 LICHROSORB COLUMN
- PARTICLE-BEAM VS. THERMOSPRAY INTERFACES
- RESULTS PROVIDE EXTENSION TO LC/MS-ICP/MS

Separation of Cu(EDTA) and Cu(HEDTA)

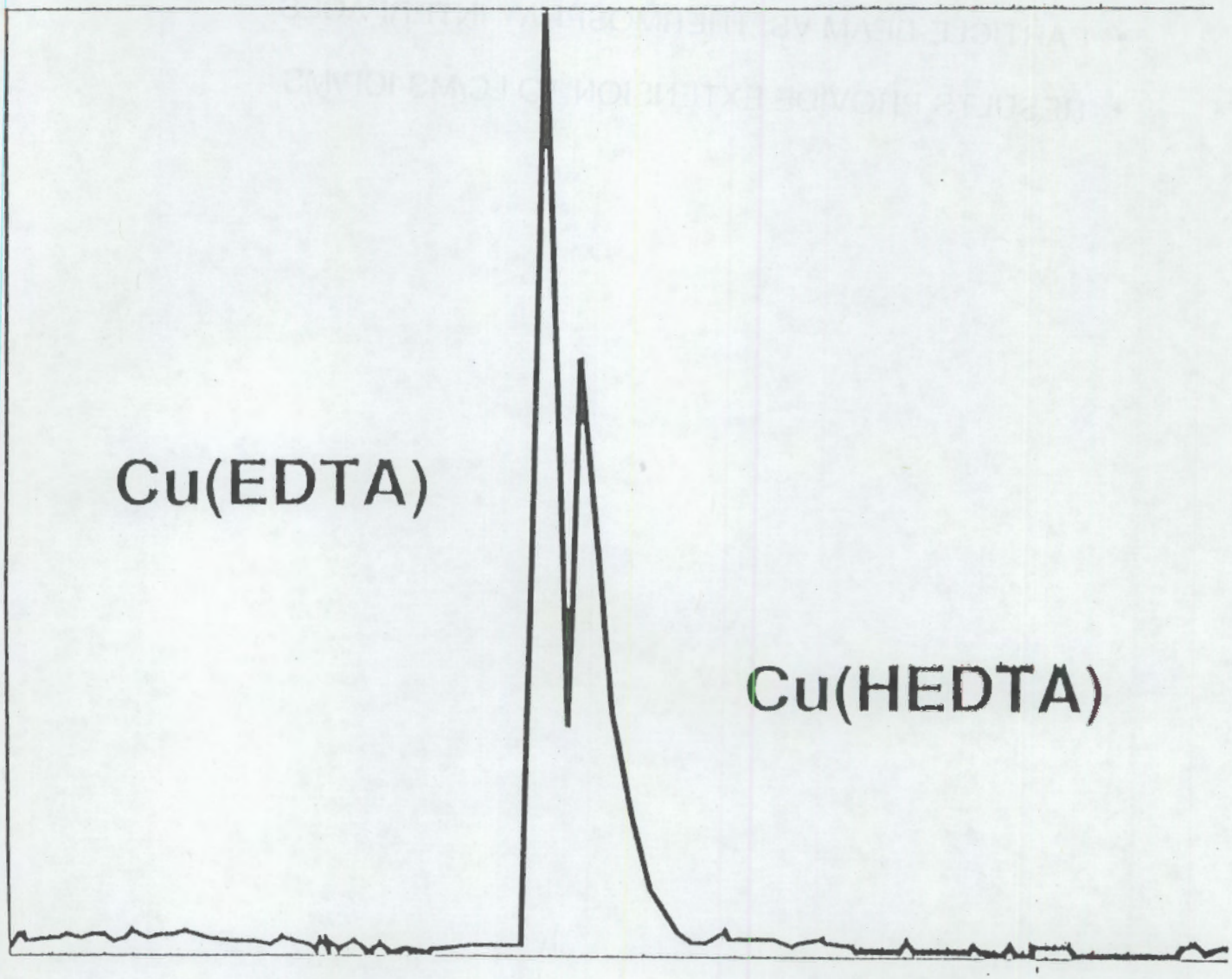

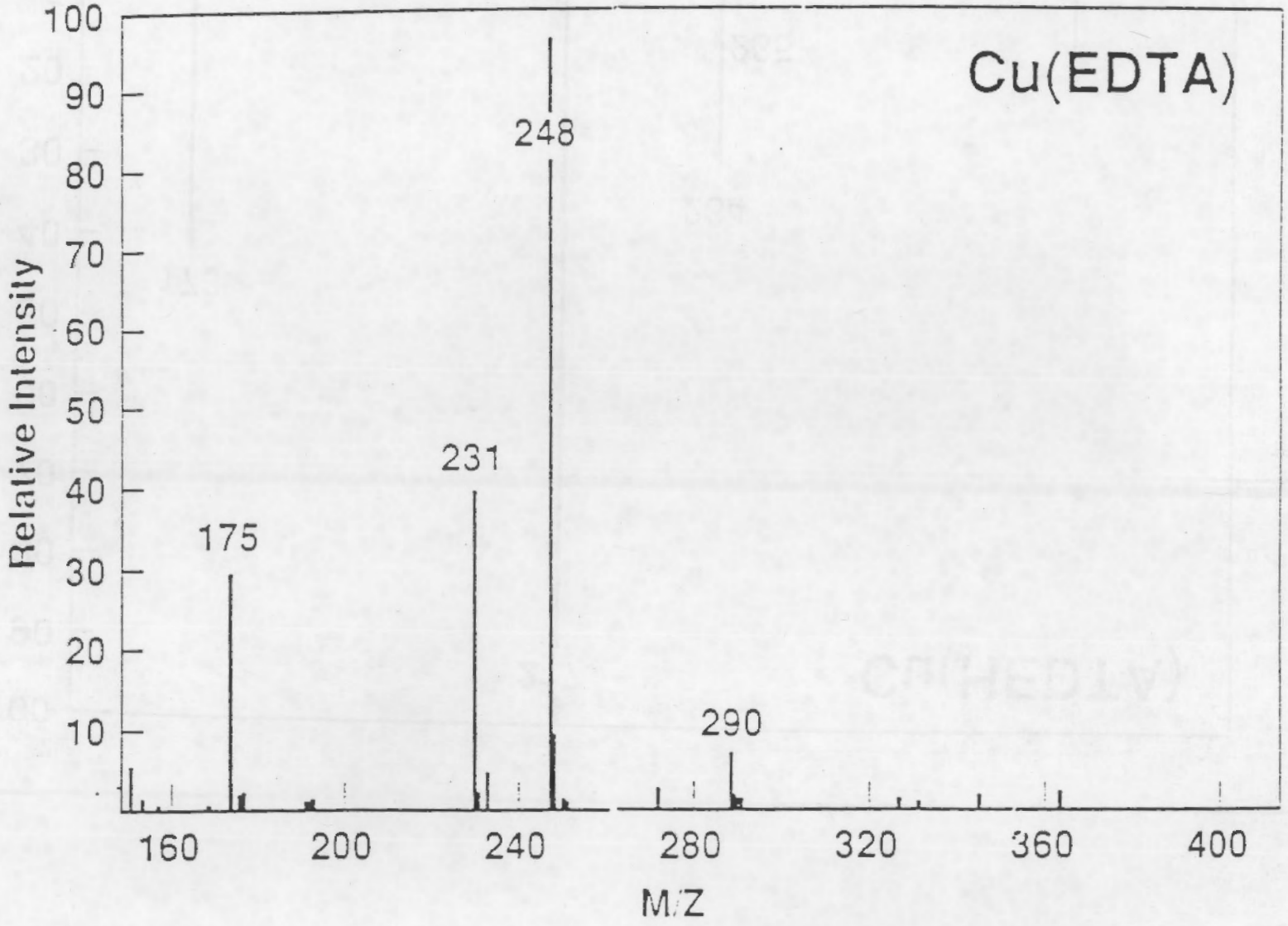
Cu(EDTA)
Relative Intensity
100
90
80
70
60
50
40
30
20
10
248
231
175
290
160
200
240
280
320
360
400
M/Z

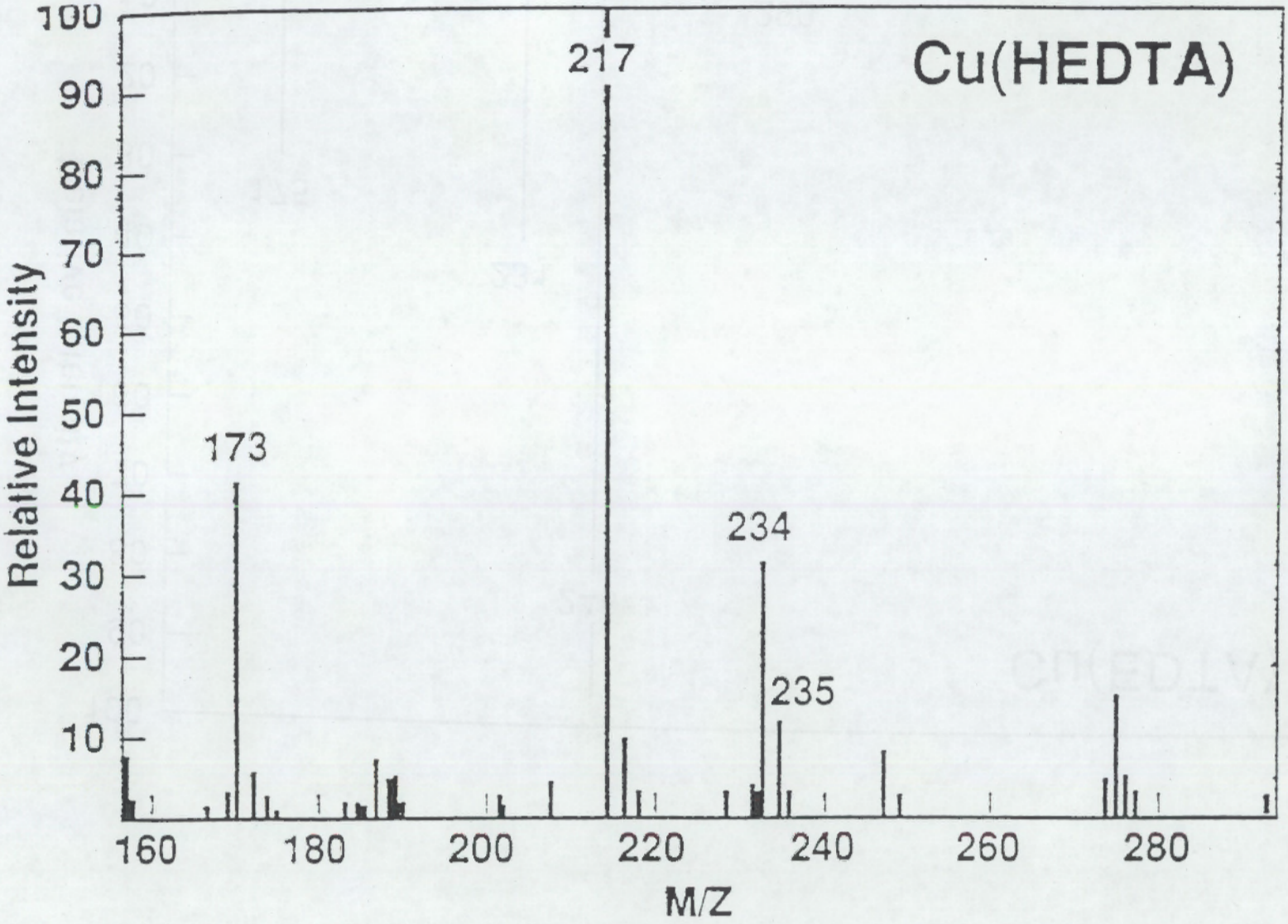
Cu(HEDTA)
217
173
234
235
Relative Intensity
100
90
80
70
60
50
40
30
20
10
160
180
200
220
240
260
280
M/Z

K60

THERMOSPRAY LC/MS OF ED3A

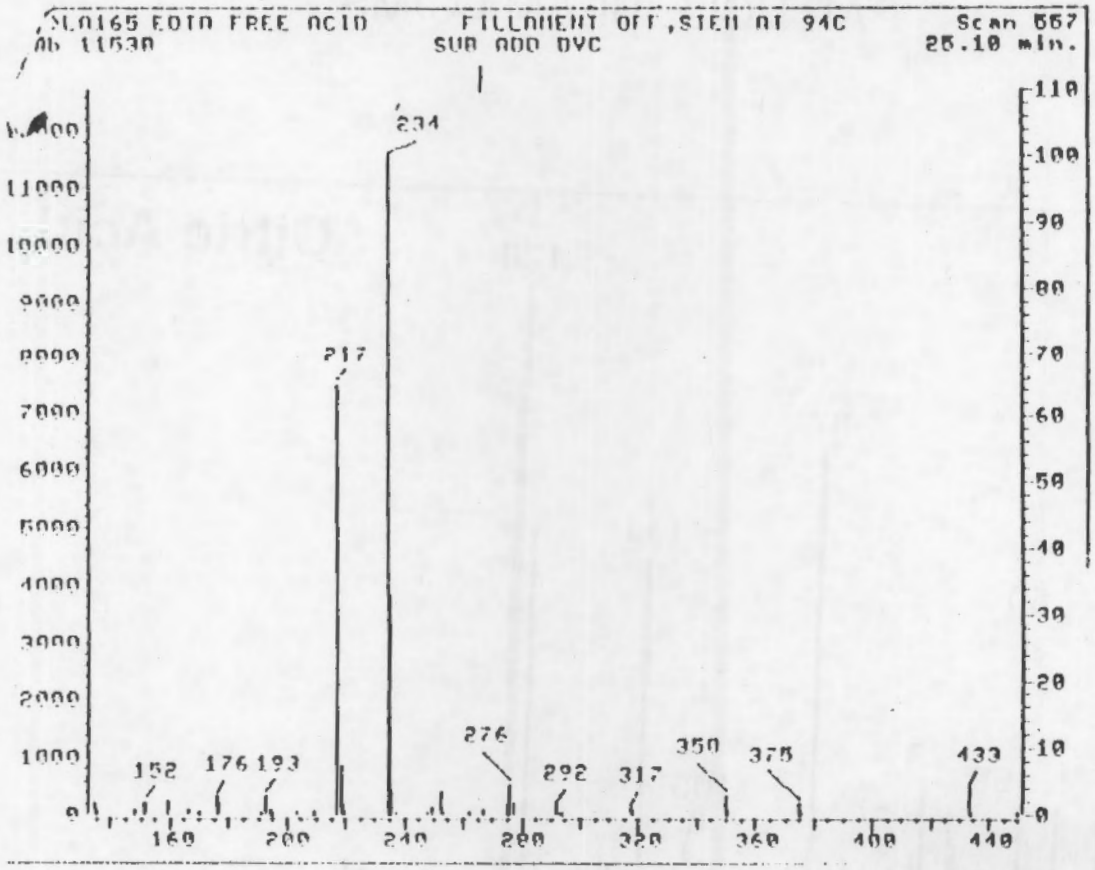

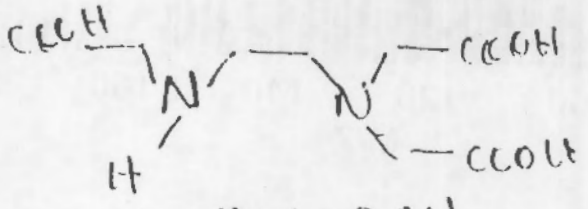

MW = 234

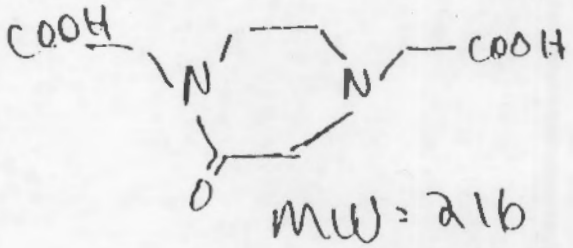

MW = 216

PARTICLE-BEAM LC/MS

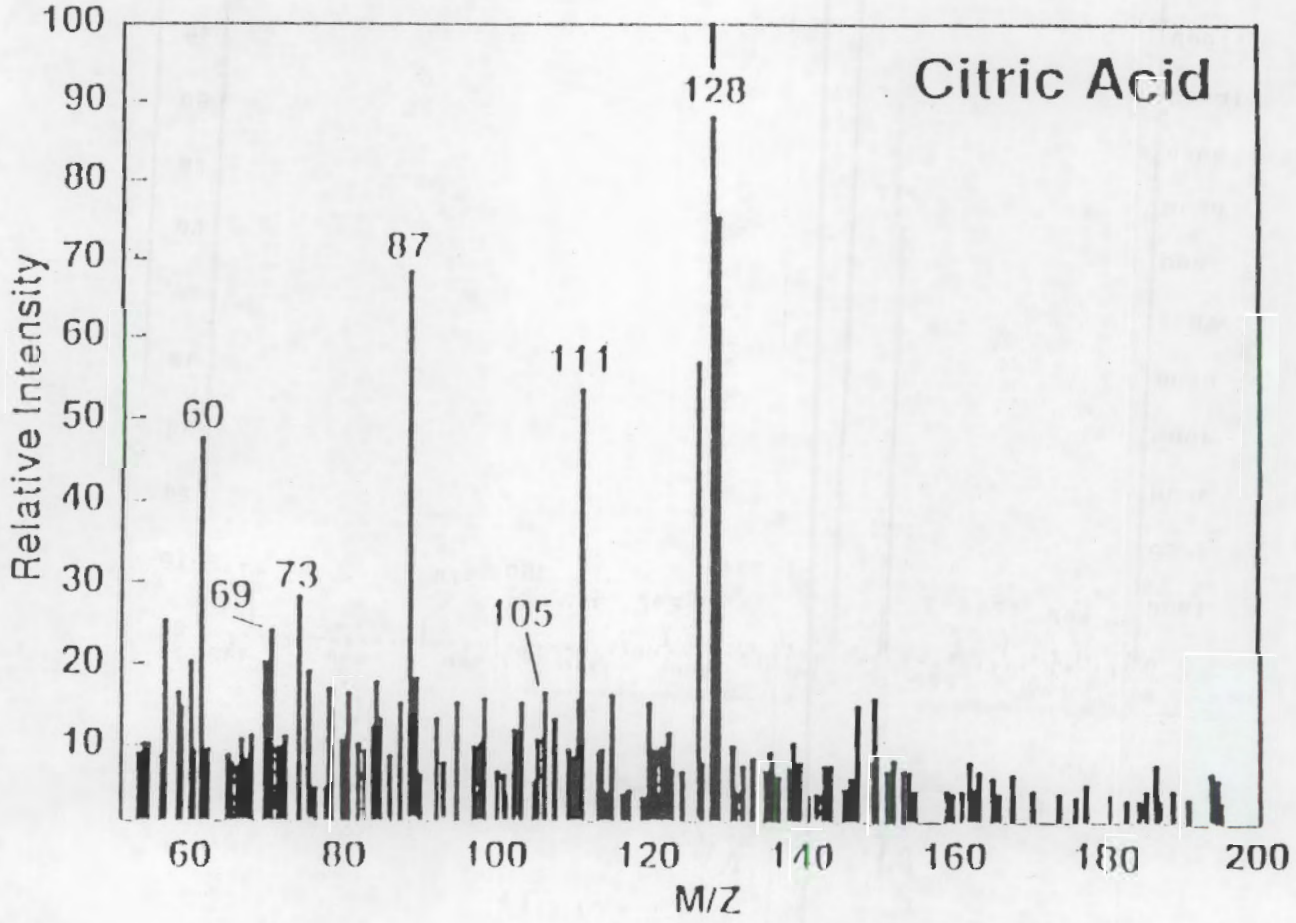

CONCLUSIONS

- Particle-Beam LC/MS Provides Extensive Fragmentation-Difficult to Unambiguously Identify
- Mass Spectra Obtained from Free Acids Different than Complexed
- Thermospray LC/MS Can be Used for Identification of Chelators and Chelator Fragments
- LC/MS Coupled to ICP/MS will Allow Organic and Metal to be Identified Simultaneously

GC ANALYSIS OF ORGANICS IN TANK 107-AN

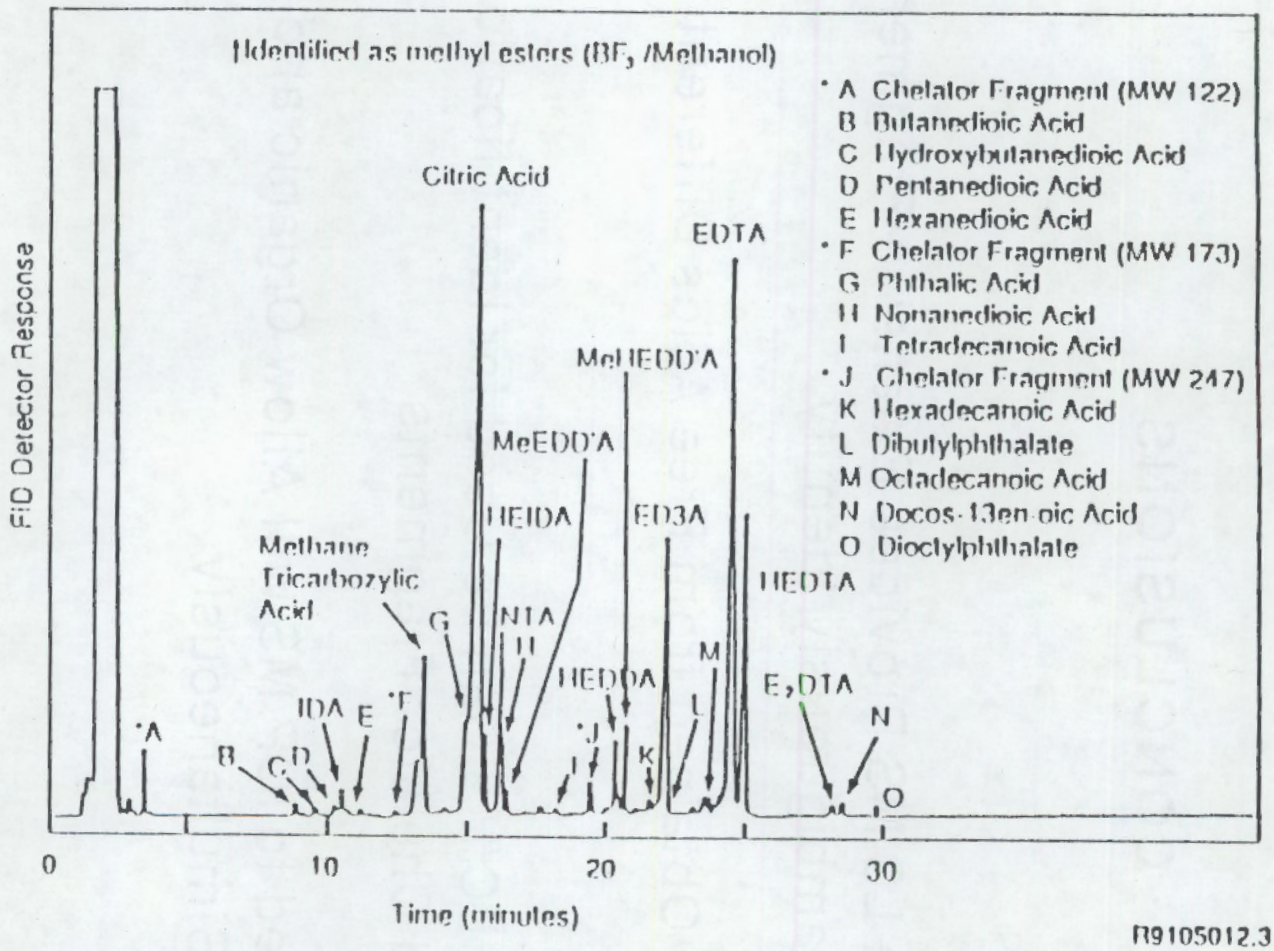

Figure 3.2. GC Analysis of Hydrophilic Organics[1] in Organic Complexant Waste from Tank 107AN

APPENDIX

Mass Spectrum of Peak #2

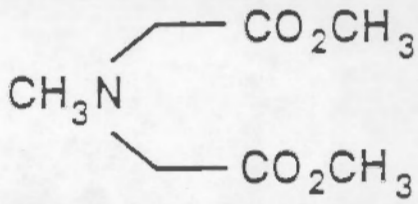

MW=175

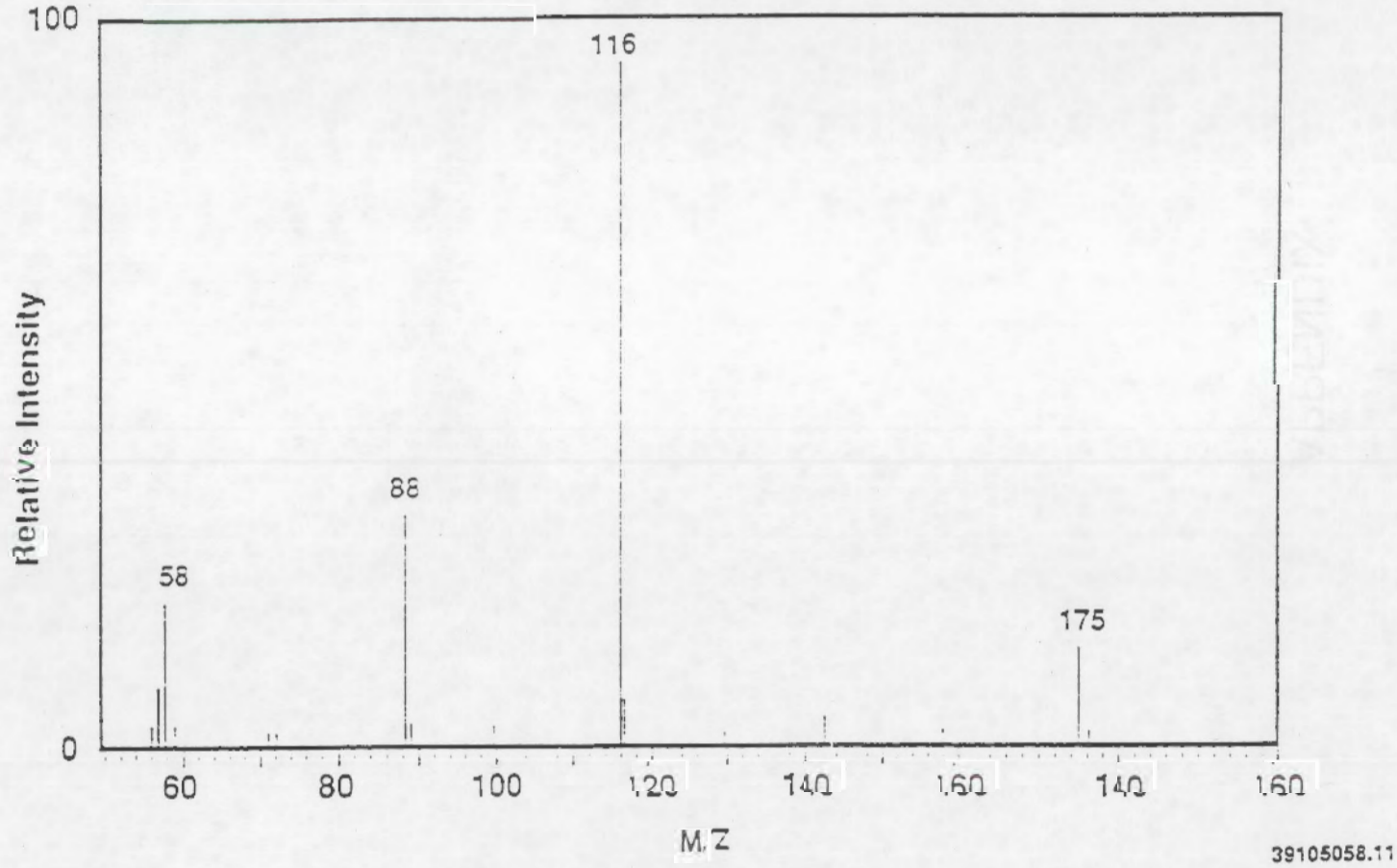

Mass Spectrum of Derivatized HEDTA

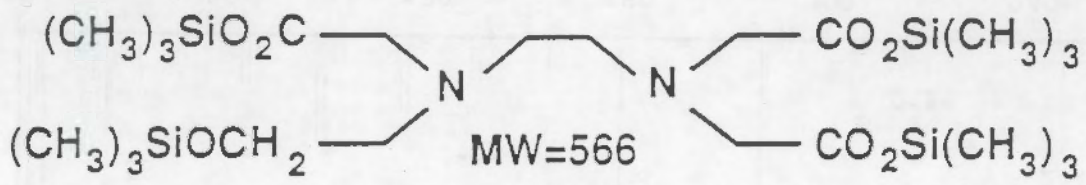

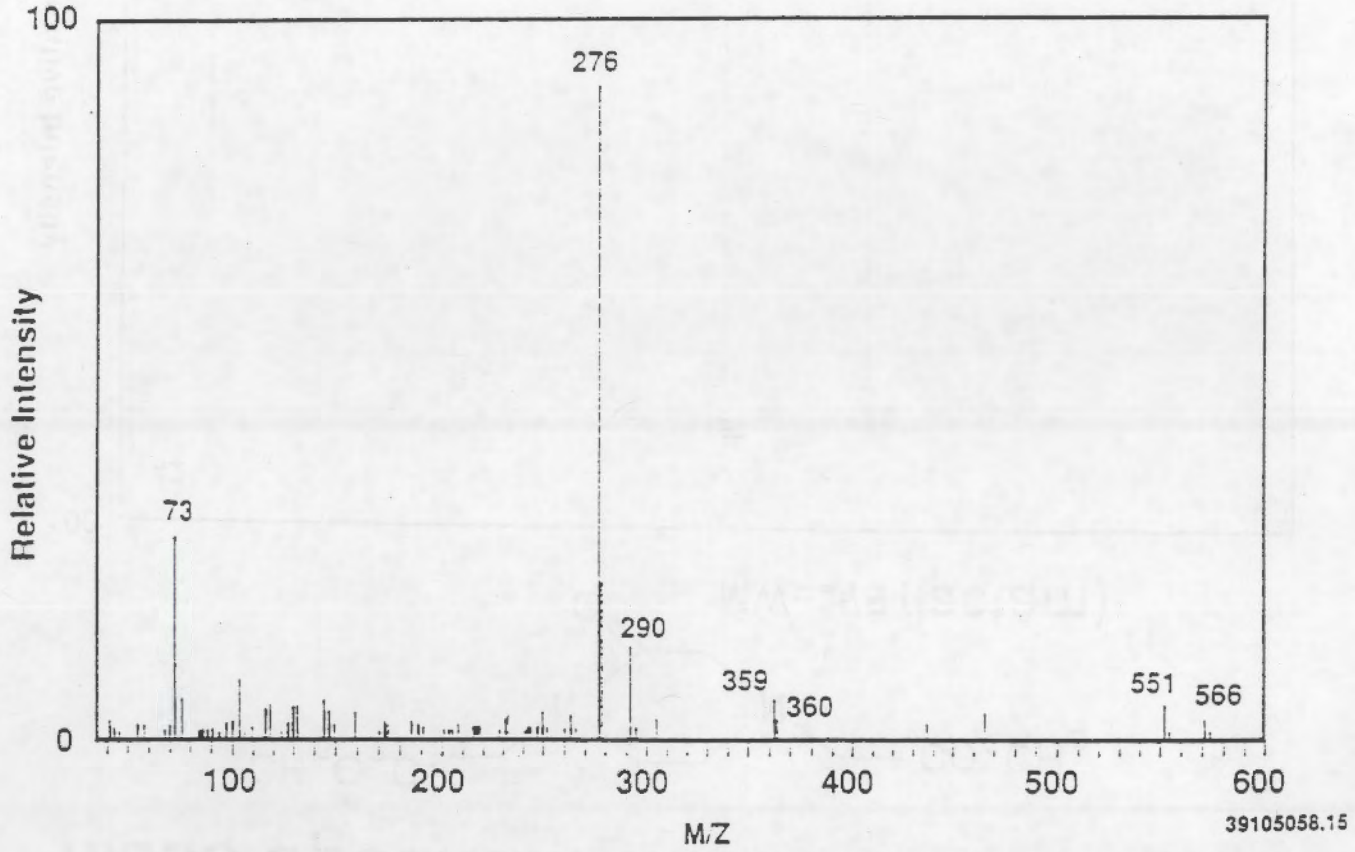

REACTION WITH BF_3/METHANOL

Mass Spectrum of Derivatized ED3A

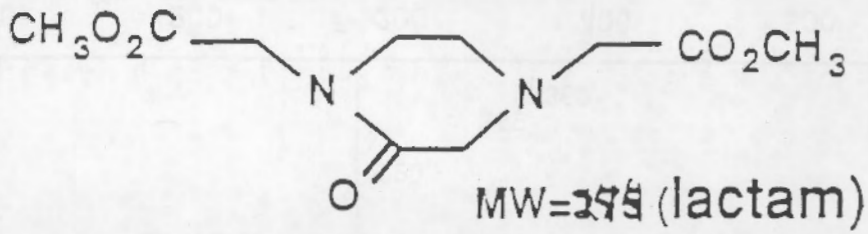

MW=275 (lactam)

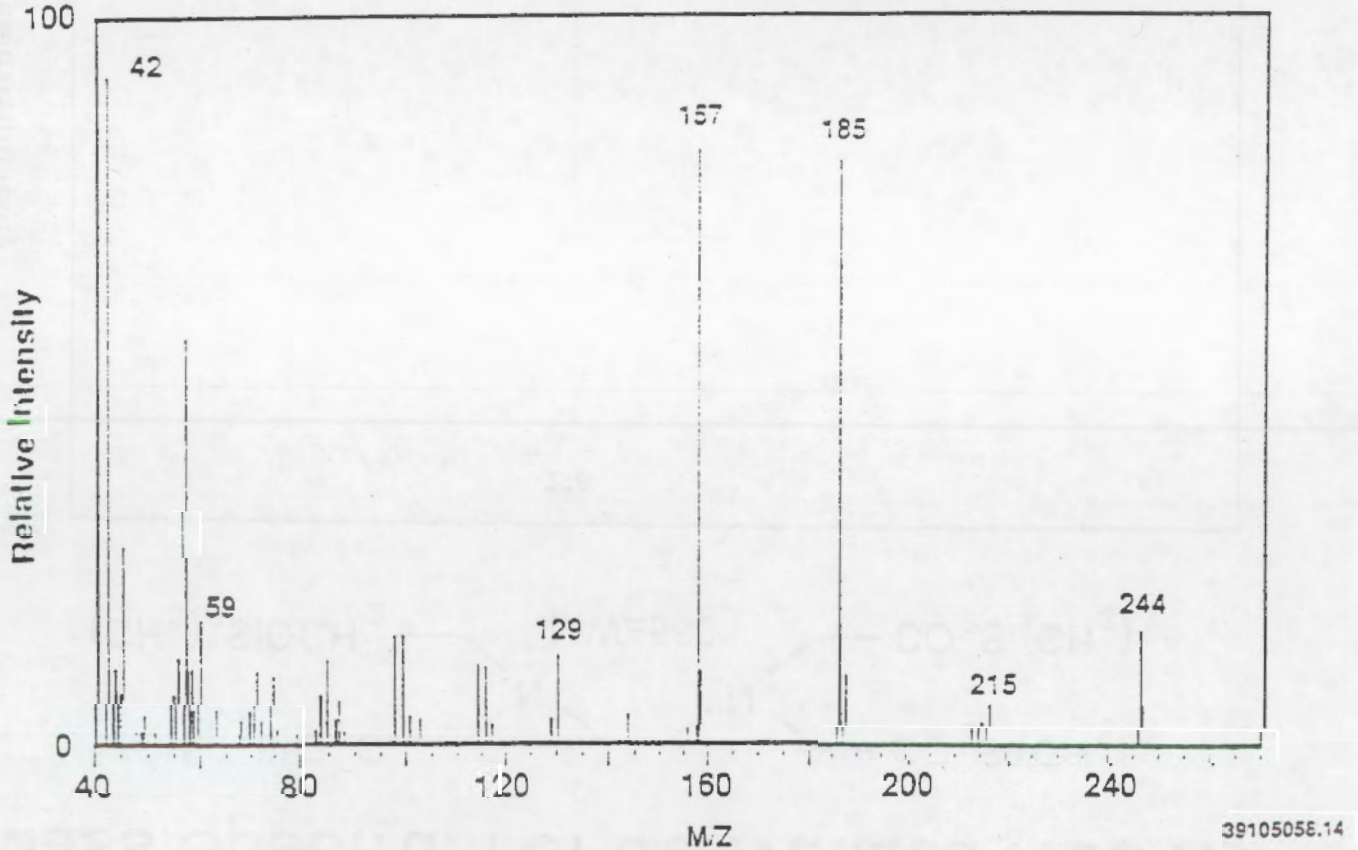

K.68

REACTION WITH BUTANOL/HCL

Mass Spectrum of Derivatized EDTA

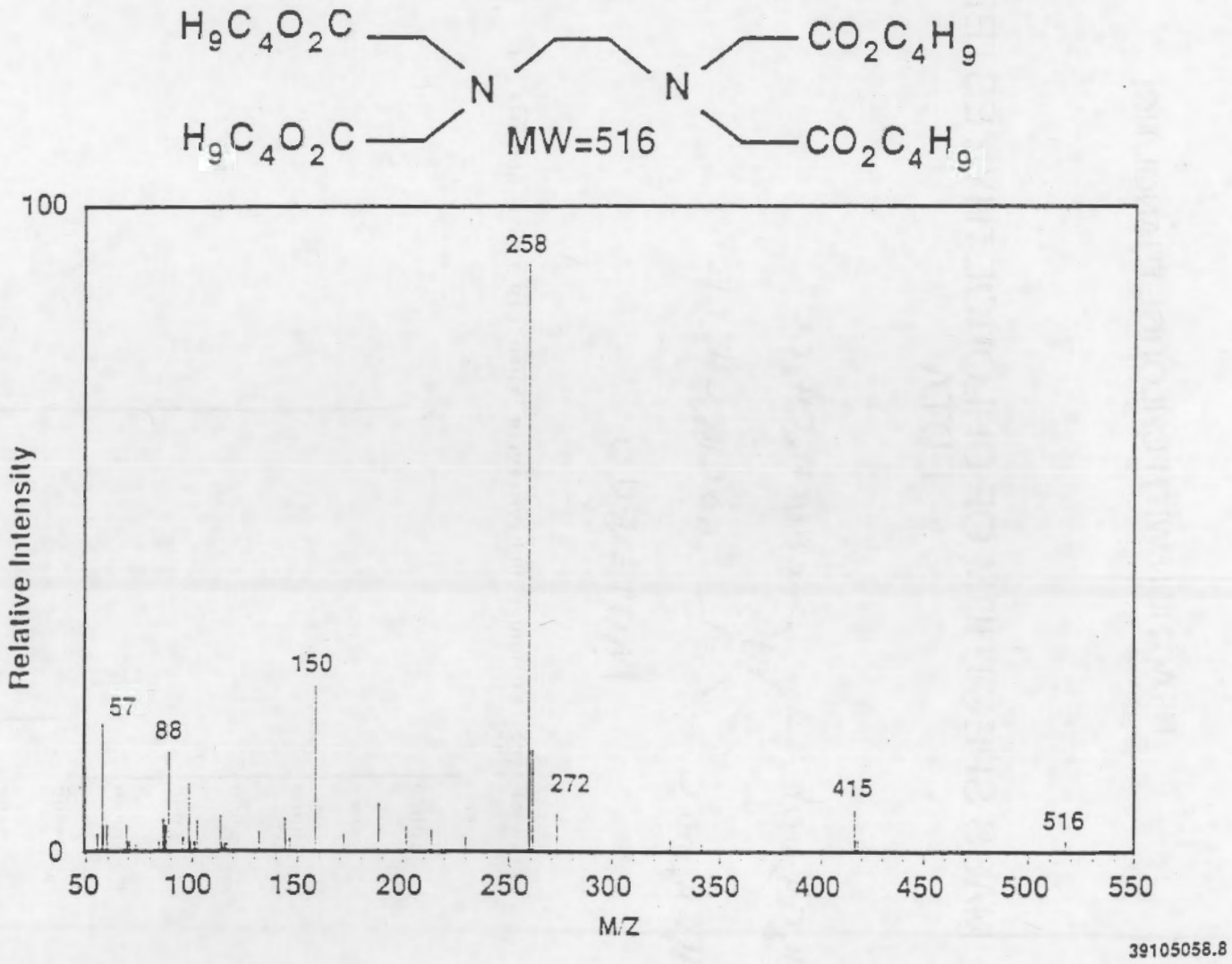

REACTION WITH CHLOROETHANOL/HCL

MASS SPECTRUM OF CHLOROETHYL ESTER OF EDTA

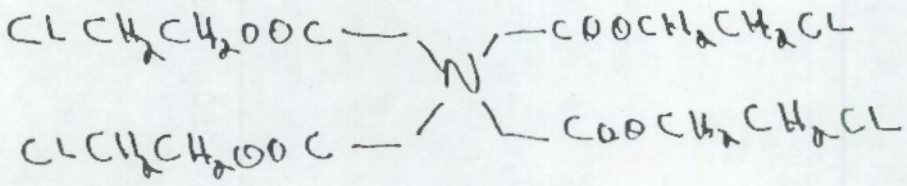

MW = 540

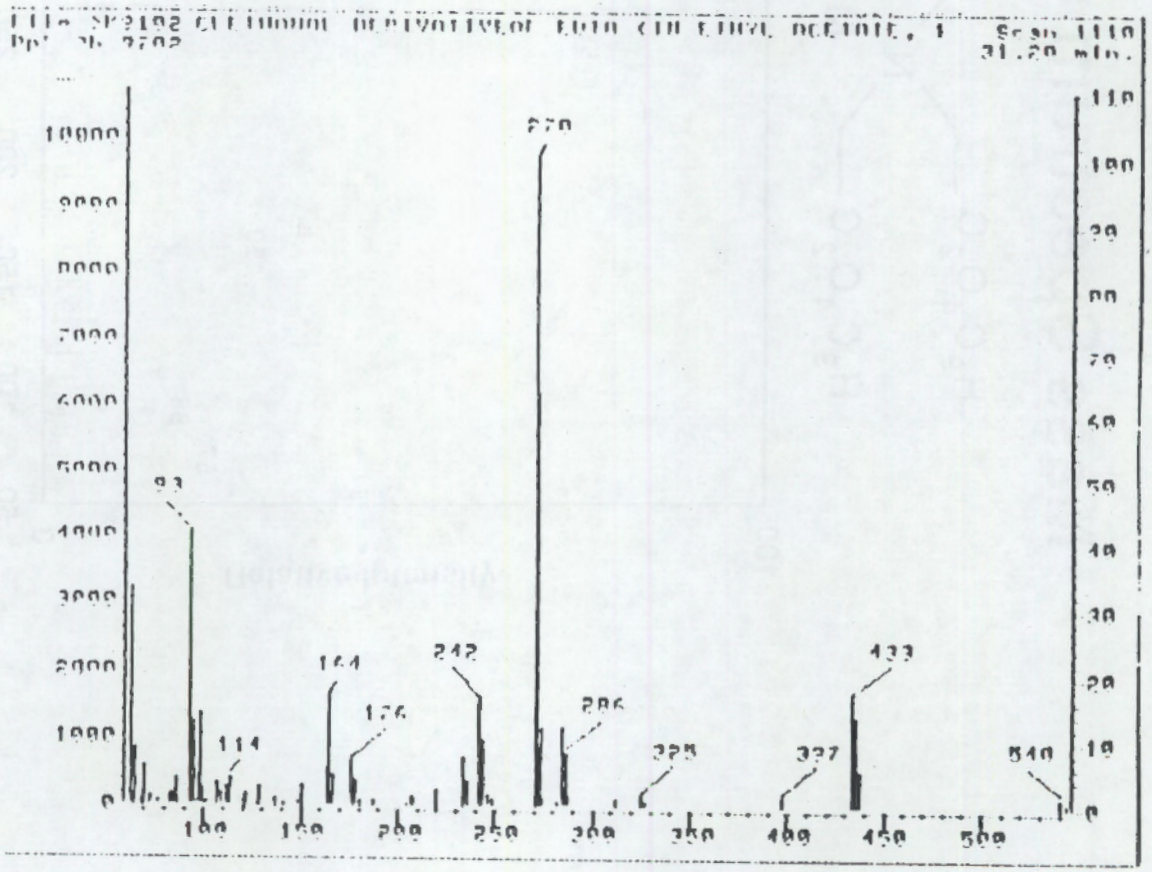

THERMOSPRAY LC/MS OF CITRIC ACID

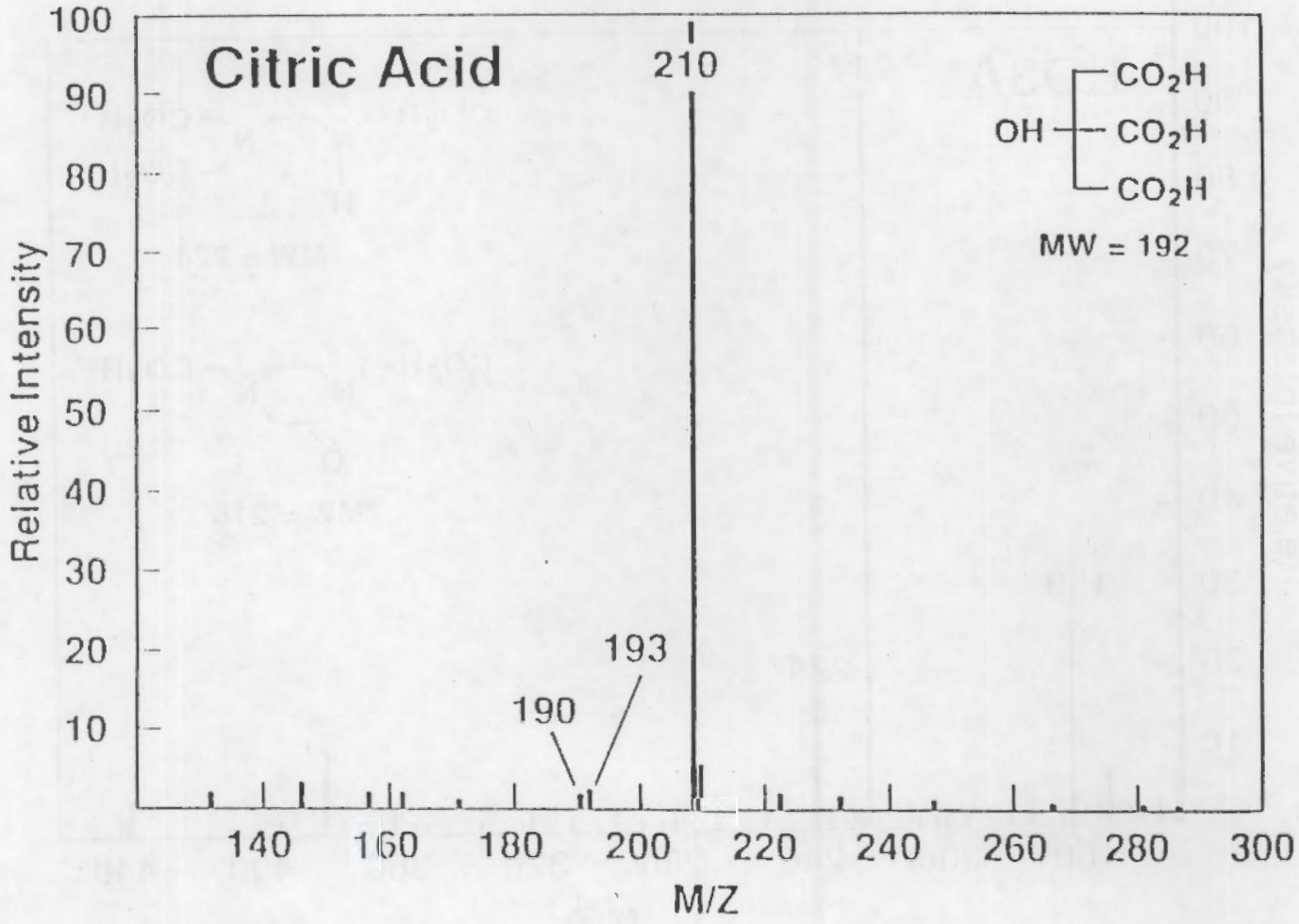

THERMOSPRAY LC/MS OF ED3A

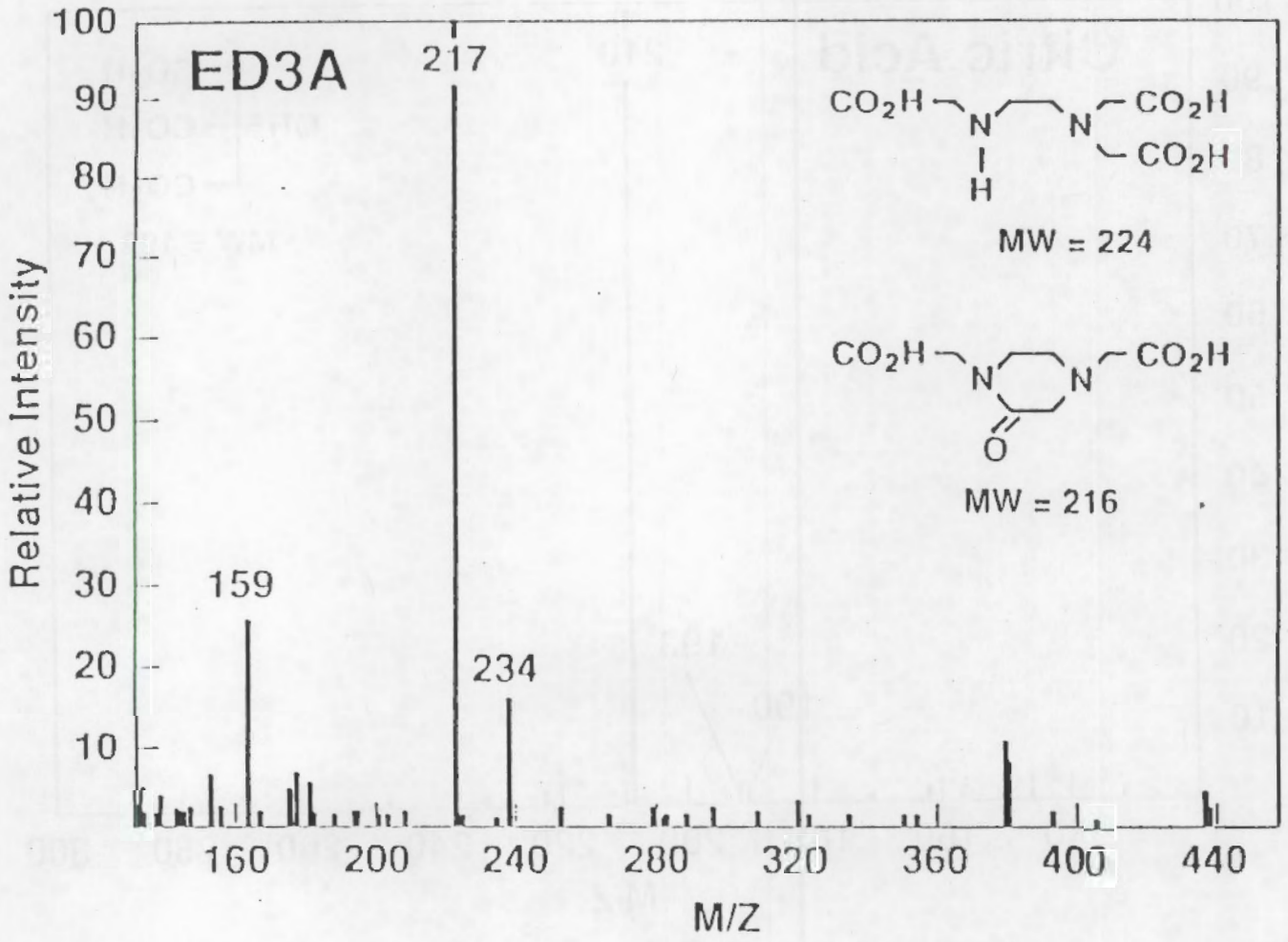

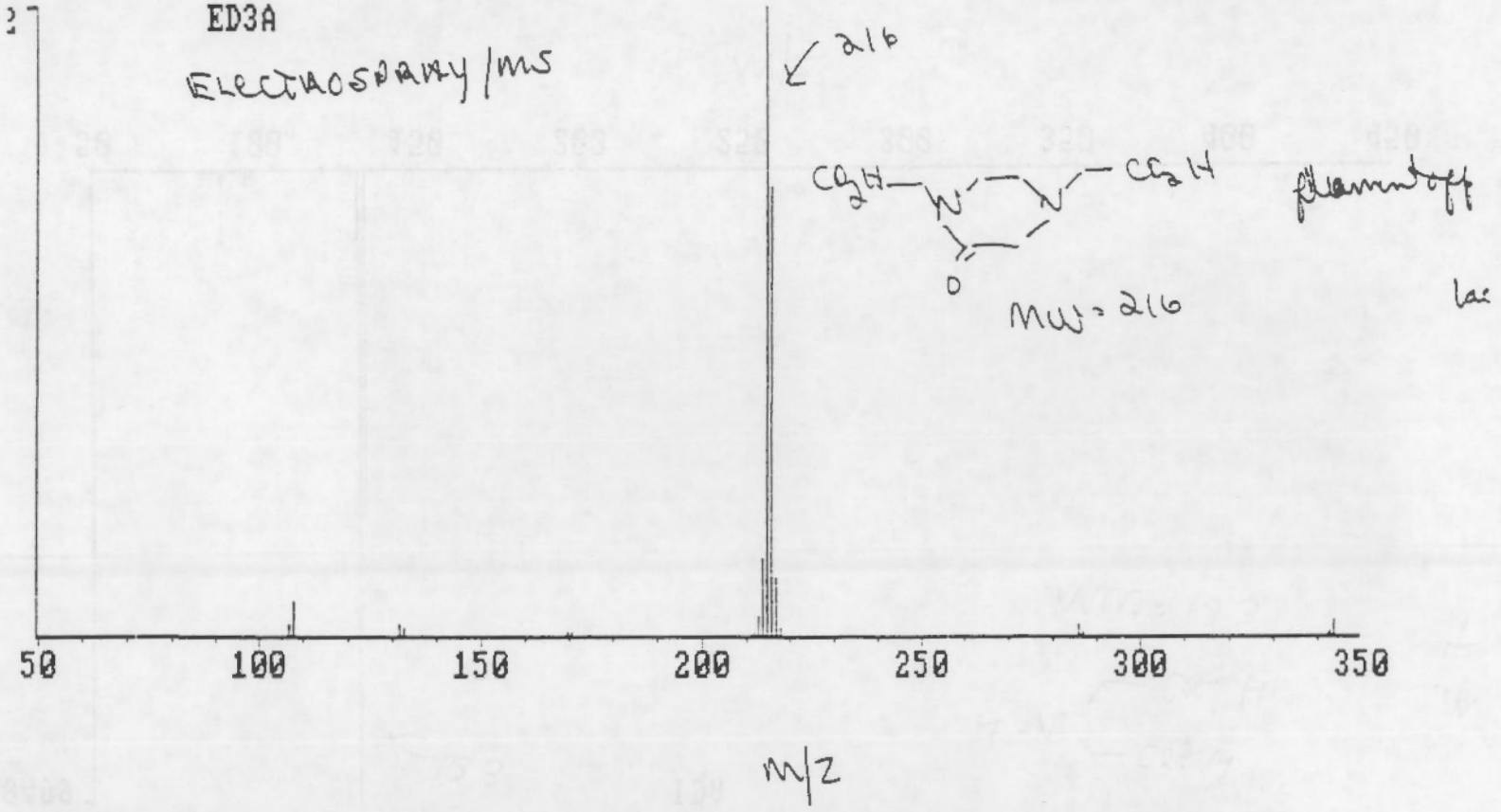

K.73

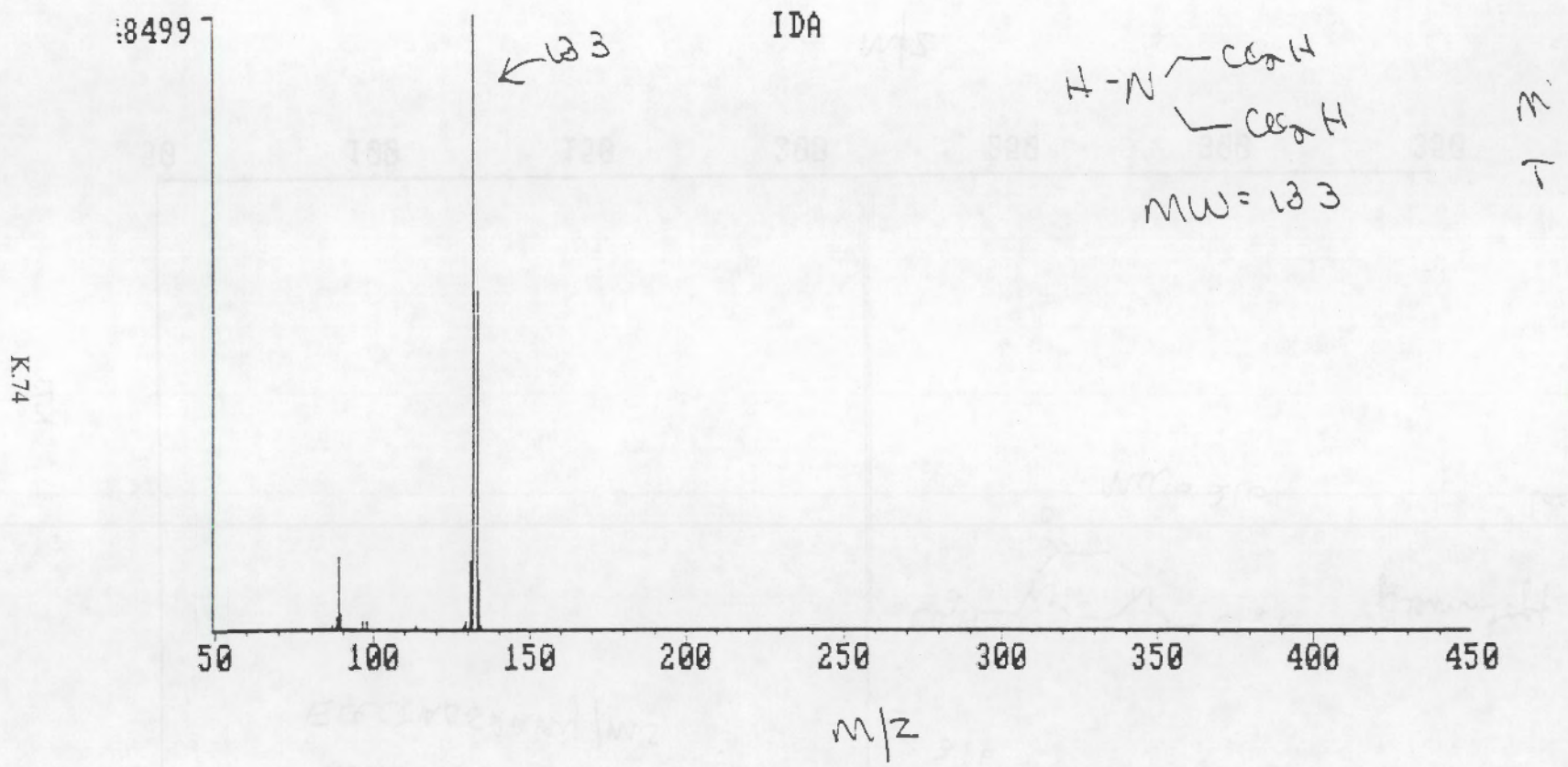
:8499
133
IDA
50
100
150
200
250
300
350
400
450
m/z
K74

H-N
CO2H
CO2H
MW = 133

STATUS OF METHOD DEVELOPMENT

- GC/MS ALMOST READY TO TRANSFER
- LC METHOD READY
- LC/MS
- μL column LC + CZE

Appendix L

Tank 101-SY Mitigation Project Experimental Plan

TANK 101-SY MITIGATION PROJECT

EXPERIMENTAL PLAN

Presented to
External Advisory Committee

BM (Ben) Johnson
March 20, 1992

MITIGATION RATIONALE

- Resulted from a study documented in WHC-EP-0516
- Both Chemical and Physical Approaches Studied -
  Physical Approaches emphasized because of uncertainty of mechanism of hydrogen generation
- 10 Methods Studied - 4 selected for further study

OUTLINE

RATIONALE

TEST APPROACH

- ♦ Jet Mixing Probe
- ♦ Enclosed (Shrouded) Probe
  - · Ultrasonic
  - · Heating
  - · Dilution

MITIGATION RATIONALE
(Continued)

Ultrasonic - Vibrate gas bubbles to cause coalescence to sufficient size to escape nonconvecting layer. Was leading contender until attenuation data was obtained.

Mixing - Jet mixing selected as best method to stir nonconvecting layer to release gas. Optimum configuration and jet power required are the uncertainties.

Heating - Synthetic waste show a marked change in nature of crystal structure in non-convecting layer on heating to ~60C - Interlocking nature of crystal disappear - May result in release of trapped gas

Dilution - 20-25% may similarly change crystal structure and cause gas release - Dilution limited by available tank space.

TEST RATIONALE

Enclosed Chamber Test Probe

Evaluate each approach in-tank because of difficulty of obtaining either

- A reliable synthetic waste or
- A reliable representative sample (unrepresentative degassing, temperature history, possible dewatering)

Use Enclosed Chamber to reduce safety concerns from committing total tank to an uncertain state, e.g. uncertainties such as

- Effect of heating on the rate of gas generation
- Temperature required
- Effectiveness of Dilution - may be marginally, resulting in greater waste volume with little benefit.

Separate probe for Jet Mixing - could not be effectively evaluated in Enclosed Chamber Probe.

TEST APPROACH - JET MIXING

Objective - Obtain information on the optimum jet configuration and minimum pump power required to adequately suspend the nonconvective layer throughout the tank so as to avoid episodic release of hydrogen

Premise - Present jet mixing pump may/may-not be of adequate size

Uncertainties - What are the important scaling parameters in designing full-scale system from small-scale tests. Depends on the critical event

- Dislodging the solids - (jet velocity) (jet diameter)
- Suspending the solids - (jet velocity)^2/(tank diameter) + particle settling velocity
- Mixing intensity - (pumping power)/(tank volume)

Approach - Extensive numerical modeling (supported by physical modeling for validation) to elucidate meager physical data from the full-scale tests

Soliciting Input - In-situ velocity & viscosity sensors

EXAMPLES OF NUMERICAL MODELING

Following Plots

1) & 2) 3-D Vel. profiles in plane of one 3" jet (of two opposing jets) at 60 ft/sec, placed 1 ft and 3 ft off tank floor. Shows the greater scouring action with lower placement. Also low velocity at tank wall (probably little effect on wall solids).

3) 3-D vel. profiles in horizontal plane of #1 jet. Show most recirculation is horizontal rather than vertical because of density gradients in the tank.

4) Color concentration of #1 jet. Show extent of suspension after 5 min. Does not include possible buoyancy of any gas attached to particulates.

5) Iso-surface of 0.5 ft/sec lateral velocity of jet #1. Shows lateral velocity mostly contained within slurry region because of density gradient.

VELOCITY VECTORS
(Vertical plane through jet)
3" jet at 60 ft/sec
3 ft. off tank floor

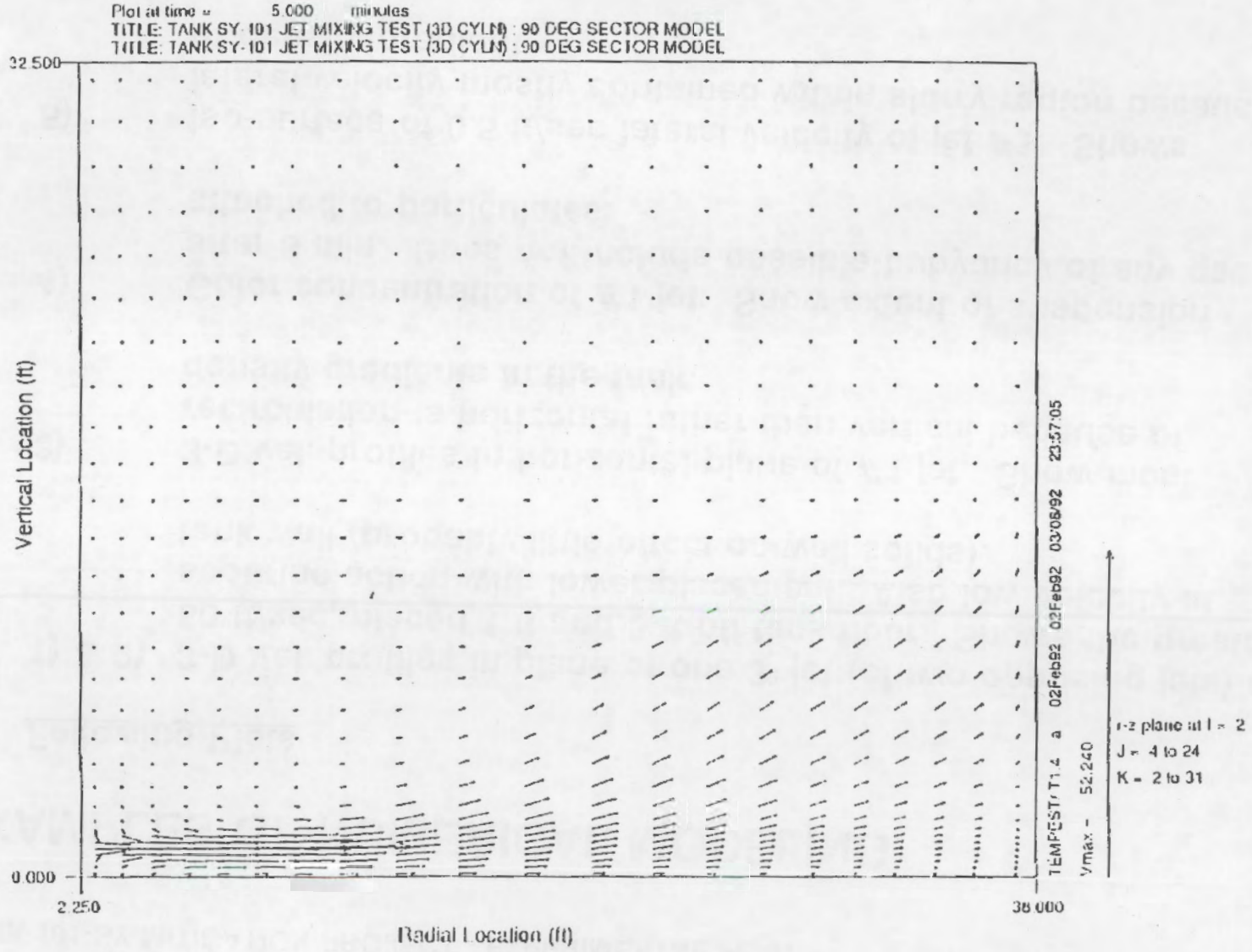

Figure 1.

VELOCITY VECTORS
(Vertical plane through jet)
3" jet at 60 ft/sec
1 ft. off tank floor

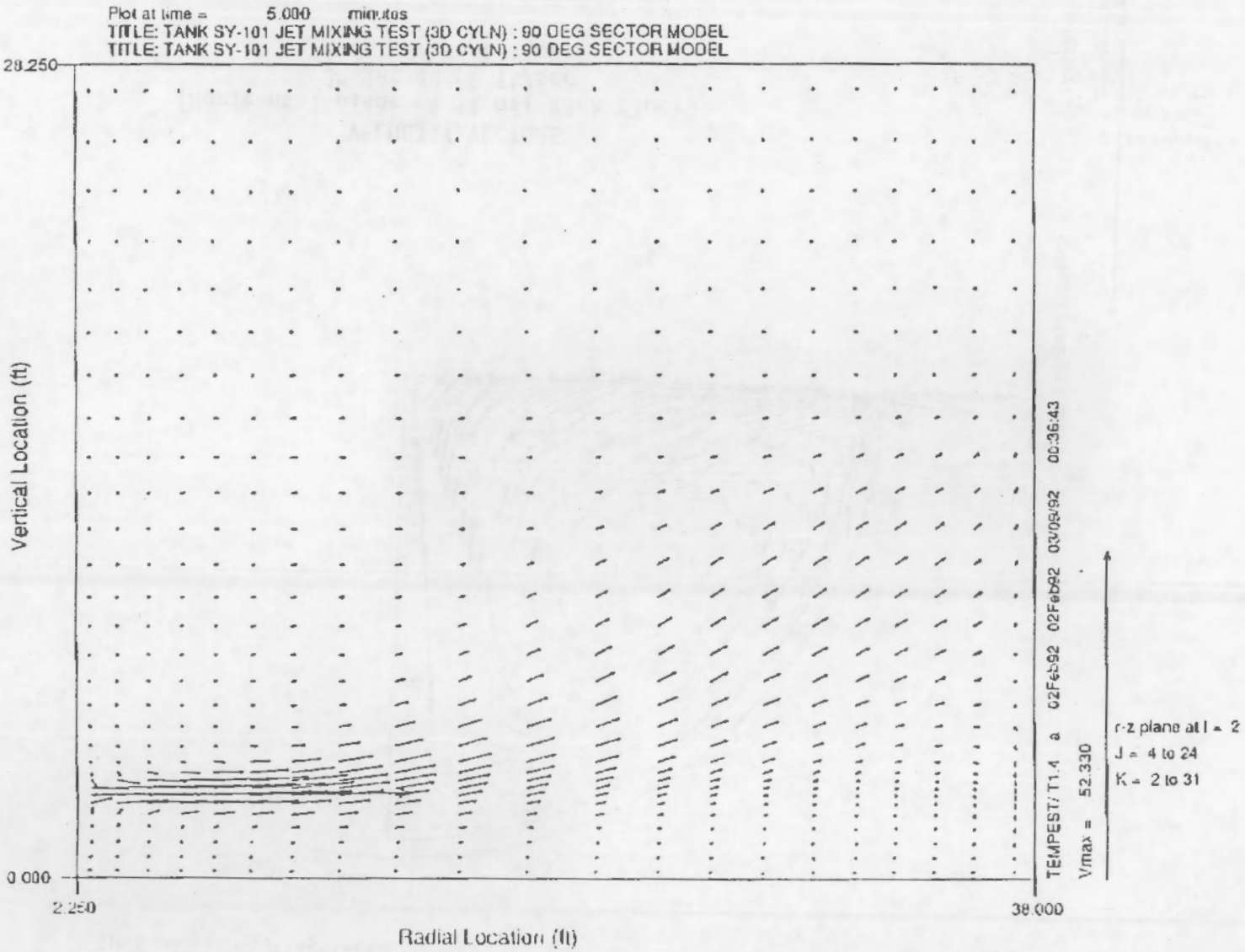

Figure 2

TEMPEST Quarter Model

Plot at time = 5.000 minutes
TITLE: TANK SY 101 JET MIXING TEST (3D CYLN) : 90 DEG SECTOR MODEL
TITLE: TANK SY 101 JET MIXING TEST (3D CYLN) : 90 DEG SECTOR MODEL

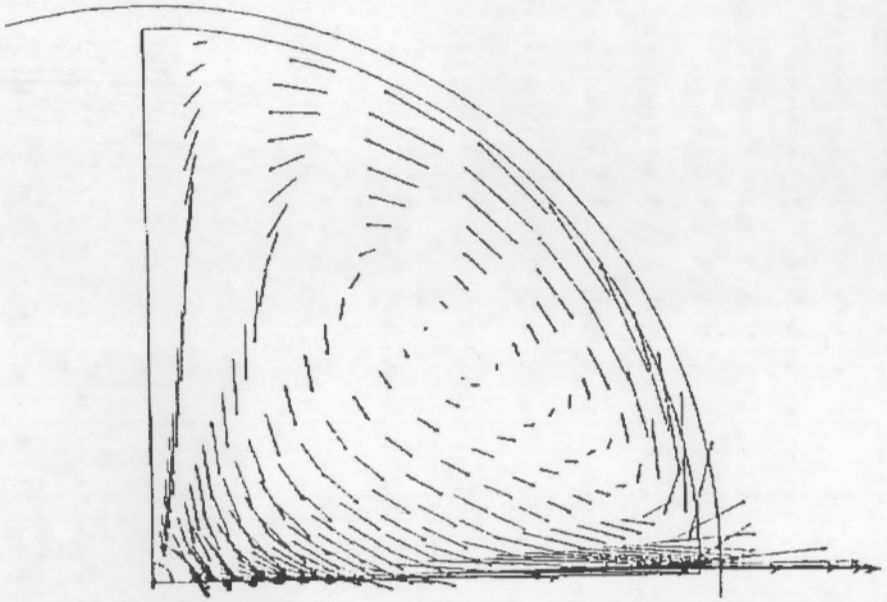

TEMPEST/T14 + 02Feb92 02Feb92 03/08/92 23:57:05
Vmax = 3.31
I x plane at K = 12
J - 1 to 25
I - 1 to 13

VELOCITY VECTORS
(Horizontal plane 4 ft off tank floor)
3" jet at 60 ft/sec
1 ft off tank floor

Figure 3

DENSITY VARIATIONS IN VERTICAL
PLANE THROUGH JET
3" jet at 60ft/sec
1 ft off tank floor

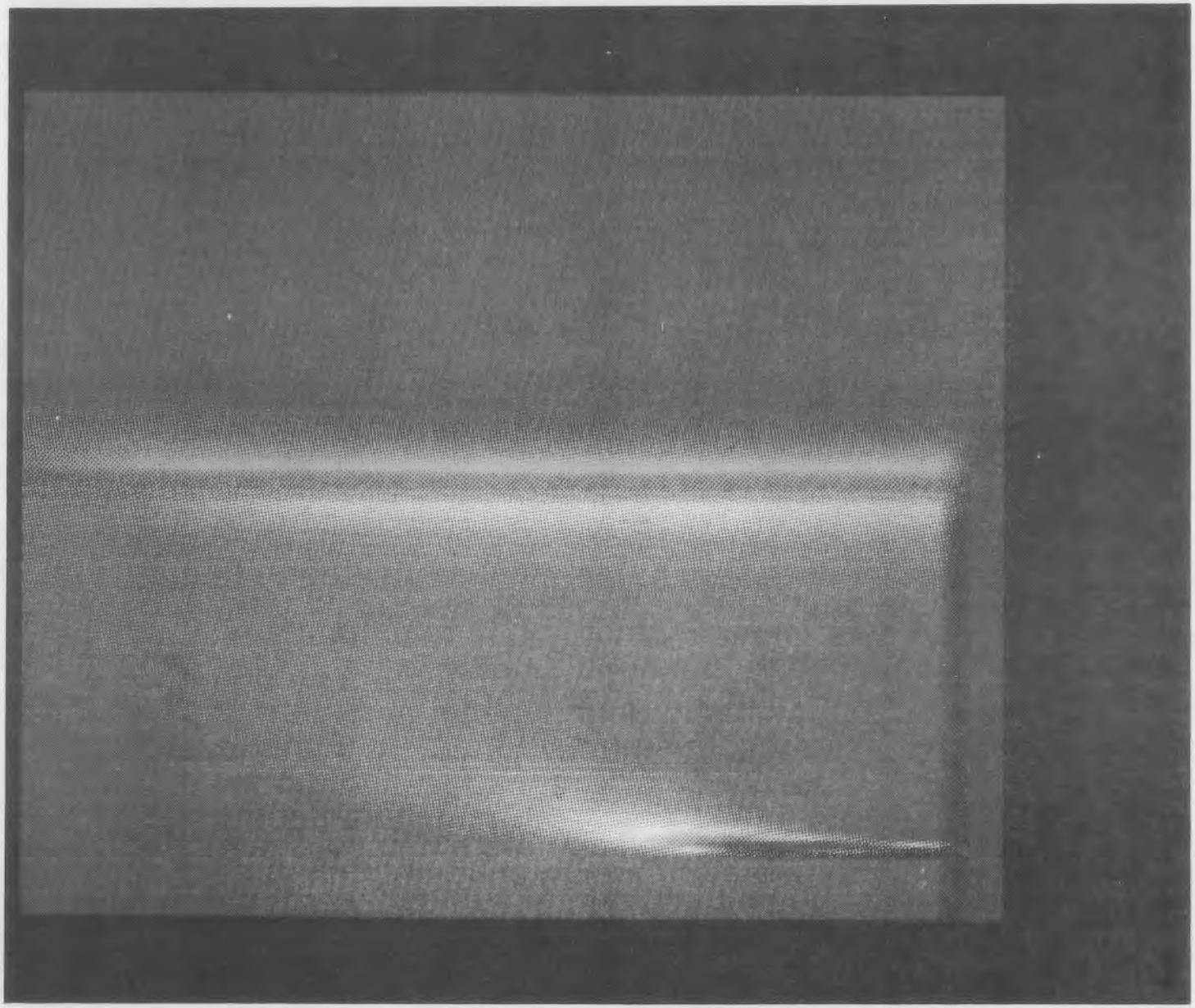

ISO-VELOCITY SURFACE OF LATERAL
VELOCITY OF 0.5ft/sec
3" jet at 60ft/sec
3 ft off tank floor

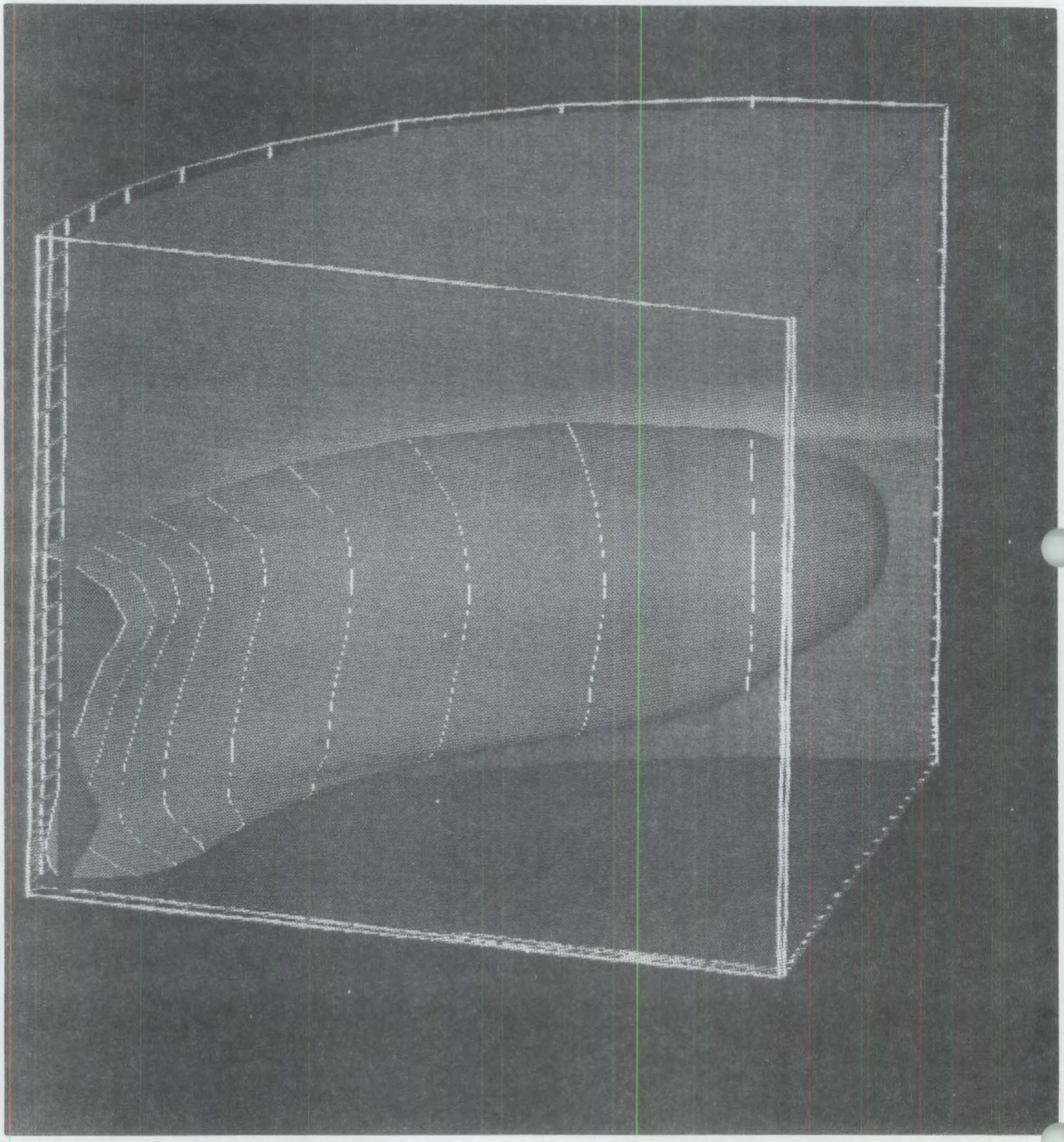

EXAMPLES OF NUMERICAL MODELING

Following Plots

6) & 7) Color concentration of "Ducted" jet with 4x flow and diameter but 1/4x velocity. #6 -5 min, #6 - 20 min. Shows more boyant character of the jet. Results in better mixing. Changes with time due to changes in fluid density.

8) Iso-surface of concentration. Shows unexpected scouring of flour near wall due to back mixing.

Potential Impact

- Ducted jet better if suspension of solids is primary interest.
- Unducted jet provides better scouring action

JET MIXING TESTING SEQUENCE
(Tentative)

1) Jet Radius vs. Pump Power

   - No rotation of jet, increase pump speed for 0 to max and note region affected

   - With jet rotation,

     - Limited, then full rotation at low flow

     - Limited, then full rotation at medium, then full flow

2) Mixing effectiveness with periodic start/stop operation

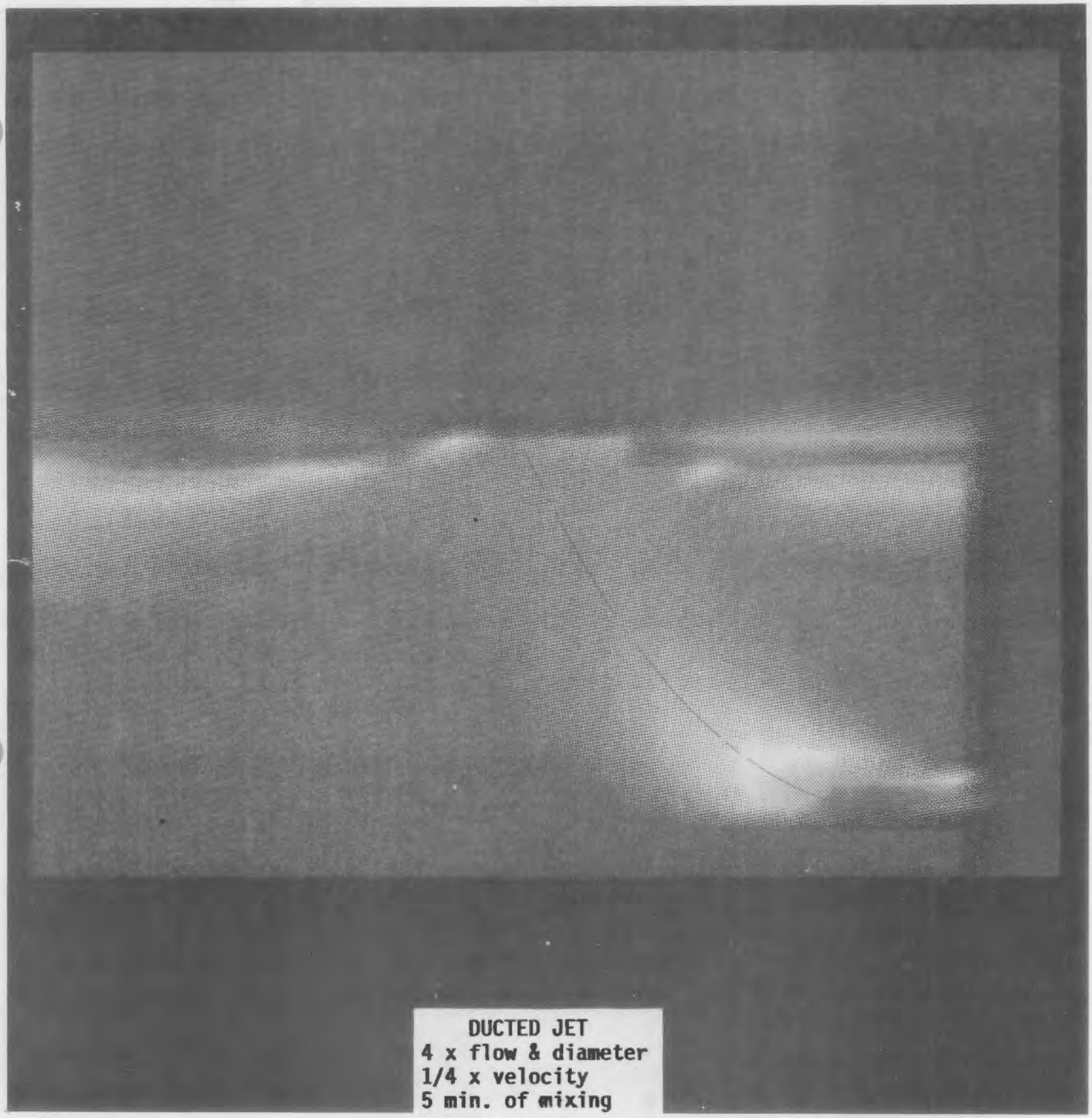

DUCTED JET
4 x flow & diameter
1/4 x velocity
5 min. of mixing

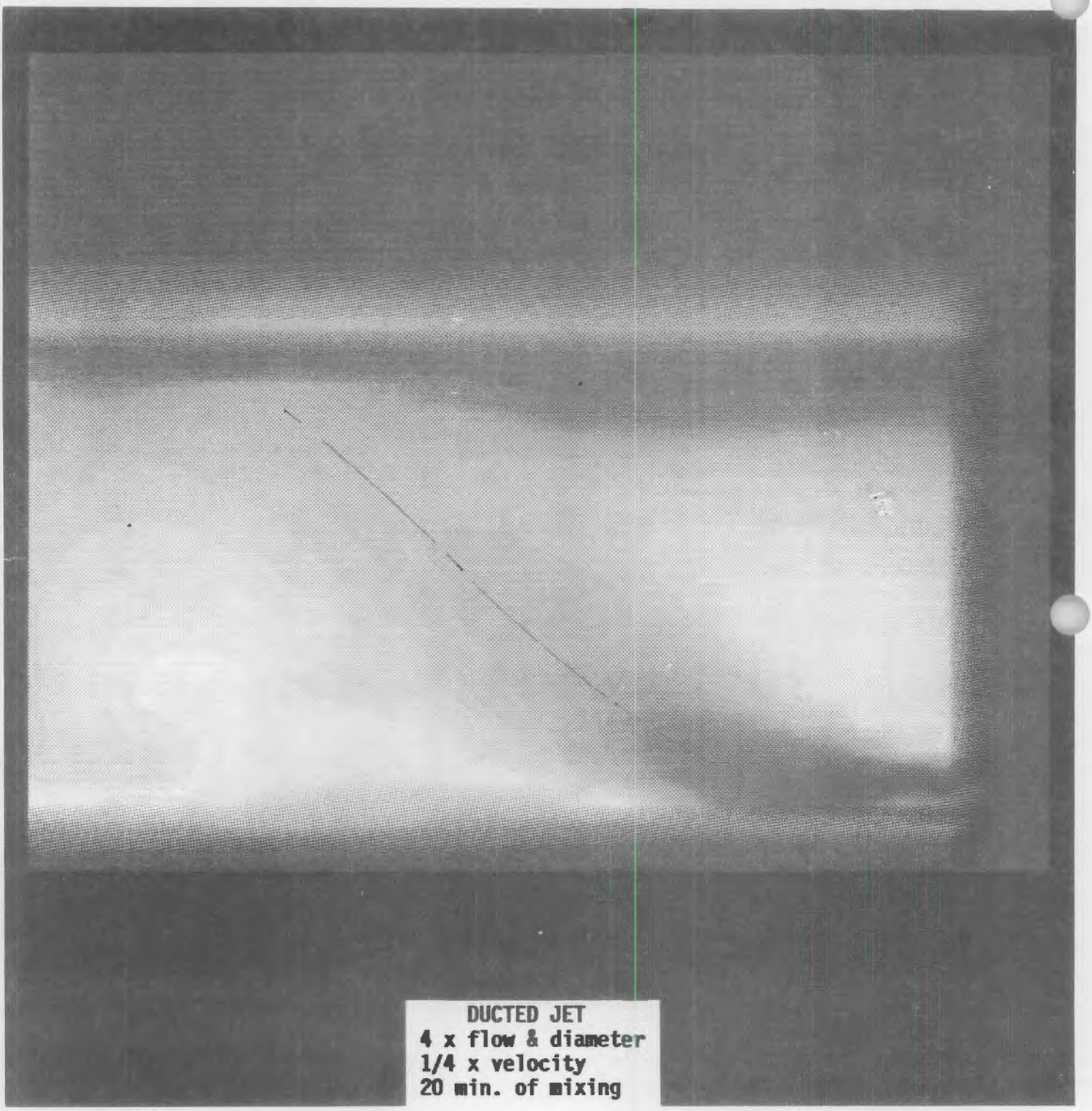
DUCTED JET
4 x flow & diameter
1/4 x velocity
20 min. of mixing

ISO-SURFACE OF CONCENTRATION

Note scouring of floor near wall

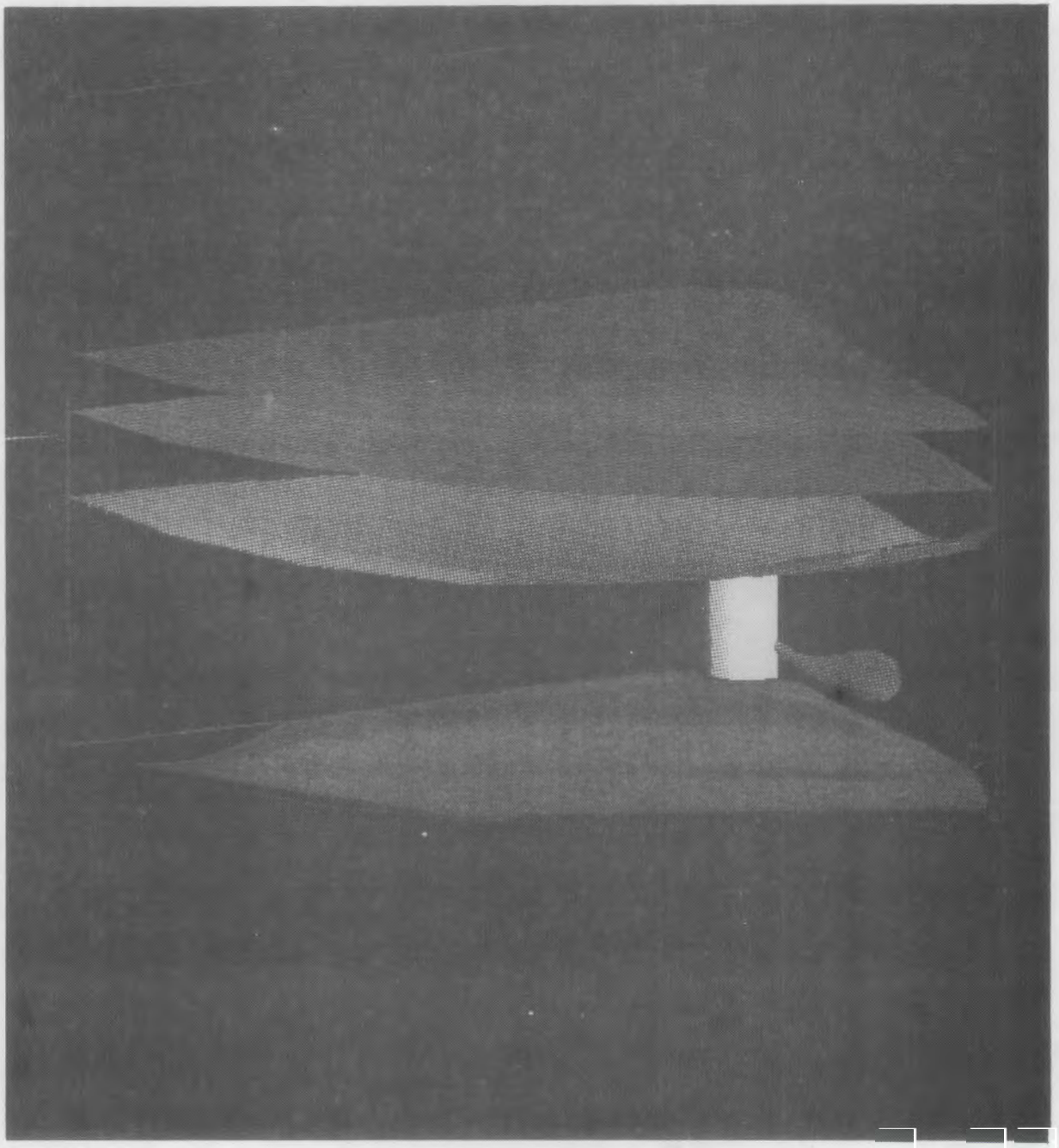

JET MIXING DATA REQUIREMENTS

Primary Data: Surface Level - Adequate mixing prevents the retention of gas indicated by no surface level rise

Secondary Data: Hydrogen Concentration - any increase above background would indicate some mixing effectiveness

Supernatant Density - An increase is evidence of suspension of solids from slurry level

Temperature (vertical gradient) - Measured at two radii will indicate mixing in the non-convecting layer

Radial Velocity - Would be primary data but for difficulty of getting any reliable method for other than relative values

In-tank Video - Note the extent of upwelling that may occur if gas is evolved from a limited region

Desired/Optional: Viscosity - Good indicator of particle density (hence mixing extent) but timely development of in-situ measurement uncertain

TEST APPROACH - ENCLOSED CHAMBER PROBE

- Objective - Determine effectiveness of three different approaches to mitigation - ultrasonic, heating, dilution

- Premise - By sequencing tests, the effectiveness of each approach can be determined

- Uncertainty - How do you proceed from one test to the next if the mitigation approach is only partially successful?

- Approach - Use the telescoping feature of the probe design to allow the re-establishment of a slurry layer within the chamber region.

Mitigation Chamber Test Sequence Logic

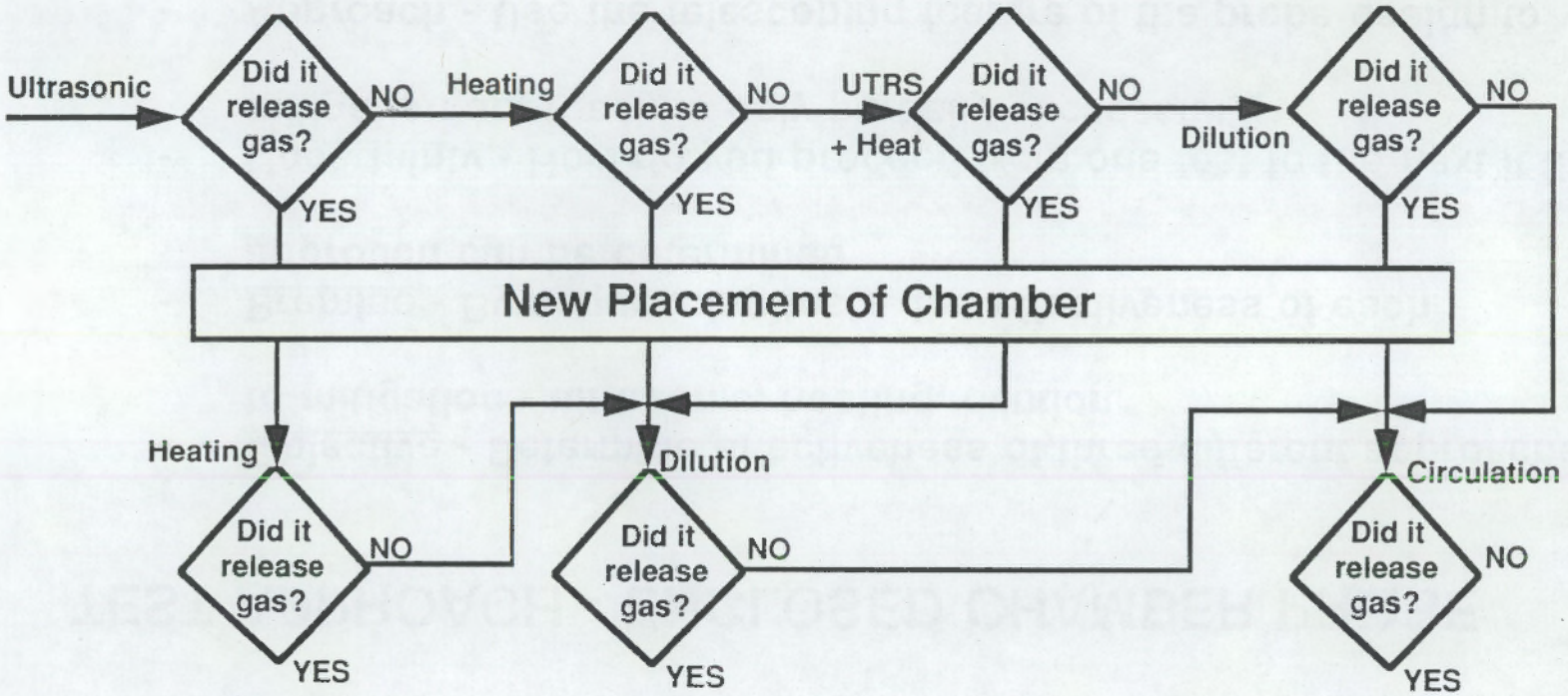

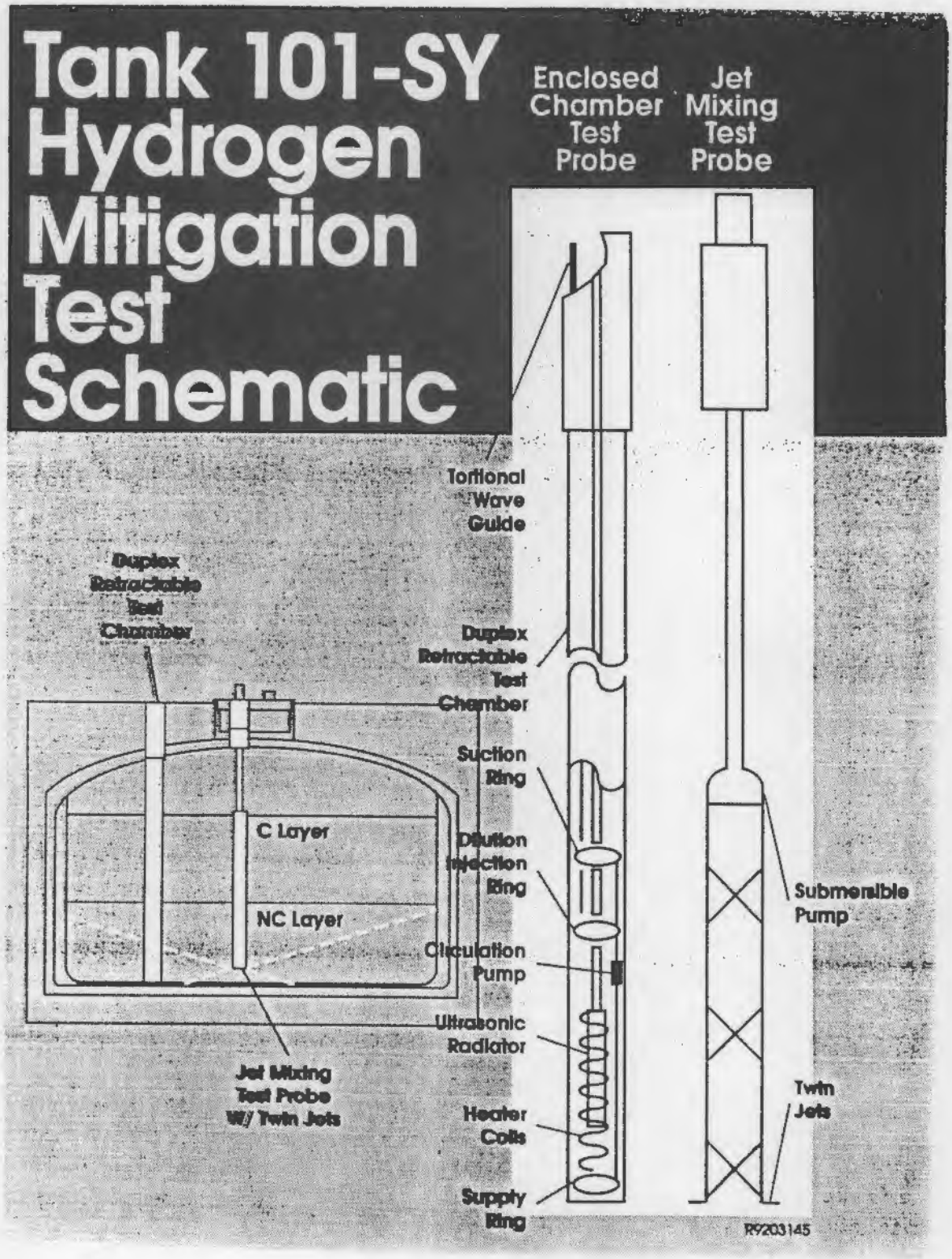
Tank 101-SY Hydrogen Mitigation Test Schematic
Enclosed Chamber Test Probe
Jet Mixing Test Probe
Torsional Wave Guide
Duplex Retractable Test Chamber
Suction Ring
Dilution Injection Ring
Circulation Pump
Ultrasonic Radiator
Heater Coils
Supply Ring
Submersible Pump
Twin Jets
C Layer
NC Layer
Jet Mixing Test Probe W/ Twin Jets
R9203145

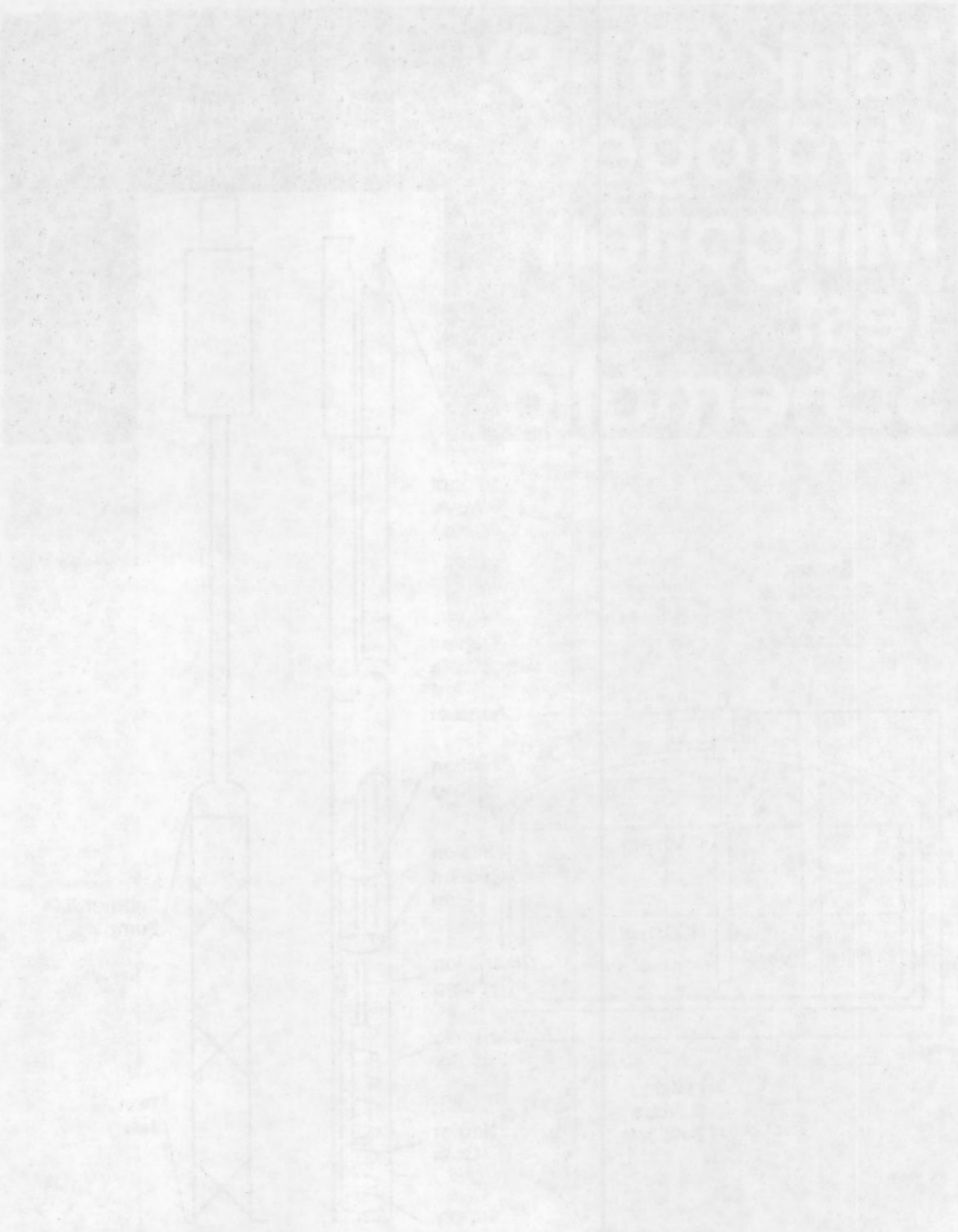

DISTRIBUTION

No. of Copies

OFFSITE

12 DOE/Office of Scientific and Technical Information

J. Tseng
U.S. Department of Energy
EM-35
Trevion II
Washington, DC 20585-0002

C. Abrams
1987 Virginia
Idaho Falls, ID 83404

S. Agnew
Los Alamos National Laboratory
MS-C345, Group INC-4
P.O. Box 1664
Los Alamos, NM 87545

J. Antizzo
U.S. Department of Energy
EM-351
Trevion II
Washington, DC 20585-0002

E. C. Ashby
225 North Avenue
Boggs Chemistry Building
Georgia Institute of Technology
Atlanta, GA 30332

K. Bandyopadhyay
Building 129
Brookhaven National Laboratory
Upton, NY 11973

N. E. Bibler
Westinghouse Savannah River
Bldg. 773A, Room 108
Aiken, SC 29802

No. of Copies

D. Campbell
Oak Ridge National Laboratory
P.O. Box 2008, MS 6268
Oak Ridge, TN 37831-6268

F. Carlson
6965 North, 5th West
Idaho Falls, ID 83401

G. R. Choppin
Department of Chemistry B-164
Florida State University
Tallahassee, FL 32306

P. d'Entremont
Westinghouse Savannah River
P.O. Box 616, Bldg. 703-H
Aiken, SC 29802

R. Daniels
SAIC
20030 Century Blvd.
Suite 201
Germantown, MD 20878

M. First
295 Upland Avenue
Newton Highlands, MA 02161

C. Forsberg
Massachusetts Institute of Technology
Room 24-109
77 Massachusetts Avenue
Cambridge, MA 02139

C. Grelecki
Hazards Research Corporation
200 Valley Rd, Suite 301
Mt. Arlington 07856

E. J. Hart
2115 Hart Road
Port Angeles, WA 98362

No. of
Copies

P. Hogroian
SAIC
20030 Century Blvd., Suite 201
Germantown, MD 20874

E. P. Horwitz
Chemistry Division
Argonne National Laboratory
Argonne, IL 60439

A. Hoskins
WINCO, MS-5217
P.O. Box 4000
Idaho Falls, ID 83403-4000

B. Hudson
Lawrence Livermore National
Laboratory, L-221
P.O. Box 808
Livermore, CA 94550

M. Kazimi
Room 24-102
77 Massachusetts Avenue
Cambridge, MA 02139

P. Kiang
BDM, Trevion I, Suite 300
12850 Middlebrook Road
Germantown, MD 20874

B. R. Kowalski
Chemistry Dept. BG-10
University of Washington
Seattle, WA 98195

T. Kress
P.O. Box 2009
MS 8088, Building 9108
Oak Ridge, TN 37381

T. Larson
Los Alamos National
Laboratory, M-1
MS C-920, P.O. Box 1663
Los Alamos, NM 87545

No. of
Copies

D. Meisel
Argonne National Laboratory
9700 South Cass Avenue
Argonne, IL 60439

D. Oakley
Los Alamos National
Laboratory
University of California,
Suite 310
409 12th Street, SW
Washington, DC 20024-2188

F. L. Parker
Vanderbilt University
P.O. Box 1596, Station B
Nashville, TN 37235

D. Ploetz
West Valley Nuclear
Services Co.
P.O. Box 191, MS 305
West Valley, NY 14171-0191

G. Powers
Design Science Inc.
163 Witherow Road
Sewickley, PA 15143

M. Reich
Building 129
Brookhaven National Laboratory
Upton, NY 11973

G. A. Russell
Department of Chemistry
Iowa State University
Ames, Iowa 50011-3111

J. Saveland
20030 Century Blvd., Suite 201
Germantown, MD 20874

G. Schmauch
Air Products & Chemicals, Inc.
7201 Hamilton Blvd.
Allentown, PA 18195-1501

No. of
Copies

A. Schneider
Massachusetts Institute of Technology
Department of Nuclear Engineering
Room 24-108
77 Massachusetts Avenue
Cambridge, MA 02139

W. W. Schulz
727 Sweetleaf Drive
Wilmington, DE 19808

B. Schutte
EG&G Idaho, Inc.
P.O. Box 1625
Idaho Falls, ID 83415-3940

D. D. Siemer
WINCO
IRC, MS 2207
Idaho Falls, ID 83403

S. Slezak
Sandia National Laboratories,
Division 6463
P.O. Box 5800
Albuquerque, NM 87185

H. Sullivan
Los Alamos National
Laboratory, N-6, MS-K557
P.O. Box 1664
Los Alamos, NM 87545

H. Sutter
SAIC
20030 Centry Blvd
Suite 201
Germantown, MD 20878

C. Terrell
U.S. Department of Energy,
Bldg. 704-S
P.O. Box A
Aiken, SC 29801

No. of
Copies

W. J. Thomson
Department of Chemical
Engineering
Washington State University
Pullman, WA 99164

E. Tuthill
Brookhaven National Laboratory
Upton, NY 11973

A. S. Veletsos
5211 Paisley
Houston, TX 77096

G. B. Wallis
Thayer School of Engineering
Dartmouth College
Hanover, NH 03755

H. Walter
U.S. Department of Energy
EM-343
Trevion II
Washington, DC 20585-0002

M. Walter
U.S. Department of Energy
EM-35
Trevion II
Washington, DC 20845-0002

D. Wiffen
U.S. Department of Energy
EM-35
Trevion II
Washington, DC 20585-0002

G. Woodall
U.S. Department of Energy,
MS-1139
785 DOE Place
Idaho Falls, ID 83402

ONSITE

No. of Copies

6 DOE Richland Field Office

R. F. Christensen, A4-02
R. E. Gerton, A5-21
N. G. McDuffie, B2-42
G. Rosenwald, A5-21
B. J. Tucker, A4-35
Reading Room, A1-65

43 Westinghouse Hanford Company

H. Babad, B2-15
D. B. Bechtold, T6-50
M. L. Bell, T5-50
R. M. Black, R1-19
R. J. Bliss, B3-04
W. F. Brehm, N2-01
T. M. Burke, H0-34
R. J. Cash, B3-68
C. Defigh - Price, R2-31
J. L. Deichman, H0-03
G. L. Dunford, R1-51
J. C. Fulton, R2-31
K. A. Gasper, B3-68
H. D. Harmon, R2-52
W. H. Hamilton, R2-40
D. L. Herting, T6-50
J. D. Hopkins, R2-08
G. D. Johnson, L5-03 (5)
N. W. Kirch, R2-11
W. L. Knecht, H0-34
W. D. Leggett, L5-04 (5)
J. W. Lentsch, R2-78
R. M. Marusich, H5-32
L. D. Muhlestein, N1-28
J. C. Person, T6-50
J. G. Propson, R2-18
D. A. Reynolds, R2-11 (5)
W. G. Ruff, R2-53
M. H. Shannon, B1-35
D. D. Stepnewski, H5-32
D. D. Wodrich, R2-23

58 Pacific Northwest Laboratory

R. T. Allemann, K5-19
R. M. Bean, P8-08
S. A. Bryan, P7-35
L. L. Burger, P7-25
J. A. Campbell, P8-08
J. B. Colson, K5-10
T. H. Dunning, K2-18
R. T. Hallen, P8-38
M. S. Hanson, K1-51
B. M. Johnson, Jr., K5-02 (5)
M. R. Kreiter, K7-90
D. K. Lemon, K2-28
G. B. Mellinger, P7-18
L. G. Morgan, P8-07
L. R. Pederson, K2-44
J. T. A. Roberts, K1-73
R. D. Scheele, P7-25
G. F. Schiefelbein, P8-38
J. C. Spanner, K2-31
J. D. Spencer, K1-40
D. M. Strachan, K2-44 (25)
R. W. Stromatt, P7-22
D. S. Trent, K1-82
H. H. Van Tuyl, P7-22
Publishing Coordination
Technical Report Files (5)